

Sustainable Aviation

T. Hikmet Karakoc · Siripong Atipan ·  
Alper Dalkiran · Ali Haydar Ercan ·  
Navatasn Kongsamutr ·  
Vis Sripawadkul *Editors*

# Research Developments in Sustainable Aviation

Proceedings of International  
Symposium on Sustainable Aviation  
2021


 **SARES**  
INTERNATIONAL SUSTAINABLE AVIATION  
AND ENERGY RESEARCH SOCIETY




Springer

# Sustainable Aviation

## Series Editors

T. Hikmet Karakoc , Eskisehir Technical University, Eskisehir, Türkiye and Istanbul Ticaret University, Istanbul, Türkiye

C. Ozgur Colpan , Department of Mechanical Engineering, Dokuz Eylül University, Buca, Izmir, Türkiye

Alper Dalkiran , School of Aviation, Süleyman Demirel University, Isparta, Türkiye

The Sustainable Aviation book series focuses on sustainability in aviation, considering all aspects of the field. The books are developed in partnership with the International Sustainable Aviation Research Society (SARES). They include contributed volumes comprising select contributions to international symposiums and conferences, monographs, and professional books focused on all aspects of sustainable aviation. The series aims at publishing state-of-the-art research and development in areas including, but not limited to:

- Green and renewable energy resources and aviation technologies
- Aircraft engine, control systems, production, storage, efficiency, and planning
- Exploring the potential of integrating renewables within airports
- Sustainable infrastructure development under a changing climate
- Training and awareness facilities with aviation sector and social levels
- Teaching and professional development in renewable energy technologies and sustainability

\* \* \*


T. Hikmet Karakoc • Siripong Atipan  
Alper Dalkiran • Ali Haydar Ercan  
Navatasn Kongsamutr • Vis Sripawadkul  
Editors

# Research Developments in Sustainable Aviation

Proceedings of International Symposium  
on Sustainable Aviation 2021


 Springer


### *Editors*

T. Hikmet Karakoc   
Faculty of Aeronautics and Astronautics  
Eskisehir Technical University  
Eskisehir, Eskisehir, Türkiye


Siripong Atipan   
Aerospace Engineering  
Kasetsart University  
Bangkok, Thailand

Information Technology Research  
and Application Centre  
Istanbul Ticaret University  
Istanbul, Türkiye

Alper Dalkiran   
School of Aviation  
Süleyman Demirel University  
Isparta, Isparta, Türkiye

Ali Haydar Ercan   
Porsuk Vocational School  
Eskisehir Technical University  
Eskisehir, Eskisehir, Türkiye

Navatasn Kongsamutr   
Aerospace Engineering  
Kasetsart University  
Bangkok, Thailand

Vis Sripawadkul   
Aerospace Engineering  
Kasetsart University  
Bangkok, Thailand

ISSN 2730-7778

ISSN 2730-7786 (electronic)

Sustainable Aviation

ISBN 978-3-031-37942-0

ISBN 978-3-031-37943-7 (eBook)

<https://doi.org/10.1007/978-3-031-37943-7>

© The Editor(s) (if applicable) and The Author(s), under exclusive license to Springer Nature Switzerland AG 2023

This work is subject to copyright. All rights are solely and exclusively licensed by the Publisher, whether the whole or part of the material is concerned, specifically the rights of translation, reprinting, reuse of illustrations, recitation, broadcasting, reproduction on microfilms or in any other physical way, and transmission or information storage and retrieval, electronic adaptation, computer software, or by similar or dissimilar methodology now known or hereafter developed.

The use of general descriptive names, registered names, trademarks, service marks, etc. in this publication does not imply, even in the absence of a specific statement, that such names are exempt from the relevant protective laws and regulations and therefore free for general use.

The publisher, the authors, and the editors are safe to assume that the advice and information in this book are believed to be true and accurate at the date of publication. Neither the publisher nor the authors or the editors give a warranty, expressed or implied, with respect to the material contained herein or for any errors or omissions that may have been made. The publisher remains neutral with regard to jurisdictional claims in published maps and institutional affiliations.

This Springer imprint is published by the registered company Springer Nature Switzerland AG  
The registered company address is: Gewerbestrasse 11, 6330 Cham, Switzerland  
Paper in this product is recyclable.

# Preface

In the past few decades, climate change and air pollution have been a source of grave concern around the globe. Both climate change and air pollution have substantial adverse effects on human health, a global problem. Expanding urban areas with extreme climate events such as heavy precipitation, high temperatures, floods, and droughts threaten human health. The amplified heat waves caused by climate change have increased temperatures, causing urban people thermal discomfort and several health problems. The majority of the world's megacities are threatened by escalating levels of air pollution above the requirements. Aerosols and PM concentrations have been investigated, and it is also essential to address the harmful health effects of particles inhaled by people and entering the respiratory system.

Airports and airspace have gotten more congested due to the fast development of air travel. Working at near-maximum capacity introduces risks that often result in operational disruptions, increased costs, and worse service quality. In addition to competing in a highly competitive market, airlines must streamline their operations to minimize costs. Several studies and applications show that the general public and policymakers seek to manage current infrastructure and activities better. Several of these projects focus on the effective allocation of resources to release unused capacity, reduce costs, and increase system resilience in the face of unforeseen events to develop sustainable transportation infrastructure. The world is also considering various options for increasing airspace capacity while lowering operational and environmental costs. Along with these activities, efficient management is critical for the aviation industry's long-term growth over the next few decades.

Over the years, sustainable aviation practices have significantly reduced greenhouse gas emissions. These efforts, however, have not maximized the aviation industry's contribution to the UN's Sustainable Development Goals. The growing air traffic volume and the profits derived from this sector have hampered the viability of airline operations. The aviation industry employs many tools and procedures for evaluating sustainability to solve this issue, which includes all socioeconomic and environmental sustainability components. Decision Support Systems examine the efficacy of eco-efficiency assessment methodologies and practices used for

sustainable airline operations using Artificial Intelligence, Deep Learning, and Neural Network models. The tools and models facilitate strategic and tactical decision-making in the aviation industry, promoting sustainable operations and mitigating present challenges.

International Symposium on Sustainable Aviation (ISSA'21), an international and multi-disciplinary symposium, was held online between November 25 and 27, 2021, to address current issues in the Research Developments in the Sustainable Aviation field. We have kindly invited academics, scientists, engineers, practitioners, policymakers, and students to attend ISSA'21 to share knowledge, demonstrate new technologies and breakthroughs, and debate the future direction, strategies, and goals in aviation sustainability. This conference featured keynote presentations by invited speakers and general papers in oral and poster sessions.

We want to thank Springer's editorial team for their support towards the preparation of this book and the chapter authors and reviewers for their outstanding efforts.

On the other hand, we would like to give special thanks to the SARES Editorial office members for their efforts in the long run for a symposium author communications, following the standards, are necessary to creating a proceedings book. Dilara Kılıç and Sinem Can have played a significant role in sharing the load and managing the chapters with Kemal Keleş.

Eskisehir, Türkiye  
Bangkok, Thailand  
Isparta, Türkiye  
Eskisehir, Türkiye  
Bangkok, Thailand  
Bangkok, Thailand

T. Hikmet Karakoc  
Siripong Atipan  
Alper Dalkiran  
Ali Haydar Ercan  
Navatasn Kongsamutr  
Vis Sripawadkul

## **Editorial Assistants**

Dilara Kılıç  
*Eskisehir Technical University*  
Kemal Keleş  
*Eskisehir Technical University*

Sinem Can  
*Eskisehir Technical University*

# Contents

<b>A Short Review on Sustainable Aviation and Public Promises on Future Prospects . . . . .</b>	<b>1</b>
Selcuk Ekici, Alper Dalkiran, and T. Hikmet Karakoc	
<b>Research on the Effects of Flight Procedures on Noise Contour Map Around Tan Son Nhat International Airport . . . . .</b>	<b>13</b>
Kiet La-Tuan and Anh Tran-Tien	
<b>Free Vibration Characteristics of a Variable-Span Morphing Wing . . . . .</b>	<b>19</b>
Damla Durmuş and Metin O. Kaya	
<b>Aero-Engine Emission Calculation Method and Its Limitation Analysis . . . . .</b>	<b>29</b>
Sanmai Su, Kaiheng Liang, and Rongzhang Xie	
<b>APC E-Rostering System . . . . .</b>	<b>37</b>
Titapong Chureeganon, Khemmarat Chunganuwat, Kacha Pinprasert, Chananporn Boonchaisiriporn, and Potchara Aungaphinant	
<b>Sustainable Aviation of Textile Industry: Life Cycle Assessment of the Pollutants of a Denim Jean Production Process . . . . .</b>	<b>45</b>
Delia Teresa Sponza and Nefise Erdiñçmer	
<b>Effects of Alternative Aviation Fuels on Environment and Enviro-economic . . . . .</b>	<b>51</b>
Selçuk Sarıkoç	
<b>Assessment of Oxygenated and Nanofluid Fuels as Alternative/Green Aviation Fuels . . . . .</b>	<b>57</b>
Selçuk Sarıkoç	



<b>An Evaluation of Particle Image Velocimetry in Terms of Correlation for Aviation</b> . . . . .	65
Onur Yasar, Selcuk Ekici, Enver Yalcin, and T. Hikmet Karakoc	
<b>Software Assessment for Particle Image Velocimetry for Aviation Industry</b> . . . . .	71
Onur Yasar, Selcuk Ekici, Enver Yalcin, and T. Hikmet Karakoc	
<b>Dye Visualization of Flow Structure of a Circular Cylinder Oscillating at <math>Re = 1000</math></b> . . . . .	77
Cemre Polat, Dogan Burak Saydam, Mustafa Soyler, and Coskun Ozalp	
<b>Aerodynamic Performance Predictions of Mars Helicopter Co-axial Rotor in Hover by Using Unsteady CFD Simulations</b> . . . . .	83
Onur Küçüköğlü, Sergen Sakaoğlu, and Nilay Sezer Uzol	
<b>Numerical Validation Study of a Helicopter Rotor in Hover by Using SU2 CFD Solver</b> . . . . .	91
Yunus Emre Sunay and Nilay Sezer Uzol	
<b>Sustainable Materials Used by Additive Manufacturing for Aerospace Industry</b> . . . . .	99
Alperen Doğru and Mehmet Özgür Seydibeyoğlu	
<b>Integration of Sustainability and Digitalization in Air Logistics: Current Trends and Future Agenda</b> . . . . .	109
Volkan Yavas and Yesim Deniz Ozkan-Ozen	
<b>Design of PI Controller for Longitudinal Stability of Fixed-Wing UAVs</b> . . . . .	117
Veena Phunpeng, Wilailak Wanna, and Thongchart Kerdphol	
<b>Effect of Work Shift Rotating on Fatigue Levels of Aircraft Mechanics in Line Maintenance</b> . . . . .	127
Monchai Suraratchai, Tutchakorn Siripanichsutha, and Pornnipa Voraprapaso	
<b>Strength Analysis of a Wing Structure for a Single Turboprop Normal Category Aircraft</b> . . . . .	135
Vis Sripawadkul and Phacharaporn Bunyawanichakul	
<b>Applying Glass Fiber-Reinforced Composites with Microsphere Particles to UAV Components</b> . . . . .	145
Veena Phunpeng, Wipada Boransan, and Thongchart Kerdphol	
<b>Decision-Making Modeling in Emergency “Unlawful Interference”</b> . . . .	151
Tetiana Shmelova, Maxim Yatsko, Yuliya Sikirda, and Eizhena Protsenko	

**Green Practices Adoption Among Leading Green Airlines . . . . .** 157  
 Teeris Thepchalerm and Phutawan Ho

**Design and Testing of Multiple Web Composite Wing Spar  
 for Solar-Powered UAV . . . . .** 163  
 Varissara Wongprasit, Nasapol Thanomwong,  
 and Chinnapat Thipyopas

**Comparative Study Between Aluminum and Hybrid Composite  
 for UAV . . . . .** 175  
 Veena Phunpeng, Karunamit Saensuriwong, and Thongchart Kerdphol

**Static and Modal Analysis of UAV Composite-Based Structures . . . . .** 181  
 Veena Phunpeng, Sireegorn Sumklang, and Thongchart Kerdphol

**A More Electric Aircraft Application: Starter/Generator . . . . .** 189  
 Ufuk Kaya and Eyyup Oksuztepe

**Safety Culture and Safety Management System in Aviation . . . . .** 199  
 Emre Nalçacıgil and Betül Kaçar

**Airline Service Quality Attributes . . . . .** 209  
 Araya Sakburanapech, Narinisara Thongpa, and Prawit Otanalai

**The Influence of Fuels Containing Fatty Acids Ethers on Fuel  
 Systems . . . . .** 215  
 Daryna Popytailenko and Olena Shevchenko

**Exposure Potential of Environment by Entropy Continuity  
 for Cruise Altitude of Aircraft Engine . . . . .** 221  
 M. Ziya Sogut

**Examining Thermo-Economic and Environmental Performance  
 of Piston Engine Considering LNG Fuel Transition of Aircraft . . . . .** 229  
 M. Ziya Sogut

**Breaking the Aircraft Vortex Wake Near the Ground:  
 Mitigation of Turbulence Wake Hazard . . . . .** 237  
 Theerawit Tekitchamroon, Watchapon Rojanaratanangkule,  
 and Vejapong Juttijudata

**Beyond Technology: Digital Transformation in Aerospace  
 and Aviation . . . . .** 243  
 Pasit Suebsuwong

**Circulation Control Flap: En Route Toward Sustainable  
 High-Lift Devices . . . . .** 249  
 Akanit Nimmanmongkol, Chinnapat Chumsing,  
 and Vejapong Juttijudata

<b>Sustainability Indices for Airport Sustainability Evaluation . . . . .</b>	<b>257</b>
Orhan Yücel, Alper Dalkiran, Seval Kardeş Selimoğlu, and T. Hikmet Karakoc	
<b>An Approach to Optimizing Aircraft Maintenance . . . . .</b>	<b>263</b>
Onyedikachi Chioma Okoro, Maksym Zaliskyi, and Serhii Dmytriiev	
<b>In Search of Environmental Protection Element in the Thai Aviation Law: A Result from CORSIA . . . . .</b>	<b>271</b>
Lalin Kovudhikulrungsri, Jantajira Iammayura, Krittika Lertsawat, Kornwara Boonsiri, Navatasn Kongsamutr, and Prangtip Rabieb	
<b>Seamless Passenger Experience for the Airport Environment: Research at DARTeC . . . . .</b>	<b>277</b>
Fatma Gul Amil, Zeeshan Rana, and Yifan Zhao	
<b>Critiques and Challenges of Air Transport Liberalisation Policy in Thailand . . . . .</b>	<b>285</b>
Navatasn Kongsamutr	
<b>Digitalization in the Way of Aviation Sustainability . . . . .</b>	<b>293</b>
Rafet Demir, Serap Gürsel, and Hakan Rodoplu	
<b>Effect of Phase Change Material Dimension on Maximum Temperature of a Lithium-Ion Battery . . . . .</b>	<b>301</b>
Uğur Morali	
<b>Global, Regional, and Local Issues of ICAO Balanced Approach to Aircraft Noise Management in Airports . . . . .</b>	<b>307</b>
Oleksandr Zaporozhets	
<b>Fuel Consumption Analysis of Gradual Climb Procedure with Varied Climb Angle and Airspeed . . . . .</b>	<b>315</b>
Siripong Atipan and Pawarej Chomdej	
<b>Investigation of Turbofan Engine Emissions at Different Cruise Conditions for Greener Flights . . . . .</b>	<b>321</b>
Ali Dinc, Ibrahim Elbadawy, Mohamed Fayed, Kaushik Nag, Rani Taher, and Yousef Gharbia	
<b>Effects of Strategic Alliance Membership on the Environmental Performance of Airlines . . . . .</b>	<b>329</b>
Serap Gürsel and Gamze Orhan	
<b>Safety Factor Analysis in Ramp Operation with AHP Approach . . . . .</b>	<b>335</b>
Ilker Inan and Ilkay Orhan	
<b>Evaluating Total Load of Aviation Operators by Analytic Hierarchy Process (AHP) . . . . .</b>	<b>341</b>
Omar Alharasees and Utku Kale	

<b>Experimental and Analytical Principles of Improving Waste Management Technologies in the Technosphere</b> . . . . .	351
Ihor Trofimov, Sergii Boichenko, Iryna Shkilniuk, Anna Yakovlieva, Sergii Shamanskyi, Tetyana Kondratyuk, and Oksana Tarasiuk	
<b>Investigation of Electromagnetic Effect of Lightning on Aircraft by Finite Element Method</b> . . . . .	363
Semen Memis, Ozcan Kalenderli, and Ozkan Altay	
<b>Research of Tribological Characteristics of Modern Aviation Oils</b> . . . . .	371
Oksana Mikosianchyk and Olga Ilina	
<b>Evaluation of Nanostructured Materials: PEM Fuel Cell Applications</b> . . . . .	379
Murat Ayar, Ozge Yetik, and T. Hikmet Karakoc	
<b>Overview of Hydrogen-Powered Air Transportation</b> . . . . .	385
Hursit Degirmenci, Alper Uludag, Selcuk Ekici, and T. Hikmet Karakoc	
<b>Evaporative Hydrocarbon Emission of Gasoline During Storage in Horizontal Tanks and Their Energy and Environmental Efficiency</b> . . . . .	395
Sergii Boichenko, Dubrovska Viktoriia, Shkyar Viktor, Iryna Shkilniuk, Anna Yakovlieva, and Oksana Tarasiuk	
<b>Technologies for Alternative Jet Fuel Production From Alcohols</b> . . . . .	407
Anna Yakovlieva, Sergii Boichenko, and Vasyi Boshkov	
<b>Analysis of World Practices of Using Liquid Hydrogen as a Motor Fuel for Aviation</b> . . . . .	413
Sergii Boichenko, Ihor Trofimov, Anna Yakovlieva, and Oksana Tarasiuk	
<b>Waste-Free Technology for the Production of Building Materials by Mining and Processing Plants</b> . . . . .	423
Oksana Vovk, Kostiantyn Tkachuk, Oksana Tverda, Andrii Syniuk, and Eduard Kukuishnyi	
<b>Index</b> . . . . .	429

# A Short Review on Sustainable Aviation and Public Promises on Future Prospects



Selcuk Ekici, Alper Dalkiran , and T. Hikmet Karakoc 

## 1 Introduction

The need to manage resources (Liu, 2003), which are the foundation of the maintenance of our generation, in such a way that the average quality of life we provide for ourselves can potentially be shared by all future generations has enabled sustainability to take place in the literature (Owusu & Asumadu-Sarkodie, 2016). This idea is based on the notion that economic concerns threaten human life in the world and that people will be deprived of many resources in the future (Anand & Sen, 2000). In other words, it also refers to items that both current and future human generations can support (Mensah, 2019). Today, the notion of sustainability is one of the most prominent subjects in social, financial, and management literature (Carter & Liane Easton, 2011). Sustainability, in concept, indicates the relationship between financial forces functioning with the evolution of civilizations (Vlek & Steg, 2007) and is impacted by environmental (Oláh et al., 2020), social (Windolph et al., 2014), cultural (Auclair & Fairclough, 2015), and economic activities (Khan et al., 2022). The first financial models have solely considered economic growth rates, not things like environmental quality or biota consciousness (Mulder & van den Bergh, 2001). The current environmental issues are reflected in financial models that have been

---

S. Ekici

Department of Aviation, Iğdır University, Iğdir, Türkiye

A. Dalkiran (✉)

School of Aviation, Suleyman Demirel University, Kecioburlu, Türkiye

e-mail: [alperdalkiran@sdu.edu.tr](mailto:alperdalkiran@sdu.edu.tr)

T. H. Karakoc

Faculty of Aeronautics and Astronautics, Eskişehir Technical University, Eskişehir, Türkiye

Information Technology Research and Application Centre, Istanbul Ticaret University, Istanbul, Türkiye

e-mail: [hkarakoc@eskisehir.edu.tr](mailto:hkarakoc@eskisehir.edu.tr)

developed by incorporating the idea of sustainability as a central theme (Morgan, 2012). In addition, sustainable development is a development that satisfies the requirements of the present without jeopardizing future generations' capacity to satisfy their own diverse demands (Basiago, 1995). As a result, today's financial institutions recognize the interconnectedness between development and the environment (Porket, 1998), and modern economic systems identify the need for ecological sustainability (Dincer, 2000).

## 2 Public Promises in Sustainable Aviation

Globally, the adoption of more sustainable paradigms is being encouraged by a growing awareness of the environmental damage caused by unsustainable economic growth models (Hall, 2010). In other words, on a global scale, there is a growing movement toward more sustainable paradigms as people become more aware of the environmental damage caused by unsustainable economic growth models (Asara et al., 2015). On the other hand, it is difficult to build an effective cooperative strategy for environmental issues stemming from financial structures owing to the expectations of many organizations and stakeholders on their activities (Diehl & Gleditsch, 2018). This makes the process of developing an effective joint strategy for environmental problems more complicated (Heikkurinen & Bonnedahl, 2013). It is anticipated that industrialized nations, in particular, will pave the way to a common policy due to the degradation of the ecological balance of the planet, which is brought on by pollution as well as the unsustainable use of resources (Water for a sustainable world, 2015). According to experts, ecological vitality is a prerequisite for economic development (Mavragani et al., 2016) as well as essential to ensuring that economic expansion can continue indefinitely, and growth is only sustainable when an environmental protection strategy program is in place (Feiock & Stream, 2001).

Nature has the capacity to purify and produce a limited quantity of food, raw materials, land, and water, therefore ensuring, preserving, and guaranteeing their availability in the future (Wellmer et al., 2019). Given that we will need resources in the future and that future generations have the right to utilize them, as well as the desire to profit from the resources we have now, one of our biggest challenges is how to use these finite resources without entirely depleting them (Pezzey & Toman, 2017). In order to address this issue and maintain environmental sustainability, the topic has gained ground in the literature (McKinnon, 2010). Environmental sustainability is described as actions that satisfy human needs without compromising biodiversity by considering the potential of ecosystems to regenerate and the concepts of resilience, adaptability, and interconnection of ecosystems (Morelli, 2011). Sustainability from an environmental perspective naturally implies sustainability from an ecological one (Brown et al., 1987). Ecological sustainability also means preserving the worth and quality of the natural environment and acknowledging that humans are a crucial component of the larger ecosystem (Brown et al., 1987).

Therefore, maintaining environmental sustainability implies supplying the resources needed by both the present and future generations without endangering the health of the planet's ecosystems (Holden et al., 2014). So, in addition to addressing climatic and environmental quality (Omer, 2008), as well as the preservation of biological variety (Marques, 2001), sustainability also includes the maintenance and/or improvement of an individual's quality of life in connection with the promotion of social equality (Moser, 2009).

The sustainability concept, targets, needs, and also mechanism maintain the recognition of sustainable aviation. Figure 1 represents those aspects of future prospects of sustainable aviation. There have been conflicting responses from major players in the air transportation sector regarding environmental sustainability (Graham & Guyer, 1999), the absence of adequate plans for expanding airport capacity, and a modal shift to address anticipated growth in air transportation issues (Nijkamp & Geenhuizen, 1997), with a particular emphasis on environmentally incompatible business practices utilized by airlines. Cooperative strategies allowed the consciousness of development policies, protection, and balance in a quality way.

As a sector that is suitable for all kinds of competition understanding and where sustainability is considered as the second element, the aviation sector, with all its components, takes its place in the literature as a sector that is frequently researched in terms of financial and environmental awareness in determining, improving, and implementing the sustainability parameters of aviation. Researchers and scientists kindly present studies of what can be done from different vantage points to assess possibilities, present new perspectives, and reveal numerous research areas to mitigate the negative effects of the aviation industry on monetary systems, governmental structures, the atmosphere, biological communities, and human societies. Studies from many different fields are addressed in all aspects as interdisciplinary in order to make the aviation sector sustainable and to ensure the long-term viability of the aviation sector. The following issues are characterized in the literature as having a significant influence and striking studies, as well as present particularly compelling questions about the extent to which the sustainability of the aviation industry lies on the eco-label gradient:

- (i) Application of alternative and renewable fuels to aviation gas turbine and reciprocating engines, including aviation ground equipment (Baroutaji et al., 2019; Bauen et al., 2020; Bicer & Dincer, 2017; Cavarzere et al., 2014; Chen et al., 2019; García-Contreras et al., 2022; Liu et al., 2021; Rochelle & Najafi, 2019; Seljak et al., 2020; Yilmaz & Atmanli, 2017)
- (ii) Supporting the use of nontraditional environmentally friendly sources and renewable sources of energy in airports (Akyuz et al., 2019; Almaz, 2022; Greer et al., 2020; Karakoc et al., 2016; Mostafa et al., 2016; Ortega Alba & Manana, 2016; Yerel Kandemir & Yaylı, 2016)
- (iii) Reducing aviation industry fuel consumption as well as increasing engine efficiency with various methods/equipment/technologies (Das et al., 2016; Johnson & Gonzalez, 2013; Nygren et al., 2009; Ryerson & Hansen, 2010; Ryerson & Kim, 2014; Seymour et al., 2020; Singh & Sharma, 2015)

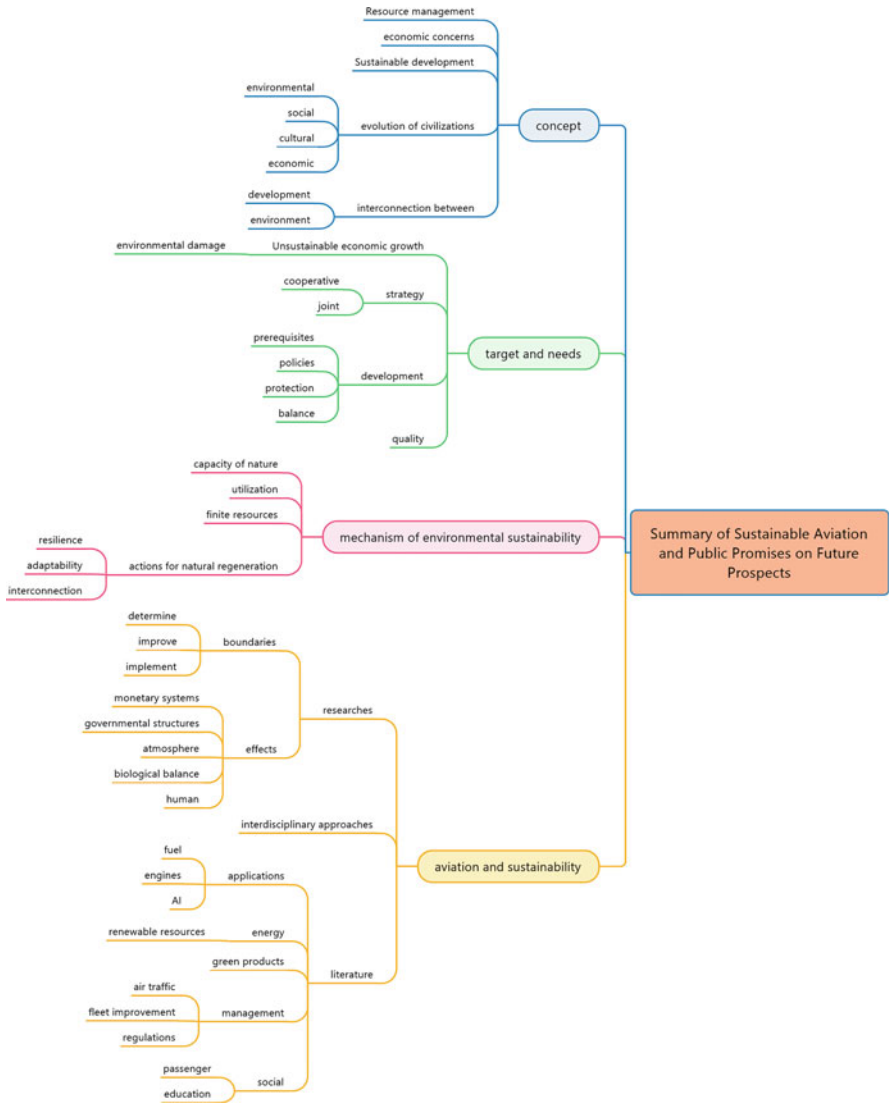


**Fig. 1** Summary of sustainable aviation and public promises on future prospects

- (iv) Developing/producing/employing green products for the aviation industry using the latest generation technologies (Barzkar & Ghassemi, 2020; Cronin, 1990; Hinnen et al., 2017; Lin, 2013; Rajjani & Kot, 2018; Sarkar, 2012a, b; Wheeler, 2016)
- (v) Air traffic management and trajectory as well as route/flight operation optimizations (Aksoy et al., 2021; Aksoy et al., 2018; Gagne et al., 2013; Jensen et al., 2013; Turgut et al., 2019; Turgut & Usanmaz, 2018)



- (vi) Putting fleets into operation with state-of-the-art gas turbine engines with low noise and gas emissions (Jansohn, 2013; Liu et al., 2017; Nemitallah et al., 2022; Zong et al., 2022)
- (vii) Application of taxation and sanctions for the externality of the effect for aircraft, airlines, and airports where the suitability of the values of noise and gas emissions is outside the scale (Berker & Böcher, 2022; Cui et al., 2022; Ekici et al., 2022; Fageda & Teixidó, 2022; Lai et al., 2022)
- (viii) Specifying the concepts of internality and externality of aviation taxes for the countries (Janić, 1999; Lu, 2009; Schipper et al., 2001; Valdés et al., 2021)
- (ix) Analyzing the travel behavior of passengers (Baumeister, 2020; Wild et al., 2021)
- (x) Application of artificial intelligence methods to ground and flight operations records (Abdul-Aziz & Hashemi, 2022; Benahmed et al., 2022; Malaek & Alipour, 2022; Tikhonov et al., 2022)
- (xi) Carrying out advertising initiatives to educate customers and society about sustainable aviation technology and using public relations efforts to enlighten the public about environmentally friendly aircraft technology (Desha & Hargroves, 2013; Dimitriou & Sartzetaki, 2020; Oto et al., 2012; Upham et al., 2012)
- (xii) Most importantly, presenting to scientists, researchers, and regulators the aviation industry data (airports, FDR data, and so on) in an easily accessible and transparent way

The stakeholders' commitments drive the recognition of sustainable aviation operations and sustainable development. The properties of the recognition can be summarized under the financial attractiveness and the obligations built on the public interests and benefits. The obligation of improved environmental sustainability is supported by the recognition of how the airlines, airports, and other stakeholders fit in the sustainability indices (Sarkar, 2012a, b). That is why the certification systems have been constructed. In partnership with businesses, academic institutions, and other EU partners, the European Commission created the Clean Sky Joint Technology Initiative in 2007, a part of sustainable aviation from an environmental perspective. Compared to the typical industry development cycles of 10 years, the goal moves more quickly when a focused effort is used.

The other aspects of sustainable aviation rely on the "green airport" approaches and regulating the resources like energy, water, and other natural reserves. Although the green airport concept regulates the project design to build phase and the operational cycles of the airport campus area, the vast majority of the air pollution was caused by aircraft's landing and take-off movements. The alternatives to the current fuel technologies reduce the environmental impacts in the aerodrome (Nelson & Reddy, 2018).

One other aspect of the green airport concept is supported by public pressure called the "willingness to pay" act (Winter et al., 2021). Several researchers have looked into whether individuals are ready to pay more for the development of an eco-friendly (green) airport vs. a conventional airport and whether the effect

mediates this relation. The participants were substantially more prepared to pay for the airport's expansion if they believed it to be environmentally friendly. In addition, they felt resentment and contempt at having to pay for a new airport that did not utilize renewable energy. Presented are practical applications of the current work and topics for future research (Walters et al., 2018). The renewable source of hydrogen has been popularly brought forward in scientific discussions (ACI, 2008; Airbus, 2002; Alder, 1987; Cecere et al., 2014; Clean Sky 2, 2020; Korycinski, 1978; Pohl & Malychevc, 1997; Schmidtchen et al., 1997; Troeltsch et al., 2020; van Zon, (n.d.)). Researchers have not conclusively determined how much more individuals are willing to pay based on the percentage of reduced greenhouse gas emissions. Examining the threshold of passengers willing to pay for the reduction of greenhouse gas emissions from commercial aircraft is necessary (Rice et al., 2020).

The green sector differs from the regular segment solely in terms of behavioral characteristics, not demographic or socioeconomic ones (Hinnen et al., 2017). Another case for Italy to test whether Italian air travellers would donate a contribution to finance these initiatives and whether the willingness to pay relies on the projects' type and on the projects' performance revealed that the volume of CO<sub>2</sub> diminished or offset by the project, as well as the respondents' gender, education level, occupational status, environmentalism, and travel habits, are significant factors (Rotaris et al., 2020). It would be beneficial for airlines to devise contribution proposals and enhance their corporate image, as well as for policymakers to support environmentally conscious air traveler behavior and environmentally sustainable airline operations.

### 3 Conclusion

For carbon-neutral air travel, most passengers hesitated to pay extra. The findings encourage public and non-profit managers to use the acknowledged key factors to inform and compose campaigns to increase public acceptance of carbon-neutral travel (Xu et al., 2022). The researches add to and expand the literature on the current debates about acceptance and willingness to pay for low-carbon jet fuels and energy transitions. The studies discovered that people are prepared to pay for renewable energy projects in poor nations since producing carbon credits can lessen a company's legal obligations (Choi & Ritchie, 2014). These projects may fit the best characteristics of offset initiatives. Airlines' mitigation efforts received widespread positive approval, with technical advancements receiving greater acceptance than operational procedures and biofuels.

The studies highlight the importance of prioritizing environmental education for aviators and demonstrate the connections between knowledge, attitude, and behavior (intention) that go beyond academic study (Lu & Wang, 2018). It is possible to increase passengers' awareness of the effects of flying and the advantages of carbon offset programs, which could encourage them to offset their flights, adopt new travel habits, and establish favorable attitudes toward carbon offsetting. Researchers asked

passengers why they were unwilling to pay to offset their flight's carbon footprint (Shaari et al., 2020). Passengers indicated that they were unwilling to pay because the flight is already expensive, making them unfavorable to an additional fee. The government and airlines should share the expense of reducing emissions since passengers believe that the responsibility should not be placed on them. Government and airline firms must work together to solve this issue.

## References

- Abdul-Aziz, Q., & Hashemi, H. H. (2022). Innovating aircraft control systems with the use of artificial intelligence and electronics. *Advanced Control for Applications*, 4, 7. <https://doi.org/10.1002/adc2.111>
- ACI. (2008). *Integration of hydrogen aircraft into the air transport system: An airport operations and infrastructure review*. ACI-ATI Report. [aci.aero/publications/new-releases](https://aci.aero/publications/new-releases)
- Airbus. (2002). *Final technical report of cryoplane liquid hydrogen fuelled aircraft-system analysis*. Airbus Deutschland GmbH. [https://www.fzt.haw-hamburg.de/pers/Scholz/dglr/hh/text\\_2004\\_02\\_26\\_Cryoplane.pdf](https://www.fzt.haw-hamburg.de/pers/Scholz/dglr/hh/text_2004_02_26_Cryoplane.pdf)
- Aksoy, H., Usanmaz, O., & Turgut, E. T. (2018). Effect of vertical profile inefficiency during descent on fuel burn, emissions and flight time. *Aeronautical Journal*, 122, 913–932. <https://doi.org/10.1017/aer.2018.41>
- Aksoy, H., Turgut, E. T., & Usanmaz, Ö. (2021). The design and analysis of optimal descent profiles using real flight data. *Transportation Research Part D: Transport and Environment*, 100, 103028. <https://doi.org/10.1016/j.trd.2021.103028>
- Akyuz, M. K., Altuntas, O., Sogut, M. Z., & Karakoc, T. H. (2019). Energy management at the airports. In T. H. Karakoc, C. O. Colpan, O. Altuntas, & Y. Sohret (Eds.), *Sustainable aviation* (Vol. 140, pp. 9–36). Springer International Publishing.
- Alder, H. P. (1987). Hydrogen in air transportation. Feasibility study for Zurich airport. *International Journal of Hydrogen Energy*, 12(8), 571–585. [https://doi.org/10.1016/0360-3199\(87\)90016-4](https://doi.org/10.1016/0360-3199(87)90016-4)
- Almaz, F. (2022). Use of renewable energy resources within the scope of sustainable energy management at airports. In H. Dinçer & S. Yüksel (Eds.), *Clean energy investments for zero emission projects* (Vol. 2, pp. 177–189). Springer International Publishing.
- Anand, S., & Sen, A. (2000). Human development and economic sustainability. *World Development*, 28, 2029–2049. [https://doi.org/10.1016/S0305-750X\(00\)00071-1](https://doi.org/10.1016/S0305-750X(00)00071-1)
- Asara, V., Otero, I., Demaria, F., & Corbera, E. (2015). Socially sustainable degrowth as a social–ecological transformation: Repoliticizing sustainability. *Sustainability Science*, 10, 375–384. <https://doi.org/10.1007/s11625-015-0321-9>
- Auclair, E., & Fairclough, G. J. (Eds.). (2015). *Theory and practice in heritage and sustainability: Between past and future*. Routledge, xvii, 218 pages.
- Baroutaji, A., Wilberforce, T., Ramadan, M., & Olabi, A. G. (2019). Comprehensive investigation on hydrogen and fuel cell technology in the aviation and aerospace sectors. *Renewable and Sustainable Energy Reviews*, 106, 31–40. <https://doi.org/10.1016/j.rser.2019.02.022>
- Barzkar, A., & Ghassemi, M. (2020). Electric power systems in more and all electric aircraft: A review. *IEEE Access*, 8, 169314–169332. <https://doi.org/10.1109/ACCESS.2020.3024168>
- Basiago, A. D. (1995). Methods of defining 'sustainability'. *Sustainable Development*, 3, 109–119. <https://doi.org/10.1002/sd.3460030302>
- Bauen, A., Bitossi, N., German, L., Harris, A., & Leow, K. (2020). Sustainable aviation fuels. *Johnson Matthey Technology Review*. <https://doi.org/10.1595/205651320X15816756012040>

- Baumeister, S. (2020). Mitigating the climate change impacts of aviation through behavioural change. *Transportation Research Procedia*, 48, 2006–2017. <https://doi.org/10.1016/j.trpro.2020.08.230>
- Benahmed, B. D., Jeffali, F., El Barkany, A., & Bakdid, A. (2022). Design and realization of an aeronautical cleaning robot for aircraft maintenance 4.0 based on artificial intelligence. *Materials Today: Proceedings*, 5, 281. <https://doi.org/10.1016/j.matpr.2022.08.254>
- Berker, L. E., & Böcher, M. (2022). Aviation policy instrument choice in Europe: High flying and crash landing? Understanding policy evolutions in The Netherlands and Germany. *Journal of Public Policy*, 42, 593–613. <https://doi.org/10.1017/S0143814X22000034>
- Bicer, Y., & Dincer, I. (2017). Life cycle evaluation of hydrogen and other potential fuels for aircrafts. *International Journal of Hydrogen Energy*, 42, 10722–10738. <https://doi.org/10.1016/j.ijhydene.2016.12.119>
- Brown, B. J., Hanson, M. E., Liverman, D. M., & Merideth, R. W. (1987). Global sustainability: Toward definition. *Environmental Management*, 11, 713–719. <https://doi.org/10.1007/BF01867238>
- Carter, C. R., & Liane Easton, P. (2011). Sustainable supply chain management: Evolution and future directions. *International Journal of Physical Distribution & Logistics Management*, 41, 46–62. <https://doi.org/10.1108/096000311111101420>
- Cavarzere, A., Morini, M., Pinelli, M., Spina, P. R., Vaccari, A., & Venturini, M. (2014). Experimental analysis of a micro gas turbine fuelled with vegetable oils from energy crops. *Energy Procedia*, 45, 91–100. <https://doi.org/10.1016/j.egypro.2014.01.011>
- Cecere, D., Giacomazzi, E., & Ingenito, A. (2014). A review on hydrogen industrial aerospace applications. *International Journal of Hydrogen Energy*, 39(20), 10731–10747. <https://doi.org/10.1016/j.ijhydene.2014.04.126>
- Chen, L., Hu, X., Wang, J., & Yu, Y. (2019). Impacts of alternative fuels on morphological and nanostructural characteristics of soot emissions from an aviation piston engine. *Environmental Science & Technology*, 53, 4667–4674. <https://doi.org/10.1021/acs.est.9b01059>
- Choi, A. S., & Ritchie, B. W. (2014). Willingness to pay for flying carbon neutral in Australia: An exploratory study of offsetter profiles. *Journal of Sustainable Tourism*, 22(8), 1236–1256.
- Clean Sky 2. (2020). Hydrogen-powered aviation, a fact based study of hydrogen technology, economics, and climate impact by 2050. <https://doi.org/10.2843/766989>
- Cronin, M. J. J. (1990). The all-electric aircraft. *IEE Review*, 36, 309. <https://doi.org/10.1049/ir:19900132>
- Cui, Q., Hu, Y.-X., & Yu, L.-T. (2022). Can the aviation industry achieve carbon emission reduction and revenue growth simultaneously under the CNG2020 strategy? An empirical study with 25 benchmarking airlines. *Energy*, 245, 123272. <https://doi.org/10.1016/j.energy.2022.123272>
- Das, D., Sharma, S. K., Parti, R., & Singh, J. (2016). Analyzing the effect of aviation infrastructure over aviation fuel consumption reduction. *Journal of Air Transport Management*, 57, 89–100. <https://doi.org/10.1016/j.jairtraman.2016.07.013>
- Desha, C., & Hargroves, K. C. (2013). *Higher education and sustainable development*. Routledge.
- Diehl, P., & Gleditsch, N. P. (2018). *Environmental conflict: An anthology*. Routledge, 352 pp.
- Dimitriou, D. J., & Sartzetaki, M. F. (2020). Social dimensions of aviation on sustainable development. In T. Walker, A. S. Bergantino, N. Sprung-Much, & L. Loiacono (Eds.), *Sustainable aviation* (Vol. 12, pp. 173–191). Springer International Publishing.
- Dincer, I. (2000). Renewable energy and sustainable development: A crucial review. *Renewable and Sustainable Energy Reviews*, 4, 157–175. [https://doi.org/10.1016/S1364-0321\(99\)00011-8](https://doi.org/10.1016/S1364-0321(99)00011-8)
- Ekici, F., Orhan, G., Gümüş, Ö., & Bahce, A. B. (2022). A policy on the externality problem and solution suggestions in air transportation: The environment and sustainability. *Energy*, 258, 124827. <https://doi.org/10.1016/j.energy.2022.124827>
- Fageda, X., & Teixidó, J. J. (2022). Pricing carbon in the aviation sector: Evidence from the European emissions trading system. *Journal of Environmental Economics and Management*, 111, 102591. <https://doi.org/10.1016/j.jeem.2021.102591>

- Feiock, R. C., & Stream, C. (2001). Environmental protection versus economic development: A false trade-off? *Public Administration Review*, *61*, 313–321. <https://doi.org/10.1111/0033-3352.00032>
- Gagne, J., Murrieta, A., Botez, R. M., & Labour, D. (2013). New method for aircraft fuel saving using flight management system and its validation on the L-1011 aircraft. In *2013 Aviation technology, integration, and operations conference*. American Institute of Aeronautics and Astronautics.
- García-Contreras, R., Soriano, J. A., Gómez, A., & Fernández-Yáñez, P. (2022). Biojet fuels and emissions. In *Sustainable alternatives for aviation fuels* (Vol. 140, pp. 177–199). Elsevier.
- Graham, B., & Guyer, C. (1999). Environmental sustainability, airport capacity and European air transport liberalization: Irreconcilable goals? *Journal of Transport Geography*, *7*(3), 165–180.
- Greer, F., Rakas, J., & Horvath, A. (2020). Airports and environmental sustainability: A comprehensive review. *Environmental Research Letters*, *15*, 103007. <https://doi.org/10.1088/1748-9326/abb42a>
- Hall, C. M. (2010). Changing paradigms and global change: From sustainable to steady-state tourism. *Tourism Recreation Research*, *35*, 131–143. <https://doi.org/10.1080/02508281.2010.11081629>
- Heikkurinen, P., & Bonnedahl, K. J. (2013). Corporate responsibility for sustainable development: A review and conceptual comparison of market- and stakeholder-oriented strategies. *Journal of Cleaner Production*, *43*, 191–198. <https://doi.org/10.1016/j.jclepro.2012.12.021>
- Hinnen, G., Hille, S. L., & Wittmer, A. (2017). Willingness to pay for green products in air travel: Ready for take-off? *Business Strategy and the Environment*, *26*(2), 197–208. <https://doi.org/10.1002/bse.1909>
- Holden, E., Linnerud, K., & Banister, D. (2014). Sustainable development: Our common future revisited. *Global Environmental Change*, *26*, 130–139. <https://doi.org/10.1016/j.gloenvcha.2014.04.006>
- Janić, M. (1999). Aviation and externalities: The accomplishments and problems. *Transportation Research Part D: Transport and Environment*, *4*, 159–180. [https://doi.org/10.1016/S1361-9209\(99\)00003-6](https://doi.org/10.1016/S1361-9209(99)00003-6)
- Jansohn, P. (Ed.). (2013). *Modern gas turbine systems: High efficiency, low emission, fuel flexible power generation*. WP Woodhead Publishing, xxi, 816 pages.
- Jensen, L., Hansman, R. J., Venuti, J. C., & Reynolds, T. (2013). Commercial airline speed optimization strategies for reduced cruise fuel consumption. In *2013 Aviation technology, integration, and operations conference* (p. 26). American Institute of Aeronautics and Astronautics.
- Johnson, M. E., & Gonzalez, A. (2013). Estimating cost savings for aviation fuel and CO2 emission reductions strategies. *Collegiate Aviation Review*, *32*, 79–102. <https://doi.org/10.22488/okstate.18.100513>
- Karakoc, T. H., Ozerdem, M. B., Sogut, M. Z., Colpan, C. O., Altuntas, O., & Açikkalp, E. (Eds.). (2016). *Sustainable aviation*. Springer International Publishing.
- Khan, M. K., Trinh, H. H., Khan, I. U., & Ullah, S. (2022). Sustainable economic activities, climate change, and carbon risk: An international evidence. *Environment, Development and Sustainability*, *24*, 9642–9664. <https://doi.org/10.1007/s10668-021-01842-x>
- Korycinski, P. F. (1978). Air terminals and liquid hydrogen commercial air transports. *International Journal of Hydrogen Energy*, *3*(2), 231–250. [https://doi.org/10.1016/0360-3199\(78\)90021-6](https://doi.org/10.1016/0360-3199(78)90021-6)
- Lai, Y. Y., Christley, E., Kulanovic, A., Teng, C. C., Björklund, A., Nordensvärd, J., Karakaya, E., & Urban, F. (2022). Analysing the opportunities and challenges for mitigating the climate impact of aviation: A narrative review. *Renewable and Sustainable Energy Reviews*, *156*, 111972. <https://doi.org/10.1016/j.rser.2021.111972>
- Lin, Z.-M. (2013). Making aviation green. *Advanced Manufacturing*, *1*, 42–49. <https://doi.org/10.1007/s40436-013-0008-3>
- Liu, Z. (2003). Sustainable tourism development: A critique. *Journal of Sustainable Tourism*, *11*, 459–475. <https://doi.org/10.1080/09669580308667216>

- Liu, Y., Sun, X., Sethi, V., Nalianda, D., Li, Y.-G., & Wang, L. (2017). Review of modern low emissions combustion technologies for aero gas turbine engines. *Progress in Aerospace Sciences*, *94*, 12–45. <https://doi.org/10.1016/j.paerosci.2017.08.001>
- Liu, R., Zhao, W., Wang, Z., & Liu, X. (2021). Investigation on performance and combustion of compression ignition aviation piston engine burning biodiesel and diesel. *Aircraft Engineering and Aerospace Technology*, *93*, 384–393. <https://doi.org/10.1108/AEAT-06-2020-0111>
- Lu, C. (2009). The implications of environmental costs on air passenger demand for different airline business models. *Journal of Air Transport Management*, *15*, 158–165. <https://doi.org/10.1016/j.jairtraman.2008.09.019>
- Lu, J. L., & Wang, C. Y. (2018). Investigating the impacts of air travellers' environmental knowledge on attitudes toward carbon offsetting and willingness to mitigate the environmental impacts of aviation. *Transportation Research Part D: Transport and Environment*, *59*, 96–107.
- Malaek, S. M., & Alipour, E. (2022). Intelligent flight-data-recorders; a step toward a new generation of learning aircraft. In *2022 8th International conference on control, decision and information technologies (CoDIT)* (pp. 1545–1549). IEEE.
- Marques, J. C. (2001). Diversity, biodiversity, conservation, and sustainability. *The Scientific World Journal*, *1*, 534–543. <https://doi.org/10.1100/tsw.2001.101>
- Mavragani, A., Nikolaou, I., & Tsagarakis, K. (2016). Open economy, institutional quality, and environmental performance: A macroeconomic approach. *Sustainability*, *8*, 601. <https://doi.org/10.3390/su8070601>
- McKinnon, A. C. (2010). In A. McKinnon et al. (Eds.), *Green logistics: Improving the environmental sustainability of logistics*. Kogan Page.
- Mensah, J. (2019). Sustainable development: Meaning, history, principles, pillars, and implications for human action: Literature review. *Cogent Social Sciences*, *5*, 1653531. <https://doi.org/10.1080/23311886.2019.1653531>
- Morelli, J. (2011). Environmental sustainability: A definition for environmental professionals. *Journal of Environmental Sustainability*, *1*, 1–10. <https://doi.org/10.14448/jes.01.0002>
- Morgan, R. K. (2012). Environmental impact assessment: The state of the art. *Impact Assessment and Project Appraisal*, *30*, 5–14. <https://doi.org/10.1080/14615517.2012.661557>
- Moser, G. (2009). Quality of life and sustainability: Toward person–environment congruity. *Journal of Environmental Psychology*, *29*, 351–357. <https://doi.org/10.1016/j.jenvp.2009.02.002>
- Mostafa, M. F. A., Abdel Aleem, S. H. E., & Ibrahim, A. M. (2016). Using solar photovoltaic at Egyptian airports: Opportunities and challenges. In *2016 Eighteenth international middle east power systems conference (MEPCON)* (pp. 73–80). IEEE.
- Mulder, P., & van den Bergh, J. C. J. M. (2001). Evolutionary economic theories of sustainable development. *Growth and Change*, *32*, 110–134. <https://doi.org/10.1111/0017-4815.00152>
- Nelson, E. S., & Reddy, D. R. (Eds.). (2018). *Green aviation: Reduction of environmental impact through aircraft technology and alternative fuels*. CRC Press.
- Nemitallah, M. A., Haque, M. A., Hussain, M., Abdelhafez, A., & Habib, M. A. (2022). Stratified and hydrogen combustion techniques for higher turndown and lower emissions in gas turbines. *Journal of Energy Resources Technology*, *144*(020801), 115. <https://doi.org/10.1115/1.4052541>
- Nijkamp, P., & Geenhuizen, M. (1997). European transport: Challenges and opportunities for future research and policies. *Journal of Transport Geography*, *5*(1997), 4–11.
- Nygren, E., Aleklett, K., & Höök, M. (2009). Aviation fuel and future oil production scenarios. *Energy Policy*, *37*, 4003–4010. <https://doi.org/10.1016/j.enpol.2009.04.048>
- Oláh, J., Aburumman, N., Popp, J., Khan, M. A., Haddad, H., & Kitukutha, N. (2020). Impact of industry 4.0 on environmental sustainability. *Sustainability*, *12*, 4674. <https://doi.org/10.3390/su12114674>
- Omer, A. M. (2008). Energy, environment and sustainable development. *Renewable and Sustainable Energy Reviews*, *12*, 2265–2300. <https://doi.org/10.1016/j.rser.2007.05.001>

- Ortega Alba, S., & Manana, M. (2016). Energy research in airports: A review. *Energies*, 9, 349. <https://doi.org/10.3390/en9050349>
- Oto, N., Cobanoglu, N., & Geray, C. (2012). Education for sustainable airports. *Procedia – Social and Behavioral Sciences*, 47, 1164–1173. <https://doi.org/10.1016/j.sbspro.2012.06.795>
- Owusu, P. A., & Asumadu-Sarkodie, S. (2016). A review of renewable energy sources, sustainability issues and climate change mitigation. *Cogent Engineering*, 3, 1167990. <https://doi.org/10.1080/23311916.2016.1167990>
- Pezzey, J., & Toman, M. A. (Eds.). (2017). *The economics of sustainability* (p. 391). Routledge.
- Pohl, H. W., & Malychevc, V. (1997). Hydrogen in future civil aviation. *International Journal of Hydrogen Energy*, 22(10–11), 1061–1069. [https://doi.org/10.1016/S0360-3199\(95\)00140-9](https://doi.org/10.1016/S0360-3199(95)00140-9)
- Porket, J. L. (1998). *Modern economic systems and their transformation*. Palgrave Macmillan, a Division of Macmillan Publishers Limited, 1 online resource.
- Rajiani, I., & Kot, S. (2018). The prospective consumers of the Indonesian green aviation initiative for sustainable development in air transportation. *Sustainability*, 10, 1772. <https://doi.org/10.3390/su10061772>
- Rice, C., Ragbir, N. K., Rice, S., & Barcia, G. (2020). Willingness to pay for sustainable aviation depends on ticket price, greenhouse gas reductions and gender. *Technology in Society*, 60, 101224.
- Rochelle, D., & Najafi, H. (2019). A review of the effect of biodiesel on gas turbine emissions and performance. *Renewable and Sustainable Energy Reviews*, 105, 129–137. <https://doi.org/10.1016/j.rser.2019.01.056>
- Rotaris, L., Giansoldati, M., & Scorrano, M. (2020). Are air travellers willing to pay for reducing or offsetting carbon emissions? Evidence from Italy. *Transportation Research Part A: Policy and Practice*, 142, 71–84.
- Ryerson, M. S., & Hansen, M. (2010). The potential of turboprops for reducing aviation fuel consumption. *Transportation Research Part D: Transport and Environment*, 15, 305–314. <https://doi.org/10.1016/j.trd.2010.03.003>
- Ryerson, M. S., & Kim, H. (2014). The impact of airline mergers and hub reorganization on aviation fuel consumption. *Journal of Cleaner Production*, 85, 395–407. <https://doi.org/10.1016/j.jclepro.2013.12.032>
- Sarkar, A. N. (2012a). Evolving green aviation transport system: A holistic approach to sustainable green market development. *American Journal of Climate Change*, 1(3), 22479. <https://doi.org/10.4236/ajcc.2012.13014>
- Sarkar, A. N. (2012b). Evolving green aviation transport system: A holistic approach to sustainable green market development. *American Journal of Climate Change*, 1, 164–180. <https://doi.org/10.4236/ajcc.2012.13014>
- Schipper, Y., Rietveld, P., & Nijkamp, P. (2001). Environmental externalities in air transport markets. *Journal of Air Transport Management*, 7, 169–179. [https://doi.org/10.1016/S0969-6997\(01\)00002-3](https://doi.org/10.1016/S0969-6997(01)00002-3)
- Schmidtchen, U., Behrend, E., Pohl, H. W., & Rostek, N. (1997). Hydrogen aircraft and airport safety. *Renewable and Sustainable Energy Reviews*, 1(4), 239–269. [https://doi.org/10.1016/S1364-0321\(97\)00007-5](https://doi.org/10.1016/S1364-0321(97)00007-5)
- Seljak, T., Buffi, M., Valera-Medina, A., Chong, C. T., Chiamonti, D., & Katrašnik, T. (2020). Bioliquids and their use in power generation – A technology review. *Renewable and Sustainable Energy Reviews*, 129, 109930. <https://doi.org/10.1016/j.rser.2020.109930>
- Seymour, K., Held, M., Georges, G., & Boulouchos, K. (2020). Fuel estimation in air transportation: Modeling global fuel consumption for commercial aviation. *Transportation Research Part D: Transport and Environment*, 88, 102528. <https://doi.org/10.1016/j.trd.2020.102528>
- Shaari, N. F., Abdul-Rahim, A. S., & Afandi, S. H. M. (2020). Are Malaysian airline passengers willing to pay to offset carbon emissions? *Environmental Science and Pollution Research*, 27(19), 24242–24252.

- Singh, V., & Sharma, S. K. (2015). Fuel consumption optimization in air transport: A review, classification, critique, simple meta-analysis, and future research implications. *European Transport Research Review*, 7, 537. <https://doi.org/10.1007/s12544-015-0160-x>
- Tikhonov, A. I., Sazonov, A. A., & Kuzmina-Merlino, I. (2022). Digital production and artificial intelligence in the aircraft industry. *Russian Engineering Research*, 42, 412–415. <https://doi.org/10.3103/S1068798X22040293>
- Troeltsch, F., Engelmann, M., Peter, F., Kaiser, J., et al. (2020). Hydrogen powered long haul aircraft with minimized climate impact. In *AIAA aviation 2020 forum* (p. 14). American Institute of Aeronautics and Astronautics Inc, AIAA. <https://doi.org/10.2514/6.2020-2660>
- Turgut, E. T., & Usanmaz, O. (2018). Effect of climb angle on aircraft fuel consumption and nitrogen oxides emissions. *Journal of Aircraft*, 55, 2392–2400. <https://doi.org/10.2514/1.C034265>
- Turgut, E. T., Usanmaz, O., Cavcar, M., Dogeroglu, T., & Armutlu, K. (2019). Effects of descent flight-path angle on fuel consumption of commercial aircraft. *Journal of Aircraft*, 56, 313–323. <https://doi.org/10.2514/1.C033911>
- Upham, P., Maughan, J., Raper, D., & Thomas, C. (2012). *Towards sustainable aviation*. Routledge.
- Valdés, R. M. A., Comendador, V. F. G., & Campos, L. M. B. (2021). How much can carbon taxes contribute to aviation decarbonization by 2050. *Sustainability*, 13, 1086. <https://doi.org/10.3390/su13031086>
- van Zon, N. (n.d.). Liquid hydrogen powered commercial aircraft: Analysis of the technical feasibility of sustainable liquid hydrogen powered commercial aircraft in 2040, p. 16. <http://www.noutvanzon.nl/files/documents/spaceforinnovation.pdf>
- Vlek, C., & Steg, L. (2007). Human behavior and environmental sustainability: Problems, driving forces, and research topics. *Journal of Social Issues*, 63, 1–19. <https://doi.org/10.1111/j.1540-4560.2007.00493.x>
- Walters, N. W., Rice, S., Winter, S. R., Baugh, B. S., Ragbir, N. K., Anania, E. C., Capps, J., & Milner, M. N. (2018). Consumer willingness to pay for new airports that use renewable resources. *International Journal of Sustainable Aviation*, 4(2), 79–98.
- Wellmer, F.-W., Buchholz, P., Gutzmer, J., Hagelüken, C., Herzig, P. A., Littke, R., & Thauer, R. K. (2019). *Raw materials for future energy supply*. Springer.
- Wheeler, P. (2016). Technology for the more and all electric aircraft of the future. In *2016 IEEE International conference on automatica (ICA-ACCA)* (pp. 1–5). IEEE.
- Wild, P., Mathys, F., & Wang, J. (2021). Impact of political and market-based measures on aviation emissions and passenger behaviors (a Swiss case study). *Transportation Research Interdisciplinary Perspectives*, 10, 100405. <https://doi.org/10.1016/j.trip.2021.100405>
- Windolph, S. E., Harms, D., & Schaltegger, S. (2014). Motivations for corporate sustainability management: Contrasting survey results and implementation. *Corporate Social Responsibility and Environmental Management*, 21, 272–285. <https://doi.org/10.1002/csr.1337>
- Winter, S. R., Crouse, S. R., & Rice, S. (2021). The development of ‘green’ airports: Which factors influence willingness to pay for sustainability and intention to act? A structural and mediation model analysis. *Technology in Society*, 65, 101576.
- World Water Development Report. (2015). *Water for a sustainable world*. UNESCO, 122 pp.
- Xu, B., Ahmad, S., Charles, V., & Xuan, J. (2022). Sustainable commercial aviation: What determines air travellers’ willingness to pay more for sustainable aviation fuel? *Journal of Cleaner Production*, 374, 133990.
- Yerel Kandemir, S., & Yaylı, M. Ö. (2016). Investigation of renewable energy sources for airports. In T. H. Karakoc, M. B. Ozerdem, M. Z. Sogut, C. O. Colpan, O. Altuntas, & E. Açıkkalp (Eds.), *Sustainable aviation* (Vol. 49, pp. 11–16). Springer International Publishing.
- Yilmaz, N., & Atmanli, A. (2017). Sustainable alternative fuels in aviation. *Energy*, 140, 1378–1386. <https://doi.org/10.1016/j.energy.2017.07.077>
- Zong, C., Ji, C., Cheng, J., Zhu, T., Guo, D., Li, C., & Duan, F. (2022). Toward off-design loads: Investigations on combustion and emissions characteristics of a micro gas turbine combustor by external combustion-air adjustments. *Energy*, 253, 124194. <https://doi.org/10.1016/j.energy.2022.124194>



# Research on the Effects of Flight Procedures on Noise Contour Map Around Tan Son Nhat International Airport



Kiet La-Tuan and Anh Tran-Tien

## Nomenclature

ANP	Aircraft Noise Performance
ECAC	European Civil Aviation Conference
ICAO	International Civil Aviation Organization
NADP	Noise abatement departure procedures
NPD	Noise-Power-Distance
RWY	Runway

## 1 Introduction

The level and extent of noise generated by flight operations in terms of noise contour map around Tan Son Nhat International Airport are presented in this study, which is based on two flight procedures recommended by the International Civil Aviation Organization (ICAO) for noise reduction purposes in the airport's vicinity, including NADP 1 and NADP 2.

The availability of certain data, such as target airport data, the number and type of aircraft operating at the airport, and representative flight path analysis for each aircraft type with specific flight procedures, is required to obtain the results of noise calculations. In this research, the noise levels around Tan Son Nhat International Airport were calculated using the flight path segmentation modelling that was recommended by ICAO, Doc 9911 (ICAO, 2008), the flight mechanics equations

---

K. La-Tuan (✉) · A. Tran-Tien  
Ho Chi Minh City University of Technology, Ho Chi Minh, Vietnam  
e-mail: [tienanh@hcmut.edu.vn](mailto:tienanh@hcmut.edu.vn)

from SAE-AIR-1845 (SAE A21 Committee, 1986) to compute the flight profile, and the Aircraft Noise Performance database from EUROCONTROL to interpolate or extrapolate the noise levels.

## 2 Method

### 2.1 Airport Data Collecting

Tan Son Nhat International Airport is one of the largest and busiest airports in Southern Vietnam, serving more than millions of passengers annually in normal operating conditions (Tan Son Nhat International Airport, 2021). RWY 25L/07R and RWY 25R/07L are two parallel runways currently in use at the airport. However, due to the limitation of this research, all flight operations were collected in March 2020 taking place in the runways 25R and 25L with RWY 25L being primarily used for take-offs and RWY 25R being primarily used for landings (Fig. 1).

For noise contour map computing, these two runways are treated as a single runway 25L for both take-off and landing operations because they are parallel and close to each other (365 m). The range of the noise map was limited to  $\pm 25$  km on the horizontal axis and  $\pm 12$  km on the vertical axis with the mesh grid of computing domain's origin O (0, 0) located at the start-of-roll point of the runway 25L.



Fig. 1 Tan Son Nhat International Airport

## 2.2 Aircraft Grouping

For noise assessment, aircraft data from Tan Son Nhat International Airport, including aircraft type and operating frequency, were collected and analysed in March 2020. Individual aircraft types having similar noise and performance characteristics are grouped so that they can be represented by a single aircraft category. The aircraft types operating at Tan Son Nhat International Airport were grouped based on two criteria that were recommended in the ECAC.CEAC Doc 29 (ECAC, 2004) and the ICAO Annex 14 (ICAO, 2013).

## 2.3 Flight Path Analysis

The flight path of each aircraft group was analysed and calculated using two noise abatement departure procedures, ICAO A and ICAO B, which are equivalent to NADP 1 and NADP 2.

The flight profile was calculated using the equations for flight performance calculations in SAE-AIR-1845 with aircraft engine coefficients from the Aircraft Noise Performance (ANP) database for these variables: engine thrust, take-off, landing ground roll, speeds, and height of each segment of the flight path. The following figure is the flight path of each aircraft group that flies out of Tan Son Nhat International Airport (Fig. 2).

## 2.4 Noise Calculation

The noise exposure level generated by each flight path segment will be obtained based on interpolation or extrapolation of the Noise-Power-Distance (NPD) table

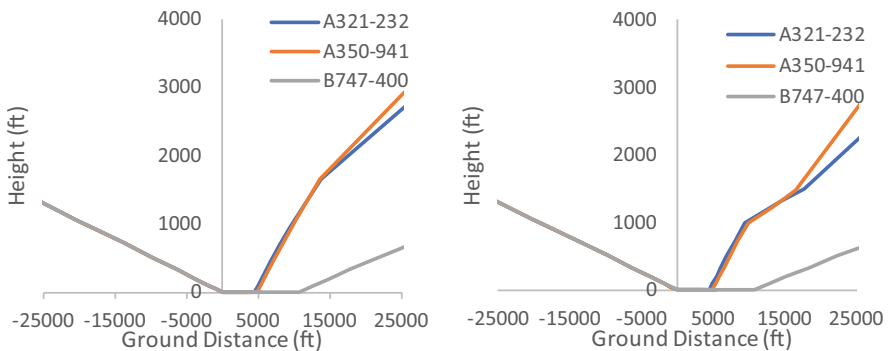


Fig. 2 NADP 1 flight path (left) and NADP 2 flight path (right)

**Table 1** The number of take-off-landing movements for each aircraft group with aircraft representatives in March 2020

A/C type	Group	Day	Evening	Night	A/C representative
Airbus A320 Family	C	2813	564	470	Airbus A321
Boeing 787, Airbus A350, Airbus A330	D	438	202	281	Airbus A350
Airbus A340, Boeing 747, Boeing 777	E	160	52	83	Boeing 747
Total		3411	818	834	

using Matlab software with two quantities: engine power ( $P$ ) and shortest slant distance between the segment and noise receiving point ( $d$ ). The contribution from one flight path segment to noise exposure level can be expressed as:

$$L_{E,seg} = L_{E,NPD}(P, d) + \Delta_v + \Delta_I(\varphi) - \Lambda(\beta, \ell) + \Delta_F(\text{dBA}) \quad (1)$$

where  $\Delta_v$ ,  $\Delta_I(\varphi)$ ,  $\Lambda(\beta, \ell)$ , and  $\Delta_F$  in Eq. (1) are called “correction terms” to account for the effects due to the difference between the NPD flight path and the actual flight path.

Based on the number of aircraft movements during the day, evening, and night as listed in Table 1, the day-evening-night equivalent sound level is then calculated based on  $L_{\text{day}}$  (0700:1900),  $L_{\text{evening}}$  (1900:2200), and  $L_{\text{night}}$  (2200:0700) by the following equation:

$$L_{\text{den}} = 10 \cdot \log \left[ \frac{1}{24} \left( 12 \cdot 10^{L_{\text{day}}/10} + 3 \cdot 10^{L_{\text{evening}}/10} + 9 \cdot 10^{L_{\text{night}}/10} \right) \right] (\text{dBA}) \quad (2)$$

The above calculation procedure was done similarly to calculate the day-evening-night sound level caused by three flight paths of three groups of aircraft, A, B, and C, at all noise receiving points in the calculation domain using Matlab software. Finally, the noise contour map for day-evening-night equivalent continuous noise level was established by interpolating the noise levels of all noise receiving points inside the calculation domain around Tan Son Nhat International Airport.

### 3 Results and Discussion

Figure 3 shows the results of noise contour maps generated by flight operations at Tan Son Nhat International Airport based on the noise abatement departure procedures ICAO A and ICAO B, respectively.

The following figure shows noise contour lines for two flight procedures ICAO A and ICAO B around Tan Son Nhat International airport (Fig. 4).

The difference between the noise levels of two flight procedures occurs within the departure area at the end of the runway. That is because those aircraft following the

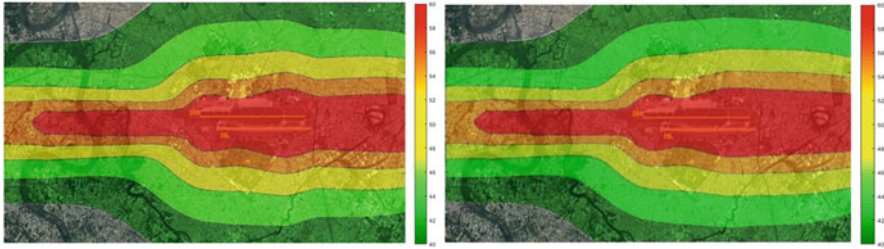


Fig. 3  $L_{den}$  noise contour maps based on ICAO A (left) and ICAO B (right) procedure

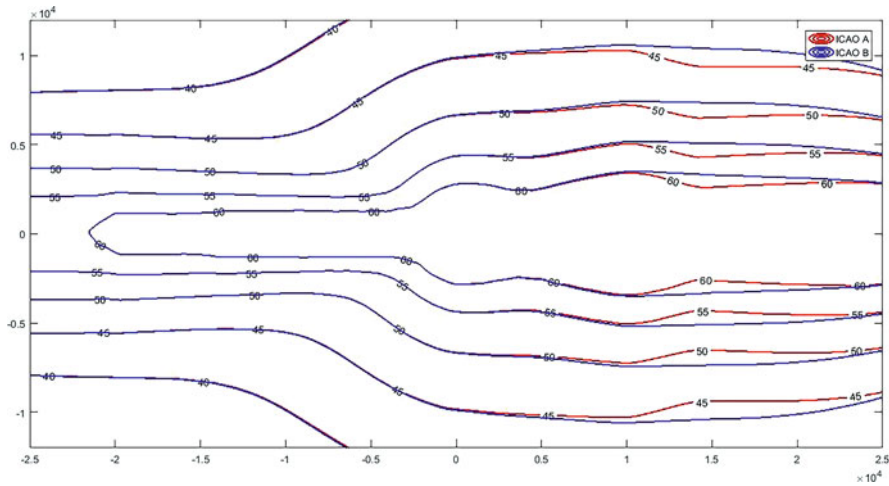


Fig. 4  $L_{den}$  noise contours based on ICAO A and ICAO B procedures

NADP 1 must climb as fast as possible to 3000 ft. and thus the contour lines of the departure area will be slightly narrower than the NADP 2 when the aircraft is far away from the runway.

### 4 Conclusion

This research has successfully simulated the noise contour map with the noise levels in the range of 40–60 dBA around Tan Son Nhat International Airport and has shown the influence of two noise abatement departure procedures ICAO A and ICAO B equivalent to NADP 1 and NADP 2 on the noise contours.

The results of this study are the basis for effectively assessing the noise level at Tan Son Nhat International Airport for the authority, thereby aiming to provide solutions for rational land use planning in the affected area by high noise levels as well as issuing regulations on noise level limits and aiming to develop noise contour maps for all major airports operating in Vietnam.

## References

- ECAC, European Civil Aviation Conference. (2004). *Methodology for computing noise contours around civil airports. Volume 1: Applications guide*.
- ICAO – International Civil Aviation Organization. (2008). Recommended method for computing noise contours around airports. ICAO Doc. 9911.
- ICAO, International Civil Aviation Organization. (2013). *Aerodromes. Volume 1: Aerodrome design and operations*. ICAO Annex 14.
- SAE A21 Committee. (1986). *Procedure for the calculation of aircraft noise in the vicinity of airports*. Technical Report SAE-AIR-1845, Society of Automotive Engineers.
- Tan Son Nhat International Airport. <https://tansonnhatairport.vn>. Accessed on 24 Sept 2021.

# Free Vibration Characteristics of a Variable-Span Morphing Wing



Damla Durmuş and Metin O. Kaya

## Nomenclature

$c$	Chord
$EI$	Bending stiffness
$GJ$	Torsional stiffness
$l$	Half span
$m$	Mass of the wing per unit length
$R_\theta$	Radius of gyration
$w$	Plunge deflection
$X_\theta$	Static unbalance
$\theta$	Pitch deflection
$\omega$	Frequency of motion

## 1 Introduction

Morphing wings are receiving a great deal of attention due to its high level of adaptability. Besides its many advantages, structural requirements of this concept may be more severe. Increasing wingspan causes to increase in wing root bending moment and structural mass requirements. Apart from that, the loading and deformation over the wing are more severe when wing extends its length (Concilio et al., 2018).

Several investigations are performed to investigate dynamics of morphing wing technology up to now. Snyder et al. (2009) utilized finite element approach to

---

D. Durmuş (✉) · M. O. Kaya  
Istanbul Technical University, Istanbul, Türkiye  
e-mail: [durmus17@itu.edu.tr](mailto:durmus17@itu.edu.tr)

analyze the natural frequencies of folding wing. Pulok and Chakravarty (2020) performed vibration analysis of the morphing wings of a hypersonic vehicle. It is concluded that the natural frequencies are decreasing by increasing the span length of the wing. Gamboa et al. (2013) carried out a modal analysis of a composite variable-span wing, and they obtained natural frequencies and mode shapes of free vibration.

The variable-span morphing wing is modeled as bending-torsion coupled three-stepped beam in this study. There are several studies about the free vibration of stepped beam model in literature. Ju et al. (1994) analyzed the free vibration of arbitrarily stepped beams. Mao et al. (2012) utilized the Adomian decomposition method to analyze the free vibration of the stepped Euler-Bernoulli beams.

## 2 Methodology

To represent the structural model of span-morphing wing, a three-stepped Euler-Bernoulli beam model is utilized. The beam is divided into three segments, main region, overlapping region, and extension region, which is shown in Fig. 1.

The equations of motion of coupled bending-torsional vibration of Euler-Bernoulli beam are obtained by Hamilton's principle which are given in the following expressions:

$$-\frac{\partial^2}{\partial y^2} \left( EI \frac{\partial^2 w}{\partial y^2} \right) + m \frac{\partial^2 w}{\partial t^2} + mX_{\theta} \frac{\partial^2 \theta}{\partial t^2} = 0 \quad (1)$$

$$\frac{\partial}{\partial y} \left( GJ \frac{\partial \theta}{\partial y} \right) + mR_{\theta}^2 \frac{\partial^2 \theta}{\partial y^2} + mX_{\theta} \frac{\partial^2 w}{\partial t^2} = 0 \quad (2)$$

The exponential solution of time is utilized as the general solution to the differential equations. The exponential form of time is described as follows:

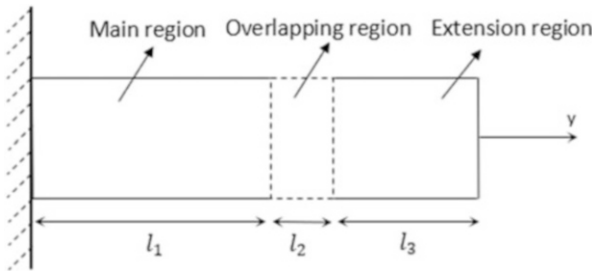


**Fig. 1** Top view of the three-stepped beam model



**Table 1** Boundary conditions of a three-stepped cantilevered beam

Fixed end		Free end	
Bending	Torsion	Bending	Torsion
$w_1 = 0$	$\theta_1 = 0$	$\frac{d^2 w_3}{dy_3^2} = 0$	$\frac{d\theta_3}{dy_3} = 0$
$\frac{dw_1}{dy_1} = 0$		$\frac{d^3 w_3}{dy_3^3} = 0$	

**Table 2** Continuity conditions of a three-stepped cantilevered beam

Bending	Torsion
$w_i(l_i) = w_{i+1}(0)$	$\theta_i(l_i) = \theta_{i+1}(0)$
$\frac{\partial w_i(l_i)}{\partial y_i} = \frac{\partial w_{i+1}(0)}{\partial y_{i+1}}$	$\frac{\partial \theta_i(l_i)}{\partial y_i} = \frac{(GJ)_{i+1}}{(GJ)_i} \frac{\partial \theta_{i+1}(0)}{\partial y_{i+1}}$
$\frac{\partial^2 w_i(l_i)}{\partial y_i^2} = \frac{(EI)_{i+1}}{(EI)_i} \frac{\partial^2 w_{i+1}(0)}{\partial y_{i+1}^2}$	
$\frac{\partial^3 w_i(l_i)}{\partial y_i^3} = \frac{(EI)_{i+1}}{(EI)_i} \frac{\partial^3 w_{i+1}(0)}{\partial y_{i+1}^3}$	

$$w = \bar{w}e^{i\omega t} \quad \theta = \bar{\theta}e^{i\omega t} \quad (3)$$

By implementing exponential solution function and nondimensionalization to Eqs. (1) and (2), the finalized nondimensional form of equations of motion are obtained as follows:

$$-\lambda_1^4 \frac{1}{\omega^2} \frac{d^4 w}{d\xi^4} + w + \frac{X_\theta}{b} \theta = 0 \quad (4)$$

$$\lambda_2^2 \frac{1}{\omega^2} \frac{d^2 \theta}{d\xi^2} + \frac{X_\theta}{b} w + \frac{R_\theta^2}{b^2} \theta = 0 \quad (5)$$

where  $\lambda_1^4$  and  $\lambda_2^2$  represent simplification coefficients that are introduced as follows:

$$\lambda_1^4 = \frac{E_0 I_o}{m l^4} \quad \lambda_2^2 = \frac{G_0 J_o}{m l^2} \quad (6)$$

The boundary and continuity conditions of a three-stepped Euler-Bernoulli beam for bending and torsion motions are given in Tables 1 and 2, respectively.

Equations of motions of the system are solved by differential transformation method (DTM), which is based on Taylor series expansion and used for solving ordinary and partial differential equations.

The function  $f(x)$  is defined by power series where the center is at  $x_0$ .  $F(k)$  is referred to as the  $k$ th order transformed function of the original function  $f(x)$  about the point  $x = x_0$ :

**Table 3** Main operations of the DTM

Original function	Transformed function
$f(x) = u(x) \pm v(x)$	$F(k) = U(k) \pm V(k)$
$f(x) = au(x)$	$F(k) = aU(k)$
$f(x) = \frac{du(x)}{dx}$	$F(k) = (k + 1)U(k + 1)$
$f(x) = \frac{d^m u(x)}{dx^m}$	$F(k) = (k + 1)(k + 2) \dots (k + m)U(k + m)$
$f(x) = u(x)v(x)$	$F(k) = \sum_{l=0}^k V(l)U(k - l)$

$$F(k) = \frac{1}{k!} \left[ \frac{d^k f(x)}{dx^k} \right]_{x=x_0} \quad (7)$$

The inverse differential transform of the original function  $f(x)$  is:

$$f(x) = \sum_{k=0}^{\infty} (x - x_0)^k F_k \quad (8)$$

Putting together Eqs. (7) and (8):

$$f(x) = \sum_{k=0}^{\infty} \frac{(x - x_0)^k}{k!} \left[ \frac{d^k f(x)}{dx^k} \right]_{x=x_0} \quad (9)$$

which is actually the expansion of the Taylor series for  $f(x)$  about  $x - x_0$ .

Table 3 summarizes some of the main operations of the DTM. Using these rules, governing equations are transformed into new expressions.

### 3 Results and Discussion

Prior to analyzing free vibration characteristics of Goland and HALE wings at 50% span extension, several validation cases are performed. Firstly, free vibration analyses of Goland and HALE wings without any extension are analyzed. Table 4 lists the structural and geometrical properties of Goland and HALE wings.

The coupled bending-torsional vibration characteristics of Goland and HALE wings are investigated and validated with literature. The comparison of obtained natural frequencies of wing models is given in Tables 5 and 6, respectively.

The other validation case is the free vibration analysis of the three-segment wing model which is composed of parts with different properties. The schematic view of the different three-stepped wing model is illustrated in Fig. 2.

In the study of Hashemi and Richard (2000), the Goland wing is also used as the basis, but some parameters are taken differently from the original ones. The

**Table 4** Structural and geometrical properties of Goland and HALE wings

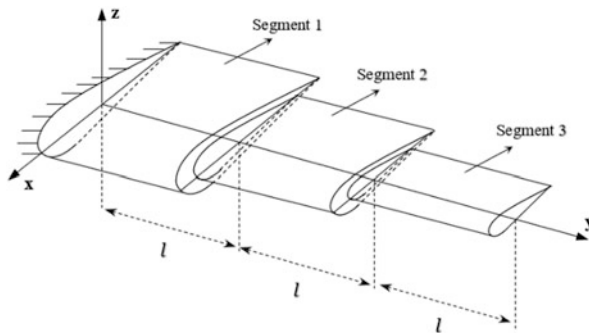
Property	Unit	Goland wing	HALE wing
Half span ( $l$ )	m	6.096	16
Chord ( $c$ )	m	1.8288	1
Bending rigidity (EI)	N. m <sup>2</sup>	$9.77 \times 10^6$	$2 \times 10^4$
Torsional rigidity (GJ)	N. m <sup>2</sup>	$0.987 \times 10^6$	$1 \times 10^4$
Mass of the wing per unit length ( $m$ )	kg/m	35.71	0.75
Static unbalance	kg	6.523	0

**Table 5** Natural frequencies of Goland wing

Frequency (rad/s)			
Mode number	Present study	Reference study (Eslimy-Isfahany et al., 1996)	Error (%)
1	49.58	49.6	0.04
2	97.28	97.0	0.29
3	248.58	248.9	0.13
4	356.32	355.6	0.20
5	451.91	451.5	0.09
6	608.24	610.0	0.29

**Table 6** Natural frequencies of HALE wing

Frequency (rad/s)			
Mode number	Present study	Reference study (Patil et al., 2001)	Error (%)
1	2.24	2.24	0
2	14.06	14.06	0
3	31.05	31.07	0.06
4	39.36	39.36	0

**Fig. 2** The schematic view of the three-stepped wing model

**Table 7** Structural and geometrical parameters of the wing model used in reference study (Hashemi & Richard, 2000)

Property	Unit	Goland wing
Half span ( $l$ )	m	6
Bending rigidity (EI)	N. m <sup>2</sup>	$9.75 \times 10^6$
Torsional rigidity (GJ)	N. m <sup>2</sup>	$0.988 \times 10^6$
Mass of the wing per unit length ( $m$ )	kg/m	35.75
Mass moment of inertia about elastic axis per unit length ( $I_{EA}$ )	kg/m	8.64
Elastic axis position from leading edge ( $y_0$ )	m	0.33c
Static unbalance	kg	6.523

**Table 8** The comparison of natural frequencies of three-stepped Goland wing

Frequency (rad/s)			
Mode number	Present study	Reference study (Hashemi & Richard, 2000)	Error (%)
1	74.02	74.43	0.55
2	131.20	128.57	2
3	248.42	253.40	1.96
4	386.16	376.59	2.48
5	425.19	431.29	1.41

parameters that are used in reference study are given in Table 7. The lengths of each segment are equal and taken as 2 m. The properties of the second segment are taken as two-thirds of segment one, and the properties of the third segment are taken as one-third of segment one.

The findings of the present study are compared with values from reference study in Table 8. The comparison shows that the findings are very close to each other.

The chord length data is not stated in the study of Hashemi and Richard (2000). Therefore, the chord lengths of each segment are taken as the same with Goland wing. Thus, it is estimated by the author that the errors may result from the missing data in reference study.

After completing validation cases, the wing at 50% span extension is analyzed for two wing models, Goland and HALE wings. Firstly, free vibration behavior of Goland wing at 50% span extension is investigated. The wingspan extends by 50% means that the semi-span length becomes 9.144 m. In this configuration, chord lengths of segments are assumed to be equal to each other. The lengths of the first, second, and third segments are taken as  $L_1 = 5$  m,  $L_2 = 1.096$  m, and  $L_3 = 3.048$  m, respectively. Table 9 compares the first six natural frequencies of Goland wing at 50% span extension with natural frequencies of Goland wing without any extension.

It is apparent from Table 9 that the natural frequencies for each mode decrease dramatically when span extends by 50%. HALE wing at 50% extension is also analyzed. The lengths of the first, second, and third segments are assigned as 13.333 m, 2.667 m, and 8 m, respectively. The first six natural frequencies of

**Table 9** The comparison of the first six natural frequencies of Goland wing at 50% extension

Frequency (rad/s)		
Mode number	50% extension	0% extension
1	21.74	49.58
2	62.64	97.28
3	130.36	248.58
4	194.76	356.32
5	283.18	451.91
6	372.23	608.24

**Table 10** The comparison of the first six natural frequencies of HALE wing at 50% extension

Frequency (rad/s)		
Mode number	50% extension	0% extension
1	0.99	2.24
2	6.25	14.06
3	17.47	31.05
4	20.70	39.36
5	27.43	77.12
6	56.79	93.14

HALE wing at 50% span extension are compared with natural frequencies of HALE wing without any extension in Table 10.

It can be seen from Table 10 that the natural frequencies of each mode decrease significantly when the HALE wing extends by 50%.

To observe the effects of span extension on free vibration, natural frequencies of Goland wing are analyzed for different extension ratios. The second mode is chosen as the basis for this case. The variation of natural frequency with span extension is given in Fig. 3.

In this case, it is considered only the third segment extends along the spanwise. The span lengths of the second and third segments are unchanged which are  $L_1 = 5$  m and  $L_2 = 1.096$  m. 0% extension represents the fully retracted wing configuration, while 100% represents the fully extended wing configuration. There is a significant difference in terms of natural frequency between fully retracted and fully extended wing configurations. The natural frequency of the second mode is found as 97.58 rad/s at 0% extension. When the wing that extends is span by 100%, the natural frequency decreases to 46.67 rad/s. These findings show that there is a significant decrease in natural frequency between 0% extension and 100% extension of Goland wing. Another important finding is that the reduction in natural frequency is relatively high in earlier stages of morphing process.

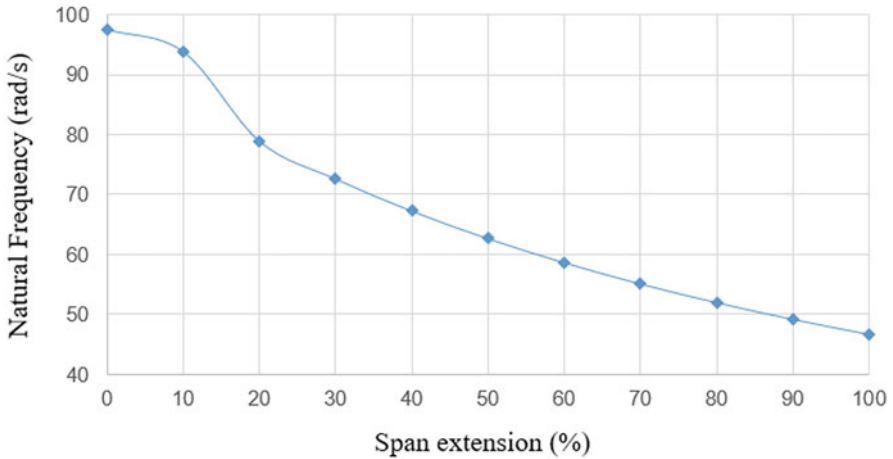


Fig. 3 Variation of natural frequency of the second mode with span extension for Goland wing

## 4 Conclusion

The aim of this paper is to analyze the free vibration behavior of variable-span morphing wings. Telescopic span morphing wing is modeled as bending-torsion coupled three-stepped Euler-Bernoulli beam. DTM is employed to solve equations of motion of the system. Goland and HALE wings are used as basis for all case studies, and three validation cases are performed. The results are compared in each case, and it is observed that the findings are in line with reference values. Then, vibration of Goland and HALE wings at 50% extension is analyzed. Natural frequencies of the wings at 50% extension are compared with natural frequencies of wings without any extension. Finally, several wing extension rates of Goland wing are investigated to observe the effects of span extension on natural frequencies. The analyses show that there is an important decrease in natural frequencies as wing extends its span length. This paper contributes to our understanding of how variable-span morphing wing affects the natural frequencies of the system.

## References

- Concilio, A., Dimino, I., Lecce, L., & Pecora, R. (2018). *Morphing wing technologies: Large commercial aircraft and civil helicopters*. Butterworth-Heinemann.
- Eslimy-Isfahany, S. H. R., Banerjee, J. R., & Sobey, A. J. (1996). Response of a bending-torsion coupled beam to deterministic and random loads. *Journal of Sound and Vibration*, 195(2), 267–283.
- Gamboa, P., Santos, P., Silva, J., & Santos, P. (2013). Flutter analysis of a composite variable-span wing. In *4th international conference on integrity, reliability and failure*, Funchal, pp. 23–27.

- Hashemi, S. M., & Richard, M. J. (2000). A Dynamic Finite Element (DFE) method for free vibrations of bending-torsion coupled beams. *Aerospace Science and Technology*, 4(1), 41–55.
- Ju, F., Lee, H. P., & Lee, K. H. (1994). On the free vibration of stepped beams. *International Journal of Solids and Structures*, 31(22), 3125–3137.
- Mao, Q. B., Nie, Y. P., & Zhang, W. (2012). Vibration analysis of a stepped beam by using adomian decomposition method. *Applied Mechanics and Materials*, 160, 292–296.
- Patil, M. J., Hodges, D. H., & Cesnik, C. E. (2001). Nonlinear aeroelasticity and flight dynamics of high-altitude long-endurance aircraft. *Journal of Aircraft*, 38(1), 88–94.
- Pulok, M. K. H., & Chakravarty, U. K. (2020). Aerodynamic and vibration analysis of the morphing wings of a hypersonic vehicle. *ASME International Mechanical Engineering Congress*, 84515, V004T04A013.
- Snyder, M. P., Sanders, B., Eastep, F. E., & Frank, G. J. (2009). Vibration and flutter characteristics of a folding wing. *Journal of Aircraft*, 46(3), 791–799.

# Aero-Engine Emission Calculation Method and Its Limitation Analysis



Sanmai Su, Kaiheng Liang, and Rongzhang Xie

## 1 Introduction

With the rapid development of modern aviation industry, the impact of air transportation on the atmospheric environment has become more and more serious. In addition to causing serious harm to the environment around the airport and public health (Masiol & Harrison, 2014; Fan et al., 2012), the emissions by aircraft during flight are more likely to lead to greenhouse effect and climate change. Therefore, the International Civil Aviation Organization (ICAO) and the airworthiness authorities of most of countries have made a series of mandatory regulations on civil aero-engines emission.

The environmental problems caused by aero-engine emission are attracting more attention by aero-engine manufacturers. The requirements for lowering the aero-engine emissions are becoming more and more stringent. Therefore, in the engine R & D stage, evaluating the emissions of the engine in different environments and service conditions is an important research work. Accurate estimating can provide decision-making assistance for engine designs, improvement, and maintenance.

The typical calculation methods of aero-engine emission mainly include two types. The first is the direct method, its main principle is to model and analyze the combustion process, and then calculate the emission of various components according to the emission generation mechanism. Representative calculation methods include single reactor model method, multi reactor model method, and computational fluid dynamics model method. The second is indirect method, its principle is to modify the aero-engine emission index under standard atmospheric conditions according to the thermal parameters of the aero-engine working process, and then estimate the emission from given working conditions. The typical methods include fuel flow method (Baughcum et al., 1996) and T3-P3 method (Mongia et al., 2001).

---

S. Su (✉) · K. Liang · R. Xie

Northwestern Polytechnical University, Xi'an, China

e-mail: [microeng@nwpu.edu.cn](mailto:microeng@nwpu.edu.cn); [khl@mail.nwpu.edu.cn](mailto:khl@mail.nwpu.edu.cn); [rongzhang\\_xie@mail.nwpu.edu.cn](mailto:rongzhang_xie@mail.nwpu.edu.cn)



Among the abovementioned engine emission calculation methods, no matter the calculation method itself or the application for actual engineering, there are certain limitations. This paper will briefly describe the current typical aero-engine emission calculation methods and then analyze their limitations, in order to provide reference for enhancing the accuracy and universality of aero-engine emission calculation.

## 2 Engine Emission Composition and Evaluation Method

The composition of aero-engine emissions mainly depends on the combustion condition in the combustion chamber and also is related to the actual operating state. Generally, the emission components mainly include  $N_2$  and  $O_2$  that completely participate in the combustion process;  $CO_2$ , water vapor, and  $SO_x$  generated by the ideal combustion process; and hydrocarbons (UHC),  $NO_x$ , CO, and other particulate matter generated by incomplete combustion.

According to statistics, the aero-engine typical combustion emission composition and proportion are shown in Fig. 1. (Penner, 1999), wherein,  $CO_2$  is about 72%,

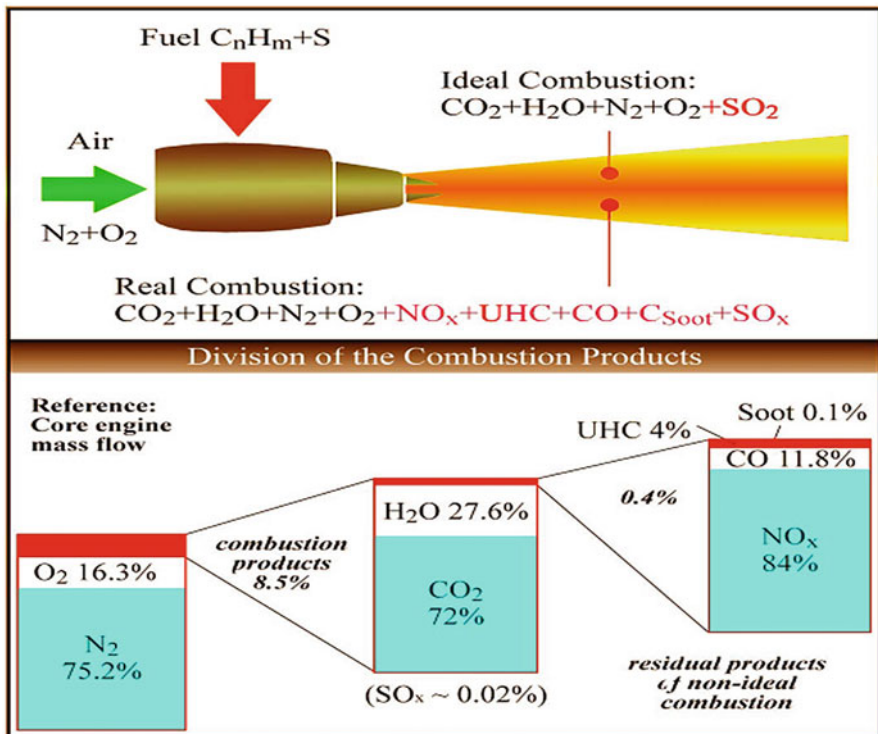


Fig. 1 Emission composition and proportion

H<sub>2</sub>O is slightly less than 27.6%, and the proportions of NO<sub>x</sub>, CO, SO<sub>x</sub>, UHC, and other components are less than 1%.

Emission index (EI) is used to describe the amount of engine emissions, which is defined as the proportion of each emission component to per kilogram of fuel burnt. The unit of EI is g/kg.

### 3 Emission Calculation Methods and Limitation Analysis

In this section, the abovementioned T3-P3 method, fuel flow method, and multi reactor model method and their limitations will be analyzed.

#### 3.1 T3-P3 Calculation Method and Its Limitation

The principle of T3-P3 method is based on engine thrust rating and emission index under standard atmospheric conditions, and then the emission index is corrected according to the engine's combustion chamber inlet total pressure P<sub>3</sub> and total temperature T<sub>3</sub> under any working conditions. Specifically, in the calculation, according to the aircraft and engine type, in the engine emission database published by ICAO, search the corresponding engine emission data under four thrust rating, and fit the data table to obtain the emission index of the engine under any thrust state.

For any working state in flight, take the emission index corresponding to the P<sub>3</sub> and T<sub>3</sub> of the engine under the standard atmosphere as the reference value and estimate the engine emission index according to the following formulas.

$$EI(\text{CO}) = EI_{\text{ref}}(\text{CO}) \times (P_{3 \text{ ref}}/P_3)^{1.5} \quad (1)$$

$$EI(\text{UHC}) = EI_{\text{ref}}(\text{UHC}) \times (P_{3 \text{ ref}}/P_3)^{2.5} \quad (2)$$

$$EI(\text{NO}_x) = EI_{\text{ref}}(\text{NO}_x) \times (P_3/P_{3 \text{ ref}})^{0.5} \times e^H \quad (3)$$

$$EI(\text{CO}_2) = 3152 - 1.5714 \times EI(\text{CO}) - 3.152 \times EI(\text{UHC}) \quad (4)$$

$$EI(\text{H}_2\text{O}) = 1290.7 - 1.2907 \times EI(\text{UHC}) \quad (5)$$

$$EI(\text{SO}_x) = 0.22(0.04\% \text{ avg fuel sample}) \quad (6)$$

In Eqs. 1, 2, 3, 4, 5, and 6, EI (XX) represents the emission index of the corresponding emission component, the unit is g/kg. In Eq. 3,  $e^H$  is the humidity correction factor, in which,

$$H = -19(\omega - 0.0063) \quad (7)$$

$$\omega = \frac{0.62198\psi P_v}{P_{\text{amb}} - \psi P_v} \quad (8)$$

$$P_v = 0.014504 \times 10^\beta \quad (9)$$

$$\beta = 7.90298 \times \left(1 - \frac{373.16}{T_{\text{amb}}}\right) + 3.00571 + 5.02808 \times \log\left(\frac{373.16}{T_{\text{amb}}}\right) + 1.3816 \times 10^{-7} \times \left[1 - 10^{11.344 \times \left(1 - \frac{T_{\text{amb}}}{373.16}\right)}\right] + 8.1328 \times 10^{-3} \times \left[10^{3.49149 \times \left(1 - \frac{373.16}{T_{\text{amb}}}\right)} - 1\right] \quad (10)$$

In Eqs. 7, 8, 9, and 10,  $\omega$  is actual humidity,  $\psi$  is relative humidity, and  $P_v$  is saturation vapor pressure.

The total emissions for a certain flight segment are calculated as follows, in which,  $W_f$  is fuel flow of engine.

$$EI_{\text{all}} = \sum EI \times W_f \times \text{time} \quad (11)$$

T3-P3 calculation method indirectly reflects the engine working conditions (by T3 and P3) at the inlet of the engine combustion chamber under flight and ground standard atmospheric conditions. In practical application, there are some limitations:

Parameter T3 and P3 cannot fully reflect the actual situation of the combustion chamber. For example, the amount of  $\text{NO}_x$  emission is closely related to the flame temperature of the main combustion zone, but the temperature of this zone and its equivalence ratio cannot be measured or difficult to calculate.

Emission index is not only closely related to thrust but also to the flight conditions (such as speed) and engine healthy (such as engine degradation).

T3-P3 calculation method is only applicable to the existing aero-engine emission calculation in ICAO database. The universality of the method is poor, especially for a newly developed or modified aero-engine.

### 3.2 Fuel Flow Calculation Method and Its Limitation

The principle of fuel flow calculation method is similar to T3-P3 method, and it is based on the relationship between engine emission index and fuel flow under standard atmospheric conditions. Different from T3-P3 method, it modifies the emission index according to fuel flow of the engine under any working conditions.

For different flight states, first, according to the aircraft and aero-engine model, the related data of fuel flow, CO, UHC, and  $\text{NO}_x$  emission index of the corresponding engine under four thrust rating can be found in the database published

by ICAO, and then interpolated by the engine current fuel flow to get emission index of each component. The calculation method is as follows:

First, calculate the fuel flow factor  $W_{ff}$

$$W_{ff} = \frac{W_f}{\delta} \times \theta^{3.8} \times e^{0.2M^2} \quad (12)$$

In which,  $\delta = T_{amb}/288.15$   $\theta = P_{amb}/101.325$ ,  $W_f$  is fuel flow,  $M$  is Mach number. Then, the emission index of main component is calculated as follows:

$$EI(\text{UHC}) = EI_{ref}(\text{UHC}) \frac{\theta^{3.3}}{\delta^{1.02}} \quad (13)$$

$$EI(\text{CO}) = EI_{ref}(\text{CO}) \frac{\theta^{3.3}}{\delta^{1.02}} \quad (14)$$

$$EI(\text{NO}_x) = EI_{ref}(\text{NO}_x) \cdot \left( \frac{\delta^{1.02}}{\theta^{3.3}} \right)^{0.5} \quad (15)$$

In Eqs. 13, 14, and 15,  $EI_{ref}(XX)$  is corresponding to  $W_{ff}$  at the emission index fitting curve.

The fuel flow method has a similar mechanism to the T3-P3 method, and it also has similar limitations. Compared with the T3-P3 method, this method uses easy-to-measure fuel flow parameters, which is easier to calculate in practical applications.

### 3.3 *Multi Reactor Model Calculation Method and Its Limitation*

The mechanism of multi reactor model emission calculation method (Cao et al., 2014) is to regard engine combustion chamber as a thermochemical reactor, which is used to simulate the combustion state when it is working, so as to reveal the generation principle, composition, and quantity of emission. When using this method to calculate emissions, it is necessary to establish a combustion air flow model according to the type, geometry, and size of the combustion chamber.

The calculation starts from the inlet of the combustion chamber. First, the initial diameter of the fuel droplets is calculated through the fuel atomization model, and then the fuel evaporation at the inlet of each reactor is calculated according to the fuel droplet evaporation model to obtain the combustion efficiency. Second, assuming that the flame is a continuous and infinitely thin reactor, emissions are formed in the continuous reactor.

Except for the initial reactor, each subsequent reactor needs to integrate reaction temperature, combustion efficiency and pressure, and equivalence ratio of each reactor. Apply the combustion chemical reaction model to calculate the adiabatic

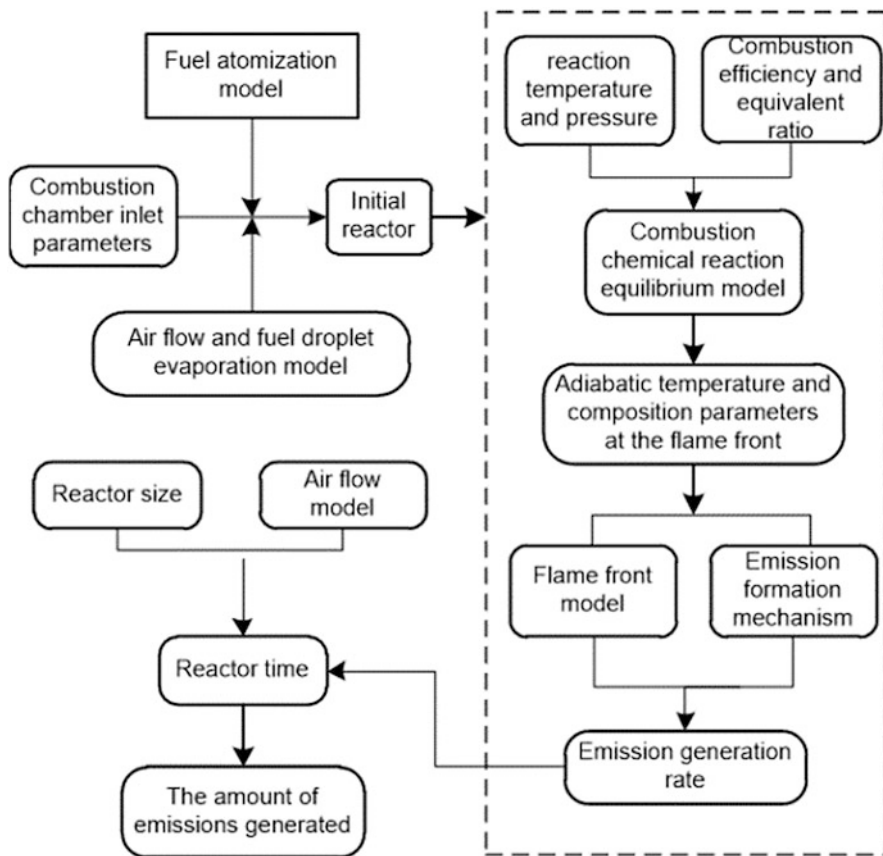


Fig. 2 The calculation flow chart of multi reactor model emission calculation method

flame temperature and the number of moles of emission components. Finally, the generation rate of various emission components is calculated according to the adiabatic flame temperature. Combined with the generation rate and reaction time, the emissions generated by each reactor are calculated. The calculation flow chart is as Fig. 2.

Furthermore, in order to improve the accuracy of the calculation, generally, the combustion chamber can be divided into multi areas according to its characteristics. Finally, the total emissions are obtained by accumulating the emission from each area.

When using multi reactor model method to calculate engine emission, it is necessary to establish fuel atomization and fuel droplet evaporation model, combustion chemical reaction equilibrium model, and flame front model. Its advantage is that it can explain the generation mechanism of emission and accurately calculate the emission components of any type of combustion chamber and engine under any working state. The calculation method has good versatility. The disadvantage is that

the modeling and calculation process are complex for different types of combustion chambers. In addition, although the emission calculation based on the multi reactor model method is mainly for the combustion chamber, when it is applied to engine emission calculation, it needs to combine the engine performance simulation model to provide the fuel gas ratio, total temperature, and total pressure.

## 4 Conclusions

Two types of typical calculation principles and three kind of methods for emission of aero-engine are analyzed, and the limitations of each calculation method in practical application are discussed. The conclusions are as follows:

T3-P3 method and fuel flow method belong to the indirect method. Its principle is to take the emission index of the existing engine under standard atmospheric conditions as a reference and then calculate the emission of the engine under any flight state according to the total pressure P3 and total temperature T3 or fuel flow. This type of calculation method is mainly used for the emission calculation of civil aircraft engines with airworthiness, and its universality is poor.

The multi reactor model method belongs to the direct method, and its principle is to establish an emission calculation model according to the emission mechanism of engine combustion chamber. The advantage is that it has good versatility, but the disadvantage is that it makes the modeling and calculation process complex. It needs to be calculated jointly with the engine performance simulation model.

In the process of aero-engine real application, it is suggested to integrating multiple methods at the same time to enhance the calculation accuracy through mutual verification.

## References

- Baughcum, S. L., Tritz, T. G., & Henderson, S. C. (Eds.). (1996). *Scheduled civil aircraft emission inventories for 1992: Database development and analysis*. NASA-Contractor Report 4700.
- Cao, M. D., Wang, Z. X., & Cai, Y. H. (2014). Civilian turbofan engine emission prediction based on combustor multi reactor model. *Journal of Aerospace Power*, 29, 1042–1052.
- Fan, W., Sun, Y., & Zhu, T. (2012). Emissions of HC, CO, NO<sub>x</sub>, CO<sub>2</sub>, and SO<sub>2</sub> from civil aviation in China in 2010. *Atmospheric Environment*, 56, 52–57.
- Masiol, M., & Harrison, R. M. (2014). Aircraft engine exhaust emissions and other airport related contributions to ambient air pollution: A review. *Atmospheric Environment*, 95, 409–455.
- Mongia, H. C., Vermeersch, M., Held, T. (2001). *A DRA modelling approach for correlating gaseous emissions of turbo-propulsion engine combustors*. 37th joint propulsion conference and exhibit. <https://doi.org/10.2514/6.2001-3419>.
- Penner, J. E. (1999). *Aviation and the global atmosphere*. Cambridge University Press.

# APC E-Rostering System



Titapong Chureeganon, Khemmarat Chunganuwat, Kacha Pinprasert,  
Chanaporn Boonchaisiriporn, and Potchara Aungaphinant

## 1 Introduction

According to the Annex 11 – Air Traffic Services, the International Civil Aviation Organization (ICAO) requires the ICAO state members to establish a regulation concerning fatigue management (ICAO, 2016, 2018). To comply with the above requirement, in Thailand, the Civil Aviation Authority of Thailand (CAAT) has published *Manual of Standards Air Traffic Management Services: Air Traffic Services (MOS-ATS)* (CAAT, 2020) and requires air traffic service providers (ATSP) to establish the prescriptive fatigue management limits for working hours and break hours as indicated in item 4.2.2 Air Traffic Controllers' rostering system(s) (Kearney et al., 2019) such as:

- Maximum duty period. Except where other limits are defined within the MOS-ATS, duty period shall not exceed 12 hours.
- Maximum monthly duty period. Within 720 consecutive hours (30 days), the aggregate of duty periods and on-call duties shall not exceed 200 hours.
- Consecutive duty period. The maximum duration of consecutive duty periods may not exceed 72 consecutive hours (6 days).
- Interval between duty period. There shall be an interval (rest period) of not less than 12 hours between the conclusion of a duty period and the commencement of the next duty period.
- Limit on and interval following consecutive periods of duty. Upon the conclusion of 6 consecutive duty periods within 144 consecutive hours (6 days), there shall be an interval (rest period) of a minimum of 60 hours before the commencement of the next duty period.

---

T. Chureeganon (✉) · K. Chunganuwat · K. Pinprasert · C. Boonchaisiriporn · P. Aungaphinant  
Aeronautical Radio of Thailand Ltd., Bangkok, Thailand  
e-mail: [Titapong.ch@aerorhail.co.th](mailto:Titapong.ch@aerorhail.co.th)

### **Time-in-position**

1. Breaks in time-in-position (partial break). Time-in-position shall not exceed a period of 2 hours without there being taken during, or at the end of, that period a partial break or breaks totaling not less than 30 minutes during which period a controller does not exercise the privileges of their license.
2. At units where workload for any part of the day is judged to be low and the activity is spasmodic rather than continuous, time-in-position, at these times, may be extended to a maximum of 4 hours, provided that the following break is taken pro rata (e.g., 45 minutes after 3 hours or 60 minutes after 4 hours):
  - Takeover of air traffic controllers. To ensure the proper transfer of functions between controllers, the ATSP may extend the maximum duration of the continuous duty period up to a maximum of 15 minutes. The time taken for orderly handover/takeover before a shift starts up to a maximum of 15 minutes shall be considered as time-in-position for the air traffic controller who finishes his/her activity and therefore shall not be considered to form part of the oncoming controller's duty period (Tello et al., 2018).
  - Night duty.
    - A duty which covers all or part of the period of night duty shall not exceed 10 hours.
    - No more than three consecutive duties which cover all or part of the period of night duty shall be performed.
    - A minimum period of 54 hours shall occur between the end of duties which cover all or part of the period of night duty and the commencement of the next period of duty.

It can be seen that the requirements set forth as mentioned above are quite complex so that it is crucial to develop any tools to help manage the working hours and break hours for air traffic control officers (ATCOs) (EUROCONTROL, 2006).

Aeronautical Radio of Thailand Ltd. (AEROTHAI), the sole air navigation service provider (ANSP) in Thailand (CANSO, 2016), is in charge of reviewing ATCOs' scheduling in accordance with the manual of standards and presenting a stagger shift model as an action figure with anticipated availability in 2023.

Previously, the Microsoft Excel program has been used to arrange the air traffic controllers' operating schedules for a long time. Additionally, the requirements of the prescriptive fatigue management limits are quite detailed, and the researchers had an idea to develop a system to simplify the scheduling procedures at the Provincial Approach Control Center, AEROTHAI, where there are a large number of air traffic control services in 17 areas (Orasanu et al., 2011). Therefore, the APC E-Rostering System was developed as a web-based application for ease of use with three objectives:



- To assist in scheduling operations in accordance with the conditions set forth in the fatigue of air traffic controllers.
- To assist in the management and supervise the operation of air traffic controllers effectively.
- To help in collecting data on the operations of air traffic controllers accurately, conveniently, and quickly and that can be examined.

## 2 Method

This research was conducted in collaboration with air traffic controllers and system developers. AEROTHAI found a way to arrange ATCOs' working schedules in accordance with the requirement of prescriptive fatigue management limits. Meetings with the officers involved in scheduling operations were conducted to collect preliminary data (Romano et al., 2008). The key data obtained from the meetings is the ATCOs' attendance pattern. It was found that the ATCOs are commonly required to work 4 days (10 hours per day) and have a break during a shift followed by 3 rest days. However, since there was an epidemic of coronavirus (COVID-19) which inevitably affects the aviation industry, the pattern was then adjusted according to the reduction of flight volumes as well as the fatigue requirements. The researchers created a tool called "the APC E-Rostering System" with the aim to help support the operations and prevent the spreading of COVID-19 among the ATCOs at AEROTHAI. Most importantly, the system was developed to support three different tasks as follows:

### 2.1 To Create a Roster

To schedule the ATCOs' operations, it is an action in the initial part of planning to arrange suitable air traffic control services workload for ATCOs and to manage fatigue for maximum efficiency. The procedure of creating roster is divided into two parts as follows:

To begin with, the first part will be the daily schedule of operations, which is to arrange the number of ATCOs in operation (opening position) based on the amount of air traffic. Once the opening position is checked abide by the fatigue requirements, position log configuration is obtained. That is in the stagger shift form. The system is not only designed to support a normal position log for working schedule but the system is also designed to accommodate a secondary schedule as a minimum schedule that can be supported in case the numbers of ATCOs need to be reduced.

For the second part, a monthly work roster is used to arrange work days and rest days for ATCOs in each month (work pattern). Once the work pattern has been assigned to each ATCO, this section is called the shift cycle. Both operations must comply with the air traffic controllers' fatigue management requirements. The

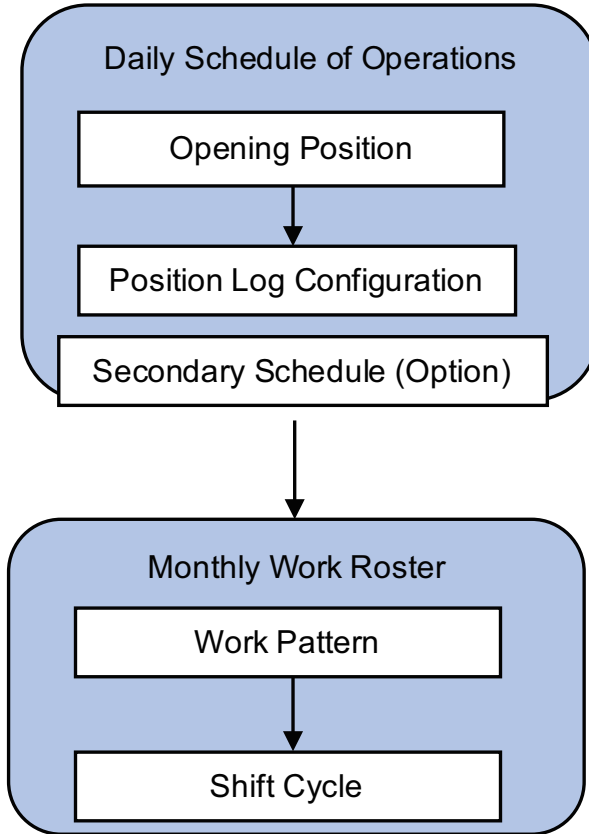


**Fig. 1** Workflow of rostering diagram

functional design of the APC E-Rostering System requires that users in all parts of the system can easily access it and use it efficiently. The summary of two parts is shown in Fig. 1.

## 2.2 To Manage and Supervise Staffs

The daily management of ATC operations is an integral duty of ATC managers. Because when we planned the arrangement of air traffic controllers in the first part, it is normal for changes to occur especially employee leave (as described in Fig. 2). In which part of the leave, the ATCOs shall follow AEROTHAI's regulations. AEROTHAI uses the System Applications & Products in Data Processing (SAP) to process leave-related activities. We therefore connect leave information from the SAP system to the APC E-Rostering System so that ATC managers can stay informed of the leave request and rearrange appropriate manpower. We make

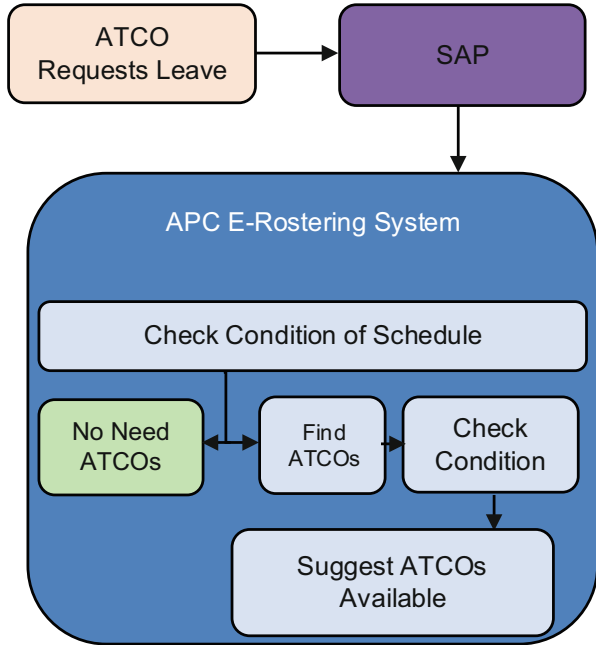


Fig. 2 Workflow of leaving management

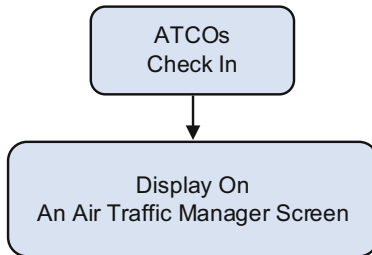


Fig. 3 Workflow of monitoring and oversight

arrangements for recruiting staff in lieu of leave, and preparations are being made for the reduction of the number of air traffic controllers.

The system will also assist in finding other ATCOs who will be available to replace those who are absent. The system will check the key conditions in terms of license rating, fatigue conditions, and the number of previous working hours in order to provide ATC managers information for taking further actions.

As shown in Fig. 3, moreover, the oversight of operations is another duty of the ATC manager. The system was also designed to include a “Check In” menu for ATCOs and ATC managers to conveniently enter registration information for each hour of operation. This information will be displayed in a “Position Log Monitoring” menu to facilitate the supervision of ATC managers.

From the operations mentioned above, the system will keep the operational data up to date regarding the record of change made in order to be able to monitor various operations easily and quickly.

### ***2.3 To Prevent Accidental Update***

The system was designed to prevent any accidental updates on the information currently in the system by specifying different rights to access its functions. According to the roles and duties, the system defines roles of a roster man, an ATC manager, and ATCOs.

A roster man is responsible for the overall scheduling planning. This position has permission to access and edit all information as ordered by the executive. This position will be primarily responsible for creating daily and monthly work schedules so that ATCOs will be informed of their own schedule in advance.

An ATC manager is a person who uses the system on a daily basis to manage manpower and supervision of air traffic control in a safe and efficient manner. Based on the manager's duty, the system allows the manager to update the ATCOs' work schedule information right after a roster man has created the work schedule. This position will also be able to oversee the operations of ATCOs in an orderly and safe manner.

Finally, an ATCO can only view the data without permissions to edit data. If an ATCO needs to make some changes on the operational data, the data shall be submitted to ATC manager who has a permission to make changes instead. Another important function for the ATCO is the use of the check-in menu when entering an assigned position.

## **3 Results and Discussion**

After testing the APC E-Rostering System, it was found that the system can support and suggest effective scheduling in stagger shift format.

According to Table 1, the system currently provides a new model that is suitable for ATCOs during the epidemic of COVID-19 called the "Shelter Operating Model" which can be divided into two types of work schedules. The first type suggests the ATCOs to have 6 work days and 6 rest days (W6R6). The second type suggests ATCOs to have 6 work days and 12 rest days (W6R12). Both types require ATCOs to work 12 hours a day divided into 8 work hours and 4 break hours. In addition, the system also suggests an additional model which allows the ATCOs to have 4 work days and 3 rest days (W4R3). The additional model requires the ATCOs to work 10 hours per day and have a break during the day according to the requirements. It can be seen that this system is flexible for modifying both working styles as well.

**Table 1** The results to comply fatigue requirements

Work model	Shelter model		W4R3
	W6R6	W6R12	
Maximum duty period	Pass	Pass	Pass
Maximum monthly duty period	Pass	Pass	Pass
Consecutive duty period	Pass	Pass	Pass
Interval between duty period	Pass	Pass	Pass
Limit on and interval following consecutive periods of duty	Pass	Pass	Pass
Time-in-position	Pass	Pass	Pass
Takeover of air traffic controllers	Pass	Pass	Pass
Night duty <sup>a</sup>	–	–	Pass

Note: <sup>a</sup>There are no air traffic control services between 01.30 and 05.29 am (night duty) since the opening and closing times for regional airports have been renovated in the current situation

**Table 2** The satisfaction surveys of the APC E-Rostering System in August 2021

Overall score	1	2	3	4	5
Number of participants	–	–	–	7	4
Percentage (%)	–	–	–	64	36

Note: 1 to 5 is poor to excellence

The APC E-Rostering System was formally tested by the participants including ATC managers and ATCOs in August 2021. Both groups were asked to evaluate the performance of the system by completing the provided satisfaction surveys. According to Table 2, the results reveal that the system can still meet the usage very well, but there are still parts that need to be improved as the advice of the test participants.

Additionally, it is expected that the APC E-Rostering System should be improved and be officially used in early 2022. The situation of the coronavirus 2019 epidemic in Thailand should be better than the present. The limitations of personnel management in the matter of the epidemic of the virus would also be relaxed. We may encounter new problems that we have not encountered at this time. However, we try to develop the system to be more responsive to automated usage.

## 4 Conclusion

The APC E-Rostering System was developed to help the Provincial Approach Control Center to arrange the work schedule of ATCOs that should be appropriate to the amount of air traffic control workload and the fatigue requirements. This system will assist in recommending the work schedule and giving notice when the information related to the schedule of ATCOs does not comply with the fatigue regulations enforced by CAAT.

Based on the results, the researchers highly expect that the APC E-Rostering System will be able to effectively assist the air traffic control agency in scheduling management tasks. If the implementation in the Provincial Approach Control Center is successful, it will be further expanded for use in other air traffic controls.

**Acknowledgments** The research reported in this paper was supported by the Provincial Approach Air Traffic Control Management Bureau, Information Technology Systems Management Department, and Human Resource Development and Learning Management Department. The authors are also grateful to all members of Fatigue Management Working Group, Provincial Approach Control Center (APC FMWG), whose expertise enhanced the conducted research.

## References

- CAAT The Civil Aviation Authority of Thailand. *Manual of standards: Air traffic management services-air traffic services*. Issued 03, September 18, 2020.
- CANSO Civil Air Navigation Services Organization. (2016). *Fatigue management guide for air traffic service providers* (1st ed.). International Civil Aviation Organization.
- EUROCONTROL. (2006). *Shiftwork practices study – ATM and related industries, DAP/SAF-2006/56*. EUROCONTROL.
- ICAO International Civil Aviation Organization. (2016). *Doc 9966 – Manual for the oversight of fatigue management* (2nd ed.). ICAO.
- ICAO International Civil Aviation Organization. (2018, July). *Annex 11 – Air Traffic Services* (15th ed.). ICAO
- Kearney, P., Li, W. C., & Braithwaite, G. (2019). Roster and air traffic controller’s situation awareness. In *Engineering psychology and cognitive ergonomics: 16th international conference, EPCE 2019, held as part of the 21st HCI international conference, HCII 2019, Orlando, FL, USA, July 26–31, 2019, Proceedings 21* (pp. 66–75). Springer International Publishing.
- Orasanu, J., Nesthus, T.E., Parke, B., Hobbs, A., Dulchinos, V., Kraft, N.O., McDonnell, L., Anderson, B., Tada, Y., & Mallis, M. (2011, September). Work schedules and fatigue management strategies in air traffic control (ATC). In *Proceedings of the human factors and ergonomics society annual meeting* (Vol. 55, No. 1, pp. 1–5). SAGE Publications.
- Romano, E., Santillo, L. C., & Zoppoli, P. (2008, May). Scheduling applied to air traffic control. In *WSEAS International Conference. Proceedings. Mathematics and computers in science and engineering* (No. 10). World Scientific and Engineering Academy and Society.
- Tello, F., Mateos, A., Jiménez-Martín, A., & Suárez, A. (2018). The air traffic controller work-shift scheduling problem in Spain from a multiobjective perspective: A metaheuristic and regular expression-based approach. *Mathematical Problems in Engineering*, 2018, 1–15.

# Sustainable Aviation of Textile Industry: Life Cycle Assessment of the Pollutants of a Denim Jean Production Process



Delia Teresa Sponza and Nefise Erdinçmer

## 1 Introduction

According to recent studies on production of a pair of jeans, the total process consumes nearly 3100 L of water and vast amounts of organic and inorganic chemicals and energy (Zhao & Chen, 2019; Kanchinadham & Kalyanaraman, 2017; Tasca & Puccini, 2019). Discharges of the chemicals increased with the amounts of denim jeans produced globally. It can be inferred that denim industry contributes highly to pollution of water by releasing harmful liquids and gases to the ecosystems (Zhao & Chen, 2019; Kanchinadham & Kalyanaraman, 2017). Textile effluents containing indigo, blue, and violet dyes cause toxicity in the surface waters for humans and animals. As a result, the balances of the aquatic systems, the food chains, and the environment are altered negatively (Tasca & Puccini, 2019). The utilization of sulfur and synthetic indigo dyes also causes serious problems in the effluents of the wastewater treatment plant discharges. The environmental impacts of denim processing are water pollution (dyeing and finishing discharge to the aquatic ecosystem), air pollution (denim cotton dust), and chemicals (in the atmosphere and aquatic ecosystems). Denim waste is classified based on its generation at different production stages as pre-consumer, post-consumer, and industrial textile waste. Pre-consumer waste can be defined as the remaining raw material discharged after the finishing processes which may include selvedge, offcuts, shearing, and organic surplus. These wastes can be reused and recycled (Proske & Finkbeiner, 2019). The post-consumer textile waste includes the textile that completed its life cycle and is not used by the consumers. Industrial textile waste contains wastes released to the environment (Zhao & Chen, 2019; Tasca & Puccini, 2019).

---

D. T. Sponza (✉) · N. Erdinçmer  
Dokuz Eylül University, Environmental Engineering Department, Izmir, Turkey  
e-mail: [delya.sponza@deu.edu.tr](mailto:delya.sponza@deu.edu.tr)

The recent studies showed that the textile waste concentrations will reach 102 million tons by 2030 which corresponds to a 60% increase between 2021 and 2030. On the other hand, the fashion wastes will reach 148 million tons in 2030. Most of the waste from clothing industry ends up in landfills or is incinerated. In landfills, decomposition of natural fibers takes hundreds of years, and during this time, methane and CO<sub>2</sub> may be released into the atmosphere. Waste management hierarchy consists of prevention, preparation for reuse, recycling, recovery, and disposal steps. Prevention of waste generation has the highest importance followed by reuse. Undamaged parts of raw materials may be reused for manufacturing of new products. After disposal of textiles by the manufacturer or consumers, its recycling provides the opportunities of recovering raw materials and saving energy as well as reducing pollution (Proske & Finkbeiner, 2019; Cabeza et al., 1998).

Life cycle assessment (LCA) is a systematic and quantitative method for evaluation of the environmental impacts of a product or a service throughout all stages of its life. Denim products depend on the use of raw fabric materials, energy, equipment, and labor, and these requirements determine the design and product development. Thus, for sustainable development, an LCA is necessary for analysis of environmental impacts that originate from each production step. Furthermore, an LCA also includes information on potential environmental impacts over the entire life of a product (i.e., cradle to grave) not only from raw material acquisition to production but also on its use and, finally, its disposal. LCAs are critical tools for interpreting the impacts on the global scale and reducing their negative effects to the environment. Currently, LCA is the most comprehensive approach that can be applied to the assessment of textile products, and it is standardized by the ISO (International Organization for Standardization) as an industry standard (14040–14043) (Proske & Finkbeiner, 2019). Life cycle of a denim jean starts when production of raw materials like fibers and chemicals begins. Then, these materials are used in fabric production where energy and water are consumed, and waste materials are emitted to the air and water.

## 2 Method

The methodology of LCA is based on consideration of all impacts that originate from a system with various inputs and outputs and expression of number of total impacts quantitatively for the system. Accordingly, in order to emphasize the importance of denim recycling from the perspective of its environmental impact, an experimental study was conducted based on LCA of a denim fabric with and without recycled fiber content. The data of this study was based on a denim production report (2021) of a facility in Turkey. For LCA, SimaPro software (developed by PRé Sustainability B.V., Amersfoort, Netherlands) was used. It is one of the leading LCA software that has been extensively used. The primary data was composed of parameters used in basic production such as amount of cotton (i.e., 0.5 kg) used in production of 1 m of denim (Tasca & Puccini, 2019; Proske &



Finkbeiner, 2019). On the other hand, the secondary data was used from the software database (Ecoinvent) which includes impacts that evolved from using raw material and other chemicals in all production steps. Ecoinvent database is supplied with software, and it is one of the most widely used life cycle inventory (LCI) databases worldwide (Tasca & Puccini, 2019; Proske & Finkbeiner, 2019). This database provides life cycle inventory (LCI) data collected from various industries such as transport, construction materials, chemical production, agriculture, energy supply, and metal production (Giannetti et al., 2015). On top of Ecoinvent database, SimaPro software not only contains all libraries in Ecoinvent but also it uses various system models and processes. System models in Ecoinvent database are “allocation at the point of substitution,” “cutoff by classification,” and “consequential.” The system model for “allocation at the point of substitution” provides proportional attribution of workloads to specific processes. Another system model “allocation, cutoff by classification” is dependent on the recycled data or cutoff methods by which the primary production of materials is always linked to the primary producer of a material. In this approach, the primary producer does not receive any credit if a material is recycled and only the impacts of the recycling processes are included. The last system model “substitution, consequential, long-term” includes some basic assumptions for analysis of the consequences of a variation in an existing system, and this approach may be used for perspective studies and prediction of future changes (Giannetti et al., 2015). In the present study, “cutoff by classification” model is used for recycled materials, and “allocation at point of substitution” model is preferred for all other data.

In this study, life cycle assessment (LCA) methodology is selected to calculate the environmental impacts of denim industry having different recycled cotton ratios. The environmental effects in the life cycle were calculated by a SimaPro software including production of the fiber, fabric production, reuse, water use, and global warming.

### 3 Results and Discussion

For life cycle assessment (LCA) of a product, the denim industry is simulated, using both consumption and production data taken from Ecoinvent database. Then the environmental impacts on the process steps were calculated. In the denim industry, the LCA consists of the raw materials, from the energy and organic chemicals used from the water consumption, from the distance to transport, from the waste, from the wastewaters from the and emissions to the atmosphere which these are primarily used data. The environmental effects originated from all the influent and effluent of the denim textile industry were secondary data.

One of the most important parts of life cycle assessment (LCA) is the environmental impacts of the product. The environmental impacts for our study were global warming potential of climate changes, acidification, eutrophication, ozone layer depletion, abiotic depletion, freshwater use, and human water toxicity consumption,

**Table 1** The environmental impact categories and calculation methodologies using SimaPro software methods

Indicator	Unit	Description	Example of impact	Methodology
Global warming potential	kg CO <sub>2</sub> eq (kilogram carbon dioxide equivalent)	Emission of greenhouse gases (GHGs)	Climate change	IPCC 2013 GWP 100a (6,7)
Freshwater use	lt (liters)	Excessive freshwater taken from the environment	Water scarcity	Life cycle inventory
Land use	m <sup>2</sup> a (meter square per annum)	The amount of agricultural area occupied	Deforestation	ReCiPe 2016 Midpoint (H) (5–7)
Eutrophication potential (EP)	kg PO <sub>4</sub> <sup>3</sup> eq (kilogram phosphate equivalent)	Emission of substances to water contributing to oxygen depletion	Nutrient loading to water stream-water pollution	CML-IA baseline (7)
Abiotic resource depletion	kg Sb eq (kilogram antimony equivalent)	Measure of mineral, metal, and fossil fuel resources used to produce a product	Mineral scarcity	CML-IA baseline (7)

**Table 2** Effects of some environmental impacts on the process steps in a denim industry process

Industry steps	Environmental impact				
	Effect of global warming (%)	Effect of water utilization (%)	Effect of land use (%)	Effect of abiotic depletion (%)	Effect of eutrophication (%)
Fiber	19	0	0	0	0
Spinning	15	0	2	4.6	0
Dyeing	16	0	0	19	5
Weaving	1	0	0	0	0
Finishing	3	1.7	0	20	3
Packaging	39	0	0	0	0
Transportation of raw materials	0	0	0	0	1

and these items were taken into consideration as environmental impact categories in this study for denim textile industry using SimaPro software (Table 1).

In denim textile, the first biggest effect was found to be fiber growth step as a result of global warming (Table 2). The abiotic resource depletion has the second highest impact. This clearly shows that the choosing of raw material is a very important tool for denim industry.

**Table 3** Effects of some environmental impacts on the process steps in a denim industry process

Industry	Environmental impacts				
	Effect of global warming (%)	Effect of water utilization (%)	Effect of land use (%)	Effect of abiotic depletion (%)	Effect of eutrophication (%)
Denim industry processes					
100% cotton	80	80	80	87	87
85% cotton + 15% recycled cotton	67	70	70	79	76
65% cotton + 35% recycled cotton	60	60	64	68	70
55% cotton + 45% recycled cotton	50	50	58	60	60
45% cotton + 45% recycled cotton	45	40	50	52	40

Global warming potential is affected by three main stages – fiber cultivation, spinning, and packaging – while abiotic depletion is mainly affected by spinning and dyeing.

In order to detect the effects of recycled cotton contents in the denim industry, different ratios of recycled cotton are used in the calculations (Table 3). The results of the life cycle assessment (LCA) calculations shown in Table 3 exhibited that as the recycled cotton ratio was increased, the effects on environmental effects decreased.

Recycling of denim in the textile industry is very important to reduce its impacts such as water consumption and land use. The use of recycled cotton with organic cotton also provides reductions in other impacts such as potential for global warming, eutrophication, and abiotic depletion. In the future, the impacts of various fibers combined with recycled cotton fibers may also be evaluated for denim fabric production. When the whole textile industry is considered, the use of recycled cotton source appears to be the major challenge. Another difficulty is the compositions of denims. Early produced denims were completely made of 100% cotton. In recent denim productions, a great number of denim products include elastane fiber. Also, new denim compositions include synthetic and regenerated cellulose fibers. As the complexity of the composition increases, it mechanically gets harder to recycle denims. Across the denim industry, only 13% of the raw material input is recycled after its use. Most of this recycled material is transferred to other industries in a cascade, and it is used in low-value applications, such as wiping cloths and insulation materials.

## 4 Conclusion

The use of recycled cotton source appears to be the major challenge when the whole textile industry is considered. Recycling of denim in the textile industry is very important to reduce its impacts such as water consumption and land use. The use of recycled cotton with organic cotton also provides reductions in other impacts such as potential for global warming, eutrophication, and abiotic depletion. Since mechanical recycling of a textile material is a challenging process, new techniques have emerged recently for use of denims and other cellulosic materials as a source/raw material. Combinations of recent technologies such as Infinited Fibers (converting multiple cellulose-rich waste materials to upcycled fibers) and Nanollose (bacterially produced nanocellulose made from waste biomass) may provide the use of recycled denims as second-hand garments by applying fiber separation and turning cellulosic part into liquid fermentation and, as a last step, processing of regenerated cellulosic fibers. Also, the use of fermentation appears to be a promising step for integration of bio-design in recycling of textiles, and it may help to eliminate most of the negative impacts of mechanical recycling.

## References

- Cabeza, L. F., Taylor, M. M., Dimaio, G. L., Brown, E. M., Marmer, W. N., Carrió, R., Celma, P. J., & Cot, J. (1998). Processing of leather waste: Pilot scale studies on chrome shavings. Isolation of potentially valuable protein products and chromium. *Waste Management*, *18*(3), 211–218.
- Giannetti, B. F., Agostinho, F., Moraes, L. C., Almeida, C. M. V. B., & Ulgiati, S. (2015). Multicriteria cost–benefit assessment of tannery production: The need for breakthrough process alternatives beyond conventional technology optimization. *Environmental Impact Assessment Review*, *54*, 22–38.
- Kanchinadham, S. B. K., & Kalyanaraman, C. (2017). Carbon trading opportunities from tannery solid waste: A case study. *Clean Technologies and Environmental Policy*, *19*(4), 1247–1253.
- Proske, M., & Finkbeiner, M. (2019). Obsolescence in LCA—methodological challenges and solution approaches. *International Journal of Life Cycle Assessment*, *25*(3), 495–507.
- SimaPro Software. <https://pre-sustainability.com>, Software use in LCA. Last accessed on 9 June 2021.
- Tasca, A. L., & Puccini, M. (2019). Leather tanning: Life cycle assessment of retanning, fatliquoring and dyeing. *Journal of Clean Production*, *226*, 720–729.
- Zhao, C., & Chen, W. (2019). A review for tannery wastewater treatment: Some thoughts under stricter discharge requirements. *Environmental Science Pollution Research*, *26*(25), 26102–26111.

# Effects of Alternative Aviation Fuels on Environment and Enviro-economic



Selçuk Sarıkoç

## Nomenclature

$c_{\text{CO}_2}$	Carbon price
$C_{\text{CO}_2}$	Economical cost of CO <sub>2</sub> emission
CO <sub>2</sub>	Carbon dioxide
G	100% gasoline
LHV	Lower heating value (MJ/kg)
M20	80% gasoline + 20% methanol (vol.)
SI	Spark-ignition
$t_{\text{working}}$	Annual working hour of the engine
$W_{\text{gen}}$	Generated power of the engine
$x_{\text{CO}_2}$	The amount of CO <sub>2</sub> emission in a year
$y_{\text{CO}_2}$	Hourly CO <sub>2</sub> emission of the engine per generated power

## 1 Introduction

Internal combustion engines are commonly used in the aviation sector. Especially, small-scale aviation vehicles such as aircraft, helicopters, and drones are powered by spark-ignition or diesel engines. Alternative liquid fuels such as methanol, ethanol, propanol, butanol, pentanol, and biodiesel were studied to improve the fuel properties, engine performance, and combustion process or to mitigate exhaust emissions in the internal combustion engines (Yesilyurt, 2019; Yilmaz et al., 2018; Atmanlı et al., 2015; Örs, 2020; Balki et al., 2014).

---

S. Sarıkoç (✉)

Department of Motor Vehicles and Transportation Technologies, Amasya University, Tasova  
Yüksel Akin Vocational School, Amasya, Türkiye

Methanol is a clean, easily biodegradable, water-soluble, clean burning fuel. These properties make it an attractive alternative fuel due to environmental and economic advantages (Methanol and Institute, 2021).

Generally, researchers have focused on land vehicles as alternative fuels, while there is not enough investigation on alternative/green aviation fuels. Therefore, methanol fuel effects on the environment and enviro-economic respect were investigated as alternative/green aviation fuel.

## 2 Materials and Methods

The experiments were conducted at full engine load, constant engine speed (2000 rpm), and lambda values ( $\lambda = 1$ ). A four-cylinder and the direct-injected spark-ignition engines were used to determine the methanol effects on the engine performance and exhaust emissions. The detailed test conditions and used pieces of equipment were explained in the previous author's study (Sarikoç, 2021). The test system and pieces of types of equipment are represented in Fig. 1. The main fuel specifications are given in Table 1.

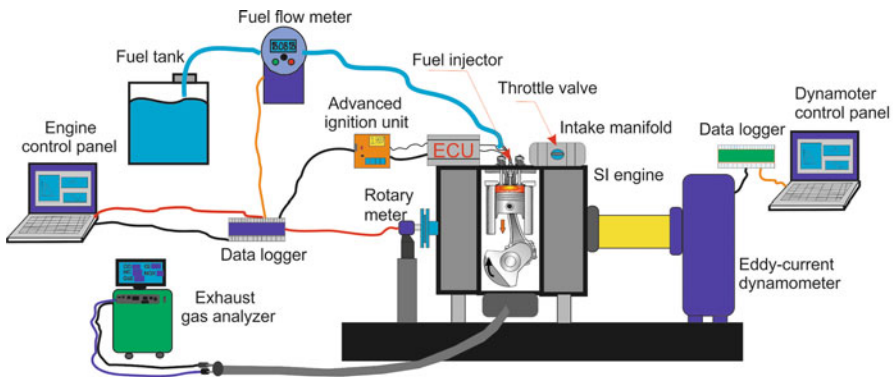


**Fig. 1** Schematic illustration of the test system and components of the equipment

**Table 1** The properties of the test fuels (Pulkrabek, 1997; Vancoillie et al., 2012; Li et al., 2017)

Fuel type	Gasoline	Methanol
Formula	$C_8H_{15}$	$CH_3OH$
Density ( $kg/m^3$ )	715–765	792
LHV(MJ/kg)	43	20.05
Octane number	92	111
Oxygen content (%)	–	50
Latent heat (kJ/kg)	307	1147
Laminar flame speed (cm/s)	33–44	52

In this study, the environmental and enviro-economic analyses of an SI engine are investigated. In this respect, the experimental results were used for calculating carbon price. For this purpose, the current Switzerland carbon price, i.e., \$19.98, was applied due to the high price of carbon emission in the Scandinavian countries (Gurbuz et al., 2019; The World Bank, 2020). Caliskan (2017) applied environmental and enviro-economic analysis method taken into account the fuels' emitting CO<sub>2</sub> emission and the CO<sub>2</sub> emission cost as follows:

$$x_{\text{CO}_2} = y_{\text{CO}_2} W_{\text{gen}} t_{\text{working}} \quad (1)$$

$$C_{\text{CO}_2} = c_{\text{CO}_2} x_{\text{CO}_2} \quad (2)$$

In Eq. (1),  $x_{\text{CO}_2}$  expresses the amount of CO<sub>2</sub> emission in a year, while  $y_{\text{CO}_2}$ ,  $W_{\text{gen}}$ , and  $t_{\text{working}}$  represent hourly CO<sub>2</sub> emission of the engine per generated power, generated power of the engine, and annual working hour of the engine, respectively. In Eq. (2),  $c_{\text{CO}_2}$  and  $C_{\text{CO}_2}$  are represented as carbon price and economical cost of CO<sub>2</sub> emission, respectively (Gurbuz et al., 2019). The total operating hour of the engine is considered to be 2190 h with respect to the assumption of 6 h working of the engine in a day.

### 3 Results and Discussion

The environmental and enviro-economic analyses are investigated to the G and MG20 fueled engine. The results of environmental and enviro-economic analyses are given in Table 2. According to the obtained results, the environmental effect of CO<sub>2</sub> per year was calculated to be 45.11 tCO<sub>2</sub>/year and 45.47 tCO<sub>2</sub>/year for G and MG20 blend. The addition of methanol slightly increased by 0.807% the release of the CO<sub>2</sub> emission. The engine system environmental analysis results are illustrated in Fig. 2. Furthermore, it was calculated to be \$901.203/year and \$908.48/year enviro-economic cost of gasoline and methanol blend, respectively. The engine system enviro-economic analysis results are presented in Fig. 3. The engine system generated power is calculated as 23.6 kW and 24 kW for G and MG20 at full engine load, respectively. However, it is obvious that the CO<sub>2</sub> per power of the engine decreased from 872.71 to 865.10 g/kWh with the addition of methanol.

**Table 2** The results of the environmental and enviro-economic analyses

Parameters	G	MG20
$y_{\text{CO}_2}$ (gCO <sub>2</sub> /kWh)	872.71	865.10
$W_{\text{gen}}$ (kW)	23.6	24
$x_{\text{CO}_2}$ (tCO <sub>2</sub> /year)	45.11	45.47
$C_{\text{CO}_2}$ (\$/year)	901.203	908.480

**Fig. 2** The environmental effect of test fuels

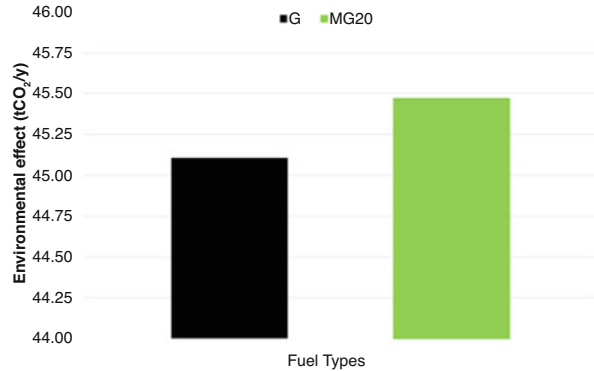
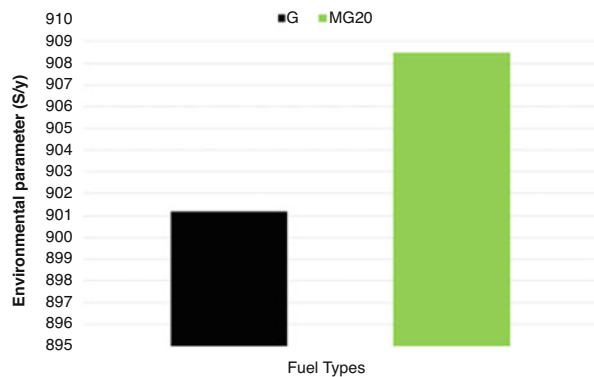


**Fig. 3** The enviro-economic effect of test fuels



## 4 Conclusion

In the present study, a four-cylinder SI engine fueled with methanol-gasoline fuel blend was evaluated in terms of environmental and enviro-economic aspects at full engine load. The main conclusions can be given as follows:

- The generated engine power increases with the addition of methanol at full engine load.
- The CO<sub>2</sub> emission value of the engine per generated power for the MG20 fuel blend decreases. However, the annual CO<sub>2</sub> emission amount slightly increases with the addition of methanol.
- The economic cost of the CO<sub>2</sub> emission increases with the addition of methanol.

It can be concluded that although the addition of methanol increased engine power, it negatively affects the environment and enviro-economic of the countries. Thus, further studies are required to better understand the cause of negative impacts. It can be recommended that further research be undertaken in the following areas: energy, exergy, thermo-economic, and thermo-environmental analysis.



**Acknowledgments** The author is grateful for the support from Amasya University and Erciyes University. The author especially wants to thank Erciyes University for providing the experimental setup facilities.

## References

- Atmanlı, A., İleri, E., & Yüksel, B. (2015). Effects of higher ratios of n-butanol addition to diesel-vegetable oil blends on performance and exhaust emissions of a diesel engine. *Journal of the Energy Institute*, 88(3), 209–220. <https://doi.org/10.1016/j.joei.2014.09.008>
- Balki, M. K., Sayin, C., & Canakci, M. (2014). The effect of different alcohol fuels on the performance, emission and combustion characteristics of a gasoline engine. *Fuel*, 115, 901–906. <https://doi.org/10.1016/j.fuel.2012.09.020>
- Caliskan, H. (2017). Environmental and enviroeconomic researches on diesel engines with diesel and biodiesel fuels. *Journal of Cleaner Production*, 154, 125–129. <https://doi.org/10.1016/j.jclepro.2017.03.168>
- Gurbuz, H., Sohret, Y., & Akcay, H. (2019). Environmental and enviroeconomic assessment of an LPG fueled SI engine at partial load. *Journal of Environmental Management*, 241, 631–636. <https://doi.org/10.1016/j.jenvman.2019.02.113>
- Li, Y., Gong, J., Deng, Y., Yuan, W., Fu, J., & Zhang, B. (2017). Experimental comparative study on combustion, performance and emissions characteristics of methanol, ethanol and butanol in a spark ignition engine. *Applied Thermal Engineering*, 115, 53–63. <https://doi.org/10.1016/j.applthermaleng.2016.12.037>
- Methanol, Institute. (2021). *About methanol*. Methanol Institute. <https://www.methanol.org/about-methanol/>. Accessed 19 Oct 2021
- Örs, İ. (2020). Experimental investigation of the cetane improver and bioethanol addition for the use of waste cooking oil biodiesel as an alternative fuel in diesel engines. *Journal of the Brazilian Society of Mechanical Sciences and Engineering*, 42(4). <https://doi.org/10.1007/s40430-020-2270-1>
- Pulkrabek, W. W. (1997). *Engineering fundamentals of the internal combustion engine* (Vol. 1, p. 07458). Prentice Hall.
- Sarkoç, S. (2021). Lifecycle-based environmental pollution cost analyses of a spark ignition engine fueled with a methanol-gasoline blend. *Energy Sources, Part A: Recovery, Utilization, and Environmental Effects*, 43(23), 3166–3183. <https://doi.org/10.1080/15567036.2021.1943568>
- The World Bank. (2020). *What we do, data, carbon pricing dashboard*. [https://carbonpricingdashboard.worldbank.org/map\\_data](https://carbonpricingdashboard.worldbank.org/map_data). Accessed 23 Dec 2020.
- Vancoillie, J., Demuynck, J., Sileghem, L., Van De Ginste, M., & Verhelst, S. (2012). Comparison of the renewable transportation fuels, hydrogen and methanol formed from hydrogen, with gasoline – Engine efficiency study. *International Journal of Hydrogen Energy*, 37(12), 9914–9924. <https://doi.org/10.1016/j.ijhydene.2012.03.145>
- Yesilyurt, M. K. (2019). The effects of the fuel injection pressure on the performance and emission characteristics of a diesel engine fuelled with waste cooking oil biodiesel-diesel blends. *Renewable Energy*, 132, 649–666. <https://doi.org/10.1016/j.renene.2018.08.024>
- Yilmaz, N., Atmanlı, A., & Vigil, F. M. (2018). Quaternary blends of diesel, biodiesel, higher alcohols and vegetable oil in a compression ignition engine. *Fuel*, 212, 462–469. <https://doi.org/10.1016/j.fuel.2017.10.050>

# Assessment of Oxygenated and Nanofluid Fuels as Alternative/Green Aviation Fuels



Selçuk Sarıkoç

## Nomenclature

Al <sub>2</sub> O <sub>3</sub>	Aluminum oxide
CNT	Carbon nanotube
CO	Carbon monoxide
LHV	Lower heating value (MJ/kg)
Mn <sub>2</sub> O <sub>3</sub>	Manganese oxide
SI	Spark-ignition
ZnO	Zinc oxide

## 1 Introduction

High-octane fuel, which is obtained by formulating gasoline and called aviation gasoline, is used in aircraft piston engines (Çetinerler, 2021). The effective oxygen concentration at sea level is 20.9%. This value is 10.5% at 18000 ft. and 6.3% at 30000 ft. (Hypoxico, 2021). At high altitudes, low oxygen density negatively affects combustion efficiency, causing incomplete combustion, thus reducing engine performance and limiting the maximum altitude.

Oxygen additives reduce the pollution of the atmosphere to a minimum by enabling the fuel to burn more efficiently. Because oxygenated fuels ensure complete combustion of the fuel in the combustion chamber they lead to reducing the amount of harmful emissions chemicals released into the atmosphere (Rashedul et al., 2014).

---

S. Sarıkoç (✉)

Department of Motor Vehicles and Transportation Technologies, Amasya University, Tasova  
Yüksel Akin Vocational School, Amasya, Türkiye

Nanomaterials have many advantages such as high energy density, ability to mix with liquid fuels, heterogeneous combustion kinetics, ignition acceleration reaction, and cost. The higher surface area-to-volume ratio and more reactive surface of the nanoparticles cause the nanofluid fuel mixture to oxidize faster. Thus, they provide higher combustion enthalpy and energy density. Nanofluids provide high evaporation rate, better atomization, more homogeneous air-fuel mixture, and better flame sustainability in fuels. This results in a shortening of the premixing and diffusion phases and a significant reduction in the ignition delay. This short ignition delay, better atomization of the fuel, and the highly reactive surface allow the combustion reaction to start faster and earlier. Thus, a higher amount of heat release rate and cylinder internal pressure are created (Saxena et al., 2017).

In the literature, many nanomaterials such as  $\text{Al}_2\text{O}_3$ ,  $\text{ZnO}$ ,  $\text{TiO}_2$ ,  $\text{CeO}_2$ ,  $\text{SiO}_2$ , and CNT (carbon nanotube) are used as fuel additives because they increase the heat transfer by radiation and enable the air-fuel mixture to oxidize faster with its high surface area-to-volume ratio (Ağbulut et al., 2020; Zhang et al., 2019; Nanthagopal et al., 2020).

There are many studies in the literature on the use of nanomaterials in the internal combustion engines. For example, there are studies in which CNT of different sizes is used as a fuel additive in diesel engines under various engine conditions (Zhang et al., 2019; Najafi, 2018). Sivakumar et al. (2018) researched on the effects of mixing  $\text{Al}_2\text{O}_3$  nanoparticles with biodiesel in a diesel engine on engine performance, combustion, and emission characteristics, Ağbulut et al. (2020) investigated the effects of mixtures of various metal oxide nanomaterials, including  $\text{Al}_2\text{O}_3$ , with biodiesel in a diesel engine, on engine performance, combustion, emission, vibration, and noise characteristics; Manigandan et al. (2020) compared the effects on emissions in diesel engines by giving hydrogen to fuel mixtures consisting of different kinds of nanoparticles, including CNT and  $\text{Al}_2\text{O}_3$  additives; and Chen et al. (2018) used CNT and  $\text{Al}_2\text{O}_3$  additives as fuel additives in diesel engines and examined the effects of nanoparticles on engine performance, combustion, and emission characteristics.

In the literature, on the use of nanomaterials in spark-ignition engines, Amirabedi et al. (2019) investigated the effects of mixtures of manganese oxide ( $\text{Mn}_2\text{O}_3$ ) nanoparticles with ethanol on engine performance and emissions. As a result of the study, it was calculated that the gasoline-10% ethanol-20 ppm  $\text{Mn}_2\text{O}_3$  fuel mixture increased the engine power by 19.56% and the specific fuel consumption decreased by 36.72% compared to gasoline.

## 2 Effect of Oxygenated and Nanofluid Fuels on Combustion Process

In the literature, it has been stated that the lack of enough oxygen in the environment during combustion causes incomplete combustion, thus reducing the performance and efficiency of the engine (Pulkrabek, 2016). In addition, alcohols with high oxygen content improve combustion, provide complete combustion, reduce CO formation, and prevent energy loss from the exhaust (Yesilyurt et al., 2020). High oxygen content of alcohols (Canakci et al., 2013) and higher laminar flame velocity than gasoline (gasoline, 33–44 cm/s; methanol, 52 cm/s; ethanol, 48 cm/s; butanol, 48 cm/s) improve the combustion process (Li et al., 2017) and increase engine torque, specific fuel consumption, thermal efficiency, and combustion efficiency (Balki et al., 2014). The high heat of evaporation caused due to the cooling effect on the combustion chamber and the higher octane number properties of alcohols considerably reduce knocking, making the combustion more uniform and thus improving the combustion process (Zhang et al., 2014). Furthermore, oxygen-rich alcohols affect the combustion process positively by improving the premix and diffusion combustion phases (Emiroğlu & Şen, 2018). However, the lower calorific value of alcohols compared to gasoline increases somewhat of the specific fuel consumption. More fuel is consumed to achieve the same engine power output due to the lower calorific value of alcohols (Li et al., 2017).

Alcohols (methanol and ethanol) have higher features than gasoline, such as oxygen content, octane number, evaporation heat, and laminar flame propagation speed, improve combustion, and provide more stable operation of the engine (Pulkrabek, 1997; Li et al., 2017; Yilmaz & Atmanli, 2017). Important properties of gasoline, methanol, and ethanol are presented in Table 1.

In spark-ignition engines, combustion starts with the ignition of the spark plug, and the flame front spreads rapidly. The temperature and pressure of the burnt gases increase as a result of compressing the unburned mixture in front of the flame front. In this compression, it increases the temperature and pressure of the unburned mixture. During the combustion process in the engines, the heat transfer by conduction and convection during combustion is not significant compared to radiation due to combustion actually occurring in a very short time per cycle. Therefore, heat

**Table 1** Important properties of gasoline, methanol, and ethanol (Pulkrabek, 1997; Li et al., 2017; Yilmaz & Atmanli, 2017)

Fuel type	Gasoline	Methanol	Ethanol
Formula	$C_8H_{15}$	$CH_3OH$	$C_2H_5OH$
Density ( $kg/m^3$ )	715–765	792	0.803
LHV (MJ/kg)	43	20.05	26.9
Octane number	92	111	129
Oxygen content (%)	–	50	34.73
Latent heat (kJ/kg)	307	1147	918.42
Laminar flame speed (cm/s)	33–44	52	48

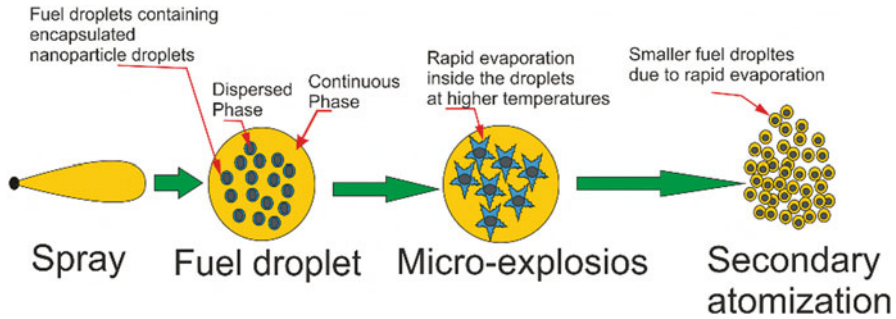


**Fig. 1** The effect of nanomaterial on the combustion process with micro-explosions

transfer by radiation is more important in heat transfer in the combustion process (Pulkrabek, 1997).

Aluminum oxide ( $\text{Al}_2\text{O}_3$ ) nanoparticles are encapsulated in the fuel mixture, causing a micro-explosion during combustion, thus providing a more homogeneous fuel-air mixture by allowing the fuel mixture to be atomized for the second time. This improves the complete combustion process positively, resulting in better combustion characteristics. With the addition of 50 ppm and 100 ppm  $\text{Al}_2\text{O}_3$  to the fuel, an increase of 28.91% and 29.7% was obtained, respectively (Sivakumar et al., 2018). CNT increased the peak pressure and heat release rate in the engine by 23.33% and 28%, respectively. It also improved the combustion process by reducing the ignition delay time by 8.98% (Najafi, 2018). CNT also caused a 23% rate reduction in specific fuel consumption. It was also stated that it provides better fuel stability (Manigandan et al., 2020). In another study, it was observed that CNT increased the maximum cylinder pressure and heat release rate by 5% and 4%, respectively (El-Seesy et al., 2019). Nanoparticles increase the heat transfer rate with their higher heat conduction properties and improve the combustion process characteristics by making a catalytic effect in the fuel (Sungur et al., 2016). In addition, the nanomaterial additive greatly affects thermal efficiency. The thermal conductivity of nanomaterials increases the heat transfer of the fuel mixture, which reduces the ignition delay, resulting in an increase in pressure rise rate and peak pressure; thus, they lead to better thermal efficiency (Kumar et al., 2017).

However, nanoparticles are likely to clog the injector as they tend to agglomerate due to their large surface area and surface activity (Saxena et al., 2017). In order to prevent the precipitation and agglomeration of nanomaterials in the fuel, they are usually added to the fuel in liquid solution (emulsion) form using a solvent and surfactant (Nanthagopal et al., 2020). Ultrasonic homogenizers are used to mix these surfactants and nanomaterials homogeneously with the fuel and to ensure the stability of the mixture (Soudagar et al., 2018). Thus, these nanomaterials can be used as additives in liquid fuels as nanofluids. The effect of nanomaterial on the combustion process is presented in Fig. 1.

### 3 Summary and Conclusions

Engine performance and combustion process characteristics can be improved by making improvements in the chemistry and technology of the fuel used in the engine. In this regard, using alcohol and nanomaterials can be improved important fuel properties so that an increase can be obtained in the engine performance and combustion efficiency. Considering the above information, the benefits of oxygenated fuels (alcohols) and nanomaterials for air vehicles can be summarized as follows:

The combustion process at a high altitude for high-flying vehicles can be improved by oxygenated fuels, which is providing extra oxygen content.

Oxygenated fuels can not only increase the fuel oxygen content of unmanned aerial vehicles but also improve cold flow characteristics. Furthermore, nanomaterials increase the fuel oxygen surface area and increase the combustion efficiency by creating a catalytic effect. In this way, engine performance and combustion efficiency increase at high altitudes, and harmful exhaust emissions and fuel consumption can be reduced.

The oxygen content, octane number, combustion surface, and heat transfer rate of the fuel can be increased with nanomaterial additives added to the fuel. Thus, performance parameters such as engine torque, engine power, thermal efficiency, and combustion efficiency can also be improved. As a result of improving the engine performance and combustion process, useful load-carrying capacity, endurance, longer range flight, higher altitude, and fuel economy can be achieved.

Considering all this, the fuel blend consisting of surfactant, nanomaterial, and alcohol can be used in the internal combustion engine. Thus, by using alcohol and nanomaterials for air vehicles, it is possible to improve fuel properties, increase engine performance, and improve phases of combustion characteristics. The author recommends for future studies should have done experimental investigations of the stability of the nanomaterials and the effects of nanomaterials on the engine performance, combustion process, and exhaust emission characteristics.

**Acknowledgment** The author would like to thank Amasya University for its support.

### References

- Ağbulut, Ü., Karagöz, M., Sandemir, S., & Öztürk, A. (2020). Impact of various metal-oxide based nanoparticles and biodiesel blends on the combustion, performance, emission, vibration and noise characteristics of a CI engine. *Fuel*, 270, 117521. <https://doi.org/10.1016/j.fuel.2020.117521>
- Amirabedi, M., Jafarmadar, S., & Khalilarya, S. (2019). Experimental investigation the effect of Mn<sub>2</sub>O<sub>3</sub> nanoparticle on the performance and emission of SI gasoline fueled with mixture of ethanol and gasoline. *Applied Thermal Engineering*, 149, 512–519. <https://doi.org/10.1016/j.applthermaleng.2018.12.058>

- Balki, M. K., Sayin, C., & Canakci, M. (2014). The effect of different alcohol fuels on the performance, emission and combustion characteristics of a gasoline engine. *Fuel*, *115*, 901–906. <https://doi.org/10.1016/j.fuel.2012.09.020>
- Canakci, M., Ozsezen, A. N., Alptekin, E., & Eyidogan, M. (2013). Impact of alcohol–gasoline fuel blends on the exhaust emission of an SI engine. *Renewable Energy*, *52*, 111–117. <https://doi.org/10.1016/j.renene.2012.09.062>
- Çetinerler, E. (2021). Uçak Motorları. <http://www.tayyareci.com/akademi/motor.asp>. Accessed 29 Oct 2021.
- Chen, A. F., Akmal Adzmi, M., Adam, A., Othman, M. F., Kamaruzzaman, M. K., & Mrwan, A. G. (2018). Combustion characteristics, engine performances and emissions of a diesel engine using nanoparticle-diesel fuel blends with aluminium oxide, carbon nanotubes and silicon oxide. *Energy Conversion and Management*, *171*, 461–477. <https://doi.org/10.1016/j.enconman.2018.06.004>
- El-Seesy, A. I., Kosaka, H., Hassan, H., & Sato, S. (2019). Combustion and emission characteristics of a common rail diesel engine and RCEM fueled by n-heptanol-diesel blends and carbon nanomaterial additives. *Energy Conversion and Management*, *196*, 370–394. <https://doi.org/10.1016/j.enconman.2019.05.049>
- Emiroğlu, A. O., & Şen, M. (2018). Combustion, performance and exhaust emission characterizations of a diesel engine operating with a ternary blend (alcohol-biodiesel-diesel fuel). *Applied Thermal Engineering*, *133*, 371–380. <https://doi.org/10.1016/j.applthermaleng.2018.01.069>
- Hypoxico. (2021). *Altitude to oxygen chart*. <https://hypoxico.com/altitude-to-oxygen-chart/>. Accessed 29 Oct 2021.
- Kumar, S., Dinesha, P., & Bran, I. (2017). Experimental investigation of the effects of nanoparticles as an additive in diesel and biodiesel fuelled engines: A review. *Biofuels*, *10*(5), 615–622. <https://doi.org/10.1080/17597269.2017.1332294>
- Li, Y., Gong, J., Deng, Y., Yuan, W., Fu, J., & Zhang, B. (2017). Experimental comparative study on combustion, performance and emissions characteristics of methanol, ethanol and butanol in a spark ignition engine. *Applied Thermal Engineering*, *115*, 53–63. <https://doi.org/10.1016/j.applthermaleng.2016.12.037>
- Manigandan, S., Sarweswaran, R., Booma Devi, P., Sohret, Y., Kondratiev, A., Venkatesh, S., Rakesh Vimal, M., & Jensis Joshua, J. (2020). Comparative study of nanoadditives TiO<sub>2</sub>, CNT, Al<sub>2</sub>O<sub>3</sub>, CuO and CeO<sub>2</sub> on reduction of diesel engine emission operating on hydrogen fuel blends. *Fuel*, *262*, 116336. <https://doi.org/10.1016/j.fuel.2019.116336>
- Najafi, G. (2018). Diesel engine combustion characteristics using nano-particles in biodiesel-diesel blends. *Fuel*, *212*, 668–678. <https://doi.org/10.1016/j.fuel.2017.10.001>
- Nanthagopal, K., Kishna, R. S., Atabani, A. E., Al-Muhtaseb, A. A. H., Kumar, G., & Ashok, B. (2020). A compressive review on the effects of alcohols and nanoparticles as an oxygenated enhancer in compression ignition engine. *Energy Conversion and Management*, *203*, 112244. <https://doi.org/10.1016/j.enconman.2019.112244>
- Pulkrabek, W. W. (1997). *Engineering fundamentals of the internal combustion engine* (Vol. 1). Prentice Hall.
- Pulkrabek, W. W. (2016). *İçten Yanmalı Motorlar Mühendislik Temelleri. I. Baskı*. İzmir Güven Kitabevi.
- Rashedul, H. K., Masjuki, H. H., Kalam, M. A., Ashraful, A. M., Ashrafur Rahman, S. M., & Shahir, S. A. (2014). The effect of additives on properties, performance and emission of biodiesel fuelled compression ignition engine. *Energy Conversion and Management*, *88*, 348–364. <https://doi.org/10.1016/j.enconman.2014.08.034>
- Saxena, V., Kumar, N., & Saxena, V. K. (2017). A comprehensive review on combustion and stability aspects of metal nanoparticles and its additive effect on diesel and biodiesel fuelled C.I. engine. *Renewable and Sustainable Energy Reviews*, *70*, 563–588. <https://doi.org/10.1016/j.rser.2016.11.067>
- Sivakumar, M., Shanmuga Sundaram, N., Ramesh Kumar, R., & Syed Thasthagir, M. H. (2018). Effect of aluminium oxide nanoparticles blended pongamia methyl ester on performance,

- combustion and emission characteristics of diesel engine. *Renewable Energy*, 116, 518–526. <https://doi.org/10.1016/j.renene.2017.10.002>
- Soudagar, M. E. M., Nik-Ghazali, N.-N., Abul Kalam, M., Badruddin, I. A., Banapurmath, N. R., & Akram, N. (2018). The effect of nano-additives in diesel-biodiesel fuel blends: A comprehensive review on stability, engine performance and emission characteristics. *Energy Conversion and Management*, 178, 146–177. <https://doi.org/10.1016/j.enconman.2018.10.019>
- Sungur, B., Topaloglu, B., & Ozcan, H. (2016). Effects of nanoparticle additives to diesel on the combustion performance and emissions of a flame tube boiler. *Energy*, 113, 44–51. <https://doi.org/10.1016/j.energy.2016.07.040>
- Yesilyurt, M. K., Aydin, M., Yilbasi, Z., & Arslan, M. (2020). Investigation on the structural effects of the addition of alcohols having various chain lengths into the vegetable oil-biodiesel-diesel fuel blends: An attempt for improving the performance, combustion, and exhaust emission characteristics of a compression ignition engine. *Fuel*, 269, 117455. <https://doi.org/10.1016/j.fuel.2020.117455>
- Yilmaz, N., & Atmanli, A. (2017). Experimental evaluation of a diesel engine running on the blends of diesel and pentanol as a next generation higher alcohol. *Fuel*, 210, 75–82. <https://doi.org/10.1016/j.fuel.2017.08.051>
- Zhang, Z., Wang, T., Jia, M., Wei, Q., Meng, X., & Shu, G. (2014). Combustion and particle number emissions of a direct injection spark ignition engine operating on ethanol/gasoline and n-butanol/gasoline blends with exhaust gas recirculation. *Fuel*, 130, 177–188. <https://doi.org/10.1016/j.fuel.2014.04.052>
- Zhang, Z., Lu, Y., Wang, Y., Yu, X., Smallbone, A., Dong, C., & Roskilly, A. P. (2019). Comparative study of using multi-wall carbon nanotube and two different sizes of cerium oxide nanopowders as fuel additives under various diesel engine conditions. *Fuel*, 256, 115904. <https://doi.org/10.1016/j.fuel.2019.115904>



# An Evaluation of Particle Image Velocimetry in Terms of Correlation for Aviation



Onur Yasar, Selcuk Ekici, Enver Yalcin, and T. Hikmet Karakoc

## 1 Introduction

Non-intrusive flow measurement techniques became significant in fluid mechanics. Visualization and measurement of velocity for fluids are accepted as quite different development in technology (Li & Hishida, 2009). Particle image velocimetry takes place in non-intrusive flow measurement techniques (Yilmaz & Nelson, 2015a).

Particle image velocimetry existed in open literature in the 1980s. Over the years, particle image velocimetry technology has been developed and made better (Adrian, 2005). The manner of work in particle image velocimetry consists of motion of tracer particles and recording camera (Todde et al., 2009). Illumination is performed via pulsed lasers in particle image velocimetry (Larsson et al., 2012; Yilmaz & Nelson, 2015b). With the realization of all mentioned processes, image acquisition and flow velocity measurement are carried out (Larsson et al., 2015). However, the acquired images are raw images that need to be processed (Yilmaz et al., 2009a; Sayeed-Bin-Asad et al., 2016).

Image processing is compulsory in particle image velocimetry applications. In image processing, interrogation windows are essential to use. Interrogation windows are utilized for dividing raw images (Prasad, 2000; Li & Hishida, 2009). Overlap ratios and correlation types are other factors in image processing. With the use of

---

O. Yasar (✉) · E. Yalcin

Department of Mechanical Engineering, Balıkesir University, Balıkesir, Türkiye  
e-mail: [onur.yasar@balikesir.edu.tr](mailto:onur.yasar@balikesir.edu.tr); [eyalcin@balikesir.edu.tr](mailto:eyalcin@balikesir.edu.tr)

S. Ekici

Department of Aviation, Iğdır University, Iğdır, Türkiye

T. H. Karakoc

Faculty of Aeronautics and Astronautics, Eskişehir Technical University, Eskişehir, Türkiye

Information Technology Research and Application Centre, Istanbul Ticaret University, Istanbul, Türkiye

overlap ratio and correlations, raw images can be converted into flow characteristics (Yilmaz et al., 2009a, b). In particle image velocimetry experiments, several overlap ratios can be selected. Correlation types can be utilized in single frame or double frame mode (Raffel et al., 2018).

## 2 Correlation Types Used in PIV

Correlations generally can be classified into four groups in particle image velocimetry applications: cross-correlation, auto-correlation, adaptive correlation, and least squares matching, respectively (Prasad, 2000; Deen et al., 2002; Kitzhofer et al., 2012; Raffel et al., 2018). Least squares matching needs good-quality images (Kitzhofer et al., 2012). The correlation type mainly depends on deformation or rotation of particle image velocimetry images (Gui & Merzkirch, 2000; Sayeed-Bin-Asad et al., 2016). Different from least squares matching, auto-correlation is accepted as expensive method (Adrian, 1991). In adaptive correlation, interrogation areas can be arranged (Adrian, 1991; Xu et al., 2006). With the use of arranged interrogation areas, better image processing can be carried out. Cross-correlation seems to be advantageous in particle image velocimetry experiments (Figueredo-Cardero et al., 2012; Ahmadi et al., 2019). Location of interrogation windows isn't a problem in cross-correlation (Riccomi et al., 2018; Raffel et al., 2018).

## 3 Results and Discussion

Correlation types with examined studies and the percentages of correlations were given in Table 1 and Fig. 1, respectively.

Figure 1 illustrates that cross-correlation has dominance over other correlation types in particle image velocimetry. The percentage of cross-correlation is 60%. Cross-correlation is generally used in double frame images. No correlation loss and direction problem are seen in cross-correlation (Riccomi et al., 2018; Raffel et al., 2018). After cross-correlation, adaptive correlation is preferred most. Adaptive correlation offers changeable interrogation windows (Figueredo-Cardero et al., 2012). On the other hand, auto-correlation has the least usage. Usage of least squares matching isn't available in examined particle image velocimetry studies. The change in percentage is possible (Tala et al., 2013; Wang et al., 2018).

**Table 1** References and correlation types

References	Mentioned correlation type
Xu et al. (2006)	Adaptive correlation
Yayla et al. (2010)	Adaptive correlation
Guo et al. (2010)	Cross-correlation
Tala et al. (2013)	Cross-correlation and adaptive cross-correlation
Jung et al. (2013)	Cross-correlation
Fujimura and Hotta (2013)	Not available
Atibeni et al. (2013)	Not available
Sergis et al. (2015)	Cross-correlation
Hongwei et al. (2015)	Cross-correlation
Tunçer et al. (2016)	Cross-correlation
Cristofano et al. (2016)	Cross-correlation and auto-correlation
Keramaris (2016)	Cross-correlation
Wang et al. (2018)	Auto-correlation
Tang et al. (2018)	Cross-correlation
Loboda et al. (2018)	Not available
Sun and Huang (2018)	Not available
Kluska et al. (2019)	Adaptive correlation
Wu et al. (2019)	Cross-correlation
Bardera et al. (2019)	Cross-correlation
Head et al. (2019)	Cross-correlation

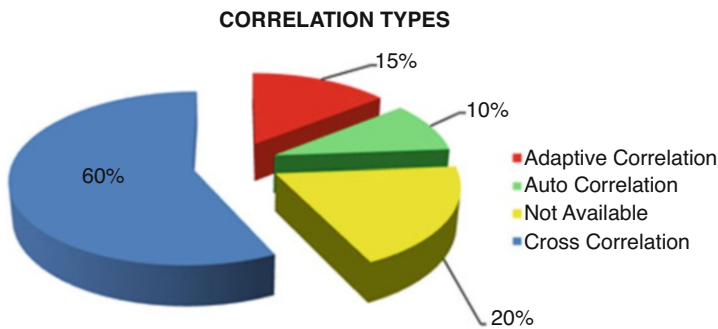


**Fig. 1** The percentages of correlation types

## 4 Conclusion

In this study, particle image velocimetry was taken into account with only correlations. Correlations have an important place in particle image velocimetry applications. Important remarks are explained below:

- The most preferred correlation type is found cross-correlation, because cross-correlation offers several advantages.
- Adaptive correlation is also utilized in particle image velocimetry studies. In adaptive correlation, interrogation areas can be changed or made smaller in order to process images better.
- Auto-correlation isn't used as much as cross-correlation and adaptive correlation.
- Usage of least squares matching isn't seen in examined studies.

Examined correlations are useful in PIV studies. In future, mentioned correlations may be viable in airships or solar aircrafts.

## References

- Adrian, R. J. (1991). Particle-imaging techniques for experimental fluid mechanics. *Annual Review of Fluid Mechanics*, 23(1), 261–304. <https://doi.org/10.1146/annurev.fl.23.010191.001401>
- Adrian, R. J. (2005). Twenty years of particle image velocimetry. *Experiments in Fluids*, 39(2), 159–169. <https://doi.org/10.1007/s00348-005-0991-7>
- Ahmadi, F., Ebrahimiyan, M., Sanders, R. S., & Ghaemi, S. (2019). Particle image and tracking velocimetry of solid-liquid turbulence in a horizontal channel flow. *International Journal of Multiphase Flow*, 112, 83–99. <https://doi.org/10.1016/j.ijmultiphaseflow.2018.12.007>
- Atibeni, R., Gao, Z., & Bao, Y. (2013). Effect of baffles on fluid flow field in stirred tank with floating particles by using PIV. *The Canadian Journal of Chemical Engineering*, 91(3), 570–578. <https://doi.org/10.1002/cjce.21652>
- Bardera, R., Barcala-Montejano, M. A., Rodríguez-Sevillano, A. A., & León-Calero, M. (2019). Conical vortices investigation and mitigation over the ski-jump ramp of an aircraft carrier by PIV. *Ocean Engineering*, 173, 672–676. <https://doi.org/10.1016/j.oceaneng.2019.01.032>
- Cristofano, L., Nobili, M., Romano, G. P., & Caruso, G. (2016). Investigation on bathtub vortex flow field by Particle Image Velocimetry. *Experimental Thermal and Fluid Science*, 74, 130–142. <https://doi.org/10.1016/j.expthermflusci.2015.12.005>
- Deen, N. G., Westerweel, J., & Delnoij, E. (2002). Two-phase PIV in bubbly flows: Status and trends. *Chemical Engineering & Technology*, 25(1), 97–101. [https://doi.org/10.1002/1521-4125\(200201\)25:1<97::AID-CEAT97>3.0.CO;2-7](https://doi.org/10.1002/1521-4125(200201)25:1<97::AID-CEAT97>3.0.CO;2-7)
- Figueredo-Cardero, A., Chico, E., Castilho, L., & de Andrade Medronho, R. (2012). Particle image velocimetry (PIV) study of rotating cylindrical filters for animal cell perfusion processes. *Biotechnology Progress*, 28(6), 1491–1498. <https://doi.org/10.1002/btpr.1618>
- Fujimura, T., & Hotta, M. (2013). A novel method to investigate the relationship between facial movements and wrinkle formation using particle image velocimetry. *Skin Research and Technology*, 19(1), e54–e59. <https://doi.org/10.1111/j.1600-0846.2011.00607.x>
- Gui, L., & Merzkirch, W. (2000). A comparative study of the MQD method and several correlation-based PIV evaluation algorithms. *Experiments in Fluids*, 28(1), 36–44. <https://doi.org/10.1007/s003480050005>
- Guo, F., Chen, B., Guo, L., & Zhang, X. (2010). Investigation of turbulent mixing layer flow in a vertical water channel by particle image velocimetry (PIV). *The Canadian Journal of Chemical Engineering*, 88(6), 919–928. <https://doi.org/10.1002/cjce.20355>
- Head, A. J., Novara, M., Gallo, M., Schrijer, F., & Colonna, P. (2019). Feasibility of particle image velocimetry for low-speed unconventional vapor flows. *Experimental Thermal and Fluid Science*, 102, 589–594. <https://doi.org/10.1016/j.expthermflusci.2018.10.028>

- Hongwei, W., Zhan, H., Jian, G., & Hongliang, X. (2015). The optical flow method research of particle image velocimetry. *Procedia Engineering*, 99, 918–924. <https://doi.org/10.1016/j.proeng.2014.12.622>
- Jung, S. Y., Park, H. W., Kim, B. H., & Lee, S. J. (2013). Time-resolved X-ray PIV technique for diagnosing opaque biofluid flow with insufficient X-ray fluxes. *Journal of Synchrotron Radiation*, 20(3), 498–503. <https://doi.org/10.1107/S0909049513001933>
- Keramaris, E. (2016). Similarities and differences between hot-film anemometry and particle image velocimetry in open channels. *Procedia Engineering*, 162, 388–395. <https://doi.org/10.1016/j.proeng.2016.11.079>
- Kitzhofer, J., Ergin, F. G., & Jaunet, V. (2012, July). 2D least squares matching applied to PIV challenge data (Part 1). In *16th International symposium on applications of laser techniques to fluid mechanics*.
- Kluska, J., Ronewicz, K., & Kardaš, D. (2019). Thermal characteristics of single wood particle pyrolysis using particle image velocimetry. *International Journal of Thermal Sciences*, 135, 276–284. <https://doi.org/10.1016/j.ijthermalsci.2018.09.020>
- Larsson, I. A., Granström, B., Lundström, T. S., & Marjavaara, B. D. (2012). PIV analysis of merging flow in a simplified model of a rotary kiln. *Experiments in Fluids*, 53(2), 545–560. <https://doi.org/10.1007/s00348-012-1309-1>
- Larsson, I. A., Johansson, S., Lundström, T. S., & Marjavaara, B. D. (2015). PIV/PLIF experiments of jet mixing in a model of a rotary kiln. *Experiments in Fluids*, 56(5), 1–12. <https://doi.org/10.1007/s00348-015-1984-9>
- Li, F. C., & Hishida, K. (2009). Particle image velocimetry techniques and its applications in multiphase systems. *Advances in Chemical Engineering*, 37, 87–147. [https://doi.org/10.1016/S0065-2377\(09\)03703-X](https://doi.org/10.1016/S0065-2377(09)03703-X)
- Loboda, E. L., Anufriev, I. S., Agafontsev, M. V., Kopyev, E. P., Shadrin, E. Y., Reyno, V. V., Vavilov, V. P., & Lutsenko, A. V. (2018). Evaluating characteristics of turbulent flames by using IR thermography and PIV. *Infrared Physics & Technology*, 92, 240–243. <https://doi.org/10.1016/j.infrared.2018.06.006>
- Prasad, A. K. (2000). Particle image velocimetry. *Current Science-Bangalore*, 79(1), 51–60.
- Raffel, M., Kähler, C. J., Willert, C. E., Wereley, S. T., Scarano, F., & Kompenhans, J. (2018). *Particle image velocimetry: A practical guide*. Springer.
- Riccomi, M., Alberini, F., Brunazzi, E., & Vigolo, D. (2018). Ghost Particle Velocimetry as an alternative to  $\mu$ PIV for micro/milli-fluidic devices. *Chemical Engineering Research and Design*, 133, 183–194. <https://doi.org/10.1016/j.cherd.2018.03.005>
- Sayeed-Bin-Asad, S. M., Lundström, T. S., Andersson, A. G., & Hellström, J. G. I. (2016). A review of particle image velocimetry for fish migration. *World Journal of Mechanics*, 6(4), 131–149. <https://doi.org/10.4236/wjm.2016.64011>
- Sergis, A., Hårdalupas, Y., & Barrett, T. R. (2015). Isothermal velocity measurements in two HyperVapotron geometries using Particle Image Velocimetry (PIV). *Experimental Thermal and Fluid Science*, 61, 48–58. <https://doi.org/10.1016/j.expthermflusci.2014.10.003>
- Sun, W., & Huang, N. (2018). A study on velocity of aeolian sand particles over leeward slope by particle image velocimetry. *Geomorphology*, 317, 157–169. <https://doi.org/10.1016/j.geomorph.2018.05.024>
- Tala, J. S., Russeil, S., Bougeard, D., & Harion, J. L. (2013). Investigation of the flow characteristics in a multirow finned-tube heat exchanger model by means of PIV measurements. *Experimental Thermal and Fluid Science*, 50, 45–53. <https://doi.org/10.1016/j.expthermflusci.2013.05.003>
- Tang, C., Li, E., & Li, H. (2018). Particle image velocimetry based on wavelength division multiplexing. *Optics & Laser Technology*, 98, 318–325. <https://doi.org/10.1016/j.optlastec.2017.08.013>
- Todde, V., Spazzini, P. G., & Sandberg, M. (2009). Experimental analysis of low-Reynolds number free jets. *Experiments in Fluids*, 47(2), 279–294. <https://doi.org/10.1007/s00348-009-0655-0>

- Tunçer, O., Kahraman, S., & Kaynaroğlu, B. (2016). Girdap vanesinden geçen akışın piv yöntemi ile incelenmesi. *Gazi Üniversitesi Mühendislik Mimarlık Fakültesi Dergisi*, 31(4). <https://doi.org/10.17341/gazimmfd.278439>
- Wang, C., Xu, Y., Wu, Y., & An, Z. (2018). PIV investigation of the flow features of double and single 45 up-pumping pitched blade turbines in a square tank. *The Canadian Journal of Chemical Engineering*, 96(3), 788–799. <https://doi.org/10.1002/cjce.22952>
- Wu, Q., Zhu, C. A., Liu, L., Liu, J., & Luo, Z. (2019). Two-dimensional flow visualization and velocity measurement in natural convection near indoor heated surfaces using a thermal image velocimetry method. *Applied Thermal Engineering*, 146, 556–568. <https://doi.org/10.1016/j.applthermaleng.2018.10.023>
- Xu, Z. F., Khoo, B. C., & Carpenter, K. (2006). Mass transfer across the turbulent gas–water interface. *AICHE Journal*, 52(10), 3363–3374. <https://doi.org/10.1002/aic.10972>
- Yayla, S., Canpolat, Ç., Şahin, B., & Akilli, H. (2010). Elmas kanat modelinde oluşan girdap çökmesine sapma açısının etkisi. *Isı Bilimi ve Tekniği Dergisi*, 30(1), 79–89.
- Yilmaz, N., & Nelson, R. (2015a). Cavity dynamics of smooth sphere and golf ball at low Froude numbers, part 2: PIV analysis. *Journal of Visualization*, 18(4), 679–686. <https://doi.org/10.1007/s12650-014-0262-x>
- Yilmaz, N., & Nelson, R. (2015b). Cavity dynamics of smooth sphere and golf ball at low Froude numbers, part 1: High-speed imaging and quantitative measurements. *Journal of Visualization*, 18(2), 335–342. <https://doi.org/10.1007/s12650-014-0234-1>
- Yilmaz, N., Lucero, R. E., Donaldson, A. B., & Gill, W. (2009a). Flow characterization of diffusion flame oscillations using particle image velocimetry. *Experiments in Fluids*, 46(4), 737–746. <https://doi.org/10.1007/s00348-008-0605-2>
- Yilmaz, N., Donaldson, A. B., Gill, W., & Lucero, R. E. (2009b). Imaging of flame behavior in flickering methane/air diffusion flames. *Journal of Visualization*, 12(1), 47–55. <https://doi.org/10.1007/BF03181942>

# Software Assessment for Particle Image Velocimetry for Aviation Industry



Onur Yasar, Selcuk Ekici, Enver Yalcin, and T. Hikmet Karakoc

## 1 Introduction

Computers are one of the technologies that take place in every aspect of our lives. Thanks to computers, many works can be carried out in a very short time and in series. With the production and development of computers, great progress was seen in the software industry. Software developers produced many software and programs for different purposes. The mentioned progresses were observed in flow measurement techniques, especially in particle image velocimetry (PIV), as in every field (Yilmaz et al., 2009a; Yilmaz & Nelson, 2015a, b; Raffel et al., 2018).

Particle image velocimetry measurements require software for various purposes like image acquisition. Namely, software packages or software programs are inevitable in particle image velocimetry experiments (Yilmaz et al., 2009a, b).

Software programs of particle image velocimetry can be regarded as TSI Insight and Dynamic Studio. TSI Insight and Dynamic Studio are useful for storing and processing images (Yamamoto et al., 2006; Hoque et al., 2014). ANSYS FLUENT and ANSYS CFX are accepted as numerical simulation software packages (Deshpande et al., 2009). In order to carry out simulation via ANSYS FLUENT or ANSYS CFX, finite element method is significant (Jeong & Seong, 2014). AutoCAD can be a good choice for drawing (Akar & Küçük, 2014). SolidWorks

---

O. Yasar (✉) · E. Yalcin

Department of Mechanical Engineering, Balıkesir University, Balıkesir, Türkiye  
e-mail: [onur.yasar@balikesir.edu.tr](mailto:onur.yasar@balikesir.edu.tr); [eyalcin@balikesir.edu.tr](mailto:eyalcin@balikesir.edu.tr)

S. Ekici

Department of Aviation, Iğdır University, Iğdır, Türkiye

T. H. Karakoc

Faculty of Aeronautics and Astronautics, Eskişehir Technical University, Eskişehir, Türkiye

Information Technology Research and Application Centre, Istanbul Ticaret University, Istanbul, Türkiye

is also good for three-dimensional modeling (Ismail et al., 2017). Apart from drawing or modeling software programs, MATLAB is another significant software. MATLAB works via several codes. MATLAB can be used for velocity field or pre-processing (Keller et al., 2014; Cortada-Garcia et al., 2018). C language is also software for coding (Ettema et al., 1997). DaVis and LabView are considered as software programs that are used in particle image velocimetry studies (Sergis et al., 2015; Keramaris, 2016).

## 2 Software Programs in PIV Experiments

Software programs that are used in particle image velocimetry applications change from study to study. The most common software packages are Dynamic Studio, TSI Insight, ANSYS, SolidWorks, and AutoCAD. Also, CLEANVEC, MATLAB, PIVlab, DaVis, C software, and LabView can be added in software group. In addition to the mentioned software programs, the number of software packages can be increased. Consequently, usage of software programs changes for purposes (Rosengarten et al., 1999; Forliti et al., 2000; Sharp & Adrian, 2001; Cho et al., 2002; Khan et al., 2004; Bown et al., 2005; Xu et al., 2006; Triep et al., 2006; Santos et al., 2008; Nordlund & Lundström, 2010; Öner et al., 2010; Satake et al., 2011; Hoque et al., 2014; Soydan et al., 2014; Decker et al., 2014; Salem et al., 2014; Ismail et al., 2017; Cortada-Garcia et al., 2018).

## 3 Results and Discussion

Software programs chosen for particle image velocimetry applications were given in Table 1:

Figure 1 indicates that Dynamic Studio is one of the most chosen software in particle image velocimetry applications. Like Dynamic Studio software, TSI Insight is the main software of particle image velocimetry (Forliti et al., 2000; Yamamoto et al., 2006). The percentages of Dynamic Studio and TSI Insight are 20% and 15%, respectively (Forliti et al., 2000; Yamamoto et al., 2006; Zhang et al., 2018).

ANSYS is generally used for simulation (Deshpande et al., 2009). Similar to ANSYS, PHOENICS software is used for simulation (Fei et al., 2003). However, usage of PHOENICS is too limited in particle image velocimetry studies (Fei et al., 2003). The percentages of ANSYS and PHOENICS are 20% and 5%, respectively (Fei et al., 2003; Deshpande et al., 2009).

AutoCAD is preferred for drawing, and CLEANVEC is utilized for post-processing step. The percentages of AutoCAD and CLEANVEC are the same (Sharp & Adrian, 2001; Akar & Küçük, 2014).



**Table 1** Software programs and references

References	Software mentioned directly
Meinhart et al. (1999)	Not available
Forliti et al. (2000)	TSI's Insight software (ver. 1.22)
Sharp and Adrian (2001)	CLEANVEC and TSI Insight 2.0
Cho et al. (2002)	Commercial software FLUENT
Fei et al. (2003)	PHOENICS-VR (version 3.3)
Yamamoto et al. (2006)	TSI Insight
Yoon et al. (2006)	Not available
Dijkhuizen et al. (2007)	Not available
Deshpande et al. (2009)	FLUENT 6.2
Pascual et al. (2009)	Not available
Körbahti (2010)	Dynamic Studio PIV
Yayla et al. (2010)	Not available
Atibeni et al. (2013)	Not available
Soydan et al. (2014)	ANSYS FLUENT
Akar and Küçük (2014)	AutoCAD
Hoque et al. (2014)	Dantec Dynamic Studio software
Öner (2016)	ANSYS® 11-Flotran
Liu et al. (2018)	Dynamic Studio
You et al. (2018)	FlowMaster
Zhang et al. (2018)	Dynamic Studio software

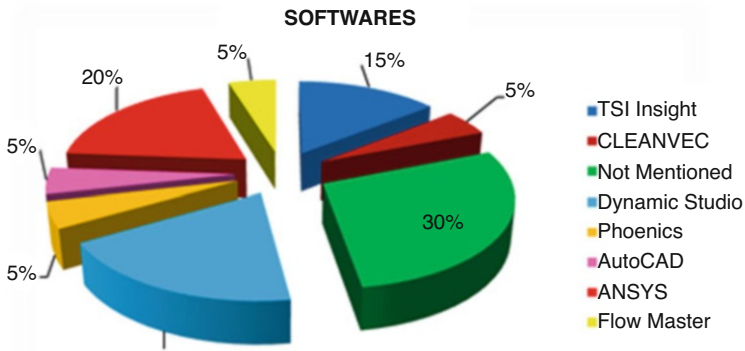


**Fig. 1** Software programs examined in studies

## 4 Conclusion

Particle image velocimetry was evaluated in terms of different aspect like software. Software programs can be used from drawing to post-processing. Concluding remarks were given below:

Dynamic Studio and TSI Insight come first for main software programs. The situation can be explained by the fact that the main PIV brands are Dantec Dynamics and TSI Insight.

ANSYS is prominent simulation software. PHOENICS isn't preferable software like ANSYS.

Usage of AutoCAD and FlowMaster is too limited in particle image velocimetry applications.

CLEANVEC can be a good choice for post-processing.

Investigated software programs can be feasible for air taxis. In studies of air taxis, utilization of the mentioned software programs and proper programs can be possible.

## References

- Akar, M. A., & Küçük, M. (2014). Silindir arkasındaki daimi olmayan akış yapısının pasif yöntemle kontrolü. *Pamukkale Üniversitesi Mühendislik Bilimleri Dergisi*, 20(4), 123–128. <https://doi.org/10.5505/pajes.2014.51523>
- Atibeni, R., Gao, Z., & Bao, Y. (2013). Effect of baffles on fluid flow field in stirred tank with floating particles by using PIV. *The Canadian Journal of Chemical Engineering*, 91(3), 570–578. <https://doi.org/10.1002/cjce.21652>
- Bown, M. R., MacInnes, J. M., & Allen, R. W. K. (2005). Micro-PIV simulation and measurement in complex microchannel geometries. *Measurement Science and Technology*, 16(3), 619. <https://doi.org/10.1088/0957-0233/16/3/002>
- Cho, S. H., Lee, I. S., Choi, J. H., & Nam, Y. S. (2002). PIV Measurement and numerical analysis of a new refrigeration compartment of a refrigerator. *Annals of the New York Academy of Sciences*, 972(1), 260–264. <https://doi.org/10.1111/j.1749-6632.2002.tb04582.x>
- Cortada-Garcia, M., Weheliye, W. H., Dore, V., Mazzei, L., & Angeli, P. (2018). Computational fluid dynamic studies of mixers for highly viscous shear thinning fluids and PIV validation. *Chemical Engineering Science*, 179, 133–149. <https://doi.org/10.1016/j.ces.2018.01.010>
- Decker, R. K., Betto, M. C., Noriler, D., & Meier, H. F. (2014). Comparison between numerical results and PIV experimental data for gas–solid flow in ducts. *The Canadian Journal of Chemical Engineering*, 92(6), 1113–1120. <https://doi.org/10.1002/cjce.21952>
- Deshpande, S. S., Sathe, M. J., & Joshi, J. B. (2009). Evaluation of local turbulent energy dissipation rate using PIV in jet loop reactor. *Industrial & Engineering Chemistry Research*, 48(10), 5046–5057. <https://doi.org/10.1021/ie8007924>
- Dijkhuizen, W. V., Bokkers, G. A., Deen, N. G., Annaland, M. V. S., & Kuipers, J. A. M. (2007). Extension of PIV for measuring granular temperature field in dense fluidized beds. *AICHE Journal*, 53(1), 108–118. <https://doi.org/10.1002/aic.11044>
- Ettema, R., Fujita, I., Muste, M., & Kruger, A. (1997). Particle-image velocimetry for whole-field measurement of ice velocities. *Cold Regions Science and Technology*, 26(2), 97–112. [https://doi.org/10.1016/S0165-232X\(97\)00011-6](https://doi.org/10.1016/S0165-232X(97)00011-6)
- Fei, W. Y., Wang, Y. D., Song, X. Y., Yin, Y. D., & Sun, L. Y. (2003). Intensification of random packing via CFD simulation, PIV measurement and traditional experiments. *Journal of Chemical Technology & Biotechnology: International Research in Process, Environmental & Clean Technology*, 78(2–3), 142–145. <https://doi.org/10.1002/jctb.715>
- Forliti, D. J., Strykowski, P. J., & Debatin, K. (2000). Bias and precision errors of digital particle image velocimetry. *Experiments in Fluids*, 28(5), 436–447. <https://doi.org/10.1007/s003480050403>

- Hoque, M. M., Sathe, M. J., Joshi, J. B., & Evans, G. M. (2014). Analysis of turbulence energy spectrum by using particle image velocimetry. *Procedia Engineering*, 90, 320–326. <https://doi.org/10.1016/j.proeng.2014.11.856>
- Ismail, M., Kabinejadian, F., Nguyen, Y. N., Wui, E. T. L., Kim, S., & Leo, H. L. (2017). Hemodynamic assessment of extra-cardiac tricuspid valves using particle image velocimetry. *Medical Engineering & Physics*, 50, 1–11. <https://doi.org/10.1016/j.medengphy.2017.08.003>
- Jeong, W., & Seong, J. (2014). Comparison of effects on technical variances of computational fluid dynamics (CFD) software based on finite element and finite volume methods. *International Journal of Mechanical Sciences*, 78, 19–26. <https://doi.org/10.1016/j.ijmecsci.2013.10.017>
- Keller, J., Möller, G., & Boes, R. M. (2014). PIV measurements of air-core intake vortices. *Flow Measurement and Instrumentation*, 40, 74–81. <https://doi.org/10.1016/j.flowmeasinst.2014.08.004>
- Keramaris, E. (2016). Similarities and differences between hot-film anemometry and particle image velocimetry in open channels. *Procedia Engineering*, 162, 388–395. <https://doi.org/10.1016/j.proeng.2016.11.079>
- Khan, F. R., Rielly, C. D., & Hargrave, G. K. (2004). A multi-block approach to obtain angle-resolved PIV measurements of the mean flow and turbulence fields in a stirred vessel. *Chemical Engineering & Technology: Industrial Chemistry-Plant Equipment-Process Engineering-Biotechnology*, 27(3), 264–269. <https://doi.org/10.1002/ceat.200401998>
- Körbahtı, B. (2010). Sesaltı akış etkisindeki delta kanadın deneysel olarak incelenmesi. *İÜ Mühendislik Bilimleri Dergisi*, 1(1), 33–44.
- Liu, K., Deng, J., & Ye, F. (2018). Visualization of flow structures in a rotary type energy recovery device by PIV experiments. *Desalination*, 433, 33–40. <https://doi.org/10.1016/j.desal.2018.01.022>
- Meinhart, C. D., Wereley, S. T., & Santiago, J. G. (1999). PIV measurements of a microchannel flow. *Experiments in Fluids*, 27(5), 414–419. <https://doi.org/10.1007/s003480050366>
- Nordlund, M., & Lundström, T. S. (2010). An investigation of particle deposition mechanisms during impregnation of dual-scale fabrics with micro particle image velocimetry. *Polymer Composites*, 31(7), 1232–1240. <https://doi.org/10.1002/pc.20910>
- Öner, A. A. (2016). Geçirimsiz Bir Taban Yakınındaki Başlıklı Bir Boru Hattı Etrafındaki Akımın Deneysel ve Sayısal Olarak İncelenmesi. *Electronic Journal of Construction Technologies/Yapı Teknolojileri Elektronik Dergisi*, 12(1).
- Öner, A. A., Çobaner, M., Kirkgöz, M. S., & Aköz, M. S. (2010). Yatay bir dairesel silindirik etrafındaki akımda maksimum hızın yapay sinir ağları ile tahmini. *Erciyes Üniversitesi Fen Bilimleri Enstitüsü Fen Bilimleri Dergisi*, 26(1), 63–70.
- Pascual, M. R., Ravelet, F., Delfos, R., Derksen, J. J., & Witkamp, G. J. (2009). Large eddy simulations and stereoscopic particle image velocimetry measurements in a scraped heat exchanger crystallizer geometry. *Chemical Engineering Science*, 64(9), 2127–2135. <https://doi.org/10.1016/j.ces.2009.01.034>
- Raffel, M., Kähler, C. J., Willert, C. E., Wereley, S. T., Scarano, F., & Kompenhans, J. (2018). *Particle image velocimetry: A practical guide*. Springer.
- Rosengarten, G., Behnia, M., & Morrison, G. (1999). Some aspects concerning modelling the flow and heat transfer in horizontal mantle heat exchangers in solar water heaters. *International Journal of Energy Research*, 23(11), 1007–1016. [https://doi.org/10.1002/\(SICI\)1099-114X\(199909\)23:11<1007::AID-ER537>3.0.CO;2-1](https://doi.org/10.1002/(SICI)1099-114X(199909)23:11<1007::AID-ER537>3.0.CO;2-1)
- Salem, H. J., Martinez, M. D., Gooding, R. W., & Olson, J. A. (2014). Experimental study of a time-varying turbulent cross-flow near a two-dimensional rough wall with narrow apertures. *The Canadian Journal of Chemical Engineering*, 92(11), 1965–1974. <https://doi.org/10.1002/cjce.22058>
- Santos, R. J., Erkoç, E., Dias, M. M., Teixeira, A. M., & Lopes, J. C. B. (2008). Hydrodynamics of the mixing chamber in RIM: PIV flow-field characterization. *AIChE Journal*, 54(5), 1153–1163. <https://doi.org/10.1002/aic.11472>

- Satake, S. I., Sorimachi, G., Masuda, N., & Ito, T. (2011). Special-purpose computer for particle image velocimetry. *Computer Physics Communications*, 182(5), 1178–1182. <https://doi.org/10.1016/j.cpc.2011.01.022>
- Sergis, A., Hardalupas, Y., & Barrett, T. R. (2015). Isothermal velocity measurements in two HyperVapotron geometries using Particle Image Velocimetry (PIV). *Experimental Thermal and Fluid Science*, 61, 48–58. <https://doi.org/10.1016/j.expthermflusci.2014.10.003>
- Sharp, K. V., & Adrian, R. J. (2001). PIV study of small-scale flow structure around a Rushton turbine. *AIChE Journal*, 47(4), 766–778. <https://doi.org/10.1002/aic.690470403>
- Soydan, A. G. N. G., Böl, Ç. İ. M., Aköz, M. S., Şimşek, A. G. O., & Kirkgöz, M. S. (2014). *Tabana oturan yatay bir boru etrafındaki türbülanslı akimin deneysel ve sayısal analizi*.
- Triep, M., Brücker, C., Schröder, W., & Siess, T. (2006). Computational fluid dynamics and digital particle image velocimetry study of the flow through an optimized micro-axial blood pump. *Artificial Organs*, 30(5), 384–391. <https://doi.org/10.1111/j.1525-1594.2006.00230.x>
- Xu, Z. F., Khoo, B. C., & Carpenter, K. (2006). Mass transfer across the turbulent gas–water interface. *AIChE Journal*, 52(10), 3363–3374. <https://doi.org/10.1002/aic.10972>
- Yamamoto, K., Inoue, S., Yamashita, H., Shimokuri, D., Ishizuka, S., & Onuma, Y. (2006). PIV measurement and turbulence scale in turbulent combustion. *Heat Transfer—Asian Research: Co-sponsored by the Society of Chemical Engineers of Japan and the Heat Transfer Division of ASME*, 35(7), 501–512. <https://doi.org/10.1002/htj.20129>
- Yayla, S., Canpolat, Ç., Şahin, B., & AKILLI, H. (2010). Elmas kanat modelinde oluşan girdap çökmesine sapma açısının etkisi. *Isı Bilimi ve Tekniği Dergisi*, 30(1), 79–89.
- Yilmaz, N., & Nelson, R. (2015a). Cavity dynamics of smooth sphere and golf ball at low Froude numbers, part 1: high-speed imaging and quantitative measurements. *Journal of Visualization*, 18(2), 335–342. <https://doi.org/10.1007/s12650-014-0234-1>
- Yilmaz, N., & Nelson, R. (2015b). Cavity dynamics of smooth sphere and golf ball at low Froude numbers, part 2: PIV analysis. *Journal of Visualization*, 18(4), 679–686. <https://doi.org/10.1007/s12650-014-0262-x>
- Yilmaz, N., Lucero, R. E., Donaldson, A. B., & Gill, W. (2009a). Flow characterization of diffusion flame oscillations using particle image velocimetry. *Experiments in Fluids*, 46(4), 737–746. <https://doi.org/10.1007/s00348-008-0605-2>
- Yilmaz, N., Donaldson, A. B., Gill, W., & Lucero, R. E. (2009b). Imaging of flame behavior in flickering methane/air diffusion flames. *Journal of Visualization*, 12(1), 47–55. <https://doi.org/10.1007/BF03181942>
- Yoon, S. Y., Ross, J. W., Mench, M. M., & Sharp, K. V. (2006). Gas-phase particle image velocimetry (PIV) for application to the design of fuel cell reactant flow channels. *Journal of Power Sources*, 160(2), 1017–1025. <https://doi.org/10.1016/j.jpowsour.2006.02.043>
- You, R., Li, H., Wu, H., & Tao, Z. (2018). PIV flow measurements for a rotating square smooth channel heated by basically uniform heat flux. *International Journal of Heat and Mass Transfer*, 119, 236–246. <https://doi.org/10.1016/j.ijheatmasstransfer.2017.11.073>
- Zhang, N., Gao, B., Li, Z., Ni, D., & Jiang, Q. (2018). Unsteady flow structure and its evolution in a low specific speed centrifugal pump measured by PIV. *Experimental Thermal and Fluid Science*, 97, 133–144. <https://doi.org/10.1016/j.expthermflusci.2018.04.013>

# Dye Visualization of Flow Structure of a Circular Cylinder Oscillating at $Re = 1000$



Cemre Polat, Dogan Burak Saydam, Mustafa Soyler, and Coskun Ozalp

## Nomenclature

$D$	Diameter
$F_R$	Rotational ratio
$G$	Gap space
PLC	Programmable logic controller
$U_0$	Free stream velocity
$\theta$	Rotation angle

## 1 Introduction

The flow structure in the wake region of a cylinder that makes a sinusoidal oscillation movement in the flow direction has an important place both in theory and in practice. The oscillation movement relative to the flow direction can be generated not only by the motion on the cylinder itself but also by an unsteady periodic disturbance superimposed on the uniform free stream and interaction on a stationary cylinder (Hu et al., 2019). Cylindrical structures are encountered in many different applications (power transmission, lines, deep water pipelines, suspension bridges, heat exchanger, towers, buildings, etc.) in the literature (Ozalp et al., 2021a, b).

---

C. Polat (✉) · D. B. Saydam · M. Soyler · C. Ozalp  
Osmaniye Korkut Ata University, Duzici Vocational High School, Motor Vehicles  
and Transport Technology, Osmaniye, Türkiye  
e-mail: [cemrepolat@osmaniye.edu.tr](mailto:cemrepolat@osmaniye.edu.tr); [doganburaksaydam@osmaniye.edu.tr](mailto:doganburaksaydam@osmaniye.edu.tr);  
[mustafasoyler@osmaniye.edu.tr](mailto:mustafasoyler@osmaniye.edu.tr); [coskunozalp@osmaniye.edu.tr](mailto:coskunozalp@osmaniye.edu.tr)

Different methods are used to examine and analyze the flow structure around objects. There are many different studies on the visualization of the flow structure in the literature. Shao et al. (2007) studied the effect of circular and square cylinder on the flow structure of a control element placed parallel to the cylinder to suppress vortex shedding. The authors performed the flow visualization using hot-wire measurement in a wind tunnel at a low Reynolds ( $Re$ ) number. As a result of the study, the authors showed that vortex shedding from both sides of the cylinder can be effectively suppressed. Sohankar et al. (2015) used a low-velocity vertical smoke tunnel to visualize the flow structure of a square cylinder positioned at different angles in the flow field. The authors examined the flow structure of a single cylinder for various angles of incidence and different parameters such as stagnation and separation points, separation angle, attachment point, and transient of the shear layer. As a result of the study, the authors showed that a maximum occurs at approximately  $\alpha = 15$  (critical angle) in the variation of the transient and turbulent lengths of the shear layer, the frequency, and the Strouhal number incidence angle. In addition, the authors found that the turbulence length of the shear layer from the upstream cylinder increased from  $G = 1$  (gap space) to  $G = 2$  and then decreased at  $G = 5.6$  relative to that for a single cylinder.

As seen in the literature review, there are different studies on the visualization of the flow structure. One of the flow visualization methods is dye experiments with dye injected into the flow field and glowing under the laser beam. In this study, the visualization of the flow structure of a cylinder that is positioned on a table and oscillates with a servo motion system has been carried out with dye experiments.

## 2 Method

The experiments were carried out in the open surface water channel in the Osmaniye Korkut Ata University Advanced Fluid Mechanics Laboratory. The field of view in the water channel is made of plexiglass material. Two speed-controlled pumps, two collecting pools, one honeycomb pattern, and mesh equipment are used to regulate the flow (Özalp et al., 2020). To obtain a laser beam, a horizontal laser beam was obtained using a cylindrical lens in front of the point laser, and the flow was visualized. In the flow visualization method, the dye/water mixture was obtained by mixing Rhodamine 6G in powder form with water, which reflects under laser light used for detailed observation of the flow structure. During the experiments, dye was injected into the flow with a thin needle from a distance without affecting the flow from the front of the cylinder. A laser beam was sent to the channel from a certain height, and images were obtained by the camera located under the channel.

A cylinder with a diameter  $D = 25$  mm was placed on the table in the midplane of the water channel at the Reynolds number  $Re = U_0 D / \nu$ , which was 1000, where  $\nu$  is the kinematic viscosity of the fluid and  $U_0$  free stream velocity. The resulting image

was recorded at a resolution of 1280 \* 720 at 100 frames per second by a digital mirrorless camera with 15–45 mm lens. The time elapsed between two frames is 0.03 seconds. A servo connected to a computer-controlled PLC system is used to make the oscillation movement of the cylinder. In this servo system, the oscillation angle and speed can be determined via computer software. In this study, 90° ( $\pi/2$ ) oscillations of the cylinder were studied.

### 3 Results and Discussion

The images obtained from the experiments carried out in a water channel at different rotational ratios at a constant oscillation angle are shown in Figs. 1 and 2. It is observed that the vortices that break off from the cylinder periphery with the effect of oscillation follow each other and become larger as they move away from the cylinder (Fig. 1a).

In the study, it is determined that the irregular flow structure around the body was controlled with the increase of the rotational ratio, in which the area of the cylinder resulted in narrowing in the flow direction (Figs. 1 and 2). It was determined that the vortices shed from the cylinder became smaller for the cases  $F_R = 2.5$  (Fig. 2a) and  $F_R = 3.3$  (Fig. 2b).

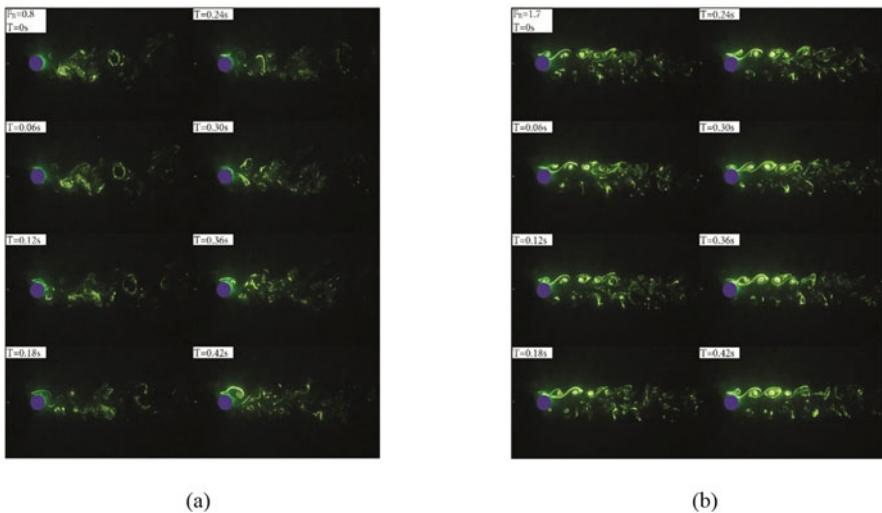


**Fig. 1** Flow structure formed behind the cylinder at (a)  $F_R = 0.8$  and (b)  $F_R = 1.7$  with  $\theta = 90^\circ$  at  $Re = 1000$

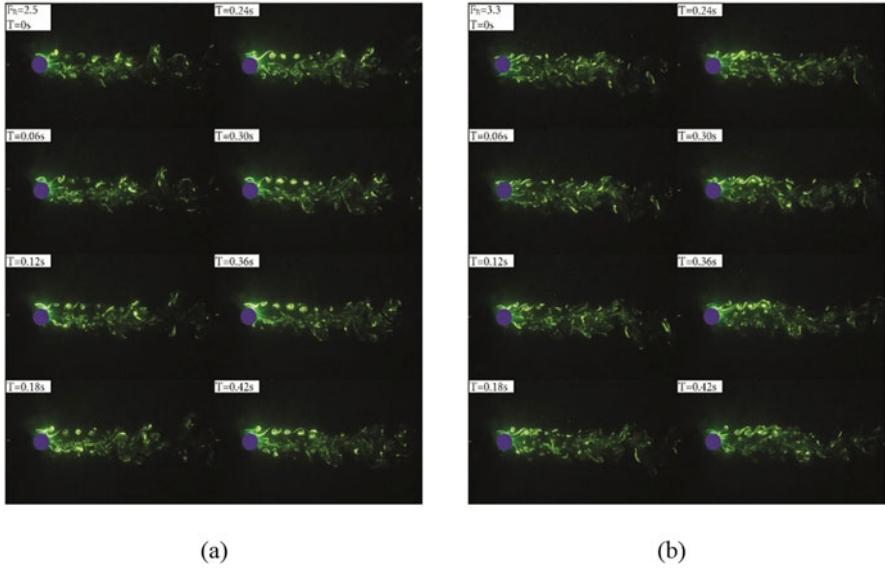


**Fig. 2** Flow structure formed behind the cylinder at (a)  $F_R = 2.5$  and (b)  $F_R = 3.3$  with  $\theta = 90^\circ$  at  $Re = 1000$

## 4 Conclusion

In this study, flow around a circular cylinder ( $D = 25$  mm) has been visualized at  $Re = 1000$  for different rotational ratios. As a result of dye experiments at different rotational ratios and constant rotation angle, it has been observed that the vortices detached from the cylinder periphery with the effect of oscillation follow each other and become larger as they move away from the cylinder. In the study, it was determined that with the increase of the rotational ratio, the vortex shedding in the cylinder wake region decreased and the irregular flow structure around the body was controlled. It has been determined that the vortices shed from the cylinder get smaller for the cases  $F_R = 2.5$  and  $F_R = 3.3$ .

**Acknowledgment** The authors would like to acknowledge the funding of the Scientific and Technological Research Council of Turkey (TUBITAK) under Contract No: 218M357. The authors acknowledge the financial support of Office of Scientific Research Projects of Osmaniye Korkut Ata University for funding under Contract No: OKÜBAP-2019-PT3-010.



## References

- Hu, Z., Liu, J., Gan, L., & Xu, S. (2019). Wake modes behind a streamwisely oscillating cylinder at constant and ramping frequencies. *Journal of Visualization*, 223(22), 505–527.
- Özalp, C., Polat, C., Saydam, D. B., & Söyler, M. (2020). Dye injection flow visualization around a rotating circular cylinder. *European Mechanical Science*, 4, 185–189.
- Ozalp, C., Saydam, D. B., Polat, C., Soyler, M., & Hürdoğan, E. (2021a). Heat transfer and flow structure around a heated cylinder by upstream installation of a grooved cylinder. *Experimental Thermal and Fluid Science*, 128, 110448.
- Ozalp, C., Soyler, M., Polat, C., Saydam, D. B., & Yaniktepe, B. (2021b). An experimental investigation of a rotationally oscillating cylinder. *Journal of Wind Engineering and Industrial Aerodynamics*, 214, 104679.
- Shao, C. P., Wang, J. M., & Wei, Q. D. (2007). Visualization study on suppression of vortex shedding from a cylinder. *Journal of Visualization*, 101(10), 57–64.
- Sohankar, A., Mohagheghian, S., Dehghan, A. A., & Dehghan Manshadi, M. (2015). A smoke visualization study of the flow over a square cylinder at incidence and tandem square cylinders. *Journal of Visualization*, 184(18), 687–703.

# Aerodynamic Performance Predictions of Mars Helicopter Co-axial Rotor in Hover by Using Unsteady CFD Simulations



Onur Küçüköğlü, Sergen Sakaoğlu, and Nilay Sezer Uzol

## 1 Introduction

Co-axial rotors have benefits over conventional tail rotor configurations as the available power is not consumed by the tail rotor to balance out the main rotor torque. However, the rotor wake and flow physics are more complicated, being unsteady due to rotor-rotor interactions of co-axial rotors. Investigating the complex flow and performance characteristics of co-axial rotors in Martian atmosphere contributes for better designs for future rotorcrafts. NASA's Mars helicopter Ingenuity with its first successful flight on 19 April 2021 demonstrates the potential of rotorcrafts in discovery of other planets. NASA's Ingenuity rotorcraft was designed to operate at Mars conditions where the atmosphere is a lot thinner than the Earth's atmosphere, causing a laminar flow over the rotors (Koning et al., 2018). Though the flow stays laminar, it is compressible having tip speeds with Mach number of 0.7. CFD emerges as a more accurate tool for simulating co-axial rotor performance compared to airfoil data-embedded models. There are few recent studies on CFD of rotorcraft applications for Mars. Previously, relative advantages of the co-axial configuration in hover, forward flight, and maneuver conditions were investigated by Kim and Brown (2010). Barbely et al. (2016) examined the performance of a co-axial rotor system numerically, both for forward flight and hover conditions, to understand the interaction between the two rotors. They showed that the thrust ratio of lower rotor to upper rotor increases as the distance between the two rotors increases. Koning et al. (2018) observed that the inclusion of transition modeling

---

O. Küçüköğlü (✉) · S. Sakaoğlu  
Middle East Technical University Department of Aerospace Engineering, Ankara, Türkiye  
e-mail: [kucukoglu.onur@metu.edu.tr](mailto:kucukoglu.onur@metu.edu.tr); [sergen.sakaoglu@metu.edu.tr](mailto:sergen.sakaoglu@metu.edu.tr)

N. S. Uzol  
Turkish Aerospace Industries Inc., Ankara, Turkey  
e-mail: [nuzol@metu.edu.tr](mailto:nuzol@metu.edu.tr)

is not necessary as the Reynolds number observed on the rotor is subcritical, which ensures laminar flow over the airfoil. Koning et al. (2019) found out that the rotor model with a transition model and with a fully turbulent solution has a similar thrust coefficient range. In this study, both steady and unsteady 3-D CFD simulations for the Mars helicopter's co-axial rotors are performed in hover by using an open-source CFD flow solver, SU2, in Martian atmospheric conditions.

## 2 Methodology

Co-axial rotor CFD simulations in Martian atmospheric conditions are performed in parallel for hover by using SU2 flow solver, and the rotor model and the numerical model used are described below.

The Ingenuity rotorcraft has co-axial rotors with 1.2 m diameter and with each rotor having two blades. The spacing between the upper and the lower rotor is 0.454 m. Airfoils of the Mars helicopter (MH) rotor are reproduced from the study by Koning et al. (2018). Mars helicopter's co-axial rotor model geometry as described in Table 1 is generated first by using CST method (Kulfan & Bussoletti, 2006) for the airfoil and by using OpenVSP software for the blade. The digitized airfoil curves are not smooth enough; therefore, to increase the quality of airfoil curves, the use of a curve fitting procedure is required.

Kulfan's Class and Shape Transformation (CST) function has emerged as a good option due to its flexibility. Hence, by implementation of an extrapolation procedure, the number of airfoil coordinates is increased to have enough points to represent the airfoil geometry accurately in the computational domain and grid. Figure 1 shows the CLF5605 airfoil, the normalized airfoil profiles for the Mars helicopter rotor at different blade stations, and the co-axial rotor model.

The experimental tests for the MH rotor were done at NASA JPL (Koning et al., 2019) with atmospheric conditions as can be seen in Table 2. The environment in JPL, using CO<sub>2</sub> as the gas in the tests, is very thin that  $Re_c$  is on the order of  $10^3$  on tip chord with a corresponding tip Mach number of 0.62. Dynamic viscosity and temperature, and speed of sound as a result, vary greatly between the Mars and the NASA JPL test conditions. Due to the availability of data, JPL conditions are used as boundary conditions.

**Table 1** Co-axial rotor model blade geometry (Koning et al., 2018)

Station	$r/R$	$c/R$	$t/c$	Twist	Airfoil
1	0.091	0.0506	0.973	16.32	Station 1
2	0.2	0.1407	0.22	17.62	Station 2
3	0.295	0.1968	0.098	15.92	Station 3
4	0.39	0.1968	0.06	12.07	Station 4
5	0.527	0.1627	0.05	8.43	CLF5605
6	0.762	0.1209	0.05	3.93	CLF5605
7	0.924	0.086	0.05	1.39	CLF5605
8	0.991	0.0341	0.05	0.06	CLF5605

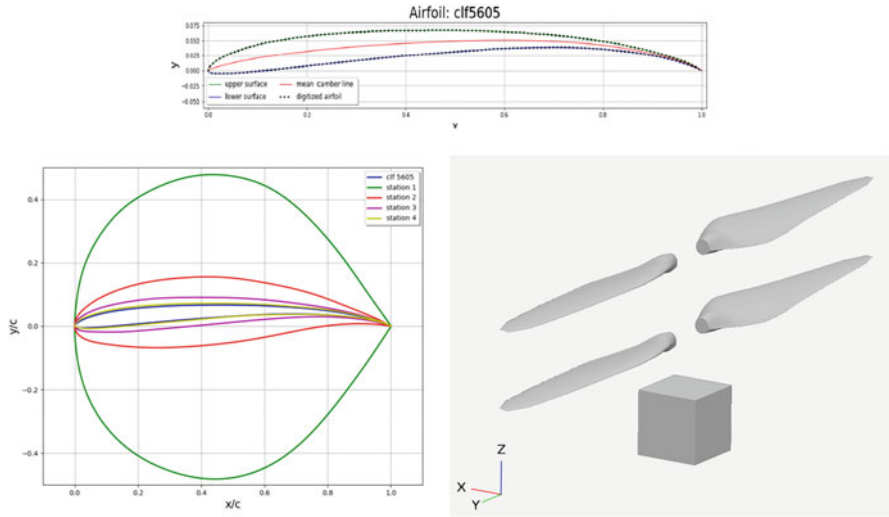


**Fig. 1** CLF5605 airfoil and the normalized airfoil profiles for the MH rotor blade and Mars helicopter co-axial rotor model

**Table 2** Atmospheric conditions for Mars

Properties	Earth SSL	JPL SS
Density	1.225	0.0185
Temperature	288.2	298.15
Gas constant	287.1	188.90
Specific heat ratio	1.4	1.289
Dynamic viscosity	$1.130 \times 10^{-5}$	$1.504 \times 10^{-5}$
Static pressure	101.3	1.04
Speed of sound	340.35	269.44

For hover flight condition, since the problem is compressible, the total pressure condition is applied to the far upstream of the inlet (Fig. 2). The total pressure of 1040 Pa is taken which is actually the static pressure in the domain, since, for the hover conditions, the free stream velocity is set to zero in order for the rotor to suck air from the inlet and there is no climb velocity for the rotor. The rotor blades are placed in two identical cylindrical inner domains as shown in Fig. 2, and the rotational speed of 2600 rpm is applied to the domains. By this way, the rotor revolutions are modeled for each time step, allowing the rotors to rotate by rotating the mesh inside the cylinders: one is rotating clockwise, and the other one is rotating counterclockwise. The boundaries near the cylindrical inner domains are modeled as the pressure outlet to let the flow go in and out of the domain without any restriction on flow direction as can be seen in Fig. 2. Likewise, pressure outlet boundary condition is also applied to the boundary on the far downstream of the rotors (Fig. 2).

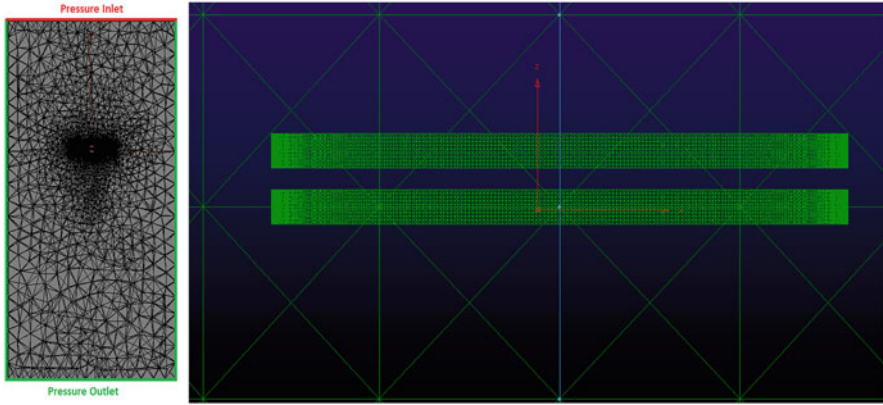


**Fig. 2** Grid boundary conditions and computational cylindrical domains for the co-axial rotors

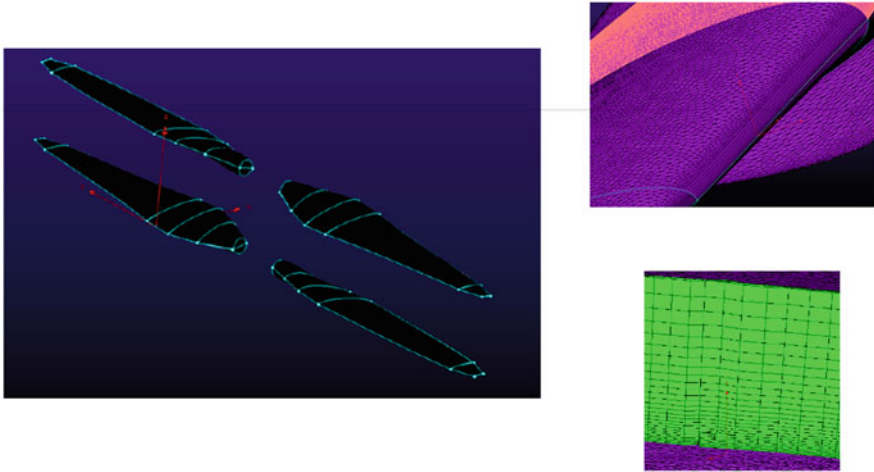


**Fig. 3** Blade surface mesh and boundary layer prism mesh

The unstructured grid with a total of 35.4 M cells, comprised of about 14.6 M tetrahedral and 20.8 M prism cells, is generated by using Pointwise. Since the flow conditions on Mars are laminar, blade surface prism layer parameters are determined based on the laminar boundary layer thickness for a flat plate. The prism layer mesh with 24 layers can be seen in Fig. 3. The numerical stability of the turbulent fluxes is ensured by generating a mesh whose first layer thickness gives  $y^+$  value of less than 1, which can be seen in Fig. 4, with a first layer thickness of 0.07 mm.

In the CFD simulations, solving RANS and URANS equations, Spalart-Allmaras one-equation turbulence model, Roe flux difference splitting scheme, and second-order discretization schemes are used. Bas-Cakmakcioglu transition model is also used. The convergence criteria of  $10e-4$  are satisfied for energy, whereas the

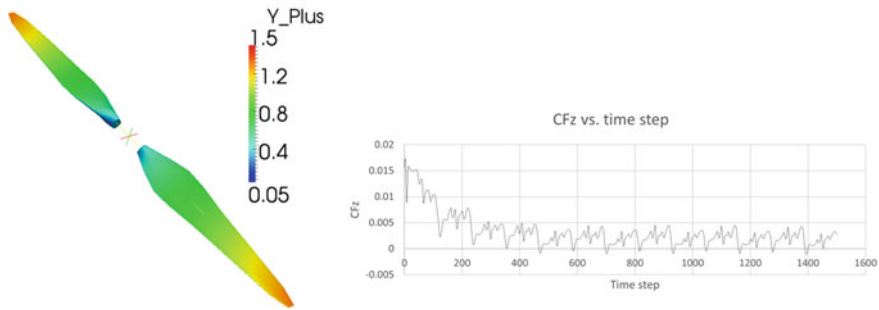


**Fig. 4** The MH rotor  $y^+$  distribution and thrust coefficient,  $C_T$  (axial force coefficient,  $C_{F_z}$ ), vs time iterations

momentum and continuity residuals fall below  $10e-5$  and even  $10e-6$ . Both moving reference frame (MRF) and sliding mesh (DM) techniques are used in SU2 for the co-axial rotor simulations.

Simulations are performed for two pitch angles of 10 and 20 degrees, and the results are compared with the experimental data from NASA JPL. The axial force coefficient,  $C_{F_z}$ , or thrust coefficient,  $C_T$ , changes with time iterations as can be seen in Fig. 4. Since the sliding mesh technique is an unsteady method, results are time averaged for seven full revolutions where the time step size,  $\Delta t$ , is 0.0001 seconds. The non-dimensional aerodynamic performance parameters are calculated by the following relations:

$$C_T = \frac{T}{\rho_\infty A_d (\Omega r)^2}, \quad C_P = \frac{P}{\rho_\infty A_d (\Omega r)^3}, \quad FM = \frac{C_T^{2/3}}{C_{P,measured}} \quad (1)$$

### 3 Results and Discussion

The steady-state and unsteady computational results are obtained for different pitch settings. Figure 5 shows the power coefficient change for different thrust coefficients, which are obtained with different pitch settings. It can be observed that the results with the transition model do not make any noticeable difference with the fully turbulent results, which are obtained from the MRF solutions. However, for the sliding mesh results, the estimates of thrust and power are higher compared to the MRF results. Figure 5 shows the figure of merit (FM) estimations for hover, and it is the ratio of ideal power required to hover to the actual power. It is calculated here from using the thrust,  $C_T$ , and power coefficients,  $C_P$ , of the analyses through using time average of  $C_{F_z}$  and  $C_{M_z}$  coefficients. The drag of rotating blades is over-estimated with RANS and U-RANS simulations, resulting in lower FM values

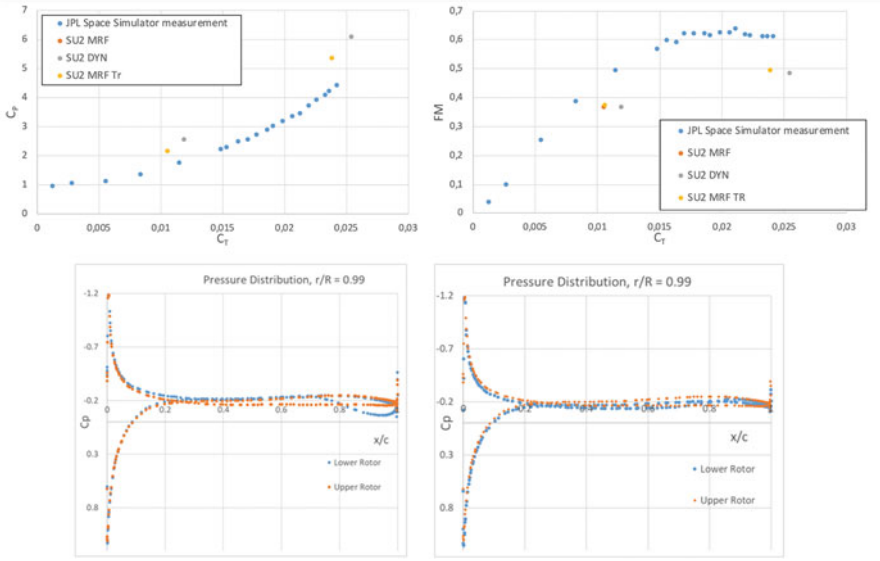


**Fig. 5** Pressure coefficient distribution at the blade tip region for upper and lower rotors and power coefficient-figure of merit vs thrust coefficient

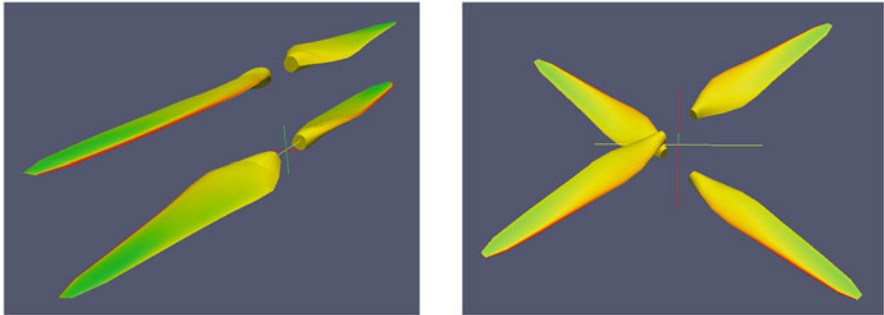


**Fig. 6** Pressure coefficient contours on rotor blades at different azimuth positions

compared to test data. This is also corresponding to the higher power consumption estimations on Fig. 5.

Upper and lower rotors' blades are aligned and positioned with 90 degrees as shown in Fig. 5. The pressure coefficient distributions near the tip of the blade are shown in Fig. 5 for both upper and lower rotors, having differences due to the flow interactions between the rotors. Figure 6 shows the pressure coefficient contours on rotor blades at different azimuth positions as the blades rotate in the unsteady simulations.

## 4 Conclusion

In this study, the steady-state and unsteady CFD simulations for the Mars helicopter's co-axial rotor model are performed by using both moving reference frame (MRF) and sliding mesh (DM) techniques. The rotor aerodynamic performance is investigated in hover condition. RANS solutions over-predict the power consumption compared to the experimental results. Over-prediction of power consumption may be due to higher calculated viscous drag. Modeling of transition in SU2 simulations does not make any noticeable difference with the fully turbulent results. In future work, different turbulence models and different flux discretization schemes will be investigated for co-axial rotor problem. Speed-up and scalability characteristics with SU2 flow solver and details of flow characteristics will be investigated.

**Acknowledgments** This study is partially supported by TUBITAK 2244 Project 118C087.

## References

- Barbely, N., Novak, L., & Komerath, N. (2016). *A study of co-axial rotor performance and flow field characteristics*. American Helicopter Society Meeting, 2016.
- Kim, H. W., & Brown, R. E. (2010). A comparison of coaxial and conventional rotor performance. *Journal of the American Helicopter Society*, 55(01), 2010.
- Koning, W. J., Johnson, W., & Allan, B. (2018). *Generation of mars helicopter rotor model for comprehensive analyses*, NASA Paper 2289, 2018.
- Koning, W. J., Johnson, W., & Grip, H. F. (2019). Improved mars helicopter aerodynamic rotor model for comprehensive analyses. *AIAA Journal*, 57(9), 3969–3979.
- Kulfan, B., & Bussoletti, J. (2006). *Fundamental parametric geometry representations for aircraft component shapes*. 11th AIAA/ISSMO multidisciplinary analysis and optimization conference, 2006.



# Numerical Validation Study of a Helicopter Rotor in Hover by Using SU2 CFD Solver



Yunus Emre Sunay and Nilay Sezer Uzol

## Nomenclature

CFD	Computational fluid dynamics
eVTOL	Electrical vertical take-off and landing
RF	Rotating frame
RM	Rigid motion

## 1 Introduction

Electrical vertical take-off and landing (eVTOL) air vehicles will be the most popular air mobility choice in the near future. Nearly 500 different design alternatives (World eVTOL Aircraft Directory, 2021) from different companies show the importance of eVTOL air mobility concept. Such concepts use many smaller rotors compared to the much larger rotors of helicopters for both vertical taking-off and forward flight capabilities. One of the challenging problems in eVTOL design is to obtain accurate solutions both for aerodynamic performance of rotors/propellers and for flow field around rotating blades. Also, there are complicated flow interactions of rotors/propellers with each other and with aircraft body for many different configurations of eVTOLs.

In this study, an open-source CFD flow solver, SU2 (SU2 Foundation, 2021), is used as a validation study for a helicopter rotor model in hover to compare two numerical approaches for rotary wings. Rotor CFD simulations in hover are

---

Y. E. Sunay (✉) · N. S. Uzol

Department of Aerospace Engineering, Middle East Technical University (METU), Ankara, Türkiye

e-mail: [emre.sunay@metu.edu.tr](mailto:emre.sunay@metu.edu.tr); [nuzol@metu.edu.tr](mailto:nuzol@metu.edu.tr)

performed by using two approaches: RM with moving grid approach and RF with moving frame approach. Inviscid simulations are performed in parallel for the validations. The results are compared with the experiments for two collective pitch angles and different rotational speed.

## 2 Methodology

A very well-known experiment by Caradonna and Tung (1981) for a helicopter rotor model is used as a test case for validation of unsteady CFD simulations by using SU2 flow solver. Rotor CFD simulations in hover are performed in parallel by using two approaches: rigid motion (RM) with moving grid and rotating frame (RF) with moving frame.

### 2.1 Test Rotor Model

Caradonna and Tung's rotor model has two rectangular blades with no twist, no taper, and an aspect ratio of 6 (1.143 m span) and with an aerofoil section of NACA 0012. A series of experimental tests are conducted for different blade collective pitch angle ( $0^\circ$  and  $8^\circ$ ) and different rotor rotational speed (650–2500 rpm) conditions. For this initial validation study, two different test cases are selected, which are a low-pitch low-speed case with  $\theta_c = 0^\circ$  and 1500 rpm and a high-pitch high-speed case with  $\theta_c = 8^\circ$  and 2500 rpm.

### 2.2 Rotor Computational Simulations

3-D solid rotor geometry is modelled by using CATIA, a solid modelling software. Gmsh, an open-source 2-D/3-D unstructured grid generator software (Geuzaine & Remacle, 2009), is used to generate computational grid for CFD analysis. For SU2 flow solver, the motion of the rotor can be modelled by two different numerical approaches by creating two computational domains, defined as an inner region containing the rotor and an outer region containing the inner domain, as shown in Fig. 1. These two different domains are identified separately in the flow solver. The interface meshes on both domain surfaces are kept the same.

3-D unstructured grid is generated for the inviscid CFD simulations, where there is a total of 204,300 triangular elements on the 2 blades. There are 300 points on the leading and trailing edges, and there are 120 points on the upper and lower surfaces of the aerofoil section. The surface meshes on the blades and on the interface are shown in Fig. 2 with homogenous distribution of triangular elements used. The volume grids are generated for the inner and outer computational domains separately

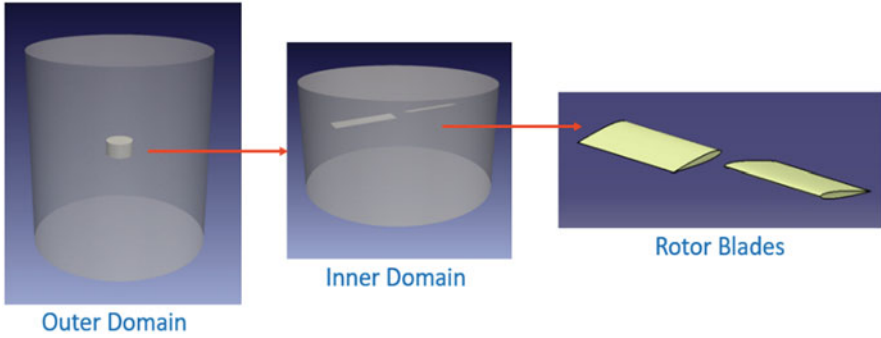


Fig. 1 Representative of computational domain

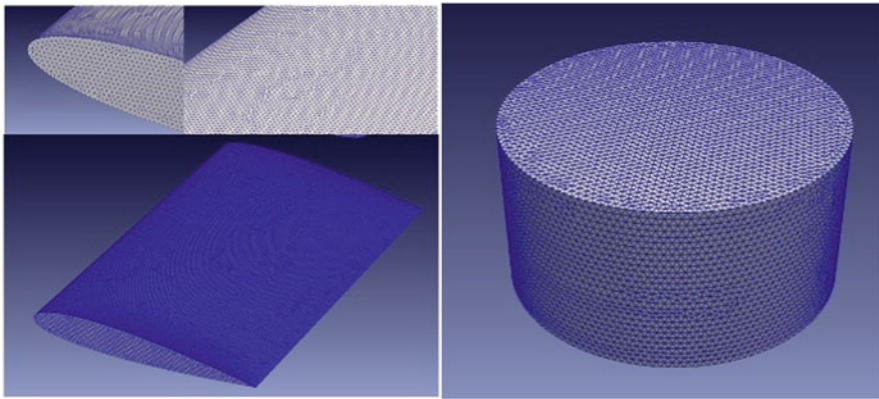


Fig. 2 Triangular surface mesh on the blades (left) and on the interface (right)

as shown in Fig. 3. The inner domain has about 2.8 million tetrahedral cells, and the outer domain has about 335 K tetrahedral cells.

Rotor CFD simulations in hover are performed by using SU2 with two approaches: rigid motion (RM) with moving grid (Sunay et al., 2011) and rotating frame (RF) with moving frame (Ramezani et al., 2013). In the first approach, rigid motion model, unsteady interaction between relative motion of the stationary and rotating components is modelled with grid regions moving with the body, and there is an interface between the stationary and moving grid regions. The second approach, rotating frame model, is used for a problem in which motion of the blade is unsteady in the stationary (inertial) frame and steady with respect to the moving frame.

For a steadily rotating body (i.e. the rotational speed is constant), it is possible to transform the equations of fluid motion to the rotating frame of reference such that steady-state solutions are possible by using the rotating frame model.

The rigid motion model is generally used for time-periodic simulations, that is, the transient solution repeats with a period related to the speeds of the moving

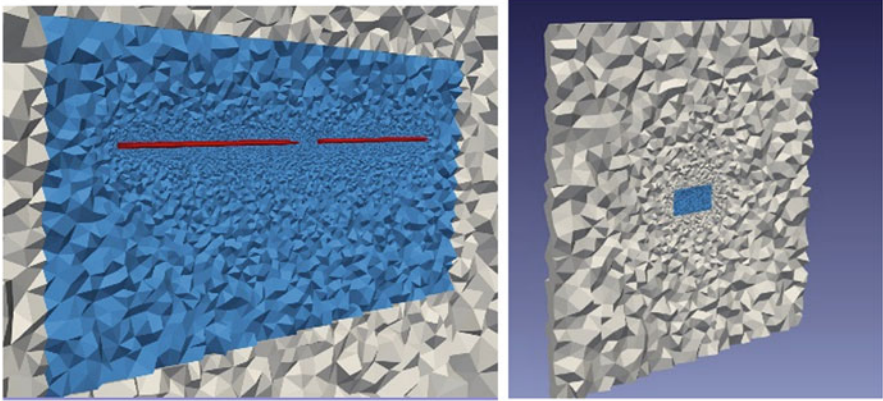


**Fig. 3** Unstructured tetrahedral volume grid in the inner (left) and outer domain (right)

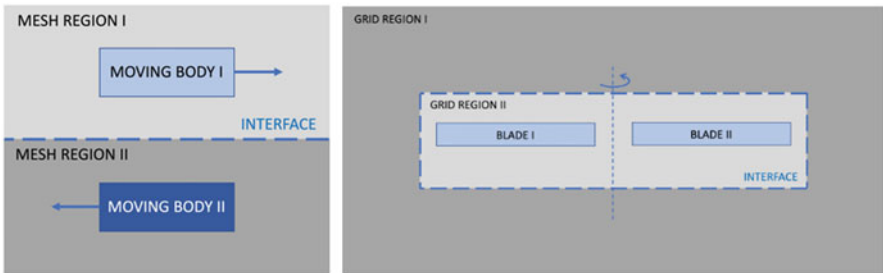


**Fig. 4** Illustrations of unsteady rigid motion with the bodies in linear motion (left) and rotating motion (right)

domains. In rigid motions, the relative motion of stationary and moving/rotating components will give rise to unsteady interactions. These interactions, similar to rotor/stator interactions in turbomachinery or rotor/fuselage interactions for helicopters, are illustrated in Fig. 4. In the rigid motion model, two or more mesh (2-D)/grid (3-D) zones (or regions) are used. Each grid region is bounded by at least one “interface zone” where it connects the grid zones and the information are interpolated and transferred between the zones.

The two different domains, inner and outer domains created during grid generation, are identified separately in the SU2 flow solver. 3-D, time-dependent (unsteady) Euler solver is used both for the inner (rotating) and outer (stationary) domains. Outer domain faces, which are located at the outer part, are identified as far-field boundary condition with sea level temperature and pressure free stream condition (300 K, 101,325 Pa). All the solid surfaces, which are blades, are identified as adiabatic Euler wall boundary condition. The interface between the outer and inner domains is identified as fluid interface. In the CFD analyses, an implicit second-order splitting method both in time and space is used with Green-Gauss

gradient numerical method for spatial gradients. FGRES for the implicit formulations and LU\_SGS for the preconditioner of the Krylov linear solver are selected. CFL number is changed adaptively from 0.5 to 5 with increasing factor 1 during unsteady simulations.

CFD simulations with both RM and RF models are performed on a PC with Intel i7-10750H 2.60 GHz CPUs. For the rotating frame case, the calculations take 5 minutes for each time step with 20 inner iterations on 6 CPU cores. For this unsteady simulation with the time step selected as 0.001 seconds, 120 time steps take nearly 10 hours. On the other hand, for the rigid motion case, the calculations take 10 minutes for each time step with 40 inner iterations on 6 CPU cores. The unsteady simulation for this case for 120 time steps corresponds to 20 hours' wall clock time.

### 3 Results and Discussion

The results discussed here for the fast Euler solutions obtained with RM and RF models can provide aerodynamic performances and flow-field details for rotor simulations. As the number of rotors increases in eVTOL configurations and flow-field interactions get more complex, obtaining solutions fast and accurately becomes important during the design of eVTOLs.

For the low-pitch low-speed case with  $\theta_c = 0^\circ$  and 1500 rpm condition, the CFD simulations are performed with the rigid motion model. The instantaneous computational results taken from the last time step are compared with the experimental data at four different spanwise stations ( $r/R = 0.5, 0.68, 0.89, 0.96$ ) as shown in Fig. 5. It

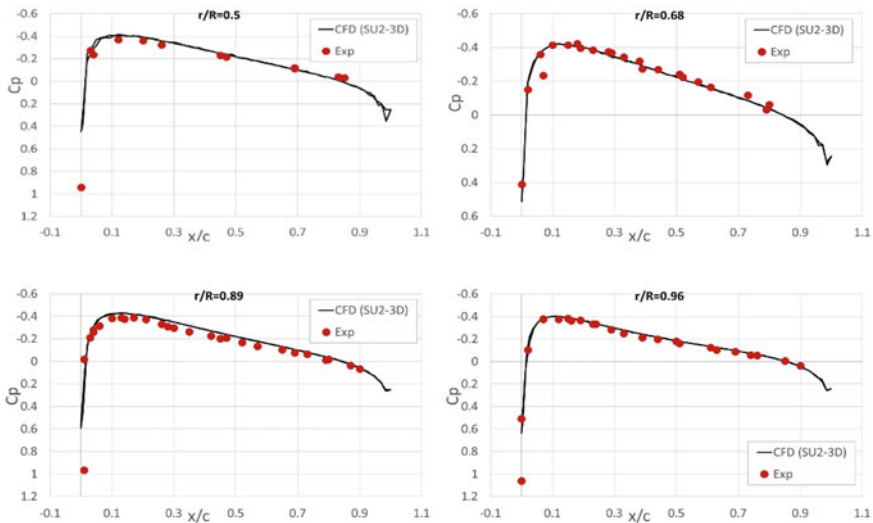


Fig. 5 Comparison of  $C_p$  for  $\theta_c = 0^\circ$  and  $\omega = 1500$  rpm

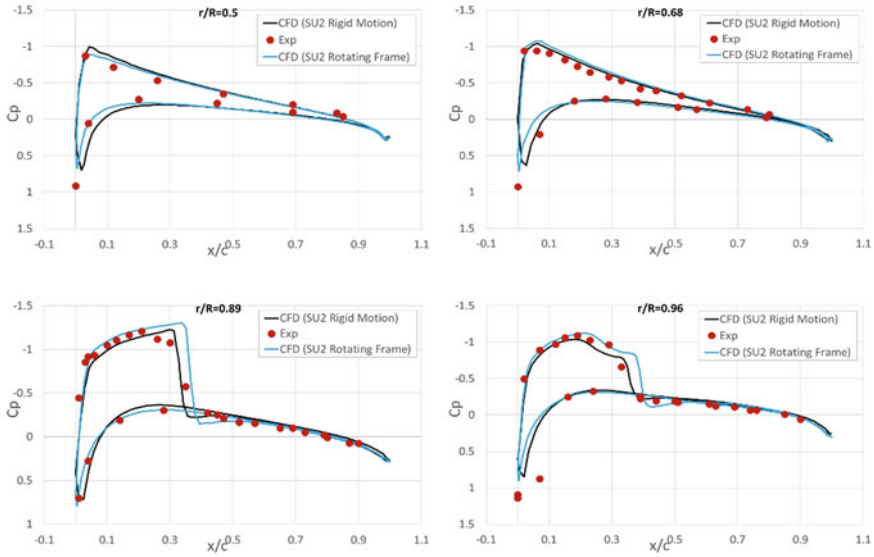


Fig. 6 Comparison of  $C_p$  for  $\theta_c = 8^\circ$  and  $\omega = 2500$  rpm

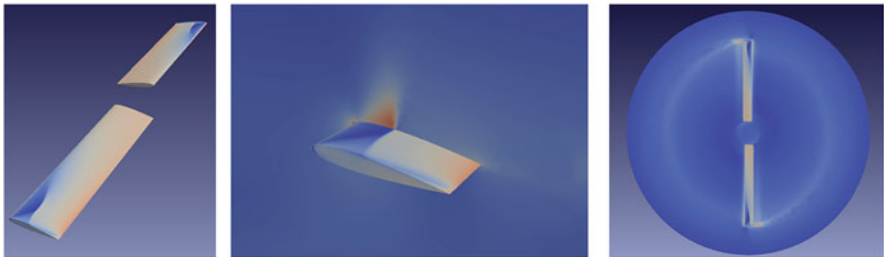


Fig. 7 Pressure contours on the rotor blades (left), Mach number contours in the vertical plane (middle), and Mach number contours in the rotor plane (right)

can be easily seen from the pressure coefficient distributions that the computational results are consistent with experimental data.

For the high-pitch high-speed case with  $\theta_c = 8^\circ$  and 2500 rpm condition, the CFD simulations are performed with the rigid motion and rotating frame approaches. The computational results taken from the last time step are compared with the experimental data as shown in Fig. 6. It can be easily seen that both models have consistent results with the experimental data. SU2 unsteady Euler solver for rotor simulations with both approaches has the capability to capture the shock and its location as can be seen in the outer spanwise stations.

The pressure contours on the rotor blades, the Mach number contours in the vertical plane near the tip, and the Mach number contours near the rotor, in the rotor plane, are presented in Fig. 7. It can be seen that the low-pressure region corresponds

to the supersonic region and the rapid change corresponds to the shock location. The grid needs to be refined to capture the wake and tip vortices more accurately.

## 4 Conclusions

Unsteady rotor CFD simulations in hover are performed with constant rotational speed by using SU2 flow solver both with rigid motion and rotating frame approaches. 3-D, unsteady, compressible, inviscid simulations are done for the Caradonna and Tung's rotor model, and the pressure coefficient distributions are compared with the available experimental data. For the low-pitch low-rpm case, no shock (low-speed case) and no separation (small angle of attack case) in the flow field are expected, and the computational results are obtained very similar with the experimental data. For the high collective pitch angle with high rotational speed case, the performance of the unsteady Euler solver for the flow field with shock conditions is investigated. Although the shock and its location are captured with the unsteady Euler simulations, there are some differences between the solutions with two models, moving grid or moving frame, used for the unsteady simulations as observed from the comparisons of pressure coefficient distributions with the experiments. This might be related with the convergence level of the simulations. The steady-state flow-field solution can be obtained more faster by using rotating frame model, which is suitable for hover conditions. On the other hand, rigid motion model allows more control on the blade motion, such as in forward flight conditions, if it can be used with adaptive or overset grids.

## References

- Caradonna, F. X., & Tung, C. (1981, September). *Experimental and analytical studies of model helicopter rotor in hover* (Technical Memorandum 81232).
- Geuzaine, C., & Remacle, J. F. (2009). Gmsh: A three-dimensional finite element mesh generator with built-in pre- and post-processing facilities. *International Journal for Numerical Methods in Engineering*, 79(11), 1309–1331.
- Ramezani, A., Remakil, L., & Suarez, J. I. A. (2013). *BBiped a SU2-based open-source: New Multiple Rotating Frame developments*. Open Source CFD International Conference, pp. 1–19. SU2 Foundation. (2021, September). <https://su2foundation.org>
- Sunay, Y. E., Akgül, A., & Kayabaşı, İ. (2011). Computational fluid dynamic simulation for rotor-body-interaction (Robin) Model and comparison with experiment, 4th Int. Sci. Conf. on Def. Tech., OTEH 2011, Oct 2011
- World eVTOL Aircraft Directory. (2021, September). <https://evtol.news/aircraft>

# Sustainable Materials Used by Additive Manufacturing for Aerospace Industry



Alperen Dođru and Mehmet Özgür Seydibeyođlu

## 1 Introduction

The source of many factors that facilitate human life has been the aerospace industry (Brothers, 2012). These are the main sectors where technologies that make our lives easier at many points, from our daily life to our professional life, emerge. The most important stakeholder in the emergence of these technologies is the developments in materials science (Mangalgiri, 1999). The aerospace industry is the sector where the technologies obtained in materials science find the first application area and where research and development studies are carried out intensively. Advances in materials science took the first place in reaching the current performance of aircraft (Ghori et al., 2018). The transition from wooden-bodied aircraft to the use of aluminum and the use of composite materials today are good examples of this process. Superalloys, ceramic matrix composites, and nano-doped materials have also led to developments in many areas from turbine engine technologies to communication technologies.

The developments in additive manufacturing technologies, which is one of today's new-generation production methods, and the applications of these technologies also play an important role in the aerospace industry (Keshavamurthy et al., 2021). Additive manufacturing technologies are another milestone for aerospace technologies. Additive manufacturing technologies offer significant opportunities, especially in the production of aircraft parts with complex geometries, where the production of these parts that is low with no mass production and lightness are at the forefront (Eichenhofer et al., 2017). As seen in Fig. 1, additive manufacturing

---

A. Dođru (✉)  
Aviation HVS, Ege University, Izmir, Türkiye  
e-mail: [alperen.dogru@ege.edu.tr](mailto:alperen.dogru@ege.edu.tr)

M. Ö. Seydibeyođlu  
İzmir Katip Çelebi University, İzmir, Türkiye  
e-mail: [ozgur.seydibeyoglu@ikcu.edu.tr](mailto:ozgur.seydibeyoglu@ikcu.edu.tr)



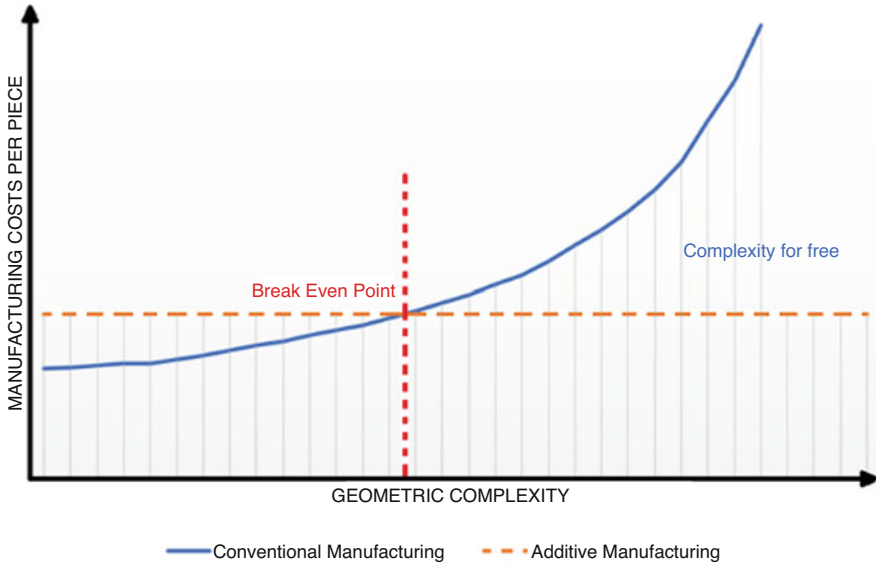


**Fig. 1** Conventional vs. additive manufacturing with per piece and geometric complexity

methods have many advantages with the per piece and geometric complexity vs. conventional manufacturing methods. A wide variety of materials can be produced in different forms with additive manufacturing methods (Parandoush & Lin, 2017). Of these, polymers are the most common. The use of additive manufacturing technologies in the manufacture of aircraft structural parts, components, and equipment, where polymer-based materials are increasingly used, offers significant sustainability, cost reduction, and topology optimization opportunities (Horn & Harrysson, 2012).

Polymer materials have many positive chemical and mechanical properties (Dizon et al., 2018). However, many types of polymer wastes cause pollution due to the inability to decompose. Especially, the negative effects of thermoset polymers in recycling and environmental pollution make these materials, which seem to be advantageous, disadvantageous (Lanzotti et al., 2019). In this regard, increasing the use of recyclable thermoplastics and replacing thermosets are critical for sustainable aviation. Aerospace structures that require high strength and stiffness have traditionally been made of metals or thermoset composites (Barile et al., 2019). However, these materials have some important limitations. Metals are heavy, limiting their use in aerospace applications where lightness is desired (Dođru et al., 2022). Thermoset composites, on the other hand, tend to be brittle and often have poor chemical resistance (Supian et al., 2018). In addition, thermoset materials cause serious problems in recycling (Post et al., 2020). The use of high-strength thermoplastic composites to reduce weight is one of the trending topics of aerospace polymers (Seydibeyođlu & Dođru). The use of thermoplastic composites in aircraft parts provides both lightness and environmentally friendly products (Dhinakaran et al.,

2020). In this context, the production of thermoplastic matrix composite materials with additive manufacturing technologies offers solutions.

In this study, short carbon fiber (SCF)-reinforced polyamide 6 (PA6) matrix specimens were produced by the fused filament fabrication (FFF) method. The changes in mechanical and thermal properties because of adding these specimens to the matrix material were investigated. Studies have been carried out to develop environmentally friendly materials that can be used in the aircraft cabin interior equipment.

## 2 Method

### 2.1 Materials

In the study, the Ultramid B 40LN PA6 product of BASF company, seen in Fig. 2a, was used as matrix material. The density of the matrix material that is PA6 is  $1.13 \text{ g/cm}^3$ , the relative viscosity value is 4, the melting temperature is  $220 \text{ }^\circ\text{C}$ , and its natural color. As for reinforcement material, AKSACA AC 41-01 product of DowAksa company, shown in Fig. 2b, was used. The diameter of the fibers is  $10 \text{ }\mu\text{m}$  and the length is 3 mm. The density of SCFs is  $1.78 \text{ g/cm}^3$ , tensile strength is  $4200 \text{ MPa}$ , and modulus value with tennis is  $240 \text{ GPa}$ . These are fibers with 1.5–2% polyamide-based sizing.

### 2.2 Production

Compounding, compounds are produced by Eurotec-EP company in a twin-screw extruder. Pre-drying was done at  $70 \text{ }^\circ\text{C}$  for 4 hours. The feed zone is  $25 \text{ }^\circ\text{C}$ , melt zone is  $220 \text{ }^\circ\text{C}$ , mixing conveying is  $220 \text{ }^\circ\text{C}$ , and die head temperature is  $225 \text{ }^\circ\text{C}$ . Compounds with PA6 matrix (SCF10PA6) reinforced with 10 wt% SCF by weight are produced. SCF10PA6 compounds are shown in Fig. 3.

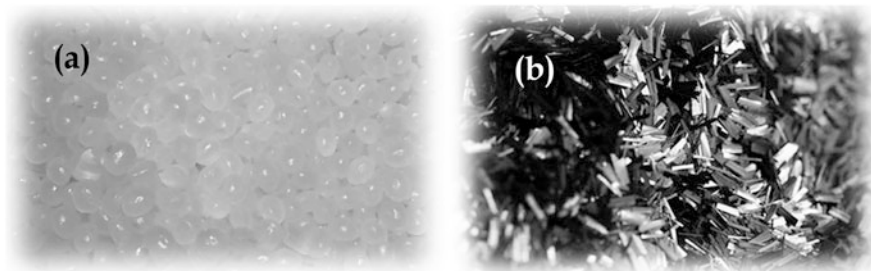
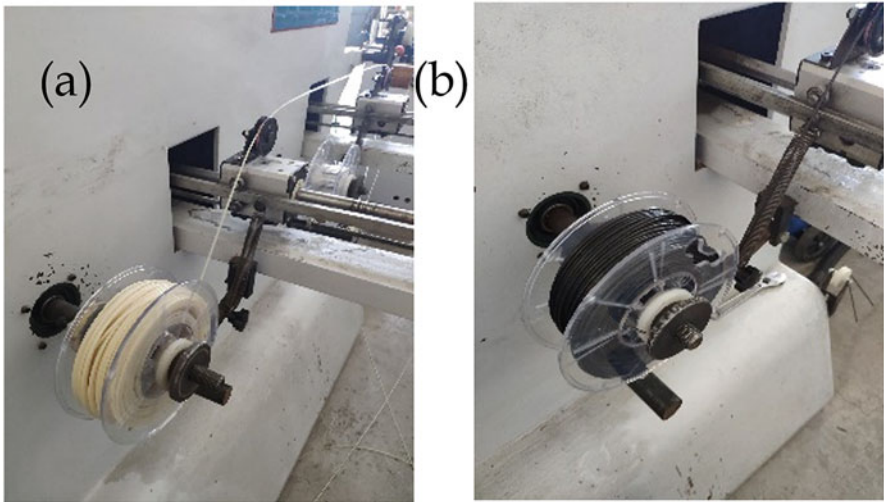


Fig. 2 (a) PA6. (b) SCF



**Fig. 3** 10 wt% SCF reinforcement PA6 compounds



**Fig. 4** (a) Pure PA6 filament, (b) SCF10PA6 filament

Filament producing, SCF-reinforced filament was produced by the extrusion method, as seen in Fig. 4b, with a single-screw extruder in EG-Plastic company by using SCF10PA6 compounds. In addition, to produce the control group, filament production was carried out with Pure PA6 compounds as seen in Fig. 4a. The filaments are 2.85 mm ( $\pm 0.15$ ) in diameter.

FFF specimens producing, specimens' production was carried out by the FFF method. Production parameters are as follows: layer height, 0.1 mm; wall thickness, 0.8 mm; nozzle diameter, 0.6 mm; infill density, 100%; infill pattern, cross; nozzle temperature, 260 °C; build plate temperature, 60 °C; flow, 105%; and print speed, 40 mm/s.

Test specimens were produced in ASTM D638 Type V dimensions as seen in Fig. 5.

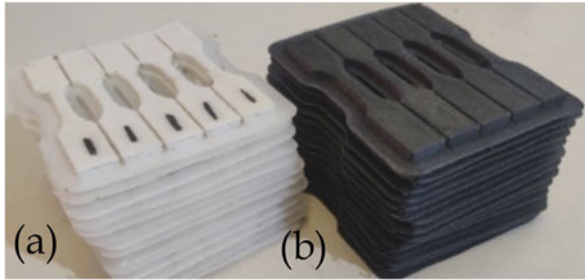


**Fig. 5** (a) Pure PA6 specimens, (b) SCF10PA6 specimens

### 2.3 Testing

Mechanical tests, thermal characterization, and morphological analyses were performed on the specimens produced by the FFF method. Tensile tests were performed using the Instron 1114 tester according to the ASTM D638 standard. Five specimens were used for each configuration. Thermogravimetric analysis (TGA) was performed to investigate the thermal properties of the specimens and to observe the reinforcement ratio. To observe the fiber distribution in the matrix and to examine the matrix fiber interfaces, microstructure image analyses were performed with Carl Zeiss 300VP scanning electron microscope (SEM).

## 3 Results and Discussion

Five pieces of each of Pure PA6 and 10 wt% SCF-reinforced specimens' groups were produced. This is for the calculation of the standard deviation. In Pure PA6 specimens, as seen in Table 1, the maximum tensile strength was measured as 46.085 MPa, and the minimum was 43.995 MPa. The average of the tensile test results is 45.062 MPa. For SCF10PA6 specimens, the maximum tensile strength is 62.109 MPa, and the minimum is 58.058 MPa. The average tensile test value is 60.086 MPa.

As seen in Fig. 6, when the average results are considered with 10 wt% SCF reinforcement in the PA6 matrix, an increase of approximately 33% in ultimate tensile strength values has been obtained.

As seen in Table 2, SCF reinforcement creates a change in density. The density value, which was 1.13 g/cm<sup>3</sup> with SCF reinforcement, increased to 1.24 g/cm<sup>3</sup> with the addition of 10 wt% SCF by weight. In addition, carbon fiber reinforcement increased tensile strength and decreased percent elongation. The percent elongation of Pure PA6 is 15.8%, while it is 10.6% in SCF10PA6 specimens.

As a result of TGA analysis, the thermal decomposition temperature for PA6 was determined to be approximately 380 °C. It was observed that it was 365 °C in SCF10PA6 specimens. It was observed that the degradation curve started at lower temperatures in the carbon fiber-reinforced specimens. The reason for this is that the

**Table 1** Tensile test results, mean, and standard deviation values of Pure PA6 and SCF10PA6 specimens

Materials	Unit	Specimens1	Specimens2	Specimens3	Specimens4	Specimens5	Avr.	Max.	Min.
Pure PA6	Mpa	45.54036	43.995035	46.085686	44.732743	44.95695	45.06215	1.02353	1.06712
SCF10PA6	Mpa	59.59183	59.009279	62.109087	58.0588307	61.66451	60.08671	2.02238	2.02788

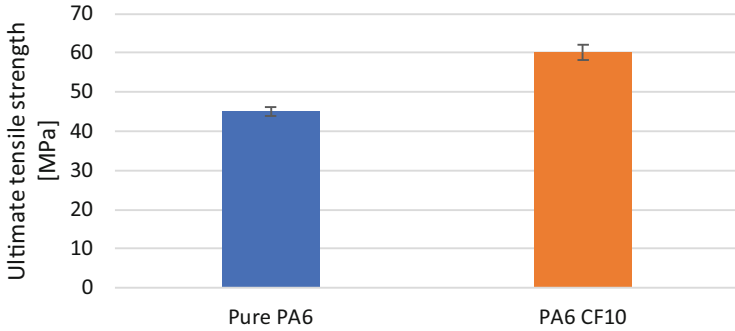


**Fig. 6** Ultimate tensile strength values of Pure PA6 and SCF10PA6 specimens

**Table 2** Stress at break values and density of Pure PA6 and SCF10PA6 specimens

Property	Condition	Unit	Standard	Results	
				Pure PA6	PA6 CF10
Stress at break	5 mm/min	Mpa	D 638	45.14	60.09
Strain at break	5 mm/min	%	D 638	15.8	10.6
Density	+23 °C	g/cm <sup>3</sup>	ISO 1183	1.13	1.24

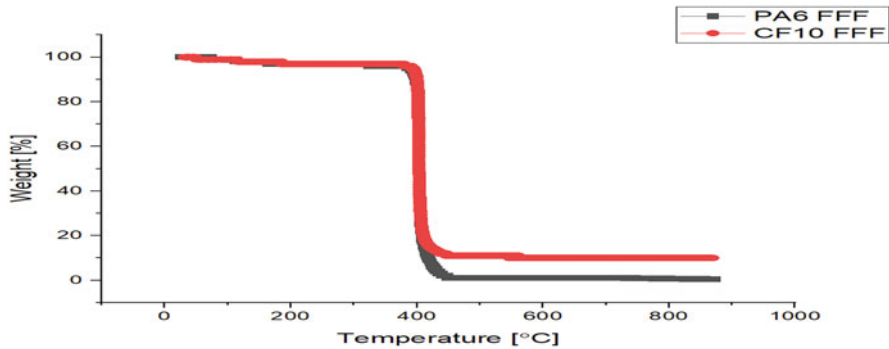


**Fig. 7** TGA results

polymer is subject to an extra melting process after preparing the compound in the filament production stage. TGA analysis also confirmed that the SCF10PA6 specimens have 10 wt% of SCF, as seen in Fig. 7.

Figure 8 shows the scanning electron microscope (SEM) image. SEM imaging was performed from the damaged areas of the specimens subjected to the tensile test. In the 20 micrometers (µm) scale image taken at 617 magnifications, it is seen that the carbon fibers have a uniform distribution. It has been observed that the fiber-matrix interfacial bonding is good.

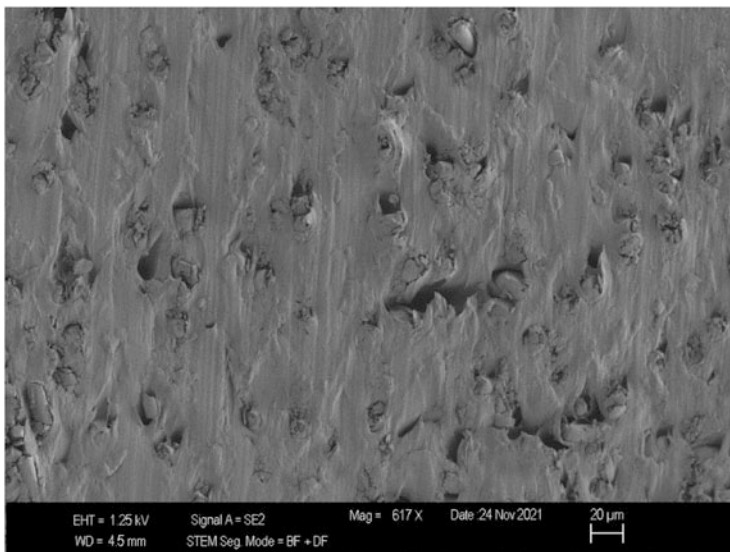


Fig. 8 SEM images of SCF10PA6 specimen

## 4 Conclusion

With the addition of 10 wt% of SCF, a 33% increase in the ultimate tensile strength of PA6 matrix material was observed compared to Pure PA6. The decomposition of PA6 at high temperatures makes its usage area widespread. It has been observed that it is possible to produce fiber-reinforced PA6 by additive manufacturing. Plastic materials are a good solution to reduce fuel consumption thanks to their low weight compared to metals. Also, the use of a thermoplastic matrix is critical for sustainability. These materials and manufacturing methods can be used for parts with small production volumes and complex geometries. Especially in aircraft cabin applications, various technical requirements must be met to limit fire inside the cabin and provide a safe environment for passengers. With the studies to be done on this subject, these materials may find use in aerospace applications. For this reason, new thermoplastic product development studies containing flame retardant additives can be carried out.

Compared to traditional manufacturing methods, the cost per unit increases as the geometric complexity increases in traditional manufacturing methods. In additive manufacturing methods, the unit cost of production is fixed. In addition, complex parts that cannot be produced with traditional manufacturing methods can be produced at the same unit costs. In additive manufacturing, the unit cost is fixed. In additive manufacturing, the number of productions is not important. This provides significant advantages in areas where there is a small number of parts production and in shortening the spare parts supply chain.

## References

- Barile, C., Casavola, C., & De Cillis, F. (2019). Mechanical comparison of new composite materials for aerospace applications [Internet]. *Composites Part B: Engineering*, 162, 122–128. Available from: <https://doi.org/10.1016/j.compositesb.2018.10.101>
- Brothers, W. (2012). Aerospace materials: Past, present and future. In *Introduction to aerospace materials* (pp. 15–38). Woodhead Publishing.
- Dhinakaran, V., Surendar, K. V., Riyaz, M. S. H., & Ravichandran, M. (2020). Review on study of thermosetting and thermoplastic materials in the automated fiber placement process [Internet]. *Materials Today: Proceedings*, 27(2), 812–815. Available from: <https://doi.org/10.1016/j.matpr.2019.12.355>
- Dizon, J. R. C., Espera, A. H., Chen, Q., & Advincula, R. C. (2018). Mechanical characterization of 3D-printed polymers [Internet]. *Additive Manufacturing*, 20, 44–67. Available from: <https://doi.org/10.1016/j.addma.2017.12.002>
- Doğru, A., Sözen, A., Neşer, G., Seydibeyoğlu, M.Ö., (2022). Numerical And Experimental Investigation of The Effect of Delamination Defect At Materials of Polyethylene Terephthalate (PET) Produced by Additive Manufacturing on Flexural Resistance. *International Journal of 3D Printing Technologies and Digital Industry*, 6(3), 382–391. Available from: <https://doi.org/10.46519/ij3dptdi.1098903>
- Eichenhofer, M., Wong, J. C. H., & Ermanni, P. (2017). Continuous lattice fabrication of ultralightweight composite structures. *Additive Manufacturing*, 18, 48–57.
- Ghori, S. W., Siakeng, R., Rasheed, M., Saba, N., & Jawaid, M. (2018). The role of advanced polymer materials in aerospace [Internet]. In *Sustainable composites for aerospace applications* (pp. 19–34). Elsevier Ltd. Available from: <https://doi.org/10.1016/B978-0-08-102131-6.00002-5>
- Horn, T. J., & Harrysson, O. L. A. (2012). Overview of current additive manufacturing technologies and selected applications. *Science Progress*, 95(3), 255–282.
- Keshavamurthy, R., Tambrallimath, V., & Saravanabavan, D. (2021). Development of polymer composites by additive manufacturing process [Internet]. In *Encyclopedia of materials: Composites* (pp. 804–814). Elsevier Ltd. Available from: <https://doi.org/10.1016/B978-0-12-803581-8.11885-5>
- Lanzotti, A., Martorelli, M., Maietta, S., Gerbino, S., Penta, F., & Gloria, A. (2019). A comparison between mechanical properties of specimens 3D printed with virgin and recycled PLA [Internet]. *Procedia CIRP*, 79, 143–146. Available from: <https://doi.org/10.1016/j.procir.2019.02.030>
- Mangalagiri, P. D. (1999). Composite materials for aerospace applications. *Bulletin of Materials Science*, 22(3), 657–664.
- Parandoush, P., & Lin, D. (2017). A review on additive manufacturing of polymer-fiber composites [Internet]. *Composite Structures*, 182, 36–53. Available from: <https://doi.org/10.1016/j.compstruct.2017.08.088>
- Post, W., Susa, A., Blaauw, R., Molenveld, K., & Knoop, R. J. I. (2020). A review on the potential and limitations of recyclable thermosets for structural applications [Internet]. *Polymer Reviews*, 60, 359–388. Taylor and Francis Inc. Available from: <https://www.tandfonline.com/doi/abs/10.1080/15583724.2019.1673406>
- Seydibeyoğlu, M. Ö., Doğru, A. (2020) *Lightweight Composite Materials in Transport Structures, Lightweight Polymer Composite Structures*, CRC Press, 103–130.
- Supian, A. B. M., Sapuan, S. M., Zuhri, M. Y. M., Zainudin, E. S., & Ya, H. H. (2018). Hybrid reinforced thermoset polymer composite in energy absorption tube application: A review. *Defence Technology*, 14(4), 291–305.



# Integration of Sustainability and Digitalization in Air Logistics: Current Trends and Future Agenda



Volkan Yavas and Yesim Deniz Ozkan-Ozen

## 1 Introduction

In today's global world, digitalization and sustainability are two major trends that shape the business environment. With the Fourth Industrial Revolution, digitalization became a significant competitive advantage element for organizations. However, while focusing on economic gains, organizations need to consider social and environmental issues as well. Therefore, sustainability and digitalization can be seen as two inseparable parts for organizations. A supporting view was given by de Sousa Jabbour et al. (2018) as "these cannot individually be considered new industrial revolutions; through their overlap and synergy they may together comprise a distinct industrial wave that will change worldwide production systems forever".

The impact of digitalization and sustainability is on the entire supply chains, and all the stages are affected from the tremendous changes. As one of the core elements of supply chains, logistics operations need to meet the sustainability goals while staying up to date through digitalization.

This research especially focuses on air logistics, due to its critical role in today's globalized world. Although digitalization has a great potential to support sustainable processes, there is a gap in the field of air logistics in terms of integration of digitalization and sustainability. Therefore, the main motivation of this research is to contribute in the air logistics field in terms of integrating sustainability and digitalization.

---

V. Yavas (✉)  
Ege University Aviation HVS, Izmir, Türkiye  
e-mail: [volkan.yavas@ege.edu.tr](mailto:volkan.yavas@ege.edu.tr)

Y. D. Ozkan-Ozen  
Yasar University Logistics Management Department, Izmir, Türkiye  
e-mail: [yesim.ozen@yasar.edu.tr](mailto:yesim.ozen@yasar.edu.tr)

From this point of view, our aim is to present current trends and future research directions for sustainable air logistics in the digital era by conducting a bibliometric analysis. To do so, VOSViewer program is used to conduct a co-occurrence analysis, and current research trends are revealed.

This paper is structured as follows: after the introduction part, a short literature review is presented. Then methodology section is included in implementation and discussions part, and conclusion section is located at the end of the study.

## 2 Literature Review

Literature that directly covers the concepts of digitalization, sustainability and air logistics is limited, and most of them include technology-based applications.

For instance, Choi et al. (2019) worked on blockchain technology and especially focused on supply chain operations risks in the air logistics sector. Similarly, Di Vaio and Varriale (2020) also focused on blockchain technology and analysed the relationship with sustainability with a case of airport industry. One of the most important question marks in terms of sustainability in the aviation logistics is energy consumption or, in other words, the traditional fuels used and the conversion process to electric fuel. In this sense, examining the general structure and energy requirement of aircraft with the concept of digital twin will be an effective approach in terms of sustainability (Portapas et al., 2021).

Furthermore, Kelemen et al. (2020) proposed an educational information software for sustainability risk assessment that can be applied to airport network and information system. On the other hand, Ordieres-Meré et al. (2020) worked on exploring the perspective of sustainability during digital transformation in manufacturing and air transport industry. They especially focused on knowledge creation and new organizational strategies. Finally, Paprocki (2021) aimed to fulfil the gap in transport sciences by proposing digital technologies and innovative solutions for sustainability purposes, especially climate policy.

As it can be seen from the brief literature summary, the field of sustainability and digitalization in air logistics industry is promising, and revealing the current trends and future research direction could be beneficial. From this point of view, a content analysis is conducted in this research. Details related to methodology, implementations and results are presented in the following section.

## 3 Methodology

This study can be called a mixed study as a method. In this sense, the study consists of two different steps. These two different methods were used together and intertwined. Related studies have been searched and listed in Web of Science and Scopus, which are databases of mostly high-quality journals. Then, an analysis was

made through the VOSViewer program for bibliometric analysis. VOSViewer is a software for creating maps based on network data and for visualizing and exploring them, mainly designed for bibliometric network analysis but used for any type of network data (Van Eck & Waltman, 2013). The network map shown in Fig. 1 was

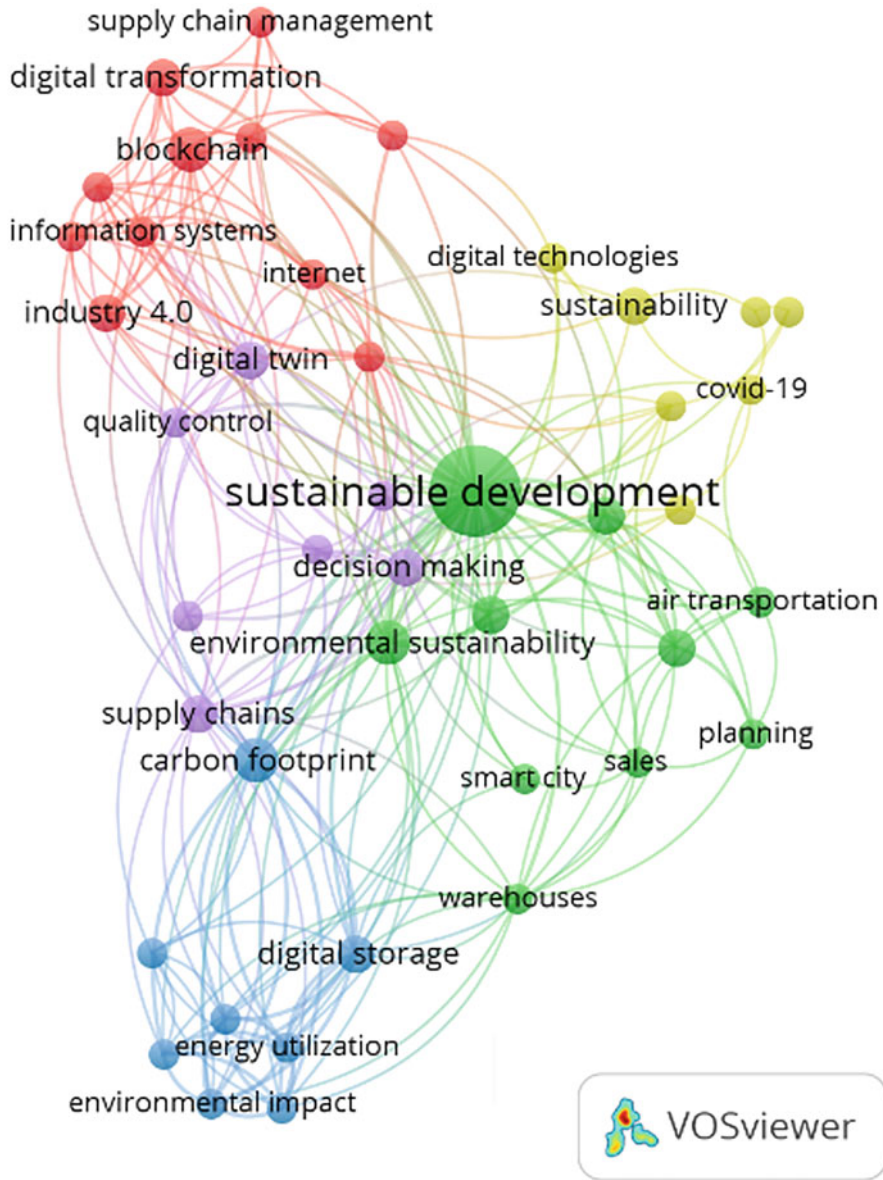


Fig. 1 Co-occurrence analysis of the listed studies

created by this software. While creating the network map, the keywords in the listed studies were used. Details about the network map are given in the next section. Afterwards, the studies to which the keywords belong were read in detail, and the studies directly related to the subject were referenced in the previous and next sections.

## 4 Findings

While there are various studies on sustainability in aviation, the field of “air logistics” was evaluated from the perspective of digitalization. For this purpose, a content analysis was carried out with academic studies obtained by literature review. In the Scopus database, the keywords “sustainable, logistics and digital” are scanned in the context of “title, abstract and keyword”. The results list studies containing the keyword “aviation”. As a result of the listing study, 31 studies were produced, and co-occurrence analysis was carried out through the VOSViewer program.

In the co-occurrence analysis revealed in Fig. 1, clusters expressed in different colours refer to keywords that are closely related to each other in studies. The thickness/size of the keywords refers to the frequency of the studies, and the lines between them refer to their relationship with each other.

Accordingly, the cluster expressed in green colour (Fig. 2) contains the keywords of sustainable development and air transport together, where words about smart cities, warehouses and automation systems stand out. The studies here are important in that they show the critical elements in ensuring sustainability in aviation. The red cluster (Fig. 3), with which keywords related to Industry 4.0 and its elements are closely related, illustrates the technical elements in the studies. Here, along with the digital transformation, information technologies and the blockchain system draw attention.

In Fig. 4, three different clusters are shown in detail. The purple cluster with keywords such as supply chain, cold chain and quality points to operational elements. It draws attention to the environmental elements of the blue cluster, which contains keywords such as energy, emissions and carbon footprint. Finally, it can be said that the yellow cluster containing keywords such as China, COVID-19 and logistics also contains current elements.

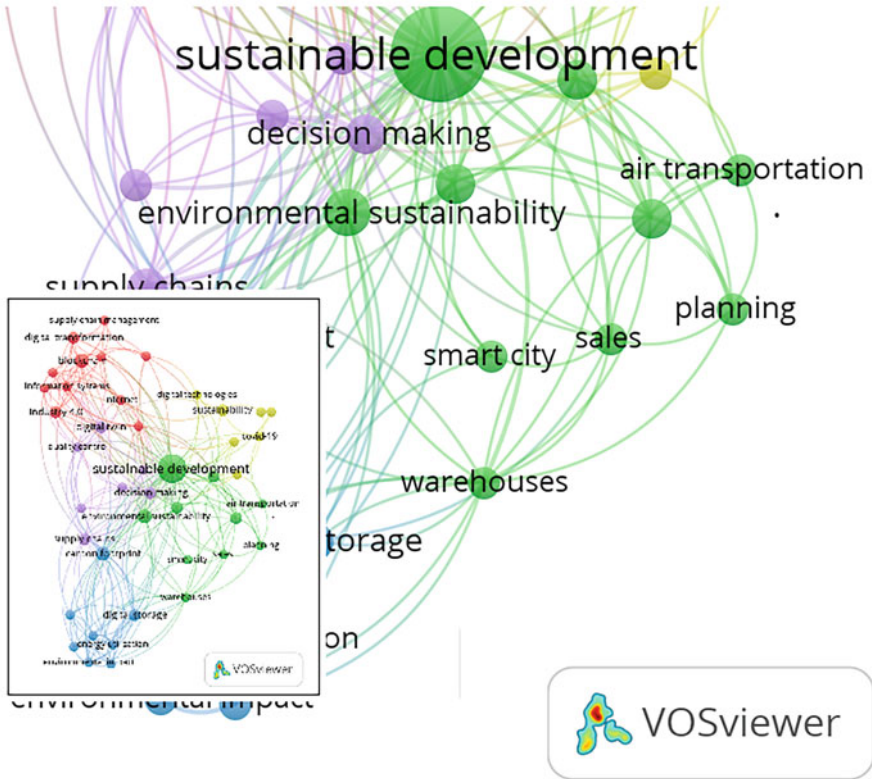
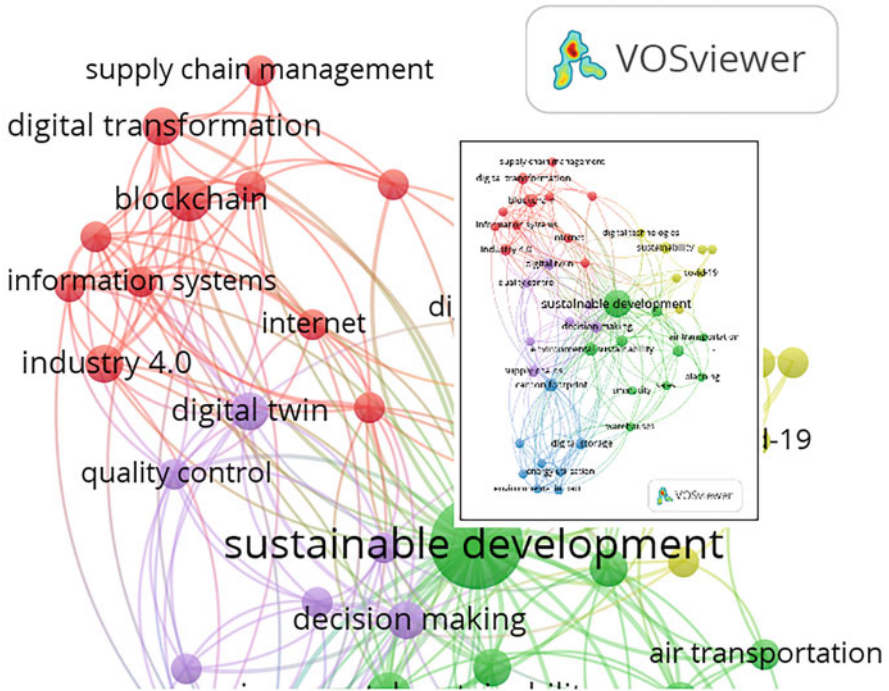


Fig. 2 Sustainability and air transport relations

## 5 Implementation and Discussions

The limitation of the number of researches on air logistics and sustainability naturally creates a limitation in keywords. It will also be possible to catch different clues in analysis to be made on the concepts of sustainable aviation or sustainable logistics. However, in essence, it is critical to consider Industry 4.0 elements with a “technical, operational and environmental” main point of view in order to ensure sustainability in air logistics processes. In this sense, it would be meaningless to consider sustainability in air logistics processes from a single point of view, and it is estimated that any improvement in any process will create a change like a whiplash effect.



**Fig. 3** Industry 4.0 elements

In addition to academic studies and theoretical knowledge, it will be important to examine the existing applications in the sector in order to see the whole picture. The reinterpretation and transformation of current problems, bottlenecks and current solution proposals in the perspective of Industry 4.0 will be one of the most logical steps to be taken in the short term for sustainability in air logistics.

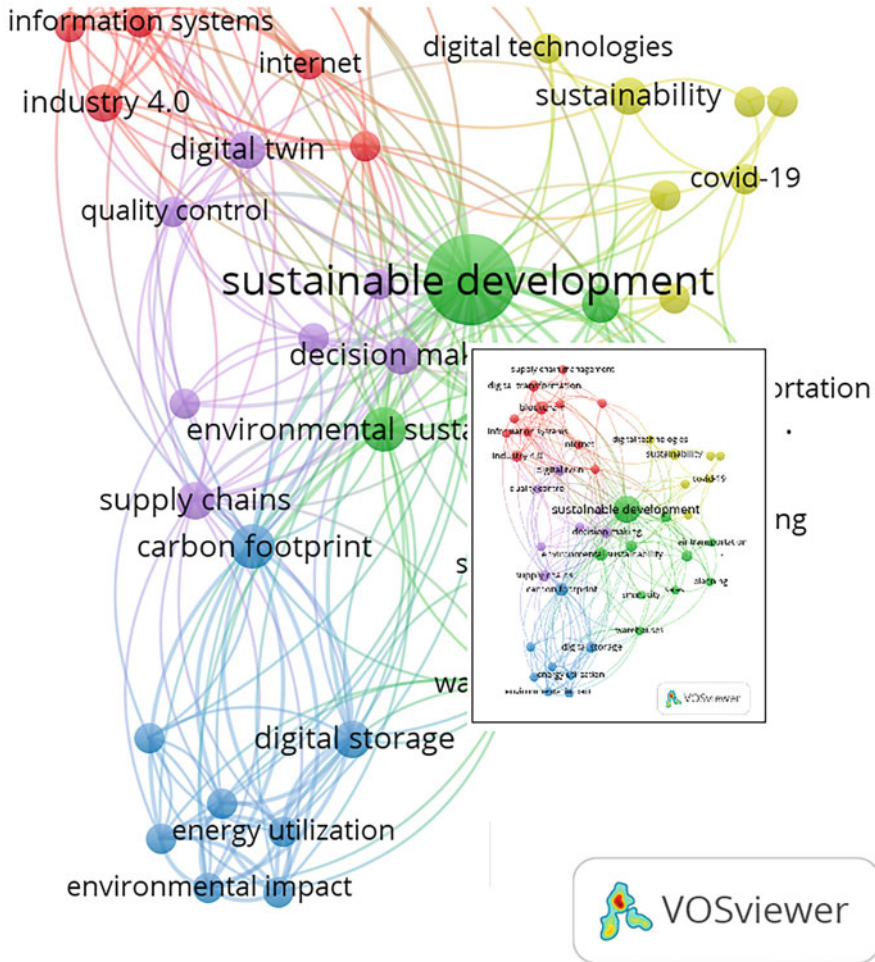


Fig. 4 Operational, environmental and current elements

## 6 Conclusion

This study is an initial attempt to present the potential of integrating of sustainability and digitalization in air logistics. A content analysis was conducted with the participation of 31 studies, and co-occurrence analysis was made by using VOSViewer program.

As a result of the study, it is revealed that there are many open research areas in the sustainable air logistics in digital era. To start with, integrating sustainable development principles with digitalized air logistics operations can be suggested

for the future research. Moreover, technology-based applications in air logistics for sustainable practices can be conducted, and new ways for minimizing environmental impacts by using digital technologies can be investigated. Finally, new business models for post-COVID-19 era in air logistics can be developed by integrating sustainability principles and digital technologies.

## References

- Choi, T. M., Wen, X., Sun, X., & Chung, S. H. (2019). The mean-variance approach for global supply chain risk analysis with air logistics in the blockchain technology era. *Transportation Research Part E: Logistics and Transportation Review*, *127*, 178–191.
- de Sousa Jabbour, A. B. L., Jabbour, C. J. C., Foropon, C., & Godinho Filho, M. (2018). When titans meet—Can industry 4.0 revolutionise the environmentally-sustainable manufacturing wave? The role of critical success factors. *Technological Forecasting and Social Change*, *132*, 18–25.
- Di Vaio, A., & Varriale, L. (2020). Blockchain technology in supply chain management for sustainable performance: Evidence from the airport industry. *International Journal of Information Management*, *52*, 102014.
- Kelemen, M., Polishchuk, V., Gavurová, B., Andoga, R., Szabo, S., Yang, W., Christodoulakis, J., Gera, M., Kozuba, J., Kaľavský, P., & Antoško, M. (2020). Educational model for evaluation of airport NIS security for safe and sustainable air transport. *Sustainability*, *12*(16), 6352.
- Ordieres-Meré, J., Prieto Remon, T., & Rubio, J. (2020). Digitalization: An opportunity for contributing to sustainability from knowledge creation. *Sustainability*, *12*(4), 1460.
- Paprocki, W. (2021). Virtual airport hub—A new business model to reduce GHG emissions in continental air transport. *Sustainability*, *13*(9), 5076.
- Portapas, V., Zaidi, Y., Bakunowicz, J., Paddeu, D., Valera-Medina, A., & Didey, A. (2021). Targeting global environmental challenges by the means of novel multimodal transport: Concept of operations. In *2021 Fifth world conference on smart trends in systems security and sustainability (WorldS4)* (pp. 101–106). IEEE.
- Van Eck, N. J., & Waltman, L. (2013). VOSviewer manual. *Leiden: Univeriteit Leiden*, *1*(1), 1–53.



# Design of PI Controller for Longitudinal Stability of Fixed-Wing UAVs



Veena Phunpeng, Wilailak Wanna, and Thongchart Kerdphol

## Nomenclature

I	Integral
P	Proportional
PI	Proportional-Integral
PID	Proportional-Integral-Derivative
UAVs	Unmanned aerial vehicles

## 1 Introduction

Unmanned aerial vehicles (UAVs) are gaining more attention in a wide range of applications of both military and civilian services (Aziz et al., 2018) such as Predator and Global Hawk (Chaoxing et al., 2019). UAVs have many applications including surveying, mapping, inspection, and security (Pakorn et al., 2018). UAVs can be divided into various classifications by the depth of action, the multiplicity of UAV application, the duration of the UAV flight, the UAV take-off weight in kg, and the way of landing the UAV (Brovchenko, 2015). The method of landing can be divided into several categories including fixed-wing, helicopter, quadcopter, hexacopter and octocopter (Jeongeun et al., 2019).

---

V. Phunpeng · W. Wanna (✉)

School of Mechanical Engineering, Institute of Engineering, Suranaree University of Technology, Nakhon Ratchasima, Thailand  
e-mail: [veenap@g.sut.ac.th](mailto:veenap@g.sut.ac.th)

T. Kerdphol

Department of Electrical Engineering, Faculty of Engineering, Kasetsart University, Bangkok, Thailand

Fixed-wing UAVs are different from quadcopters. Fixed-wing UAVs require a runway for take-off and landing. Fixed-wing UAVs have main advantages in controlling hover ability/ranges, flying at a high altitude, improving flight endurance, and carrying more payloads (Junyu et al., 2020). The wings of such UAVs are fixed, and the bodies are rigid structures (Prithvi et al., 2021). Fixed-wing UAVs easily lose their stability when facing a sudden change of disturbances. The disturbances mainly involve weather conditions and wind gusts, which can cause the fixed-wing UAVs to lose their control of direction and attitude. A significant disturbance can cause rapid changes related to the wing lift force, leading to the stalling of UAVs (Jun et al., 2019). Thus, controlling the stability of the UAVs is a critical issue.

For the autonomous control of the fixed-wing UAVs, the controller must be robust to wind gust disturbances (Erdal et al., 2017). Therefore, fixed-wing UAVs need a suitable controller that can compensate immediately for the sudden disturbances to enhance UAV performance and stability (Chenggong et al., 2009).

In control systems, adaptive feedback controllers (e.g., Proportional-Integral (PI) and Proportional-Integral-Derivative (PID)) are widely used in industrial systems to control errors in manufacturing plants (Thongchart et al., 2018, 2019). Such controllers can also be applied to control the UAV system. Most of the feedback controllers in UAVs are used for attitude stability control (Hongru et al., 2019). To reduce the designed complexity, the PI controller can be used to improve the performance of the longitudinal motion and disturbance rejection (Ahmed et al., 2015). The PI controller consists of proportional and integral controllers. The proportional term immediately impacts the error of the system, while the integral term continually sums up an error (Lalitesh et al., 2014), stabilizing the system.

In previous research, the authors developed a completed function of the UAV platform to develop a suitable flight control system. The fixed-wing UAVs (i.e., ARF60 model) are used for longitudinal modeling (Amer et al., 2009). The model was thoroughly analyzed using the linearized state space (Amer et al., 2009).

This paper focuses on the design of the PI controller for the longitudinal stability of fixed-wing UAVs. To study the longitudinal stability, the UAV pitch motion is linearized in terms of the state-space modeling. To analyze the PI control effects, the gains of  $K_P$  and  $K_I$  are varied by  $\pm 50\%$  of their original values after disturbances. Then, the optimal gains of  $K_P$  and  $K_I$  are obtained by the build-in tuner in MATLAB/Simulink<sup>®</sup>. The optimal gains of  $K_P$  and  $K_I$  are chosen from the settling time.

The remaining part of the paper is organized as follows: the system modeling part presents the pitch motion behavior, longitudinal state-space model, and pitch angle transfer function. The design of the controller part proposes the tuning of PI controller for longitudinal stability of the fixed-wing UAV. The discussion part shows the simulation results of the pitch angle control system with the designed PI controller. The conclusion comes at the end of the last section.

## 2 System Modeling

The movements of fixed-wing UAVs can be divided into the sections of roll, pitch, and yaw that follow the UAV axes of  $X$ ,  $Y$ , and  $Z$  (Jin et al., 2018). The UAV movements are characterized by the rotation around the axes of the UAVs. Each axis ( $X$ ,  $Y$ , and  $Z$ ) is an imaginary line that passes through the center of gravity (CG) point (see Fig. 1).

The pitch process is characterized by the UAVs moving around the  $Y$ -axis. The  $Y$ -axis runs from the left wingtip to the right wingtip. The pitch relates to the nose of the UAVs, indicating the nose up or nose down. The pitch is controlled by an elevator that is installed on the tail section in the horizontal. The moving up or moving down of the elevator (the elevator deflection angle,  $\delta_e$ ) can cause the change of pitch angle ( $\theta$ ) (Jun et al., 2019); see Fig. 2. The UAV movements can be explained using the dynamic equation of motion. This equation relates to the stability and control of the UAVs. The action of the system is described by a derived state-space model (Michale, 2007).

The state-space model represents the mathematical relationship that uses the matrix method to solve the equation of motion (e.g., linear dynamic system problems) (Soliman & Kandari, 2010). The longitudinal model of ARF60 UAV (see Eq. 1) can be described by the derived state-space model with typical flight control parameters ( $V_a = 20$  m/s,  $h = 100$  m,  $\varnothing = 0$ ) (Ahmed et al., 2015).

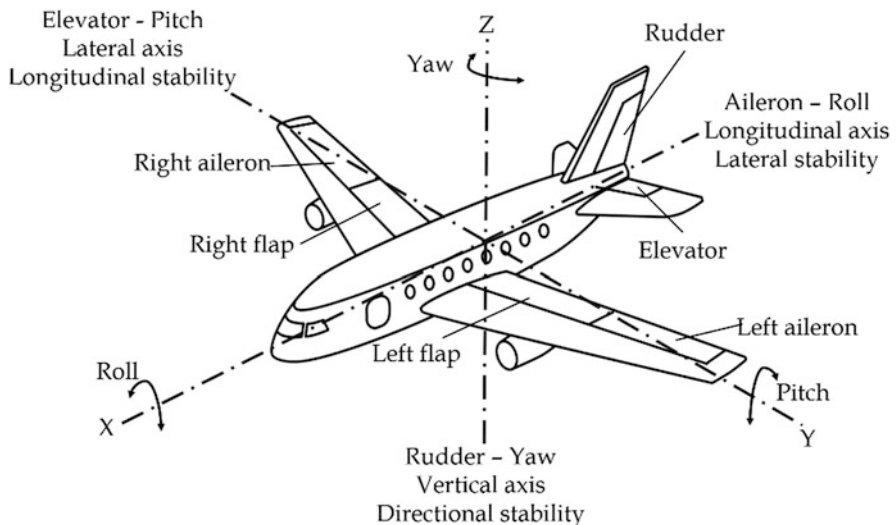


Fig. 1 The control axes of fixed-wing UAVs

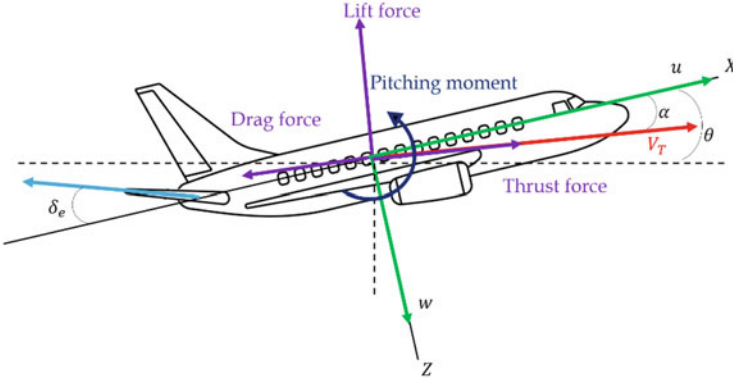


Fig. 2 Longitudinal control motion of UAVs

$$\begin{bmatrix} \dot{u} \\ \dot{w} \\ \dot{q} \\ \dot{\theta} \\ \dot{h} \end{bmatrix} = \begin{bmatrix} -0.2289 & 0.3712 & 0 & -9.81 & 0 \\ -1.8772 & -10.1512 & 20 & 0 & 0 \\ 0.9219 & -7.0403 & -26.072 & 0 & 0 \\ 0 & 0 & 1 & 0 & 0 \\ 0 & -1 & 0 & 20 & 0 \end{bmatrix} \begin{bmatrix} u \\ w \\ q \\ \theta \\ h \end{bmatrix} + \begin{bmatrix} 0 & 51.5 \\ -14.0042 & 0 \\ -147.6913 & 0 \\ 0 & 0 \\ 0 & 0 \end{bmatrix} \begin{pmatrix} \delta_e \\ \delta_t \end{pmatrix} \quad (1)$$

The pitch angle transfer function can be obtained by solving Eq. (1), which can be written as:

$$\frac{\theta(s)}{\delta_e(s)} = \frac{-147.7s^2 - 1434s - 428.3}{s^4 + 36.45s^3 + 113.2s + 221.5} \quad (2)$$

### 3 Design of Controller

Usually, the controller is employed to compensate changes (i.e., error) from the input of the system (i.e., disturbance) and generates a suitable signal to control the output. The adaptive feedback controller measures the output of the system to compare with the input. Then, the difference value (error) is used to modify the system to achieve the desired setpoint (input) (Peter et al., 2020).

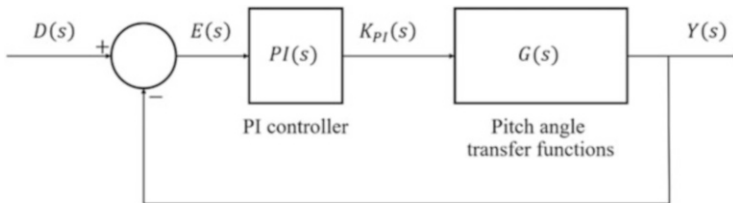


**Fig. 3** The designed PI control for pitch angle system

The PI controller consists of the Proportional (P) and Integral (I) parts. The P controller provides a proportional gain ( $K_P$ ) to modify the error signal of the system. The I controller provides an integral gain ( $K_I$ ) to improve the transient response and overshoot of the system (Kiam et al., 2005). In this study, the step input is set as the sudden disturbance to the system. The optimal gains of  $K_P$  and  $K_I$  are obtained from the MATLAB<sup>®</sup> tuning. The optimal gains are varied by  $\pm 50\%$  of original values against the applied disturbances. The overview of PI control for UAV pitch angle is shown in Fig. 3.

The rule of the PI controller for pitch angle can be written as:

$$Y(s) = D(s) - E(s)K_{PI}(s) \quad (3)$$

where  $D(s)$  is the disturbance (input),  $Y(s)$  is the output of the system,  $K_{PI}$  is the output of PI controller, and  $E(s)$  is the error of the system.

The dynamic transfer function of PI control can be written as (Andrei et al., 2018):

$$K_{PI}(s) = K_P + \frac{K_I}{s} \quad (4)$$

where  $K_P$  is the proportional gain and the  $K_I$  is the integral gain.

## 4 Results and Discussion

In this section, the optimal gains of P and I controllers are tuned by the build-in tuner-based MATLAB/Simulink<sup>®</sup>. The optimal gains of  $K_P$  and  $K_I$  are chosen from the desired constraints. The constraints are set to deal with an overshoot of less than 20% of its original value and a settling time of less than 1 s. The applied disturbance refers to the change of  $1^\circ$  of pitch angle.

To evaluate a suitable trade-off between system stability and controller gains, the gains of  $K_P$  and  $K_I$  are varied by  $\pm 50\%$  of original values against the applied disturbance.

Figure 4 shows the system response of the UAV pitch angle against the variations of proportional control ( $\pm 50\%$  of its original value), while  $K_I$  is a constant value. The zoom-in view of Fig. 4 is shown in Fig. 5. The result indicates that increasing  $K_P$  improves the response of the system by reducing the rise and settling time. However, the increasing  $K_P$  also increases the overshoot of the system. On the other hand, reducing  $K_P$  increases the rise time, overshoot, and settling time that affects the large oscillations of the system.

Then, the system response of the UAV pitch angle is varied against the variations of integral control (see Fig. 6). When the  $K_I$  is varied by  $\pm 50\%$  of its original value, while  $K_P$  is a constant value. The zoom-in view of Fig. 6 is shown in Fig. 7. It is found that the increasing  $K_I$  reduces the rise time and settling time of the system, but it also increases the overshoot of the system. Vice versa, the reducing  $K_I$  increases the rise time and settling time, but it also reduces the overshoot of the system.

Finally, the system response with the optimal PI controller is shown in Fig. 8. Without the PI controller, the system has a very large overshoot over  $-5.5^\circ$  with a long settling time of over 40 s. The result shows that the system without the controller has a prolonged response in dealing with overshoot and setting time, leading to an unstable system.

By applying the optimal gains of  $K_P$  of  $-2.5919$  and  $K_I$  of  $4.9355$  obtained from the built-in tuner, it is found that the system overshoot is reduced to  $1.18^\circ$  and the

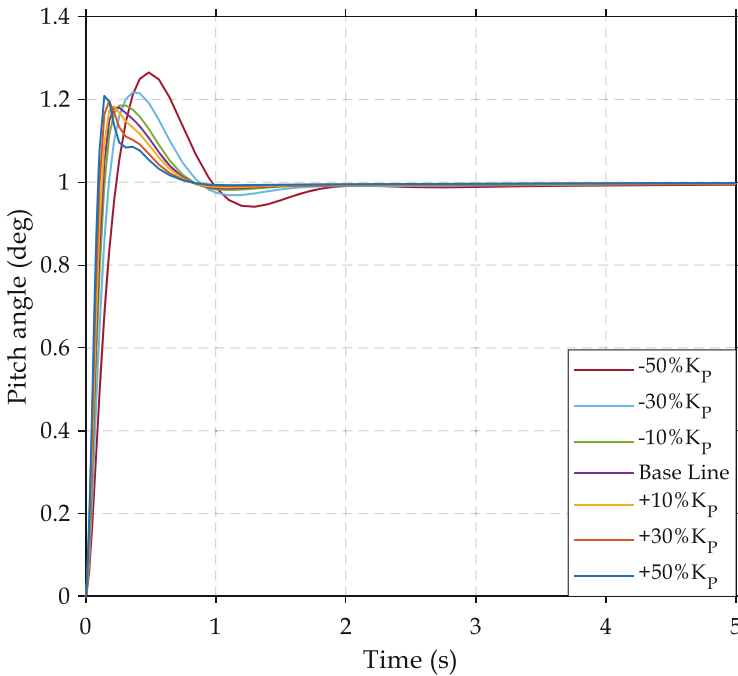


Fig. 4 Response of the UAV pitch angle with variations of P control (constant  $K_I$ )

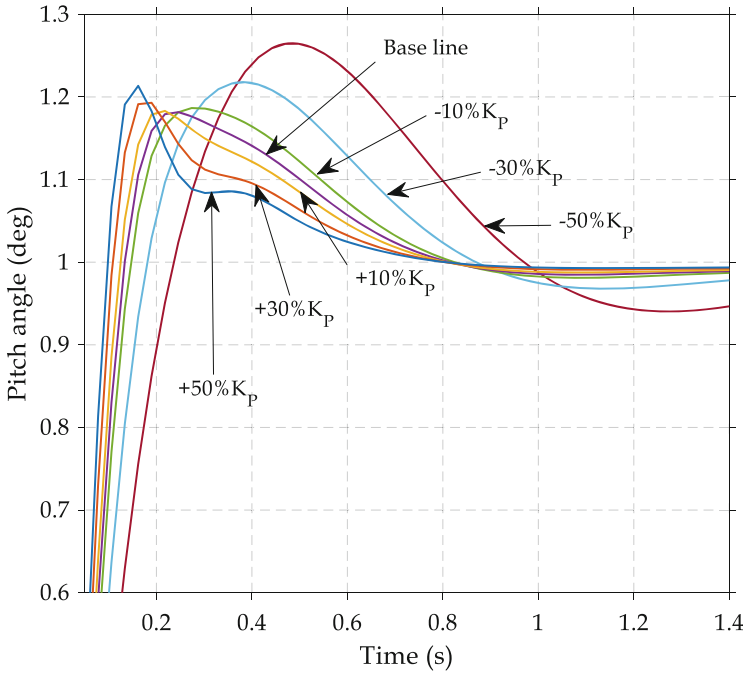


Fig. 5 Zoom-in view of the response of the UAV pitch angle with variations of P controller

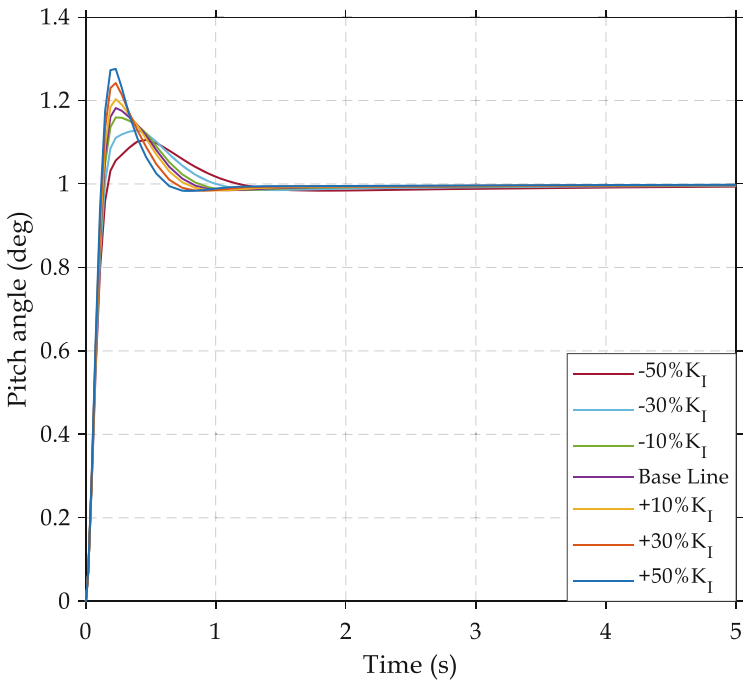


Fig. 6 Response of the UAV pitch angle with variations of I control (constant  $K_P$ )

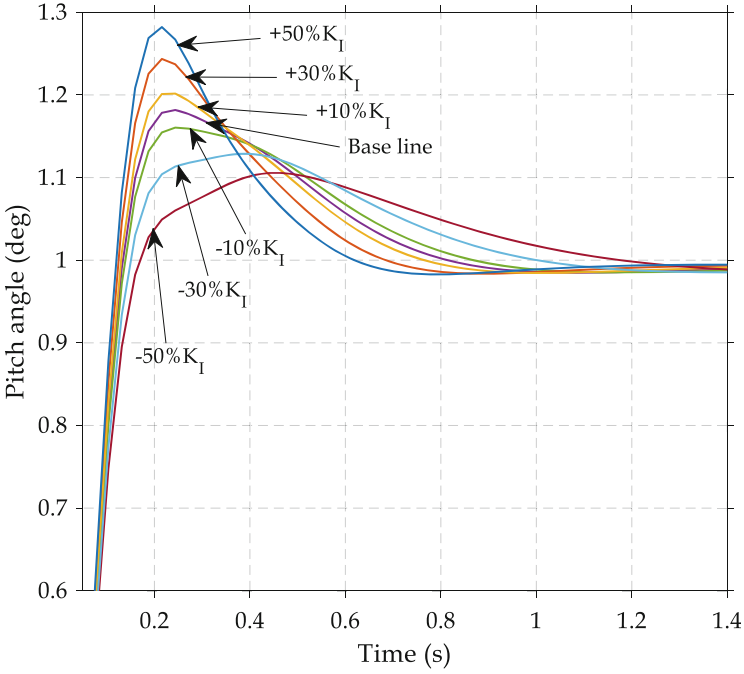


Fig. 7 Zoom-in view of the response of the UAV pitch angle with variations of I control

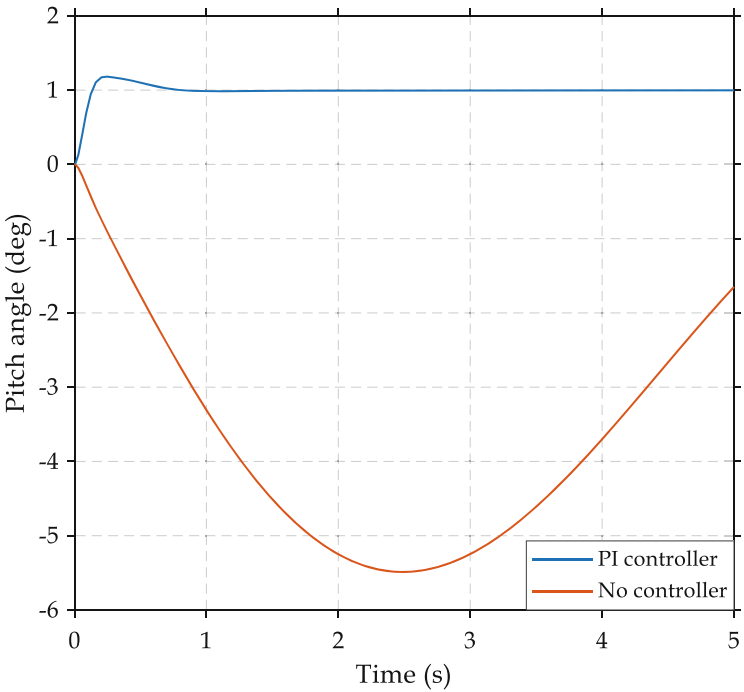


Fig. 8 Response of the UAV pitch angle with and without PI control



settling time is also suppressed to 0.713 s. Therefore, it is confirmed that the desired PI controller could reduce the overshoot and settling time of the system, leading to the improvement of UAV stability.

## 5 Conclusion

Fixed-wing UAVs easily lose stability when facing sudden disturbances. Disturbances can cause fixed-wing UAVs to lose control of direction and attitude. It can cause rapid changes in wing lift force, leading to the stalling of UAVs. Therefore, controlling the stability of the UAVs is a critical issue. To enhance the stability of the longitudinal dynamic system, the PI controller is applied to the UAV pitch angle system. The optimal gains of  $K_P$  and  $K_I$  are  $-2.5919$  and  $4.9355$ , respectively. To analyze the dynamics of the PI controller, the gains of  $K_P$  and  $K_I$  are varied by  $\pm 50\%$  of original values after the disturbance. It is found that the increasing  $K_P$  reduces rise time, overshoot, and settling time of the system. The increasing  $K_I$  reduces the rise time and settling time of the system, but it also increases the overshoot of the system. From the results, the PI controller can reduce the overshoot and settling time of the system. The optimal PI controller gives a faster response system than the system without the controller, leading to the improvement of the longitudinal stability of UAVs. In future work, the longitudinal stability system can be further extended to robust control to deal with more uncertain parameters in UAVs.

## References

- Ahmed, E., Ashraf, E., Ouda, A. N., & Hossam, A. (2015). Design of longitudinal motion controller of a small unmanned aerial vehicle. *International Journal of Intelligent Systems Technologies and Applications*, 7, 37–47.
- Amer, A., Jarrah, M. A., Ali, J., & Dhaouadi, R. (2009). ARF60 AUS-UAV modeling system identification, guidance and control validation through hardware in the loop simulation. In *2009 6th International symposium on mechatronics and its applications (ISMA09)*. IEEE.
- Andrei, P., Sergiu, O., Adriana, F., & Ștefan, G. R. (2018). Simple and digital implementation of PI controller used in voltage-mode control. In *2018 10th International conference on electronics, computers and artificial intelligence (ECAI)*. IEEE.
- Aziz, A. K., Yunfei, C., Nan, Z., et al. (2018). A survey of channel modeling for UAV communications. *IEEE Communications Surveys & Tutorials*, 20, 2804–2821.
- Brovchenko, D. V. (2015). Application features of UAVs different types. In *IEEE APUAVD proceedings* (pp. 26–29). IEEE.
- Chaoxing, Y., Jiankang, Z., & Jingjing, W. (2019). A comprehensive survey on UAV communication channel modeling. Special section on advances in statistical channel modeling for future wireless communications networks. *IEEE Access*, 7, 107769–107792.
- Chenggong, H., Qionglng, S., Pengfei, J., et al. (2009). Pitch attitude controller design and simulation for a small unmanned aerial vehicle. In *2009 International conference on intelligent human-machine systems and cybernetics*. IEEE.

- Erdal, K., Mojtaba, A. K., Jaime, R., & Mahmut, R. (2017). Learning control of fixed-wing unmanned aerial vehicles using fuzzy neural networks. *Hindawi International Journal of Aerospace Engineering*, 2017, 1–12.
- Hongru, J., Yuanqing, X., Rui, H., Dailiang, M., & Chenxi, H. (2019). A feedback linearization and saturated control structure for quadrotor UAV. In *IEEE proceedings of the 38th Chinese control conference* (pp. 8277–8282). IEEE.
- Jeongeun, K., Seungwon, K., Chanyoung, J., & Hyoung, I. S. (2019). Unmanned aerial vehicles in agriculture: A review of perspective of platform, control, and applications. IEEE special section on new technologies for Smart Farming 4.0: Research challenges and opportunities. *IEEE Access*, 7, 105100–105115.
- Jin, Z., Lijun, R., Huaxia, D., Mengchao, M., Xiang, Z., & Pengcheng, W. (2018). Measurement of unmanned aerial vehicle attitude angles based on a single captured image. *Sensors (Basel)*, 18, 2655.
- Jun, Y., Ximan, W., Simone, B., et al. (2019). A software-in-the-loop implementation of adaptive formation control for fixed-wing UAVs. *IEEE/CAA Journal of Automatica Sinica*, 6, 1230–1239.
- Junyu, L., Min, S., Ruiling, L., et al. (2020). Access points in the air: Modeling and optimization of fixed-wing UAV network. *IEEE Journal on Selected Areas in Communication*, 38, 2824–2835.
- Kiam, H. A., Gregory, C., & Yun, L. (2005). PID control system analysis, design, and technology. *IEEE Transactions on Control Systems Technology*, 13, 559–576.
- Lalitesh, K., Prawendra, K., & Subhojit, G. (2014). Design of PI controller: A multiobjective optimization approach. In *International conference on advances in computing, communications and informatics (ICACCI)* (pp. 834–838). IEEE.
- Michale, V. C. (2007). *Flight dynamics principles*. Butterworth-Heinemann Publications.
- Pakorn, P., Liuping, W., & Abdulghani, M. (2018). Gain scheduled attitude control of fixed-wing UAV with automatic controller tuning. *IEEE Transactions on Control Systems Technology*, 26, 1192–1203.
- Peter, W., et al. (2020). *Chemical process dynamics and controls, feedback control*. LibreTexts.
- Prithvi, K. C., Bhartiraja, C., & Lucian, M. (2021). A review on UAV wireless charging: Fundamentals, applications, charging techniques and standards. *IEEE Access*, 7, 69235–69266.
- Soliman, S. A., & Kandari, A. M. (2010). Mathematical background and state of the art. In *Electrical load forecastin* (pp. 1–44). Butterworth-Heinemann.
- Thongchart, K., Fathin, S. R., Veena, P., Masayuki, W., & Yasunori, M. (2018). Demonstration of virtual inertia emulation using energy storage systems to support community-based high renewable energy penetration. In *2018 IEEE global humanitarian technology conference (GHTC)*. IEEE.
- Thongchart, K., Masayuki, W., Yasunori, M., & Veena, P. (2019). Applying virtual inertia control topology to SMES system for frequency stability improvement of low-inertia microgrids driven by high renewables. *Energies*, 12, 3902.

# Effect of Work Shift Rotating on Fatigue Levels of Aircraft Mechanics in Line Maintenance



Monchai Suraratchai, Tutchakorn Siripanichsutha,  
and Pornnipa Voraprapaso

## 1 Introduction

The aviation industry was rapidly growing in recent years. High demand in aircraft usage along with competition push the need of aircraft mechanics to work as shift, especially the maintenance work that done daily at ramp area which are call the line maintenance. High pressure due to schedule induces stress and fatigue to mechanics.

Fatigue is generally referred to as a physiological condition, which causes a decrease in physical and mental performance. A consensus definition of fatigue is difficult. And it is generally accepted that fatigue and fatigue-related impairment are influenced by prior sleep history, work hours, workload, and length of time spent awake (Dorrian et al., 2011; Dawson & McCulloch, 2005). Measuring fatigue is subjective, and the rating scales are the only available tools to assess fatigue (Shahid et al., 2010). The Swedish Occupational Fatigue Inventory (SOFI) was developed to understand the concept of fatigue by measuring the subjective dimensions of work-related fatigue in different occupations (Åhsberg, 1998). SOFI consists of 20 expressions, distributed on the dimensions of lack of energy, physical exertion, physical discomfort, lack of motivation, and sleepiness (Åhsberg, 2000). Shift workers are at risk of fatigue or sleepiness caused by work-related fatigue, which was a result of insufficient restorative sleep due to circadian disruption (Costa, 1996; Hossain et al., 2003; Shen et al., 2006). Recovery durations are an important factor to reduce fatigue, since on the first day of the rest period, shift workers scored poorer on the sleep quality (Merkus et al., 2015).

“Shift work system” is introduced in aircraft maintenance process to respond to the rapidly growing aviation industry today and to be able to use resources and

---

M. Suraratchai (✉) · T. Siripanichsutha · P. Voraprapaso  
Department of Aerospace Engineering, Faculty of Engineer, Kasetsart University, Bangkok,  
Thailand  
e-mail: [monchai.s@ku.th](mailto:monchai.s@ku.th)

manpower for existing maintenance to be more efficient and cost-effective. It is used in scheduling operations in the aviation industry to change the time characteristics of the aviation personnel resulting in continuity in operations. Different shift systems are used, resulting in different fatigue (Åhsberg et al., 2000; Hakola & Härmä, 2001; Shen et al., 2006). Fatigue is part of human factors that will reduce human performance and increase the chance of accidents while performing maintenance work. It also causes negative effects on aircraft organizations or even aircraft technicians themselves. Thus, this study aims to evaluate the effect of work shift system on fatigue in order to improve shift management to reduce the risk of accidents that may occur from fatigue.

## 2 Method

### 2.1 Participants and Data Collection

The participants are aircraft mechanics working on the line maintenance at Don Mueang International Airport. The aircraft mechanics include 164 males and 20 females; the age distribution is 61 (33%) from 20 to 24 years old, 65 (35%) from 25 to 29 years old, 28 (15%) from 30 to 34 years old, and 30 (16%) older than 35 years old. There are three types of shift system examined in this research. Shift systems *P1* and *P2* are slow-rotating shifts, and shift system *P3* is a fast-rotating shift, and all shift systems are listed in Table 1.

### 2.2 Dependent Variables

**Fatigue** The paper used the Swedish Occupational Fatigue Inventory (SOFI) to assess fatigue level of the aircraft mechanics. The SOFI was developed by Åhsberg et al. (1997) to contribute to the understanding of the concept of fatigue by measuring the subjective dimensions of work-related fatigue in people from different

**Table 1** Shift system

No.	Shift system
<i>P1</i> (slow-rotating shift)	Two 12-h morning shifts Two 12-h night shifts Four days off
<i>P2</i> (slow-rotating shift)	Four 12-h night shifts Four days off
<i>P3</i> (fast-rotating shift)	Two 12-h morning shifts Two days off Two 12-h night shifts Two days off

occupations. The SOFI consists of 20 items belonging to the 5 dimensions: lack of energy (items: worn out, spent, drained, overworked), physical exertion (items: palpitations, sweaty, out of breath, breathing heavily), physical discomfort (items: tense muscles, numbness, stiff joints, aching), lack of motivation (items: lack of concern, passive, indifferent, uninterested), and sleepiness (items: falling asleep, drowsy, yawning, sleepy). The feelings of being tired are graded from 0 (not had such feelings at all) to 6 (had such feelings to a very high degree). Lack of energy is general qualitative fatigue which reflects both the physical (the factors of physical exertion and physical discomfort) and mental (the factors of lack of motivation and sleepiness) (Åhsberg et al., 2000). In this study, the SOFI dimension was translated to local language and was proven by expertise in human factor and high experience mechanics. The pilot test was conducted to verify the reliability with Cronbach's alpha ( $\alpha$ ), which was measured as 0.861.

### 2.3 *Independent Variables*

**Shift system** The duration of work shifts that is designed to cover the day is usually either 8 h or 12 h; however, the aircraft line maintenance mostly uses 12 h shift work. Three types of shift system were examined in this study: two shift systems (*P1* and *P2*) are classified as slow-rotating shift and the other (*P3*) is fast-rotating shift.

**Sleep durations** Sleep is a mechanism to recover from work-related fatigue. The study of Dorrian (2011) suggests that sleep duration less than 5 h or more than 16 h of wakefulness can significantly increase the likelihood of fatigue. This study collected sleep duration by dividing into three groups: less than 5 h, 5 h–8 h, and more than 8 h.

**Work experience** Work experience represents the duration that participants experience in shift work. Higher work experience means higher duration in shift system.

### 2.4 *Statistical Analysis*

Descriptive statistics were used to obtain a simple measure of each dimension, a mean of five SOFI fatigue ratings. Analysis of variance (ANOVA) and two-way analysis of variance and analysis of covariance (ANCOVA) were performed on the data collected to test the differences between groups (shift system and work experience).

### 3 Results and Discussion

#### 3.1 Participant Demographics

Difference in participant demographic and work-related background variables between the shift pattern groups is shown in Table 2. Most of the participants were male due to the nature of job. Shift systems *P1* (49 participants) and *P2* (52 participants), which are slow-rotating shifts, are equal to 55% of samples, and shift system *P3* (83 participants) is 45% of samples.

#### 3.2 Difference Between Shift Systems

Results show that shift systems *P1* and *P2*, which are slow-rotating shifts, have the higher rating in lack of energy dimension than shift system *P3*, which is a fast-rotating shift. But, in the lack of motivation and sleepiness dimensions, the rating from shift systems *P1* and *P2* (slow-rotating shift) is less than shift system *P3* (fast rotating), as shown in Table 3. Analysis of variance (ANOVA) is used to test the differences, and the results show that the difference between shift systems *P1* (swing shift: 2 day shifts and two night shifts) and *P2* (permanent shift: four night shifts) was not significant. This result is consistent with the finding from Merkus et al. (2015) that the swing shift had no effect on fatigue.

But the fatigue was affected by the shift rotating system, as found in the study of Hakola, T., and Härmä, M. (2001). Fast-rotating shift had less fatigue in terms of lack of energy ( $P3 < P2$ ). However, some contradictions had been found, and the

**Table 2** Demographic characteristics within each shift pattern

		Shift system						Total	
		<i>P1</i> (slow rotating)		<i>P2</i> (slow rotating)		<i>P3</i> (fast rotating)			
Total		49	(27%)	52	(28%)	83	(45%)	184	(100%)
Gender	M	38	(21%)	46	(25%)	80	(43%)	164	(89%)
	F	11	(6%)	6	(3%)	3	(2%)	20	(11%)
Age (years old)	20–24	15	(8%)	11	(6%)	35	(19%)	61	(33%)
	25–29	20	(11%)	21	(11%)	24	(13%)	65	(35%)
	30–34	3	(2%)	8	(4%)	17	(9%)	28	(15%)
	>35	11	(6%)	12	(7%)	7	(4%)	30	(16%)
Work experience (years)	<2	13	(7%)	11	(6%)	28	(15%)	52	(28%)
	2–4	12	(7%)	8	(4%)	29	(16%)	49	(27%)
	>4	24	(13%)	33	(18%)	26	(14%)	83	(45%)
Sleep duration	<5 h	6	(3%)	15	(8%)	5	(3%)	26	(14%)
	5–8 h	37	(20%)	35	(19%)	53	(29%)	125	(68%)
	>8 h	6	(3%)	2	(1%)	25	(14%)	33	(18%)

**Table 3** Demographic characteristics within each shift pattern

SOFI fatigue dimension	<i>P1</i> (slow); <i>n</i> = 49		<i>P2</i> (slow); <i>n</i> = 52		<i>P3</i> (fast); <i>n</i> = 83		Total; <i>n</i> = 184		<i>F</i> ; <i>df</i> = 2	<i>p</i>
	Mean (SD)	Mean (SD)	Mean (SD)	Mean (SD)	Mean (SD)	Mean (SD)	Mean (SD)	Mean (SD)		
Lack of energy	3.7 (0.9)	4.1 (1.1)	3.5 (1.6)	3.7 (1.4)	3.809	0.024* ( <i>P2</i> > <i>P3</i> )				
Physical exertion	2.2 (1.2)	2.6 (1.4)	2.7 (1.8)	2.6 (1.6)	1.494	0.227				
Physical discomfort	2.3 (1.3)	2.6 (1.4)	2.6 (1.8)	2.5 (1.6)	1.007	0.367				
Lack of motivation	1.7 (1.5)	2.1 (1.3)	2.7 (1.9)	2.2 (1.7)	5.982	0.003* ( <i>P1</i> < <i>P3</i> )				
Sleepiness	2.7 (1.5)	3.2 (1.5)	3.7 (1.7)	3.3 (1.6)	6.290	0.002* ( <i>P1</i> < <i>P3</i> )				

Remark: \**p* < 0.05

result in this study shows that the slow-rotating shift is more suitable to reduce the mental fatigue, and age of population and shift pattern may be the reason of difference.

### 3.3 Effect of Work Shift Rotating and Work Experience

Some studies have shown that gender also had an effect on fatigue (Åhsberg, 2000); however, there is a small amount of female sampling in shift system *P3*, and to exclude the effect of gender and prevent bias result, only male respondents were considered. The fatigue rating of shift systems *P1* and *P2* had been merged as the slow-rotating shift and was compared to the fast-rotating shift. Two-way analysis of variance and analysis of covariance (ANCOVA) was used to study the different five fatigue dimensions of two independent variables (work experience and shift rotating), while sleep duration was used as covariate.

The results are shown in Table 4. It demonstrates that there is no difference in lack of energy dimension, but both physical fatigue (physical exertion and physical discomfort dimensions) and mental fatigue (lack of motivation and sleepiness dimensions) ratings of the slow-rotating shift are significantly less than the fast-rotating shift. Since the fast-rotating shift has less recovery duration, this may be the main factor (Merkus et al., 2015) that causes higher fatigue.

Lack of energy and physical fatigue (physical exertion and physical discomfort) are also dependent on the work experience. As shown in Fig. 1, work experience between 2 and 4 years has experience in highest level of lack of energy and physical fatigue (physical exertion and physical discomfort). A correlation exists between work experience and the fatigue rating; however, whether this correlation is causal cannot be concluded.

**Table 4** Significant test of SOFI fatigue dimensions of work experience and shift rotating

SOFI fatigue dimension		Work experience	Shift rotating	Work experience × shift rotating
Lack of energy	<i>F</i>	5.018	1.094	3.343
	<i>p</i>	0.008*	0.297	0.038*
Physical exertion	<i>F</i>	4.451	7.862	1.313
	<i>p</i>	0.013*	0.006*	0.272
Physical discomfort	<i>F</i>	5.136	6.119	1.506
	<i>p</i>	0.007*	0.014*	0.225
Lack of motivation	<i>F</i>	1.400	20.381	2.104
	<i>p</i>	0.250	0.000*	0.125
Sleepiness	<i>F</i>	1.236	10.723	1.476
	<i>p</i>	0.293	0.001*	0.232

Remark: \**p* < 0.05

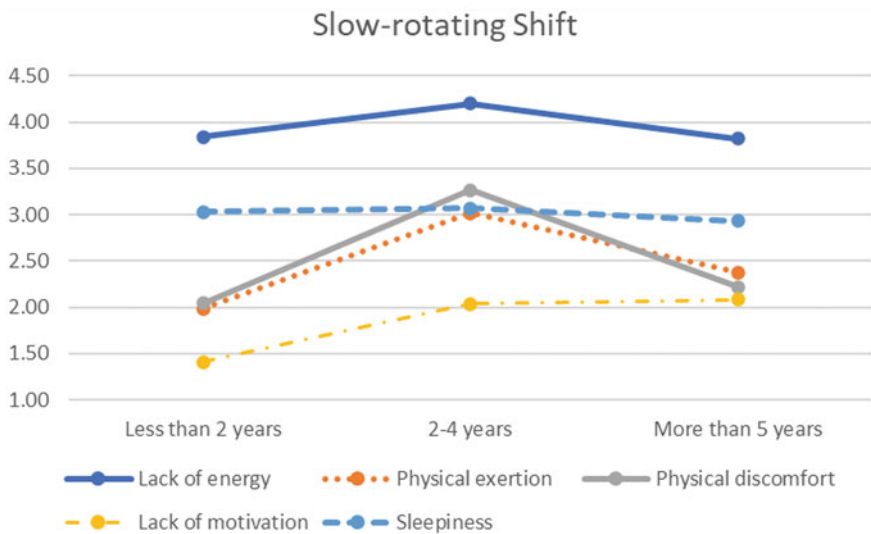


**Fig. 1** SOFI fatigue dimensions of work experience for slow-rotating shift

Considering the interaction between work experience and shift rotating, the high work experience with fast-rotating shift and the fatigue rating in lack of energy tended to increase significantly. This reflects that high exposure to fast-rotating shift can cause high level of fatigue rating in lack of energy (Fig. 2).



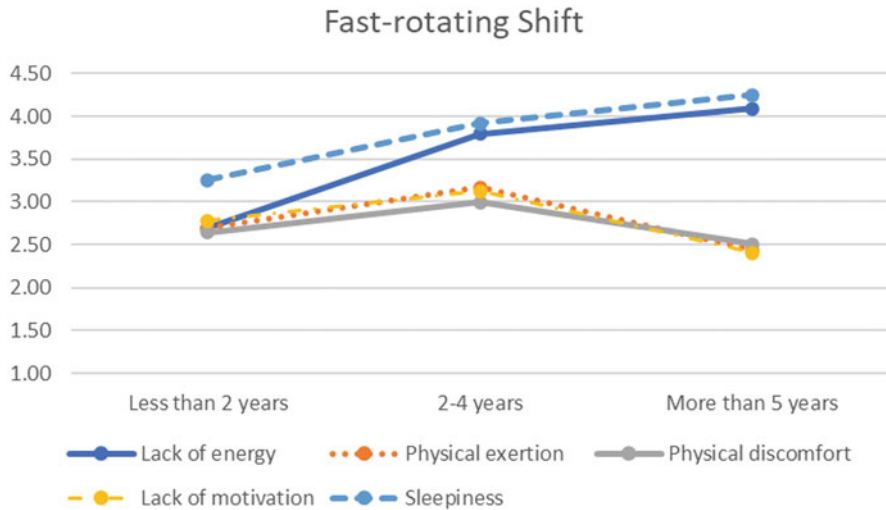


Fig. 2 SOFI fatigue dimensions of work experience for fast-rotating shift

### 3.4 Limitation

There are some limitations to the current study that must be noted. First, this study focused on subjective fatigue, and no objective performance indicators were analyzed for this study. Such measures may be of benefit, particularly access to performance record, incidents, accidents, or near-misses. These data would have been of benefit had they been available. Second, case study was selected from two companies, although these two companies were quite similar in terms of location and operations, but there may be some latent factors that cannot be controlled in this study. Generalization should be done with caution.

Finally, the Swedish Occupational Fatigue Inventory (SOFI) was chosen for this study as it has been validated (Åhsberg et al., 2000) and widely used (Shen et al., 2006) and was considered to be the optimal choice at the time the studies were conducted. Other tools that are available could be used to compare and confirm the results of the study.

## 4 Conclusion

In conclusion, the fast-rotating shift had more negative impact on physical fatigue and mental fatigue than slow-rotating shift. Overall fatigue in slow-rotating shift was higher than fast-rotating shift due to the extended shift work, but the difference was not statistically significant. Extended shift work might have a negative effect on overall fatigue and physical fatigue; especially, extended fast-rotating fatigue might increase significantly than overall fatigue.

Finally, this research contributes to the understanding of the effect of shift rotating on subjective fatigue. Therefore, in shift system design, the recovery durations might be one of the main factors to reduce risk of work-related fatigue.

**Acknowledgments** The authors acknowledge aircraft mechanics who participated and the companies who distributed surveys. Assistance in the distribution of the surveys was provided by the Thai Air Asia and Thai Lion Air.

## References

- Åhsberg, E. (1998). *Perceived fatigue related to work*. Arbetslivsinstitutet.
- Åhsberg, E. (2000). Dimensions of fatigue in different working populations. *Scandinavian Journal of Psychology*, *41*, 231–241.
- Åhsberg, E., Garnberale, F., & Kjellberg, A. (1997). Perceived quality of fatigue during different occupational tasks development of a questionnaire. *International Journal of Industrial Ergonomics*, *20*(2), 121–135.
- Åhsberg, E., Kecklund, G., Åkerstedt, T., & Gamberale, F. (2000). Shiftwork and different dimensions of fatigue. *International Journal of Industrial Ergonomics*, *26*, 457–465.
- Costa, G. (1996). The impact of shift and night work on health. *Applied Ergonomics*, *27*(1), 9–16.
- Dawson, D., & McCulloch, K. (2005). Managing fatigue: It's about sleep. *Sleep Medicine Reviews*, *9*(5), 365–380.
- Dorrian, J., Baulk, S. D., & Dawson, D. (2011). Work hours, workload, sleep and fatigue in Australian Rail Industry employees. *Applied Ergonomics*, *42*(2), 202–209.
- Hakola, T., & Härmä, M. (2001). Evaluation of a fast forward rotating shift schedule in the steel industry with a special focus on ageing and sleep. *Journal of Human Ergology*, *30*(1–2), 315–319.
- Hossain, J. L., Reinish, L. W., Kayumov, L., Bhuiya, P., & Shapiro, C. M. (2003). Underlying sleep pathology may cause chronic high fatigue in shift-workers. *Journal of Sleep Research*, *12*(3), 223–230.
- Merkus, S. L., Holte, K. A., Huysmans, M. A., van de Ven, P. M., van Mechelen, W., & van der Beek, A. J. (2015). Self-reported recovery from 2-week 12-hour shift work schedules: A 14-day follow-up. *Safety and Health at Work*, *6*(3), 240–248.
- Shahid, A., Shen, J., & Shapiro, C. M. (2010). Measurements of sleepiness and fatigue. *Journal of Psychosomatic Research*, *69*(1), 81–89.
- Shen, J., Botly, L. C. P., Chung, S. A., Gibbs, A. L., Sabanadzovic, S., & Shapiro, C. M. (2006). Fatigue and shift work. *Journal of Sleep Research*, *15*, 1–5.

# Strength Analysis of a Wing Structure for a Single Turboprop Normal Category Aircraft



Vis Sripawadkul  and Phacharaporn Bunyawanichakul

## 1 Introduction

Developing an aircraft involves a lot of effort regarding the market, technical data, commercial analysis, payload, range, and mission. The aviation sector had been growing rapidly prior to the pandemic in 2019 that has had a major impact not only on aviation but also on the world economy. Now, after almost 2 years, the general aviation sector has started to make a good recovery. The General Aviation Manufacturers Association recently released its aircraft shipment report that indicated a 45.4% increase in turboprop aircraft in the first 6 months of 2021 compared to the same period in 2020, as the highest growth among all types (Table 1).

The objective of this study was to develop a wing geometric model (3D) and perform structural analysis to determine the wing structural requirements and mass for a single turboprop aircraft in the normal category according to 14 Code of Federal Regulations (CFR) Part 23. These requirements are:

- Symmetrical positive and negative limit maneuvering load factor
- Mid-wing stiffness: wing tip displacement <5% of the wing's half span
- Wing mass estimation <12% of maximum take-off weight
- Margin of safety >0.5

In this study, the simplified model of the wing structure was composed of a single box-shaped spar, ribs, and skin with some cutouts excluding stringers and dimensions of control surfaces. The analysis was performed using aluminum as the material, with its structural response for overall strength and tip deformation obtained using finite element analysis.

---

V. Sripawadkul · P. Bunyawanichakul (✉)  
Kasarsart University, Bangkok, Thailand  
e-mail: [fengvisp@ku.ac.th](mailto:fengvisp@ku.ac.th); [phacharaporn.b@ku.ac.th](mailto:phacharaporn.b@ku.ac.th)

**Table 1** First half aircraft shipments and billings

Aircraft type	2020	2021	% change
Piston airplanes	503	565	+12.3%
Turboprops	152	221	+45.4%
Business jets	244	264	+8.2%
Total airplanes	899	1050	+16.8%
Total airplane billing	\$7.9B	\$8.6B	+9.4%
Piston helicopters	63	83	+31.7%
Turbine helicopters	194	258	+33%
Total helicopters	257	341	+32.7%
Total helicopter billing	\$1B	\$1.4B	+37.7%

Source: General Aviation Manufacturers Association

## 1.1 Wing External Geometry

The aircraft had the following specifications:

• Maximum take-off weight	2200 lbs
• Basic empty weight	990 lbs
• Maximum usable fuel	616 lbs
• Maximum usable load	264 lbs
• Engine power	240 hp
• Take-off	1312 ft
• Take-off over 50 ft obstacle	1968 ft
• Climb rate	3000 ft/min
• Maximum operating altitude	28,000 ft
• Stall speed with flaps	61 KCAS
• Maximum cruise speed	320 KTAS
• Landing ground roll	1148 ft
• Wingspan	28.5 ft
• Length	21.0 ft
• Height	8.92 ft
• Cabin width	4.13 ft
• Wing area	95.1 ft <sup>2</sup>
• Taper ratio	0.6
• Airfoil	NACA 65 <sub>2</sub> -415

The wing structural mass was 264 lbs, with the wing incidence angle at root 3 degrees with a  $-3$ -degree twist angle.

## 1.2 Forces on the Wing

### 1.2.1 Aircraft Flight Envelope (Gust Included)

Referring to Title 14 Code of Federal Regulations (CFR) Part 23, the maximum positive and negative load factors for the normal category are +3.8 and  $-1.5$ , respectively. The stall speed was determined at the corresponding maximum lift coefficient of the NACA 65<sub>2</sub>-415 airfoil (Airfoil Tools, 2021), while the dive speed was 1.4 times the cruise speed. Gust wind speeds of 50 and 25 fps were included to determine the load factors at cruise speed and dive speed, respectively. The combined flight envelope is shown in Fig. 1.

### 1.2.2 Critical Forces and Moments

Spanwise lift distribution was calculated using the lifting-line theory initially developed by Prandtl (Sadraey, 2013). First, the wing was divided into  $N$  segments along the span with each corresponding angle  $\theta$ , as shown in Fig. 2.

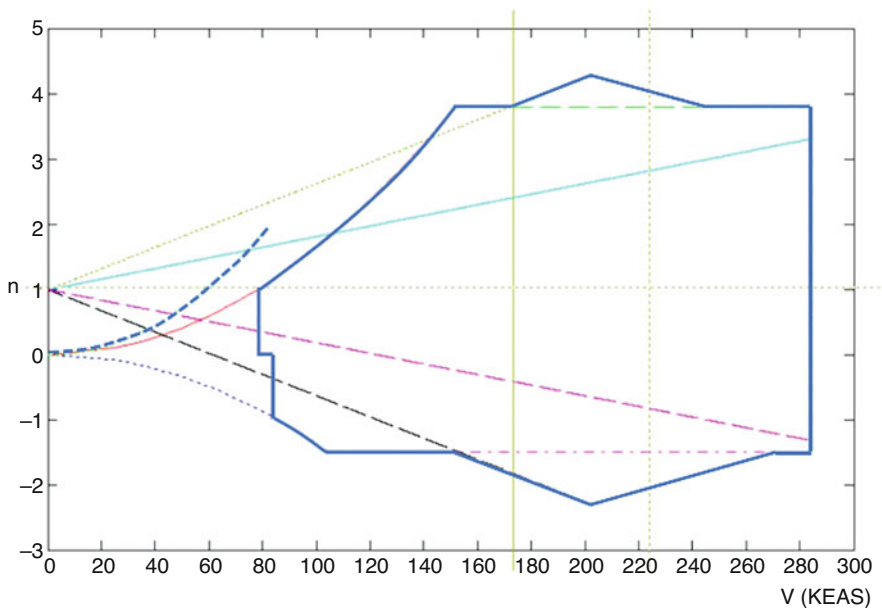


Fig. 1 Combined flight envelope

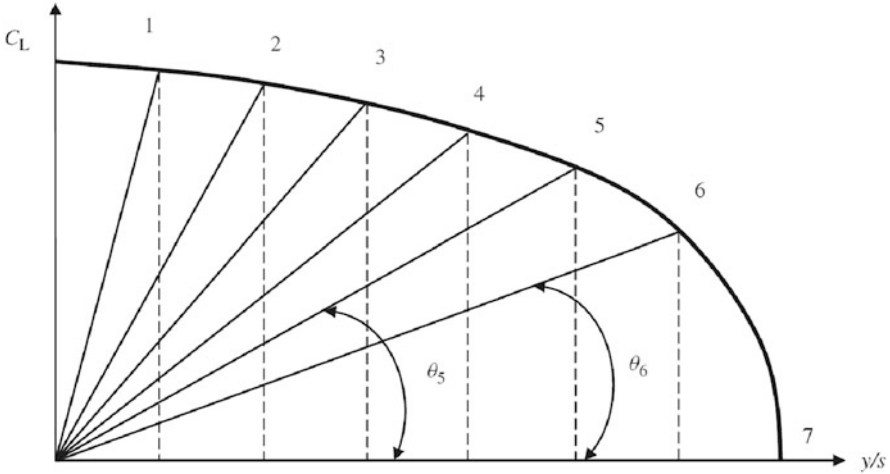


Fig. 2 Angles corresponding to each segment in lifting-line theory

The aim was to solve for coefficients  $A_1$  to  $A_n$  using the following equation:

$$\mu(\alpha - \alpha_0) = \sum_{n=1}^N A_n \sin(n\theta) \left(1 + \frac{\mu n}{\sin\theta}\right) \tag{1}$$

where  $\alpha$  is the segment's angle of attack and  $\alpha_0$  is the segment's zero-lift angle of attack. The parameter  $\mu$  is defined as:

$$\mu = \frac{C_i C_{l,\alpha}}{4b} \tag{2}$$

where  $C_i$  is the segment's mean geometric chord,  $C_{l,\alpha}$  is the segment's lift curve slope, and  $b$  is the wingspan. Each segment's lift coefficient was finally determined using the equation:

$$C_{Li} = \frac{4b}{C_i} \sum A_n \sin(n\theta) \tag{3}$$

The shear force and bending moments due to wing structure weight and lift were calculated along spanwise positions at the maximum load factor and with a margin of safety of 0.5 for two flight conditions: cruise and dive. The results of the level flight condition ( $n = 1$ ) are shown in Fig. 3, where the critical shear force and bending moment occur at a dive condition corresponding to 4407 lbs and 312,555 in-lb compared to 2207 lbs and 155,970 in-lb for the dive and maximum cruise speed, respectively. These loads were used as requirements for the wing structure design in the later simulation.

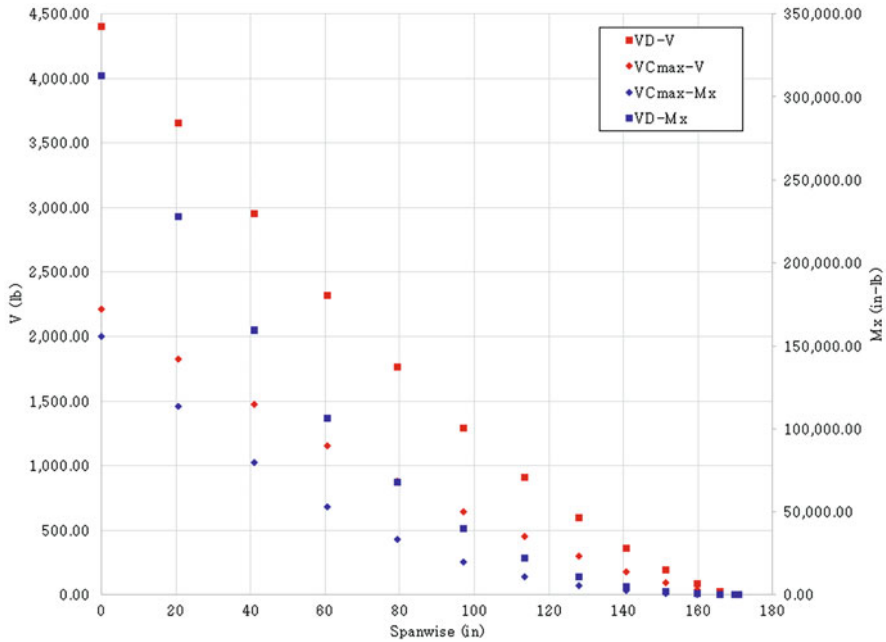


Fig. 3 Wing-bending moment diagram at  $n = 1$

## 2 Wing Structure Analysis

### 2.1 Wing Structural Layout

Only the half wing was modeled due to the symmetry related to the mid-fuselage. The wing model was developed with constant taper and twist and used 7075T6 aluminum sheets, with its material properties shown in Table 2. All wing components in the model were initially developed based on the available thicknesses of the sheet: 0.04", 0.063", and 0.125" (Aircraft Spruce, 2021).

From the wing loading calculation above, all wing components were initially designed and sized using basic theory (Megson, 1999; Brandt et al., 2004) within the framework. Then, several simplified models were developed. For each model, the structural response was simulated and analyzed to fulfill the objectives of this study in terms of strength, deformation, and weight. The wing components were finalized under a skin surface consisting of a single spar and nine ribs (Fig. 4). The spar box running along the wingspan had its center located at 40% of the chord. All ribs were set with uneven spacing according to the non-uniform load distribution with some lightening holes. The model was prepared as a surface with no defined thickness, which was later identified in the pre-processing tool.

**Table 2** Properties of 7075T6 aluminum sheet

Property	Value
Density, lb/in <sup>3</sup>	0.101518
Young's modulus, Msi	10
Poisson's ratio	0.33
Yield strength, ksi	64
Ultimate tensile strength, ksi	75

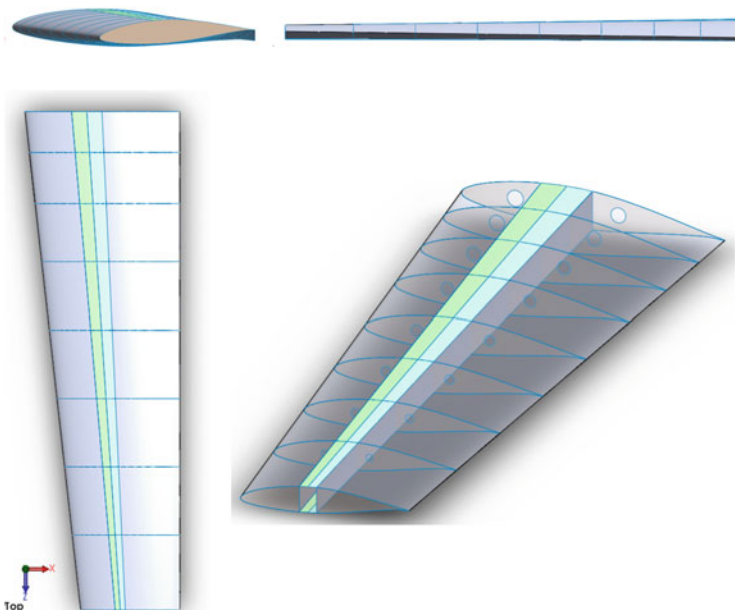


**Fig. 4** Wing model from top, side, front, and 3D view

## 2.2 Thickness Attribution

From the wing simplified model, all wing components were created as 2D shells. The thickness of each part was defined using different colors, as shown in Fig. 5. The identification of the shell type was “thick” when attributing the material to each surface. All skins had a thickness of 0.04”, and the spar webs had a thickness of 0.125”. The thickness of the spar flanges corresponding to bays 1 to 3 from the wing root used three layers of 0.125” aluminum plate, while the rest of the flanges had only two layers. The four ribs on the root side had a thickness of 0.063”, while the rest had a thickness of 0.04”. The total structural weight was estimated to be 117.97 lbs, which was less than the wing mass estimation (132 lbs).



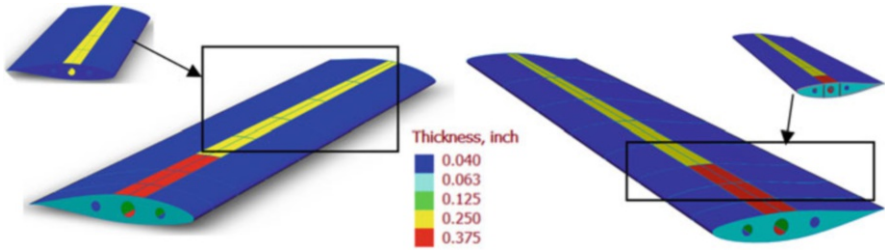


**Fig. 5** Thickness of each surface: from top view (left) and bottom isometric view (right)

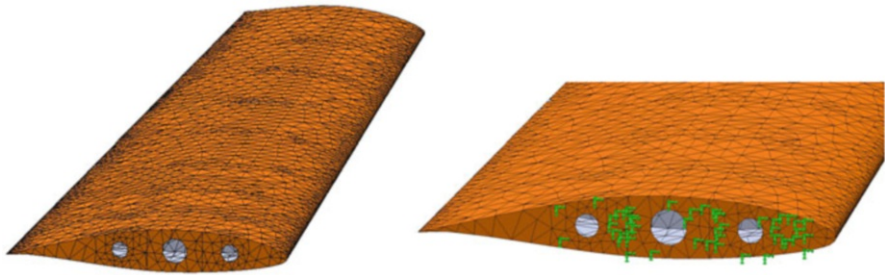


**Fig. 6** Wing structure mesh (left) and boundary condition as cantilever beam (right)

### 2.3 Meshing

All surfaces were divided into several small elements using a curvature-based mesh. The maximum and minimum element sizes were 3" and 1", respectively. The general shape of the mesh for the whole wing is shown in Fig. 6. (left) and shows that the outer surface of the model meshing was smooth enough to perform the calculation. The orange color represents the bottom surface of the element, while gray represents the top surface of the element.

### 2.4 Boundary Conditions

The wing structure was considered as a cantilever boundary condition. The root location was fixed throughout the root rib boundary with no rotation and no displacement to simulate the mounting location to the fuselage as shown by green color in Fig. 6 (right).

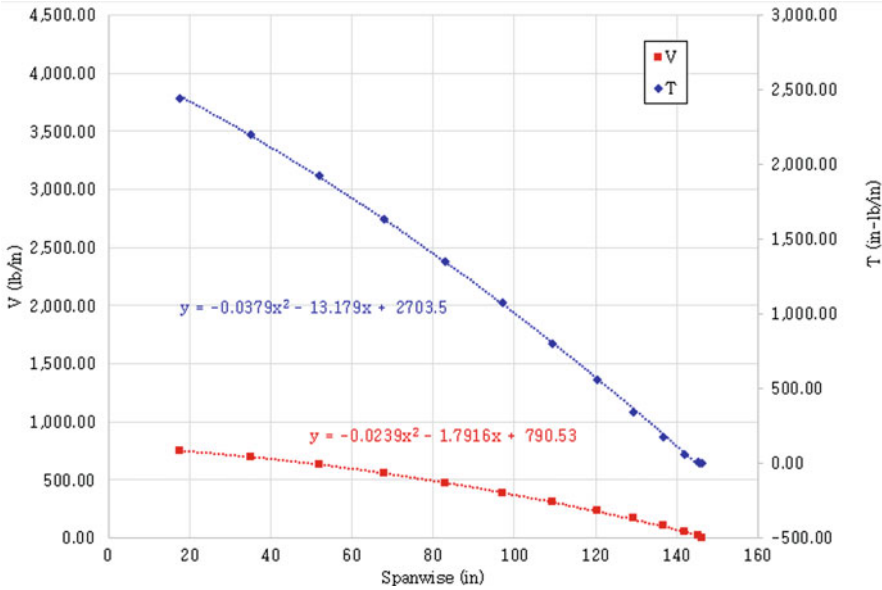


Fig. 7 Shear and torsion along spanwise direction

### 2.5 Shear Forces and Torsions

The force identified in the previous calculation was applied to the wing model, which was fixed at the root edge as a cantilever beam boundary condition. Figure 7 shows the shear and torsion distribution acting on the wing along a spanwise direction (the  $z$  axis as defined in the model).

At a dive speed with the maximum load factor ( $n = 3.8$ ), the total shear force applied on the wing structure was 16,747 lbs. The shear force ( $V$ ) was varied along the  $z$ -direction using the reference coordinates, which were originally located at 40% of the chord length, and was calculated using the equation:

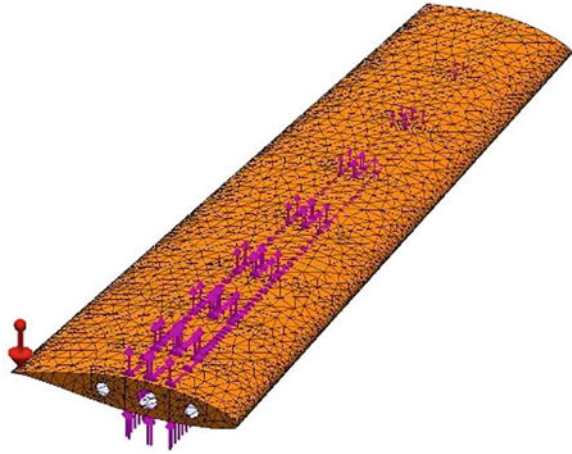
$$V(z) = -2.39 \times 10^{-2}z^2 - 1.792z + 790.53 \tag{4}$$

In the same manner, the pitching moment distribution function was applied to the wing spar about 40% of the chord length with a total intensity of 57,762 in-lb using the equation:

$$T(z) = -3.79 \times 10^{-2}z^2 - 13.18z + 2704 \tag{5}$$

Both the shear and torsion functions were applied to the structure using the non-uniform distribution command. The analysis was performed including gravitational force, as shown in Fig. 8.

**Fig. 8** Shear, torsion, and structural body force applied on the structure



### 3 Results and Discussion

Static structural analysis was performed, and the outputs in terms of Von Mises stress and displacement are shown in Fig. 9 (left) and Fig. 9 (right), respectively. It was clear that the Von Mises stress was locally high at the wing root because this was the fixed end location from the defined boundary condition. There were some localized stresses at the skin, spar, and rib connection, but the intensity of the stress was not severe. The stress contour showed the region having a margin of safety of 0.5 at the wing-fuselage junction. This region could be reinforced during the manufacturing process.

It was noted that the maximum displacement of 6.48" occurred at the wing tip which satisfied the constraint of being less than 5% of the wing's half span. The wing gradually twisted and deformed along its spanwise direction.

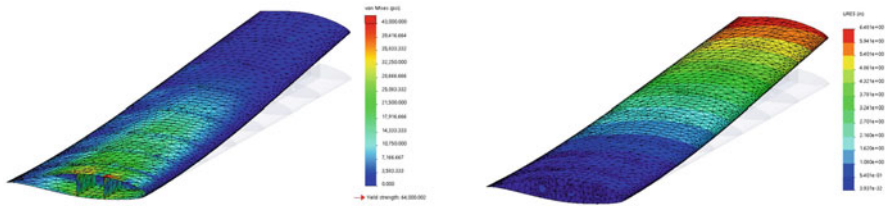


Fig. 9 Von Mises stress of the wing (left) and wing displacement (right)

## 4 Conclusion and Future Work

Based on the information presented in the flight envelope and the critical wing loading, an initial wing structure was developed that met all aircraft structural and operational requirements according to Title 14 Code of Federal Regulations (CFR) Part 23. The simplified model developed successfully achieved the objectives of this study in terms of strength, displacement, and weight. Further study could include:

- Analysis to include stringers, cutouts, and control surfaces
- Detail design in the high stress concentration region
- Wing design and optimization
- Buckling analysis
- Flutter analysis
- Composite material replacement
- Unsymmetrical flight condition
- Construction and testing of individual components for structural integrity behavior

## References

- Aircraft Spruce. *General aluminum information*. <https://www.aircraftspruce.com/catalog/mepages/aluminfo.php/>. Accessed on 10 Mar 2021.
- Airfoil 652-415. (2021). *Airfoil tools*. [Online]. Available: <http://airfoiltools.com/airfoil/details?airfoil=naca652415-il>. Accessed on 1 Mar 2021.
- Brandt, S. A., Stiles, R. J., Bertin, J. J., & Withford, R. (2004). *Introduction to aeronautics: A design perspective* (2nd ed.). AIAA Educational Series.
- “GAMA”, General Aviation Manufacturers Association. <https://gama.aero/news-and-events/press-releases/gama-publishes-second-quarter-2021-aircraft-shipments-and-billings-report/>. Accessed on 13 Sept 2021.
- Megson, T. (1999). *Aircraft structures for engineering students* (3rd ed.). Elsevier.
- Sadraey, M. H. (2013). *Aircraft design: A systems engineering approach*. Wiley.

# Applying Glass Fiber-Reinforced Composites with Microsphere Particles to UAV Components



Veena Phunpeng, Wipada Boransan, and Thongchart Kerdphol

## Nomenclature

GC	Glass fiber chopped strand mat
GM	Glass microsphere
GP	Glass fiber plain-woven fabric
UAV	Unmanned aerial vehicle
wt%	Percent of weight

## 1 Introduction

UAVs are widely employed in urban and remote areas due to their specific ability. UAVs are developed and improved to provide better responsiveness by using mathematical models (i.e., fuzzy control system, PID control) and equipping them with mission-specific equipment to perform a variety of missions (Sudtachat et al., 2017; Kerdphol et al., 2021; Phunpeng & Kerdphol, 2021). The structure and surface of the UAV must be lightweight to reduce the load on the UAV, leading to longer operating and more productive UAVs.

The design and material selection for UAV manufacturing has a significant impact on operational efficiency. Polymer-based composites have strength-to-

---

V. Phunpeng (✉) · W. Boransan  
School of Mechanical Engineering, Institute of Engineering, Suranaree  
University of Technology, Nakhon Ratchasima, Thailand  
e-mail: [veenap@g.sut.ac.th](mailto:veenap@g.sut.ac.th)

T. Kerdphol  
Department of Electrical Engineering, Faculty of Engineering, Kasetsart University, Bangkok,  
Thailand

weight advantages over other materials. As a result, polymer-based composites are used to make various parts for UAVs including landing gear and wings. Reinforcement fibers such as carbon, aramid, and glass fibers are also employed in polymer composite materials. According to Wong et al., plain weave laminates have higher tensile, bending, and inter-sheet shear strength than chopped strand mat (Wong et al., 2018).

One approach to improve composite properties is to combine fibers with fillers. Carbon nanotubes and glass microspheres have been widely used as fillers to enhance characteristics and satisfy application requirements (Megahed & Megahed, 2017; Phunpeng & Baiz, 2015). To reduce the cost of composite components, accessible fillers might be utilized. Glass microspheres (GM) are used in the epoxy matrix because they have a lower density than epoxy, resulting in a lighter product. The fracture and impact behavior of hollow microsphere/epoxy resin composites were investigated by Kim et al. The results show that the amount of GM content affects the properties of composite materials (Kim & Khamis, 2001). J.A.M. Ferreira studied the mechanical performance of epoxy matrix composites using hollow glass microsphere fillers and short fiber reinforcement. According to previous research, increasing the filler content in unreinforced composites reduces the flexural impact including absorbed energy (Ferreira et al., 2010; Huichao et al., 2018).

A multitude of techniques may be used to manufacture composite materials. Hand lay-up comes out as a standout approach due to its inexpensive cost and less complex technology (Chandramohan et al., 2019). In terms of cost and time reduction, the hand lay-up method is the most outstanding choice in student UAV. Mohan et al. present a hand lay-up technique using glass fibers and polyester resins. According to the results, the composite had an ultimate tensile strength of 306 MPa, flexural stress of 209 MPa, and impact strength of 151 MPa (Mohan et al., 2018). In terms of production, vacuum bagging techniques are equivalent to hand lay-up. Vacuum is used to aid in resin dispersion (Arpitha et al., 2017; Saensuriwong et al., 2021). This study presents a hand lay-up and vacuum bagging process at 100 °C to fabricate glass fiber-reinforced laminated composites with GM. The flexural characteristics of glass fiber-reinforced laminate composites with GM were compared. The flexural characteristics of the specimens fabricated are investigated by a universal testing machine (UTM).

## 2 Method

This section covers the materials utilized in composite fabrication, manufacturing process, and flexural testing according to ASTM D790.

## 2.1 Material Preparation

Chopped strand mats are randomly oriented and have similar strength in all directions. Chopped strand mats are less expensive than plain weave mats and have a lower strength. Because of its flexibility and strength, a plain weave mat is ideal for reinforcing materials. Glass fibers in the form of chopped strands and plain weave mats are used as reinforcing materials in this experiment, and ER550 epoxy resin and hardener are used as a matrix. Glass microspheres (GM) are used as a filler particle to evaluate the flexural properties when the filler content is modified.

## 2.2 Experiment Preparation

The polymer composite is produced by mixing the particles with epoxy resin (0%, 5%, 10%, and 15% by weight) and stirring by hand for 30 minutes with a glass rod before adding the hardener (100:35). Fiber-reinforced plastic laminates consist of eight layers of glass fiber oriented in the direction of  $[0]_8$ , following the hand lay-up approach. The curing temperature will be varied to perform the vacuum bagging process. The peel ply collects any excess resin before a vacuum pump connection to press the resin at  $-0.8$  bar pressure. The temperature at  $100$  °C is used in the curing process (Table 1).

## 2.3 Flexural Test

Test specimens are prepared in accordance with ASTM D790. The subsequent procedure for testing is a three-point bend test. The universal testing machine is used for flexural testing with a displacement velocity of  $5$  mm/min. The rectangular test specimen is  $191$  mm  $\times$   $20$  mm  $\times$   $2$  mm.

**Table 1** A designed method for experimental study (Phunpeng et al. 2022)

Fiber type	Glass microspheres as particles (wt%)	Specimens
Glass fiber chopped strand mat (GC)	0	GCF00
	5	GCF05
	10	GCF10
	15	GCF15
Glass fiber plain-woven fabric (GP)	0	GPF00
	5	GPF05
	10	GPF10
	15	GPF15

### 3 Results and Discussion

A study of the influence of GM particles on the bending properties of glass fiber-reinforced composites is performed using UTM in accordance with ASTM D790. In a flexural test, the force applied to the specimen causes strain and bending stress. This is because the strength value is affected by the amount of filler used and the curing temperature. The fillers generate more flexural stress, which improves fiber and matrix adhesion in the composite (see Fig. 1b).

The effect of GM on the deflection behavior of glass epoxy composites is shown in Fig. 1a. The composite deflection without GM filler is 25 mm. The stress behavior of fiber-reinforced epoxy composites is enhanced by adding 5% GM. On the other hand, when the GM content of the composites increases, the deflection behavior of the composites decreases. This might be due to the fact that fillers and resins interact less.

The addition of GM particles to glass fiber-reinforced composites increases the load tolerance of the composites significantly. This is due to the composite glass fiber and particle working together. The load is initially received by the matrix and transferred to the particles and fibers during the bending test. The fibers are supported by fillers that distribute the load throughout the network fillers. The interfacial bonding between fibers and fillers could effectively support the matrix in epoxy composites to endure bending strength. Figure 2 presents the load and strength values of materials obtained from flexural testing. Aluminum alloy has the maximum loading capacity (225 N), followed by GPF10 (100.93 N) and GCF10 (89.45 N). GPF10 has the ultimate flexural strength (189.24 MPa), followed by aluminum alloy (174.12 MPa) and GCF10 (131.23 N).

The landing gear of UAVs is generally produced by the aluminum alloy. Flexural tests are performed on it. Aluminum has a greater load tolerance and strength than

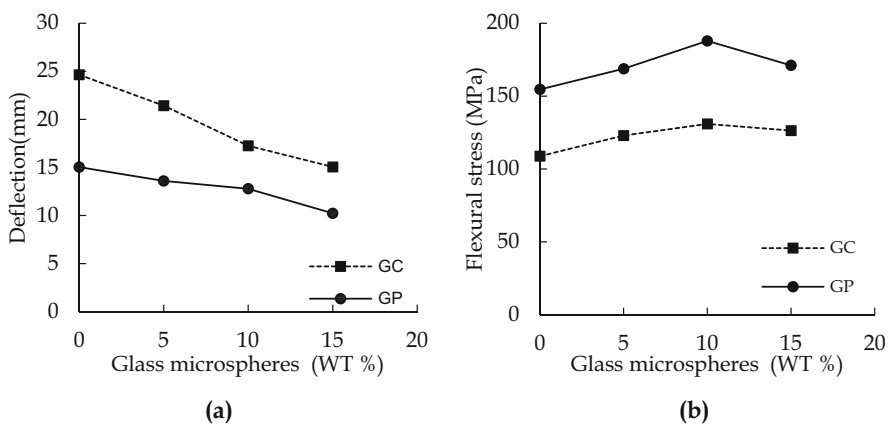


**Fig. 1** (a) Flexural stress variation with the percentage of GM content. (b) Flexural deflection variation with the percentage of GM content



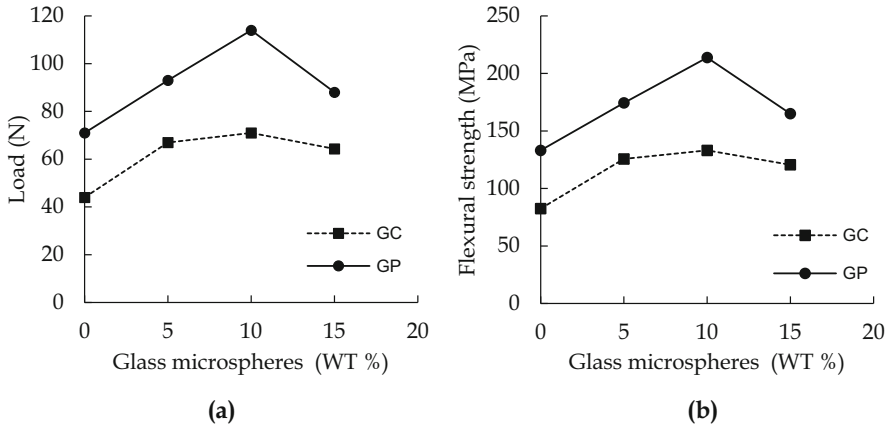


**Fig. 2** (a) Flexural load variation with the percentage of GM content. (b) Flexural strength variation with the percentage of GM content

glass fiber-reinforced composites with GM particles when compared to the previous composite material flexural test. The UAV structure weighs 4 kg with a payload capacity of 1 kg. The material is utilized to create the landing gear support at least 5 kg of its weight. The glass fiber-reinforced composite with GM particles has a maximum load capacity of 10 kg, which is enough to support the weight of a 5 kg UAV.

## 4 Conclusion

The influence of glass microspheres on the bending characteristics of glass fiber-reinforced composites (chopped strand mat and plain-woven fabric  $1 \times 1$ ) is investigated in this research. This work is carried out using UTM in compliance with ASTM D790 standards. The impact of adding glass microsphere particles is studied. It is found that adding microparticles could enhance the flexural strength. Glass fiber plain-woven fabric is found to be more effective than chopped strand mat. Adding glass microspheres to glass fiber-reinforced composites dramatically improves the load performance of the composites. Also, the glass fiber plain-woven fabric attributes the interaction between glass fibers and glass microspheres. This enables the composite to support greater payloads. The maximum load capacity of conventional glass fiber plain-woven fabric composites with GM particles is 10 kg, which is sufficient to support the weight of a 5 kg UAV. As a result, the alternative material can be glass fiber plain-woven fabric composites with GM particles. The landing gear is made of a composite material rather than T6 aluminum alloy. This reduces the UAV production costs and weight, allowing more extended operation with more efficiency.

## References

- Arpitha, G., Sanjay, M., Senthamarai Kannan, P., Barile, C., & Yogesha, B. (2017). Hybridization effect of sisal/glass/epoxy/filler based woven fabric reinforced composites. *Experimental Techniques*, 41(8), 577–584.
- Chandramohan, D., Murali, B., Vasantha-Srinivasan, P., & Dinesh, K. S. (2019). Mechanical, moisture absorption, and abrasion resistance properties of bamboo–jute–glass fiber composites. *Journal of Bio- and Tribo-Corrosion*, 5(3), 1–8.
- Ferreira, J. A. M., Capela, C., & Costa, J. D. (2010). A study of the mechanical behaviour on fibre reinforced hollow microspheres hybrid composites. *Composites Part A Applied Science and Manufacturing*, 41(3), 345–352.
- Huichao, Y., Zhou, G., Wang, W., & Peng, M. (2018). Silica nanoparticle-decorated alumina rough platelets for effective reinforcement of epoxy and hierarchical carbon fiber/epoxy composites. *Composites Part A Applied Science and Manufacturing*, 110(2), 53–61.
- Kerdphol, T., Rahman, F. S., Watanabe, M., Mitani, Y., Hongesombut, K., Phunpeng, V., Ngamroo, I., & Turschner, D. (2021). Small-signal analysis of multiple virtual synchronous machines to enhance frequency stability of grid-connected high renewables. *The Institution of Engineering and Technology Generation, Transmission and Distribution*, 15(8), 1273–1289.
- Kim, H. S., & Khamis, M. A. (2001). Fracture and impact behaviours of hollow micro-spheres/epoxy resin composites. *Composites Part A Applied Science and Manufacturing*, 32(9), 1311–1317.
- Megahed, A., & Megahed, M. (2017). Fabrication and characterization of functionally graded nanoclay/glass fiber/epoxy hybrid nanocomposite laminates. *Iranian Polymer Journal*, 26(9), 673–680.
- Mohan, K. S., Ravikiran, K. R., & Govindaraju, K. H. (2018). Development of e-glass woven fabric/polyester resin polymer matrix composite and study of mechanical properties. *Materials Today*, 5(5), 13367–13374.
- Phunpeng, V., & Baiz, P. M. (2015). Mixed finite element formulations for strain-gradient elasticity problems using the FEniCS environment. *Finite Elements in Analysis and Design*, 96(1), 23–40.
- Phunpeng, V., & Kerdphol, T. (2021, August). Comparative study of Sugeno and Mamdani fuzzy inference systems for virtual inertia emulation. In *Proceedings of 8th annual IEEE PES/IAS PowerAfrica conference, Nairobi, Kenya* (pp. 1–5). IEEE.
- Phunpeng, V., Saensuriwong, K., & Kerdphol, T. (2022). Comparative Manufacturing of Hybrid Composites with Waste Graphite Fillers for UAVs. *Materials*, 15(19), 1–15.
- Saensuriwong, K., Kerdphol, T., & Phunpeng, V. (2021). Laboratory study of polypropylene-based honeycomb core for sandwich composites. *Spektrum Industri*, 19(2), 97–104.
- Sudtachat, K., Tantrairatn, S., & Phunpeng, V. (2017, February). The queuing model for perishable inventory with lost sale under random demand, lead time and lifetime. In *Proceedings of IASTED international conference on modelling, identification and control. Innsbruck, Austria* (Vol. 848, pp. 13–20). Actapress.
- Wong, M. M., Azmi, A. I., Chuan, L. C., & Ahmad, F. M. (2018). Experimental study and empirical analyses of abrasive waterjet machining for hybrid carbon/glass fiber-reinforced composites for improved surface quality. *Advanced Manufacturing Technology*, 95(9), 3809–3822.

# Decision-Making Modeling in Emergency “Unlawful Interference”



Tetiana Shmelova, Maxim Yatsko, Yuliya Sikirda, and Eizhena Protsenko

## Nomenclature

ACFT	Aircraft
ATCO	Air traffic control officer
CDM	Collaborative decision-making
DM	Decision-making
DMM	Decision-making model
ICAO	International Civil Aviation Organization

## 1 Introduction

Civil aviation, as an integral part of the transport system, is important for the economy and is playing an increasing role in the globalized economy. At the same time, aviation objects remain one of the most vulnerable to various hazards and can pose a significant threat to the public and the environment, even if all safety standards are met. Aviation is a source of increased danger to humans. From the second half of the last century, special attention has been paid to the fight against acts of unlawful interference in the activities of civil aviation – the most dangerous crimes in this area. Evidence of this is the numerous terrorist attacks on aircraft that have not stopped since the second half of the twentieth century.

One of the forms of unlawful interference in the activities of civil aviation is the hijacking of an aircraft (ACFT), which can take place both in the air and on the ground. According to the Aviation Safety Network (Aviation Safety Network,

---

T. Shmelova (✉) · M. Yatsko · Y. Sikirda · E. Protsenko  
National Aviation University, Kyiv, Ukraine

Flight Academy of National Aviation University, Kropyvnytskyi, Ukraine

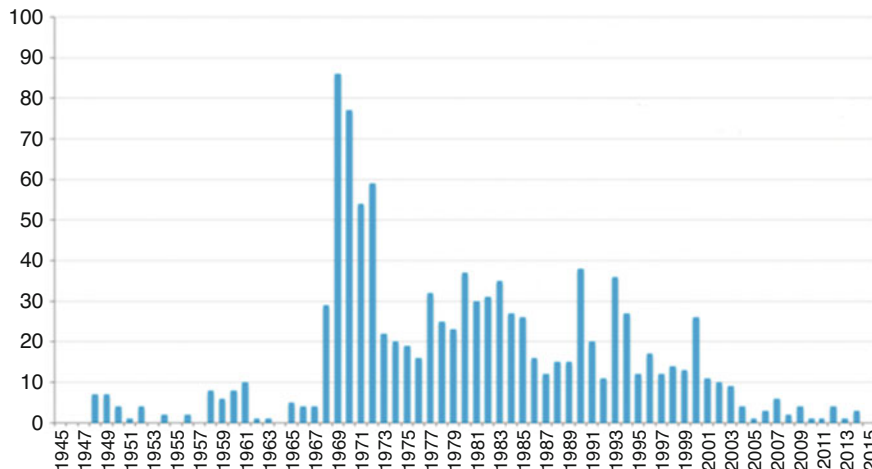


**Fig. 1** Aircraft hijackings per year, 1945–2015

2021), hijackings are less common these days. In 1969, 86 aircraft (maximum) were hijacked. From 2002, the average is only 3.5 per year (Fig. 1).

Of particular importance in these situations is the coherence of all participants (flight crew (pilot, co-pilot, flight attendant), air traffic control officer (ATCO), supervisor, flight dispatcher, ground handler, aviation security and airport rescue service, military, Security Service of Ukraine, etc.), due to the acute shortage of time for decision-making (DM), incompleteness and lack of information, and significant psychophysiological load. Decision-making models (DMM)s by human operators in conditions of certainty, risk, and uncertainty were developed to timely diagnose the aircraft in emergency flight situations, to predict their development, and to be able to promptly provide appropriate assistance to air navigation system operators. Unexpected notification of a special accident in flight, acute shortage of time, and a sudden awareness of an emergency can lead aircraft crewmembers to erroneous actions (Shmelova & Sikirda, 2021a).

The goal of the work is to increase the effectiveness of air navigation system operators' actions in an emergency with the help of working out of operators' DMM under conditions of certainty, risk, and uncertainty on an example of emergency "unlawful interference" (an example from the scientific work of the bachelor of the National Aviation University (Ukraine) Eizhena Protsenko, the fourth year of study, specialty "Aviation Transport," qualification "Air Traffic Services," discipline "Informatics of Decision-Making").

## 2 Decision-Making by Operators in Emergency “Unlawful Interference”

### 2.1 Integration of Deterministic, Stochastic, and Non-stochastic Uncertainty Models in Emergency

In the recent documents, ICAO defined new approaches for effectiveness in aviation – application of artificial intelligence models for the organization of collaborative decision-making (CDM) by all participants using collaborative DMM on the basis of common information about the flight and characteristics of emergency (ICAO, 2014). In the process of analysis of the emergency are building DMMs to complexity from deterministic to stochastic models (Shmelova, 2019). In the process of synthesis of models and for effectiveness of DM in emergencies, there is a sense to simplify complex models and solutions. So, for example, stochastic and non-stochastic uncertainty, neural, the Markov, GERT (Graphical Evaluation and Review Technique), and dynamic models may be integrated into deterministic models (Fig. 2).

Collaborative DMMs in individual and collective information by various interacting participants, such as pilots, flight dispatchers, and ATCOs, in professional solutions and optimal solutions were obtained using the method of the objective-subjective decision in conditions of uncertainty (Shmelova, 2019). The integration of DMM in conditions of certainty, risk, and uncertainty is the basis for the building of a decision support system for a human operator in the event of a flight emergency. For the modeling of DM, human operator can apply different levels of DM complexity depending on the factors that influence the DM. For example, the technologies of ATCO work ASSIST (Acknowledge, Separate, Silence, Inform, Support, Time) are presented by EUROCONTROL as an online emergency training package (SKYbrary, 2021). The form of individual DM matrix in uncertainty for operators  $O_k$  is presented in Table 1 (Shmelova & Sikirda, 2021b).

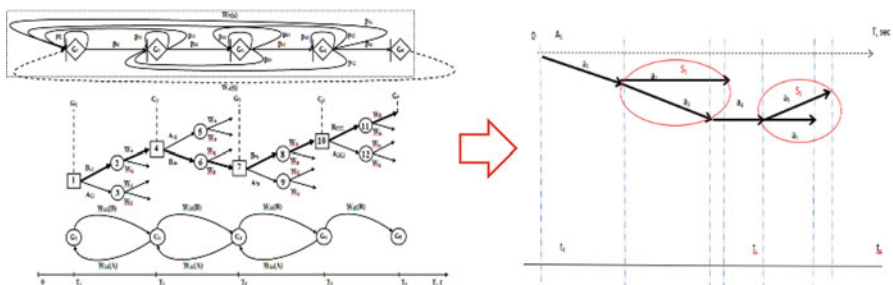


Fig. 2 The integration of the stochastic DMM in the deterministic model

**Table 1** DM matrix in uncertainty for  $O_1$  operator

Alternatives	Factors influencing DM					
	$\lambda_1$	$\lambda_2$	...	$\lambda_j$	...	$\lambda_n$
$\{A\}$	$U_{11}$	$U_{12}$	...	$U_{1j}$	...	$U_{1n}$
$A_1$	$U_{21}$	$U_{22}$	...	$U_{2j}$	...	$U_{2n}$
$A_2$	...	...	...	...	...	...
...	$U_{i1}$	$U_{i2}$	...	$U_{ij}$	...	$U_{in}$
$A_i$	...	...	...	...	...	...
...	$U_{m1}$	$U_{m2}$	...	$U_{mj}$	...	$U_{mn}$
$A_m$						

In Table 1,  $\{A\} = \{A_1, A_2, \dots, A_j, \dots, A_m\}$  are the alternative solutions of the operators;  $\{\lambda\} = \{\lambda_1, \lambda_2, \dots, \lambda_j, \dots, \lambda_n\}$  are the objective and subjective factors that affect DM by operators; and  $\{U\} = \{U_{11}, U_{12}, \dots, U_{ij}, \dots, U_{mn}\}$  are the outcomes of DM matrix ( $i = 1, \dots, m; j = 1, \dots, n$ ).

## 2.2 Decision-Making in Emergency Under Uncertainty

The methods (criteria for analyzing the DM problem) of DM under uncertainty are Wald criterion (maxmin), Laplace criterion, Savage criterion, and Hurwicz criterion. For DM in the emergency under uncertainty in case of “unlawful interference” during the flight on-route are the next initial data: emergency landing, “Continue” ( $A_1$ ), and emergency landing, “Allow” ( $A_2$ ). The following are a set of factors that affect the decision  $\lambda = \{\lambda_1, \lambda_2, \dots, \lambda_n\}$ : the availability of fuel onboard ( $\lambda_1$ ), the remoteness of the aerodrome ( $\lambda_2$ ), the technical characteristics of the runway ( $\lambda_3$ ), the weather conditions ( $\lambda_4$ ), the approach lighting system ( $\lambda_5$ ), the navigation approach system ( $\lambda_6$ ), and the subjective factor ( $\lambda_7$ ). The factors  $\lambda_1$ – $\lambda_6$  are the same for all participants of CDM objective factors, and the subjective factor  $\lambda_7$  differs from each other for the different participants of CDM: pilot ( $O_1$ ), co-pilot ( $O_2$ ), flight attendant ( $O_3$ ), ATCO ( $O_4$ ), supervisor ( $O_5$ ), military sector of the air traffic services ( $O_6$ ), flight dispatcher ( $O_7$ ), ground handler ( $O_8$ ), aviation security ( $O_9$ ), airport rescue service ( $O_{10}$ ), Alpha unit of the Security Service of Ukraine ( $O_{11}$ ), etc. ( $O_k$ ).

The interaction of services, in which pilots have the opportunity to participate in emergency “unlawful interference,” is fully dependent on the flight attendants. In the event of unlawful actions on board, they must, by all means and capabilities, prevent intruders from entering the aircraft cockpit. If, nevertheless, it did not work out, then there is a high probability that pilots will fall out of this interaction of services. The aircraft becomes completely uncontrollable or is controlled by the terrorists. Then the interaction will take place only between ground services, and the ATCO becomes the main source of information. For example, DM matrix for the optimal solution of ATCO in emergency “unlawful interference” is presented in Table 2.

According to obtained matrices, we see that by three criteria (Wald, Laplace, Hurwicz) the most optimal solution is to continue the flight, by Savage criteria – to perform an emergency landing at the aerodrome.

**Table 2** DM matrix in emergency “unlawful interference”

	Factors							Results			
	$\lambda_1$	$\lambda_2$	$\lambda_3$	$\lambda_4$	$\lambda_5$	$\lambda_6$	$\lambda_7$	Wald	Laplace	Hurwicz	Savage
$A_1$	8	3	8	2	6	9	8	2	6.28	5.5	7
$A_2$	6	7	2	1	1	3	1	1	3	4	6

### 3 Results and Discussion

DMMs are built for many types of emergencies (engine failure, fire onboard, rejected take-off, decompression, etc.) and for many air navigation system operators (pilots, unmanned aerial vehicle operators, ATCOs, flight dispatchers, etc.). Integrated DMMs for several operators are proposed (Shmelova, 2019). The problem of optimizing the CDM of the pilot (remote pilot), flight dispatcher, and ATCO in emergencies with the help of consolidated deterministic, stochastic, and non-stochastic models is studied (Sikirda et al., 2021; Shmelova & Sikirda, 2021b). The algorithms of CDM by different aviation operators during the selection of the optimal solution in an emergency are developed. The example of choosing the optimal solution by ATCO in emergency “unlawful interference” using the methods of decision-making under certainty, risk, and uncertainty is presented.

### 4 Conclusion

The optimal DM for both a single operator and a group of operators is determined by the objective and subjective factors. The effective use of CDM is providing synchronization of decisions taken by participants, the exchange of information between them, and the effective balancing between safety and cost in collective solutions. It is important to ensure the possibility of making a joint, integrated solution with partners at an acceptable level of efficiency. The direction of further research is working out DMM for all CDM participants within the airport CDM concept that can combine the interests of partners in united work, to create the basis for effective DM through more exact and timely information that provides all co-workers at the airport a single operational view of air traffic.

### References

- Aviation Safety Network. (2021). *ASN Wikibase*. <https://www.aviation-safety.net/wikibase/>. Accessed 26 Aug 2021.
- ICAO. (2014). *Manual on collaborative decision-making (CDM)*, Doc. 9971 (2nd ed.). Author.
- Shmelova, T. (2019). Integration deterministic, stochastic and non-stochastic uncertainty models in conflict situations. *CEUR Workshop Proceedings*, 2588, 47–56.

- Shmelova, T., & Sikirda, Y. (2021a). Socio-technical approaches for optimal organizational performance: Air navigation systems as sociotechnical systems, chapter 49. In D. B. A. Mehdi Khosrow-Pour (Ed.), *Research anthology on reliability and safety in aviation systems, spacecraft, and air transport* (pp. 1201–1232). IGI-Global Publ. <https://doi.org/10.4018/978-1-7998-5357-2.ch049>
- Shmelova, T., & Sikirda, Y. (2021b). Collaborative decision-making models for UAV operator's intelligent decision support system in emergencies. In *Artificial intelligence and information systems (ICAIS 2021). Proceedings of the 2nd international conference, Chongqing, China, May 28–30, 2021* (pp. 1–7). ACM. <https://doi.org/10.1145/3469213.3469222>.
- Sikirda, Y., Shmelova, T., Kharchenko, V., & Kasatkin, M. (2021). Intelligent system for supporting collaborative decision making by the pilot/air traffic controller in flight emergencies. *CEUR Workshop Proceedings*, 2853, 127–141.
- SKYbrary Aviation Safety. (2021). *Main page*. [http://www.skybrary.aero/index.php/Main\\_Page](http://www.skybrary.aero/index.php/Main_Page). Accessed 3 Sept 2021.



# Green Practices Adoption Among Leading Green Airlines



Teeris Thepchalerm and Phutawan Ho

## 1 Introduction

In 2015, the United Nations (UN) had announced the Sustainable Development Goals (SDGs), including climate action, among other goals (United Nations, 2021). Air transport can place negative effects on the environment, mostly from greenhouse gases emission. According to Calderon-Tellez and Herrera (2021), aircraft engine combustion can emit carbon dioxide (CO<sub>2</sub>), carbon monoxide (CO), nitrogen oxide (NO<sub>x</sub>), and nitric oxide (NO), all of which can contribute to global warming. The aircraft emit up to 3.16 kg of CO<sub>2</sub> for each kilogram of jet fuel burnt (ICAO, 2016). In response to the SDGs and environmental impacts caused by air transport, the International Civil Aviation Organization (ICAO) and the International Air Transport Association (IATA), as the leading bodies in the aviation industry, have announced their policies regarding environmental protection. The ICAO has introduced the Carbon Offsetting and Reduction Scheme for International Aviation (CORSIA) to put the cap on CO<sub>2</sub> emission from air transport aiming for carbon-neutral air transport (ICAO, 2020). The IATA also proposed its strategy for sustainable aviation, including sustainable aviation fuel, clean technology, improving flight operation, and market-based policy (IATA, 2021).

Aiming to reduce the negative impact on the environment, the airlines have recognized the need for environment-friendly or green practices, and many have adopted green practices (Amankwah-Amoah, 2020). There are various practices that can be considered green practices. However, these practices can be categorized into different categories (ICAO, 2020; Migdadi, 2020; Walker et al., 2020; IATA, 2021).

---

T. Thepchalerm (✉) · P. Ho

Business Excellence and Logistics Research Centre, School of Management, Mae Fah Luang University, Chiang Rai, Thailand

e-mail: [teeris.the@mfu.ac.th](mailto:teeris.the@mfu.ac.th); [phutawan.ho@mfu.ac.th](mailto:phutawan.ho@mfu.ac.th)

## 1. Practices for flight operation:

- 1.1. Alternative Fuels – besides the conventional jet fuel, there are several cleaner fuel choices for aircraft operation. Biofuels are more environmentally friendly alternatives since the combustion of such fuel emits less greenhouse gases and consume less energy in production (Janic, 2017).
- 1.2. Aircraft Improvement – the advancement in aircraft efficiency mostly depends on technology development. Lighter materials and better engine performance lead to better fuel efficiency (Sakar, 2012; Walker et al., 2020). As a result, there is less greenhouse gases emission. For example, some state-of-the-art technology, the sustainable aircraft operating with sustainable energy, is the new hope for sustainable air transport (Baharozu et al., 2017).
- 1.3. Flight Operation – improving in flight operation can lead to shorter flight time and less fuel consumption, for example, the “linear holding” procedure for reducing fuel consumption during aircraft flight delay holding (IATA, 2021).
- 1.4. Supporting Units – the airlines can reduce emission not only from the aircraft but also from other sources such as the vehicles used during flight preparation, e.g., truck, passenger coach, etc.

## 2. Practices not related to flight operation:

- 2.1. Energy stewardship – jet fuel is not the only energy that airlines consume. To become more environmentally friendly, the airlines need to reduce energy consumption in their facilities or seek for sustainable sources of energy or approach for reducing energy consumption. For instance, the airline can use electricity produced by a sustainable process such as wind turbines or solar cells (Migdadi, 2020).
- 2.2. Water stewardship – water resource is one of the SDGs (United Nations, 2021). The airlines should also concern about their water usage for improving environmental performance (Walker et al., 2020).
- 2.3. Waste management – operating an airline can cause a huge number of wastes. The airlines can recycle or upcycle these wastes, so they can mitigate negative effects from the wastes.

Despite various available green practices for air transportation, the insight regarding green practices adoption among airlines is still imprecise. Thus, this article aims to explore the current green practices adoption among worldwide leading green airlines.

## 2 Method

This article is a secondary qualitative research article. The authors collected data from environmental reports of scheduled airlines listed in the top 10 green airlines by the Atmosfair Airline Index 2018 (Atmosfair, 2018). The authors chose Atmosfair Airline Index because it has been used in many studies regarding green aviation (Mayer et al., 2015). The index was published by the atmosfair, which is a non-profit organization based in Berlin. The index indicates the “efficiency point” based on greenhouse gases emission of the airlines and ranks the airlines based on such points. First, the authors purposively selected the top 10 scheduled airlines ranked by the index, since the leader company, especially in the environmental aspect, has more potential to adopt green practices (Margaret, 2017). Then, the authors extracted data regarding green practices adopted by the airlines from the latest airlines’ environmental reports. The authors selected only the airlines which provided their full enclosure environmental reports (Table 1).

The authors used the content analysis method for analyzing the collected data. The content analysis is a suitable method for analyzing written text (Krippendorff, 2013). First, the authors identified the green practices of each airline reported in the environmental report. The authors then separately categorized each practice into different categories based on the practice’s attributes. The authors acquired these categories from the literature review consisting of two main categories and six sub-categories. The categories and sub-categories are shown in Table 2. After categorization, the authors made a discussion and conclusion based on the finding.

**Table 1** List of top 10 scheduled airlines ranked by Atmosfair Airline Index

Airline ranks in Atmosfair Airline Index (scheduled airline only)	Airline’s name
1	TUI
2	LATAM
3	Transavia
4	Air New Zealand
5	KLM
6	Virgin Atlantic
7	Alaska Airlines
8	Thai Airways International
9	Air Transat
10	Air China

Source: atmosfair

**Table 2** Categories and sub-categories of green practices of airlines

Categories	Sub-categories
Practices related to flight operation	Sustainable fuel
	Aircraft improvement
	Flight operation improvement
Practices not related to flight operation	Energy stewardship
	Water stewardship
	Waste management

### 3 Results and Discussion

The content analysis results are reported in Table 3. For reliability testing, the authors have calculated kappa's value, and it indicates strong reliability at 0.81. The authors identified, in total, 55 green practices. Thirty (54.55%) practices are related to flight operation, and the other 25 (45.45%) practices are not related to flight operation. For practices related to flight operation, 5 (9.09%) sustainable fuel, 8 (14.55%) aircraft improvement, and 17 (30.91%) flight operation improvement practices were identified. For practices not related to flight operation, 5 (9.09%) energy stewardship, 10 (18.18%) water stewardship, 7 (12.73%) waste management, and 3 (5.45%) carbon offsetting practices were identified. The carbon offsetting sub-category was introduced because the authors found the practices that do not belong to any other sub-categories; thus, the researchers generated a new sub-category based on the data content as suggested by Krippendorff (2013).

The results indicate that the airlines are now focusing on both practices related and not related to flight operation. For practices related to flight operation, flight operation improvements such as one engine taxi, continuous landing approach, route planning optimization, etc. are highly adopted. The reason behind this finding could be that these practices require lower investment compared to other practices such as fleet or aircraft upgrading. Both aircraft and flight operation improvements basically aim for reducing fuel consumption. Therefore, less fuel would be burnt, leading to less GHGs emission. According to the finding, sustainable fuel is not widely used because the production scale of such fuel is still far from full commercial scale (Virgin, 2020). In addition, the airlines use sustainable fuel only in some flights and with a specific amount. For practices not related to flight operation, the airlines have adopted various practices regarding energy, water, and waste management, for example, reducing electricity and water consumption in the office buildings. The reason could be that the airlines are trying to meet or maintain some standard or accreditation, for instance, national standard, ISO 14001, etc. (Thai Airways, 2020). Interestingly, these practices can also provide financial benefit, that is, the airlines can save their cost by reducing energy and water consumption. The airlines also started to implement carbon offsetting practices, for example, forestation and solar

**Table 3** Descriptive results

Categories	Sub-categories	Freq.	Percentage
Practices related to flight operation	Sustainable fuel	5	9.09
	Aircraft improvement	8	14.55
	Flight operation improvement	17	30.91
	Sum	30	54.55
Practices not related to flight operation	Energy stewardship	5	9.09
	Water stewardship	10	18.18
	Waste management	7	12.73
	Carbon offsetting	3	5.45
	Sum	25	45.45
Total sum		55	100

cell installation. These practices are meant to offset the CO<sub>2</sub> emission from airlines' operations. This practice might be the response to the Carbon Offsetting and Reduction Scheme for International Aviation (CORSIA) which will be fully implemented worldwide in 2024 (ICAO, 2020).

## 4 Conclusion

Currently, environmental issue has gained significant attention from every sector. The airlines need to take action to reduce their negative impacts on the environment. There are various environmentally friendly practices both related and not related to flight operation. The results of this article revealed that the leading green airlines have adopted different green practices. Practices regarding flight operation improvement are commonly adopted, while sustainable aviation fuel will require significant improvement before it is widely used in commercial air transport. Apart from practices related to flight operation, the airlines also implement green practices in other areas of activities such as energy and water management in their facilities. The finding also reveals that some airlines have implemented carbon offsetting practices which might be the preparation for ICAO's CORSIA initiative. This article certainly has limitations. Firstly, this article does not separate the airlines by their characteristics, for instance, business model, region, or size. Secondly, this article collects data from only the latest environmental reports. Therefore, future studies should take the different airline characteristics into account. Future studies can also compare the results with this article to identify the change or development of green practices adoption in the airline business.

## References

- Amankwah-Amoah, J. (2020). Stepping up and stepping out of COVID-19: New challenges for environmental sustainability policies in the global airline industry. *Journal of Cleaner Production*, 271, 123000. <https://doi.org/10.1016/j.jclepro.2020.123000>
- Atmosfair. (2018). *Atmosfair airline index 2018*. Bonn.
- Baharozu, E., Soykan, G., & Ozerdem, M. (2017). Future aircraft concept in terms of energy efficiency and environmental factors. *Energy*, 140, 1368–1377.
- Calderon-Tellez, J., & Herrera, M. (2021). Appraising the impact of air transport on the environment: Lessons from the COVID-19 pandemic. *Transportation Research Interdisciplinary Perspectives*, 1, 1–10.
- IATA. (2021). *Action for the environment*. Montreal.
- ICAO. (2016). *Environmental report 2016*. Montreal.
- ICAO. (2020). *Introduction to CORSIA*. Montreal.
- Janić, M. (2017). An assessment of the potential of alternative fuels for “greening” commercial air transportation. *Journal of Air Transport Management*, 69, 235–247.
- Krippendorff, K. (2013). *Content analysis: An introduction to its methodology*. SAGE.
- Margaret, R. (2017). *Sustainability principle and practices*. Routledge.
- Mayer, R., Ryley, T., & Gillingwater, D. (2015). Eco-positioning of airlines: Perception versus actual performance. *Journal of Air Transport Management*, 44, 82–89.
- Migdadi, Y. K. (2020). Identifying the effective taxonomies of airline green operations strategy. *Management of Environmental Quality: An International Journal*, 31, 146–166.
- Sarkar, A. (2012). Evolving green aviation transport system: A holistic approach to sustainable green market development. *American Journal of Climate Change*, 1, 164–180.
- Thai Airways. (2020). *Sustainability report 2019*. Bangkok.
- United Nation. (2021). *Sustainable development goals*. New York.
- Virgin. (2020). *Sustainability report 2019*. Australia.
- Walker, T., Bergantino, A., Sprung-Much, N., & Loiacono, L. (2020). *Sustainable aviation greening the flight path*. Springer.

# Design and Testing of Multiple Web Composite Wing Spar for Solar-Powered UAV



Varissara Wongprasit, Nasapol Thanomwong, and Chinnapat Thipyopas

## Nomenclature

$A$	Cross-sectional area, $m^2$
$b$	Sandwich width, mm
$c$	Core thickness, mm
$d$	Sandwich thickness, mm
$dY$	Perpendicular distance between the centroidal axis and the parallel axis, mm
$E_1$	Longitudinal Young's modulus, GPa
$E_{1c}, E_{2c}$	Compressive modulus, GPa
$E_2$	Transverse Young's modulus, GPa
$F$	Force, N/m
$G_{12}$	In-plane shear modulus, GPa
$I_A$	Actual moment of inertia, $m^4$
$I_R$	Required moment of inertia, $m^4$
$L$	Span length, mm
$M$	Maximum bending moment, Nm
$N_x, N_y$	Normal force per unit length, kN/m
$N_{xy}$	Shear force per unit length, kN/m
$t$	Facing thickness, mm
$t_c$	Web thickness, mm
$W$	Weight, g
$\gamma_{xy}^0$	Midplane shear strains
$\epsilon_{1c}, \epsilon_{2c}$	Major Poisson's ratio
$\epsilon_x^0, \epsilon_y^0$	Midplane strains

---

V. Wongprasit · N. Thanomwong · C. Thipyopas (✉)  
Department of Aerospace Engineering, Kasetsart University, Bangkok, Thailand  
e-mail: [fengcpt@ku.ac.th](mailto:fengcpt@ku.ac.th)

$\nu_{12}$	Major Poisson's ratio
$\sigma_{1c}, \sigma_{2c}$	Compressive shear, MPa
$\sigma_f$	Facing bending stress, MPa

## 1 Introduction

Solar-powered unmanned aerial vehicle used solar power to charge a Li-Po battery to extend the flight period, for environment monitoring application (Thipyopas et al., 2019). A high aspect ratio wing is used in solar-powered UAV to reduce drag and increase endurance. As a result, it is vulnerable to a variety of structural problems. Because of its large span, it has a substantial structural weight (Rumayshah et al., 2017). To solve this problem, the UAV wing material was changed from wood with a foam core section to composite material. Composite materials are a great option because they possess a high strength-to-weight ratio, especially for polymer matrix with fiber reinforcement. This material is commonly used in the aerospace industry due to their high specific strength, specific stiffness, lightweight, high fatigue resistance, and high corrosion resistance. For instance, Helios, Pathfinder, Zephyr, and most solar-powered UAV platforms are based on lightweight carbon fiber construction (Alsahlani & Rahulan, 2017). Carbon fiber reinforcement is commonly used for primary wing structure components (i.e., main spar, wing skin, ribs) due to very high strength. Moreover, epoxy resins/polymer matrix provides the better mechanical and thermal properties (Boransan et al., 2021).

The design of composite material demands accurate experimental result of the mechanical properties of the composite materials (Carlsson et al., 2013). Fiber is a crucial factor in the composite materials' final properties, which include orientation, shape, and volume ratio. Furthermore, the mechanical properties of the composites are also very sensitive to the manufacturing as well (Turgut, 2007). The testing adheres to ASTM standards to determine mechanical properties of the material for designing a wing spar structure. Using multiple web architectures for wing spars allows for an increase in specific ultimate strength while maintaining a low weight requirement (Urik & Malis, 2008). The primary function of a spar is to carry the bending load acting on the wing. The design is carried out as per the external bending moment at each station (Girenavar et al., 2017). To ensure that the wing spar is strong enough to handle from aerodynamic load, wing spar prototype without skin is used for static structural testing with sandbag.

The test specimen and wing spar prototype used a hand lay-up and vacuum bagging technique, similar to wing production, at room temperature. The wing is manufactured using Styrofoam male and female molds with a co-curing technique. Co-curing is an integral molding technique and another bonding approach in which composite subcomponents are produced in a single-shot manufacturing (Akin, 2018). Co-curing composite structures can decrease manufacturing time while creating lighter and more accurate parts (Patterson & Grenestedt, 2018).



## 2 Method

### 2.1 Mechanical Testing of Composite

Vacuum bagging with hand lay-up technique was utilized to fabricate composite plates, and a CNC machine was used to cut composite plates' specimen to a standard size. From weighing the reinforcement and matrix materials, the average fiber volume ratio of composite plates was 40 percent. The material properties would be estimated using ASTM standards, with at least five specimens required for each test condition. Table 1 shows the test methods for determining composite material properties, and Table 2 shows the composite component materials. Tensile, compression, and bending tests are all performed on universal testing machines. Table 5 shows the composite test results, where the face bending stress of the core material can be calculated using Eq. (1).

$$\sigma = \frac{PL}{2t(d+c)b} \quad (1)$$

### 2.2 Structural Design of Wing Spar

The wing spar is a spanwise structure that distributes wing aerodynamic loads. The selected structure concept for spar is a multiple web sandwich structure. Symmetric 45-degree plain weave carbon fiber laminate, that can provide the maximum shear strength, with a PU foam core is insert in the middle. To improve strength and load

**Table 1** Test method for measured composites' properties

Loading	ASTM	Measured properties
Longitudinal tension	D 3039	$E_1, \nu_{12}$
Transverse tension	D 3039	$E_2$
45-degree tension	D 3039	$G_{21}$
Longitudinal compressive	D 695	$E_{1c}, \epsilon_{1c}, \sigma_{1c}$
Transverse compressive	D 695	$E_{2c}, \epsilon_{2c}, \sigma_{2c}$
Flexure	C 393	$\sigma_f$

**Table 2** Material used in the wing spar

Reinforcement	Plain weave carbon fiber 160 g Unidirectional carbon fiber 80 g
Matrix	Epoxy resin ER 550
Core material	PU foam 3 mm

distribution, an additional unidirectional plain weave carbon fiber is placed at the top portion of the spar web. This alteration allows the wing to withstand the entire load. The cross-sectional wing design of a solar-powered UAV is shown in Fig. 1.

The spar design is based on the UAV wing configuration as shown in Table 3. For the initial stage of structural design consideration, only maximum bending moment and maximum shear stress are used for determine sizing of wing spar. As a result, the number of ply stacking along the spar is the same. Assumed that the wing bending moment is carried by the wing spar and maximum bending moment acts from the center of pressure along the span. The design load uses critical load with 1.3 safety factor and 2.5 load factor. Multiple webs are considered as a beam is split into three parts to share the entire load between each web. The bending moment acting on each web must be calculated to obtain the required moment of inertia using Eq. (2). Figure 2 shows a moment diagram of the wing spar, and each web height is determined by the thickness of the airfoil in that segment.

$$\sigma_f = \frac{Mt_c}{2I_R} \tag{2}$$

Depending on the shape of the web cross section, the actual moment of inertia can be calculated using Eq. (3). Assuming the thickness of 45 degrees plain weave

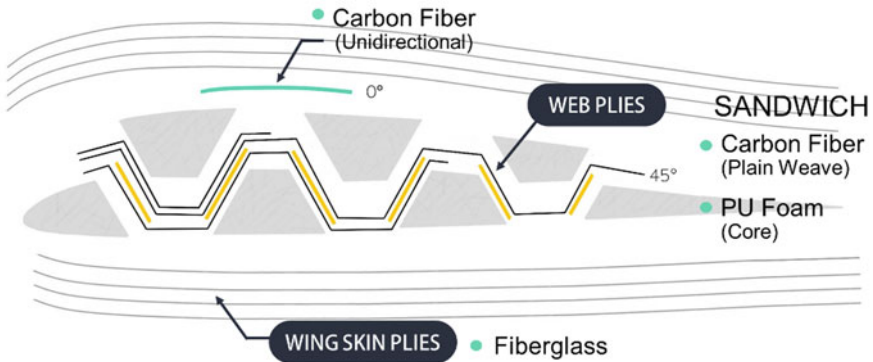


Fig. 1 Cross section of wing model

Table 3 Wing design parameters (Thipyopas et al., 2019)

Wing chord	0.45	m
Wing span	4.3	m
Wing area	1.935	m <sup>2</sup>
Maximum take-off mass	5.83	kg
Load factor	2.5	
Safety factor	1.3	
Airfoil	HS-520	

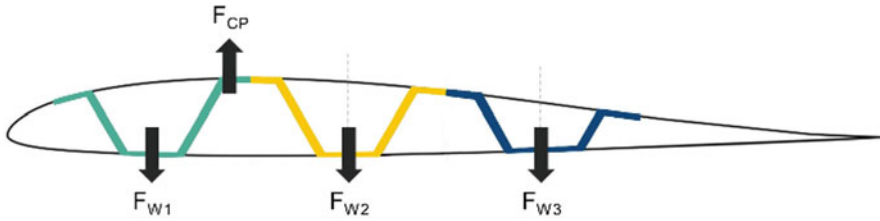


Fig. 2 Moment diagram of the wing spar

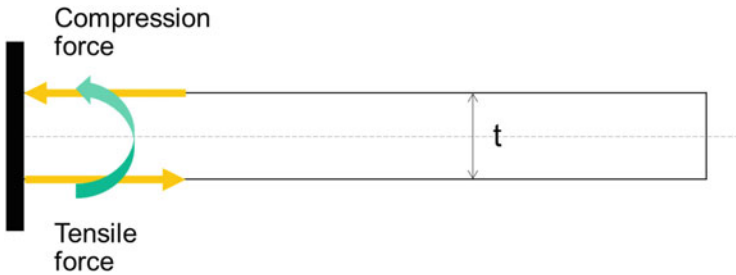


Fig. 3 Fixed cantilever beam spar subjected to bending moment

carbon fiber ply stacking on each web is known. Comparison of each web required moment of inertia to its actual moment of inertia. The design is acceptable if the actual value exceeds the required value but not be optimum.

$$I_A = \sum I = \sum I' + \sum (A_i d y_i^2) \tag{3}$$

Equation (4) is used to calculate the tensile force acting on the lower portion of the wing and the compression force acting on the upper part of the wing. Using the sum of bending moments along a spanwise transform to compression and tensile force on the wing root, as shown in Fig. 3. Assuming with the assumption of the web of the wing spar is a thin laminate. From laminate theory, mechanical properties can be used to assess the stiffness value of matrices A and B, where A is the extensional stiffness matrix and B is the bending-extension-coupling stiffness matrix. Substituting all values into Eq. (5) results in shear force per unit length, allowing Eq. (6) to be used to estimate the fabric minimum width. The top and bottom ply of each web were designed with a minimal width to obtain an optimal value where the actual and required moments of inertia are approximately equal. The number of plain weave ply stacking calculated for each web is shown in Table 4.

$$F = \frac{M}{t_c} \tag{4}$$

**Table 4** The number of plain weave ply stacking calculated for each web

Web	Required moment of inertia	Actual moment of inertia	Ply stacking
1	$11 \times 10^{-9}$	$13.12 \times 10^{-9}$	3
2	$5.72 \times 10^{-9}$	$9.35 \times 10^{-9}$	2
3	$1.93 \times 10^{-9}$	$2.47 \times 10^{-9}$	1

$$\begin{bmatrix} N_x \\ N_y \\ N_{xy} \end{bmatrix} = \begin{bmatrix} A_{11} & A_{12} & A_{16} \\ A_{12} & A_{22} & A_{26} \\ A_{16} & A_{26} & A_{66} \end{bmatrix} \begin{bmatrix} \varepsilon_x^0 \\ \varepsilon_y^0 \\ \gamma_{xy}^0 \end{bmatrix} + \begin{bmatrix} B_{11} & B_{12} & B_{16} \\ B_{12} & B_{22} & B_{26} \\ B_{16} & B_{26} & B_{66} \end{bmatrix} \begin{bmatrix} \kappa_x \\ \kappa_y \\ \kappa_{xy} \end{bmatrix} \quad (5)$$

$$W_m = \frac{F}{N_{xy}} \quad (6)$$

If the total width of the ply stacking fabric at the top or bottom of the web is smaller than the minimum width, the wing will not be able to sustain the tension or compression force from the bending moment. Carbon fiber ply with a 90-degree unidirectional orientation will be placed at the top or bottom web at the maximum thickness of the airfoil because of its high strength along the fiber. The width of unidirectional fabric can be determined similarly to plain weave ply design by calculating from the difference between the load that is carried by plain weave fabric and the entire load.

### 2.3 Wing Spar Prototype

For static structure testing with sandbag, the spar web prototype without skin must be manufactured from the design to verify that the structure can withstand the design load. Because the wing spar has no skin to ensure that only bending forces occur, the multiple web design is changed to a close section of trapezoid shape, as shown in Fig. 4, with the constraint that the moment of inertia and fabric width of the trapezoid spar must be equivalent to multiple web spar.

A vacuum bag lay-up with a co-cured mold method for producing wing spar prototype is shown in Fig. 5. The male and female molds were made of Styrofoam and cut to final shape with a hot wire cutter before being wrapped with mold release tape. Hand lay-up technique is used to lay up the wing spar on the female mold in accordance with the design. To produce the trapezoid shape of the wing spar, the male mold is placed at the top. After the laying-up procedure, vacuum bagging film was used to cover the mold. The wing spar cures for 12 hours under vacuum pressure at ambient temperature before being removed from the molds.

The 2.45 m wing spar weighs 675 g after curing, with 30 cm added from the half span length to accommodate grip during sandbag testing. Figure 6 shows a trapezoid composite wing spar after it was released from the mold.

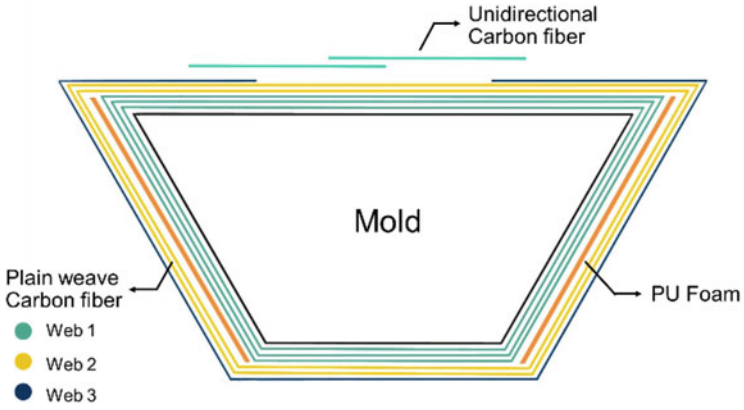


Fig. 4 Cross section of trapezoid spar

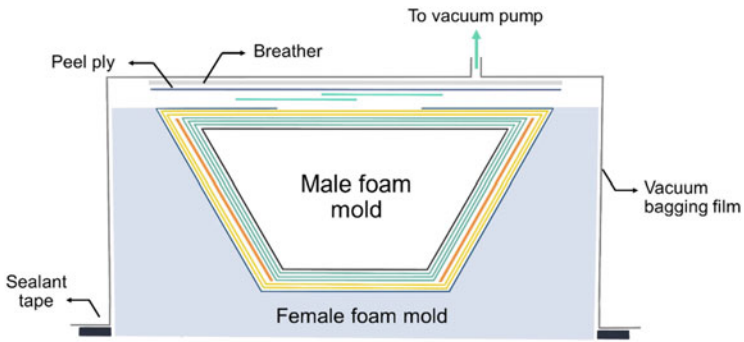


Fig. 5 Schematic of a vacuum bag lay-up with a co-cured mold technique



Fig. 6 Trapezoid composite wing spar

## 2.4 Wing Spar Static Structure Testing

Trapezoid wing spar prototype is used for static testing with sandbags to simulate load distribution throughout the span under flight conditions. Wing load distribution on the half of span is divided into 18 stations. The weight of sandbags to apply to each station can be calculated using Eq. (7).

$$W_{\text{sandbag}} = \text{load distribution} - W_{\text{spar}} \quad (7)$$

The wing spar is propped upside down, and the root of the spar is fixed during static testing. From the root to the tip station, sandbags are placed on the wing spar, and deformation of every station is recorded by vernier caliper. For the next test, the weight of the sandbag is generally increased by 0.5 times until it fails, or the spar is permanently distorted. The spar during the static test procedure is shown in Fig. 7.

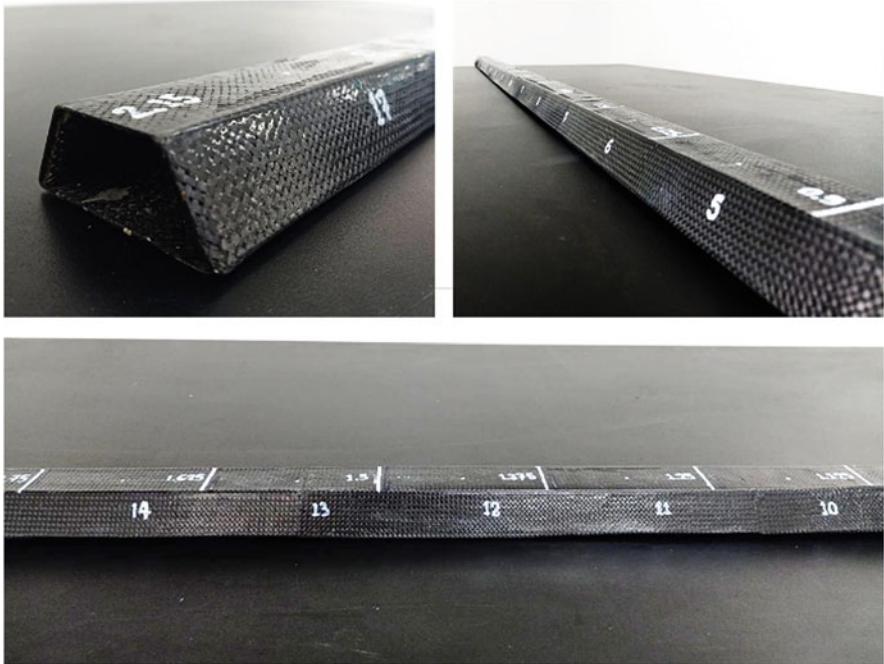


Fig. 7 The spar during static test with 3.25 multiplication factor

### 3 Results and Discussion

#### 3.1 Mechanical Test Result

Table 5 shows the mechanical properties testing result.

For example, Table 6 shows a comparison of mechanical properties between testing results and micromechanical theory (the fiber/matrix is assumed with no voids or disbands) for unidirectional fiber reinforcement with epoxy resin. The result shows that the values are quite different: longitudinal Young's modulus from testing result is less than the micromechanical theory 3.9 times, and the transverse Young's modulus is less than 1.6 times.

The major reasons is due to specimen preparation and manufacturing process. The hand lay-up technique with vacuum bagging is strongly dependent on the experience of the person preparing (Turgut, 2007). There is a change in air leakage during the vacuum bagging process, and the resin injection pressure is restricted between ambient pressure and vacuum. Furthermore, due to the curing process that began before the vacuum procedure, the vacuum is unable to remove the voids that have already formed in the laminate (Abduruohman et al., 2018). Voids can lower the fiber-to-volume ratio, affecting the composite material mechanical characteristics.

**Table 5** Test results

Material type	Properties
Plain weave carbon/epoxy	$E_1 = 13.48$ GPa, $E_2 = 13.48$ GPa, $G_{12} = 3.48$ GPa, $\nu_{12} = 0.33$ GPa, $E_{1c} = 35.7$ GPa, $E_{2c} = 33.2$ GPa, $\sigma_{1c} = 255$ MPa, $\sigma_{2c} = 239$ MPa, $\varepsilon_{1c} = 0.9$ , $\varepsilon_{2c} = 0.9$
Unidirectional carbon/epoxy	$E_1 = 20.78$ GPa, $E_2 = 3.43$ GPa, $G_{12} = 3.48$ GPa, $\nu_{12} = 0.276$ GPa, $E_{1c} = 44.9$ GPa, $E_{2c} = 14.8$ GPa, $\sigma_{1c} = 255$ MPa, $\sigma_{2c} = 83.4$ MPa, $\varepsilon_{1c} = 0.7$ , $\varepsilon_{2c} = 1.7$
PU foam	$\sigma_f = 59.93$ MPa

**Table 6** Mechanical properties between testing results and micromechanical theory

Material type	Micromechanical theory	Mechanical testing
Unidirectional carbon/epoxy	$E_1 = 81.70$ GPa	$E_1 = 20.78$ GPa
	$E_2 = 3.93$ GPa	$E_2 = 3.43$ GPa

### 3.2 Static Test Result

The structure of the spar on each station is considered based on its deformation due to the applied loads. The result of static testing is shown in Fig. 8.

The results show that the wing spar can sustain loads up to 3.75 multiplication factors and that there are no visible failures on the outside surfaces. However, as shown in Fig. 9, when the load exceeds the design limit (1.3 safety factor and 2.5 load factor or 3.25 multiplication factors), the spar becomes permanently deformed.

As a result, when multiplication factors are increased to 3.5 and 3.75, the load on the spar is predicted to be beyond the linear elastic relationship of the material, or a microscopic scale failure of composite structure occurs. According to ply stacking design calculations, the spar can withstand the entire load with a safety factor of 1.3 and a load factor of 2.5. Based on this design, the estimated weight of the 4.3 m solar-powered UAV wing is 2.15 kg.

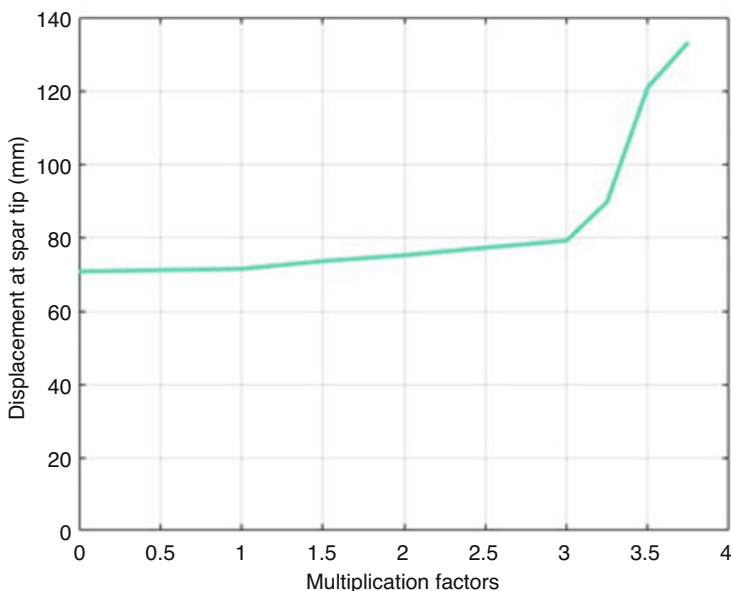


Fig. 8 Comparison of different load and displacement curve



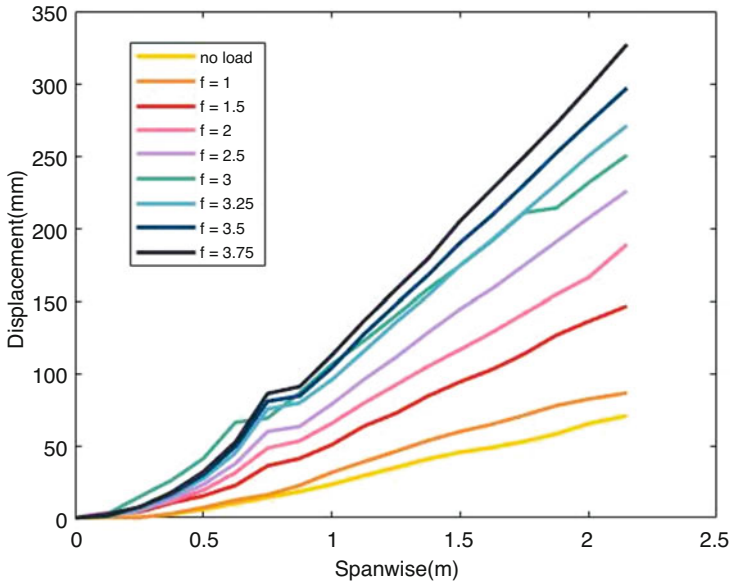


Fig. 9 Displacement at spar tip versus multiplication factors

## 4 Conclusion

Mechanical properties of in-house hand lay-up carbon composite coupon tested by ASTM standard is obtained and they are used for design wing's spar of low-cost solar cell UAV. Multiple web structure concept is selected due to the lightweight benefit. Then three-web-spar structures are transformed to a trapezoid shape spar, with identical moment of inertia and area, for sandbag testing. Based on the static test results, the wing spar prototype can withstand design load without structural failure, in accordance with the calculations. This demonstrated the ability to calculate the minimal laminate ply and web spar dimensions. To lower structural weight while maintaining a high strength-to-weight ratio, the manufacturing method must be enhanced in the future to achieve a higher fiber-to-volume ratio of composite material. Moreover, this design model can be enhanced due to the bending moment that is not uniform along the spar, and it increases from tip to root and reaches its maximum at the root. So, laminate ply along spanwise can be reduced by considered ply stacking on each wing station and use bending moment on that station for calculation of ply thickness. With good mechanical characteristics of material and an improved design model that can reduce the weight of the structure, a 4.3 m solar-powered UAV wing can be developed in the future.

**Acknowledgments** Authors sincerely appreciate Asst. Prof. Dr. Pongtorn Prombut (Kasetsart University, Thailand) for composite theory advice and Galaxi Laboratory of GISTDA (Thailand) for composite material testing guidance. Finally thank to Department of Mechanical Engineering, Kasetsart University, Bangkok, Thailand, for kindly support the space for Advance Composite Manufacturing in Aerospace Centre (ACMAC).

## References

- Abdurohman, K., Satrio, T., Muzayadah, N. L., & Teten. (2018). A comparison process between hand lay-up, vacuum infusion and vacuum bagging method toward e-glass EW 185/lycal composites. *Journal of Physics: Conference Series*, 1130, 012018.
- Akin, M. (2018). *Co-cured manufacturing of advanced composite materials using vacuum assisted resin transfer molding*. Mechanical Engineering Department, Missile East Technical University.
- Alsahlani, A., & Rahulan, T. (2017). Composite structural analysis of a high altitude solar powered unmanned aerial vehicle. *International Journal of Mechanical Engineering and Robotics Research*, 6, 71–76.
- Boransan, W., Kerdphol, T., & Phunpeng, V. (2021, August 6). Experimental manufacturing methods of glass fiber composites considering flexural behavior. In *SUT international virtual conference on science and technology*, Nakhon-Ratchasima, Thailand.
- Carlsson, L. A., Adams, D. F., & Pipes, R. B. (2013). Basic experimental characterization of polymer matrix composite materials. *Polymer Reviews*, 53, 277–302.
- Girenavar, M., Soumya, H. V., Subodh, H. M., Heraje, T. J., & Deepak Raj, P. Y. (2017). Design, analysis and testing of wing spar for optimum weight. *International Journal of Research and Scientific Innovation*, IV, 104–112.
- Patterson, J. B., & Grenestedt, J. L. (2018). Manufacturing of a composite wing with internal structure in one cure cycle. *Composite Structures*, 206, 601–609.
- Rumayshah K. K., Prayoga, A., & Moelyadi, M. A. (2017, September 27–29). Design of high altitude long endurance UAV: Structural analysis of composite wing using finite element method. In *5th international seminar on aerospace science and technology*, Medan, Indonesia.
- Thipyopas, C., Sripawadkul, V., & Warin, N. (2019). Design and development of a small solar-powered UAV for environment monitoring application. In *IEEE Eurasia Conference on IOT, Communication and Engineering (ECICE)* (pp. 316–319). International Institute of Knowledge Innovation and Invention.
- Turgut, T. (2007). *Manufacturing and structural analysis of a lightweight sandwich composite UAV wing*. Aerospace Engineering Department, Missile East Technical University.
- Urik T., & Malis M. (2008). Innovative composite structures for small aircraft. In *26th International congress of the aeronautical sciences*. American Institute of Aeronautics and Astronautics.

# Comparative Study Between Aluminum and Hybrid Composite for UAV



Veena Phunpeng, Karunamit Saensuriwong, and Thongchart Kerdphol

## Nomenclature

CFRP Carbon fiber-reinforced polymers  
RG Carbon fiber reinforcement with graphite fillers  
UAV Unmanned aerial vehicle

## 1 Introduction

Nowadays, aircraft are used for several purposes (e.g., military, civil transportation, and survey). Aviation industries encompass significant aspects of air travel and activity by stabilization control, in which a mathematical model is defined for the control (i.e., fuzzy control, PID control) (Sudtachat et al., 2017; Kerdphol et al., 2021; Phunpeng & Kerdphol, 2021). One of the most essential sectors relies on aircraft manufacture (Boransan et al., 2021). In aviation manufacturing, carbon fiber-reinforced polymers (CFRP) are widely used in airframes including UAV components due to remarkable properties (i.e., strength and lightweight). For a structure, lighter weight and strength in materials are key factors of modern aircraft design (Fanran et al., 2020).

---

V. Phunpeng (✉) · K. Saensuriwong  
School of Mechanical Engineering, Institute of Engineering, Suranaree University of  
Technology, Nakhon Ratchasima, Thailand  
e-mail: [veenap@g.sut.ac.th](mailto:veenap@g.sut.ac.th)

T. Kerdphol  
Department of Electrical Engineering, Faculty of Engineering, Kasetsart University, Bangkok,  
Thailand

Composite materials are a combination between fiber and matrix, providing superior levels of strength and stiffness. The matrix can bind the reinforcements together with the virtue of its cohesive and adhesive characteristics. To improve the matrix property, additives and fillers are used (Phunpeng & Biaz, 2014). As a result of coordination, composite materials can increase mechanical properties. To select an appropriate filler, the same type of fiber material is recommended (e.g., carbon fiber with graphite and glass fiber with silica oxide) (Cho et al., 2007). When graphite fillers are embedded in the epoxy resin matrix, it is called a hybrid composite material. The mechanical properties of carbon fiber/epoxy embedded with graphite fillers can provide more extraordinary mechanical properties in terms of the mechanism for adhesion in the material (Hulugappa et al., 2016).

Carbon fiber shows greater tensile strength than glass fiber or other fibers. As a result, the capability of the material can handle a higher load (Bin et al., 2020). Additionally, the changing angle of ply orientation also affects the mechanical properties because of the orientation of the fibers. This orientation could allow the material to guide a load direction along with fiber length. Therefore, different ply orientations are studied to allow the composites subjected to multi-direction loads. When the material is subjected to external force, an initial crack is formed on the surface of the matrix and propagated until the fracture. The propagated fracture line depends on the weave pattern of the fiber fabric. The fracture in the material would follow the fiber orientation and weave pattern of the fabric (Neumeister et al., 1996).

There are various methods to create composite materials. The manual lay-up technique is one of the most common methods, which is low-cost and requires fewer manufacturing tools. However, the disadvantage includes the occurring air bubbles in the composite workpiece, affecting the mechanical properties (Baran et al., 2017). To correctly solve the problem, the vacuum bagging process is required to remove the air bubbles. The curing temperatures and pressure show a significant role in the mechanical properties and fiber and matrix adherence (Hoda et al., 2015).

To enhance the material properties, the hybrid composite material is introduced to perform superior properties (e.g., stiffer and lighter). The purpose of this research is to study the mechanical properties of hybrid composites, carbon fiber/epoxy, with graphite fillers. To provide an alternative material, hybrid composite is introduced and utilized by UAV components and aircraft structure manufacture.

## 2 Method

In this section, material and specimen preparation are discussed. A forming process of specimens is conducted under an ASTM standard to achieve standard mechanical properties.

## 2.1 Materials

Epoxy resin (ER550) and hardener are used as a matrix in this research due to their suitability for wet lay-up type. The fiber selected for this research is carbon fiber, which is the fiber that was selected the most because of its high strength and lightweight suitable for use in UAVs. Therefore, the 3K plain weave carbon fiber is used as a reinforcement. The graphite particles (with a mean particle size of 5  $\mu\text{m}$ ) are also used as the filler.

## 2.2 Prepared Specimens

The 3K carbon fiber woven fabric is prepared with the fiber orientation of  $-45^\circ$ ,  $0^\circ$ ,  $45^\circ$ , and  $90^\circ$ . The ER550 epoxy resin and hardener are mixed at a ratio of 100:35 called the polymer matrix. The graphite filler is added to the epoxy resin/hardener with the different filler concentrations shown in Table 1. To fabricate composite laminates, the hand lay-up process is used together with vacuum bagging to reduce the air bubbles within lamination. Two different ply orientations are applied (i.e.,  $[0^\circ/90^\circ]_{4s}$  and  $[-45^\circ/45^\circ]_{4s}$ ). The polymer matrix of each specimen has different filler contents (i.e., 0%, 5%, 7.5%, and 10% of its weight). The carbon fiber/epoxy laminates are placed in an oven by controlling the temperature at 100  $^\circ\text{C}$ .

## 2.3 Bending Test

The flexural test is performed under three-point bending. According to ASTM D790-02 using Universal Testing Machine (UTM) 100 kN, the size of specimens is  $191 \times 20 \times 2 \text{ mm}^3$ , while the crosshead speed of testing is 5 mm/min, and the span length is

**Table 1** Preparation of specimens with graphite filler

Specimens	Reinforcement	Graphite filler (wt%)
0_90-RG 0%	$[0^\circ/90^\circ]_{4s}$	0
0_90-RG 5%		5
0_90-RG 7.5%		7.5
0_90-RG 10%		10
-45_45-RG 0%	$[-45^\circ/45^\circ]_{4s}$	0
-45_45-RG 5%		5
-45_45-RG 7.5%		7.5
-45_45-RG 10%		10

RG carbon fiber reinforcement with graphite fillers, wt% percent of the weight

100 mm. The flexural strength is considered and calculated by the following equation (ASTM International, 1970):

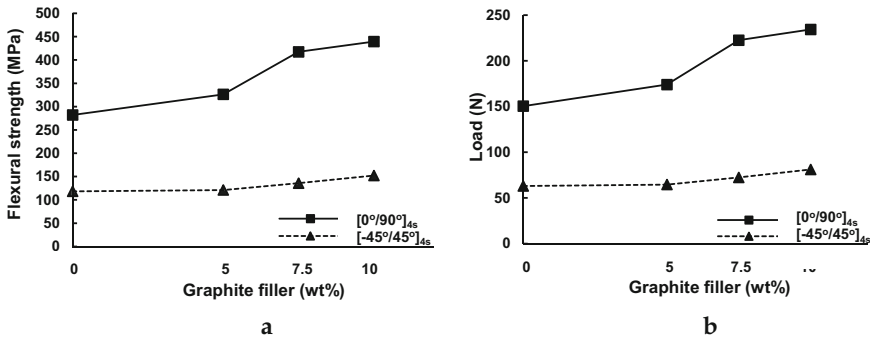
$$\sigma = 3FL/2bt^2 \quad (1)$$

where  $F$  is the maximum load of a test,  $L$  is the length of supports,  $b$  is the width of specimens, and  $t$  is the thickness of specimens.

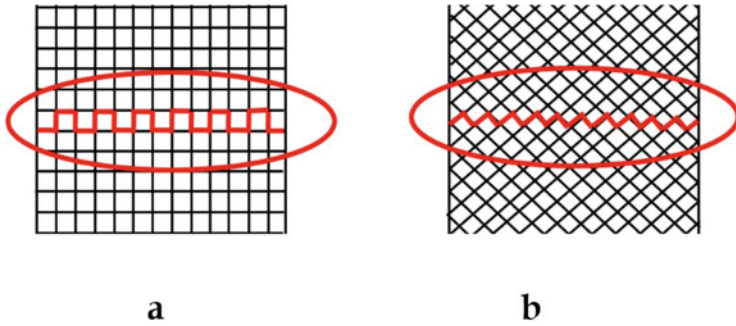
### 3 Results and Discussion

Figure 1a shows the relationship between flexural strength and graphite filler. It was found that when graphite filler is added to carbon fiber/epoxy, the flexural strength is increased. Flexural strength is increased by graphite fillers at 5 wt%, 7.5 wt%, and 10 wt%, respectively. Due to the addition of the graphite filler, air gaps are reduced between the fiber and matrix. Ply orientation affects flexural strength. It can be seen that carbon-fiber ply orientation with  $[0^\circ/90^\circ]_{4s}$  provides greater flexural strength than those of the ply orientation  $[-45^\circ/45^\circ]_{4s}$  in the three-point bending test (see Fig. 1a). This is because of the characteristic of the fabric orientation  $[0^\circ/90^\circ]_{4s}$ , which is oriented vertically and horizontally, and it can absorb the load applied from the bending test. The  $[-45^\circ/45^\circ]_{4s}$  ply orientation is oriented in a diagonal direction absorbing shear strength.

Figure 1b shows the relationship between ultimate load and different graphite filler concentrations. When the graphite filler was added into the composite matrix, it affected the ultimate strength and loads. The orientation  $[0^\circ/90^\circ]_{4s}$  at 5 wt%, 7.5 wt%, and 10 wt% filler contents exhibits the increase of ultimate loads by 15.7%, 48%, and 55.8% compared with 0 wt% graphite fillers. The orientation has a better load than laminates without the graphite filler. At  $[-45^\circ/45^\circ]_{4s}$  orientation, the graphite



**Fig. 1** (a) The relationship between flexural strength and graphite filler concentrations. (b) The relationship between ultimate load and different graphite filler concentrations



**Fig. 2** Fracture lines of ply orientation: (a)  $[0^\circ/90^\circ]_{4s}$ , (b)  $[-45^\circ/45^\circ]_{4s}$

**Table 2** Flexural strength of aluminum and hybrid composite

Materials	Flexural strength (MPa)
Aluminum alloy 6061	187.5
Hybrid composite	439.4

fillers of 5 wt%, 7.5 wt%, and 10 wt% exhibit the ultimate load increase by 12.2%, 25.7%, and 28.7% when compared with 0 wt% graphite fillers.

The fracture characteristics of the hybrid composite specimen can be observed. Figure 2 shows the final fracture line of the ply orientation of  $[0^\circ/90^\circ]_{4s}$  and  $[-45^\circ/45^\circ]_{4s}$ . This is caused by force acting on the filler matrix firstly. The force from the matrix is distributed over the fiber. Consequently, it exhibits different fracture patterns related to the fiber orientations.

Then, the flexural strength of the hybrid composite with the 10 wt% filler content of ply orientation  $[0^\circ/90^\circ]_{4s}$  and aluminum alloy 6061 (conventional aircraft structure) are compared in Table 2, which shows higher flexural strength in the hybrid composite rather than the aluminum alloy. When the strength-to-weight ratio is considered, it can be observed that hybrid composite provides a higher strength-to-weight ratio, resulting in higher strength with lightweight material. Thus, hybrid composite can be used as an alternative material for UAV frames or aircraft components, allowing the lightweight and durable UAVs.

## 4 Conclusion

Hybrid composite materials are introduced by adding graphite fillers into the carbon fiber/epoxy composite. When the strength-to-weight ratio is considered, hybrid materials can be used instead of aluminum. The mechanical properties of the hybrid composite are tested to verify the fractures and performance using the three-point bending approach. It is found that applying the ply orientation of fabric affects the flexural strength of the hybrid material. The ply orientation of the fabric shows the capability of the composite subjected to load directions. For the fracture

characteristics in terms of different ply orientations, the final fracture shows different fracture patterns with regard to the fiber angle. The filler dispersion is capable of transferring bending loads to the fibers, which are the core reinforcement. Finally, it is confirmed that the hybrid composite materials show superior properties in terms of strength-to-weight ratio, which can be further employed to replace a conventional UAV material, such as aluminum.

## References

- ASTM International. (1970). *D790-02 Standard test methods for flexural properties of unreinforced and reinforced plastics and electrical insulating materials* (pp. 1–12). ASTM Int<sup>l</sup>.
- Baran, I., Cinar, K., Ersoy, N., Remko, A., & Jesper, H. H. (2017). A review on the mechanical modeling of composite manufacturing processes. *Archives of Computational Methods in Engineering*, *24*(1), 365–395.
- Bin, H., Boyao, W., Zhanwen, W., Shengli, Q., Guofeng, T., & Dezhen, W. (2020). Mechanical properties of hybrid composites reinforced by carbon fiber and high-strength and high-modulus polyimide fiber. *Polymer*, *204*(1), 122830–122838.
- Boransan, W., Kerdphol, T., & Phunpeng, V. (2021). Experimental manufacturing of glass fiber composites considering flexural behaviour. *Spektrum Industri*, *19*(2), 87–95.
- Cho, J., Chen, J., & Daniel, I. M. (2007). Mechanical enhancement of carbon fiber/epoxy composites by graphite nanoplatelet reinforcement. *Scripta Materialia*, *56*(8), 685–688.
- Fanran, M., Yuanlong, C., Steve, P., & Jon, M. (2020). From aviation to aviation: Environmental and financial viability of closed-loop recycling of carbon fibre composite. *Composites Part B Engineering*, *200*(1), 108362–108369.
- Hoda, K., Seyed, A. S., Bob, M., & Melanie, V. (2015). Effects of variation in autoclave pressure, temperature, and vacuum-application time on porosity and mechanical properties of a carbon fiber/epoxy composite. *Composite Materials*, *46*(16), 1985–2004.
- Hulugappa, B., Achutha, M. V., & Suresha, B. (2016). Effect of fillers on mechanical properties and fracture toughness of glass fabric reinforced epoxy composites. *Journal of Minerals and Materials Characterization and Engineering*, *4*(1), 1–14.
- Kerdphol, T., Rahman, F. S., Watanabe, M., Mitani, Y., Hongesombut, K., Phunpeng, V., Ngamroo, I., & Turschner, D. (2021). Small-signal analysis of multiple virtual synchronous machines to enhance frequency stability of grid-connected high renewables. *The Institution of Engineering and Technology Generation, Transmission and Distribution*, *15*(1), 1273–1289.
- Neumeister, J., Jansson, S., & Leckie, F. (1996). The effect of fiber architecture on the mechanical properties of carbon/carbon fiber composites. *Acta Materialia*, *44*(2), 573–585.
- Phunpeng, V., & Biaz, P. M. (2014). Mixed finite element formulations for strain-gradient elasticity problems using the FEniCS environment. *Finite Elements in Analysis and Design*, *96*(1), 23–40.
- Phunpeng, V., & Kerdphol, T. (2021, August). Comparative study of Sugeno and Mamdani fuzzy inference systems for virtual inertia emulation. In *Proceedings of 8th Annual IEEE PES/IAS PowerAfrica Conference, Nairobi, Kenya* (pp. 1–5). IEEE.
- Sudtachat, K., Tantrairatn, S., & Phunpeng, V. (2017, February). The queuing model for perishable inventory with lost sale under random demand, lead time and lifetime. In *Proceedings of IASTED international conference on modelling, identification and control, Innsbruck, Austria* (Vol. 848, pp. 13–20). Actapress.



# Static and Modal Analysis of UAV Composite-Based Structures



Veena Phunpeng, Sireegorn Sumklang, and Thongchart Kerdphol

## Nomenclature

AL-2024	Aluminum 2024
CFRP	Carbon-fiber-reinforced polymers
FEM	Finite Element Method
GFRP	Glass-fiber-reinforced polymers
UAV	Unmanned aerial vehicle

## 1 Introduction

The main UAV component is the wing structure, which generates lift force, maintaining UAV stability in the air. The wing structure is connected to the fuselage and is subjected to repeat external force or continuous force. The wings must be strong to withstand the mentioned force. However, when the wing is too heavy, it affects the lift of a UAV. There are several materials to construct UAV wings. The majority of the material used in most aircraft types is aluminum alloy due to its strength and low density (compared with steel). Nowadays, the enhanced materials called composite materials have played an essential role in the aviation industry including UAV structures.

---

V. Phunpeng (✉) · S. Sumklang  
School of Mechatronics Engineering, Institute of Engineering, Suranaree University of  
Technology, Nakhon Ratchasima, Thailand  
e-mail: [veenap@g.sut.ac.th](mailto:veenap@g.sut.ac.th)

T. Kerdphol  
Department of Electrical Engineering, Faculty of Engineering, Kasetsart University, Bangkok,  
Thailand

A composite material is a combination of two materials with different physical and chemical properties. When there is a combination, it provides a novel material that improves the performances and properties (i.e., stronger, lighter, more resistant to electricity, and so on) (Boransan et al., 2021; Saensuriwong et al., 2021). Therefore, composite materials are used to build UAV wings due to the weightlessness and strength. For analyzing the UAV structure, the finite element method (FEM) is commonly used. The FEM is a method based on mathematical principles to solve engineering problems. It has been used to analyze various engineering topics (e.g., material behavior, strength in structures, and fluid flow). Most of the engineering problems can be expressed in terms of partial differential equations. To solve system of equations, the numerical method is applied to determine an approximated solution (Aabid et al. 2021; Serkan et al., 2020).

This research work studies a UAV wing structure based on well-known composite materials (i.e., Carbon-fiber-reinforced polymers (CFRP) and glass-fiber-reinforced polymers (GFRP)). To investigate the strength of the wing structure (i.e., stress, strain, and deformation), the static structural module based on ANSYS software is used to simulate the strength of various types of material. To determine the natural mode shape and frequency of the wing structure during free vibration, the natural frequency is examined by the modal analysis. Finally, the obtained results are compared with the results of conventionally used material (i.e., aluminum alloy (Al)).

## 2 Method

In the design of the UAV structure, stability is taken into account. It is necessary to analyze the strength and aerodynamics of the UAV especially the main structures. This research focuses on the finite element method for strength and natural frequency analysis of UAV wings.

### 2.1 Materials

This research studies the strength of wing structures based on composite materials. The materials used to construct a wing are described as follows: carbon-fiber-reinforced plastic (CFRP), glass-fiber-reinforced polymers (GFRP), and aluminum 2024 (AL-2024). The properties of materials are shown in Table 1 (Nielsen, 2005).

**Table 1** Material properties

Material	Young's modulus (GPa)	Density (kg/m <sup>3</sup> )	Poisson ratio
AL-2024	73.8	2770	0.34
CFRP	121	1490	0.27
GFRP	45	2000	0.3

## 2.2 Wing Design

Previously, several research works have studied wing construction, while the cross-sectional area of the wing is an airfoil shape (Gotten et al. 2021; Sullivan et al. 2009; Thomas and Roy 2015). The airfoil commonly used for UAV wing is NACA-4412 (Sharma et al., 2013). Thus, the airfoil of NACA-4412 is examined in this study. Figure 1 shows the shape and dimensions of a rib with 3 mm of thickness. The ribs, spars, and skin are structured together as described in Fig. 2.

The material for the studied model is applied while the structure's overall weight is calculated. The total weight of the structure is shown in Table 2. The CFRP represents the lightest material, while aluminum 2024 is the heaviest material.

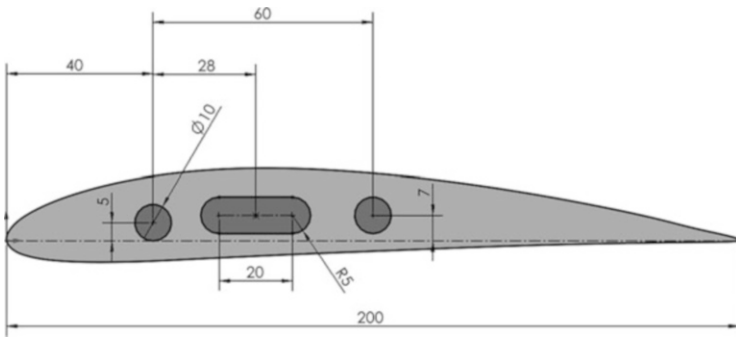


Fig. 1 An airfoil shape (NACA-4412) for a rib

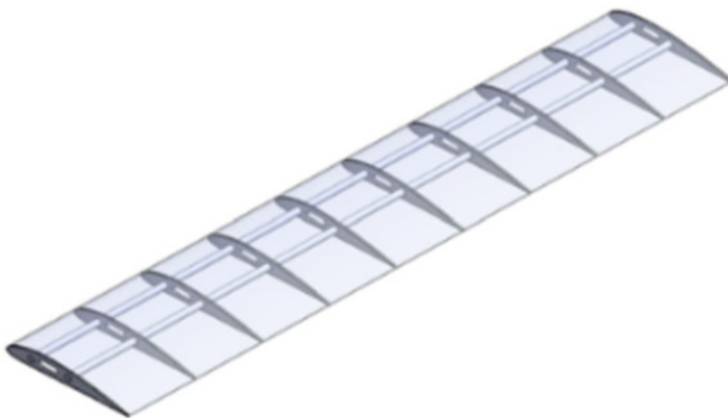
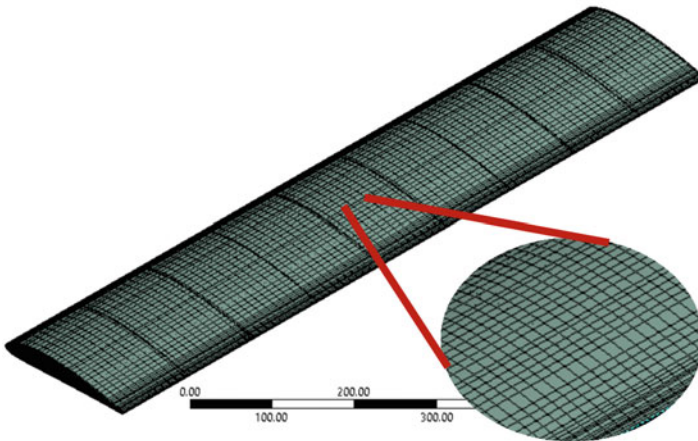


Fig. 2 A CAD model of UAV wing without surface

**Table 2** Weight of the structure

Material	Total weight (kg)
AL-2024	1.826
CFRP	0.982
GFRP	1.220

**Fig. 3** Hexahedral mesh

### 2.3 Numerical

The numerical method has been used to determine an approximated solution of engineering principles. The model validation must be performed to verify idealization. By applying a smaller mesh, a more accurate result can be obtained, while it requires a longer running/simulation time. Following the previous research (Ting et al., 2019), the proper mesh size has been verified. Thus, this study has mainly evaluated the mesh in three criteria, that is, skewness, aspect ratio, and orthogonal quality (Ting et al., 2019). The hexahedral mesh is shown in Fig. 3.

In addition to the evaluated meshes, results were also validated by comparing the results with the number of elements (Phunpeng & Biaz, 2014). It was found that with the element number higher than 150,000, the result became invariable, and when the number of elements increased, the result remained the same as shown in Fig. 4.

Considering a wing structure, the lift force is induced by the aerodynamics based on an airfoil shape. The velocity of the UAV is defined at 20 m/s, which is an average (standard) velocity of small UAVs during a flight operation (Theys & Schutte, 2020). The lift coefficient can be obtained from airfoil data (Anderson, 2010) and formulation shown below:

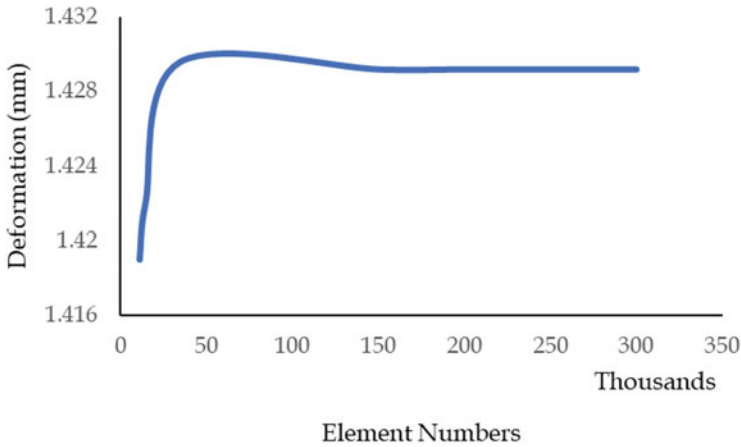


Fig. 4 Validation number of elements

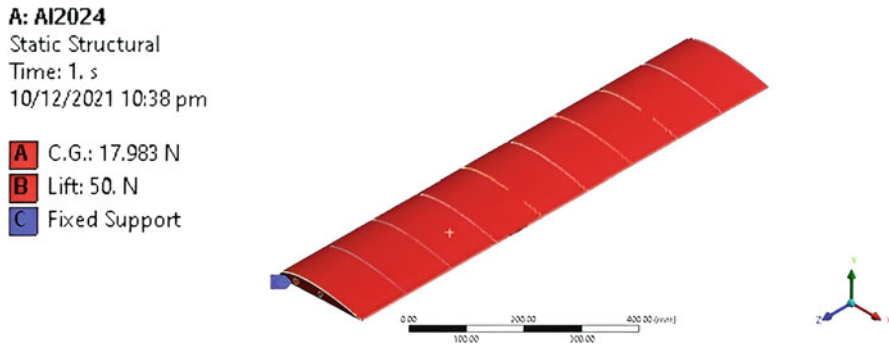


Fig. 5 External and body force with boundary

$$L = \frac{1}{2} \rho V^2 A C_l \tag{1}$$

$$L = \frac{1}{2} (1.225)(20)^2 (0.41636431)(0.4741) \tag{2}$$

$$L = 48.3626 \approx 50 \text{ N} \tag{3}$$

The wing structure is connected to the fuselage, which acts as a cantilever beam. The external force, body force, and boundary are applied in the simulation model (see Fig. 5), while the one end at area C is fixed. The body force acts on the center gravity of the wing structure, and the top surface is subjected to the distributed load of 50 N (Ramesh et al., 2013).

Next, the modal analysis is used to determine natural mode shapes and frequencies of the structure during free vibration. The modal analysis of wing structure is analyzed without a permanent stress condition. The configuration setting of modal

analysis is similar to static structural analysis. To determine the natural frequency and displacement at the free end, the ANSYS Workbench® software is used.

### 3 Results and Discussion

In static structural analysis, the total deformation, maximum equivalent stress, and maximum equivalent strain with various types of materials are observed, as shown in Table 3. The CFRP provides the highest deformation, equivalent stress, and equivalent strain, while the AL-2024 exhibits the lowest deformation, equivalent stress, and equivalent strain.

Figures 6 and 7 show the simulation results of an AL-2024 wing structure, where the gradient color displays the variation of deformation, equivalent stress, and equivalent strain. Figure 6 demonstrates the total deformation of the wing structure under static structural analysis. At the one end, it yields the maximum deformation highlighted in red color, while the blue color signifies the minimum deformation. Similarly, the red color and blue color in Fig. 7 indicate the maximum and minimum equivalent stress of AL-2024 wing structures. Based on the static structural analysis, it is confirmed that the maximum equivalent stress and strain occur at the wing root. The CFRP has the advantage of a high strength-to-weight ratio for use in lightweight.

**Table 3** The results of static structural analysis

Material	Total deformation (mm)	Maximum equivalent stress (MPa)	Maximum equivalent strain (mm/mm)
AL-2024	1.4004	7.374	1.00E-04
CFRP	15.104	15.196	1.85E-03
GFRP	13.373	12.116	1.52E-03

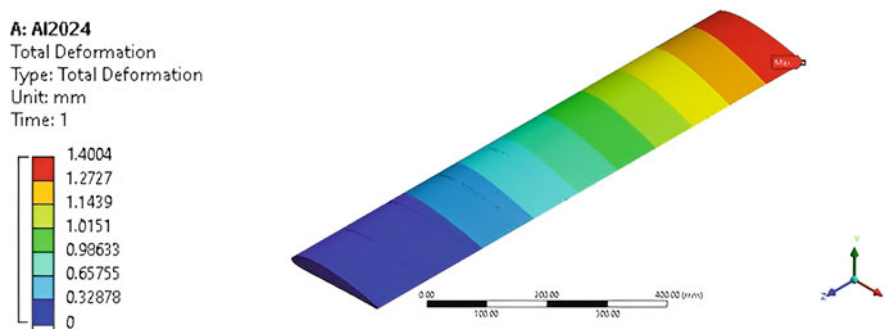


**Fig. 6** Total deformation of AL-2024 wing under static structural analysis

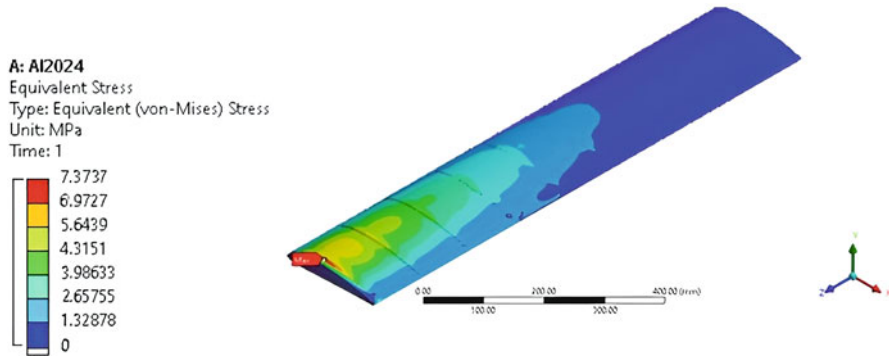


**Fig. 7** Equivalent stress of AL-2024 wing under static structural analysis

**Table 4** The results of modal analysis

Material	Natural frequency (Hz)	Total weight (kg)
CFRP with skin	10.163	0.982
GFRP with skin	9.455	1.220
CFRP without skin	4.748	0.373
GFRP without skin	4.266	0.463

Due to the resonance factor affecting the failure of UAV wing structures, the maximum deformation is determined without pre-stress conditions using the modal analysis. Table 4 examines the natural frequency and maximum deformation of the wing structure. By obtaining the natural frequency of the aircraft wing, it would be useful to calculate the resonance of the wing structure used to prevent the failure of the wing structure.

## 4 Conclusion

Conventionally, UAV wing structures are made of heavy metal or high-density materials, which could significantly affect the lift force and durability of UAVs. This paper proposes a sustainable utilization of composite materials for constructing UAV wings. The typical wing model is analyzed using the ANSYS Workbench® to determine the high performance and lightweight structure. Compared with the glass-fiber-reinforced plastic and aluminum, the Carbon-fiber-reinforced polymers (CFRP) provides superior performances in terms of lightweight, flexibility, and external load. In modal analysis, the lowest frequency mode is considered. The natural frequency of the CFRP wing structure is higher than those of GFRP, resulting in the delay of resonance. Consequently, the CFRP can be utilized and extended to apply in other aviation structures, i.e., fuselage, empennage, nacelle, cowling structures, and other structures such as automotive parts, motorcycle frames, and sports equipment.

## References

- Aabid, A., Zakuan, M. A. M. B. M., Khan, S. A., & Ibrahim, E. Y. (2021). Structural analysis of three-dimensional wings using finite element method. *Aerospace Systems*, 5, 1–17.
- Anderson, J. D. (2010). *Fundamentals of aerodynamics*. McGraw-Hill.
- Boransan, W., Kerdphol, T., & Phunpeng, V. (2021). Experimental manufacturing of glass fiber composites considering flexural behaviour. *Spektrum Industri*, 19(2), 87–95.
- Gotten, F., Finger, D. F., Havermann, M., Braun, C., Marino, M., & Bil, C. (2021). Full configuration drag- estimation of short-to-medium range fixed-wing UAVs and its impact on initial sizing optimization. *CEAS Aeronautical Journal*, 12(1), 589–596.
- Nielsen, L. F. (2005). *Composite Theory — Elasticity composite materials*. Berlin: Springer.
- Phunpeng, V., & Biaz, P. M. (2014). Mixed finite element formulations for strain-gradient elasticity problems using the FEniCS environment. *Finite Elements in Analysis and Design*, 96(1), 23–40.
- Ramesh, K., Balakrishnan, S. R., & Balaji, S. (2013). Design of an aircraft wing structure for static analysis and fatigue life prediction. *International Journal for Engineering Research & Technology*, 2(5), 129–135.
- Saensuriwong, K., Kerdphol, T., & Phunpeng, V. (2021). Laboratory study of polypropylene-based honeycomb core for sandwich composites. *Spektrum Industri*, 19(2), 97–104.
- Serkan, C., Kadir, G., Mustafa, A., & Ikbali, O. (2020). Finite element method based structural analysis of quadcopter UAV chassis produced with 3D printer. *Journal of Scientific Report-A*, 44(1), 24–32.
- Sharma, H., Roshan S. A., G. Ramesh, A. Sajeer, & Narayan P. (2013). Design of a high-altitude fixed wing mini-UAV – aerodynamic challenges, Conference or Workshop Item, Jaipur, India
- Sullivan, R. W., Hwang, Y., Rohani, M., & Lacy, T. (2009). Structural analysis and testing of an ultralight unmanned-aerial-vehicle carbon-composite wing. *Journal of Aircraft*, 46(3), 814–820.
- Theys, B., & Schutte, J. D. (2020). Forward flight tests of a quadcopter unmanned aerial vehicle with various spherical body diameters. *International Journal of Micro Air Vehicles*, 12(1), 1–8.
- Thomas, B., & Roy, T. (2015). Vibration and damping analysis of functionally graded carbon nanotubes reinforced hybrid composite shell structures. *Journal of Vibration and Control*, 23(11), 1711–1738.
- Ting, K. S., Balasubramanian, E., Surendar, G., & Sachin, S. (2019). Finite element analysis, prototyping and field testing of amphibious unmanned aerial vehicles. *UPB Scientific Bulletin, Series D*, 18(2), 125–140.



# A More Electric Aircraft Application: Starter/Generator



Ufuk Kaya and Eyyup Oksuztepe

## Nomenclature

I	Phase current
i	Stator current
V	Phase voltage
v	Stator voltage

## 1 Introduction

The electrification of transportation systems is very popular nowadays and essentially aims to use electric power as the main energy source. But when it comes to aviation, this goal is not very feasible due to regulations and technological constraints. Hence, the aviation industry and researchers studied feasible electrification applications called More Electric Aircraft (MEA). The MEA concept defines the extensive usage of electric power on conventional aircrafts instead of pneumatic, hydraulic, and mechanical power. By doing so, the goal of efficient and environmentally friendly aircrafts will be more achievable. The narrow-body and wide-body aircrafts are responsible for 76% of the total greenhouse gas emission due to aviation activities (International Council on Clean Transportation, 2018). Also the International Council on Clean Transportation states that 2.4% of the total greenhouse gas emission in the United States during 2018 is originating from aviation actions. Therefore, using electric power as an alternative of present power sources is very vital. Moreover, the electric-powered aircraft systems are more efficient, robust, and

---

U. Kaya (✉) · E. Oksuztepe  
Department of Avionics, Firat University, Elazig, Türkiye  
e-mail: [u.kaya@firat.edu.tr](mailto:u.kaya@firat.edu.tr); [eoksuztepe@firat.edu.tr](mailto:eoksuztepe@firat.edu.tr)

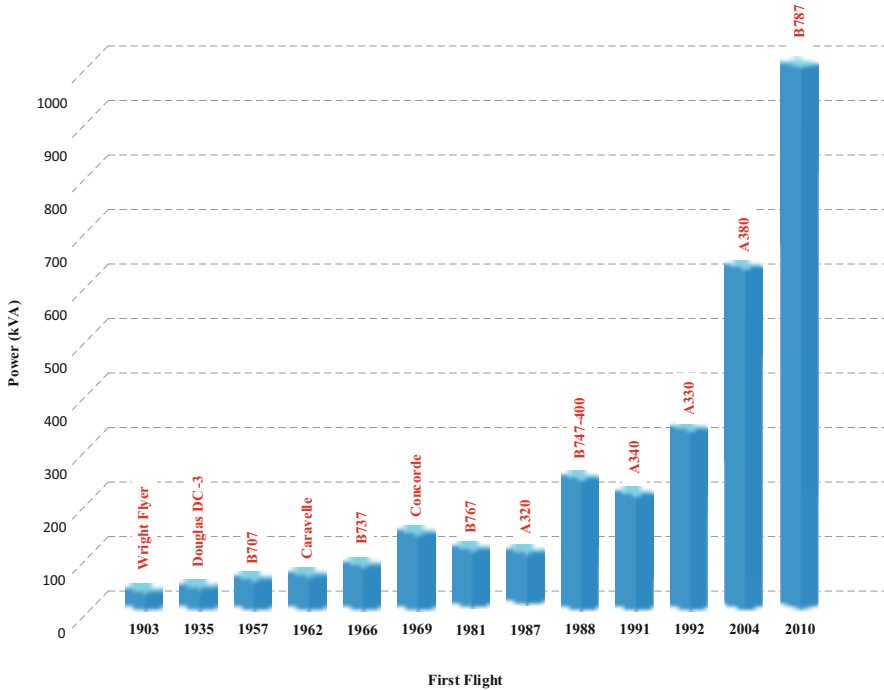


**Fig. 1** The increased demand for electric power by years

cost-effective. They usually require less maintenance, which leads to shorter maintenance time and less maintenance costs. As mentioned above, the conventional aircrafts use pneumatic and hydraulic power for subsystems such as main engine starters, actuators, and air conditioning system. Using electric power for this system comes with a big consequence: the increased demand for electric power on aircraft. Hence, the installed total electric power on an aircraft has increased over the years. As is seen in Fig. 1, Boeing 787 has almost 1000 kVA installed electric power (Madonna et al., 2018).

The main engine generators and auxiliary power unit (APU) are responsible for electric power production in conventional aircrafts. The subsystems of this conventional electric generation system vary with aircraft type. But the electric generation system with three stages is very common in commercial aircrafts. This three-staged system consists of an alternative current generator, constant speed drive, voltage regulator, field windings, excitation winding, and rotating rectifier. The conventional electric generation system given in Fig. 2 is complex and demands high maintenance. This increases costs and decreases system efficiency and reliability. Also this complex system is only used for electric power generation. The aircraft is still dependent on ground units or APU for main engine starting. For eliminating this dependency and compensating for the required electric power demand, the new-generation aircraft use Starter/generators (SG). The SG is basically an electric

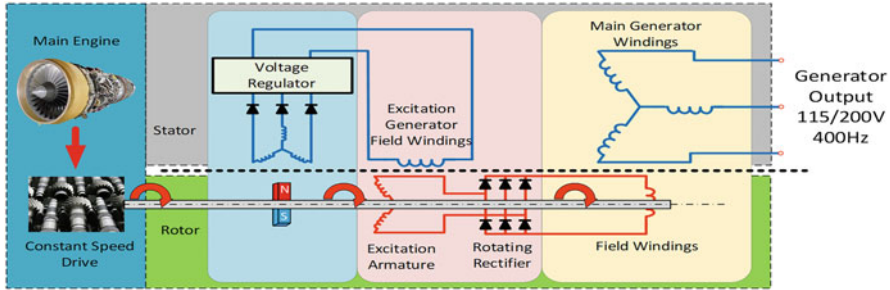


Fig. 2 The conventional three-staged electric generation system

machine and is capable both of main engine starting and electric power generating. For this reason, the SG has a key role in MEA concept. The SG increases aircraft efficiency in terms of electric power generation and starting main engine. Also it is lighter and smaller than conventional system. Besides the efficient and fault-tolerant SG design, the operation control of SG is very important. The second section comprises a short brief of candidate electric machine types for SG. The third section gives the operation control of SG regarding the chosen machine type. While the fourth section gives the results and discussions, the final section concludes the SG operation in a manner of future studies.

## 2 Starter/Generator

The main jet engines need an external accelerator until idle speed. This first motion of jet engine is named as starting operation. The conventional starting operation of jet engines can be accomplished with starter, pressurized air from APU or ground units. On the other hand, the generators are coupled with main engine or APU responsible for electric power generation on speeds above idle speed. Briefly, the SG is an electric machine, which can operate as starter and generator simultaneously. In contrast to conventional electric power generation system, the SG operation is less complex and plain. The operation differences of these predecessor and successor systems are summarized in Fig. 3.

According to aviation regulations and technical demands such as power level, fault tolerance, weight, and volume constraint, one can use different types of machines as SG. But in detail, Ganev et al. (2014) indicated 14 different criteria for the SG operation. Hereby, there are three types of electric machines suitable for SG. These are induction motor (IM), switched reluctance motor (SRM), and permanent magnet synchronous machine (PMSM). The induction motors are simple and controller-free machines. They also have good fault tolerance. Friedrich and Girardin (2009) point its fault tolerance in high temperatures. The IM has some disadvantages that limit its usage as a SG. Besides other competitor machines, the

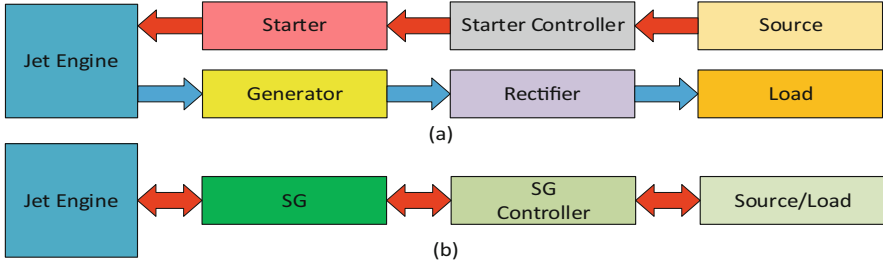


**Fig. 3** (a) The conventional system. (b) The new-generation SG

IM has higher rotor losses, which makes cooling of the machine harder. Also, high rotor losses decrease machine efficiency. The high speed limitation of IM is not suitable for SG operation. The second candidate machine SRM is a good choice for higher temperature operations. But the SRMs also suffer from rotor losses, and additionally they have high ventilation losses due to their unique structure. This structure also causes high torque vibrations which affects the starting operation of the SG. When it comes to military applications, the SRM is a good choice for SG (Ferreira and Richter, 1993). The SRM machine efficiency is lower than the next competitor machine, PMSM. The last and chosen machine type PMSMs are famous for their high efficiency in wide operating speed range. The flux-weakening applicable structure of the rotor enables efficient operation. The magnets used in rotor provide good power/torque density. But using magnets in rotor comes with some disadvantages. First of all, these magnets are not tolerant for high operating temperatures. Therefore, the machine needs to be cooled. Moreover, flux-weakening should be applied with caution. Otherwise, the magnets will be demagnetized. But these disadvantages can be taken care of. Also high thermal tolerant magnets are available for use in harsh environments like aviation. The PMSM is widely used as SG on new-generation aircraft. For example, Lockheed Martin's F-22 has six PMSM-based SGs on board. There are surface-mounted and interior magnet types of PMSMs used as SG. They can work in wide speed ranges with high efficiency. Ismagilov and Vavilov (2019) optimized a three-phase 150 kW PMSM-based SG. The optimized machine can speed up to 9000 rpm.

### 3 The Operation of SG

The operation of SG is dimerous. The first part of this operation is the starter (motoring) operation, and the second part is the generator (generating) operation. The starter and generator operations should be cascaded and meet aircraft operation demands. For robust starter operation, the actual speed of the SG should be known. The actual speed can be measured with an encoder. The operating envelope of the SG is shown in Fig. 4. Points 1 and 2 of the operating envelope correspond to

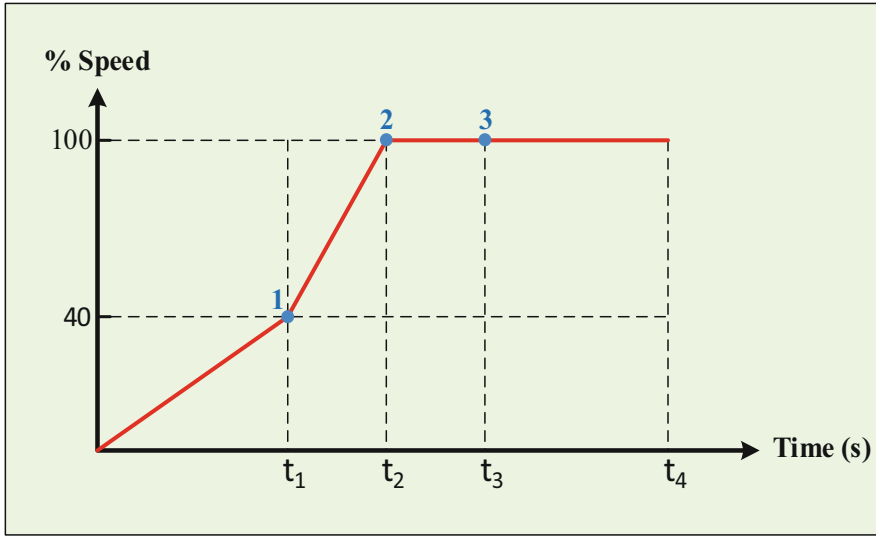


Fig. 4 The operating envelope of the SG

ignition speed and idle speed, respectively. The generator operation starts at point 3. The starter operation of SG usually occurs until the ignition speed. When the SG reaches that speed, the main jet engine is capable of self-operating. Hence, there is no need of the starter operation, and the SG is switched off. At point 2, the main jet engine reaches idle speed. From that point, the SG can operate as generator. But the SG is still kept offline until point 3 for the regulation of shaft speed. When point 3 is achieved, the SG can safely operate as generator. The controller manages both starter and generator operations. The starter operation takes place during the  $0 - t_1$  seconds. In this time region, the SG accelerates until the ignition speed. The controller uses field-oriented control technique with no flux-weakening. In order to do that, the  $d$ -axis current  $i_d$  is set to 0, and the  $q$ -axis current  $i_q$  is calculated instantaneously. Then, the controller algorithm produces proper switching signals for the gates of IGBTs according to space vector pulse width modulation technique. The generator operation of SG is efficient in high speeds owing to its flux-weakening capability. The flux- or field-weakening technique is simply applying reverse field to magnets on rotor. The reverse field should be utilized properly to avoid permanent demagnetization of magnets. Unlike the starter operation, the controller calculates both  $i_d$  and  $i_q$  currents during the generator operation. For efficient flux-weakening operation, the controller also considers Eqs. (1) and (2) (Lang et al., 2021).

$$i_d^2 + i_q^2 \leq I_{\max}^2 \tag{1}$$

$$v_d^2 + v_q^2 \leq V_{\max}^2 \tag{2}$$

The power management and distribution system is responsible for stored or generated electric power in new-generation aircrafts (Maldonado et al., 1999). Also, this system decides the amount of generated electric power on aircraft by the power consumption of loads. The loads on an aircraft can be resistive, capacitive, or inductive. Therefore, the generator operation of the SG is secured with the controller, and the controller regulates DC bus voltage to 270 VDC. This regulation is independent from load type and shaft speed. The whole SG system designed and verified with MATLAB/Simulink is given in Fig. 5. According to the operating envelope of the SG given in Fig. 4, the SG is accelerated to 15,000 rpm. The speed and torque graphs are given in Fig. 6 a and b, respectively. The starter operation occurs between

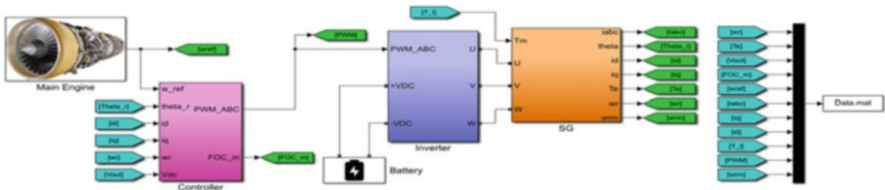


Fig. 5 The modeled SG system in MATLAB/Simulink

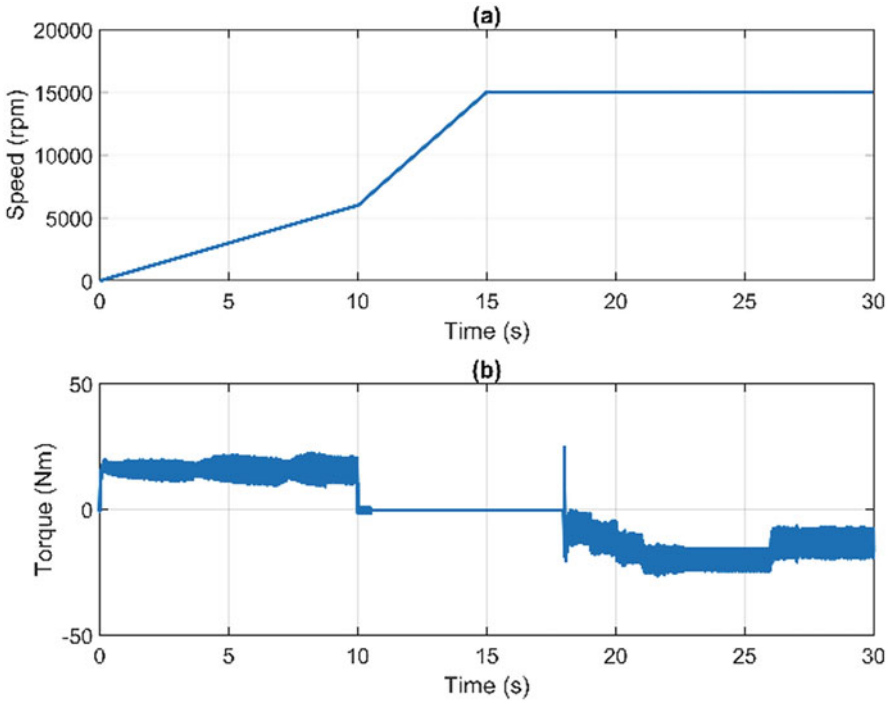
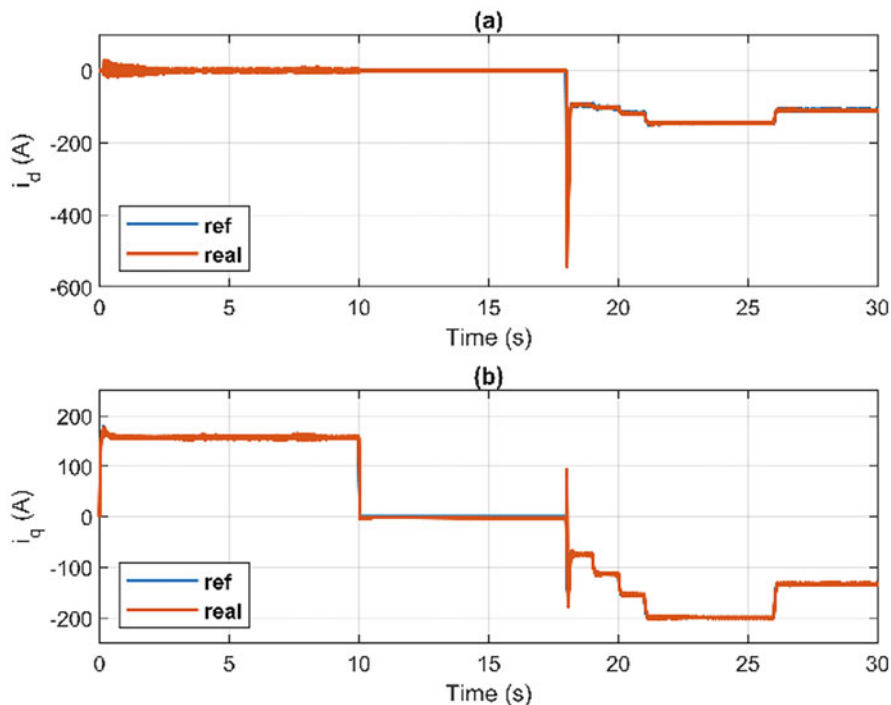
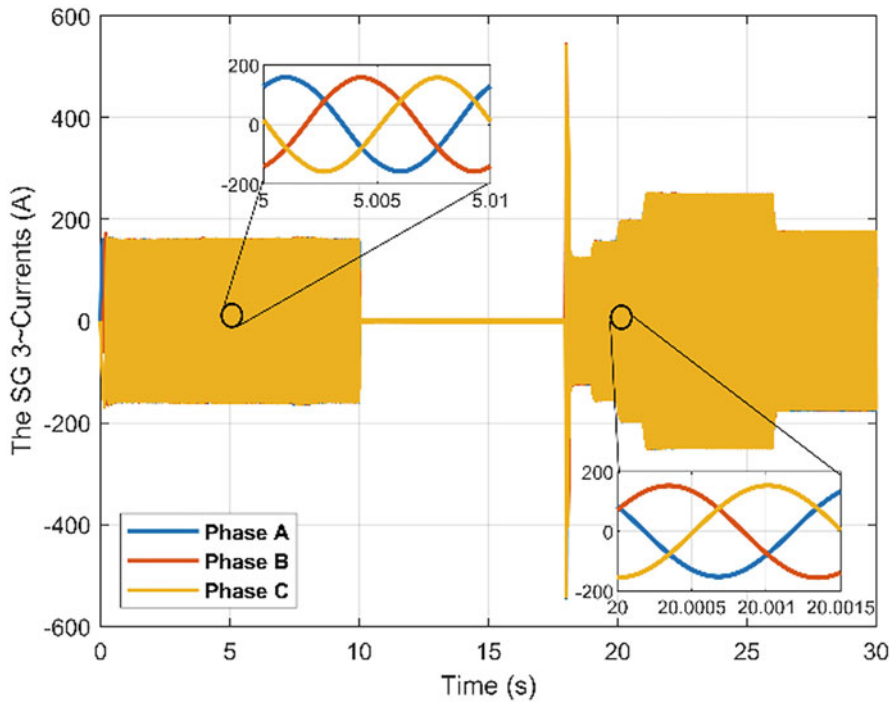


Fig. 6 (a) The speed of the SG. (b) The torque of the SG



**Fig. 7** (a) The  $i_d$  current. (b) The  $i_q$  current

0 and 10 seconds and generator 18 and 30 seconds. The main jet engine is fired at 10 seconds and starts to accelerate idle speed of 15,000 rpm. Hence, the SG is offline. The  $i_d$  and  $i_q$  currents of SG are given in Fig. 7a and b, respectively. The mean value of  $i_d$  is  $-50.41$  A and the  $i_q$  is  $-10.65$  A. Figure 8 shows three phase currents with zoomed perspective both for starter and generator operations. The currents are stable and vary between  $\pm 156.25$  A approximately during the starter operation. The mean and peak values of phase currents vary during generator operation due to changing load conditions. As it can be seen from the figure, there are five different load conditions. The final figure of Fig. 9 shows the battery current and the battery voltage. The battery current direction changes with the SG operation. During the starter operation, the SG operates as motor and consumes electric power. For generator operation, the SG generates electrical power and the battery current is positive. The controller regulates common bus voltage to 270 VDC.



**Fig. 8** The three-phase SG currents

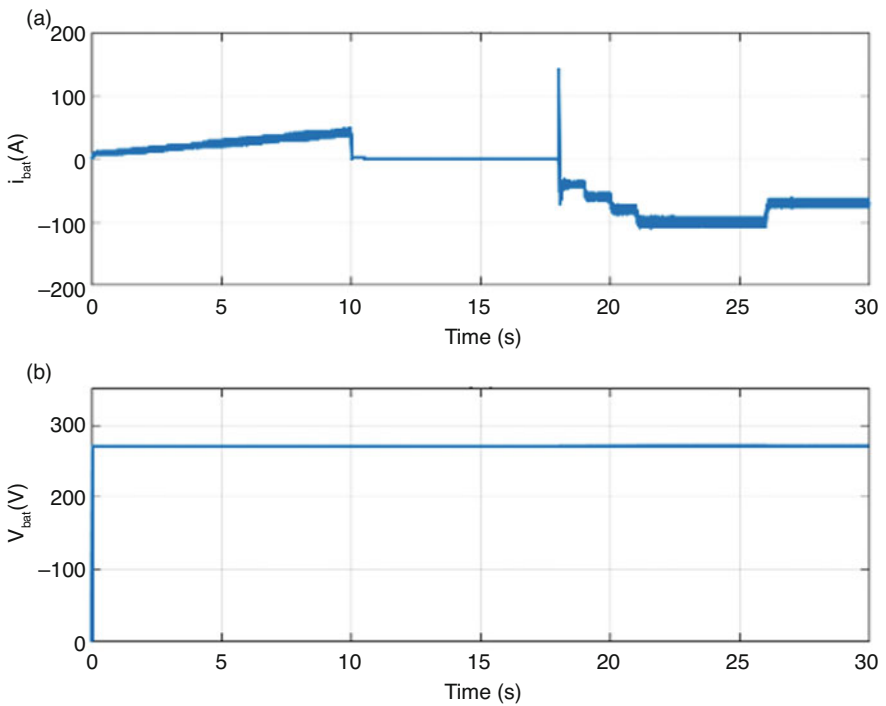


**Fig. 9** (a) The battery current. (b) The battery voltage



## 4 Conclusion

This study has revealed very important findings for future study areas such as SG machine design. Due to demagnetization of magnets, the flux-weakening operation is limited. The desired iq current for such operation may not be suitable for the SG. Hence, it is highly recommended to simulate the whole SG system before electromagnetic machine design.

On the controller side, the conventional control technique is not satisfactory and not recommended due to high speed region flux-weakening operation. Also, sufficient switching frequency needs to be determined properly with respect to controller gains and power electronics. So, it would be better to choose a feedforward controller than a conventional feedback controller.

**Acknowledgments** This work was funded by the Scientific and Technological Research Council of Turkey (TUBITAK) with project number 121E370.

## References

- Ferreira, C. A., & Richter, E. (1993). Detailed design of a 250-kW switched reluctance starter/generator for an aircraft engine. *SAE Transactions*, 289–300. <https://doi.org/10.4271/931389>
- Friedrich, G., & Girardin, A. (2009). Integrated starter generator. *IEEE Industry Applications Magazine*, 15(4), 26–34.
- Ganev, E. (2014). Selecting the best electric machines for electrical power-generation systems: High-performance solutions for aerospace more electric architectures. *IEEE Electrification Magazine*, 2(4), 13–22.
- International Council on Clean Transportation. (2018). [https://theicct.org/sites/default/files/publications/ICCT\\_CO2-commercl-aviation-2018\\_20190918.pdf](https://theicct.org/sites/default/files/publications/ICCT_CO2-commercl-aviation-2018_20190918.pdf). Accessed on 22 Sept 2021.
- Ismagilov, F. R., & Vavilov, V. E. (2019). Optimization of a high-temperature starter—Generator of inverted design for aircraft. *Russian Electrical Engineering*, 90(5), 391–396.
- Lang, X., Yang, T., Li, C., Yeoh, S. S., Bozhko, S., & Wheeler, P. (2021). *An enhanced feedforward flux weakening control for high-speed permanent magnet machine drive applications* (Vol. 14, p. 2179). IET Power Electronics.
- Madonna, V., Giangrande, P., & Galea, M. (2018). Electrical power generation in aircraft: Review, challenges, and opportunities. *IEEE Transactions on Transportation Electrification*, 4(3), 646–659.
- Maldonado, M. A., & Korba, G. J. (1999). Power management and distribution system for a more-electric aircraft (MADMEL). *IEEE Aerospace and Electronic Systems Magazine*, 14(12), 3–8.

# Safety Culture and Safety Management System in Aviation



Emre Nalçacıgil and Betül Kaçar

## Nomenclature

CAA	Civil Aviation Authority
EASA	European Aviation Safety Agency
GDCA	General Directorate of Civil Aviation
ICAO	International Civil Aviation Organization
OECD	Organization for Economic Co-operation and Development
SMICG	Safety Management International Collaboration Group
SMS	Safety Management System
SSP	State Safety Program
UK	United Kingdom

## 1 Introduction

Aviation is basically a sector with a highly complex structure that houses interdependent operational activities, such as airline operations, flight services, ground handling, fuel, maintenance, customer service, catering, management and security. In such a large, global, dynamic and fast-evolving industry, risk cannot be addressed as the most important factor, which is zero-based, during the operation of any error, omission or misstatement that could lead to disasters that are executed in a safe manner to avoid the process. For these reasons, the International Civil Aviation Organization (ICAO), according to all the institutions that operate in the aviation, airports, airlines and other companies to be able to perform operations safely,

---

E. Nalçacıgil (✉) · B. Kaçar  
Cappadocia University, Nevşehir, Türkiye  
e-mail: [emre.nalcacigil@kapadokya.edu.tr](mailto:emre.nalcacigil@kapadokya.edu.tr); [betul.kacar@kapadokya.edu.tr](mailto:betul.kacar@kapadokya.edu.tr)

including, to the elimination of accidents or to minimize the possibility of accidents in 2005, published by the International Civil Aviation Organization safety management system is implementing in light of the instructions.

Nowadays, in order for the safety management system in aviation to fully achieve the set goals, the development of a safety culture in aviation has begun to be considered an important element in achieving the goals, due to the fact that a person is always at the centre. The International Civil Aviation Organization aims to make the safety management system applicable in the same way and at the same level all over the world. Therefore, when implementing it, there should be a standardized international safety culture in every part of the world.

### ***1.1 Safety Culture in Aviation***

Zero accidents are the goal of international civil aviation organizations, aircraft manufacturers and other civil aviation organizations. In order to achieve this, it equips the aircraft produced by aircraft manufacturers with very advanced technologies every day. International civil aviation organizations, by setting international standards for the subject countries to closely follow the issue of compliance with these standards and the country's legal infrastructure necessary for the preparation of national civil aviation authorities in this regard, are engaged in a very serious study (Erdag, 2013:1).

Research shows that 10% of accidents are caused by unsafe conditions, and the remaining 90% are caused by corporate and human factors. Since the greatest threats to aviation safety are caused by organizational problems, organizations have taken action to make the system more secure. An effective safety management system generates a developed safety culture and provides the necessary management environment for an organization to easily identify and solve systemic safety problems (Zealand, 2009:1).

Safety culture is the perception, value and priority of safety in an institution. This reflects the real commitment to safety of all departments of all levels that exist in the organization. At the same time, the safety culture is defined as "doing the right thing even when no one is watching you". Safety culture is not something that is bought and sold; it is a phenomenon that occurs as a product of the combined effects of an organization's organizational culture, professional culture and, in general, national culture (Skybrary, 2017:1).

### ***1.2 Historical Development of Safety Culture***

The term safety culture first appeared in 1987 with the publication of the OECD Nuclear Agency's report on the 1986 Chernobyl disaster. However, most companies with high-risk jobs thought that making money was a higher priority than safety until

the last few years (Cooper, 2002:30). After a short while, the concept of safety culture, among other things, in transport (the Kings Cross Underground fire in London 1987; the Clapham Junction rail crash in London 1988) and in offshore oil production (the Piper Alpha platform explosion in the North Sea in 1988), has emerged again with a major disaster. The UK nuclear safety panel defines safety culture, which has become the industry standard definition of a developed country (Goldenhar, 2014:18): “The safety culture of an organization and its commitment to an organization’s health and safety management, style and competence that determine individual and group values, attitudes, perceptions, competencies and patterns of behaviour of the product”.

### ***1.3 Important Elements of Safety Culture***

The culture of an organization is defined by what people/employees do. The decisions people make reflect the values of the organization. While the following sections reflect the critical elements of the safety culture, these activities will be a conscious culture in which the managers and operators of the systems have up-to-date information. The following important elements of the safety culture are evaluated within the scope of human, technical, organizational and environmental factors that determine the safety of the system as a whole (Ross, 2009:19).

- **Reporting Culture**

People are encouraged to express their concerns about safety, to report their mistakes and events up to a point.

When safety concerns are reported, they are analysed and appropriate measures are taken.

- **Flexible Culture**

A culture that can effectively adapt to changing demands.

The ability to switch from bureaucratic, centralized mode to a more decentralized professional mode.

- **Learning/Information Culture**

People are encouraged to develop and apply their knowledge and skills to improve corporate safety.

The staff is updated by the management on safety issues.

Feedback is provided to the staff about safety reports so that everyone can learn lessons.

- **Fair Culture**

People are even rewarded for providing basic information about safety.

Mistakes should be understood, but deliberate violations cannot be tolerated.

The workforce knows and accepts what is acceptable and unacceptable.

The Fair Culture is according to James Reason, “A questioning attitude against thoughtlessness resistant, safety idea dedicated to excellence, and safety issues both personal and corporate accountability encourages self-regulation” (Reason, 2004). A

fair organizational culture promotes security by supporting the fact that people are open to mistakes; mistakes always arise, and some mistakes should not carry a personally harsh, punitive resolution with them in cases where the system itself may be flawed. However, a clear line should be drawn that distinguishes between the common one of ordinary human error and deceptive and deliberate violations that can be dealt with more rigidly and not taken by force (Ross, 2009:21).

## 2 Safety Management System in Aviation

According to the definition of the dictionary, safety means: to be free from risk or danger, to move away, to be exempt. However, if the nature and inherent risks of aviation are to be taken into account, this dictionary definition remains restrictive and inadequate in terms of its actually applied meaning. The statement to get out of danger will most likely not allow the operation of any aircraft. For this reason, the International Civil Aviation Organization defines aviation safety as a state of being free, removed and exempt from unwanted risks or injuries that may occur against aircraft, assets or people. In other words, aviation safety is called the situation when the risks remain at the desired level (International Civil Aviation Organization [ICAO], 2013:14).

Although the elimination of accidents and/or serious incidents and the achievement of absolute control are desirable, these are the goals that cannot be achieved in open and dynamic operational contexts. Hazards are integral components in the context of aviation operations. Although the best efforts are being made to prevent it, malfunctions and operational errors will occur in aviation. No human activity or human structure system can be guaranteed to be completely free from hazards and operational errors. Aviation safety has a dynamic structure. New safety hazards and risks are constantly emerging and should be reduced as much as possible. As long as safety risks are kept at an appropriate level of control, an open and dynamic system such as aviation can always be kept at a safe level. It is important to note that acceptable safety performance is usually defined and influenced by national/international norms and cultures (ICAO, 2018:1–1).

### 2.1 *Development of the Concept of Safety*

Although the application of safety rules in aviation dates back to the time of the first military and commercial flights in writing, in fact, safety measures were also taken at the end of the 1700s, when there were primitive methods used to fly such as balloons and wings. For example, hot air balloons can be flown in open and dirt areas without hard hats, knee pads, etc.; the use of personal protective equipment was actually a safety measure taken without realizing it (BASOL, 2013).

In its early years, safety was based on such elements as undeveloped technology, lack of appropriate infrastructure, limited foresight and insufficient understanding of the dangers inherent in aviation operations. Therefore, it was an event that had no available opportunities to meet the demands and was not subject to strict regulations (SHGM, 2011:3).

Technological advances (largely due to accident reviews) and, accordingly, the development of appropriate infrastructure have led to a gradual, continuous decrease in the frequency of accidents, as well as an increasing need for regulation (SHGM, 2011:4).

The systematic consideration of safety dates back to the beginning of the 1950s. Other progress on the subject can be explained by four approaches that are consistent with the period of activity (ICAO, 2018:2–1):

- **Technical Factors:** From the early 1900s to the late 1960s, aviation was a type of transport in which the source of safety shortcomings was associated with technical factors and technological failures. The focus of safety studies was therefore based on the research and improvement of technical factors. In the 1950s, technological advances led to a gradual decrease in the frequency of accidents, and the safety processes were expanded to comply with legal regulations and inspections.
- **Human Factors:** In the early 1970s, the frequency of aviation accidents decreased significantly due to major technological advances and improvements in safety regulations. Aviation has become a safer and safer form of transport, and the focus of safety work has been expanded to include human factors, including elements such as the human/machine interface. Despite investments in resources used to reduce errors, human factors continue to appear as a recurrent factor in accidents. Human factors tended to focus on the individual without fully considering the operational and organizational context. Until the early 1990s, it was not accepted that individuals work in a complex environment with a large number of factors that can affect their behaviour.
- **Organizational Factors:** In the mid-1990s, safety began to be viewed from a systematic perspective. It began to be considered in such a way as to cover human and technical factors, as well as organizational factors. The concept of “organizational accident” was introduced. This perspective has addressed the impact of safety risk controls on the organizational culture and policies of such elements. In addition, the collection and analysis of routine safety data using reactive and proactive methods allowed organizations to monitor known safety risks and identify emerging safety trends. These improvements provided the basis for learning the current safety management approach.
- **Total Systemic Factors:** Since the beginning of the twenty first century, many state and aviation organizations have adopted safety approaches in the past and reached the next level by developing the approach that they adopted later. SSPs or SMS were started to be implemented, and they saw the benefit of the safety management system. This has led to the complexity of the aviation system and the growing recognition of different organizations that play a role in aviation safety.

There are many examples of accidents and incidents that show that the interfaces between organizations cause negative consequences.

The steady and integrated evolution of safety has led governments and aviation organizations to a point where they are seriously considering the interactions and interfaces between the components of the system: people, processes and technologies. In addition, the states have begun to define the role that the total aviation system approach can play in the development of SSP (ICAO, 2018:2–4).

A safety management system is a defined set of processes implemented throughout a company/institution or organization that ensure more effective risk-based decision-making in a company's daily business (EASA-ICAO Annex 19, 2010). The rapid change and development of technology, increasing efficiency and confusion due to the growth of global aviation, and new challenges are the main reasons for the formation of a risk-based approach to safety (Civil Aviation Authority [CAA], 2015:12).

SMS works on maximizing the opportunities for continuous improvement and improvement of aviation safety (Safety Management International Collaboration Group [SM ICG], 2010:1). In other words, a safety management system is a holistic form of system in which a number of processes or components are combined to form a safety management system. Specifically, it is the interaction of these processes or components that reveals the safety management system. In addition, the October management system is a set of ideas, applications and processes for monitoring and continuously improving the safety within the organization. It is also a system that requires a feedback loop (Transport Canada Civil Aviation Communications Centre, 2004:5).

It is a fact that SMS with the support of senior management cannot be executed only with senior management. In addition, all personnel of aviation organizations and the sectoral information flow in general should be included in SMS activities (SHGM, 2012:4). On the other hand, SMS, with a reactive approach, accidents waiting to happen, and the investigation of the accident after the accident in order to prevent similar accidents investigation by doing the lessons that classic in a completely different way from accident investigations, proactive and predictive approach, the cause of the accident the safety risks of the consequences of the hazards by creating safety risks before they are identify, analyse, mitigate and continuously evaluate ways to control activity (SHGM, 2012:4).

The safety management system also provides enterprises with the opportunity to make more informed decisions, increase safety by reducing accident risks, reduce costs, provide better resource planning that will result in increased efficiency and strengthen the common culture and conduct joint due diligence (Kaliten Consulting, 2012:1).

## 2.2 *The Purpose of the Safety Management System*

The purpose of SMS is to provide organizations with a systematic approach to managing security. It is designed for the continuous improvement of safety performance through the identification of hazards, the collection, analysis of safety data and safety data and the continuous assessment of safety risks. SMS is aimed at proactively reducing aviation accidents and safety risks before they result in incidents. It allows organizations to effectively manage their activities, safety performance and resources and to better understand their contribution to aviation safety (ICAO, 2018:2–13).

According to another source, the purpose of SMS is (CAA, 2015:8):

- Managing risks within the company
- Ensuring continuous monitoring and evaluation of safety performance
- To make continuous improvements in order to achieve an adequate level of safety in the operations performed
- To develop and improve the in-house safety culture

According to the information obtained from the source of Anadolu University, Airport Security Management System, the objectives of the security management system are as follows (Anadolu Üniversitesi, 2021):

- Ensure that the safety risks that may occur in all areas of activity and in all processes that may affect aviation safety can be reduced to acceptable levels.
- SMS focuses more on processes than outputs, trying to understand and find solutions to problems without compromising safety more with a proactive approach rather than a reactive approach.
- SMS predicts that it will fall by constantly measuring safety performance and making it possible to prevent it without an accident.
- In order to manage risks, it is also necessary to try to manage crises arising from risks.

Awareness of the scope of the safety management system in aviation organizations should be high. In general, SMS should include all customer service and operational activities of the relevant aviation organization. SMS is a great job for establishing security in the aviation system. The occurrence of an accident in the aviation system indicates that there is a failure in the middle, and this failure indicates SMS (SHGM, 2012:6).



### 3 Results and Discussion

Safety has been the most important element in aviation since the moment of the first attempts to fly. In particular, when losses of lives and property began to appear as a result of accidents, it became the topic that was most focused on and was at the top of the list.

After the implementation of the safety management system, it was found that a significant decrease was recorded in the accident and death rates in all world civil aviation, including Turkey. However, since there can be no zero accidents or a completely risk-free state in aviation, even if the events cannot be reset, this decrease clearly demonstrates the success of the safety management system application.

One of the most important elements that benefit in reducing negative events and accidents in aviation is the safety culture. Nowadays, the safety culture is also discussed as thoroughly as the safety management system and is almost one of the most focused topics. In fact, the International Civil Aviation Organization safety management system manual safety in the most recently published as a separate part of the culture as a title and not a broader way of dealing has made many recommendations for improving safety culture has been investigated.

In order to ensure an environment of trust in safety, voluntary notifications sent should be handled systematically, and employees should be informed about the process. In order to develop a safety culture in organizations, it should be ensured that all employees from the top management to the lowest level are included in the safety management system process and that the employees' knowledge skills support this issue.

In order to ensure an environment of trust in safety, voluntary notifications sent should be handled systematically and employees should be informed about the process. In order to develop a safety culture in organizations, it should be ensured that all employees from the top management to the lowest level are included in the safety management system process and that the employees' knowledge skills support this issue. Organizations need to have a sufficient number of employees in accordance with their man/hour plans in order to carry out a healthy safety culture in organizations (He, 2012).

As a result of recent studies, it is seen that approximately 84% of employees positively evaluate the safety culture in their organizations. The results obtained make it clear that the safety culture in general is approaching the level of positive safety culture and the safety culture is developing rapidly. In general, it has been observed that airport employees have a high level of safety culture, but there are differences in perceptions of safety culture according to the type of business. The results are that employees of the higher-risk business type have more perceptions of safety. It has also been observed that the perception of aviation employees also differs according to their titles. It has been concluded that the perception of safety culture increases as we move from the lower level to the upper management, but it has been found that non-shift employees have a higher perception of safety than shift employees. There was no significant difference in the perceptions of safety culture according to the gender, age level and educational status of the employees (Galloway, 2010).

## References

- Anadolu Üniversitesi. (2021). *Anadolu Üniversitesi Havaalanı Emniyet Yönetim Sistemi*. <https://eys.anadolu.edu.tr/node/4>. 6 Oct 2021.
- Basol, S. (2013). *Havacılık Kronolojisi*. <http://www.servetbasol.com/Kitaplar/Krono/160530-Krono.pdf>. 6 Oct 2021.
- CAA. (2015). *Advisory Circular AC100-1 (Cilt Volume:0.4)*. Mongolia. <https://mcaa.gov.mn/wp-content/uploads/2018/03/AC-100-1-R.2-1-1.pdf>. 5 Oct 2021.
- Cooper, D. (2002). *Safety culture: A model for understanding & quantifying a difficult concept*. [http://www.behaviouralsafety.com/articles/safety\\_culture\\_understanding\\_a\\_difficult\\_concept.pdf](http://www.behaviouralsafety.com/articles/safety_culture_understanding_a_difficult_concept.pdf). 5 Oct 2021.
- EASA-ICAO Annex 19 – Safety Management. (2010). <http://web.shgm.gov.tr/tr/kurumsal-yayinlar/6082-icao-ek-19-emniyet-yonetimi>. 5 Oct 2021.
- Erdagi, O. (2013). *Emniyet Yönetim Sistemi (SMS)*. <http://havadaahkam.blogspot.com/2013/02/emniyet-yonetim-sistemi-sms.html>. 5 Oct 2021.
- Galloway, S. (2010). Assessing your safety culture in seven simple steps. *EHS Today*. <https://www.ehstoday.com/safety/news/assessing-safety-cultureseven-simple-steps-9093>. 5 Oct 2021.
- Goldenhar, S. H. (2014). *Understanding safety culture and safety climate in construction: Existing evidence and a path forward*. [https://www.cpwr.com/sites/default/files/publications/hecker\\_goldenhar\\_lit\\_review\\_summary\\_final.pdf](https://www.cpwr.com/sites/default/files/publications/hecker_goldenhar_lit_review_summary_final.pdf). 5 Oct 2021.
- He, A. (2012). *Study on the basic problems of safety culture*. <https://www.sciencedirect.com/science/article/pii/S1877705812030536>. 6 Oct 2021.
- ICAO. (2013). *Safety management manual 3*. Cilt.
- ICAO. (2018). *Safety management manual 4*. Cilt.
- Kaliten Danışmanlık. (2012). *Emniyet Yönetim Sistemi SMS Nedir?* <http://www.kaliten.com/emniyet-yonetim-sistemi-sms-nedir.html>. 5 Oct 2021.
- Reason, J. (2004). *Global Aviation Information Network*. <https://flightsafety.org/toolkits-resources/past-safety-initiatives/global-aviation-safety-network-gain/>. 5 Oct 2021.
- Ross, G. (2009). *Safety culture: Concepts*. New Zealand. <https://www.mcnz.org.nz/assets/standards/b71d139dca/Statement-on-cultural-safety.pdf>. 5 Oct 2021.
- SHGM. (2011). *Emniyet Yönetimi El Kitabı (Cilt HADT/T-16)*. Pegem Akademi Yayıncılık.
- SHGM. (2012). *Emniyet Yönetim Sistemi Temel Esaslar (Cilt HAD/T-18)*. Pegem Akademi Yayıncılık.
- SKYbrary. (2017). *Safety culture*. SKYbrary. [https://www.skybrary.aero/index.php/Safety\\_Culture](https://www.skybrary.aero/index.php/Safety_Culture). 5 Oct 2021.
- SM ICG. (2010). *10 Things you should know about SMS*. [https://www.skybrary.aero/index.php/10\\_Things\\_You\\_Should\\_Know\\_About\\_SMS](https://www.skybrary.aero/index.php/10_Things_You_Should_Know_About_SMS). 6 Oct 2021.
- Transport Canada/Civil Aviation Communications Centre. (2004). *Safety management system for small aviation operations*. Canada. <https://aviationsolutions.net/wp-content/uploads/TP14135E.pdf>. 6 Oct 2021.
- Zealand, C. A. (2009). *Safety culture: Concepts*. Aviation Knowledge: <http://aviationknowledge.wikidot.com/aviation:safety-culture>. 5 Oct 2021.

# Airline Service Quality Attributes



Araya Sakburanapech, Narinisara Thongpa, and Prawit Otanalai

## 1 Introduction

Although the airline industry has been hit hard from the global outbreak of COVID-19 since the beginning of 2020, it realises that improving airline services without compromising safety is vital to fulfil passengers' needs and expectations. This supports airlines to increase their competitiveness to respond to the fierce competition. Monitoring quality of services become important not only from operator perspectives but also from regulator perspectives to assure that passengers receive the level of service worth the value of money spent and to raise awareness among those passengers in choosing services of airlines suitable for their needs. This paper aims to explore quality attributes widely accepted in the airline industry. How to monitor quality services provided by airlines will be described.

## 2 Research Method

With the objectives determined above, the research is seen as exploratory research to collect data from primary data sources and secondary data sources. The review of academic and industrial papers had been carried out to understand the differences. This was then used for as a foundation to conduct the semi-structured interviews with Thai-registered air carriers. In addition, focus-group meetings with government agencies relevant were proceed. This helps to understand the perspectives of both parties involved.

---

A. Sakburanapech (✉) · N. Thongpa · P. Otanalai  
Department of Aerospace Engineering, Kasetsart University, Bangkok, Thailand  
e-mail: [araya.sa@ku.ac.th](mailto:araya.sa@ku.ac.th); [narinisara@to70.co.th](mailto:narinisara@to70.co.th); [prawit.o@to70.co.th](mailto:prawit.o@to70.co.th)

### 3 Results and Discussion

#### 3.1 Airline Services

Variations of airline business models are currently seen across the globe. In Thailand, there are three models: full-services carriers (FSC), light-premium carriers (LPC) and low-cost carriers (LCC). The comparison of passenger activities serviced by airlines with the three business models shows in Table 1.

Along the passenger journey comprised of six phases (International Air Transport Association: IATA and Airports Council International: ACI, 2020), there are six different services among the three models. Services provided by full-service carriers are free of charges while some of services provided by low-cost carriers are fully charged to passengers. In the meantime, services provided by light-premium carriers rely on strategies of each individual airlines. Most of optional services by light-premium carriers and low-cost carriers does not involve minimum rights from consumer perspectives.

In addition to the airline business model, flight range influences the type and variety of services provided, for example, baggage allowance without fee, seat classes and variety of foods served in-flight. Quality of services expected from passengers would be in line with the airline business models and flight ranges. Otherwise, it seems not to be fair for those airlines pursuing different approaches for different target market.

#### 3.2 Dimensions of Airline Service Quality

One of the key features of services is intangible, which is difficult for the service providers to continuously monitor the quality of services meet the customer satisfaction. Airlines realise that the quality of services provided along the passenger journey is vital for fulfilling requirements of passengers and raising their loyalty.

**Table 1** Classification criteria of airline business model

Passenger activity	Airline services	FSC	LPC	LCC
Check-in	Baggage allowance	●	●	○
	Business class lounge	●	⊙	✖
In-flight	In-flight entertainment	●	⊙	✖
	In-flight amenity kits	●	⊙	✖
	Dining	●	⊙	○
	Special meal	●	●	✖

- Standard service
- ⊙ Option without fee
- Option with fee
- ✖ No service

**Table 2** Airline service quality matrix along passenger journey

Phase of journey	Pax activity	Passenger need				
		Reliability	Assurance	Tangible	Empathy	Responsiveness
Off airport	Reservation and ticketing			●		●
	Travel preparation	●		●	●	
At airport departure	Check-in	●	●	●	●	
	Baggage drop		●	●		
	Lounge at main base airport			●		
	Boarding	●			●	
In-flight	Cabin service	●		●		
	Seat			●		
	Amenity and entertainment			●		
	Meal	●			●	
	Cabin crew	●	●			
At airport arrival	Disembark		●			
	Baggage claim	●	●		●	
At destination	Passenger service			●	●	

They continue to integrate the quality system to the journey of passenger starting from reservation and ticketing at the origin to baggage claim at the destination. Quality standards are determined regarding to services provided by the airline.

A review and analysis of airline services quality had been carried out to understand quality standards widely used in the global airline industry, and focus-group meetings with airlines currently operating in Thailand had been conducted. The research result shows that five quality dimensions are deployed for assuring that services provided in each phase of passenger journey meet the passenger requirements, as shown in Table 2. They include reliability, assurance, tangible, empathy and responsiveness, which are known as service quality evaluation criteria in the SERVQUAL (Wang et al., 2011). Parasuraman et al. (1988) provided the definition of the five quality attributes as follows:

Reliability: ability to perform the promised service dependably and accurately

Assurance: knowledge and courtesy of employees and their ability to inspire trust and confidence

Tangible: physical facilities, equipment and appearance of personnel

Empathy: caring, individualized attention provided to customers

Responsiveness: willingness to help customers and provide prompt services

### 3.3 Monitoring Quality of Airline Services

Rights of consumer is currently recognized as the mandatory measure that shall be fulfilled by airlines. They involve only vital dimensions of quality services that have huge impacts on minimum rights of passengers. It includes, for example, on-time performance (OTP), flight delays, flight cancellations and complaint handling. Nevertheless, there are numbers of service quality standards voluntary for airlines to increase the satisfaction of their passengers.

Figure 1 presents a comparison of monitoring system of airline service quality, which is currently executed and widely accepted. European Union has set minimum rights of air passenger, known as “air passenger rights”, as the guideline for the aviation authorities of EU countries to regulate all flights to/from the EU countries (European Commission, 2019). The monitoring results have been published with the purpose of raising knowledge and awareness of passengers in some countries, such as the United Kingdom, Germany and Switzerland. Similarly, aviation consumer protection in the United States of America is used as the based mechanism to ensure

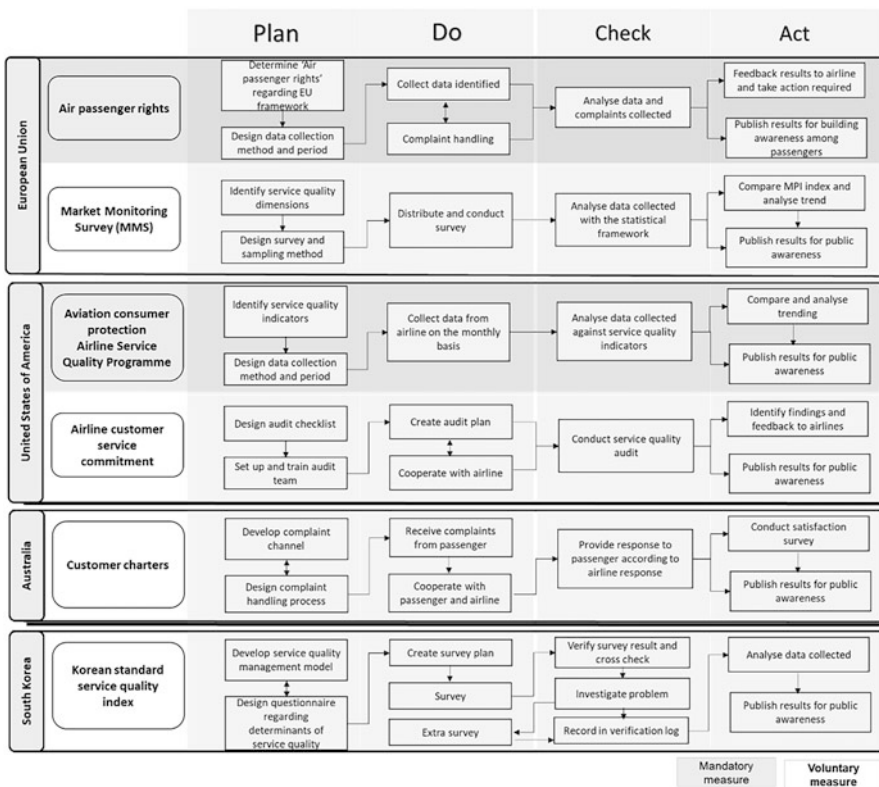


Fig. 1 Comparison of process for monitoring airline service quality

that airlines fulfil the minimum rights of passengers (U.S. Department of Transportation, 2019). Airline service quality programme is another mandatory measure executed by the Federal Aviation Administration. The two mandatory measures focus on the minimum rights of passenger travelled to/from the United States of America. In Australia and South Korea, handling of complaints from air passenger is regulated to assure the complaints are properly handled according to consumer protection law (Australian Competition and Consumer Commission, 2014; Kim et al., 2015).

In addition to mandatory monitoring systems, a number of voluntary systems have been widely implemented to raise the quality levels of services provided by airlines. For example, the market monitoring system (MMS) is an annual satisfaction survey of air passenger travelling to/from the EU region (European Commission, 2021). Based on the three service quality programs shown below, quality attributes of airline services are determined responding to the types and characteristics of services provided along the passenger journey.

Although various service quality programs are implemented across the world, they are all aligned with the continuous improvement circle, called as PDCA cycle (Jonker & Faber, 2020). They begin with identifying quality standards, collecting quality data, comparing results against quality standards set and providing feedback to airlines for improving their services.

## 4 Conclusion

Airlines continue to improve the quality of services to improve and sustain passenger experiences along the travel journey. Services provided by each airline rely on the airline business models. Full-service air carriers, light premium carriers and low-cost carriers serve different services in phase of check-in and in-flight.

Despite the differentiation of services, quality assessment remains crucial for airlines to improve service level to meet passenger expectations. The research result shows that five service quality attributes of SERVQUAL are widely applied in the airline industry. In addition, these five quality attributes are integrated with PDCA cycle not only to solve quality problems but also to identify room for improvements.

## References

- Australian Competition and Consumer Commission. (2014). *Guideline for quality of service monitoring at airports*. Australian Competition and Consumer Commission.
- European Commission. (2019). *Passenger rights*. <https://ec.europa.eu/transport/themes/passengers/air>. Accessed on September 26, 2021.
- European Commission. (2021). *Market monitoring: Consumer market monitoring objectives and results*. [https://ec.europa.eu/info/policies/consumers/consumer-protection-policy/evidence-based-consumer-policy/market-monitoring\\_en](https://ec.europa.eu/info/policies/consumers/consumer-protection-policy/evidence-based-consumer-policy/market-monitoring_en). Accessed on September 26, 2021.

- International Air Transport Association: IATA and Airports Council International: ACI. (2020, October). *The NEXTT vision in a post-COVID-19 world*.
- Jonker, J., & Faber, N. (2020). *Organising for sustainability: A guide to developing new business models*. Palgrave Macmillan.
- Kim, J.-c., Kim, Y. M., Han, J.-H., et al. (2015). *Korea's aviation policies* (Issue 20). The Korea Transport Institute (KOTI).
- Parasuraman, A., Zeithaml, V. A., & Berry, L. L. (1988). SERVQUAL: A multiple-item scale for measuring consumer perceptions of service quality. *Journal of Retailing*, 64(1), 12–40.
- U.S. Department of Transportation. (2019, December). *Air travel consumer report*.
- Wang, R., Hsu, S.-L., Lin, Y. H., et al. (2011). Evaluation of customer perceptions on airline service quality in uncertainty. *Procedia – Social and Behavioral Sciences*, 25, 419–437.



# The Influence of Fuels Containing Fatty Acids Ethers on Fuel Systems



Daryna Popytailenko and Olena Shevchenko

## Nomenclature

FAME                      Fatty acid methyl esters

## 1 Introduction

The reduction of world oil reserves, as well as the solution of modern environmental problems, requires the search for alternative energy sources. This is due not only to the need to reduce environmental pollution but also to the importance of switching from fossil fuels to renewable resources. Biodiesel, which is produced from oils and fats by alcoholysis, is the most promising alternative to diesel fuel. Fatty acid methyl esters (FAME) have calorific value, viscosity, and density close to diesel fuel. Its main advantage lies in the reduction of the concentration of harmful substances emitted with exhaust gases in comparison with diesel fuel by 25–50%. FAME can also be produced from fat-containing industrial waste, which will partially solve the problem of waste disposal and environmental protection. However, their corrosive effects on fuel system materials and higher biodegradation are of serious concern. Microorganisms use FAME as an energy source, so their addition to diesel fuel accelerates its decomposition several times. A significant part of corrosive damage to materials is caused by microorganisms, which in the course of their vital activity release metabolic products and accelerate corrosion.

---

D. Popytailenko (✉) · O. Shevchenko  
Ukrainian State University of Chemical Technology, Dnipro, Ukraine

## 1.1 Corrosiveness of Biofuels

FAME are good solvents. Plaque that forms when operating on mineral diesel fuel is destroyed when switching to biofuels, which causes clogging of filters and injectors. During the operation of the engines, the fuel comes into contact with rubber products (gaskets, seals). FAME dissolves rubber engine parts with prolonged contact on unadjusted vehicles. The least resistant to the corrosive effects of biodiesel are polypropylene, polyvinyl.

Motor fuel must not corrode metal parts of the engine that come into contact with fuel and its combustion products. It is necessary to distinguish corrosion caused by fuel during its storage, transportation, and use in the engine from corrosion caused by exposure to combustion products on the surfaces. Despite that FAME has many similar properties to diesel fuel, they are inferior in oxidation stability, low-temperature characteristics, and influence on structural materials. To solve these problems, the influence of FAME and composite fuels on the materials of fuel systems was studied (Shevchenko & Danilov, 2018).

The main indicators that can affect the corrosiveness are the content of sulfur, water-soluble acids, and alkalis and copper plate test.

FAME is more susceptible to microbiological damage due to hygroscopicity and higher bioavailability (Shkilniuk, 2015). As a result of the development of microorganisms, the following problems arise: accumulation of sludge in the tank, changes in the physical and chemical properties of fuel, deposition on the walls of the tank, damage to paints and varnishes, increased engine wear, intensification of corrosion of structural materials, and clogged filters.

The species composition and properties of strains (aggressiveness to materials) are different. More than half of all cases of microbiological destruction of oils and greases occur as a result of the action of fungi of the genus *Aspergillus*, *Penicillium*, *Fusarium*, and *Scopulariopsis*. Microbiological damage to polymer and paint and varnish materials is a consequence of the activity of fungi of the genera *Penicillium*, *Stemphylium*, *Chaetomium*, and *Trichoderma*.

*Cladosporium resinae* (kerosene fungus) is most commonly found in diesel fuels. Its spores can enter the fuel during transportation and remain in a passive state until favorable conditions for growth. Unlike other genera of fungus, the “kerosene fungus” produces significantly more biomass, which causes technical malfunctions in the fuel system.

## 2 Research Methods

To carry out investigations of corrosivity, samples of FAME obtained from fish oil, chicken fat, palm oil, soybean oil, rapeseed oil, sunflower oil, and blended fuels based on pre-hydrotreated diesel fuel with 30% of the above FAME addition were used.

## 2.1 Study of the Corrosion Effect on Metals

The corrosiveness of FAME to metals was assessed by the reduction in plate weight before and after testing using standard methodic. The following metal samples were used in the study: copper grade M1, aluminum alloy D16, steel St1, and brass L63.

The metal plates were processed and sanded with emery paper until a uniform surface was obtained, without roughness and chipping. The dimensions of the plate were measured with a caliper with an accuracy of 0.1 mm. The prepared plates were treated with alcohol to remove fat from the surface and dried between sheets of filter paper in a desiccator for 1 hour. Then, the plates were weighed on an analytical balance with an accuracy of 0.0002 g.

The tested fuel samples were poured into test tubes; metal samples were placed in them and kept in a thermostat at a temperature of  $120 \pm 0.5$  °C. The test was carried out in five stages, each lasting 5 hours. After each stage, the tubes were cooled for 30–40 minutes in air. After the fifth stage of heating, the plates were taken out of the thermostat and placed one by one in the isoctane bottles with lids. The formed deposits were removed from the plates and treated with solutions, depending on the metal. A 10% citric acid solution was used for steel, a 5% nitric acid solution for aluminum, and a 5% sulfuric acid solution for copper and brass. Then, the plates were dried and weighed on an analytical balance.

The corrosiveness of the fuel ( $K$ ) was calculated by the formula (Eq. 1):

$$K = \frac{m_1 - m_2}{S \times \tau} \quad (1)$$

where  $m_1$  is the initial mass of the metal sample, g;  $m_2$  is the sample mass after testing and removal of corrosion products, g;  $S$  is the sample surface,  $\text{cm}^2$ ; and  $\tau$  is the test time, hour.

## 2.2 Microbiological Damage to Fuels

A microbiological damage study was carried out by cultivation of solid nutrient media in Petri dishes. The tests were carried out by cultivation of solid nutrient media in Petri dishes. Pre-purified fuel was seeded under sterile conditions in Petri dishes and kept at a temperature of  $25 \pm 2$  °C during the incubation period. To improve the accuracy, parallel crops were carried out. During and after incubation, the number of colonies of each class of microorganisms was counted. Measurement of bacterial contamination was carried out after an incubation period of 48 hours, mycologically, 7 days.

To count the number of colonies of forming elements (CFE), the Petri dish was placed on a light background. To calculate the amount of CFE in 1 L of the fuel sample, the results of parallel inoculations were summed up, and the average COE was determined using the formula (Eq. 2):

$$M = \frac{a \times 1000}{V} \quad (2)$$

where  $a$  is the average number of colonies at inoculation and  $V$  is the volume of fuel taken for inoculation, mL.

The identification of microbiological contamination was carried out on the basis of morphological characteristics. The assessment of the morphological and cultural characteristics of microorganisms was carried out on solid nutrient media using microscopic examination. Bacteria and fungi were characterized and identified based on colony morphology and microscopic features.

### 2.3 Corrosive Effect on Rubber

A study of the effect of mixed fuels on oil and petrol-resistant (special) rubbers of different compositions was carried out. We studied samples of standard rubber compounds based on butadiene-nitrile rubbers SKN-18 (with a low content of acrylic acid nitrile) and SKN-40 (with a high content of acrylic acid nitrile), as well as research samples of C1 cipher (based on SKN-40 rubber with the addition of polyvinyl chloride (PVC) plasticate) and A1 (based on SKN-40 rubber with the addition of PVC plasticate (polychloride)).

For testing, rectangular samples were made. Rubber samples were placed in test tubes with mixed fuels in a suspended state in a thermostat with a constant temperature of  $50 \pm 0.5$  °C for 12 hours. Samples were periodically removed and weighed on an analytical balance with an accuracy of 0.0002 g. In parallel, control tests were carried out under similar conditions using diesel fuel as a working medium.

## 3 Results and Discussion

FAME samples were practically free of sulfur, except for chicken fat FAME, which contains 9 mg/kg. It follows from this that the sulfur content does not affect the corrosivity of biodiesel fuel. The copper plates in all fuel samples did not darken but became dull without shine. The corrosion rate of copper plates in diesel fuel was  $0.4 \times 10^{-7}$  g/cm<sup>2</sup> × h; in samples of fuels with alternative components, it was within  $0.5$  to  $4 \times 10^{-7}$  g/cm<sup>2</sup> × h for samples with sunflower oil FAME, soybean oil FAME, palm oil FAME, and chicken fat FAME.

The corrosion rate of brass in the mixed fuel samples ranged from 1 to  $6 \times 10^{-7}$  g/cm<sup>2</sup> × h. During the study, it was found that brass samples do not corrode in diesel fuel and chicken fat and palm oil FAME.

Palm oil FAME had a slight corrosive effect on the samples of steel St1 structural carbon steel of ordinary quality. The rest of the fuel samples did not have an

aggressive effect. The study determined that aluminum samples remained intact in blended fuels that contain FAME.

Soybean oil FAME, sunflower oil FAME, palm oil FAME, and chicken fat FAME had practically no corrosive effect on the metals studied in the work. All test results of the corrosion effect of fuel samples on metals are shown in Table 1.

The test results for the determination of microbiological contamination of fuel samples are presented in Table 2.

Analyzing the results obtained during the determination of microbiological contamination, it can be concluded that diesel fuel and sunflower oil FAME had medium contamination with fungal spores and strong bacteria. Rapeseed oil FAME was heavily contaminated with bacterial and fungal spores.

All fuel samples were contaminated with bacteria of the genus *Pseudomonas*, which do not significantly affect the performance of the fuel. The fungus *Cladosporium resinae* was present in diesel fuel, and *Cladosporium resinae* and *Aspergillus* were present in rapeseed oil FAME. Both types of fungi have an aggressive effect on construction materials; in addition, fungi of the genus *Aspergillus* are pathogenic in relation to the human body.

**Table 1** Corrosion rate of metal plates in fuel samples

Fuel samples	The corrosion rate, $\times 10^{-7}$ , g/cm <sup>2</sup> × h			
	Copper	Brass	Steel St1	Aluminum
Diesel fuel 100%	0.4	–	3.9	–
100% soybean oil FAME	4	2	2	1
70% diesel fuel + 30% soybean oil FAME	2	1	–	–
100% sunflower oil FAME	3	4	–	1
70% diesel fuel + 30% sunflower oil FAME	2	6	–	–
100% chicken fat FAME	2	–	–	1
70% diesel fuel + 30% chicken fat FAME	2	3	–	–
100% palm oil FAME	1.3	–	6.5	–
70% diesel fuel + 30% palm oil FAME	0.65	–	0.7	–

**Table 2** Microbiological contamination

Fuel sample	Sample volume (mL)	Bacteria		Fungus	
		Number of colonies	Contamination CFE/L	Number of colonies	Contamination CFE/L
Diesel fuel	0.15	42	280,000	1	6667
	0.24	150	625,000	1	4167
Average result		–	452,500	–	5417
Sunflower oil FAME	0.15	17	113,333	0	0
	0.24	58	241,667	1	4167
Average result		–	177,500	–	2083
Rapeseed oil FAME	0.15	34	226,667	3	20,000
	0.24	76	316,667	6	25,000
Average result		–	271,667	–	22,500

**Table 3** Increase in the mass of rubber samples in mixed fuels, %

Fuel samples	The increase in the mass of the rubber sample (%)			
	A1	S1	SKN – 18	SKN – 40
Diesel fuel 100%	50.8	4.41	3.87	0.6
70% diesel fuel + 30% fish oil FAME	62.39	7.62	8.58	1.22
70% diesel fuel + 30% palm oil FAME	53.25	7.05	7.42	1.41
70% diesel fuel + 30% chicken fat FAME	51.1	6.13	6.34	0.95
70% diesel fuel + 30% soybean oil FAME	62.69	7.85	8.45	1.31
70% diesel fuel + 30% sunflower oil FAME	63.29	7.91	8.56	1.29

The test results showed that in rubber sample A1, the most resistant SKN-40, turned out to be the least resistant to the aggressive effects of mixed fuels. The corrosiveness of composite fuels toward rubbers increases with increasing FAME concentration.

Compared to traditional diesel fuel, samples of blended fuels affect rubber. When using fuels with alternative components, rubber seals should be made from rubber compounds based on nitrile butadiene rubbers. The results of the tests performed are presented in Table 3.

## 4 Conclusion

D16 aluminum alloy samples are corrosion resistant in mixed diesel fuels. FAME, except for palm biodiesel, reduces the corrosion rate of St10 steel due to the formation of a protective film on the surface. The addition of FAME to diesel fuel reduces the corrosive effect on copper. FAME has no corrosive effect on the surface of brass or has a negligible effect, except for sunflower oil FAME. The increased corrosiveness of which is associated with a high content of oleic acid. FAME is corrosive to rubbers, causing swelling and weight loss. The least resistant to corrosion of FAME are rubbers of grade A1, and the most resistant are rubber compounds based on nitrile butadiene rubbers. The degree of microbiological damage to composite fuels was determined in the study. FAME and mixed fuels with their addition are more prone to microbiological contamination.

## References

- Shevchenko, O. B., & Danilov, A. M. (2018). Use of bio-diesel as an additive to petroleum fuel. *Chemistry and Technology of Fuels and Oils*, 53(6), 823–829.
- Shkilniuk, I. (2015). Investigation of the microbiological stability of traditional and alternative aviation fuels. In *First international symposium on sustainable aviation*, p. 4.

# Exposure Potential of Environment by Entropy Continuity for Cruise Altitude of Aircraft Engine



M. Ziya Sogut

## 1 Introduction

The aviation industry intensively discusses the change due to carbon management in its corporate strategies and producing alternatives to fossil fuel-based consumption. Basically, it is seen that there is a lot of work and development in aircraft technologies, from material to technology. Especially the changes in engine technologies have affected this process positively, and many gains have been achieved due to technological improvements. However, it is a fact that there is a need for more effective strategies for carbon management in the aviation industry, which has approximately 3% of the total emissions in the fight against global climate change (IATA, 2013, 2016).

In sectoral studies, especially changes in engine technologies, very different changes have been achieved from weight to combustion performance. These design developments have been significant changes for fossil fuel-burning engines in terms of effective combustion performance, power generation, and life cycles. However, despite all these processes, the production of entropy and the irreversibility that contribute to its formation still have an important potential. This effect defines the potential of direct and indirect emissions and engine-related environmental pollution. In this study, primarily in the cruise condition of a piston engine, depending on the operating performance of the engine, primarily thermodynamic analyses were made, and the effects of entropy-induced environmental pollution caused by the engine were investigated. In this context, the speed-fuel relationship of the engine and the fuel-environment relationship in cruise processes were discussed separately.

---

M. Z. Sogut (✉)  
Maritime Faculty, Piri Reis University, Istanbul, Türkiye

## 2 Flight Process Environment

Increasing flight traffic in the world directly or indirectly interacts with the environmental structures connected to the route relationship. In airplanes operating with different pressure and temperature values, depending on climatic conditions, especially components with thermal processing processes and their performances are affected by environmental conditions. In particular, engine performances represent an important potential due to the irreversibility it causes together with fossil fuel consumption.

Aircraft engines follow a course depending on the general flight plan given in Fig. 1 with a minimum of 26.7 kN propulsion power loads in the general structure. Especially in this process where power management distribution changes depending on environmental conditions, the International Civil Aviation Organization (ICAO) has brought important limitations in the fight against global climate change (Annex 16 of the Civil Aviation Convention – Environmental Protection – Trunk II – Aircraft Engine Emissions). ICAO and related studies have shown the effect of fuel-related inefficiencies, especially due to the flight process, on the sectoral emission potential.

Temperature-dependent operational parameters are an effective tool for engine performance. The manageability of this engine with thermal control at every stage of the engine, including the combustion temperature, is important in terms of performance values. In particular, the relationship between the thrust produced in engine performance and environmental parameters shows the extent of the irreversibility produced. Therefore, thrust optimization and power reduction due to thrust conditions are directly related to performance. Temperature is inversely proportional to density. The high-temperature flight process of the aircraft causes more power consumption and hence fuel consumption. This is the reason for the inefficiency, especially in climbing and descending. Especially uncontrolled heat overload is the cause of this irreversibility.

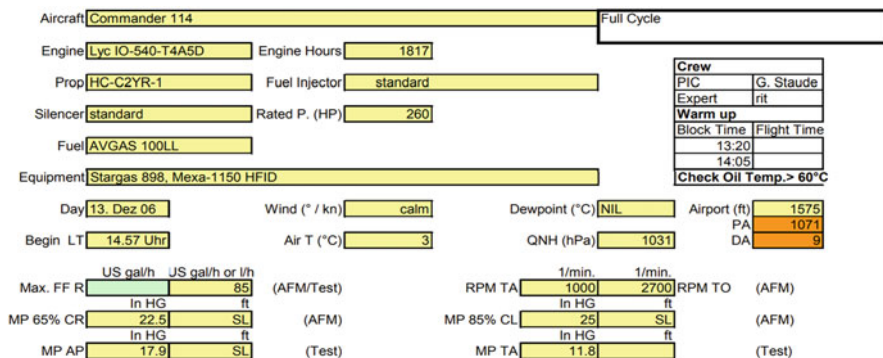


Fig. 1 Reference engine parameters (DETEC, 2007)



Atmospheric conditions vary with altitude. These values are important in terms of engine performance. As the working environment, the temperature and pressure values associated with altitude directly affect the combustion performance. However, this process definition is related to the entropy that occurs due to the irreversibility of the engine. However, for basic structures, the manageability of entropy provides advantages in terms of performance.

### 3 Entropy and Conceptual Framework

Global warming causes the temperature of the earth and biosphere to increase in particular. The entropy of the universe is constantly increasing due to the effective direction and the increasing load condition and the principle of increasing entropy. This is increasing chaos. Especially in this context, it is important to control the fossil fuel consumption. This is provided by entropy management is taken into consideration along with energy management in all system approaches (Jing, 2012).

Based on these concepts of reversibility and absolute temperature, entropy generation is a measure of system disorder due to the exergy destruction produced from the system. For this approach, the second law of thermodynamics and relations criteria such as improvement potential and exergy losses must be prioritized (Dincer & Rosen, 2012; Cornelissen, 1997; Moran et al., 2011; Van Gool, 1997).

In this study, firstly, an index study was conducted to evaluate the environmental effects of entropy production caused by irreversibility. In this context, Environmental Performance Index (EPI) has been seen as a function of entropy due to current engine consumptions under ambient temperature.

$$\text{EPI} = \left( \frac{\sum S_{\text{gen}}}{\sum \dot{E}x_{\text{in}}} \right) \times T_0 \quad (1)$$

The EPI developed here has a value in the range of zero to one. It should be close to zero in terms of environmental impact. However, it is important to use a reference criterion in this evaluation. This value gives us Carnot efficiency. The Carnot efficiency of the engine is the target efficiency of the exergy efficiency as a reference criterion. In this respect, IP has been re-modified and evaluated.

$$\text{IP} = (\eta_{\text{Carnot}} - \eta_m) \cdot (\dot{E}x_{\text{in}} - \dot{E}x_{\text{out}}) \quad (2)$$

where the improvement potential is referenced by the Carnot efficiency for each thermodynamic system. In this study, the Sustainability Index (SI) was developed based on this performance.

$$SI = \left( \frac{\sum S_{gen,c}}{\sum \dot{E}x_{in}} \right) \times T_0 \tag{3}$$

The total entropy production in the system is related to the IP ratio of the engine, which depends on the Carnot efficiency (Sogut, 2021).

### 4 Results and Discussion

This study primarily includes thermodynamic analyses based on the power and speed performance of a piston engine. In the study, exergy analyses were made with reference to the piston engine parameters along with its thermal efficiency. The entropy produced according to the revolutions and fuel consumptions defined in the study and the optimal conditions for them are discussed. For this purpose, the reference motor data is given in Fig. 1.

Depending on the altitude conditions of the engine, the RPM values vary between 980 and 2620 RPM. The altitude load values of the engine vary between 75%, 65%, and 55%. Its velocity relationship is defined as 2510 RPM for 6500 ft, 2450 RPM for 5500 ft, 2300 RPM for 6000 ft, and 2400 RPM for 11,000 ft for cruise altitude criteria. The analyses in this study were used for 18 different process flows of the reference engine between 980 and 2620 RPM. Accordingly, RPM and fuel consumption distribution are given in Fig. 2.

The fuel consumption of the engine ranges from 12 to 81 gal/h. This performance shows a variation between 70 and 188 kW. While the air fuel ratio was 54.4, the ambient temperature was 284.5 K on average. According to these data, the thermal efficiency and RPM change of the motor are given in Fig. 3.

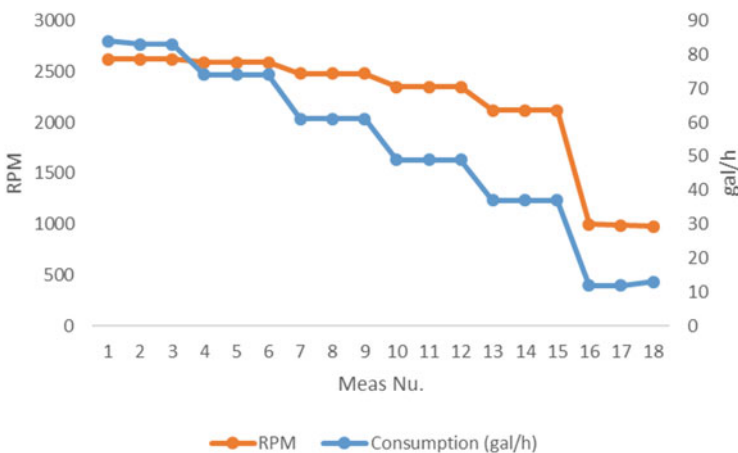


Fig. 2 Fuel consumption and RPM values of engine

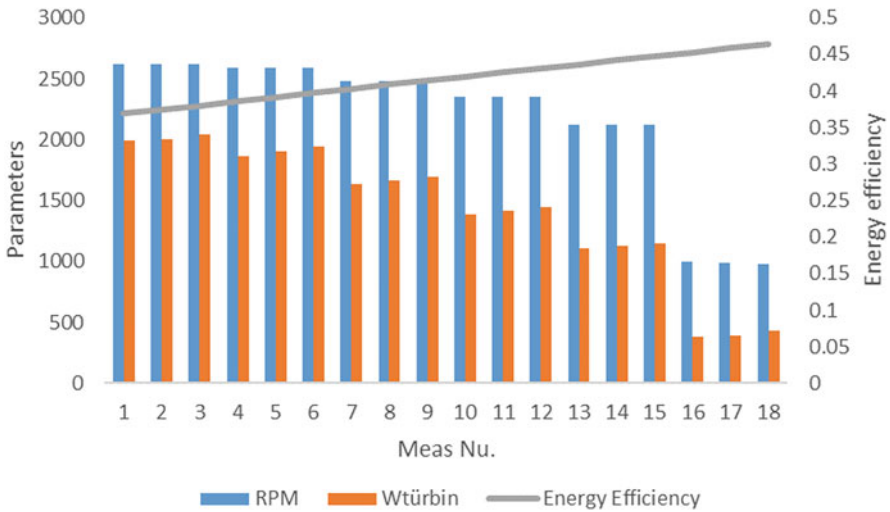


Fig. 3 Thermal efficiency and RPM

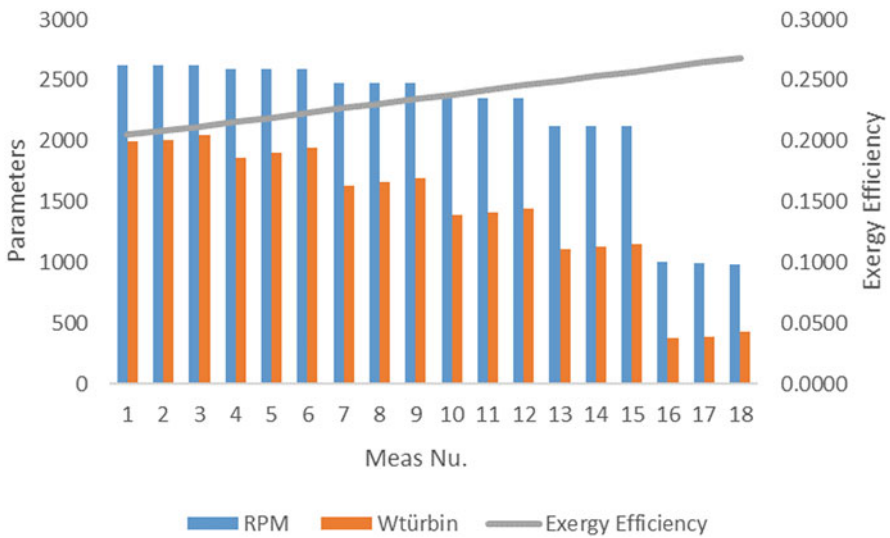


Fig. 4 Exergy efficiency and RPM

The efficiency of the engine was found to be 36.94–46.36%. The average efficiency of the engine is 41.67%, and there is a performance decrease for high RPMs according to the engine’s rpm values. It is not sufficient to describe the extent of reversibility based on quantitative assessment. In this context, the exergy performance of the engine was examined, and the results are given in Fig. 4.

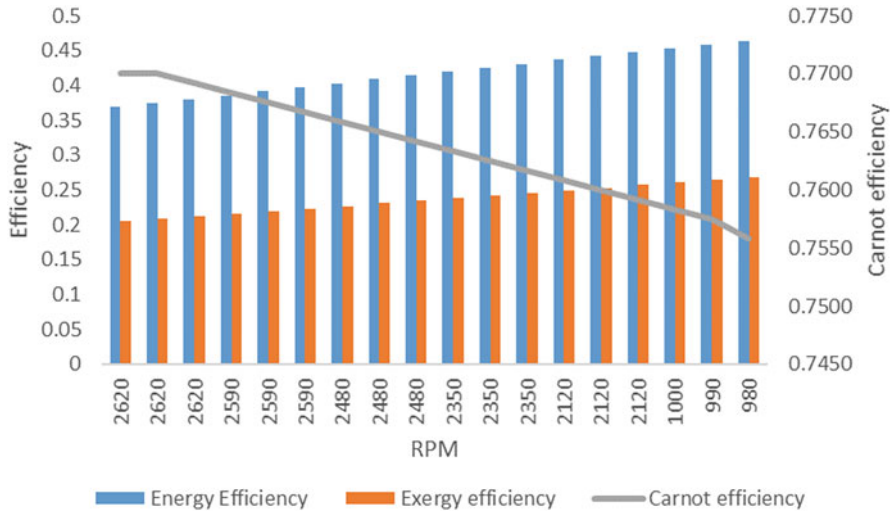


Fig. 5 Efficiencies and RPM

While the exergy efficiency of the engine has an average of 23.65% potential, this change shows a change of 20.51–26.83% according to the RPM values. In the performance distribution, the RPM change depending on both efficiency values was evaluated (Fig. 5).

Depending on the engine’s Carnot change RPM data, 1.85% change is seen, while this change in energy and exergy efficiencies is 25.5% and 30.8%, respectively. In these values, it is seen that there is a 5.31% higher value, especially in qualitative change. The exergy destruction caused by the losses due to the exergy consumption of the engine was examined, and its effect on the Carnot efficiency was evaluated (Fig. 6).

The exergy destruction produced by the real engine is 2.29 times higher than the Carnot value. The exergy breakdown of the engine shows an average potential of 4804.56 kW. The entropy production due to the exergy destruction of the engine was considered together with each RPM value, and the results are given in Fig. 7.

The entropy production of the engine shows a potential of 3.97 kW/K, with 27 kW/K according to the RPM distributions. Entropy production is important in terms of direct environmental impact. According to these data, EPI was found to be 0.76, while SI was found to be 0.24. These data show the 69.04% entropy pollution effect on the environmental performance of the engine.

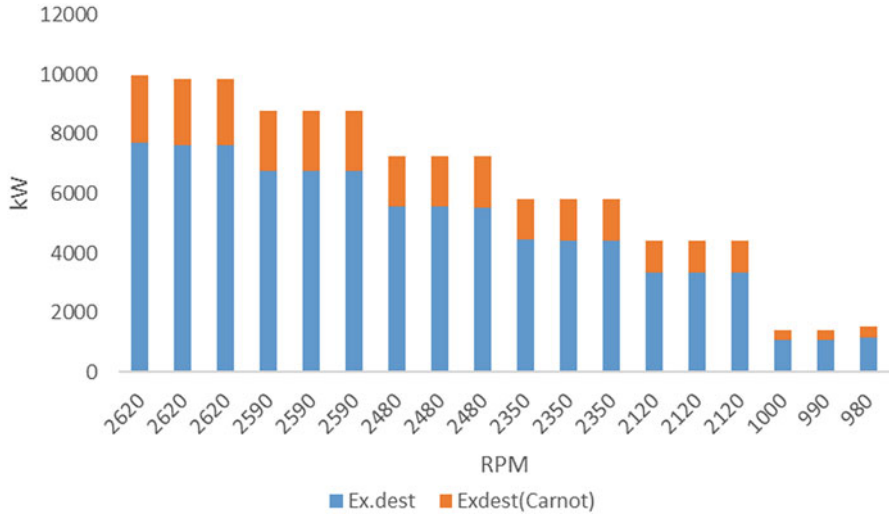


Fig. 6 Exergy destruction and RPM

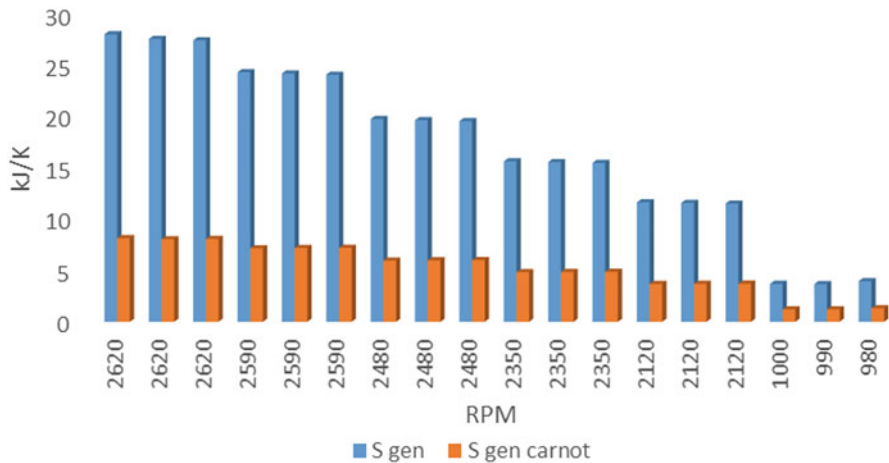


Fig. 7 Entropy generation and RPM

## 5 Conclusion

In this study, the potential of entropy-induced environmental pollution was evaluated with reference to a piston engine, and it was found that it had an effect of 69.04%. According to the RPM values of the aircraft, the energy and exergy efficiencies were found to be 41.64% and 23.65%, respectively. Based on the two indices produced according to these parameters, the impact boundary conditions

depending on the total entropy production of the aircraft should be determined. In this context, analyses should be made in terms of environmental and cost effects.

## References

- Cornelissen, R. L. (1997). *Thermodynamics and sustainable development: The use of exergy analysis and the reduction of irreversibility* [PhD thesis, University of Twente, The Netherlands].
- DETEC. (2007). *Aircraft piston engine emissions: Appendix 3: Power settings and procedures for static ground measurements*. Federal Department of the Environment, Transport, Energy and Communications DETEC. Federal Office of Civil Aviation FOCA, Aviation Policy and Strategy Environmental Affairs. [https://www.bazl.admin.ch/dam/bazl/de/dokumente/Fachleute/Regulationen\\_und\\_Grundlagen/appendix\\_3\\_proceduresforstaticgroundmeasurements.pdf.download.pdf/appendix\\_3\\_proceduresforstaticgroundmeasurements.pdf](https://www.bazl.admin.ch/dam/bazl/de/dokumente/Fachleute/Regulationen_und_Grundlagen/appendix_3_proceduresforstaticgroundmeasurements.pdf.download.pdf/appendix_3_proceduresforstaticgroundmeasurements.pdf)
- Dincer, I., & Rosen, M. A. (2012). *Exergy: Energy, environment and sustainable development*. Elsevier.
- IATA. (2013). *Technology roadmap* (4th ed.). International Air Transport Association (IATA). <http://www.iata.org/pressroom/pr/Pages/2017-02-02-01.aspx>
- IATA. (2016). *Another strong year for air travel demand in 2016*. International Air Transport Association (IATA). <http://www.iata.org/pressroom/pr/Pages/2017-02-02-01.aspx>
- Jing, D. (2012). The study on business growth process management entropy model. *Physics Procedia*, 24, 2105–2110.
- Moran, M. J., Shapiro, H. N., Boettner, D. D., & Bailey, M. B. (2011). *Fundamentals of engineering thermodynamics*. Wiley.
- Sogut, M. Z. (2021). New approach for assessment of environmental effects based on entropy optimization of jet engine. *Energy*, 234, 121250. ISSN 0360-5442.
- Van Gool, W. (1997). Energy policy: Fairy tales and factualities. In *Innovation and technology – Strategies and policies* (pp. 93–105). Springer.

# Examining Thermo-Economic and Environmental Performance of Piston Engine Considering LNG Fuel Transition of Aircraft



M. Ziya Sogut

## 1 Introduction

Piston engines, which have taken place in all transportation sectors with the change in technology since the seventeenth century, have become the preferred engines in private and commercial aircraft with the multicylinder engine applications developed by Czarnigowski et al. (2010). However, they are engines that have left their place to alternatives in sectoral preferences due to their low system performance. Despite its 3% effect on the total emission potential, the aviation sector is the sector that contributes to continuous emission production with the effect of high-intensity transportation. Although the current Covid-19 pandemic process provides a significant decrease in sectoral potentials, the future projections of the sector, which has reached the potential to transport approximately 4.5 billion people according to 2019 data, show that it will increase (Lee et al., 2020; Pearce, 2020). Considering the sectoral projections, it is seen that the consumption of fossil fuels and the related emission potential will increase rapidly. It examines all aspects of alternative approaches based on reducing fossil consumption, with sectoral responsibilities based on potentially reducing the emission threat.

Depending on the increase in sectoral competition, engine technologies are an important indicator as technology management elements for aircraft in the cost management of aviation enterprises. As a matter of fact, in the future scenarios of the sector, the development of existing engine technologies has provided significant gains in sectoral competition. Especially in the aviation industry, which gained importance as an economic value in the cyclical economies in the 1960s, this technology change in recent years has resulted in a reduction of up to 60% in fuel consumption per mile (Daley, 2012). However, sectoral projections indicate that the demand for fossil fuel consumption will continue to increase. Depending on the

---

M. Z. Sogut (✉)

Maritime Faculty, Piri Reis University, Istanbul, Türkiye

value of environmental indicators in the sector, the search for alternative fuels continues in all aspects. According to the latest data, an annual average 3% increase in fossil fuel consumption in the sector, which consumes an average of one billion liters of jet fuel (approximately 300 Mton/year), is remarkable. In this context, alternative studies in the sector have been handled in many ways, and important developments have been achieved.

In this study, the performance data of LNG fuel was examined in order to contribute to alternative fuel studies. Natural gas can be an important choice in engine systems. In particular, natural gas, as a clean fuel, reduces NO<sub>x</sub> formation and has a reduction of more than 20% in emissions (Kumar et al., 2011). It is predicted that the choice of LNG, which will provide significant gains when evaluated with existing aviation fuels, may be an important gain, especially for piston engines. In this study, the energy and environmental performance effects of LNG exchange were investigated by considering the consumption potentials of a piston engine depending on the flight process.

## 2 Sectoral Perspective of Piston Engines

The development of the aviation sector due to the increase in demand is also seen with the change of deliveries. As a matter of fact, according to 2019 data, general aviation deliveries represent a 10.2% change compared to the previous year, with a potential of approximately 27 billion dollars. However, this potential reached a higher value in piston engines. With a 16.4% change in annual potential, the number of deliveries, which was 1137 in 2018, reached 1324 in 2019. These values show a decrease of 15.08% to 809 units in jet engines and 11.3% in turboprops. On the other hand, with 2019 data, the piston engine ratio has a significant share of 30.16% in the potential of 31,839 rotor airplanes worldwide (GAMA, 2019). Piston engines are highly dispersed despite an increasing trend in sectoral deliveries. The distributions of engine deliveries (1994–2019) depending on engine type of piston engines are examined, and the results are given in Fig. 1.

Fuel used in piston engines is basically Avgas and Mogas, known as aviation gas. Energy production in piston engines is a process that generally develops depending on the Otto cycle. Energy efficiency in these engines, which operate with explosion ignition depending on thermal management, is a feature that depends on the compression ratio and fuel-air mixture as well as environmental effects. Piston engines, defined as small piston airplanes, have low fuel consumption on an international scale. Avgas has two main classes, 100 and 100LL low carbon, based on ASTM D910 and UK DEF STAN 91–90 specifications. In these fuels, tetraethyl Pb is added to increase the octane, and lead content is up to 100LL, 0.56 g Pb L<sup>-1</sup> (Masiol & Harrison, 2014). As a matter of fact, emissions from aviation have a share of less than 1%, approximately 1% in NO<sub>x</sub>, 40% in CO, and 100% in lead (Pb) (Robert et al., 2015). LNG proposed as a fuel in this study is a cryogenic gas and has a boiling temperature of 112 K in standard atmosphere. In addition, with an effective



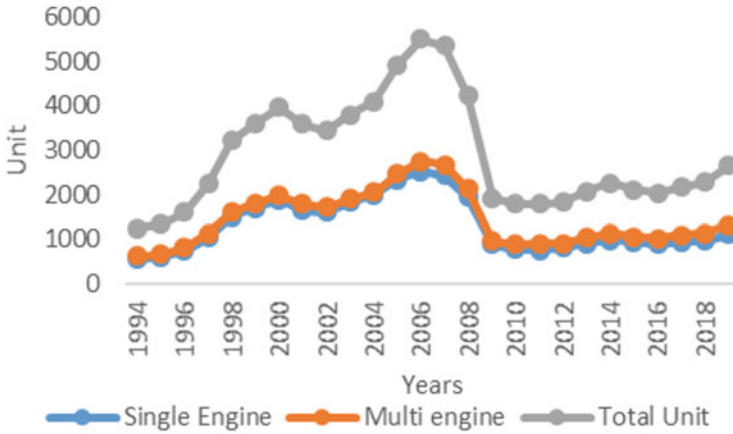


**Fig. 1** Distribution of piston engine shipments by Type of Airplane Manufactured Worldwide (1994–2019) (GAMA, 2019)

thermal management feature, the latent heat from liquid to vapor is 509 kJ/kg. Today, there are advanced control technologies based on the use of LNG for aircraft. There is also an air-to-air thermal management structure for the thermal conversion of cryogenic fuel (Robert et al., 2015). LNG has heating values ranging from 27.5 to 48.7 MJ/m<sup>3</sup> due to its different compositions, fuel, and production characteristics (MANDATE, 2021).

### 3 Methodological Background

Thermo-economics analysis is an important method for evaluating the relationship between energy performance and cost in such system evaluations. The performance relationship of the engine is directly related to the power produced, as well as the thermal efficiency, which is defined based on the fuel consumed. Accordingly, the energy efficiency of the system:

$$\eta = \frac{\dot{W}_{\text{net}}}{\dot{Q}_{\text{in}}} \quad (1)$$

where  $\eta$  is the thermal efficiency,  $\dot{W}_{\text{net}}$  is the net power of the engine, and  $\dot{Q}_{\text{in}}$  is the total heat load of system fuel consumption. Accordingly, an assessment can be made to the engine's consumption parameters, depending on the total amount of fuel consumed by the engine. This evaluation is the instantaneous or temporal total value according to the data feature. In this case, the energy given to the system can be expressed as the following:

$$-\dot{Q}_{in} = \dot{m}_{fuel} \cdot H_{LHV} \quad (2)$$

Located in the formula,  $\dot{m}_{fuel}$  is the mass flow rate of fuel consumed and  $H_{LHV}$  is the expressed low heat value of the fuel. The total amount of fuel ( $M_{fuel}$ ) depending on the total energy load in a system can be calculated as follows (Cengel & Boles, 2006):

$$M_{fuel} = \frac{\dot{Q}_{in}}{H_{LHV} \cdot \eta} \quad (3)$$

The energy cost effect is a defined economic value for each fuel. The cost and value of the energy produced in a thermal system is mostly defined by the cost of the resource.

$$C_{total} = \dot{m}_{fuel} \cdot C_{fuel, cost} \quad (4)$$

In this study, unit costs are made directly over the purchasing costs of fuels. One of the main causes of greenhouse gas emissions is emissions due to fossil fuel consumption. Although it contains many different pollutants in its components, the definition of pollutant potential for thermal processes that consume fossil fuels is defined by the CO<sub>2</sub> equivalent (Hepbasli, 2012). Although many approaches have been developed in this regard, the most valid one is the definition of the emission potential depending on the fuel type developed by the IPCC. According to this:

$$SEG = m_{fuel} \cdot F_{SEG} \quad (5)$$

Here, FSEG is CO<sub>2</sub> which defines the emission factor of the defined fuel. In this study, it was defined for LNG with Avgas100LL.

## 4 Results and Discussion

In this study, firstly, the thermodynamic performance of a reference piston engine was investigated. The reference engine has 180 hp at 2700 RPM, a compression ratio of 8.5:1, and a propeller driver ratio of 1:1 (Superior Air Parts, 2005), and AVGAS100LL is used as fuel. Flight parameters and technical data of the engine (FOCA, 2007). The fuel consumption of the engine was evaluated according to rpm, and the distributions are given in Fig. 2.

The fuel consumption distribution of the engine was defined in an altitude-related structure. In this context, power generation and fuel consumption according to the rpm values of the engine are given in Fig. 3.

The variation between the engine's power generation and fuel consumption was studied in many ways. While there is an 82.27% change in engine performance, there

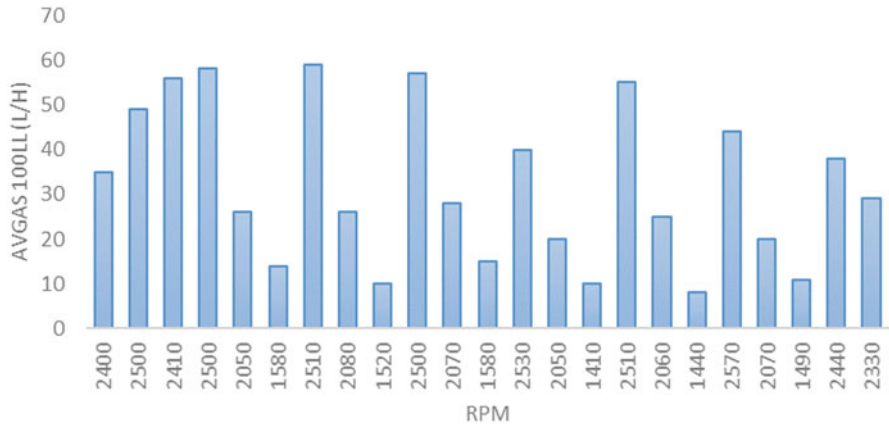


Fig. 2 Fuel consumption of the piston engine

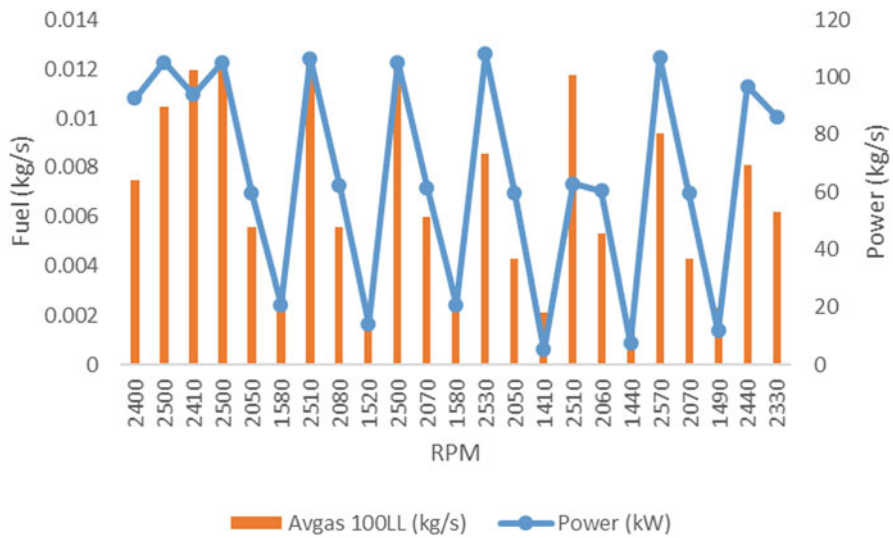


Fig. 3 Power generation and fuel consumption of the piston engine

is a 6.37-fold change in fuel consumption. There is a 19.98% change in power generation. Considering the fuel change consumed per unit of power, it was seen that the fuel consumption has a very dispersed structure. Considering the performance of the engine in consumption, the changes between energy efficiency and power generation are also remarkable. Along with the potential power of the engine, performance analyses were made considering the actual efficiency, and the results are given in Fig. 4.

It was observed that the efficiency of the engine varies between 5.52% and 31.95%. However, when evaluated together with power performance, a nonlinear

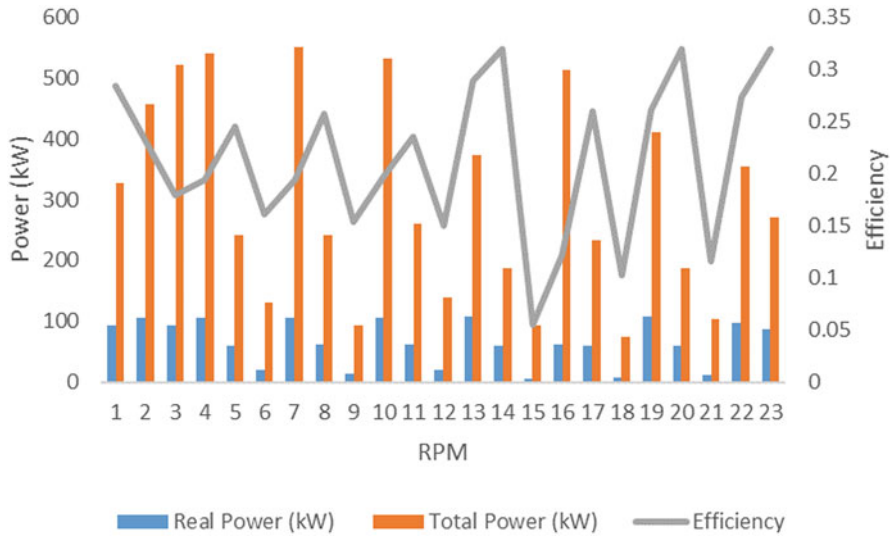


Fig. 4 Power and efficiency consumption of the piston engine

relationship was seen between fuel consumption and efficiency of the engine. The loss rate in power generation of the engine was found an average of 78.60% potential. In this potential consumption, LNG consumption as an alternative fuel was evaluated, and a potential analysis was made. In this respect, LNG comparison was made over the current potential. In this context, the LHV value for the LNG potential was defined as 48,600 kJ/kg. The LNG mass flow comparison in the study is given in Fig. 5.

Depending on the mass flow difference in the LNG consumption of the engine, an advantage of 10.06% over AvgasLL stands out. It has a 44.28% difference in density in terms of total mass flow. Thus, LNG has the opportunity to store higher fluids in total mass. The emission emission due to the total mass flow was examined depending on both fuel potentials, and the distribution of the emission potentials is given in Fig. 6.

In both fuel consumption, the emission emission due to LNG consumption represents a potential of 53.72%. While a total of 2419.015 tons of CO<sub>2</sub> is released in AvgasLL, especially in emission release, depending on the flight process, this value was defined as a potential of 1119.6 tons of CO<sub>2</sub> in LNG. In the study, another examination was handled in terms of fuel costs. In the cost effect, very different price flows in terms of the market draw attention. This price range varies between \$2.95 and \$8.5/l for AvgasLLL and between \$2.25/l and 3.5 l/h for LNG. In the study, 5.73\$/l for AvgasLLL and 2.88\$/l for LNG were taken as reference prices. Accordingly, the total cost based on consumption of the flight process was found to be 4196.25 \$ for AvgasLLL and 3400.98 \$ for LNG consumption. An advantage of 18.96% in total consumption of LNG usage came to the fore.

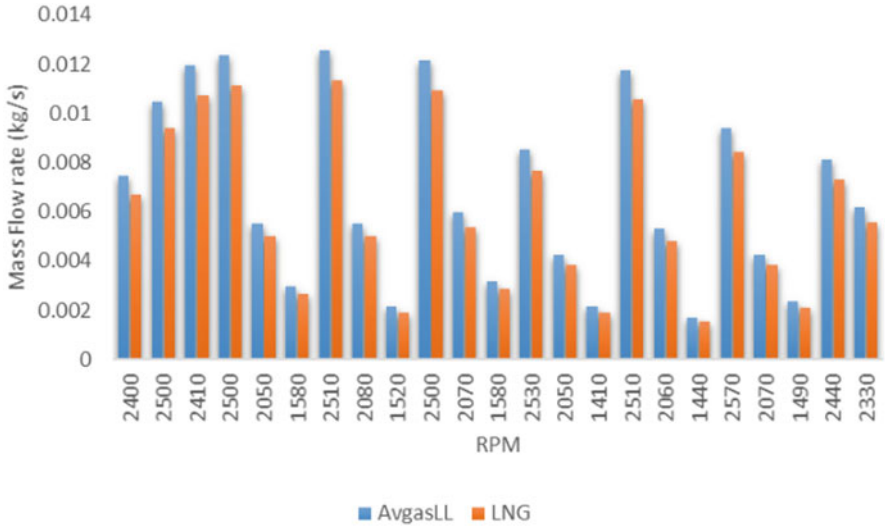


Fig. 5 AvgasLL and LNG consumption

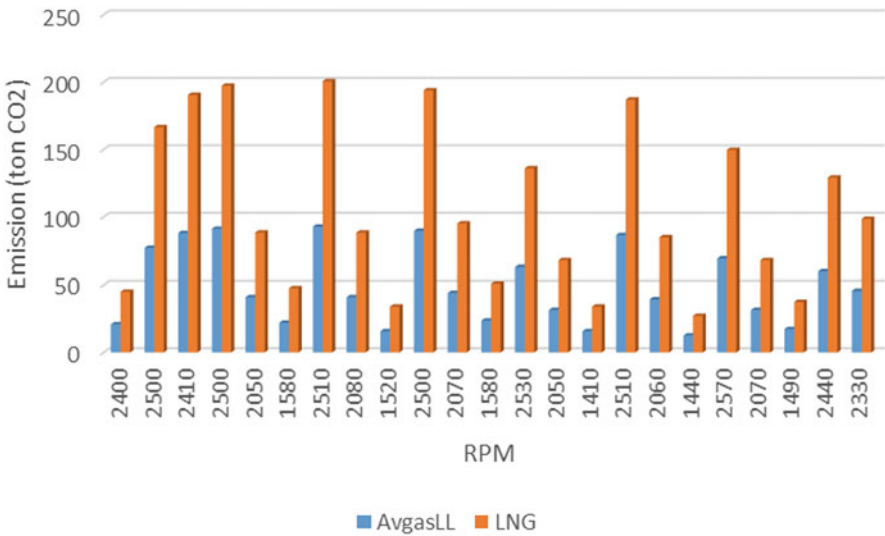


Fig. 6 AvgasLL and LNG emission potential

## 5 Conclusion

In this study, first of all, the energy efficiency of a piston engine is evaluated, and the thermo-economic performance of the use of LNG as an alternative fuel in the engine was discussed. In the analyses made, the average energy efficiency of the engine was found to be 21.4%, and the fuel mass advantage in LNG use is 10.06%. The emission advantage of LNG was determined as 53.72%, and the consumption cost advantage, depending on the fuel preference of the engine, is 18.96%. While the study makes the use of LNG particularly advantageous, it is also important to consider the costs of conversion and sustainability in existing engine technologies. For this purpose, evaluating the studies from this aspect may be an opportunity for future studies.

## References

- Cengel, Y., & Boles, M. (2006). *Thermodynamics: An engineering approach* (5th ed.). McGrawHill.
- Czarnigowski, J., Jakliński, P., & Wendeker, M. (2010). Fuelling of aircraft radial piston engines by ES95 and 100LL gasoline. *Fuel*, 89(11), 3568–3578.
- Daley, B. (2012). *Air transport and the environment*. Ashgate.
- FOCA. (2007). *Aircraft piston engine emissions, Appendix 3: Power settings and procedures for static ground measurements* (0/3/33/33-05-003 ECERT). Federal Office of Civil Aviation FOCA.
- GAMA. (2019). *2019 Databook: General Aviation Manufacturers Association*. Available at: [https://gama.aero/wp-content/uploads/GAMA\\_2019Databook\\_ForWebFinal-2020-02-19.pdf](https://gama.aero/wp-content/uploads/GAMA_2019Databook_ForWebFinal-2020-02-19.pdf)
- Hepbasli, A. (2012). Low exergy (LowEx) heating and cooling systems for sustainable buildings and societies. *Renewable and Sustainable Energy Reviews*, 16, 73–104.
- Kumar, S., Kwon, H.-T., Choi, K.-H., Lim, W., Cho, J. H., Tak, K., & Moon, I. (2011). LNG: An eco-friendly cryogenic fuel for sustainable development. *Applied Energy*, 88, 4264–4273. <https://doi.org/10.1016/j.apenergy.2011.06.035>
- Lee, D. S., Fahey, D. W., Skowron, A., Allen, M. R., Burkhardt, U., Chen, Q., Doherty, S. J., Freeman, S., Forster, P. M., Fuglested, J., et al. (2020). The contribution of global aviation to anthropogenic climate forcing for 2000 to 2018. *Atmospheric Environment*, 244, 117834. <https://doi.org/10.1016/j.atmosenv.2020.117834>
- MANDATE E.U. M/400 to CEN “gas quality”: CEN BT WG 197 N 0310 final report. Available online: [http://portailgroupe.afnor.fr/public\\_espacenormalisation/BNG234/FprEN16726%20\(E\).pdf](http://portailgroupe.afnor.fr/public_espacenormalisation/BNG234/FprEN16726%20(E).pdf). Accessed on 13 May 2021.
- Masiol, M., & Harrison, R. M. (2014). Aircraft engine exhaust emissions and other airport-related contributions to ambient air pollution: A review. *Atmospheric Environment*, 95, 409–455. <https://doi.org/10.1016/j.atmosenv.2014.05.070>
- Pearce, B. (2020). *COVID-19 outlook for air travel in the next 5 years*. Available online: <https://www.iata.org/en/iata-repository/publications/economic-reports/covid-19-outlook-for-air-travel-in-the-next-5-years/>. Accessed on 4 September 2020.
- Robert, R. A., Nuzum, S. R., & Wolff, M. (2015). Liquefied natural gas as the next aviation fuel. In *13th International energy conversion engineering conference, propulsion and energy forum*, July 27–29, 2015, Orlando, Canada. American Institute of Aeronautics and Astronautics, Inc.
- Superior Air Parts. (2005). *O-360 & IO-360 series engines overhaul manual*. Available online: [http://rvplane.com/pdf/XP360\\_OverhaulManual.pdf](http://rvplane.com/pdf/XP360_OverhaulManual.pdf). Accessed on 13 May 2021.

# Breaking the Aircraft Vortex Wake Near the Ground: Mitigation of Turbulence Wake Hazard



Theerawit Tekitchamroon, Watchapon Rojanaratanangkule,  
and Vejapong Juttijudata

## Nomenclature

$A_0$	Initial amplitude
$b_0$	Initial vortex separation distance
$E_k$	Kinetic energy
$E_\omega$	Enstrophy
$h_0$	Initial vortex height from ground plane
PVS	Primary vortex structures
Re	Reynolds number
SVS	Secondary vortex structures
$\mathbf{u}$	Velocity vector
$\Delta$	Initial vortex core perturbation
$\Gamma_0$	Initial circulation
$\theta$	Angle of instability
$\lambda$	Wavelength
$\omega$	Vorticity

## 1 Introduction

One of the significant fluid dynamic features, vortex flow, has been studied for a long time. Many types of research studies cover from small-scale fields to large-scale fields. In the aviation industry, aircraft produce a large, long-lived counterrotating

---

T. Tekitchamroon (✉) · V. Juttijudata  
Kasetsart University, Bangkok, Thailand  
e-mail: [theerawit.te@ku.th](mailto:theerawit.te@ku.th); [vejapong.j@ku.ac.th](mailto:vejapong.j@ku.ac.th)

W. Rojanaratanangkule  
Mechanical Engineering, Chiang Mai University, Chiang Mai, Thailand

vortex pair structure left behind during flight phases. This vortex induces a roll moment that causes stability and control loss to the following aircraft, particularly during an approach phase. For encounter avoidance, the distance between aircraft must be restricted by the separation standard regarding the ICAO regulations affecting the air traffic limitation. Previous studies attempted to research their dynamics and methodologies for vortex hazard alleviation. The vortex decay factors combine with ambient turbulence, viscous interaction, buoyancy, instability, and secondary vorticity structures (SVS) (Hallock & Holzäpfel, 2018). Especially, ambient, instability, and SVS play a dominant role in exciting the vortex dissipated rate. Long-wavelength instability (Crow instability) arises from a vortex pair's self-induced and mutual interaction (Crow, 1970). This phenomenon results in a sinusoidal distortion for each vortex, which subsequently becomes periodically large vortex rings (contrail). Short-wavelength instability, namely, elliptic instability, is the interaction between the perturbation waves and external strain produced from another vortex. As a result, each vortex core deforms into small unstable waves. When a vortex pair approaches the wall, the boundary layer forms the opposite-signed vorticity at the wall beneath. Then, this boundary layer rolls up into the secondary vortices due to adverse pressure gradient. This formulation induces upward velocity into the primary vortices, which causes the rebound of the primary vortices. The secondary vortices are also induced by the primary vortices that warp the primary ones. Ultimately, the primary vortices merge with the secondary vortices generates the vortex dissipation.

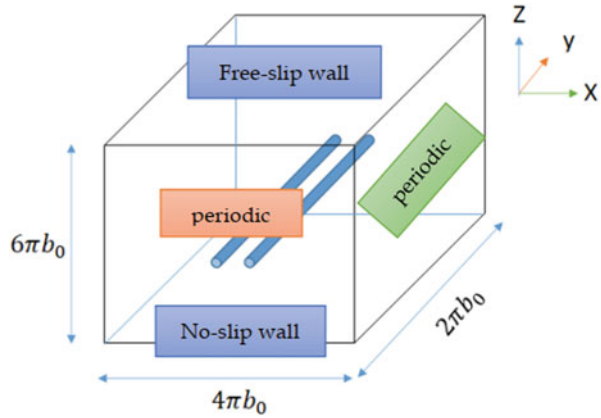
A Crow instability in ground proximity is one of the significant breakdown mechanisms. Including the interaction of the secondary vortices from the ground remains knowledge to understand the complexities of the dynamics. This study seeks to study the inhibited Crow instability evolution under the ground effect via flow visualization and mitigation of turbulence hazard to reduce flight separation en route to more sustainable aviation.

## 2 Method

The direct numerical simulation (DNS) applies to create the vortex pair model in this study. The governing equations for incompressible flow used Navier-Stokes equations with a second-order Adams-Bashforth scheme. The second-order central finite-difference method was employed to discretize all spatial derivatives on a staggered grid. A small-time step of the simulations was selected to control the maximum Courant–Friedrichs–Lewy number (CFL), which is located at maximum velocity and grid size, below the criteria at 0.15. The investigations of vortex pair dynamics and interaction in ground proximity used the counterrotating Lamb-Oseen pair as a base flow for trailing vortices model from aircraft. The individual Lamb-Oseen vortex model can be expressed as:



**Fig. 1** Schematic domain of simulation and boundaries implementation



$$V_{\theta,t=0}(r) = \frac{\Gamma_0}{2\pi r} \left( 1 - \exp\left[-\frac{r^2}{a_0^2}\right] \right) \tag{1}$$

where  $\Gamma_0$  is initial circulation,  $r$  is radial distance, and  $a_0$  is characteristic vortex core radius. The initial height of the vortex pair from the ground is set to be  $h_0/b_0 = 5$ . With Crow instability implementation, the vortex cores are initially perturbed by a sinusoidal wave with amplitude  $A_0$  and wavelength  $\lambda$  that satisfy:

$$\Delta = (A_0 \cos \theta) \sin\left(\frac{2\pi}{\lambda} y\right) e_x + (A_0 \sin \theta) \sin\left(\frac{2\pi}{\lambda} y\right) e_z \tag{2}$$

where  $\Delta$  is the initial perturbation at core located in  $r = \pm b_0/2 e_x + \Delta$  and  $\theta$  is the angle to the plane of pair. With Crow instability  $\theta$  approximate to  $45^\circ$ , the schematic domain of the simulation is shown in Fig. 1. The domain size is defined as  $(x, y, z) = (4\pi b_0, 2\pi b_0, 6\pi b_0)$  for spanwise, streamwise, and vertical, respectively, with uniform grid resolution of  $384 \times 192 \times 576$ . The size of the simulation domains was designated to ensure the boundaries won't affect the vortex pair, except for the ground plane fixed by the initial height of the vortex pair and streamwise axis fixed by one-wavelength of vortex pair. Periodic boundary conditions were employed at the streamwise axis and the spanwise axis. The ground plane applied a no-slipped wall condition, and a top surface was implemented as a free-slipped wall.

In-house C++ code to perform DNS was modified from the code that was well-validated and used in Tunkeaw and Rojanaratanangkule's study (2018). To identify the vortex pair evolution, the second invariant of velocity gradient tensor and vorticity component are used to visualize the vortex structures.

### 3 Results and Discussion

The spatial discretization error can be shown in terms of the rate of change of global kinetic energy comparing with global enstrophy in domain due to proportionality (Doering & Gibbon, 1995). Therefore, the rate of change of global kinetic energy is prescribed as:

$$\frac{dE_k}{dt} = -\frac{1}{\text{Re}} E_\omega \quad (3)$$

where Re is the Reynolds number, enstrophy is  $E_\omega = \iint |\boldsymbol{\omega}|^2 d\Omega$ , and global kinetic energy is defined as  $E_k = \frac{1}{2} \iint |\mathbf{u}|^2 d\Omega$ .

Figure 2 illustrates the comparison plot between global kinetic energy and global enstrophy. Two minimum local peaks describe maximum energy decay as a consequence of the interaction between the vortex and the wall. The maximum discrepancy is approximately 10%, which appears while the vortex pair descends nearest to the wall.

The vortex pair with Crow perturbation becomes more noticeable sinusoidal waves while descending into the ground. The amplification of the vortex pair amplitude provides two regions flow, the peak and the trough (Fig. 3). At the trough, vortices approach each other; thus, the external strain from another one induces vorticity cancellation. Because of this, both vortex strength reduces and pressure increases which causes the pressure difference between peak and trough, arise axial

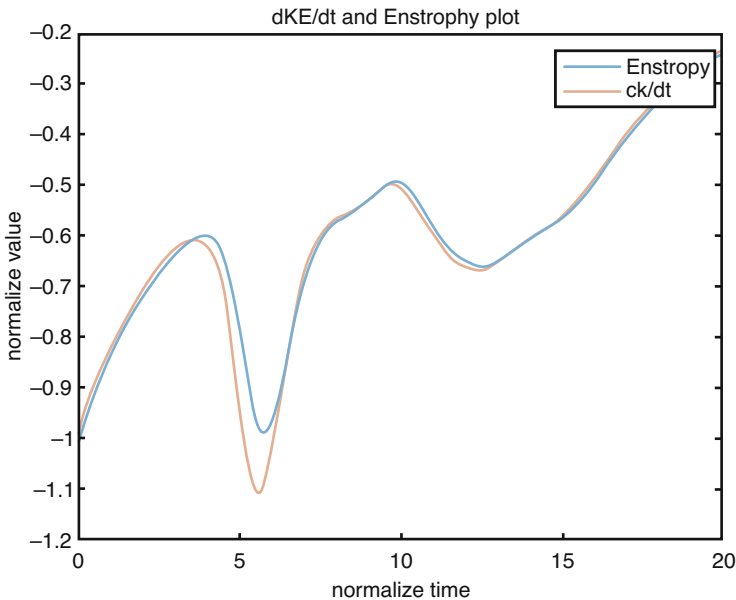
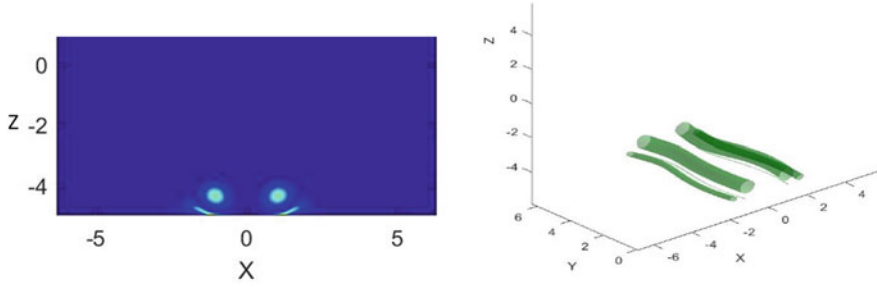
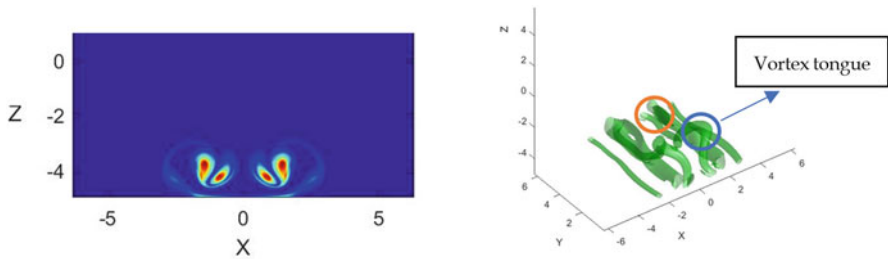


Fig. 2 The results of the validation study using equation (3) under time normalization



**Fig. 3** Vorticity magnitude at  $y = \lambda/2$  and second invariant at normalized time 5.8



**Fig. 4** Vorticity magnitude at  $y = \lambda/2$  and second invariant at normalized time 9.8

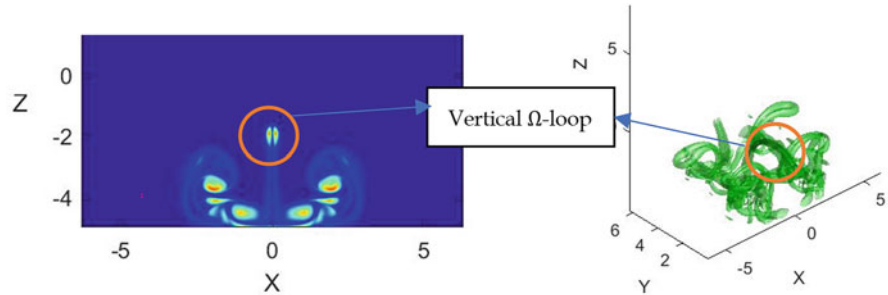


**Fig. 5** Vorticity magnitude at  $y = \lambda/2$  and second invariant at normalized time 15

flow. When the vortex pair approaches the ground, SVS are generated by the boundary layer, which occurs at the trough first come after the peak. The SVS strength at the peak regions distinguishes from the trough regions due to the PVS vorticity cancellation. Thus, the pressure at the SVS peak regions is lower than the trough ones that generate the axial flow. SVS distort their structure like vertical loops at the peak regions, which are called vortex tongue (blue circle, Fig. 4) and also small vortex tongue for the trough regions (orange circle, Fig. 4). The SVS also obtain strain induction from the PVS, hence moving upward and wrapping around the PVS. Ultimately, vortex tongues interact with each other and slowly decay in time; Fig. 5 illustrates the formation of vertical  $\Omega$ -loop structures between the PVS.

## 4 Conclusion

The study performed a direct numerical simulation of an inhibited Crow instability vortex pair in a ground vicinity. The initial vortex height was fixed at  $h_0/b_0 = 5$  to investigate the dynamics of small-amplitude mode. The expectation is further to consider the interaction of an inhibited Crow instability with obstacles implementation. With Crow perturbation, SVS are affected by changing their structure. The inequality vortex's strength and a sinusoidal wave of PVS make SVS from boundary layers that are similar to PVS conditions. SVS subsequently arise axial flow in their structure and shape into a vertical loop structure, called "vortex tongue" at peak regions. Upward strains from PVS induce SVS rotating around PVS. While vortex tongues approach together, vortex tongues mutually interact with each other. Vertical  $\Omega$ -loop structures are produced as a result of the interaction and eventually slowly decay in time. The maximum decay rate occurs when the vortex approaches the ground, and the second occurs while the SVS interact into large vertical loop. The point of energy decay is the foundation of SVS that generates significant dynamic outcomes. It's interesting to observe more characteristics of the Crow perturbation and the additional ground obstacle implementation. Since the vortex pair behaves like waves, perturbing with specific wavelengths may excite the vortex pair instabilities. Consequently, this dissipates the vortex and reduces the separation distance of approach aircraft.

**Acknowledgments** This work was supported by Kasetsart University for high-resource computational equipment. And, we literally appreciate and thank Jiratrakul Tunkeaw for DNS usage and analysis tool consulting.

## References

- Crow, S. C. (1970). Stability theory for a pair of trailing vortices. *AIAA Journal*, 8, 2172–2179.
- Doering, C. R., & Gibbon, J. D. (1995). *Applied analysis of the navier-stokes equations*. Cambridge University Press.
- Hallock, J. N., & Holzäpfel, F. (2018). A review of recent wake vortex research for increasing airport capacity. *Progress in Aerospace Sciences*, 98, 27–36.
- Tunkeaw, J., & Rojanaratanangkule, W. (2018). Effect of external turbulence on the short-wavelength instability of a counter-rotating vortex pair. *Physics of Fluids*, 30, 064105.

# Beyond Technology: Digital Transformation in Aerospace and Aviation



Pasit Suebsuwong

## 1 Introduction

Today, as never before, the productivity, efficiency, and competitiveness of enterprises depend on the rapid and flexible use of key digital management systems and technologies. The digital model of development envisages not only complete economic transformation but also the adoption of the three key requirements of global markets today: faster decision-making, more rapid project completion and compressed product development times.

Halpern et al. (2021) identify four stages that can be applied to airports: (1) analogue, where the majority of processes are manually captured data; (2) digitization, where some digital technologies are used; (3) digitalization, where digital technologies are used for the majority of processes; and (4) digital transformation, where value is created from data and used in real-time via smart data capabilities.

There are countries that are leaders of digitalization and countries that only now recognize the need for that change. Nine basic trends of digital aviation are proposed by Tikhonov et al. (2019). The trends are on the basis of design, manufacturing, and management. The nine areas of the trends are enterprise's information platform; modelling and optimization; partnership with educational platforms; digital twins, corporate innovation centres and laboratories; intellectual property; manufacturing; digital reverse engineering; digital logistics management; and cross-disciplinary cooperation.

---

P. Suebsuwong (✉)

Aerospace Engineering Department, Kasetsart University, Bangkok, Thailand

e-mail: [fengttw@ku.ac.th](mailto:fengttw@ku.ac.th)

## 2 Digitalization in Aerospace and Aviation

The aerospace and aviation sectors are exploring the benefits of digitalization on operational efficiency and cost-effectiveness through IoT, predictive analytics and digital twin technologies. In aerospace, there is the need for global communication infrastructure and the information management innovations and the defence sector. Aerospace faces many challenges such as maintaining and communicating, in the characteristic of accessible and interoperable, with assets in remote and difficult conditions. Aviation is a highly competitive sector that relies on data sharing partnerships for gaining a competitive edge on customer experiences while ensuring the safety of passengers' data and travel. Another key challenge is for service providers, which have to create an environment that is intelligent enough to anticipate customer needs and feeling superior, seamless experience while not being invasive or insecure.

On the whole, aerospace has a stronger innovative focus in design, building and maintenance, while aviation is generally more innovative with integrating data. Digital challenges in aerospace and aviation are categorized by Lamb (2018), with a wider perspective rather than focusing on technical solution, into the following topics: data, security, human factors, social outcomes, role of regulation and investment.

The aviation sector has suffered and been dramatically destroyed by the coronavirus disease (Covid-19) pandemic. Some airlines are forced to bankruptcy process, such as Virgin Australia. COVID-19 forces people to make a considerable behaviour change and places significant psychological difficulty on individuals. Due to economic problems, people intend to tighten the leisure travel budget. Liang (2020) presents the future of aviation in post-Covid-19 in the following aspects: air travel behaviour and social changes, application of automation in flight operation and air transport route network reshaping.

## 3 Digital Transformation

It is a fact that recent technologies are highly disruptive and subject to constant change. It is expected to be significant for the overall predisposition of an organization to adopt technologies (Ferreira et al., 2014). Digital transformation represents the strategic transformation of all aspects of the business, creating a new ecosystem where technology creates and delivers value to the stakeholders (Ross, 2019). The process of digital transformation in each country takes place in its own way, it depends on political, economic and social factors.

Digital transformation is about more than technology, which is widely supported in the literature: Kane et al. (2016) state that it is not just about implementing more and better technologies but about digital congruence that aligns culture, people, structure and tasks of a company. Digital transformation discusses about all those

series of events and processes, which individuals, business organizations, societies and nations practice globally for technology adoption (Collin et al., 2015). Many companies still understand digital transformation only as “advance digitization” and not as a continuous process of changes, adaptation and improvements (Ross, 2019).

Digital transformation needs the data, and sharing data with key stakeholders is the most important part. Each stakeholder has its own responsibilities and priorities regarding data and may be inclined to protect their own interests rather than working towards a common goal. The structural/psychological approach infers that organizations with similar resources and organizational structures can present different results when implementing changes resulting from how they plan, aggregate and utilize the resources and processes available (Weiner et al., 2009).

## 4 Digital Transformation Readiness

It is unlikely that digital transformation can be realized if the organization itself is not ready for it. Most of new ideas fail to translate into new products or services due to a lack of organizational readiness (Lokuge et al., 2019). Tabrizi et al. (2019) state that rather than being about technology, it is about developing an organizational readiness to succeed.

Organizational readiness can be defined as a state of preparedness that an organization attains prior to commencing an activity (Helfrich et al., 2011). The organizational readiness has a significant direct effect on digital change and innovation, which are studied by Halpern et al. (2021). There are several approaches to develop organization readiness for digital transformation.

ACI (2017) and Halpern et al. (2021) present four key needs: strategic clarity and visible leadership, effective partnering and collaboration associated, internal capabilities in terms of digital skills and resources (as well as Mullan, 2019) and a digital mindset and culture (as well as Mullan, 2019).

Results published by Pessot et al. (2020) indicate that manufacturing companies still need to develop adequate organizational structures and managerial capabilities in the following domains: strategy, lack of clear vision/strategy; organization, lack of talented/skilled people and leadership from top management; management, adopt digital solutions for enriching customer service, and technology, implementing and embedding data analysis across company business processes and functions.

## 5 Technologies and Beyond

A review of the possibility to use current digital technologies in the aviation industry is given by Molchanova (2020). The recent digital technologies, potentially adopted in aviation, are blockchain technology, augmented reality and virtual reality, artificial intelligence, beacon technology, robotics, big data and analysis and biometrics.

The survey from global executives in digital business reports that the key success is the leader who cultivates a culture of change and leads organization to digital transformation (Kane et al., 2015). The business outcome depends on effectiveness of these organizations integrating their business operations with digital technology.

Kodak failed to understand consumers' changing requirements because of its overconfidence on consumer brand loyalty. Company's people, knowledge and infrastructure became obsolete feasibly company was denying to take decisions timely to adapt to changing business scenarios. Fujifilm leaders successfully planned to survive by not only developing adaptability towards potential technological advancement in the field of photographic domain and taking timely decisions of infusing ongoing technologies but also making radical changes in its existing business model.

It is also clear that technology alone is nothing to drive organization towards its intended objectives. It is essential that leader creates such a culture and environment where people get empowered by technology to adapt and drive changes. Lokuge et al. (2019) claim that most new ideas fail to bring into new products or services due to a lack of organizational culture which develop internal digital capabilities and encourage collaboration for innovation.

In aviation, most of organizations desire to acquire high reliability and high performance. Members of the human envelope for the sociotechnical system in aviation industry are as follows (Wise et al., 2016): designer, manufacturers' regulation, operators, quality controllers, support personnel, supplier, crew members and passengers. They have examined the main activities for each member that provide the high-integrity human envelope including the following: design process, operating process, organizational culture, maintaining people as human assets, managing the interfaces internally between the members of the system and externally and evaluation and learning.

## 6 Conclusion

There are many levels of digital technology adoption to organization for achieving the business goal. The latest stage is digital transformation, which uses the digital technology with extensive potential through the value chain. Trends of the digital technology in aviation cover the whole industrial domains: design, manufacturing and managements.

For industrial characteristic, the aerospace directs to the high performance for design, manufacturing and maintenance, while the aviation intends to the high reliability, as minimum incidents and accidents. This requires a different challenge in digital transformation. In aviation, the main challenge is data sharing partnerships for enhancing customer experiences. But for the aerospace industry the technologies are necessary, and it has been developed for the aviation requirements. The main common challenges are data, security, people, social, regulation and investment.



The effect of coronavirus pandemic is immense for the aviation industry. It catalyses changes in the industry, such as industrial structure, passenger behaviour, flight operation and route network.

Numerous studies show that the digital transformation is more than just implementing more or better technologies. The digital transformation is about the strategic transformation of all aspects of the business, which is influenced by political, economic and social factors. Besides, the results of digital transformation depend on the psychological approach.

Organization readiness helps us determine the organization aspects that need to be improved for digital transformation. Although there are several approaches to develop organization readiness, the common indicators are the following: clear vision/strategy, effective partnering and collaboration, skilled people and leadership and a digital mindset/culture.

The latest digital technologies can be adopted along the value chain in aviation industry. Meanwhile, many studies show that the primary key for digital transformation is the leader and effectiveness of organization integrating the business operations with digital technology.

People in organizations resist every change, which includes digital transformation. It is essential to study in more detail each activity in organization, which are proposed by Wise et al. (2016), for successful digital transformation. We need the implementation with both structural approach and psychological approach. In addition, companies require to invest in both formal, hard skill and informal, soft skill, learning to meet the challenge of workforce skill gap.

## References

- ACI. (2017). *Airport digital transformation: Best practice*. Airports Council International (ACI).
- Collin, J., Halen, M., Juhanko, J., Jurvansuu, M., Koivisto, R., Kortelainen, H., Simons, M., Tuominen, A., & Uusitalo, T. (2015). *Finland – The Silicon Valley of industrial internet* (Publications of the Government's Analysis, Assessment and Research Activities) (Vol. 10/2015). Valtioneuvoston kanslia.
- Ferreira, J. B., da Rocha, A., & Ferreira da Silva, J. (2014). Impacts of technology readiness on emotions and cognition in Brazil. *Journal of Business Research*, 67(5), 865–873. <https://doi.org/10.1016/j.jbusres.2013.07.005>
- Halpern, N., Mwesiumo, D., Suau-Sanchez, P., Budd, T., & Bråthen, S. (2021). Ready for digital transformation? The effect of organisational readiness, innovation, airport size and ownership on digital change at airports. *Journal of Air Transport Management*, 90, 101949. ISSN 0969-6997.
- Helfrich, C. D., Blevins, D., Smith, J. L., Kelly, P. A., Hogan, T. P., Hagedorn, H., Dubbert, P. M., & Sales, A. E. (2011). Predicting implementation from organizational readiness for change: A study protocol. *Implementation Science*, 6(76), 1–12. <https://doi.org/10.1186/1748-5908-6-76>
- Kane, G. C., Palmer, D., Phillips, A. N., Kiron, D., & Buckley, N. (2015). *Strategy, not technology, drives digital transformation* (MIT Sloan Management Review). Deloitte University Press.
- Kane, G. C., Palmer, D., Phillips, A. N., Kiron, D., & Buckley, N. (2016). *Aligning the organisation for its digital future* (MIT Sloan Management Review). Deloitte University Press.

- Lamb, K. (2018). *Challenges of digitalisation in the aerospace and aviation sectors* (CDBB\_REP\_002). CDBB. <https://doi.org/10.17863/CAM.26276>
- Liang, A. (2020). *Applying behavioural science and automation in future of aviation*. Project: Future Airspace Management System for Emerging Operations in Urban Environment. <https://doi.org/10.13140/RG.2.2.28640.92168/1>
- Lokuge, S., Sedera, D., Grover, V., & Xu, D. (2019). Organizational readiness for digital innovation: Development and empirical calibration of a construct. *Information Management*, 56(3), 445–461. <https://doi.org/10.1016/j.im.2018.09.001>
- Molchanova, K. (2020). A review of digital technologies in aviation industry. *Logistics and Transport*, 47–48, 69–77.
- Mullan, M. (2019). The data-driven airport: How data created data and analytics capabilities to drive business growth, improve the passenger experience and deliver operational efficiency. *Journal of Airport Management*, 13(4), 361–379.
- Pessot, E., Zangiacomini, A., Battistella, C., Rocchi, V., Sala, A., & Sacco, M. (2020). What matters in implementing the factory of the future: Insights from a survey in European manufacturing regions. *Journal of Manufacturing Technology Management*, 32, 795–819.
- Ross, J. (2019, July). *Digital success requires breaking rules*. MIT Sloan Management Review. <https://sloanreview.mit.edu/article/digital-success-requires-breaking-rules/>. Accessed 29 October 2019.
- Tabrizi, B., Lam, E., Girard, K., & Irvin, V. (2019, March 13). Digital transformation is not about technology. *Harvard Business Review*.
- Tikhonov, A. I., Sazonov, A. A., & Novikov, S. V. (2019). Digital aviation industry in Russia. *Russian Engineering Research*, 39(4), 349–353.
- Weiner, B. J., Lewis, M. A., & Linnan, L. A. (2009). Using organization theory to understand the determinants of effective implementation of worksite health promotion programs. *Health Education Research*, 24(2), 292–305.
- Wise, J. A., Hopkin, V. D., & Garland, D. J. (Eds.). (2016). *Handbook of aviation human factors*. CRC Press.

# Circulation Control Flap: En Route Toward Sustainable High-Lift Devices



Akanit Nimmanmongkol, Chinnapat Chumsing, and Vejapong Juttijudata

## Nomenclature

$c$	Chord length
$C_d$	Drag coefficient
$C_{l_{max}}$	Maximum lift coefficient
$C_\mu$	Momentum coefficient
CC	Circulation control
CFD	Computational fluid dynamics
Cs	Coanda surface
DRF	Dual-radius flap
$h$	Slot height
$\dot{m}$	Mass flow rate
$P$	Pressure
$q$	Dynamics pressure
$r_1$	First flap radius
$r_2$	Second flap radius
$S$	Reference surface area
TE	Trailing edge
$V_\infty$	Free stream velocity
$V_{jet}$	Exit slot jet velocity
$\Delta C_d$	Change of drag (compared with clean configuration)

---

A. Nimmanmongkol · C. Chumsing (✉) · V. Juttijudata  
Department of Aerospace Engineering, Faculty of Engineering, Kasetsart University, Bangkok, Thailand  
e-mail: [akanit.n@ku.th](mailto:akanit.n@ku.th); [chinnapat.chum@ku.th](mailto:chinnapat.chum@ku.th); [vejapong.j@ku.ac.th](mailto:vejapong.j@ku.ac.th)

$\Delta C_d^*$	Change of drag (compared with no-blown configuration)
$\Delta C_l$	Lift augmentation respective to clean airfoil configuration
$\Delta C_l^*$	Lift augmentation respective to no-blown configuration
$\alpha$	Angle of attack
$\rho$	Density

## 1 Introduction

The significant increase in aviation growth rate and the drive to sustainable aviation in recent years have had a profound influence on development and technology in this field, including high-lift systems. Conventional high-lift systems use flaps and leading-edge slats, resulting in significant weight and volume penalties of a typical wing assembly. These assemblies are also complex (up to three and four sub elements) and very sensitive to location relative to the main element of the wing. Alternatively, Coanda-driven circulation control has met with varying degrees of enthusiasm as the requirements for improved high-lift systems continue to increase (Jones, 2005).

Circulation control (CC) as a lift augmentation device is traditionally used on the main wing of an aircraft. This technology has been in the research and development phase for over 60 years, primarily for fixed-wing aircraft, with the early models referred to as “blown flaps” (Jonathan et al., 2015). With the Coanda effect induced by the circulation control, the jet sheet remains attached along the curved surface. The rear stagnation point location moves toward the lower airfoil surface, producing an additional increase in circulation around the entire airfoil. The outer irrotational flow is also substantially turned, leading to a high value of lift coefficient comparable to that achievable from conventional high-lift systems (Alexandru, 2014).

With the aim to achieve sustainable aviation, circulation control flap as a route toward sustainable high-lift systems was explored and investigated by means of computational fluid dynamics (CFD) via ANSYS-FLUENT 2021 R2 in this study with the outline as followed. Details of flap configuration, circulation control, and computational model are given in Sect. 2. The computational results of different flap configurations and circulation control were presented in Sect. 3 with the discussion. Section 4 concluded the study and discussed the ongoing and future work.

## 2 Approach and Methodology

### 2.1 Flap Configuration and Circulation Control Parameters

For the research, a dual-radius flap (DRF) configuration shown Fig. 1 was selected, with the first radius ( $r_1$ ) turning the slot exit jet stream to take advantage of the small radius as well as travel along the second radius with a larger radius to the trailing edge. The flap’s radii of curvature ( $r_1$  (mm) –  $r_2$  (mm)) were varied from 36–77, 36–115, 36–188, to 36–298 on NASA SC(2)-0414. Note that  $r_1$  is kept unchanged at 36 mm in this study. The deflection angle of flap was fixed at 30° throughout the study.

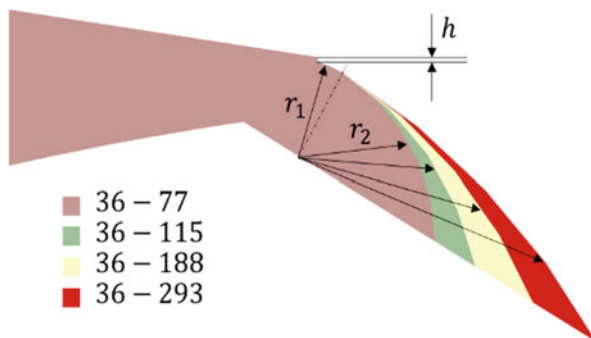


**Fig. 1** Schematic of the dual-radius flap configuration and geometry of the trailing edge of the airfoil that  $r_1$  was fixed at 36 mm, while  $r_2$  was varied to be 77, 115, 188, and 293 mm. The jet slot height  $h$  was set at 1.6 mm

The circulation control was achieved by means of blowing jet stream at the curved surface through the jet slot at a height of 1.6 mm to promote flow attachment along the flap, as illustrated in Fig. 1. The strength of the blowing jet was characterized by momentum coefficient:

$$C_\mu = \frac{\dot{m}V_{\text{jet}}}{0.5\rho V_\infty^2 S} \quad (1)$$

## 2.2 Computational Model

### 2.2.1 Geometry and Grid Setting

The semi-structured mesh was appointed to capture all highly intricated details as shown in Figs. 2 and 3. The unstructured mesh was created in the region adjacent to the airfoil to achieve proper compatibility around the airfoil and slot region, which has sharpened edges or quirk angles. Further away from the airfoil, the structured mesh was chosen to reduce the computational time. The domain region extended six times of the chord-length forward, 11 times of the chord-length backward, and 6.5 times of the chord-length up and down direction.

### 2.2.2 Flow Model and Boundary Conditions

The flow was assumed to be in a low-speed regime, i.e., an incompressible flow. Complex boundary layer/jet flap interaction was modeled by SST  $k - \omega$  turbulence model. A no-slip boundary condition with an appropriate value for the SST  $k - \omega$

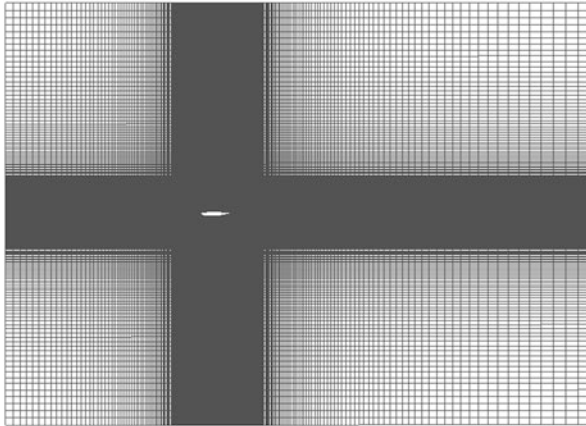


**Fig. 2** Rectangular computational domain and overall grid detail

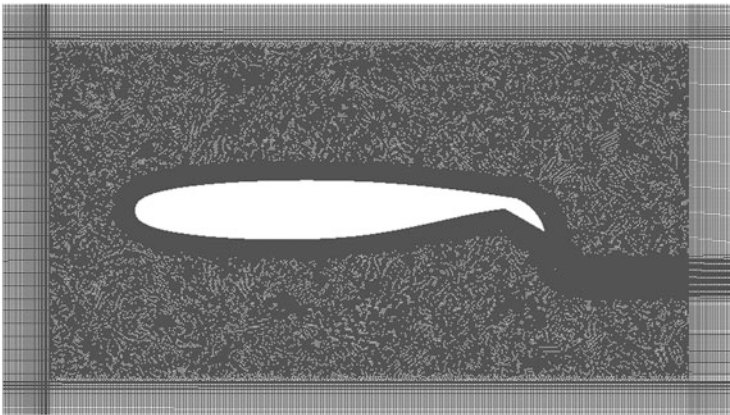


**Fig. 3** Detail for semi-structured mesh around airfoil

**Table 1** Boundary condition for inlet

Freestream (inlet)	
$M_\infty$	0.1
$\rho_\infty$ (kg/m <sup>3</sup> )	1.225
$T_\infty$ (K)	288.15
$P_\infty$ (Pa)	101,325
$\mu_\infty$ (kg/ms)	1.789e-5
Turbulence model	SST $k\omega$

model was applied to the airfoil and flap surfaces. Inlet boundary condition shown in Table 1 was applied at inlet, upper, and lower boundaries. A pressure outlet boundary condition was applied at the downstream boundary.

### 3 Results and Discussion

#### 3.1 Validation

To validate the computational model, the lift coefficient for different momentum coefficients from the CFD model was compared against the data from the research (Lee-Rausch et al., 2006), as shown in Fig. 4. Note that the DRF configuration for the flap was 34–154. The airfoil was set at zero angle of attack with the flap deflection of 30°. The momentum coefficient was varied from 0 to 0.14. Table 2 showed the freestream condition for the validation. The computational cells were carried out at 400,000. Figure 4 showed excellent agreement with the reference data suggesting that the computational model was well-valid (Fig. 5).

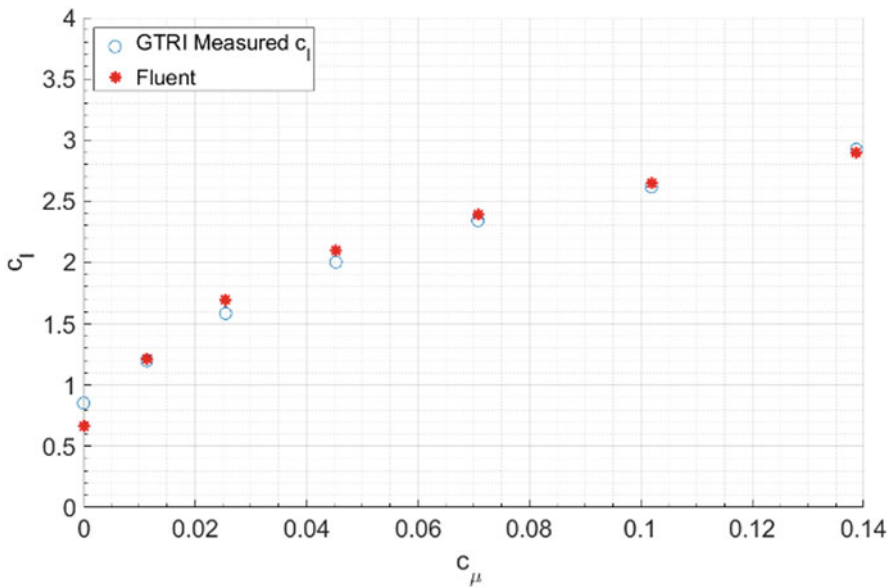


**Fig. 4** Lift coefficient from this study (Fluent) in comparison to GTRI data from Lee-Rausch et al. (2006) (GTRI measurement)

**Table 2** Setting for solver validation

$P_\infty$ (Pa)	97,906
$\rho_\infty$ (kg/m <sup>3</sup> )	1.1596
$V_\infty$ (m/s)	28.74

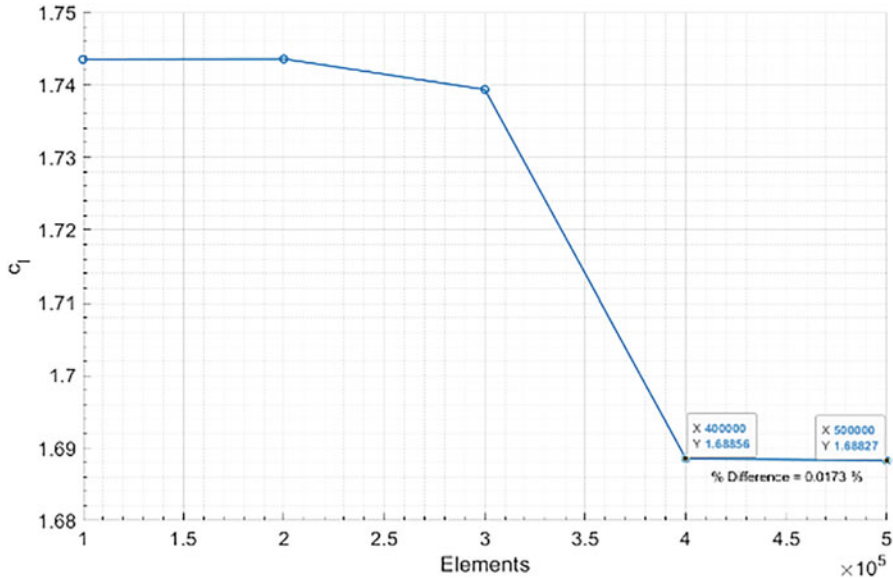


**Fig. 5** Mesh independent study for lift coefficient via a consecutive mesh refinement from 100,000 to 400,000 cells

### 3.2 Analysis

Figure 6 showed the (typical) velocity of magnitude of flow near the trailing edge of the flap with the momentum coefficient at 0.092 and the angle of attack of  $0^\circ$ . The  $r_1 - r_2$  DRF configuration was 36–188. Flow at the slot exit reached the speed of 182.54 m/s corresponding to the Mach number of 0.53. The incompressibility assumption was locally violated within this thin jet flap boundary layer on the flap surface. However, a rapid mixing of the turbulent boundary layer with surrounding air reduced the airspeed below the Mach number of 0.3 close to the trailing edge, restoring the validity of the incompressible assumption. Such results were also observed in Montanya and Marshall (2007). Figure 6a also suggested the flap jet enhanced the Coanda effect and maintained flow attachment over the airfoil, resulting in an increase of the lift augmentation  $\Delta c_l$  (with respect to maximum lift of a clean wing) as the momentum coefficient.

Comparing the effect of blown jet via lift augmentation  $\Delta c_l^*$  with respect to maximum lift of flap without blown jet (i.e.,  $\Delta c_l^* = 0$  at  $C_\mu = 0$ ) in Fig. 6b revealed that the Coanda effect induced by blown jet shifted its preference from a high to low  $r_2$  DRF configuration as the momentum coefficients increased. This turned out to be the results of a higher potential to create stronger suction pressure along the flap surface and ability to negotiate a sharper curve (small  $r_2$ ) flap surface as the momentum coefficient increased, as shown in Fig. 6.



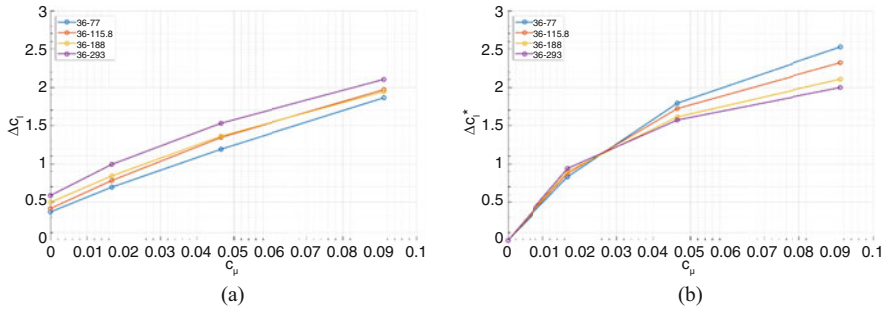


**Fig. 6** Lift augmentation for different  $C_\mu$  and DRF configuration with respect to (a – left) maximum lift of clean wing ( $\Delta C_l$ ) and (b – right) maximum lift of a flapped wing without a blown jet ( $\Delta C_l^*$ ), i.e.,  $\Delta C_l^* = 0$  for  $C_\mu = 0$

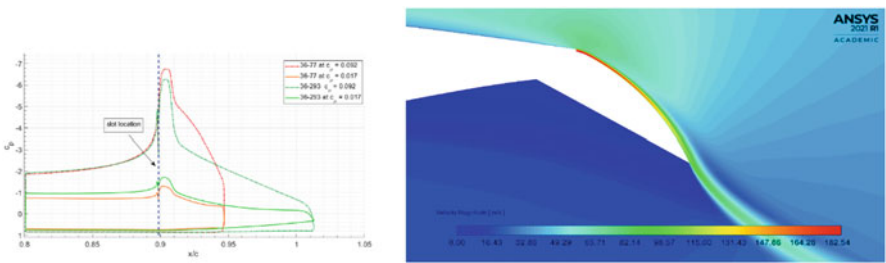


**Fig. 7** Pressure coefficient of largest and smallest  $r_2$  with different momentum coefficient (L), Velocity contour of flow exits slot area (R)

Drag increase at maximum lift (with respect to drag of a clean wing at maximum lift) in Fig. 7 showed that the blown jet reduced the drag at maximum lift for all DRF configuration. This was due to a blown jet promoting an attached boundary layer over the flap; form drag was reduced. As the momentum coefficient increased, the drag was monotonically increased. This was a result of a stronger suction pressure as the momentum coefficient increased, as discussed above; boundary layers were susceptible to stronger adverse pressure gradients and stronger form drag (Fig. 8).

### 4 Conclusion

This paper studied the effect of flap geometry and momentum coefficient of blown flap jet via CFD. Preliminary results suggested lift could be augmented by the Coanda effect induced by blown flap jet. Low momentum coefficients tend to prefer large  $r_2$  DRF configuration, while high momentum coefficients tend to prefer small

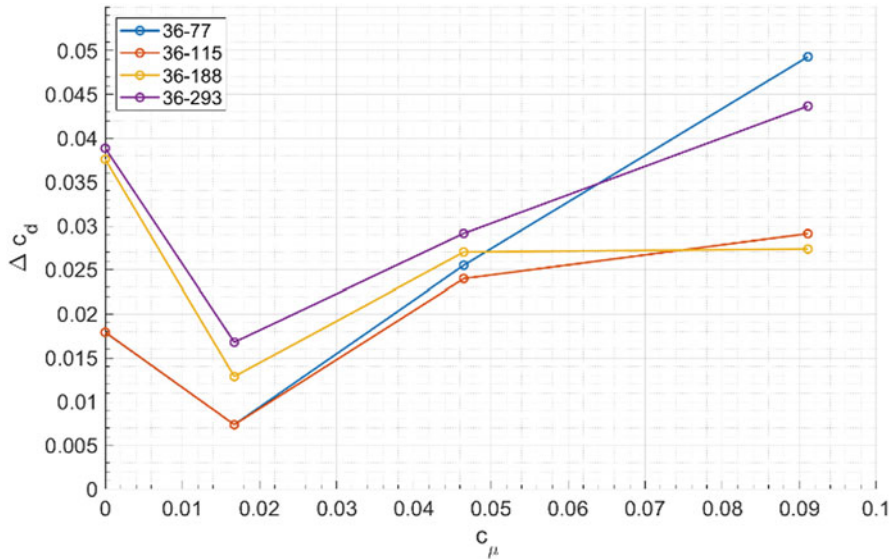


**Fig. 8** Increase of drag at maximum lift (compared with clean configuration) with respect to momentum coefficient

$r_2$  DRF configuration. In addition, blown flap jet also affected the adverse pressure gradient and form drag, i.e., it reduced drag compared to flap jet without blown jet, and drag increased as the momentum coefficient of blown jet increased.

The concept of circulation control could be further examined and equipped on aircraft in order to augment maximum lift while potentially reducing wing weight; hence, it may lead us the way to the future sustainable aviation in the future.

## References

- Alexandru, D. (2014). Blowing jets as a circulation flow control to enhancement the lift of wing or generated power of wind turbine. *INCAS Bulletin*, 6(2/2014), 33–49.
- Jonathan, K., et al. (2015). Applications of circulation control, yesterday and today. *International Journal of Engineering and Advanced Technology (IJEAT) Exploring Innovation*, 4(5), 411–429.
- Jones, G. S. (2005). Pneumatic flap performance for a 2D circulation control airfoil, steady & pulsed. In *Proceedings of the 2004 NASA/ONR Circulation control workshop* (pp. 845–888). Langley Research Center.
- Lee-Rausch, E. M., et al. (2006). Computational analysis of dual radius circulation control airfoils. In *36th AIAA fluid dynamics conference*, June 5–8, 2006, San Francisco, CA.
- Montanya, J. B., & Marshall, D. D. (2007). Circulation control and its application to extreme short take-off and landing vehicles. In *45th AIAA aerospace science meeting and exhibit*, January 8–11, 2007. American Institute of Aeronautics and Astronautics.

# Sustainability Indices for Airport Sustainability Evaluation



Orhan Yücel, Alper Dalkiran , Seval Kardeş Selimoğlu,  
and T. Hikmet Karakoc

## Nomenclature

GRI	Global Reporting Initiative
IATA	International Air Traffic Association
MCDM	Multi Criteria Decision-Making
UN SDG	United Nations Sustainable Developments Goals

## 1 Introduction

Technological advances and the development of global trade increase the demand for air transportation. Due to this increase in demand, the air transport sector is among the sectors that grow steadily.

According to the IATA, the number of passengers traveling annually will grow by an average of 3.7% every year and will reach 8.2 million in 2037, almost doubling compared to 2017 (IATA, 2018).

---

O. Yücel (✉)  
Cappadocia University, Nevşehir, Türkiye  
e-mail: [orhan.yucel@kapadokya.edu.tr](mailto:orhan.yucel@kapadokya.edu.tr)

A. Dalkiran  
Suleyman Demirel University, Isparta, Türkiye

S. K. Selimoğlu  
Anadolu University, Eskisehir, Türkiye

T. H. Karakoc  
Eskisehir Technical University, Eskisehir, Türkiye

Information Technology Research and Application Centre, Istanbul Ticaret University, Istanbul, Türkiye

The increase in air transport demand requires extra growth in capacity and new infrastructure expansions. However, due to growth, problems such as additional air and environmental pollution, noise, land use and construction, and urban traffic cause both local and international concerns and reactions (Graham & Guyer, 1999).

The understanding of sustainable aviation, which states that environmental and social impacts should be taken into account as well as economic concerns in the development of air transport services, has gained prevalence in this direction.

In order for businesses to evaluate their sustainability performance both by themselves and by all stakeholders, it is important to determine the change in their performance over time and the situation compared to other businesses. For this purpose, the use of sustainability indices is important.

Although there are a limited number of studies in the literature evaluating the airports in terms of performance, service quality, and environmental impacts, there exist very few studies on sustainability indices that consider the three basic pillars of sustainability, namely the economic, environmental, and social dimensions.

### ***1.1 Airport Sustainability Indices and Indicators***

Environmental capacity in airports, especially in big cities, has now taken precedence over physical capacities (runways, aprons, terminal areas, taxiways, etc.). Noise, air pollution, land use around the airport, wastes left to the environment, traffic in the land transportation connection, etc. are the main issues of these effects (Graham & Guyer, 1999).

In the literature, the issue of CO<sub>2</sub> emissions, which has the highest share in air pollution caused by aviation, is examined in detail. In addition to the air pollution caused by aviation activities in the general environment, the effects on the air of the residential areas around the airports are also the basis of research (Irvine et al., 2016).

The degradation of the ozone layer is seen as one of the most threatening phenomena awaiting humanity for the future. The airline industry has an important role in the formation of this problem, and this share is increasing in parallel with the growth of the industry (Upham et al., 2003).

In order to control the emissions that cause climate change, limits and future reduction targets are set by some airports. In this context, managing the traffic effectively has gained importance in airports (Irvine et al., 2016).

The most effective method in providing solutions to the criticisms directed at airports in terms of sustainability and environmental aspects is to communicate transparently with the public about the plans and practices of the airports (Upham et al., 2003). For this purpose, sustainability reports are published, and it is not possible for an airport establishment or expansion project to progress without agreeing with the relevant stakeholders (Freestone, 2009).

GRI Sustainability Reporting Frame is the most common sustainability reporting tool for large airport operators as well as for large and important businesses. For this reason, the sustainability reports of the large airports on the GRI Database for the past years were a very important data source for this research (GRI, 2021).

The sustainability data reported with these reports provide both quantitative and qualitative data in terms of evaluating business sustainability performances.

United Nations Sustainable Development Goals (UN SDG) also constitute an important base for every sustainability report (UNDP Turkey, 2021). These goals are also considered during the indicator determination phase of this research.

There are limited number of articles on the use of indices for airports to cover the three main dimensions of sustainability, and these articles have been examined in detail. In addition, studies that partially cover these three dimensions and include the use of indices on service quality, economic, environmental, and social sustainability at airports are also examined in detail.

## 2 Methodology

Both quantitative and qualitative research methods are used for this research.

For this purpose, an extensive literature research for determining the sustainability indices for airports was performed. Among the indices studied and used in the said studies, the most common and effective ones were analyzed.

Additionally, sustainability reports of large airports that publish annual reports were analyzed from the GRI Database and airport websites. UN Sustainable Development Goals were also considered during the indicator determination phase.

Based on the literature review and GRI reports, a unique set of indices and indicators that can perfectly reflect the sustainability status of airports is proposed. The research model is given in Fig. 1.

## 3 Results and Discussion

The sustainability issues in airports are spread over a wide range, and it is very difficult to make an assessment by covering all of them. In this respect, it is important to select indices and metrics that are sufficient to produce coherent knowledge on the subject.

Fig. 1 Research model



**Table 1** Airport sustainability index set

Social index Customer satisfaction Employee well-being and involvement Employee satisfaction Human rights and abuse Corporate governance and business ethics Social responsibility projects Supporting local people	Environmental index Waste management Water pollution Noise management Energy management Emissions and air pollution Resource usage Environment friendly building design Systematic efforts Green outdoors
Economy index Direct economic contributions Growth Indirect economic effects Debt status Distribution of economic value to stakeholders Efficiency and innovation	Operational indicators Number of passengers Aircraft movements, number of landings, and takeoffs Annual cargo carried Annual allocated passenger km, ton-km Aircraft movement per fate

As a result of the literature research and the review of the airport sustainability reports, an original index set (Table 1) was created. This set, which forms the basis of this study, consists of economic, environmental, and social sustainability indices and supporting operational indicators. Operational indicators, although not considered as an index, have the feature of shaping all the indices.

## 4 Conclusion

Airports create large sustainability impacts, both locally and globally. Managing these effects sustainably can only be possible by comparing airports with the use of certain sustainability indices.

Currently, indices used for airport sustainability evaluation are very few, and there are very few studies on this subject in the literature.

In this study, by using a literature review, GRI reports, and expert opinion, a unique set of sustainability indices and indicators for airports is proposed.

Later, research can involve the use of suitable MCDM (multi-criteria decision-making) methods to determine the weights of each index and indicator, which has not been applied to the sustainability of airports.

Additionally, the index set can be tested with the case studies on some sample airports using real airport data.

Both airport managements and all airport stakeholders can benefit from the comparative information to be obtained through the use of sustainability indices and indicators developed as a result of this research. It will also contribute to the scientific literature on aviation management and sustainability.

## References

- Freestone, R. (2009). Planning, sustainability and airport-led urban development. *International Planning Studies*, 14(2), 161–176. <https://doi.org/10.1080/13563470903021217>
- Graham, B., & Guyer, C. (1999). Environmental sustainability, airport capacity and European air transport liberalization: Irreconcilable goals? *Journal of Transport Geography*, 7(3), 165–180. [https://doi.org/10.1016/S0966-6923\(99\)00005-8](https://doi.org/10.1016/S0966-6923(99)00005-8)
- GRI. (2021). *Register your report*. <https://www.globalreporting.org/how-to-use-the-gri-standards/register-your-report/>
- IATA. (2018). *IATA annual review 2018*.
- Irvine, D., Budd, L., Ison, S., & Kitching, G. (2016). The environmental effects of peak hour air traffic congestion: The case of London Heathrow Airport. *Research in Transportation Economics*, 55, 67–73. <https://doi.org/10.1016/j.retrec.2016.04.012>
- UNDP Turkey. (2021). *Sustainable development goals*. <https://www.tr.undp.org/content/turkey/en/home/sustainable-development-goals.html>
- Upham, P., Thomas, C., Gillingwater, D., & Raper, D. (2003). Environmental capacity and airport operations: Current issues and future prospects. *Journal of Air Transport Management*, 9(3), 145–151. [https://doi.org/10.1016/S0969-6997\(02\)00078-9](https://doi.org/10.1016/S0969-6997(02)00078-9)

# An Approach to Optimizing Aircraft Maintenance



Onyedikachi Chioma Okoro, Maksym Zaliskyi, and Serhii Dmytriiev

## Nomenclature

IATA International Air Transport Association  
PDF Probability density function

## 1 Introduction

According to IATA (2021), global aircraft maintenance, repair, and overhaul expenditure represent 10.83% of airlines' operational costs. This significantly high cost highlights the need for the optimization of aircraft maintenance without compromising on reliability and flight safety. Aircraft maintenance optimization is typically a multi-objective solution that aims to maximize revenue by maintaining high availability while simultaneously minimizing cost (Yang et al., 2021). To optimize aircraft maintenance, many researchers have suggested and evaluated a range of techniques based on aspects of aircraft maintenance processes such as planning, scheduling, maintenance task allocation, aircraft maintenance routing, spare parts inventory, use of aircraft prognostics and health management data, personnel, and skill management. However, considering that the goal of an aircraft operator is to retain or restore the reliability levels of an aircraft at a minimum cost using a reliability control program, there is a gap in research devoted to reliability-centered models for optimizing the maintenance of aircraft systems.

---

O. C. Okoro (✉) · M. Zaliskyi · S. Dmytriiev  
National Aviation University, Kyiv, Ukraine  
e-mail: [sad@nau.edu.ua](mailto:sad@nau.edu.ua)



### 1.1 An Overview of Aircraft Reliability

Aircraft are expensive industrial systems that at the same time have the highest reliability and safety requirements. Maximizing aircraft availability and minimizing cost are best achieved by designing the aircraft to be reliable and maintainable. Reliability requirements are typically determined during the research and development phase of the aircraft life cycle and are applied to the other three phases of the aircraft life cycle: manufacturing and acquisition, operation and support, and disposal (Ren et al., 2017). During the operation and support phase, the reliability of the aircraft and its components is of paramount importance to flight safety and availability – the need for an optimal maintenance task interval with minimal costs arises during this phase.

The reliability process allows aircraft operators to analyze data of aircraft and component parts. An operator can compare the reliability of the entire fleet to understand the cost of schedule interruptions, analyze solutions, and prioritize service bulletins based on impact to the fleet. Maintenance optimization tasks of aircraft systems can be conducted based on analytical, numerical, or simulation approaches (Fig. 1). The analytical approach is based on the determination of an exact equation; the numerical approach is based on descent methods, evolutionary methods, and pattern search methods; the simulation approach is based on Monte Carlo methods (Ostroumov et al., 2021a, b).

## 2 Method

To solve the problem of determining an optimal maintenance task interval, the average operational cost per unit time  $E(C/t_M)$  is considered a measure of efficiency, where  $C$  is the operational costs and  $t_M$  is the maintenance interval. The average operational cost per unit time is function (1)

$$E(C/t_M) = \phi(C_R, C_M, t_M, n, f(t)) \tag{1}$$

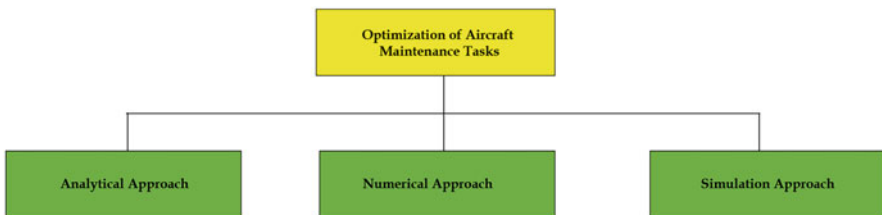


Fig. 1 Approaches for optimizing aircraft maintenance tasks

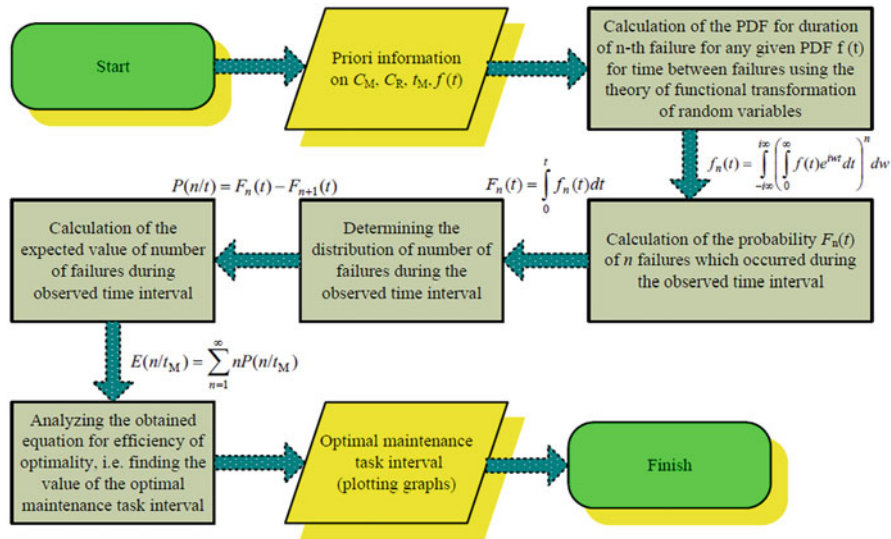


Fig. 2 Flowchart for finding an optimal maintenance task interval for aircraft systems

where  $C_R$  is the repair cost,  $C_M$  is the maintenance cost,  $f(t)$  is the probability density function (PDF) of time between failures, and  $n$  is the number of observed failures. It is assumed that based on operational experience and documentation, the priori information on  $C_R$ ,  $C_M$ , and  $f(t)$  is known and the methodology for finding the optimal maintenance task interval is shown in Fig. 2.

### 2.1 Calculation

Reliability theory considers various PDFs to describe the process of failure and deterioration of aircraft systems. The most used PDFs are exponential, Erlang, Weibull, Gaussian, inverse Gaussian, and Birnbaum-Saunders.

If time between failures of aircraft systems is determined using exponential PDF, the average operational cost per unit time is

$$E(C/t_M) = \lambda C_R + \frac{C_M}{t_M} \tag{2}$$

With an increase in  $t_M$ , efficiency decreases and does not have an optimum point. Therefore, it is impossible to develop an optimal maintenance strategy,  $t_M \rightarrow \infty$ .

If time between failures of aircraft systems is determined by Erlang PDF, the average operational cost per unit time will be

$$E(C/t_M) = \frac{(2\lambda t_M + e^{-2\lambda t_M} - 1)C_R + 4C_M}{4t_M} \tag{3}$$

To find an approximate optimal value for maintenance task interval, the numerical method can be used. In this case, we applied the Newton-Raphson method.

$$t_{Mk+1} = t_{Mk} - \frac{\phi'(t_{Mk})}{\phi''(t_{Mk})},$$

where,

$$\begin{aligned} \phi'(t_M) &= \frac{\partial E(C/t_M)}{\partial t_M} = \frac{-2\lambda C_R t_M e^{-2\lambda t_M} - C_R e^{-2\lambda t_M} + C_R - 4C_M}{4t_M^2}, \\ \phi''(t_M) &= \frac{\partial^2 E(C/t_M)}{\partial t_M^2} \\ &= \frac{2\lambda^2 C_R t_M^2 e^{-2\lambda t_M} + 2\lambda C_R t_M e^{-2\lambda t_M} + C_R e^{-2\lambda t_M} - C_R + 4C_M}{2t_M^3}, \\ t_{M0} &= \sqrt{\frac{C_M}{\lambda^2 C_R}}. \end{aligned}$$

The initial value  $t_{M0}$  for the first iteration was calculated based on asymptotical presentation of Eq. (3) using the Taylor series.

$$t_{Mk+1} = t_{Mk} \left( 1 - \frac{2C_R - 8C_M - 4\lambda C_R t_{Mk} e^{-2\lambda t_{Mk}} - 2C_R e^{-2\lambda t_{Mk}}}{2\lambda^2 C_R t_{Mk}^2 e^{-2\lambda t_{Mk}} + 2\lambda C_R t_{Mk} e^{-2\lambda t_{Mk}} + C_R e^{-2\lambda t_{Mk}} - C_R + 4C_M} \right).$$

The optimal maintenance task interval in case also can be found using Lambert function  $L(x)$ . The exact solution can be presented as follows:

$$t_{M \text{ opt}} = -\frac{1}{2\lambda} - \frac{1}{2\lambda} L\left(\frac{4C_M - C_R}{C_R}\right). \tag{4}$$

### 3 Results and Discussion

To analyze our proposed approach, simulation using the Monte Carlo method was carried out in MathCAD software. The initial data for simulation are:

- Failure rate  $\lambda = 0.0008 \text{ hours}^{-1}$  (for exponential and Erlang PDFs)
- Mean  $m = 3000$  and standard deviation  $\sigma = 600$  (for normal PDF)

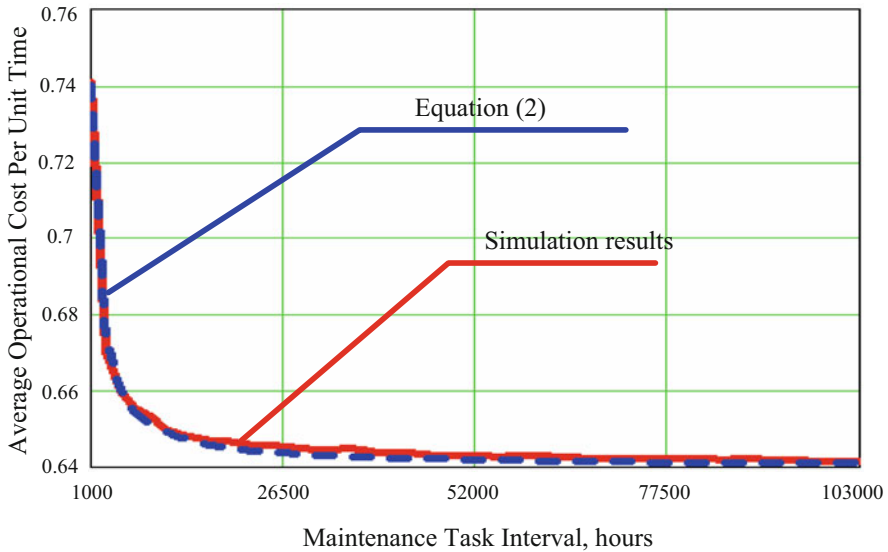


**Fig. 3** The dependence of efficiency on maintenance task interval obtained based on analytical equation (blue line) and statistical simulation (red line) for exponential time between failures

- Costs for maintenance  $C_M = 100$  and repair  $C_R = 800$
- Sample size  $n = 1000$
- Number of iterations  $N = 10000$

Figures 3, 4, and 5 show the dependence of the average operational cost per unit time on maintenance task interval obtained according to analytical equations and statistical simulations for exponential, Erlang, and normal PDFs.

Figure 3 confirms that for the exponential time between failures, an optimal maintenance interval does not exist, because there is no minimum and optimal maintenance task interval tends to infinity. Simulation results and analytical calculations using Eq. (2) almost coincide.

For the Erlang model for time between failures shown in Fig. 4, the minimum for average operational cost per unit time exists. The values of the optimal maintenance task interval obtained according to Eq. (4), numerical optimization, and simulation results are approximately the same.

Figure 5 demonstrates the general methodology for the normal PDF of time between failures. For this distribution, there is an optimal maintenance task interval. The optimal values of this interval using analytical calculation and statistical simulation are approximately same.

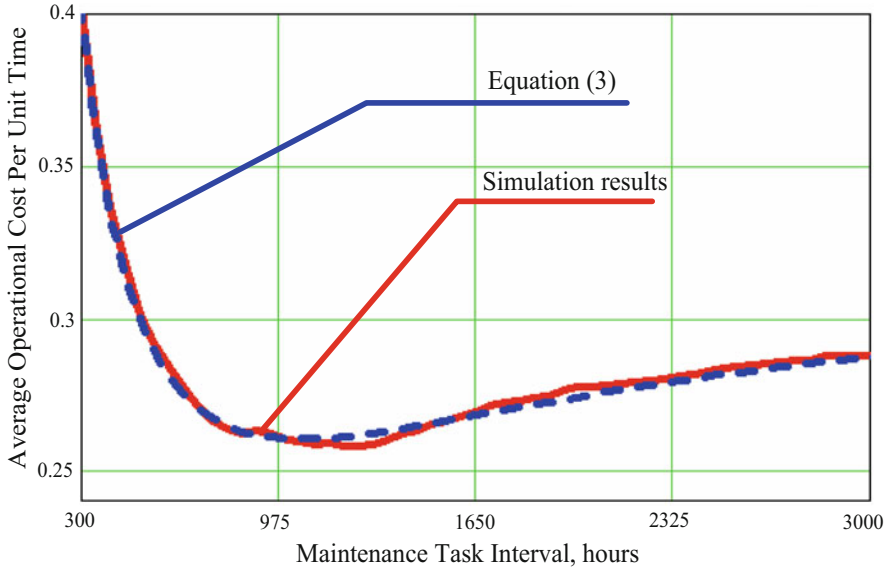


**Fig. 4** The dependence of efficiency on maintenance task interval obtained based on analytical equation (blue line) and statistical simulation (red line) for Erlang PDF of time between failures

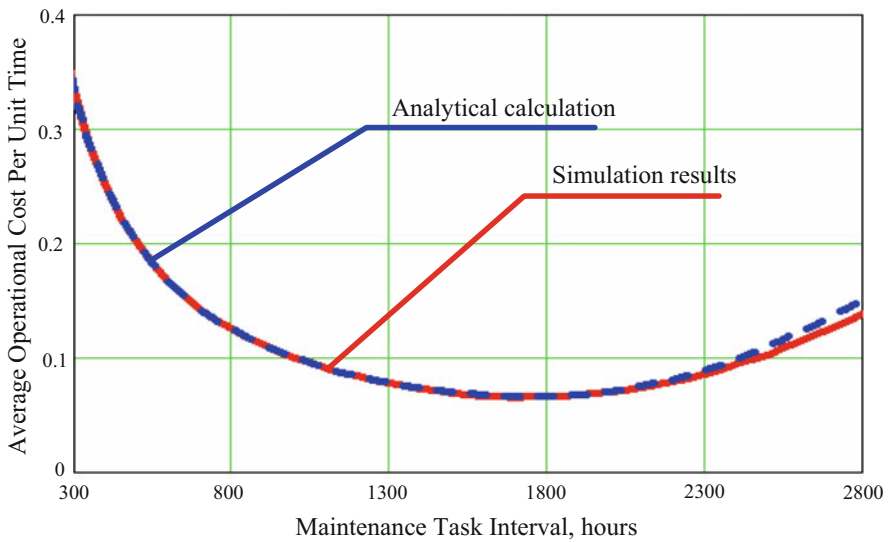


**Fig. 5** The dependence of efficiency on maintenance task intervals obtained based on the analytical equation (blue line) and statistical simulation (red line) for normal PDF of time between failures

## 4 Conclusion

This study presents the optimization of maintenance task intervals for aircraft systems using the average operational cost per unit time as an efficiency measure. This paper considered the exponential and Erlang model. For the exponential model, a minimum does not exist; hence, this model cannot be used to find an optimal interval for maintenance. On the other hand, a minimum exists for the Erlang model, which proves that this model can be used for the optimization of maintenance task intervals of aircraft systems.

The accuracy of our findings was checked using MathCAD software and the simulation results compared favourably with the obtained equations.

## References

- IATA. (2021). *Airline maintenance cost executive commentary FY2019 data*. [https://www.iata.org/contentassets/bf8ca67c8bcd4358b3d004b0d6d0916f/fy2019-mctg-report\\_public.pdf](https://www.iata.org/contentassets/bf8ca67c8bcd4358b3d004b0d6d0916f/fy2019-mctg-report_public.pdf). Accessed 18 Oct 2021.
- Ostroumov, I., et al. (2021a). A probability estimation of aircraft departures and arrivals delays. In O. Gervasi et al. (Eds.), *Computational science and its applications – ICCSA 2021. Lecture notes in computer science* (Vol. 12950). Springer. [https://doi.org/10.1007/978-3-030-86960-1\\_26](https://doi.org/10.1007/978-3-030-86960-1_26)
- Ostroumov, I., et al. (2021b). Modelling and simulation of DME navigation global service volume. *Advances in Space Research*, 68(8), 3495–3507. <https://doi.org/10.1016/j.asr.2021.06.027>
- Ren, H., Chen, X., & Chen, Y. (2017). *Reliability based aircraft maintenance optimization and applications* (pp. 1–3). Elsevier Inc.
- Yang, H., Miao, X., Zhang, J., Liu, J., & Pan, E. (2021). Reinforcement learning-driven maintenance strategy: A novel solution for long-term aircraft maintenance decision optimization. *Computers and Industrial Engineering*, 153. <https://doi.org/10.1016/j.cie.2020.107056>

# In Search of Environmental Protection Element in the Thai Aviation Law: A Result from CORSIA



Lalin Kovudhikulrungsri, Jantajira Iammayura, Krittika Lertsawat, Kornwara Boonsiri, Navatasn Kongsamutr , and Prangtip Rabieb

## Nomenclature

CORSIA Carbon offsetting and reduction scheme for international aviation  
GMBM Global Market-Based Measure  
ICAO International Civil Aviation Organization

## 1 Introduction

The Convention on International Civil Aviation (Chicago Convention) is silent on the environmental aspect due possibly to the fact that international civil aviation law had been developed before the existence of international environmental law. Nonetheless, the International Civil Aviation Organization (ICAO), as a specialized agency under the United Nations, adopted Annex 16 on Environment Protection to set standards on environmental pollution arising from civil aviation. As of 2021, the latest volume of Annex 16 is devoted to a carbon offsetting and reduction scheme for international aviation (CORSIA). This initiative follows the United Nations Framework Convention on Climate Change and the Paris Agreement (ICAO Assembly

---

L. Kovudhikulrungsri (✉) · J. Iammayura  
Faculty of Law, Thammasat University, Bangkok, Thailand  
e-mail: [lalin@tu.ac.th](mailto:lalin@tu.ac.th)

K. Lertsawat  
ENLAWTHAI Foundation, Bangkok, Thailand

K. Boonsiri · P. Rabieb  
Office of the Council of State, Bangkok, Thailand

N. Kongsamutr  
Faculty of Engineering, Kasetsart University, Bangkok, Thailand

Resolution A40-19) and Goals 7 and 13 of the United Nations Sustainable Development Goals (ICAO, Environmental Protection's Contribution to Sustainable Development Goal 7; ICAO, Environmental Protection's Contribution to Sustainable Development Goal 13).

In the 39th ICAO Assembly in 2016, Thailand's Minister of Transport has undertaken to join the Global Market Based Measure (GMBM) in 2021 (ICAO, CORSIA States for Chapter 3 State Pairs). With the short timeline to pass its regulation on CORSIA, Thailand has been grappling with two major legal questions: (1) Which law provides a legal basis for passing a subordinate regulation on CORSIA and other Volumes of Annex 16, and (2) how is the law equipped with legal measures to address aviation environmental problems including CORSIA-related activities? This paper aims to bring light to both issues that were swept under the carpet prior to the commitment towards CORSIA.

## 2 Method

By applying documentary research, this paper examines ICAO documents and primary sources, i.e., laws and regulations from four countries from four continents, namely, France, the United States of America, Australia, and Thailand. The selection criteria are based on their membership in the ICAO and their approach to implementing environmental law relating to aviation. The comparative method is applied to propose the appropriate legal measures for Thailand.

## 3 Results and Discussion

### 3.1 *Legal Basis for CORSIA*

In any rule-of-law country, a regulation must be passed by due process of law which critically entails a legal basis established by an act of parliament. An analysis of laws and regulations from four selected countries reveals that many statutes are governing environmental issues in aviation. General environmental law, civil aviation law, and zoning law are all examples of laws that try to regulate airports and aircraft as shown in Table 1. In Thailand's case, the legislation that implements the Chicago Convention, as part of its compliance with international obligations, should be the foundation for CORSIA regulation.

Thailand implements the Chicago Convention through the Air Navigation Act, B.E. 2497 (1954), and the Civil Aviation of Thailand Emergency Decree, B.E. 2558 (2015) (Emergency Decree). After being audited under the Universal Safety Oversight Audit Program, the Emergency Decree was promulgated in response to the urgent need to "improve the form, structure, powers and duties of civil aviation bodies of Thailand" (The Emergency Decree, Remark).



**Table 1** Law and regulation on environmental aviation

Law/ Regulation	Australia	EU France	Thailand	United States of America
Civil Aviation Law	Air Navigation (Aircraft Noise) Regulations 2018	Acoustic Certifi- cation under Ministre Chargée de L'aviation Civile	Air Navigation Act, B.E. 2497 (1954);	14 CFR Part 36 Aircraft noise
	Air Navigation (Aircraft Engine Emissions) Regulations 1995	Autorité de contrôle des nui- sances aéroportuaires – ACNA (Phase-out loud noise aircraft)	(1) Phase-out loud noise aircraft (Noise Certificate) (2) Noise abatement measures under the air navigation (Technical mea- sures) (3) Airport Operation Certificate	14 CFR Part 34 Air emis- sions from air- craft engine
	Air Navigation (Fuel Spillage) Regulations 1999	EU Directive 2003/87/EC (EU ETS + ICAO CORSIA)		40 CFR Part 87 and 1068 GHGs
	Curfew Act (specific airport: Sydney Airport Curfew Act 1995)	Noise restrctions: Noise curfew, ban loud noise aircraft type		Federal Register vol.80 No.126 on 1st July 2015 ICAO CORSIA
General Envi- ronmental Law	Airports (Envi- ronmental Pro- tection) Regula- tions 1997	EU Directive (related on air pollutants and air quality)	Enhancement and Conservation of National Environ- mental Quality Act, B.E.2535 (1992) (Emission standards)	40 CFR 1500- 1508 NEPA Act 1969 Envi- ronmental Impact Statement
		DIRECTIVE 2003/87/EC EU ETS	Environmental Impact Assess- ment of Airport Project	
		Noise permissi- ble limits for specific airport		
Zoning Law			Town Planning Act, B.E.2562 (2019): Specific Town Plan	14 CFR Part 150 Airport Noise Compat- ibility Planning
				24 CFR Part 51 Subpart B Noise Abate- ment Control (HUD)

The Air Navigation Act, B.E. 2497 (1954), has been amended 14 times, with the most recent addition of Chapter 1/1 on Civil Aviation Overseeing in 2019. Nevertheless, it appears that the term “environmental protection” was mentioned inconsistently. The CAAT is obliged to prescribe standards on safety, security, and facilitation under the Chicago Convention and its Annexes (the Emergency Decree, Article 15/7 (9)). This provision omits the term “environmental protection.” On the other hand, Section 15/9 (1) includes the word “environmental protection” in the CAAT’s responsibility, which reads:

Section 15/9 in the implementation of Section 15/7 and Section 15/8, the Civil Aviation Authority of Thailand shall proceed to comply with or take into account the conventions and annexes including the obligations under the International Agreement on Civil Aviation that Thailand is a Party, as the case may be, and including the following actions:

(1) Covenant and comply with the conventions and annexes including obligations according to the international agreement related to . . . *Environmental Protection* . . . that Thailand is a Party ... (The Emergency Decree, Article 15/9 (1) emphasis added).

Section 15/9 is subject to the application of Section 15/7; as a result, the strict interpretation of Sections 15/7 and 15/9 leaves the CAAT without a legal basis to enact subordinate regulations on environmental protection.

Turning to Article 37(1)(p) of the Emergency Decree authorizes the CAAT to issue environmental regulations to comply with international standards (the Emergency Decree, Article 37 (1)(p)). Thus, this article establishes the groundwork for passing other regulations from Annex 16 to the Chicago Convention.

### ***3.2 The Sufficiency of the Legal Basis***

Upon closer examination, this paper discovers that the Emergency Decree differs from the laws of the other selected countries. While the Thai law provides the CAAT with the power to create any subordinate laws, it also disables the CAAT by offering neither carrot nor stick initiatives. On the contrary, the Air Navigation Act imposes sanctions. The analysis also concludes that incentive measures are under the purview of the Ministry of Finance.

ICAO recommends economic tools to combat environmental pollution. In the case of aircraft noise, a variety of financial measures are found in Australia, France, and the United States as shown in Table 2. The Thai Air Navigation Act authorizes the collection of environmental charges under Sections 60/37, 60/44, and 56(5). However, they do not comply with the ICAO Doc 9082 key charging principles, namely, cost-relatedness, transparency, and consultation with users, due to the lack of stated rationale, a requirement on the publication of the financial statement, and a requirement for allocating the charge for environmental pollution mitigation.

**Table 2** Economic measures

Measures	ICAO	Australia	EU France	United States of America
Economic measures	Airport economics manuals (Doc9562)	Aircraft Noise Levy Collection Act 1995	Pollution complaints management	Airport Improvement Program (AIP)
	Airport and air navigation facility charge (Doc7100)		Taxes sur les nuisances sonores aériennes	Passenger Facility Charges (PFC)

While both criminal and administrative charges are incorporated in Thailand's Air Navigation Act, only administrative fines are adopted in France and Australia (see *Code de l'aviation civile*; Air Navigation (Aircraft Noise) Regulations 2018 and in Air Navigation (Fuel Spillage) Regulations 1999). These two countries' approach is consistent with Section 77 of the Constitution of the Kingdom of Thailand, B.E. 2560 (2017), which attempts to curb overcriminalization.

## 4 Conclusion

Although the Emergency Decree can serve as a basis for a regulation on CORSIA and other aviation environmental laws, it lacks incentives and sanctions to enforce the regulation. Meanwhile, the Air Navigation Act does not expressly authorize the enactment of environmental regulation, though it includes criminal and administrative punishments. Therefore, the authors propose that a CORSIA regulation be passed under the Emergency Decree, assuring Thailand's adherence to the ICAO's timeline. In the long run, Section 15/7 of the Air Navigation Act should be updated to explicitly mention "environmental protection," amend its economic measures to reflect ICAO policy, and abolish the criminal penalty for violating aviation environmental provisions. At the same time, the CAAT should cooperate with other agencies to create financial incentives for airlines and airports to become more environmentally friendly.

**Acknowledgments** This paper is a brief and partial summary of the research titled Legal Framework for the Global Market-Based Measure (GMBM) and Legal Concept for Thai Aviation Environmental Law funded by the Civil Aviation Authority of Thailand.

## References

International Civil Aviation Organization. (2019). *Resolution A40-19 Consolidated statement of continuing ICAO policies and practices related to environmental protection - Carbon Offsetting and Reduction Scheme for International Aviation (CORSIA)*. Available via ICAO. [https://www.icao.int/environmental-protection/Documents/Assembly/Resolution\\_A40-19\\_CORSIA.pdf](https://www.icao.int/environmental-protection/Documents/Assembly/Resolution_A40-19_CORSIA.pdf)

- International Civil Aviation Organization. (2020). *CORSIA States for Chapter 3 State Pairs*. [https://www.icao.int/environmental-protection/CORSIA/Documents/CORSIA\\_States\\_for\\_Chapter3\\_State\\_Pairs\\_Jul2020.pdf](https://www.icao.int/environmental-protection/CORSIA/Documents/CORSIA_States_for_Chapter3_State_Pairs_Jul2020.pdf)
- International Civil Aviation Organization. *Environmental protection's contribution to sustainable development goal 7*. <https://www.icao.int/about-icao/aviation-development/SDGen/ENV7.pdf>
- International Civil Aviation Organization. *Environmental protection's contribution to sustainable development goal 13*. <https://www.icao.int/about-icao/aviation-development/SDGen/ENV13.pdf>

# Seamless Passenger Experience for the Airport Environment: Research at DARTeC



Fatma Gul Amil, Zeeshan Rana, and Yifan Zhao

## Nomenclature

Covid-19    Coronavirus disease

DARTeC    The Digital Aviation Research and Technology Centre at Cranfield University

## 1 Introduction

Security demands of airports have been increased more and more with the increasing volume of people. Visual tracking, facial recognition at gateways, and biometric recognition at borders are popular not only in the digital aviation industry but also among researchers to provide the highest possible safety for passengers. Face detection has a key role in face analysis, tracking, and recognition. Over the years, it has progressed from traditional computer vision techniques all the way to advanced artificial neural networks. Learned-Miller et al. (2016) examined traditional approaches for face detection and received satisfactory results. However, these methods are not well enough with complex images; deep learning models have better results.

Especially, the success of deep learning in feature extraction and classification has been accepted by most of the researchers (Ahmed et al., 2020). Several studies, by Huang et al. (2021), Li et al. (2018), and Masi et al. (2019), have been carried out on the occlusion problem. To solve this problem, many researchers have proposed

---

F. G. Amil (✉) · Z. Rana · Y. Zhao  
School of Aerospace, Transport and Manufacturing (SATM), Cranfield University,  
Bedfordshire, UK  
e-mail: [fatma-gul.amil@cranfield.ac.uk](mailto:fatma-gul.amil@cranfield.ac.uk); [zeeshan.rana@cranfield.ac.uk](mailto:zeeshan.rana@cranfield.ac.uk);  
[yifan.zhao@cranfield.ac.uk](mailto:yifan.zhao@cranfield.ac.uk)

various methods of deep learning like Fast R-CNN (Girshick, 2015), SSD (Liu et al., 2016), YOLO (Redmon et al., 2016), and Cascade CNN (Ahmed et al., 2020). Fast R-CNN comprises two subnetworks that have caused longer computational time. YOLO and SSD consist of a single network, making them faster but less precise than the algorithms listed above. SSDs have lower localization errors compared with R-CNN. However, they have more classification errors dealing with similar categories. Nevertheless, they do not have a good performance on smaller objects. Cascaded CNN is explained next section in detail.

As regards of face recognition model, significant progress has been achieved with large-scale training data (Guo et al., 2016), sophisticated network structures (Peng et al., 2020), and advanced loss designs (Deng et al., 2018). These existing systems are typically provided with non-occluded faces that include main facial characteristics like the eyes, nose, and mouth. The main challenge faced by many researchers is occlusion, which is the case when wearing a mask. In addition to this, other difficulties are the quality of data, illumination variation, complex background, abrupt motion, pose variations, and multi-camera correlation. The purpose of this research is to investigate and develop advanced deep learning algorithms for robust and real-time face recognition to overcome partial or full occlusion. We have intended to develop novel face recognition and tracking system to handle occlusion. Initially, we developed new large-scale datasets of faces with occlusion. On the other hand, it is important to be lightweight and memory-efficient, which preferred model.

## 2 Methodology

There are two basic approaches currently being adopted in research and experimental. One is FaceNet, by Schroff, Kalenichenko, and Philbin (2015), which is the primary algorithm for our facial recognition, and the second one is MTCNN, which is beneficial for detecting bounding boxes of faces (Kaziakhmedov et al., 2019).

### 2.1 FaceNet

In 2015, the FaceNet model was enhanced by Schroff, Kalenichenko, and Philbin, which is one of the popular algorithms in classification, detection, face verification, and recognition. The model uses 128 low-dimensional embeddings instead of high-dimensional vector analysis for each image frame. That is a vital difference between FaceNet and other state-of-the-art methods (Li et al., 2018). In order to match faces, they calculate Euclidean distance, which is a scalar scale value of the embedding of each image. FaceNet uses deep convolutional networks and triplet loss to achieve good accuracy, which is known as one-shot learning. The embeddings can be considered as feature vectors, which could be a benefit for the simultaneous implementations. Additionally, FaceNet can train any difficult learning system of

any single model that illustrates an entire goal system by collecting all the factors at the same time, and this is the most significant part of the FaceNet model.

## 2.2 *MTCNN*

MTCNN contains a cascade structure of CNN. Cascade CNN-based algorithms have operated at multiple resolutions and distinguished the background regions in low resolution quickly. This system of classification includes three networks, which are P-net, R-net, and O-net. P-Net proposes facial regions, R-Net filters the bounding boxes, and O-Net proposes facial landmarks. This approach is designed for high performance, which is convenient for face detection and camera capture applications.

## 2.3 *Triplet Loss*

Triplet loss architecture helps us to learn distributed embedding by the notion of similarity and dissimilarity. For triplet loss, the objective is to build triplets consisting of an anchor image, a positive image (which has similarity to the anchor image), and a negative image (which has dissimilarity to the anchor image).

The cost function for triplet loss is as follows:

$$\text{Loss} = \sum_i^N \left[ \left\| f(x_i^a) - f(x_i^p) \right\|_2^2 - \left\| f(x_i^a) - f(x_i^n) \right\|_2^2 + a \right]_+ \quad (1)$$

$x_i$ : It represents an image.

$f(x_i)$ : It represents the embedding of an image (Euclidean space).

$a$ : It represents the margin between positive and negative pairs.

The objective of this function is to keep the distance between the anchor and positive smaller than the distance between the anchor and negative.

## 3 Experimental Performance: Evaluation Metrics

### 3.1 *Implementation Details*

There are three major factors influencing the performance of the face recognition model: lightweight models which are capable of running real-time, large-scale dataset, and retrained models to prevent computational and memory cost. The

**Table 1** Training specifications and results of the implementation of our proposed model

Input image type	Model shape	Model	Loss Function	Feature number	Batch size	Epochs	Best accuracy
Without mask	$112 \times 112 \times 3$	Inception-Resnet v1	Cross entropy	128	96	100	61.6
With and without mask	$112 \times 112 \times 3$	Inception-Resnet v1	Cross entropy	128	96	200	96.93
With and without mask	$112 \times 112 \times 3$	Inception-Resnet v1	ArcFace loss	128	64	100	96.8

FaceNet model was chosen considering these features. For the face recognition process, our FaceNet model was retrained with different configurations and datasets (as shown in Table 1). Our implementation evaluated the TensorFlow deep learning framework. The model was trained using NVIDIA Quadro T1000 (12GB) GPU. For evaluation of the model, we use the VGG19 convolution network configuration. Inception V1 layer adopted the model in which this concept uses different kernel sizes to extract different-sized features. Inception-Resnet-v1 layer is used as the latest model with residual blocks, which help to improve training speed (Peng et al., 2020). The model size has been increased with residual connections in order to outperform. We used a smaller input size, which is  $112 \times 112$  instead of the original pretrained input model  $160 \times 160$ . Hence, a reduction dimension means fewer weights of embeddings and faster inferences.

### 3.2 Dataset

We evaluated our model on two datasets. We used LFW datasets (Learned-Miller et al., 2016) for testing and Casia-WebFace datasets (Yi et al., 2014) for training, and we evaluated our own model. The Casia-WebFace dataset had a preprocessing part before the evaluation of the model. The first step in this process was to remove mislabeled images and align faces from the dataset. Once the mislabeled ones were extracted, we created a dataset with facial masks. Data arrangements and analysis were performed using PyCharm software (version 2020.2.3).

### 3.3 Location of the Cameras

In this section, we are going to design the planning by deciding criteria for camera position, within the DARTeC building. Cameras are positioned for different purposes, and they create a route for passengers in the airport environment. One camera is located at the entrance of the airport environment for the collection of facial



information and database. One camera is located in stairways that are connected with the entrance and passenger experience environment. The rest of the cameras are located in the passenger experience environment. This presented plan has been designed for the airport environment, whereas it can be suited with other communal places such as industrial areas, working places, and universities.

## 4 Results and Discussion

Retrained FaceNet model was used to detect and recognize the masked face images. The table above presents some of the main characteristics of the training process in our model. “Input image type” refers to the training dataset, which has a significant rise in accuracy with masked images. The results, as shown in Table 1, indicate that the relation between dataset and accuracy are remarkable aspect for the research. In further examination, the original model with pretrained analysis accuracy achieved 61.6%, while the accuracy of retrained model reaches up to 96.3%. The results obtained from the pretrained model analysis of the FaceNet model and our retrained model is shown in Fig. 1.

Other aspects of the research indicate that there are difficulties in distinguishing various occlusion accurately in real-world applications. As a result of our implementation, which is shown in the Fig. 2, our model recognizes masked or without masked faces in real time.

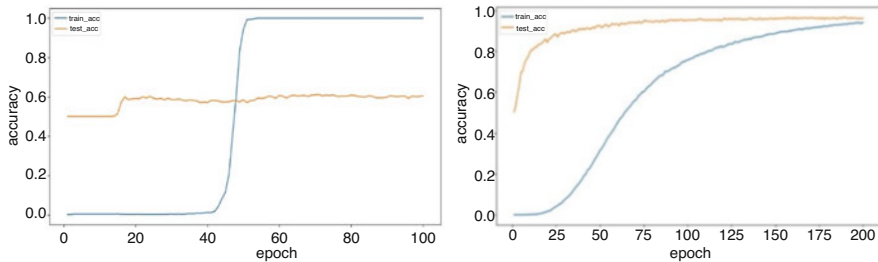


**Fig. 1** Statistic for (a) accuracy of our model dataset without mask and (b) accuracy of our model dataset with masked



Fig. 2 Experimental results from the entrance camera

## 5 Conclusion

In the performance of facial recognition, one of the most crucial aspects is the large-dataset. On the other hand, there are certain drawbacks associated with the computational time and memory, which are caused by dataset. It is very difficult to adopt real-time scenarios in many deep learning methods, whereas these have been leading us to investigate more lightweight algorithms. The overall analysis shows that our lightweight face recognition model gets excellent results even with a masked face, as shown in Fig. 2.

Future work will be evaluation of the other large-scale datasets with our model and develop visual tracking with this could be enhanced passenger experience at airport.

## References

- Ahmed, T., Das, P., Ali, M. F., & Mahmud, M.-F. (2020). A comparative study on convolutional neural network based face recognition. In *2020 11th international conference on computing, communication and networking technologies (ICCCNT)* (pp. 1–5). IEEE.
- Deng, J., Guo, J., & Zafeiriou, S. (2018). *ArcFace: Additive angular margin loss for deep face recognition*. IEEE.
- Girshick, R. (2015). Fast R-CNN. In *Proceedings of the IEEE international conference on computer vision, 2015 Inter* (pp. 1440–1448). IEEE.

- Guo, Y., Zhang, L., Hu, Y., He, X., & Gao, J. (2016). MS-Celeb-1M: A dataset and benchmark for large-scale face recognition. In B. Leibe, J. Matas, N. Sebe, & M. Welling (Eds.), *Computer vision – ECCV 2016* (pp. 87–102). Springer International Publishing.
- Huang, B., Wang, Z., Wang, G., Jiang, K., Zeng, K., Han, Z., Tian, X., & Yang, Y. (2021, June). When face recognition meets occlusion: A new benchmark. In *ICASSP, IEEE international conference on acoustics, speech and signal processing – proceedings* (pp. 4240–4244). IEEE.
- Kaziakhmedov, E., Kireev, K., Melnikov, G., Pautov, M., & Petiushko, A. (2019). Real-world attack on MTCNN face detection system. In *2019 International multi-conference on engineering, computer and information sciences (SIBIRCON)* (pp. 422–427). IEEE.
- Learned-Miller, E., Huang, G. B., RoyChowdhury, A., Li, H., & Hua, G. (2016). Labeled faces in the wild: A survey. In M. Kawulok, M. E. Celebi, & B. Smolka (Eds.), *Advances in face detection and facial image analysis* (pp. 189–248). Springer International Publishing.
- Li, P., Wang, D., Wang, L., & Lu, H. (2018). Deep visual tracking: Review and experimental comparison. *Pattern Recognition*, 76, 323–338. Elsevier Ltd.
- Liu, W., Anguelov, D., Erhan, D., Szegedy, C., Reed, S., Fu, C. Y., & Berg, A. C. (2016). SSD: Single shot multibox detector. In *Lecture notes in computer science (including subseries lecture notes in artificial intelligence and lecture notes in bioinformatics)*, 9905 LNCS (pp. 21–37). Springer.
- Masi, I., Wu, Y., Hassner, T., & Natarajan, P. (2019). Deep face recognition: A survey. In *Proceedings – 31st Conference on Graphics, Patterns and Images, SIBGRAPI 2018* (pp. 471–478).
- Peng, S., Huang, H., Chen, W., Zhang, L., & Fang, W. (2020). More trainable inception-ResNet for face recognition. *Neurocomputing*, 411, 9–19.
- Redmon, J., Divvala, S., Girshick, R., & Farhadi, A. (2016, December). You only look once: Unified, real-time object detection. In *Proceedings of the IEEE computer society conference on computer vision and pattern recognition* (pp. 779–788). IEEE.
- Schroff, F., Kalenichenko, D., & Philbin, J. (2015, June 7–12). FaceNet: A unified embedding for face recognition and clustering. In *Proceedings of the IEEE computer society conference on computer vision and pattern recognition* (pp. 815–823). IEEE.
- Yi, D., Lei, Z., Liao, S., & Li, S. Z. (2014). *Learning face representation from scratch*. CoRR, abs/1411.7.

# Critiques and Challenges of Air Transport Liberalisation Policy in Thailand



Navatasn Kongsamutr 

## 1 Introduction

In the global air transport marketplace, which favours full market access, concentration, competition, and multilateralism, bilateral agreements with the restrictions on ownership and control of airlines are no longer relevant. Some nations are slow to react to the new economic era, mainly to protect their national interests. In contrast, some governments have been initiating deregulation and liberalisation. Through borderless investment, airlines progressively become “global”, following the trend of many other industries (Lelieur, 2003).

Several economic concepts are relevant to the theoretical discussion of industrial liberalisation. Many traditional neoclassical economic models are predicated on the assumption of perfect or pure competition, which there should not be a need for government regulation in a perfectly competitive market because the market is subject to monopoly abuse (Goetz & Vowles, 2009). The deregulation and liberalisation in many countries and regions show remarkable impacts. The deregulation of many domestic markets initiates the increased number of seats supplied but decreased the number of routes served; by contrast, the deregulation of most international markets stimulates the radical change in a rising number of both seats supplied and routes operated (Williams, 1993). There is an argument on the negative side of deregulation. In Canada, this has been more apparent in addition to the impact of deregulation and liberalisation policy on the airline industry; Canada’s peculiar geopolitical characteristics have intensified the new pressures to which it has had to respond. By the fifth year of deregulation, Canada’s airlines were in crisis. They

---

N. Kongsamutr (✉)

Air Transport Research and Consulting Centre, Department of Aerospace Engineering,  
Faculty of Engineering, Kasetsart University, Bangkok, Thailand  
e-mail: [navatasn.k@ku.ac.th](mailto:navatasn.k@ku.ac.th)

faced the distinct possibility of the collapse of the domestic airline industry, necessitating the opening of the home market to foreign carriers.

The other aspect towards the deregulation is about the passengers. Obviously, in terms of airfare, there are many significant shreds of evidence that show the remarkably declined fares. In contrast, according to ground access fares, the potential benefits to passengers from increased airline competition will, in general, be partially absorbed by increased airport charges at unregulated airports. In some circumstances, this may even result in increases in overall charges, not reductions. Similarly, unilateral deregulation leading to increased airport competition in one country may lead to the majority of the gains going abroad. A claim of significant passenger gains from deregulation and competition may be exaggerated, and achieving these gains, in reality, may need subtle and quite far-reaching government intervention.

There are also some significant differences in deregulation and competition between the developed and developing countries. The developed country has had more significant opportunities and capabilities to undertake the prior evaluation of policy changes, and it has been able to monitor the performance of deregulation. However, the government of the developing country has to react in a dynamic market without the benefit of a full, public evaluation of the alternatives (Hooper, 1998). Especially in the hugely diversified markets in Asia, the countries differ widely in many aspects, for instance, economic, social, country size, and aviation policies. However, developing countries have the following details of airline deregulation and liberalisation experiences in the USA and Europe.

Liberalisation has been one of the main drivers of the continuous growth of air traffic, and measures enabling expanded market and capital access for air transport have resulted in enhanced connectivity with the corresponding benefits of sustainable economic development at the state and regional levels and the emergence of active carriers and airports that are more passenger-friendly. The opening-up of the air transport market has furthermore led to increased and more efficient utilisation of airspace, more competitive fares, and more choices for the travelling public (ICAO, 2016).

### ***1.1 Air Transport Liberalisation in Thailand***

Thailand is one of a few countries in Asia that have a long history of commercial air transport. The first commercial air transport service provider for Thailand was founded on 13 July 1930 under the name Aerial Transport of Siam Co. Ltd., which was a pioneer in commercial aviation. Despite the long history of commercial air transport in the country, the period should be focused starts in 1973, when all air services belonged to the civil government for a decade. After that, the first privately owned airline was allowed and successfully established in 1986. Deregulation and liberalisation have proceeded gradually since then. The national airline industry witnessed another remarkable change in 1994, when the government allowed the

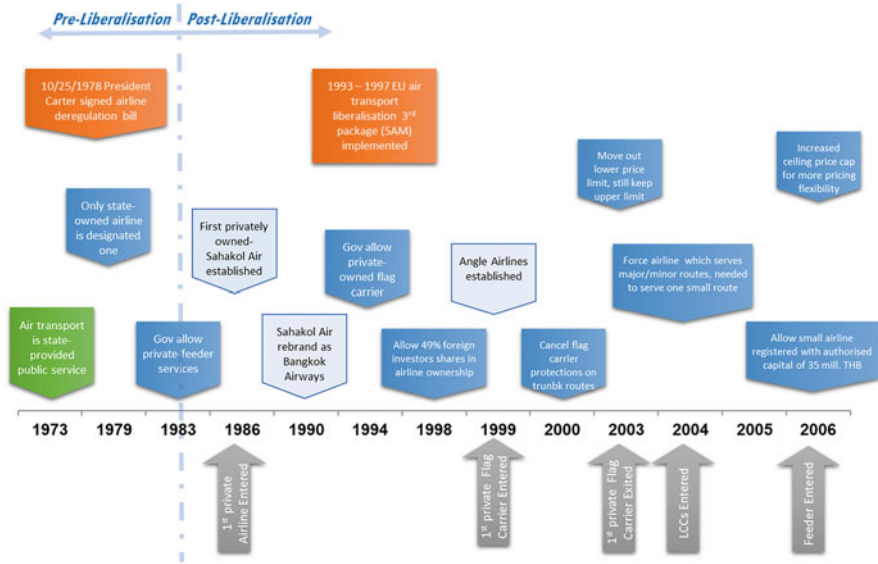


**Fig. 1** Evolution of deregulation and liberalisation evolution in Thailand (selected years during 1973–2006) (Kongsmutr, 2021)

establishment of a second privately owned national carrier, resulting in the launch of the first privately owned flag carrier, Angel Airlines, in September 1999 (Kongsmutr, 2021). Since that time, the government has implemented a number of deregulation packages and liberalised policies that have led to significant changes in the airline industry structure and market landscape. Especially during 2003–2004, a number of deregulations were implemented, allowing low-cost carrier business models to enter the market. Since then, Thailand’s airline market landscape has been remarkably changed (Fig. 1).

## 2 Method

The study was designed by using a mixed research method, administering a series of in-depth interviews with 25 major airlines’ experts and executives, the director general of the Civil Aviation Authority of Thailand, and three experts from the Office of the National Economic and Social Development Council. The interview transcripts were analysed by content analysis to analyse content meanings and context-context relationships of the country’s air transport liberalisation policy and its impact. The critiques and challenges of the policy are elevated and summarised (Table 1).

**Table 1** Summary of the number of interviewees, classified by organisation and position

Organisation	Experts	Executives	Total
Bangkok Airways	5	1	6
Civil Aviation Authority of Thailand	–	1(DG)	1
Nok Scoot	–	1(CEO)	1
Office of the National Economic and Social Development Council	3	–	3
Thai Airways	6	4	10
Thai AirAsia	2	–	2
Thai AirAsia X	–	2	2
Thai Lion Air	1	1	2
Thai Smile Air	1	1(COO)	2
Total	18	11	29

### 3 Results and Discussion

During the studied period (2012–2019), Thailand has experienced remarkable growth of air travel traffic in both international and domestic market. In order to gain more understanding and knowledge towards the market, an in-depth market analysis was conducted to explore three main aspects. This topic presents the first aspect, showing the results from the market structure and competition analysis. The study surfaces key changes at route-level market in view of competitive landscape by considering the number of airline player in particular market.

HHI of the international flight market is less than that of the domestic flight market. It is pointed out that the international market is more competitive than the domestic one, which is related to the number of operators in both markets. In the international flight market, the number of operators is 12.02 times higher than in the domestic flight market. HHI between 2012 and 2019 for domestic and international flight markets has decreased continuously at an average rate of 2.80% and 9.35%, respectively, showing the tougher environment expected in the international market (see Fig. 2). In addition, average fare per distance of domestic route has been declined to almost the same level as the international ones. The gap between average fare per distance flown of domestic and international route markets has been dropped from 36.36% difference to 14.28% difference (see Fig. 3).

Conclusion of the airlines' experts and executives' interview on the drivers of changes in air transport market from past to present in both domestic routes and international routes are divided into the following issues.

*The open skies policy:* The open skies policy makes freedom in air transport and gives the airlines opportunities to serve new destinations for the passengers. For domestic market, the thick route protection were eliminated and opened for free access and competition from Thai nationality carriers. For international market, the expansion of unlimited bilateral agreements with many countries, including middle-east countries, brings capacity and players in various route

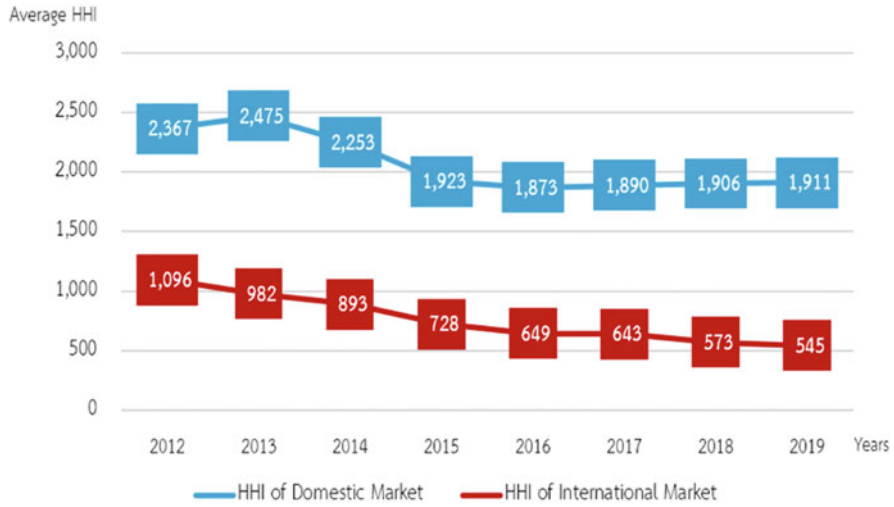


Fig. 2 Market concentration level of Thailand’s domestic and international markets (2012–2019)

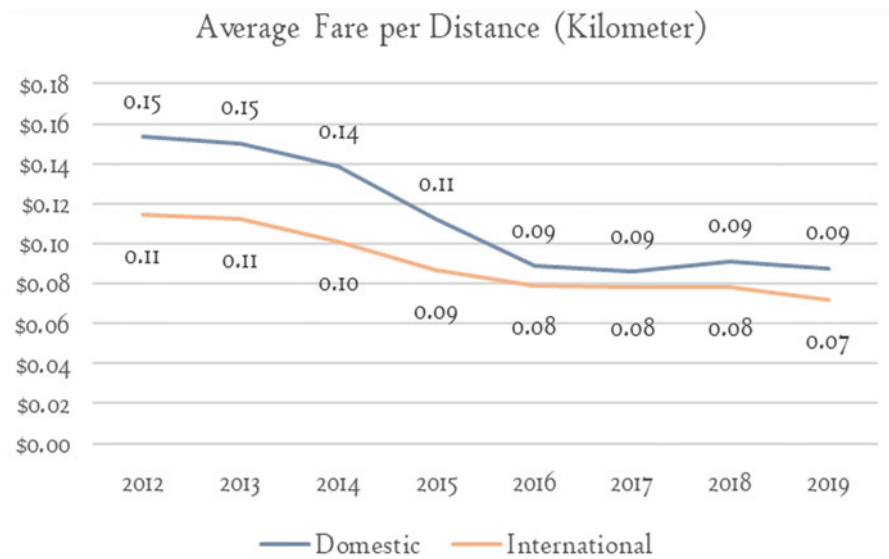


Fig. 3 Average yield of airlines’ domestic and international routes (2012–2019)

markets, but also intense competition on South East Asia-Europe region pair market between nonstop services and connecting services at middle east hub airports.

*Economic condition:* The economic cooperation as well as stronger economy of each country and region promotes trade and business. It has also created more travels in air transport.



*Tourist market:* Since Thailand first tourism promotion policy rolled out in 1988, it has created a collaboration between the stakeholders to promote the tourist market and develop the infrastructure of the cities to make them have more attractions for the tourists. These created fast growing derived demand in air transport services.

*Technology:* Many new technologies enrich the performance of aircraft, such as a better engine or payload capacity. That means the airplane can fly longer and more fuel efficiently. Also, the new technologies of air traffic services increased the airspace capacity and improved the safety of the airspace usage. Moreover, the technologies also affect the behaviour of people. They changed air travel market landscape from agent and airline centric to consumer centric through easy-to-access online ticket search, compare, and booking.

*The development of low-cost airlines:* From the promotion policy in the tourist industry as well as open skies policy, the development technologies, and new customer behaviour, low-cost airlines expand their markets rapidly and play an important role in making air transport easier to access and more affordable for travellers.

*The development of airport and transport infrastructure:* The increased capacity of airports made the airport able to handle larger number of passengers and flights. Also, the development of other modes of transport infrastructure created better integrated networks and connectivity for air transport.

*Regulation:* Many new and loosen regulations accommodate the establishment of new airlines. These made the air transport market more available choices as well as extensive competition on trunk route markets.

*Other drivers:* Many countries created new strength in business. For example, Japan in the past was only famous for the electronic industry, but nowadays, Japan is also famous for tourists because of the new free visa for tourist policy that can attract many tourists around the world. This thing inevitably created a new demand for air transport. Moreover, new distribution channels, such as online selling and the digital marketing of airlines, are also the key to increasing demand for air transport.

Regarding the critiques of the country's open skies policy from the past to the present in terms of failure issues. Key failure issues are as follows: The first is the negative impact of the open skies policy. Although the open skies policy made a growing number of newly registered airlines in Thailand recently, the policy has some conditions or agreements that let other dialogue partners gain the advantages. Thai airlines do not get the balanced right as they should get from the other countries. These created disadvantages for Thailand's air transport, as if the open skies policy nowadays were untrue. The second is the inattentive regulatory function. The regulation influenced by open skies policy is inattentive to regulate and not adequate, such as the regulation to register new airlines. It is too easy to register new airlines, so it created the room for the lack of standards for many new airlines. Many regulations do not accord with the main government policy. There are too few policies and regulations in the operation and development of air transport infrastructure, such as airport and air navigation service, compared to the excessive and unnecessary regulations for airlines. The lack of policy to support the ground service made the airline unable to fully handle passengers. The last key issue is the aviation

policy does not synergise with other industries' policy and direction, because of the lack of understanding of the aviation industry ecosystem and its impact to the country's economic, social, and environment. To create a reliable, competitive, and sustainable aviation industry, policy maker needs to see the roles of air transport are both enabler and producer. Focusing on air transport as only being travel means for tourists is not enough because the air transport could be important producer that add more value to economic and social system.

## 4 Conclusion

The conclusions are that having better policy and regulation in air transport by setting the agendas to promote and support for the development and operation of both Thai airline industry and its ecosystem could be more beneficial for the country. It also could create fairness thorough competition and create more value for traveller and public. The infrastructure of the airport and other modes of transport should be developed and regulated accordingly. Airport facilities should be improved in order to meet international standards and be able to handle passenger and flight growth in the future.

The government should set strategic objectives clearly and holistically. As mentioned before, focusing on only particular sector, such as tourism sector, would not bring the great benefits to the country. The focal sector and other sectors considered as its ecosystem need to be inclusively combined and assessed before policy formulation. Policy options and designs by careful selection of proper interventions and instruments would bring more value added to the country. Further, sharing knowledge among sectors in air transport system is a key to continuous improvement.

## References

- Goetz, A. R., & Vowles, T. M. (2009). The good, the bad, and the ugly: 30 years of US Airline deregulation. *Journal of Transport Geography*, 17, 251–263.
- Hooper, P. (1998). Airline competition and deregulation in developed and developing country contexts – Australia and India. *Journal of Transport Geography*, 6, 105–116.
- International Civil Aviation Organization. (2016). *Overview of regulatory and industry developments in international air transport*.
- Kongsamutr, N. (2021). Impact on Thai Airways of air transport liberalisation in Thailand. In J. W. Lee (Ed.), *Aviation Law and Policy in Asia: Smart regulation in liberalized markets*, Brill's Asian Law series (Vol. 10, pp. 221–234). Brill | Nijhoff.
- Lelieur, I. (2003). *Law and policy of substantial ownership and effective control of airlines*. Routledge.
- Williams, G. (1993). *The airline industry and the impact of deregulation*, Ashgate. Cambridge University Press.

# Digitalization in the Way of Aviation Sustainability



Rafet Demir, Serap Gürsel, and Hakan Rodoplu

## Nomenclature

ALAQS	Airport Local Air Quality Studies
IoT	Internet of Things
RFID	Radio Frequency Identification
SDG	Sustainable Development Goals

## 1 Introduction

Digitalization causes the change of existing services and products and the creation of many new products and services in a way that affects all sectors on a global scale. In this process, the aviation industry is among the sectors most affected by this change. While digitalization enables people to access the information and services they want more easily, it also creates a platform where they can present their problems, concerns, and ideas. In all sectors shaped by digitalization, besides many benefits, new and difficult-to-solve problems also arise. Environmental sustainability studies, which have seriously affected the aviation industry in recent years, sometimes get help from digitalization and sometimes get into a dead end due to digitalization. Thanks to well-developed digitalization, the information shared will influence and guide sustainability efforts in the future. With the concept of sustainability gaining importance in aviation, as it is all over the world, environmental sustainability practices in the sector have become quite remarkable. Today's aviation industry is affected by many factors. One of the most important of these is digitalization.

---

R. Demir (✉) · S. Gürsel · H. Rodoplu  
Aviation Management Department, Aviation and Space Science Faculty, Kocaeli University,  
Izmit, Türkiye

Correctly designing the interaction between the concepts of sustainability and digitalization, which affect the industry at the same time, will both help in overcoming the digitalization process easily and gain in achieving sustainability.

## 2 Digitalization and Sustainability Relationship

Sustainability in general means the balance of the relationship between the growth rate of societies and the consumption of resources. The negative consequences that will result in the unsustainability of the development in the future, which occur with the consumption of world resources faster than their renewal, are examined. The most important dimension in sustainability, especially after climate change, is environmental sustainability (Akanke et al., 2019). Environmental sustainability does not only include the problem of scarcity of resources. In addition to this problem, there is also the pollution of the environment by harmful wastes and gases that occur during production and consumption. Greenhouse gases cause the climate crisis by heating the atmosphere. The resulting situation is called climate change or global warming (IPCC, 2018). The impact of digitalization, which is another concept that seriously affects the aviation industry, on sustainability will be the subject of our research. It refers to the whole of the methods applied for the technological transformation of the information-based businesses on the basis of digitalization and the acceleration of the activities of the enterprises by making them more efficient (Klymenko et al., 2019).

As a global threat, climate change will negatively affect future life and the activities of airline companies. Sustainability efforts become essential for the continuity of production and social welfare. At this point, it is quite clear that rapidly developing technology will play a key role for environmental sustainability. In the research and analysis, it is accepted that digitalization has a positive effect on sustainability. In addition, sustainability will be easily followed through digital technologies (Gouvea et al., 2017; Wu & Raghupathi, 2018).

Techniques such as efficient use of resources, equipping company assets with smart systems, and realizing production capacity with new technologies increase the sustainability of industries. Digital transformation is an integral part of corporate sustainability too. Thanks to digital technologies, businesses can perform sustainable operations, achieve balanced growth, create awareness in their capacity, and achieve this by spending less resources, thanks to smart systems (Castro et al., 2021; Klymenko et al., 2019). Today, the concepts of digital management and digital transformation have gained importance in transportation policy. It is seen that the air transportation industry, which is an important supporter of the economy on a global scale, is one of the sectors that adapts most easily to the said digital transformation. In technology-intensive sectors such as aviation, sustainability practices are more tiring and costly than digital transformation practices.

Among the digitalization applications, there are technologies such as cloud-based management, deep learning, artificial intelligence, virtual reality, robotic coding,

additive manufacturing, Internet of Things (IoT), big data processing, and digital decision-making. Although these concepts were seen as far from daily life in the past, they have been included in everyone's daily life today (The World in 2050, 2019). Although it is preferred by businesses to facilitate, especially the information-based business on the basis of digitalization, it is beneficial in processing the data of all businesses. It provides marginal benefit by making the use of resources efficient in the field of production and service (Lange et al., 2020). Thanks to these technologies, the data transferred to the digital environment ensures that the operation is faster and more effective, and a more efficient production process emerges by increasing the connection of operations.

Digitalization means changing the evolutionary way of doing business in this field, rather than being accepted as an auxiliary tool for sustainability. In the aviation industry, digitalization is already heavily used in management activities, operations, and maintenance activities. There are studies stating that digitalization also has negative environmental effects. For this reason, it is necessary to examine the effects of digitalization in detail (Chen et al., 2020). By closely monitoring the implementation of the digital transformation process in the aviation industry through change management, the process can be completed successfully, and the negative aspects of environmental sustainability can be eliminated in this process (WEF, 2017). While it is generally accepted that digitalization is the most important method to reduce environmental impacts, today digitalization is used on the basis of business development and business strategy (Sparviero & Ragnedda, 2021).

### 3 Digitalization Practices in Aviation

Advances in the aviation industry are experienced very quickly, mainly thanks to the development of technology. Parallel to the developments in technology and communication, the aviation industry was adversely affected first of all, but when this situation was overcome industrially, the air transportation sector surpassed other sectors. The first use of digital technologies in the aviation industry started with the collection of passenger data by airline companies, and this data was processed and shared with industry stakeholders. Thus, passenger satisfaction was tried to be achieved by personalizing the services provided to the passengers (WEF, 2017). At the same time, flights are smoother and safer thanks to data technologies. Digitalization increases efficiency, reduces costs, and improves operations in the highly competitive aviation industry (Kuisma, 2017). In aviation, especially augmented reality, artificial intelligence, blockchain, and IoT are the most used technologies (George et al., 2021).

Digitalization processes implemented by airline companies and airports, which are the main actors of the aviation industry, attract more attention than the efforts of other stakeholders. Although digitalization has had an important place in aircraft production since the early days of air transportation, digitalization has been seen in the digital transformation efforts of the last period in the management function of all aviation enterprises.

### ***3.1 Airlines and Digitalization***

Airline companies need intensive information transfer and sharing processes while continuing their activities. The management of this data is provided by digital technologies and storage areas and data transfer networks. Today, almost all airlines provide their ticketing and reservation activities through digital channels, maximizing the passenger experience while reducing many costs. While these applications are the most common examples of digitalization, they have also led to gains in the field of environmental sustainability. Along with the airline companies that have advanced on the path of digitalization, there are also airlines that have not assimilated digitalization in the sector.

The steps of the International Air Transport Association (IATA) on sustainability coincide with those on digitalization. Digitalization steps bring benefits related to environmental sustainability. The leading ones in digitalization efforts are FRED+, Trajectory Sharing Platform (TSP), and e-Freight (Meré et al., 2020). With the FRED+ platform, airlines are provided with information on fuel, emission rates, and operational efficiency with benchmark reports and analytical tables (IATA, 2019). This platform is a website on a digital basis. Access to all countries included in CORSIA, as well as IATA member airlines, is open and free. TSP, on the other hand, can be defined as a platform to share the routes generally used by airlines and to minimize the damage to the environment by ensuring fuel efficiency.

### ***3.2 Airports and Digitalization***

Digitalization activities, which are applied primarily to increase efficiency and customer experience in airports as in airlines, have been used extensively in aviation safety and aviation security in the past. Especially the airports, which are known as pioneers in the field of sustainability (Schiphol, Heathrow, Munich, Frankfurt, Copenhagen, Zurich, Stockholm Arlanda), are taking great digital steps in the field of efficiency of operations, security, and passenger experience (Zaharia & Pietreanu, 2018). The use of cloud base, big data flow, and IoT technologies mostly focuses on instant monitoring of existing processes and improving the human-machine interface. Such technologies are suitable for use at airports that are willing to increase process automation (Little, 2018).

The main purpose of digitalization of airports is to increase efficiency in production, as in airlines. It seems possible to fulfill the duties of airports in the field of sustainability through digitalization activities. Basically, what is expected from an airport is to focus on sustainability: reduction of emissions; efficient use of resources; reduction of environmental noise, light, and visual pollution; waste management; and selection of used energies from renewable sources. Airports that meet these expectations exist today. There are some digital database applications to measure the data to be used in environmental sustainability activities at airports and

to make future forecasts. These applications are made available by EUROCONTROL. These are named as OPEN ALAQS, AMP, IMPACT, and V-PATH (SESAR, 2020). As explained, digitalization applications provide information to users by measuring emissions from fuel consumption at airports during takeoff, taxiways, and aprons. Of course, one of these applications specifically designed for airport monitoring is OPEN ALAQS. This application is integrated with the AUSTAL2000 tool developed by Germany, which is also used to analyze carbon values.

### ***3.3 Stakeholders and Sustainability***

When we look at the stakeholders of the sector outside of the airline and airport, it is seen that the steps of digitalization have started to be taken in every field to a large extent. Kovynyov and Mikut (2019) conducted a study on the usage areas of digital technologies used in ground operations at airports in the aviation industry and grouped these technologies. In the passenger group, there are applications such as check-in with kiosk devices, automatic boarding devices, terminal navigation, smart wheelchairs, fingerprint, and face recognition. In the baggage group, there are applications such as RFID, a kind of barcode system, automatic baggage delivery, and lost baggage kiosks. In the team planning and programming group, there are applications such as smart crew allocation method, congestion reduction method, and shift change method. In the human resources and training group, there are applications such as digital processing of personnel data, web-based training, mobile applications and corporate communication, and personnel cycle management. (Kovynyov & Mikut, 2019).

## **4 Results and Discussion**

The sources used and examined in this study are, in particular, sustainability, digitalization, sustainability in aviation, digitalization in aviation, sustainable digitalization, the effects of digitalization on sustainability, and finally, the effects of digitalization on sustainability activities in aviation, which have been reached with the deductive method. As understood from the literature and aviation companies examined throughout the study, the environmental dimension of sustainability in aviation has not yet been integrated with the digital age. Outside of aviation, it is seen that the importance of digitalization for environmental sustainability or the environmental effects of digital technologies are frequently researched and analyzed.

## 5 Conclusion

The concepts of sustainability and digitalization are processes that affect businesses both in the aviation industry and in the global market and that should be carried out together at a fundamental level. The reason why these concepts are trending together is the care given to the livable environment by the increasing environmental awareness and the immutability of technological developments.

In addition to the positive effects of digitalization, its negative effects also affect the aviation industry and environmental sustainability. In particular, the issue of digital waste may reach alarming proportions (Arushanyan et al., 2014). There are also challenges that airlines and airports will face while managing their digitalization processes. Inadequate infrastructure, the cost of technology, the forces that can be experienced in the adaptation of employees, the increase in the consumption of energy resources, and social effects are among the problems that digitalized businesses will experience (Pohl, 2017). Considering the aviation industry, digitalization process data is not shared due to competition, trust issues, and data security. For this reason, sectoral problems arise in digital transformation. The lack of information sharing among airline companies can be solved by national and international institutions making arrangements on this issue. With the digitalization of businesses, the issue of cyber security has also gained importance. Businesses have become more susceptible to theft of their data. Another obstacle to digitalization is the human factor. Business personnel may feel that their jobs are in jeopardy. The use of new technology can cause resistance in employees. It is normal to encounter problems on the way to digitalization. Industry stakeholders seek common solutions to these problems. The sectoral benefits of digitalization are many. Less fuel consumption, energy savings, and reduction in inputs, thanks to paperless operations, are the most well-known of these benefits.

## References

- Akande, A., Cabral, P., & Casteleyn, S. (2019). Assessing the gap between technology and the environmental sustainability of European cities. *Information Systems Frontiers*, 21, 581–604.
- Arushanyan, Y., Petersen, E. E., & Finnveden, G. (2014). Lessons learned – Review of LCAs for ICT products and services. *Computers in Industry*, 65(2), 211–234.
- Castro, G. D., Fernández, M. C., & Colso, Á. U. (2021). Unleashing the convergence amid digitalization and sustainability towards pursuing the Sustainable Development Goals (SDGs): A holistic review. *Journal of Cleaner Production*, 280, 1–40.
- Chen, X., Despeisse, M., & Johansson, B. (2020). Environmental sustainability of digitalization in manufacturing: A review. *Sustainability*, 12(24), 10298.
- George, G., Merrill, R. K., & Schillebeeckx, S. J. D. (2021). Digital sustainability and entrepreneurship: How digital innovations are helping tackle climate change and sustainable development. *Entrepreneurship Theory and Practice*, 45(5), 999–1027.
- Gouvea, R., Kapelianis, D., & Kasscieh, S. (2017). Assessing the nexus of sustainability and information & communications technology. *Technological Forecasting and Social Change*, 130, 39–44.



- IATA. (2019). FRED+. [Online]. Available at: <https://www.iata.org/en/programs/environment/fred/#tab-1>. Accessed 2 Oct 2021.
- IPCC. (2018). *Global warming of 1.5°C*. s.l.
- Klymenko, O., Halse, L. L., Jæger, B., & Nerger, A. J. (2019). Digitalization and environmental sustainability: What are the opportunities? In *26th EurOMA conference – Operations adding value to society* (pp. 3880–3889).
- Kovynyov, I., & Mikut, R. (2019). Digital technologies in airport ground operations. *Netnomics*, 20, 1–30.
- Kuisma, N. (2017). *Digitalization and its impact on commercial aviation*. Aalto University School of Business.
- Lange, S., Pohl, J., & Santarius, T. (2020). Digitalization and energy consumption. Does ICT reduce energy demand? *Ecological Economics*, 176, 106760.
- Little, A. D. (2018). *Airport digital transformation, from operational performance to strategic opportunity*. Amadeus.
- Meré, J. O., Remón, T. P., & Rubio, J. (2020). Digitalization: An opportunity for contributing to sustainability from knowledge creation. *Sustainability*, 12(1460), 1–21.
- Pohl, J. (2017). Digitalisation for sustainability? Challenges in environmental assessment of digital services. In *Informatik 2017 Conference*.
- SESAR. (2020). *Environment assessment process*. SESAR.
- Sparviero, S., & Ragnedda, M. (2021). Towards digital sustainability: The long journey to the sustainable development goals 2030. *Digital Policy, Regulation and Governance*, 23(3), 216–228.
- The World in 2050. (2019). *The digital revolution and sustainable development: Opportunities and challenges. Report prepared by The World in 2050 initiative*. International Institute for Applied Systems Analysis, IIASA.
- WEF. (2017). *Digital transformation initiative aviation, travel and tourism industry*. World Economic Forum.
- Wu, S. J., & Raghupathi, W. (2018). The strategic association between information and communication technologies and sustainability: A country-level study. In *Sustainable development: Concepts, methodologies, tools, and applications* (pp. 694–719). IGI Global.
- Zaharia, S. E., & Pietreanu, C. V. (2018). Challenges in airport digital transformation. *Transportation Research Procedia*, 35, 90–99.

# Effect of Phase Change Material Dimension on Maximum Temperature of a Lithium-Ion Battery



Uğur Morali

## Nomenclature

NTGK Newman, Tiedemann, Gu, and Kim

PCM Phase change material

## 1 Introduction

Lithium-ion batteries have been used more and more frequently in mobile applications, especially in electric vehicles, in recent years (Swornowski, 2017). Lithium-ion batteries have been used in aviation, thanks to their high energy density and high power density (Panchal et al., 2016). On the other hand, the incidents concerning overheating under high-rate discharge conditions restrict their use. Battery manufacturers suggest a temperature range to be used the lithium-ion batteries safely. The suggested temperature range is generally between  $-15$  and  $40$  °C (Choudhari et al., 2020). The temperature of lithium-ion batteries needs to be controlled, especially during operation in extreme conditions, to obtain maximum performance from lithium-ion batteries.

In the literature, there have been various studies performed to control battery temperature. In (Wang et al., 2018), the effect of phase change storage energy unit casing, the thermal conductivity of the composite phase change material (PCM), geometric parameters, discharge/charge rate, and ambient temperature on the battery temperature were investigated. Results indicated that the PCM cooled system could maintain the battery temperature at  $42$  °C for the lithium-ion battery discharged at

---

U. Morali (✉)

Department of Chemical Engineering, Eskisehir Osmangazi University, Eskisehir, Türkiye

e-mail: [umorali@ogu.edu.tr](mailto:umorali@ogu.edu.tr)

4C-rate. In (Weng et al., 2019), the performance of the PCM cooling system was examined under different operation parameters, including PCM thickness, PCM temperature, and laying aside time. The optimum thickness of PCM was determined to be 10 mm. Moreover, the authors noted that one should be considered the lower heat dissipation observed at the bottom of the battery. In (Jilte et al., 2019), a modified cooling system was proposed to control the temperature of each battery in the module. The sufficient PCM thickness was found to be 4 mm. The results showed that the modified cooling system could be used to control the temperature of each battery cell in the module.

Battery thermal models provide valuable information in analyzing battery temperature. Thus, their uses in simulations not only provide a cost-effective approach but also ensure reliable data without dangerous experimentation. Therefore, in this study, the multi-scale multidimensional NTGK model was applied to simulate the maximum battery temperature. A PCM cooled thermal management system for a single lithium-ion battery was proposed. The effect of the PCM dimension on the cooling system performance was investigated for the battery discharged at 3C-rate.

## 2 Method

Maximum temperature of a prismatic lithium-ion battery was simulated by using the NTGK model. The battery was discharged from 4.30 to 3.00 V at 3C-rate. The temperature of the battery and PCM was assumed to be equal to the ambient temperature of 300 K at the initial stage of simulation. The convective heat transfer coefficient of the battery was accepted as  $5 \text{ W m}^{-2} \text{ K}^{-1}$ . Thermophysical properties of phase change material was obtained from (Choudhari et al., 2020). Density, heat capacity, and thermal conductivity of the PCM were  $820 \text{ kg m}^{-3}$ ,  $2000 \text{ J kg}^{-1} \text{ K}^{-1}$ , and  $0.2 \text{ W m}^{-1} \text{ K}^{-1}$ , respectively. Melting heat and dynamic viscosity of the PCM were  $165,000 \text{ J kg}^{-1}$  and  $0.02 \text{ kg m}^{-1} \text{ s}^{-1}$ . Solidus and liquidus temperatures are 311.15 K and 316.15 K, respectively. PCM was assumed to exhibit adiabatic boundary conditions.

ANSYS Fluent Workbench was used to perform simulation. Geometry was edited in DesignModeler. Battery geometry with two different PCM cooling designs is presented in Fig. 1. The width of PCM was 10 mm and 40 mm for the PCM cooled battery system presented in Fig. 1a, b respectively.

## 3 Results and Discussion

Maximum battery temperatures are shown in Fig. 2. The highest maximum battery temperature was obtained for the battery cooled by 10 mm PCM and was 310.9477 K. On the other hand, the single battery discharged at 3C-rate exhibited the lowest maximum battery temperature (309,2439 K). The maximum battery

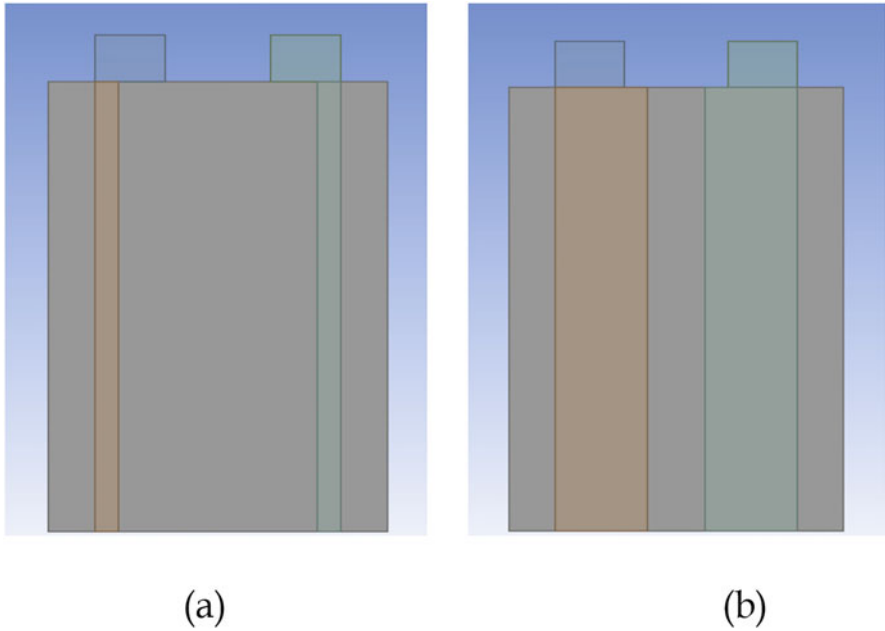


Fig. 1 Geometry of PCM cooled battery: (a) 10-mm-width PCM, (b) 40-mm-width PCM

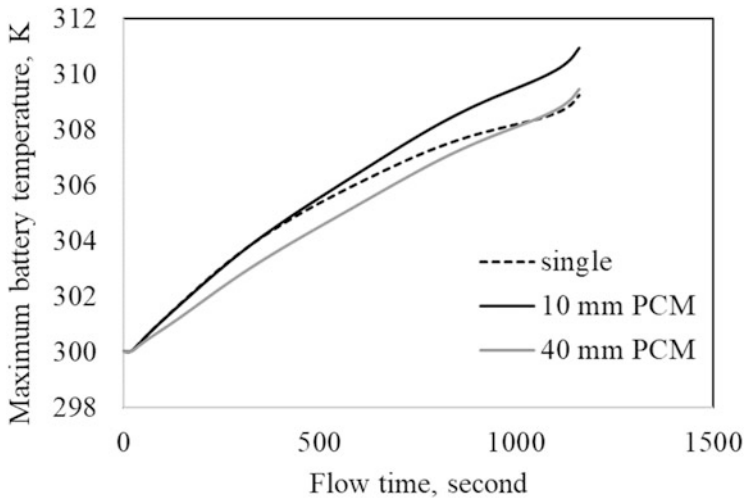
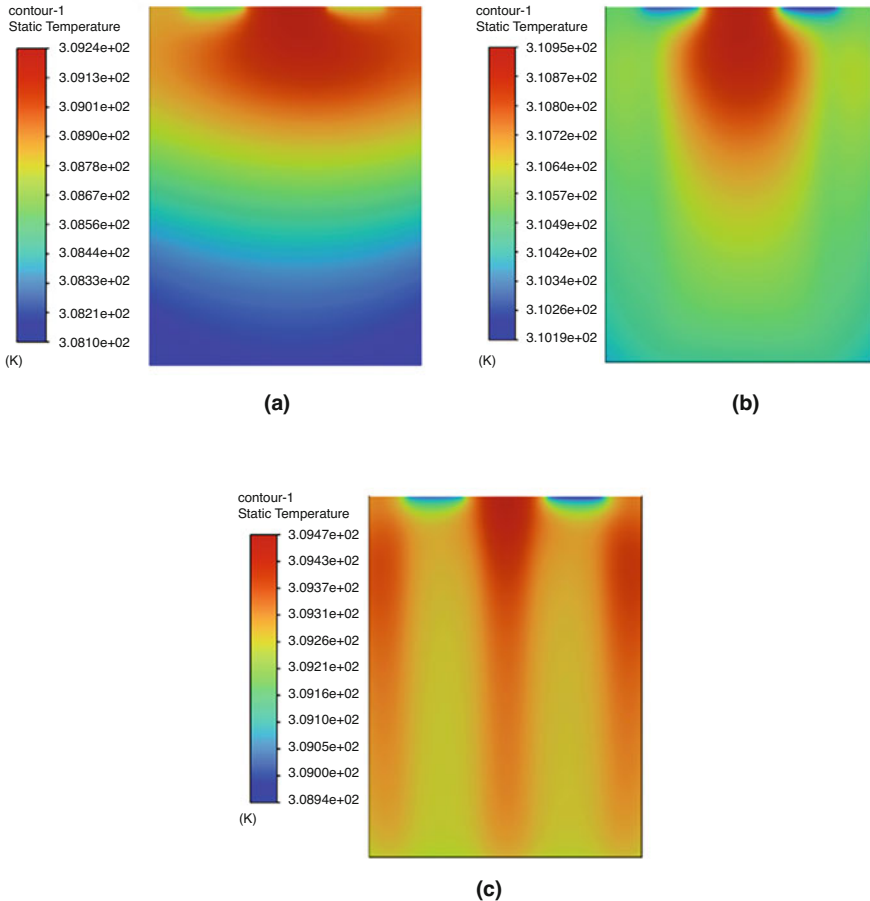


Fig. 2 Maximum battery temperature at 3C-rate with and without PCM

temperature of the battery cooled with 40 mm PCM (309,4706 K) was slightly higher than the single battery. However, the point to be noted here is that the maximum battery temperature of the single battery is higher than the battery cooled



**Fig. 3** Temperature counters for static temperature at 3C-rate: (a) without PCM, (b) with 10-mm-width PCM, (c) with 40-mm-width PCM

by 40 mm PCM, except after the 1000th second of the flow time. This can be attributed to the lower heat transfer from the battery to the PCM (40 mm) than the heat transferred from the single battery surface to the surrounding air when the flow time is greater than 1000 seconds. Another reason can be the adiabatic heat transfer condition of PCM. In other words, the heat transferred from the battery to the PCM was absorbed by PCM and not transferred from PCM to the surrounding air. Thus, the maximum battery temperature of the single battery could be lower than the PCM cooled batteries at the end of discharge operation.

Another performance parameter of a battery cooling system to be considered was the heat dissipation throughout the battery. Figure 3 shows the temperature counters for the static temperature. Figure 3a indicated that the single battery exhibited a heterogeneous temperature distribution. The higher battery temperatures were

observed in the upper center of the battery. On the other hand, the lower temperatures were observed at the bottom of the battery. Furthermore, the wall temperature adjacent to the tab zones showed moderate temperatures. It is important to note that heterogeneous temperature distribution affects the battery performance adversely. Figure 3b displayed the temperature distribution of 10 mm PCM cooled battery. The lowest temperatures for 10 mm PCM cooled battery was observed at the edge locations. Similarly, the highest temperatures were obtained in the upper center of the battery. However, the temperature distribution of the 10 mm PCM cooled battery was more homogeneous compared to the single battery. The 40 mm PCM cooled battery exhibited a more uniform temperature distribution compared to others. The higher temperatures were observed near the PCM, as shown in Fig. 3c. Similarly, the edges near the tab zones exhibited lower temperatures.

## 4 Conclusion

The effect of phase change material dimension on maximum battery temperature was investigated in this study. The single battery exhibited the lowest maximum battery temperature compared to the PCM cooled batteries. The 40 mm PCM cooled battery showed lower maximum battery temperatures than the single battery up to 1000 seconds. The 40 mm PCM cooled battery showed a more uniform temperature distribution throughout the battery compared to the 10 mm PCM cooled battery and the single battery. From maximum battery temperature and temperature distribution perspectives, the 40 mm PCM cooled battery showed better cooling performance owing to its low maximum battery temperature and more uniform temperature distribution.

## References

- Choudhari, V., Dhoble, A., & Panchal, S. (2020). Numerical analysis of different Fin structures in phase change material module for battery thermal management system and its optimization. *International Journal of Heat and Mass Transfer*, *163*, 120434.
- Jilte, R. D., Kumar, R., Ahmadi, M. H., & Chen, L. (2019). Battery thermal management system employing phase change material with cell-to-cell air cooling. *Applied Thermal Engineering*, *161*, 114199.
- Panchal, S., Dincer, I., Agelin-Chaab, M., Fraser, R., & Fowler, M. (2016). Thermal modeling and validation of temperature distributions in a prismatic lithium-ion battery at different discharge rates and varying boundary conditions. *Applied Thermal Engineering*, *96*, 190–199.
- Swornowski, P. J. (2017). Destruction mechanism of the internal structure in lithium-ion batteries used in aviation industry. *Energy*, *122*, 779–786.

- Wang, X., Xie, Y., Day, R., Wu, H., Hu, Z., Zhu, J., & Wen, D. (2018). Performance analysis of a novel thermal management system with composite phase change material for a lithium-ion battery pack. *Energy*, *156*, 154–168.
- Weng, J., Yang, X., Zhang, G., Ouyang, D., Chen, M., & Wang, J. (2019). Optimization of the detailed factors in a phase-change-material module for battery thermal management. *International Journal of Heat and Mass Transfer*, *138*, 126–134.

# Global, Regional, and Local Issues of ICAO Balanced Approach to Aircraft Noise Management in Airports



Oleksandr Zaporozhets

## Nomenclature

BA	Balanced Approach
ICAO	International Civil Aviation Organization
NAP	Noise Abatement Procedures
NPZ	Noise Protection Zones

## 1 Introduction

Noise has always been a major environmental issue in the field of aviation, primarily affecting residential communities close to airports. It still is the most significant local environmental impact associated with aircraft operation (ICAO Resolution A40-17, 2019a, b). Aircraft noise exposes and affects communities within an airport influence area, defined by the level of noise exposure or for a specific flyby or for a specific interval (during the overall day or during mostly sensitive to noise periods) of observation. In general, aircraft noise exposure varies with the type and size of the aircraft, the power the aircraft is using at the moment, and the altitude or distance of the aircraft from the receptor. A higher distance from the source provides a lower noise exposure level; this is an essential condition for all noise protection programs. To minimize aircraft noise problems through preventive measures, ICAO policy, first of all, recommends locating the new airports at an appropriate place, such as away from noise-sensitive areas. But each airport requires its own solutions based on its specific characteristics, as in noise hazard generation and propagation effects, as

---

O. Zaporozhets (✉)  
National Aviation University, Kyiv, Ukraine  
e-mail: [zap@nau.edu.ua](mailto:zap@nau.edu.ua)





**Fig. 1** Example of noise contours for NPZ at Kyiv/Zhuliany International Airport – Kyiv, Ukraine: red contour, 85 dBA  $L_{Amax}$ ; yellow contour, 80 dBA  $L_{Amax}$ ; pink boarded zones, residential areas of the Kyiv city

well as in noise exposure influence on all elements at risk with their vulnerability and coping capacity performances (Zaporozhets & Blyukher, 2019). The circumstances of each airport vary significantly between themselves, so an effective operational procedure or even mitigation measure at one airport may not be appropriate (or even feasible) at another.

Airports are usually located within or close to the limits of large urban areas (Fig. 1); in better case, a distance to existing noise-sensitive land usage (residential or recreational) may provide human protection from noise exposure and minimise the adverse impacts of their operations. The overlap of urban areas within the noise protection zones (NPZ) around aerodrome (as shown in Fig. 1, especially on the east from the runway) may exist, and in such a case, it indicates that a population inside the zones is exposed and vulnerable and even impacted (at least annoyed) by noise and needs additional protection (due to noise insulation schemes, etc.).

## 2 General Considerations on Noise Management

The national legal system declares the noise limits (standard values for noise in the environment) usually in practice, which are prohibited for overloading inside the area of any human activity – especially inside residential and rehabilitation areas. Somewhere, particularly in Ukraine, there are few criteria used for environmental noise assessment and management, emphasizing that noise may impact the population in a few ways, including the effects during long-term and short-term exposures. Particularly for aviation noise, short-term exposure is important in the case of a contribution of the noisiest flight events to overall exposure and especially in conditions of quite small flight intensity, which are observed in regional airports at

the first stage of their development. For them, the noise contours for a single flight event, defined for maximum sound level  $L_{Amax}$ , are larger in size (area also) in comparison with equivalent sound levels  $L_{Aeq}$ .

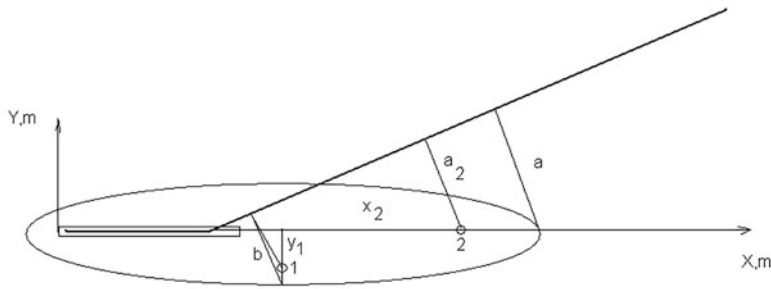
### 3 Balanced Approach to Aircraft Noise Management

In 2001, the 33rd Session of the ICAO Assembly adopted a new policy for aircraft noise control globally, referred to as the “balanced approach” (BA) to noise management. The ICAO BA guidance (ICAO Document 9829, 2004) contains the explanation of all elements in general details, namely: reduction of aircraft noise at source – manufacturing quieter aircraft in accordance with ICAO standard requirements; noise zoning, land-use planning, and management; noise abatement procedures for aircraft operation; and usually partial restrictions for noisy aircraft operation. The goal also is to identify the noise-related measures that achieve the maximum environmental benefit (minimum environmental risk), using objective and measurable criteria, at any specific airport most cost-effectively. If the main goal in aircraft noise control is to reduce the noise level at the source of its generation, the main goal for noise zoning and land-use management is to prevent people from levels that are inconsistent with their health and welfare.

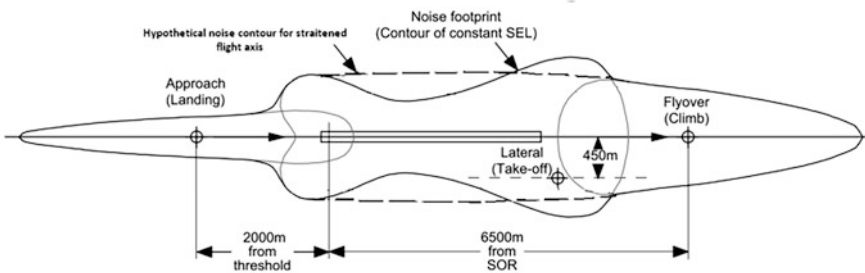
#### 3.1 ICAO Standard Requirements to Aircraft Noise and Management of Noise Exposure Around the Airports

The area and sizes of noise zones are the subjects of aircraft noise calculation (ICAO 9829, 2004). To imagine the sizes of noise zones around the aerodrome (or separately for the runway), a simple approach may be proposed (Zaporozhets et al., 2011; Zaporozhets & Levchenko, 2021) – to consider the noise contours as a result of the intersection of the cylindrical surface of equal sound level (equal to the limit used for the noise zoning board) with the ground surface around the aerodrome and flight paths. It was shown that this simplified contour will be an ellipse, whose small radius is equal to the noise radius  $R_N$  and whose big radius is equal to the  $R_N/\sin\gamma$  for the aircraft type under consideration at this flight mode, where  $\gamma$  is an angle of climbing/descending, depending on the character flight stage (Fig. 2a).

The main simplification in the concept of noise radius  $R_N$  (its concept is fully described in (Zaporozhets et al., 2011; Zaporozhets & Levchenko, 2021)) is that it is considered as constant, at least during the definitive for noise contour assessment flight stages of the aircraft. The results of numerous researches show that  $R_N$  is varying all the time, it is mostly dependent on engine operation mode (engine power) and noise level (type and value) to be considered, but a number of operational factors is also influencing the value of noise radius and its derivatives (Zaporozhets & Levchenko, 2021).



a)



b)

**Fig. 2** A simplified form of noise footprint having the shape of an ellipse under the takeoff flight path: (a) simplified contour will be an ellipse (Zaporozhets et al., 2011); (b) transformation of INM contours into ellipse

The most sensitive violation of the simplification of the concepts of constant noise radius and ellipse for the noise contour occurs at the point of intersection of the segments of the flight path of the altitude, which changes the mode of operation of engines (it corresponds to a distance of  $\sim 4$  km usually, Fig. 2b). But, in general, the error (inaccuracy) of these changes does not seem significant in strategic assessments and decisions. A more significant impact on the assessment should be expected from a further reduction in noise levels at the source, when the sound levels at the control points and for the noise contours with the normative value of the sound level (e.g. 75 dBA  $L_{Amax\ night}$ ) will not be displayed on the airport noise map. Particularly for the airplanes with noise performances in accordance with the requirements of FAR 36 stages 3–5 – the dimensions/areas of the contours for departure flight are within 10% of the accuracy of INM data (or ANP database) (Fig. 3).

During the 50 years of aircraft noise standardization from ICAO (1st Edition of Annex 16 – Aircraft Noise was published in 1969) and continuous strengthening of

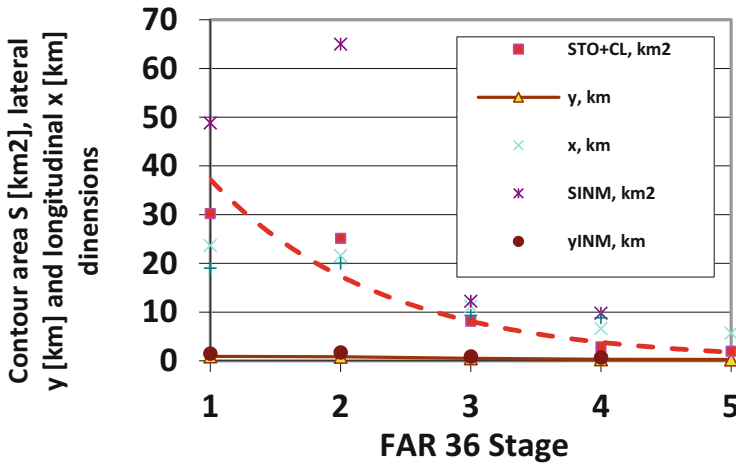


**Fig. 3** Comparison between the dimensions and area for noise contour 75 dBA  $L_{A_{max}}$  defined simplified model and INM for Boeing-737 at departure with noise performances in accordance with FAR-36 requirements (from B737-100 for stage 1 till Boeing-737MAX for stage 5)

the requirements from Chapter 2–14, the cumulative reduction was gained up to ~35 dB; close to this value is necessary to be reached till the aircraft noise goal at 2050 (ICAO Document 10127, 2019).

### 3.2 Land-Use Planning

The need for land-use planning in the vicinity of an airport was recognized in the early history of civil aviation and focused on the use and control of land. The manual (ICAO Document 9184, 2018) is focused on land-use and environmental management on and around an airport. Airport operators can reduce the environmental impacts – noise, air emission/pollution, and safety issues of their operations by incorporating environmental management plans and procedures with land-use compatibility planning with a broad appreciation of their relative sensitivity of the population to the aircraft operational safety, local third-party risk, and noise exposure. Among land-use planning measures, noise zoning around airports is the primary, main, and mostly effective to be protected from noise exposure (Fig. 4). But compatible land-use planning and management should be based on appropriate *forecasted* aircraft noise contours, rather than *current* contours, which must prevent encroachment of residential development at airports where future aircraft noise levels are projected to increase.

The control measures may be divided into three categories, as follows: planning instruments, mitigating instruments, and financial instruments. There are only some examples of these instruments listed in Fig. 4. Noise zoning is a core regulation in

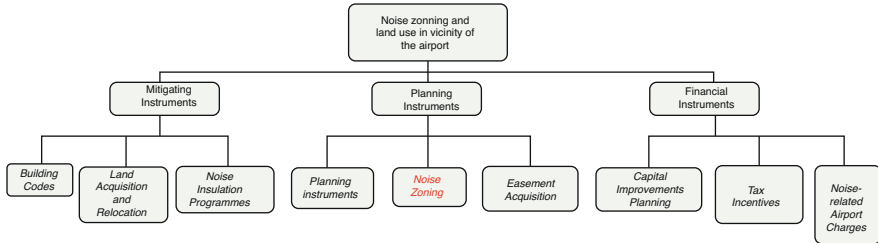


**Fig. 4** Noise zoning and land usage instruments in airport environment

noise exposure/impact management on population and should specify land development depending on the level of noise exposure and use restrictions, based on certain noise levels – the limits, which are incompatible with human activities inside the zones. Some of the airports due to their specific place in air transportation system of the state (or inside the region) may use/implement different from the state rules noise limits, which may or mitigate or allow a specific land usage inside the zone. Noise monitoring systems (Chyla et al., 2020) are the instrument for objective noise exposure assessment of the air traffic inside the specific zone (where a noise monitor is installed) or to be used for assessing the efficiency of any implemented noise protection measure.

### 3.3 *Noise Abatement Procedures and Aircraft Operating Restrictions*

Operational low-noise procedures are intended for use by aircraft of the existing fleet and have the potential to make an immediate improvement in the environmental impact of aviation, as a rule locally emphasized at airports where the noise zoning and land-use procedures are realized with omissions (ICAO Document 8168, 2020; ICAO Document 9888, 2007). Operational NAPs in use today can be categorized into three broad components: noise abatement flight procedures, spatial management, and ground movement management. Any progress in designing low-noise aircraft would therefore relax the stringency of the NAP to be used (Zaporozhets & Blyukher, 2019).

## 4 Results and Discussion

Brief analysis of all the elements of ICAO BA shows that ICAO noise standards accompanied by technological improvements in aircraft noise performances provide a reduction of aircraft noise exposure globally, at least for international air

transportation. The second BA element – noise zoning and land usage – is mostly a subject of regional/national noise exposure management, predefined by regional (like Directive inside EU) or/and national rules.

Numerous violations of noise limits may be observed inside the zones in the vicinity of the airport: for their control, a third element is included – the NAPs. Airport and airline authorities must find the best solution to what kind of NAP will be most efficient in any specific case. There is a subject for local consideration. Flight restrictions are mostly the subjects of local decisions and only in cases if the efficiency of the first three BA elements is insufficient. There are also a number of regional and global restriction that exist – they are effective for all airports if implemented for the whole (national, regional, or global) system at the same time.

Besides the technical elements, which are based on noise intensity metrics completely, the noise annoyance (and other types of outcomes of aircraft noise exposure to neighbouring residents) must now be addressed. This evolution may lead to a new vision of the balanced approach to aircraft noise control in very near future. Up to now, annoyance was mainly explained through acoustical factors like sound intensity, peak levels, duration of time in-between sound events, and number of events (Janssen et al., 2011). The non-acoustical factors (“moderators” and/or “modifiers” of the effect) have still received empirical attention but without a deep theoretical approach, despite the fact that various comparative studies reveal that they play a major role in defining the impact on people (Job RFS, 1988). Addressing such human-centric concerns, encompassing fear, negative health effects, and other environmental issues may lead to adding a fifth element to the ICAO BA to aircraft noise management around the airports (Zaporozhets & Blyukher, 2019).

## References

- Chyla, A., et al. (2020). Portable and continuous aircraft noise measurements in vicinity of airports // Systemy s SrodkiTransportu. Bezpieczenstwo I MaterialyEkspluatacyjne. Red. Naukowa Leida K., Wos P. Monografia, WydawnictwoPolitechniliRzeszowskiej, Rzeszow. pp. 69–80.
- ICAO Document 10127. (2019). *Final report of the independent expert integrated technology goals assessment and review for engines and aircraft*. ICAO, Montreal.
- ICAO Document 8168. (2020). *Aircraft Operations (PANS OPS) volume I flight procedures* (6th ed., p. 214). ICAO, Montreal.
- ICAO Document 9184. (2018). *Airport planning manual, part 2 — Land use and environmental control.Doc 9184 - part 2* (4th ed., p. 124). ICAO, Montreal.
- ICAO Document 9829. (2004). *Guidance on the balanced approach to aircraft noise management. Doc 9829, AN/451*. ICAO, Montreal.
- ICAO Document 9888. (2007). *Review of noise abatement procedure research & development and implementation results*. ICAO, Montreal.
- ICAO Resolution A40-17. (2019a). 2019 to the convention on International Civil Aviation — environmental protection: Volume I — aircraft noise; Volume II — aircraft engine emissions; Volume III — aeroplane CO2 emissions; Volume IV — Carbon Offsetting and Reduction Scheme for International Aviation (CORSA), 2019.
- ICAO Resolution A40-17. (2019b). *Consolidated statement of continuing ICAO policies and practices related to environmental protection – General provisions, noise and local air quality*.

- Janssen, S. A., Vos, H., van Kempen, E. E., Breugelmans, O. R., & Miedema, H. M. (2011). Trends in aircraft noise annoyance: The role of study and sample characteristics. *The Journal of the Acoustical Society of America*, *129*(4), 1953.
- Job, R. F. S. (1988). Community response to noise: A review of factors influencing the relationship between noise exposure and reaction. *The Journal of the Acoustical Society of America*, *83*, 991–1001.
- Zaporozhets, O., & Blyukher, B. (2019). Risk methodology to assess and control aircraft noise impact in vicinity of the airports. In T. H. Karakoc, C. O. Colpan, O. Altuntas, & Y. Sohret (Eds.), *Sustainable aviation* (pp. 37–79). Springer International Publishing, Springer Nature Switzerland AG. Print ISBN: 978-3-030-14194-3. [https://doi.org/10.1007/978-3-030-14195-0\\_3](https://doi.org/10.1007/978-3-030-14195-0_3)
- Zaporozhets, O., & Levchenko, L. (2021). Accuracy of noise-power-distance definition on results of single aircraft noise event calculation. *Aerospace*, *8*(5), 121. <https://doi.org/10.3390/aerospace8050121>
- Zaporozhets, O., Tokarev, V., & Attenborough, K. (2011). *Aircraft noise: Assessment, prediction and control*. Glyph International, Taylor & Francis.

# Fuel Consumption Analysis of Gradual Climb Procedure with Varied Climb Angle and Airspeed



Siripong Atipan  and Pawarej Chomdej

## Nomenclature

$CD_0$	Zero lift drag coefficient
$CD_2$	Induced drag factor
$C_{f1}$	1st thrust specific fuel consumption coefficient
$C_{f2}$	2nd thrust specific fuel consumption coefficient
$F_{nom}$	Nominal fuel flow [kg/min]
$g$	Gravitational acceleration [ $m/s^2$ ]
$m$	Aircraft mass [kg]
THR	Thrust [N]
VTAS	True airspeed [m/s] or [knots]
$\gamma$	Angle of climb [rad] or [deg]
$\eta$	Thrust specific fuel flow [kg/(min·kN)]
$\rho$	Air density [ $kg/m^3$ ]

## 1 Introduction

Climate change becomes a very serious issue today as it has vast and strong impact on humanity securities. One of the major causes of this problem is  $CO_2$  emission which largely produced from global aviation industry. To contribute on this concern, IATA issued a guidance material and best practices for fuel and environmental management (IATA, 2008) and issued a guidance material for sustainable aviation fuel management (IATA, 2015). A variety flight operation techniques for emission

---

S. Atipan (✉) · P. Chomdej  
Faculty of Engineering, Kasetsart University, Bangkok, Thailand  
e-mail: [siripong.a@ku.ac.th](mailto:siripong.a@ku.ac.th); [fengpac@ku.ac.th](mailto:fengpac@ku.ac.th)



reduction were suggested such as engine out taxi, reduced takeoff flaps, reduced landing flaps, reduced acceleration altitude, optimum CG position, and continuous climb and continuous descent operation known as CCO and CDO.

For the past decades, there have been many researchers working and focusing on emission reduction during climbing and descending phases. Panklam and Kowanichkul (2011) performed flight simulation with RAMS PLUS software for A320 and B737 descending flights. It was found that with continuous descent operations, fuel consumption could be reduced 15.8% for A320 and 14.8% for B737 when descending from FL350. Ming et al. (2019) studied on fuel consumption of climbing phase of A320 aircraft based on flight data analysis. The continuous climb operation was simulated to climb from sea level to FL240 at standard temperature and with constant angle of climb. The results were compared with the flight of conventional climb procedure and show obviously that continuous climb operations provide fuel consumption reduction by 12.3%. Mori (2020) proposed a new fuel-saving climb procedure by reducing thrust near top of climb. 20–50 lbs of fuel could be saved for a large jet airliner.

## 2 Fuel Consumption Model

### 2.1 BADA Model

The calculation of fuel consumption and flight trajectory prediction in this study is based on the BADA aircraft performance model revision 3.8 (EUROCONTROL, 2010). The aircraft aerodynamics and fuel consumption model in the climbing phase are expressed as follows:

Total energy model

$$(T_{HR} - D)V_{TAS} = mg \frac{dh}{dt} + mV_{TAS} \frac{dV_{TAS}}{dt} \quad (1)$$

Rate of climb

$$ROC = \frac{dh}{dt} = V_{TAS} \cdot \sin(\gamma) \quad (2)$$

Angle of climb

$$AOC = \gamma = \sin^{-1} \left( \frac{T_{HR} - D - mV_{TAS} \frac{dV_{TAS}}{dt}}{mg} \right) \quad (3)$$

Lift coefficient

$$C_L = \frac{2mg}{\rho V_{TAS}^2 S \cdot \cos(\gamma)} \quad (4)$$

Drag coefficient

$$C_D = C_{D0} + C_{D2} \times (C_L)^2 \quad (5)$$

True airspeed (m/s)

$$V_{TAS} = \sqrt{\frac{2mg}{C_L \rho S \cdot \cos(\gamma)}} \quad (6)$$

Thrust specific fuel flow (kg/(min·kN))

$$\eta = C_{f1} \times \left(1 + \frac{V_{TAS}}{C_{f2}}\right) \quad (7)$$

Nominal fuel flow (kg/min)

$$f_{nom} = \eta \times T_{HR} \quad (8)$$

Cruise fuel flow (kg/min)

$$f_{cr} = \eta \times T_{HR} \times C_{fcr} \quad (9)$$

## 2.2 Optimization and Numerical Models

The optimal true airspeed for gradual climb flight that varied with altitudes can be calculated from the lift coefficient which is determined from the optimization models (Anderson, 2014). The models are expressed as follows:

Lift coefficient for minimum thrust required

$$C_{L_{TR, \min}} = \sqrt{\frac{C_{D0}}{C_{D2}}} \quad (10)$$

Lift coefficient for best range (jet propelled airplane)

$$CL_{R, \max} = \sqrt{\frac{C_{D0}}{3C_{D2}}} \tag{11}$$

The numerical model is formed for estimation of the acceleration of the aircraft and is given as follow:

$$\frac{dV_{TAS}}{dt} \approx ROC \times \frac{\Delta V_{TAS}}{\Delta h} \tag{12}$$

### 2.3 Flight Simulation

In this study, climbing flights of three different cases were generated. These are continuous climb with constant angle of climb (CCO), gradual climb with minimum thrust required airspeed (GCO1), and gradual climb with best range airspeed (GCO2). All flights were simulated for A320 aircraft climbing from sea level to 24,000 ft. under the international standard atmosphere condition and at MTOW of 77,000 kg and then cruising to reach the distance of 120 km.

In gradual climb simulation, two different optimal airspeeds were examined, which are minimum thrust required airspeed and best range airspeed using Eqs. 10 and 11, respectively. The acceleration is then determined using Eq. 12 for altitude step of 1000 ft. Reduced thrust is applied with gradually reduced rate of 2% per 1000 ft. At every step of altitude, the aircraft mass is recalculated for the reduction due to fuel consumption. The flight trajectories of the studied cases were predicted and as shown in Fig. 1.

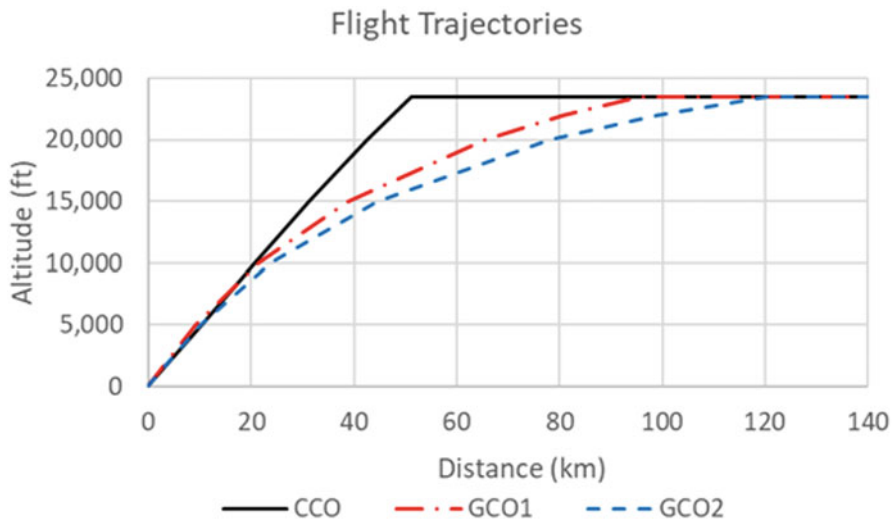


Fig. 1 Predicted flight trajectories of the tested cases, CCO, GCO1, and GCO2

**Table 1** Validation of the calculation model used in this study

Model	Climb distance (km)	Cruise distance (km)	Total fuel consumption (kg)
Present calculation model	53.2	66.8	1084.9
Ming et al. (2019)	51.0	69.0	1116.0

**Table 2** Fuel consumption of climbing phases, continuous climb (CCO), gradual climb with minimum thrust required airspeed (GCO1), and gradual climb with best range airspeed (GCO2)

Trajectories	Climb distance (km)	Fuel during climb (kg)	Cruise distance (km)	Fuel during cruise (kg)	Total fuel consumption (kg)
CCO	53.2	740.5	66.8	344.4	1084.9
GCO1	95.4	695.5	24.6	332.7	1028.2
GCO2	120.2	993.4	–	–	993.4

The fuel consumption model was validated with the calculation and the data analysis of Ming et al. (2019) for the case of continuous climb with constant angle of climb of 8 deg. The comparisons are shown in Table 1. The results of the present calculation model agree well with the reference model which has accuracy falling into 97.2%.

### 3 Results and Discussion

The calculation model for the flight trajectories of CCO, GCO1, and GCO2 was simulated and executed with a PC to give the climb distance, cruise distance, fuel flows during climb and cruise, and the total fuel consumption. The results are presented in Table 2.

The results in Table 2 show obviously that with gradual climb procedure, the fuel consumption is reduced when compared to the continuous climb procedure. The reduction of fuel consumption of GCO1 flight trajectory is 56.9 kg or 5.24%, while GCO2 flight trajectory provides even more fuel reduction of 91.5 kg or 8.43%. This agrees well with the works of Mori (2020).

### 4 Conclusion

The study of fuel consumption of aircraft flight with gradual climb procedure showed that the gradual climb procedure can improve fuel consumption up to 8.43%. To maximize fuel-saving, climbing with best range true airspeed is suggested. However, this suggestion should be further studied deeply to confirm the solutions. Actually, the optimization of the fuel consumption with gradual climb

procedure is challenging as the fuel consumption of the climbing flight still has various variables to play with such as true airspeed, acceleration, angle of climb, and thrust of the aircraft, which can be written as in Eq. 13.

$$f_{\text{nom}} = f\left(T_{\text{HR}}, \gamma, V_{\text{TAS}}, \frac{dV_{\text{TAS}}}{dt}\right) \quad (13)$$

There are still a lot of works that can be done further on the development on the optimization with these variables.

## References

- Anderson, J. D. (2014). *Introduction to flight* (8th ed.). McGraw Hill.
- EUROCONTROL. (2010). User Manual for Base of Aircraft Data (BADA) Revision 3.8. 2010; EEC Technical/Scientific Report No. 2010-003; Eurocontrol Experimental Centre; Les Bordes, France.
- IATA. (2008). *Guidance material and best practices for fuel and environmental management* (3rd ed.). International Air Transport Association.
- IATA. (2015). *Guidance material for sustainable aviation fuel management* (2nd ed.). International Air Transport Association.
- Mori, R. (2020). Fuel-saving climb procedure by reduced thrust near top of climb. *Journal of Aircraft*, 57(5), 1.
- Ming, Z., Qianwen, H., Sihan, L., & Yu, Z. (2019). Fuel consumption model of the climbing phase of departure aircraft based on flight data analysis. *Sustainability*, 11, 4362. <https://doi.org/10.3390/su11164362>
- Panklam, P., & Kowanichkul, L. (2011). *Fuel consumption calculation of flight procedures and time saving analysis*. B.Sci. in Aviation Technology Thesis, Faculty of Engineering, Kasetsart University.

# Investigation of Turbofan Engine Emissions at Different Cruise Conditions for Greener Flights



Ali Dinc, Ibrahim Elbadawy, Mohamed Fayed, Kaushik Nag, Rani Taher, and Yousef Gharbia

## Nomenclature

CO	Carbon monoxide
CO <sub>2</sub>	Carbon dioxide
EI	Emission index
GHG	Greenhouse gases
GWP	Global warming potential
H <sub>2</sub> O	Water vapor
HC	Unburned hydrocarbons
$m_f$	Fuel mass flow rate
NO <sub>x</sub>	Nitrogen oxides
SE	Specific endurance
SR	Specific range
$V$	Flight velocity

## 1 Introduction

Aviation industry has been putting extensive research and development efforts to implement green strategies to reduce aviation's environmental effects for a sustainable future. Global warming and climate change pose a significant threat to society (EASA, 2019). Any potential reduction in emissions with the help of technological

---

A. Dinc (✉) · I. Elbadawy · M. Fayed · K. Nag · R. Taher · Y. Gharbia  
College of Engineering and Technology, American University of the Middle East, Egaila, Kuwait  
e-mail: [Ali.Dinc@aum.edu.kw](mailto:Ali.Dinc@aum.edu.kw); [Ibrahim.Mohamed@aum.edu.kw](mailto:Ibrahim.Mohamed@aum.edu.kw);  
[Mohamed.Fayed@aum.edu.kw](mailto:Mohamed.Fayed@aum.edu.kw); [Kaushik.Nag@aum.edu.kw](mailto:Kaushik.Nag@aum.edu.kw); [Rani.Taher@aum.edu.kw](mailto:Rani.Taher@aum.edu.kw);  
[Yousef.Gharbia@aum.edu.kw](mailto:Yousef.Gharbia@aum.edu.kw)

advancements should be able to counterbalance the rise in emissions caused by the future growth of aviation in addition to today's fleet sizes. As a result, more efforts are needed to develop solutions to cut emissions down. In an integrated approach, efforts are needed from all parties including design, operation, management, etc. Consequently, many researches have focused on environment-friendly engine selection/modeling and modeling the aviation fuel burn and corresponding emissions (Schwartz & Kroo, 2009; Wasiuk et al., 2015; Dinc, 2017, 2021; Pagoni & Psarakikalouptsidi, 2017; Pawlak et al., 2018; Dinc & Elbadawy, 2020; Dinc & Gharbia, 2020).

This study focuses on predicting and finding regions of lower engine emissions in flight envelop in terms of flight speed and altitude which can be used during fleet operation for the Trent 892 turbofan engine based on ICAO ground test data and cruise flight emission predictions.

## 2 Method

### 2.1 Turbofan Engine Performance Model

For the basis of this study, a performance model was constructed for the Trent 892 turbofan engine (Meier, 2020) which was certified in 1995 with a thrust rating of 409.2 kN (92,000 lbf). Trent 892 is one of the alternative engines that power B777 commercial airplanes. For the validation of the performance model, data from literature was used at the two points as given in Table 1.

### 2.2 Engine Emissions

The sum of individual CO<sub>2</sub>, H<sub>2</sub>O, NO<sub>x</sub>, CO, and HC emissions determines the total global warming potential (GWP) value. CO<sub>2</sub> and H<sub>2</sub>O are major contributors, and the others are typically less than 1 or 2% of the total in mass. Some emission indices are directly related with fuel flow; for CO<sub>2</sub> and H<sub>2</sub>O emission, indices are 3.155

**Table 1** Validation points of Trent 892 turbofan engine performance model

Parameter	Literature data	Calculated value	Flight speed	Flight altitude	Deviation (%)
Thrust <sup>a</sup>	57,824 kN (13,000 lb)	58,975 kN	0.83 Mach	10.67 km (35,000 ft)	1.9%
Fuel flow <sup>b</sup>	0.882 kg/s (7000 lb/hr)	0.875 kg/s	0.84 Mach	11.89 km (39,000 ft)	0.8%

<sup>a</sup>Source: (Meier, 2020)

<sup>b</sup>Source: (Dubois & Paynter, 2006)

(kg/kg fuel) and 1.237 (kg/kg fuel), respectively (Kim et al., 2005). Therefore, total GWP (kg) can be determined using Eqs. 1 and 2 where  $i$  stands for the pollutant gas.

$$GWP_{total} = \Sigma GWP_i \tag{1}$$

$$GWP_i = EI_i m_f \tag{2}$$

The experimental data for Trent 892 turbofan engine is available based on sea level static tests by ICAO (ICAO, 2015). For NOx, CO, and HC emissions, the mentioned test data is given in Table 1. In order to predict cruise flight emissions, ICAO data can be used together with Boeing Fuel Flow Method2 (BFFM2). BFFM2 is used to estimate NOx, CO, and HC emissions for any given flight speed and altitude (Baughcum et al., 1996; Dubois & Paynter, 2006; Dinc, 2020).

### 3 Results and Discussion

In the first part of the study, BFFM2 was used to estimate NOx, CO, and HC emissions for an interval of 0.7–0.9 Mach and 9–13 km altitude. Figure 1 shows NOx and CO emission prediction results. HC emission is not depicted since the values were found to be zero based on ICAO data and BFFM2 calculations for this particular engine. Figure 1a illustrates that NOx emission index increases with Mach number; however, it decreases as altitude increases. Figure 1b displays that CO emission does not change with altitude and it increases in higher altitudes for the Trent 892 engine case (may not be same trend for other engines). Baseline point was selected as 0.84 Mach and 11.89 km (39,000 ft) as this point is a validation point for calculations to be compared with a reference study (Dubois & Paynter, 2006).

The second part of the study was about calculating engine performance parameters such as SFC, thrust, fuel flow, etc. This is necessary because NOx and CO emission indices given in Fig. 1 are per kg fuel and therefore fuel consumption or fuel flow values are needed to be calculated by engine performance model.

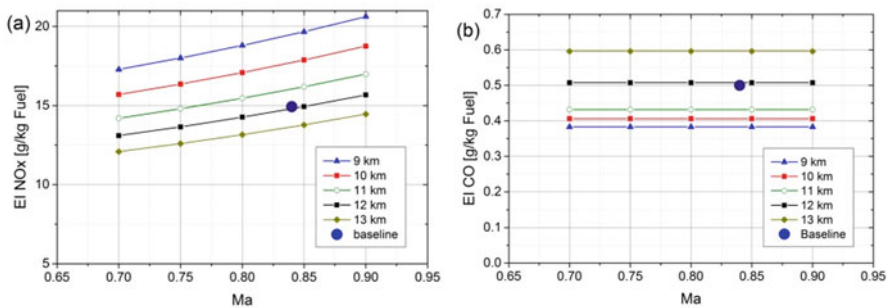


Fig. 1 (a) NOx emission index; (b) CO emission index



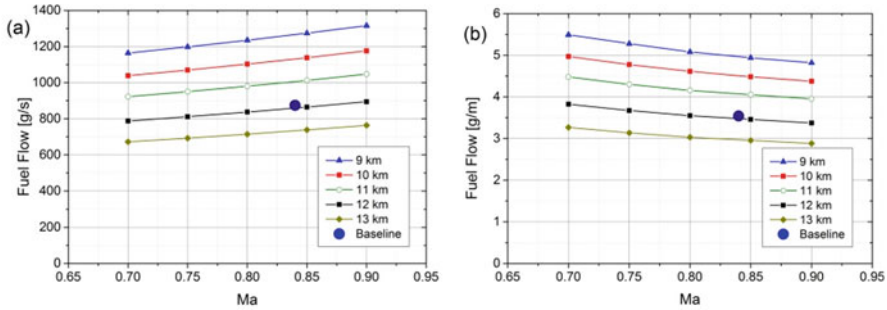


Fig. 2 (a) fuel flow per time; (b) fuel flow per distance

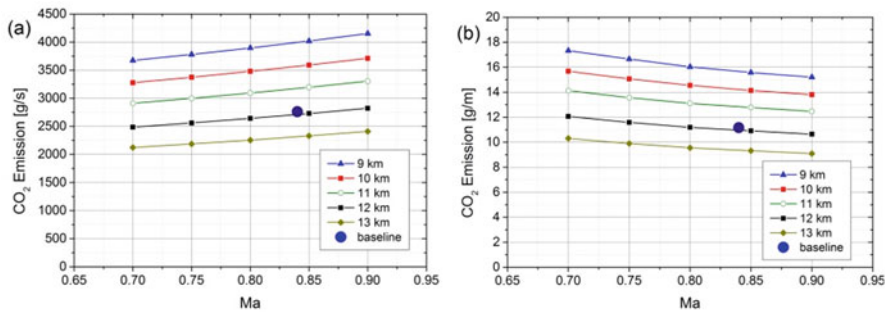


Fig. 3 (a) CO2 emission per time; (b) CO2 emission per distance

In Fig. 2 both fuel flow per time and fuel flow per distance were calculated which have the same trend for altitude. However, they have the opposite trend when it comes to flight Mach number. Fuel flow per time (Fig. 2a) is related with the endurance of aircraft which is something more desirable for a UAV during loiter or reconnaissance flight and specific endurance (endurance per unit mass of fuel) is simply the inverse of fuel flow per time. On the other hand, fuel flow per distance (Fig. 2b) is more useful for commercial airliners where a minimum amount of fuel per km or mile is wanted. Figure 3 shows CO<sub>2</sub> emissions. The trend is similar to the fuel flow which was given earlier in Fig. 2. Since the CO<sub>2</sub> and H<sub>2</sub>O emissions are directly proportional to the amount of fuel burned, there should be a minimum where the fuel flow is minimum. Therefore, minimizing fuel consumption also minimizes the CO<sub>2</sub> and H<sub>2</sub>O emissions.

Figure 4a, b shows NOx emissions calculated per time and per distance, respectively. The behavior of NOx with respect to airspeed (Mach) is somewhat different than CO<sub>2</sub> and H<sub>2</sub>O emissions where it shows slower speeds are advantageous for NOx.

Figure 5a, b illustrates total GWP emissions (sum of CO<sub>2</sub>, H<sub>2</sub>O, NOx, CO, HC) calculated per time and per distance, respectively. Due to the dominance of CO<sub>2</sub> and H<sub>2</sub>O emissions (around 99%), the general trend of total GWP emissions is similar to CO<sub>2</sub> and H<sub>2</sub>O. For maximum endurance, GWP emissions will be lower at lower speeds and higher altitudes which could be more suitable for UAV applications where maximum loiter or airborne time is required. For maximum range, GWP

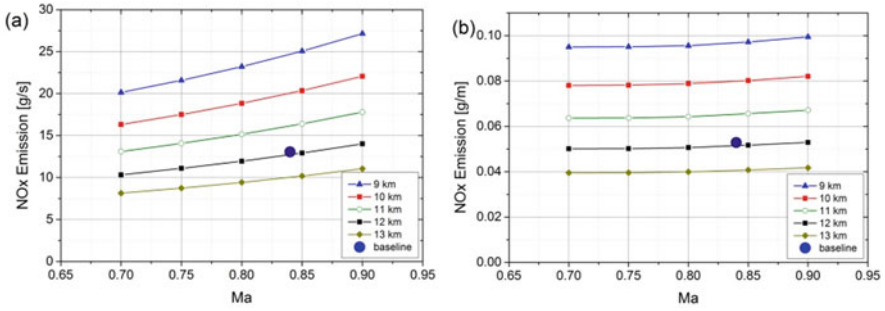


Fig. 4 (a) NOx emission per time; (b) NOx emission per distance

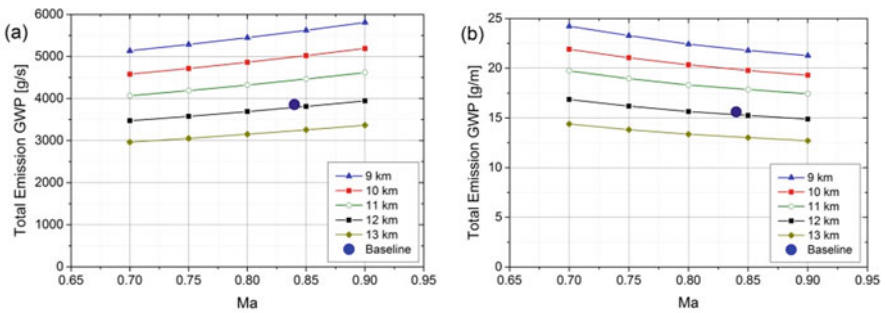


Fig. 5 (a) total GWP per time; (b) total GWP per distance

emissions will be lower at higher subsonic speeds and higher altitudes which could be more suitable for commercial aircraft where maximum distance per unit mass of fuel burned is desired.

### 4 Conclusion

In summary, this study examined the emissions of turbofan engines under various cruise conditions using an engine-only model, ICAO test data, and the BFFM2 method for cruise flight emission predictions. The following key findings have been derived from this investigation. Optimizing flight Mach number and altitude can effectively reduce greenhouse gas emissions from turbofan engines. Operating at appropriate levels allows for the reduction of these emissions. It is essential to calculate and evaluate emissions per time or per distance separately, considering the specific design mission of the aircraft. Commercial aircraft, focusing on emissions per distance, and unmanned aerial vehicles (UAVs), focusing on emissions per time, should be treated differently from this perspective. CO<sub>2</sub> and H<sub>2</sub>O emissions exhibit a proportional relationship with the amount of fuel consumed. Consequently,

minimizing fuel consumption during flights leads to the reduction of CO<sub>2</sub> and H<sub>2</sub>O emissions. NO<sub>x</sub> emissions demonstrate different magnitudes and trends compared to CO<sub>2</sub> and H<sub>2</sub>O emissions in relation to Mach number and altitude. They require specific attention and consideration in emission reduction strategies. Total GWP emissions, which encompass CO<sub>2</sub>, H<sub>2</sub>O, NO<sub>x</sub>, CO, and HC emissions, predominantly follow the trends observed in CO<sub>2</sub> and H<sub>2</sub>O emissions due to their dominance in the total emissions. Hence, minimizing fuel consumption by adopting higher subsonic speeds and higher altitudes during flights also minimizes total GWP emissions. These conclusions emphasize the significance of optimizing flight conditions, fuel consumption, and emissions per time or distance for turbofan engines to mitigate their environmental impact. Implementing strategies based on these findings can contribute to achieving greener and more sustainable aviation.

## References

- Baughcum, S. L., Tritz, T., Henderson, S. C., & Pickett, D. (1996). *Scheduled civil aircraft emission inventories and analysis for 1992: Database*. NASA Contractor Report 4700. NASA Contract Rep.
- Dinc, A. (2017). Optimization of turboprop ESFC and NO<sub>x</sub> emissions for UAV sizing. *Aircraft Engineering and Aerospace Technology*, 89, 375–383. <https://doi.org/10.1108/AEAT-12-2015-0248>
- Dinc, A. (2020). NO<sub>x</sub> emissions of turbofan powered unmanned aerial vehicle for complete flight cycle. *Chinese Journal of Aeronautics*, 33, 1683–1691. <https://doi.org/10.1016/j.cja.2019.12.029>
- Dinc, A. (2021). The effect of flight and design parameters of a turbofan engine on global warming potential. *IOP Conference Series: Materials Science and Engineering*, 1051, 012051. <https://doi.org/10.1088/1757-899X/1051/1/012051>
- Dinc, A., & Elbadawy, I. (2020). Global warming potential optimization of a turbofan powered unmanned aerial vehicle during surveillance mission. *Transportation Research Part D: Transport and Environment*, 85. <https://doi.org/10.1016/j.trd.2020.102472>
- Dinc, A., & Gharbia, Y. (2020). Global warming potential estimations of a gas turbine engine and effect of selected design parameters. In *Proceedings of the ASME 2020 international mechanical engineering congress and exposition volume 8: Energy*. American Society of Mechanical Engineers (p. 1–7).
- Dubois, D., & Paynter, G. C. (2006). “Fuel flow method2” for estimating aircraft emissions. SAE Tech Pap 776–790. <https://doi.org/10.4271/2006-01-1987>
- EASA. (2019). *European aviation environmental report 2019*.
- ICAO. (2015). *Aircraft Engine Emissions Databank*. <https://www.easa.europa.eu/easa-and-you/environment/icao-aircraft-engine-emissions-databank>. Accessed 12 May 2020.
- Kim, B., Fleming, G., Balasubramanian, S., et al. (2005). *Global aviation emissions inventories for 2000 through 2004*.
- Meier, N. (2020). *Jet engine specification database*. <http://www.jet-engine.net/>. Accessed 24 May 2020.
- Pagoni, I., & Psaraki-Kalouptsidi, V. (2017). Calculation of aircraft fuel consumption and CO<sub>2</sub> emissions based on path profile estimation by clustering and registration. *Transportation Research Part D: Transport and Environment*, 54, 172–190. <https://doi.org/10.1016/j.trd.2017.05.006>

- Pawlak, M., Majka, A., Kuźniar, M., & Pawluczy, J. (2018). Emission of selected exhaust compounds in jet engines of a jet aircraft in cruise phase. *Combust Engines*, 173, 67–72. <https://doi.org/10.19206/CE-2018-211>
- Schwartz, E., & Kroo, I. M. (2009). *Aircraft design: Trading cost and climate impact*. 47th AIAA Aerosp Sci Meet Incl New Horizons Forum Aerosp Expo. <https://doi.org/10.2514/6.2009-1261>.
- Wasiuk, D. K., Lowenberg, M. H., & Shallcross, D. E. (2015). An aircraft performance model implementation for the estimation of global and regional commercial aviation fuel burn and emissions. *Transportation Research Part D: Transport and Environment*, 35, 142–159. <https://doi.org/10.1016/j.trd.2014.11.022>

# Effects of Strategic Alliance Membership on the Environmental Performance of Airlines



Serap Gürsel and Gamze Orhan

## 1 Introduction

An undergoing change endangered in aviation industry between the years of 1980 and 2000 by deregulation, privatization, and globalization affected the airline sector severely. These pressures forced airlines to form alliances. First form of these partnerships has been defined as joint ventures, networks, and strategic alliances (Bennett, 1997). Strategic alliances became an important management strategy. They represent cooperative approach to increase market accessibility and operational capacity, ensure passenger loyalty, and help reducing costs (Semercioz & Kocer, 2008). Although tactical alliances are still used very frequently today, the demand for global alliances is increasing day by day (European Commission and US DOT Report, 2010).

Airlines expect six basic benefits from strategic alliances. These benefits are to achieve scale economy, to use other airlines' assets, to reduce risk, to help form of the market, to survive in the market, and to increase the speed of reaching the market (Bennett, 1997). Members of global alliances aim to reach the most comprehensive flight network in the world. The joint strategy of global alliance and the existing flight network of member airlines are vital in achieving this goal. Even members participating in only one service of global alliances (frequent flyer program, code share agreements, lounge access) benefit from global collaboration synergies (European Commission and US DOT Report, 2010). Airline alliances ensure a win-win situation for member airlines (Hall & Eppink, 1992).

---

S. Gürsel  
Aviation Management, Kocaeli University, Kocaeli, Türkiye

G. Orhan (✉)  
Aviation Management, Eskisehir Technical University, Eskisehir, Türkiye  
e-mail: [gozsoy@eskisehir.edu.tr](mailto:gozsoy@eskisehir.edu.tr)

Airlines rely on alliance synergies for all aspects of core business activities (Hall & Eppink, 1992). Environmental strategies do not count in core business activities, but in the future, because of the climate change, environmental issues will be a core airline activity. International regulations are very important in sustainability. Especially the European Union and International Civil Aviation Organization (ICAO) are taking many steps in this regard. Among the steps taken in the world, the first international study to separately touch on the aviation sector was carried out by the European Union. In fact, the European Union has influenced airline cooperation since its establishment. Europe-based airline collaborations are affected by the European Union's environmental regulations. By developing a joint sustainability plan, a dependency relationship is necessary in order to achieve long-term goals in airline alliances (Hall & Eppink, 1992).

## 2 Environmental Performance of Airlines

Many international regulatory institutions, especially the ICAO, have recently established regulations regarding the environmental efficiency and environmental performance of airline companies. Since the 2000s, the importance of climate change has been understood, and environmental performance has gained importance all over the world in this direction. Due to the magnitude of the environmental impacts of the aviation industry, international regulatory agencies encourage airline companies, airports, and all other stakeholders to take steps regarding environmental sustainability.

Sustainability in the aviation industry is mostly studied through the concept of environmental efficiency. To increase environmental efficiency, there are practices such as reducing energy consumption, recycling waste, reducing the use of single-use plastics, reducing weight in flights, promoting biofuels, and reducing carbon emissions (Kim & Son, 2021). Alliances make environmental commitments on many of these issues.

On a global scale, aircraft emissions of carbon dioxide and nitrogen oxides that harm the climate and atmosphere cause ozone depletion. At the local level, the environmental impact of aviation is related to the noise that occurs during aircraft takeoff and landing. The environmental impacts of airline companies are examined under two main headings. These are noise and gas emissions during aircraft operations and gas emissions and noise during ground operations (Skurla et al., 2002).

The environmental performance of airline companies is improving day by day. Today's airplanes produce an average of 20 decibels less noise than airplanes 30 years ago. This reduced noise complaints by 75%. Airplanes are 65% more fuel efficient than planes in 1975. Even between 1990 and 2000, fuel efficiency increased by 17% (Skurla et al., 2002). Airlines buy planes that produce less gas emissions in order to have a green image. They also plan their maintenance activities by paying attention to the environmental impacts.

Load factor is an important data for environmental performance of airlines. The load factor can be achieved by increasing the passenger capacity of the aircraft and improves the airline business in an environmental sense. There are different load factor ratios for different airline business models, and this is demand related. In particular, it is accepted that the load factor of scheduled airlines is lower. Charter airlines and low-cost airlines have a higher load factor, and this is more positive in terms of environmental sustainability. It is also known that mainline carriers have a higher load factor than regional carriers (Mayer et al., 2015).

Biofuels can help airlines in achieving environmental sustainability goals. Airlines can reduce their carbon dioxide emissions between 6.6% and 17% by using biofuels (Mayer et al., 2015).

Aircraft age can be a decisive factor for environmental performance. The biggest decrease in fuel consumption in the airline industry is thought to be due to airlines renewing their fleets. For this reason, it is foreseen that there will be a serious reduction in carbon emissions of aircraft even with the retirement of old aircraft. It is known that strategic global alliances create a marketing advantage in aircraft purchase. The fact that the aircraft produced with the new aircraft technology are both more environmentally friendly and advantageous in fuel consumption is the reason why airline companies want new aircraft (Mayer et al., 2015).

### **3 Oneworld Alliance and Sustainability Commitment**

Oneworld Alliance is one of the three global airline alliances. Oneworld Alliance, together with its members, aims to reach net zero emissions gradually by 2050. In this direction, it has determined a roadmap with its 14 members.

In September 2020, the roadmap of alliance was announced. In this way, Oneworld was the first alliance to announce its carbon neutral target. It has been explained that this goal will be achieved through various applications. Initiatives in line with the objectives supported by ICAO, such as fleet modernization, operational efficiency improvements, and the expansion of sustainable aviation fuel (SAF), will be implemented.

Calling all aviation industry and countries on behalf of its members, the alliance gathers support for decarbonizing in aviation. The roadmap will be renewed with the development of technology in aviation and the widespread use of SAF. Oneworld member airlines are actively involved in many sustainability and environmental initiatives. These initiatives may take place within the alliance (in environmental and sustainability management activities) or outside the alliance (Table 1).

**Table 1** Commitments of Oneworld Alliance members

Member Airline	Commitment
Alaska Airlines	Net zero emissions by 2040.
American Airlines	An intermediate, science-based target for reducing emissions by 2035.
IAG (parent of British Airways and Iberia)	Power 10% of its flights with SAF by 2030 and has extended its net zero emissions target to its supply chain.
Cathay Pacific	Cut their ground emissions by 32% from their 2018 baseline before the end of 2030, through enhancing energy-saving measures and exploring renewable energy options in its premises and ground operations as part of its net-zero carbon emissions commitment.
Finnair	Carbon neutrality by 2045 and to halving its net emissions by 2025 from 2019 levels.
Japan Airlines	Use SAF at 10% of its total fuel consumption, reducing total emissions in 2030 by 10% compared to 2019.
Malaysia Airlines and sister companies under the Malaysia Aviation Group (MAG)	Launched the MAG Sustainability Blueprint in April 2021, with the aim to promote socio-economic development and achieve net zero carbon emissions by 2050. MAG has also set a goal for 50% of the materials used for inflight operations to be biodegradable by 2025.
The Qantas Group	Reaching net zero carbon emissions by 2050 and investing A\$50 million in developing a sustainable aviation fuel industry.
Qatar Airways	Enhanced environmental sustainability education for its employees, including engaging with LATA on additional sustainability training.
S7 Airlines	Launched its Green Steps edutainment program. It includes short lessons in the S7 Airlines mobile app on how to make travel more environmentally friendly and users could earn S7 Priority miles when they pass tests after lessons. S7 Airlines uses blankets on board which are made from recycled plastic bottles and has reduced the packaging for business-class travel kits.
Sri Lankan Airlines	Its aviation fuel efficiency enhancement program, conservation through education program and waste upcycling project.



## 4 Conclusion

Accelerated primarily by economic pressures and assisted by globalization, deregulation, and privatization, alliances became a global trend. Airlines enjoy many benefits from global alliances. These benefits, which generally result from the creation of economies of scale, cause airline companies to gain competitive advantage in the global market. When environmental sustainability, which is one of the important issues of recent years, is supported by strategic alliances, it becomes easier for airline companies to fulfill their responsibilities to national and international regulatory institutions.

It is considered more important for airlines in developing countries to participate in strategic alliances. Thus, they can compete with the airlines of developed countries and increase their bargaining power in areas such as aircraft maintenance, fuel prices, and airport fees. All these benefits can also positively affect the environmental performance of airline companies.

Airlines join strategic global alliances because of all-round benefits of alliances. Environmental strategy and commitments bring airlines a perspective in eco-positioning in the market. Today, countries give importance to environmental issues in order to cope with the problem of climate change. In this direction, efforts are made to achieve environmental targets on a sectoral basis. It is seen that airline companies, like businesses in all other sectors, are completely focused on environmental sustainability issues such as green marketing, ecology, environmental performance, and environmental efficiency.

Airline alliances are highly influenced by the regulations of national authorities. For this reason, airline companies belonging to countries or regions with more internal regulations on environmental issues are in a more advantageous position in strategic cooperation.

In an environmental sense, airlines support the environmental commitments of its belonging alliance to provide competitive advantage. Alliances would not guarantee environmental success for member airlines. However, airlines that are involved in an alliance become more strategically dependent in terms of environmental policies than airlines that are not involved in an alliance. As in the case of the Oneworld group, the environmental commitment of cooperation can become binding on all members. Voluntary work of the participants at the beginning of all regulations facilitates compliance later when the regulation becomes mandatory.

## References

- Bennett, M. M. (1997). Strategic alliances in the world airline industry. *Progress in Tourism and Hospitality Research*, 3, 213–223.
- European Commission and the United States Department of Transportation. (2010). *Transatlantic airline alliances: Competitive issues and regulatory approaches*. Retrieved from [http://ec.europa.eu/competition/sectors/transport/reports/joint\\_alliance\\_report.pdf](http://ec.europa.eu/competition/sectors/transport/reports/joint_alliance_report.pdf).
- Hall, W., & Eppink, D. J. (1992). Strategic alliances in the airline industry. *Strategic Change*, 1(6), 341–348.
- Kim, H., & Son, J. (2021). Analyzing the environmental efficiency of global airlines by continent for sustainability. *Sustainability*, 13, 1571.
- Mayer, R., Ryley, T., & Gillingwater, D. (2015). Eco-positioning of airlines: Perception versus actual performance. *Journal of Air Transport Management*, 44–45, 82–89.
- Semercioz, F., & Kocer, B. (2008). Strategic alliances in the aviation industry: An analysis of Turkish airlines experience. *Journal of Transnational Management Development*, 9(2–3), 29–45.
- Skurla, R., Kolar, V., & Takac, A. (2002). *Environmental management system: current airline trends and practices in the EU with prospects for Croatia*. 10th international symposium on electronics in traffic proceedings, 9, p. 406–410.

# Safety Factor Analysis in Ramp Operation with AHP Approach



Ilker Inan and Ilkay Orhan

## Nomenclature

AHP	Analytic hierarchy process
IATA	International Air Transport Association
IGOM	IATA Ground Operations Manual
MCDM	Multi-criteria decision-making

## 1 Introduction

Ramp operation in civil aviation is considered as one of the most important processes by airlines. Providing on-time ground operation is very essential, and any delay during this process will affect other steps, respectively, that might push ramp agents to be hurry. Therefore, time pressure on ramp may cause accidents or injury.

An airport ramp is the place where planes are parked, unloaded or loaded, refueled, or boarded. Both the airports and the carriers are responsible for the ramp area. By providing gates, cargo hard stands, passenger loading bridges, and fueling facilities to enable aircraft operations at the terminal, the airport gives passenger and cargo access to air transportation. Airlines are granted access to leased gates and are allowed to utilize the amenities. Ground operations, which include a range of

---

I. Inan

Department of Civil Aviation, Graduate School of Sciences, Eskişehir Technical University, Eskişehir, Türkiye

I. Orhan (✉)

Faculty of Aeronautics and Astronautics, Eskişehir Technical University, Eskişehir, Türkiye  
e-mail: [iorhan@eskisehir.edu.tr](mailto:iorhan@eskisehir.edu.tr)

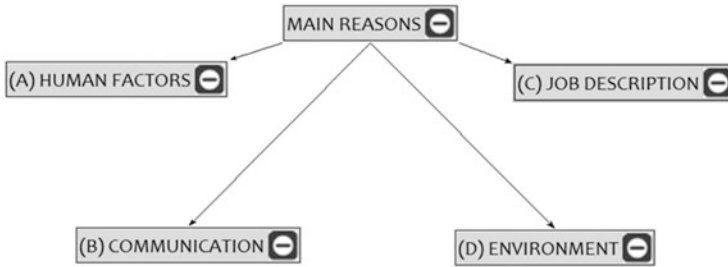


**Fig. 1** General safety factors

services, take place at the ramp regions. The airlines may operate these activities themselves or contract them out to subcontractors (Landry & Ingola, 2011).

All ground service personnel must have operational and safety training in order to assist aircraft servicing. The training also includes the use of ground service equipment such as belt loaders, tugs, carriers, unit loaders, baggage carts, track loaders, and portable ground power units. Regardless of required training, the presence of a large number of people operating a variety of equipment in a small space, sometimes under time constraints, creates an environment prone to accidents and fatalities, as well as aircraft and equipment destruction (GAO, 2007).

This study aims to determine safety risks on the ground and measure them in order of importance among each other. Multi-criteria decision-making (MCDM) method is used to analyze these priorities under four main items, namely, human factor, communication, job description, and environment, as it is shown in Fig. 1. These main factors are mentioned in IGOM (IATA Ground Operations Manual) in Chapter 6 (IGOM, 2021).

## 2 Method

We present the analytic hierarchy process (AHP) to develop a weight model of safety factors by assessing and choosing the relevance of all sorts of factors, due to the complexity and unpredictability of factors.

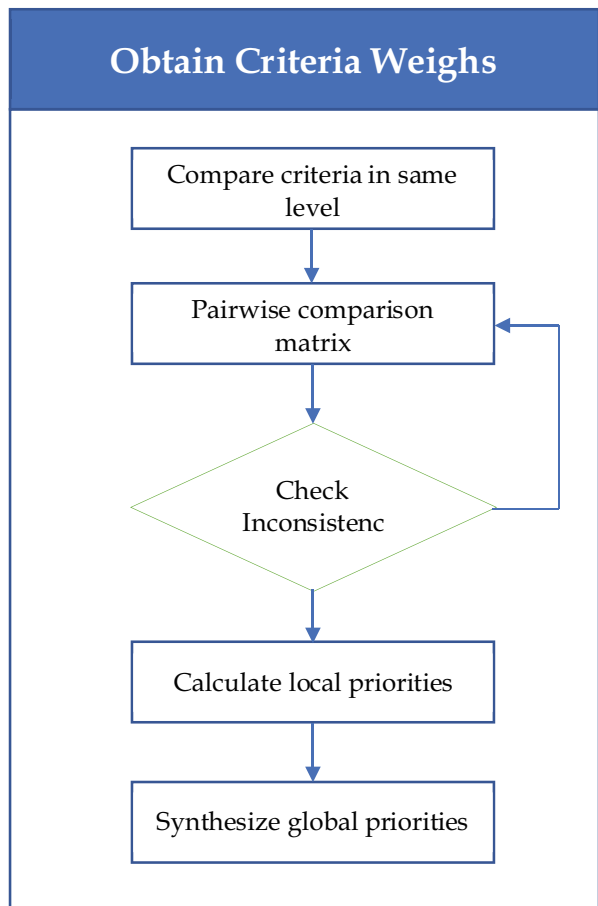
AHP is a theory of relative measurement of criteria which are intangible, and it is proposed by Saaty (Saaty, 1980; Aragonés-Beltrán et al., 2014; Saaty, 1994). He proposes to use the ratio scales to compare the decision-maker's preferences and his Saaty's fundamental scale view that is shown in Table 1 (Saaty, 1980; Aragonés-Beltrán, 2014).

Figure 2 shows main steps of MCDM in order to find out AHP process (Aragonés-Beltrán et al., 2014; Saaty, 2001).

**Table 1** Saaty’s fundamental scale (Saaty, 1980)

Intensity of importance	Definition
1	Equal importance/preference
2	Weak
3	Moderate importance/preference
4	Moderate plus
5	Strong importance/preference
6	Strong plus
7	Very strong or demonstrated importance/preference
8	Very, very strong
9	Extreme importance/preference

**Fig. 2** AHP method scheme (Aragonés-Beltrán et al., 2014)



### 2.1 Data and Analyses

A survey is applied to experts who have experience in ramp operations in Istanbul Airport. The survey questions are asked with nine-point Likert scale to provide results in enough wide range. Each risk factor is matched with other in the same group, and the participants are required to answer them in terms of comparative degree.

The module of hierarchical safety considerations in the apron operation, as indicated in Table 2, is based on expert advice and a survey.

### 2.2 Determine Weight Value of Each Factor

We can specify a set of elements’ weights sorted by the important degree based on expert opinion and surveys. The outcomes are represented in Table 3.

**Table 2** The hierarchy module of safety factors in apron operation

First level	Second level	Third level
<i>Effect factor</i>	Human factors	Fatigue (A1)
		Overconfidence (A2)
		Unattending (A3)
	Communication	Lack of communication (B1)
		Marshaling (B2)
		Work shift (B3)
	Job description	Kneeling/bending (C1)
		Overtime work (C2)
		Repetitive work (C3)
	Environment	Bad weather (D1)
		Low visibility (D2)
		Noise (D3)

**Table 3** The weight value of each factor

	w		w
A1	0.70886	B1	0.31081
A2	0.17862	B2	0.49339
A3	0.11252	B3	0.19580
(a) Human factor		(b) Communication	
C1	0.68698	D1	0.45996
C2	0.18648	D2	0.22113
C3	0.12654	D3	0.31892
(c) Job description		(d) Environment	

### 3 Results and Discussion

It is seen that ramp accidents occurring under “human factor” reasons are mostly caused by “fatigue” and take the first place with a rate of 70% in the whole process among the ramp operations. Overconfidence which has a rate of roughly 17% is in the second place. Finally, the “unattending” effect is in the last place with 11% (Table 3(a)).

Experts who answered the questions evaluated “marshaling” as the first among the communication-based reasons. Wrong hand signals used by marshalers might be thought of as a cause of why this rate is so high comparing to others. “Lack of communication” factor ranked second with 30%. The accidents caused by “work shift” are in the last place with approximately 20% (Table 3(b)).

The “kneeling/bending” body movement in the job description has been evaluated as the most remarkable risk factor for ramp operations, especially for ramp agents who are responsible for loading/offloading and technicians working in hangar. In addition to this, “overtime work” factor which is very common in aviation has taken the second place. Accidents caused by “repetitive work” follow them with a rate of 12% (Table 3(c)).

“Bad weather” effect comes first with a rate of 45% among the safety factors originating from environment. This triggers a significant risk for handling personnel working in very hot and cold weather conditions. The noise factor is considered in the second place with a rate of 31%. It is known that the ramp agents especially working very close to the aircrafts are being exposed to a great extent of noise from APU and engines. Finally, the “low visibility” factor ranks third with 22% due to heavy snowfall in winter (Table 3(d)).

### 4 Conclusion

We may utilize AHP as a form of convenient and effective evaluation method in the investigation of human factors in apron operation since it has features of dependable conclusion, practicability, and accuracy. It's tough to assess aviation operations because of their intricacy, especially when they're linked to the operators' psyche and physiology, which is difficult to quantify. However, if we use the AHP to quantize all elements using the judgment matrix, we can address the problem.

We may logically judge the influencing elements and obtain the priority order of all factors' effect on the final occurrences if the judgment matrix fulfills the consistency condition requirement. As a result, decision-makers may easily identify areas that need to be addressed as well as concealed dangers.

## References

- IGOM. (2021). *IATA ground operations manual*, <https://www.iata.org/en/publications/store/iata-ground-operations-manual/>
- Saaty, T. L. (1980). *The Analytic Hierarchy Process. Planning, priority setting, resource allocation*. McGraw-Hill.
- Aragonés-Beltrán, P., Chaparro-González, F., Pastor-Ferrando, J. P., & Pla-Rubio, A. (2014). An AHP (Analytic Hierarchy Process)/ANP (Analytic Network Process)-based multi-criteria decision approach for the selection of solar-thermal power plant investment projects. *Energy*, *66*, 222–238.
- Saaty, T. L. (1994). *Fundamentals of decision making and priority theory with the Analytic Hierarchy Process* (1st ed.). RWS Publications.
- Saaty, T. L. (2001). *Decision making with dependence and feedback. The Analytic Network Process. The organization and prioritization of complexity* (2nd ed.). RWS Publications.
- Landry, J., & Ingola, S. (2011). *Ramp safety practices: A synthesis of airport practice*. Transportation Research Board.
- U.S. Government Accountability Office. (2007). *Aviation runway and ramp safety: sustained efforts to address leadership, technology, and other challenges needed to reduce accidents and incidents*. Washington, DC. GAO-08-29.



# Evaluating Total Load of Aviation Operators by Analytic Hierarchy Process (AHP)



Omar Alharasees and Utku Kale

## Nomenclature

AHP	Analytical hierarchy process
MCDC	Multi-criteria decision making
PCM	Pairwise comparison matrix
ATCO	Air traffic controller
CR	Consistency ratio

## 1 Introduction

As the avionics system evolves to be more dynamic, automated, and complicated, assessing the aviation operators' total loads becomes more critical to the system's applicability and reliability in the aviation world.

The adaption of the current complex and dynamic aviation system needs to balance operator's loads in the innovative systems, which require feasible frameworks and concepts (Kale et al., 2020). In such an environment, operator performance is measured more intricately. Aviation operators deal with enormous data and relevant information as flight systems, including aircraft capabilities, radar, sensor systems, and many other appliances.

The future operator environment (cockpit, future ground control tower of pilots, and towers) and avionics systems need to be redesigned by considering various psychological parameters, human factors, and operator loads (Jankovics & Kale,

---

O. Alharasees (✉) · U. Kale

Department of Aeronautics and Naval Architecture, Budapest University of Technology and Economics, Budapest, Hungary

e-mail: [oalharasees@edu.bme.hu](mailto:oalharasees@edu.bme.hu); [kale.utku@kjk.bme.hu](mailto:kale.utku@kjk.bme.hu)

2019). Therefore, this study focuses on evaluating operators' total loads using the analytic hierarchy process.

The analytic hierarchy process (AHP) is a well-known "multi-criteria decision-making (MCDM)" technique for multiple objective ranking procedures and an excellent approach for dealing with complicated decision-making (Saaty, 2008). This method can help decision-makers define priorities and make the optimal option (Saaty, 1990). Another advantage of the AHP is to capture both subjective and objective components of choice by reducing complicated judgments to a series of pairwise comparisons and then synthesizing the findings. Furthermore, the AHP includes a beneficial approach for assessing the consistency of the decision-maker's judgments, therefore eliminating decision-making bias.

The AHP is a theory of relative measuring on absolute scales of both actual and potential criteria based on a familiar involved participant's opinion as well as current measurements and relevant information. The primary focus of the AHP's mathematics is how to measure entities evaluating and weighing the critical characters. Because decision-making is diverse, the AHP has mainly been used to multi-objective, multi-criteria, and multiparty decisions, specifically in the engineering field (Nakagawa & Sekitani, 2004). The judgments generally made in qualitative terms are stated mathematically to create compromises among the various intangible objectives and criteria, rather than assigning a score based on a person's subjective judgment (Saaty, 2008). Finally, to cope with the difficulties, integrating repetitive and broad experiences would pour into a system of priorities. The AHP is built on four axioms: reciprocal judgments, homogenized characters independent within each level, hierarchical structure, and rank order expectations.

Many previous studies employed AHP in aviation in the literature. Bruno et al. assessed planes to maintain planned choices, demonstrating that cabin baggage compartment volume is the best aspect (Bruno et al., 2015). Chao & Kao discovered that policy and dependability were necessary standards for service quality (Chao & Kao, 2015).

Rezaei et al. (2014) assessed and designated the supplier in the airline retail business; the result of this research suggested that economic steadiness is a considerable standard in supplier selection (Rezaei et al., 2014). Chen et al. (2014) utilized AHP procedures to assess the significance of weighting the technical elements in aviation safety (Chen et al., 2014).

Other AHP studies were specified for the aviation operators, for example, Oktal H. and Onrat A. used AHP for characterizing the critical factors in airline pilots' candidates' selection (Oktal & Onrat, 2020). Havle and Kılıç (2019) identified and examined the circumstances that impact navigation errors in the North Atlantic region by combining a fuzzy analytic hierarchy process (FAHP) into the Human Factors Analysis and Classifying System framework (Havle & Kılıç, 2019). Kilic and Ucler (2019) applied AHP techniques to weigh stress factors among student pilots (Kilic & Ucler, 2019).

The research aims to evaluate the elements that influence and shape the total loads of aviation operators. The current study examines the preferences of the three operator categories (less skilled pilots, skilled pilots, and ATCOs) based on the

primary criteria. In order to create a general hierarchical model, the analytic hierarchy process (AHP) is employed in this research. These decision-making models are primarily built on three layers in order to develop evaluator preference loads for (i) the assessment procedure, (ii) preventing complication, and (iii) lacking information from other AHP functions. In this study, the Saaty Scale was utilized for scoring to depict lost data utilizing matrices that could be computed using a particular technique.

## 2 Method

The MCDM technique demands that decision alternatives or sub-criteria be chosen or selected based on their qualities. In MCDM scenarios, a preset, restricted number of choice possibilities is assumed. Sorting, ranking, and scoring are all steps in the MCDM process.

The primary technique employed in the research is the analytic hierarchy process (AHP), one of the popular multi-criteria decision-making (MCDM) techniques, to investigate the major and main characteristics of pilots and ATCOs.

The current authors created a two-level hierarchy model containing the five main types of aviation operators' loads: (i) workload is the work done by an operator in a given time interval as it relies on human factors, skills, knowledge, practice, etc.; (ii) task load is the level of complexity and toughness when completing a task, which depends on the degree of difficulty, traffic demand, traffic regulations, etc.; (iii) information load is the volume of information and data collected from complex systems, which highly depends on the level of technology, weather conditions, and other aspects, as information overload might create confusion among operators; (iv) communication load is the level of awareness and understanding among operators and is highly altered by cultural norms, social relations, etc.; and (v) mental load is the physical and psychophysiological situation of the operators during operation and highly depends on the level of stress, performance action, etc.

Figure 1 shows the hierarchical model for the total loads of operators with the components of each level:

Because the AHP utilizes the unique properties of pairwise comparison matrices (PCM), the choice of decision-makers between specific pairs of options illustrates the importance and priority of a particular aspect over another based on a scale (see Table 1). The matrix of pairwise comparisons (see Eq. 1)  $A = [a_{ij}]$  represents the strength of the decision-maker's preference between individual pairs of alternatives ( $A_i$  versus  $A_j$ , for all  $i, j = 1, 2, \dots, n$ ). The pairwise comparison matrix can be given as follows (Eq. 1):

**Fig. 1** Hierarchical model of the operators' total load

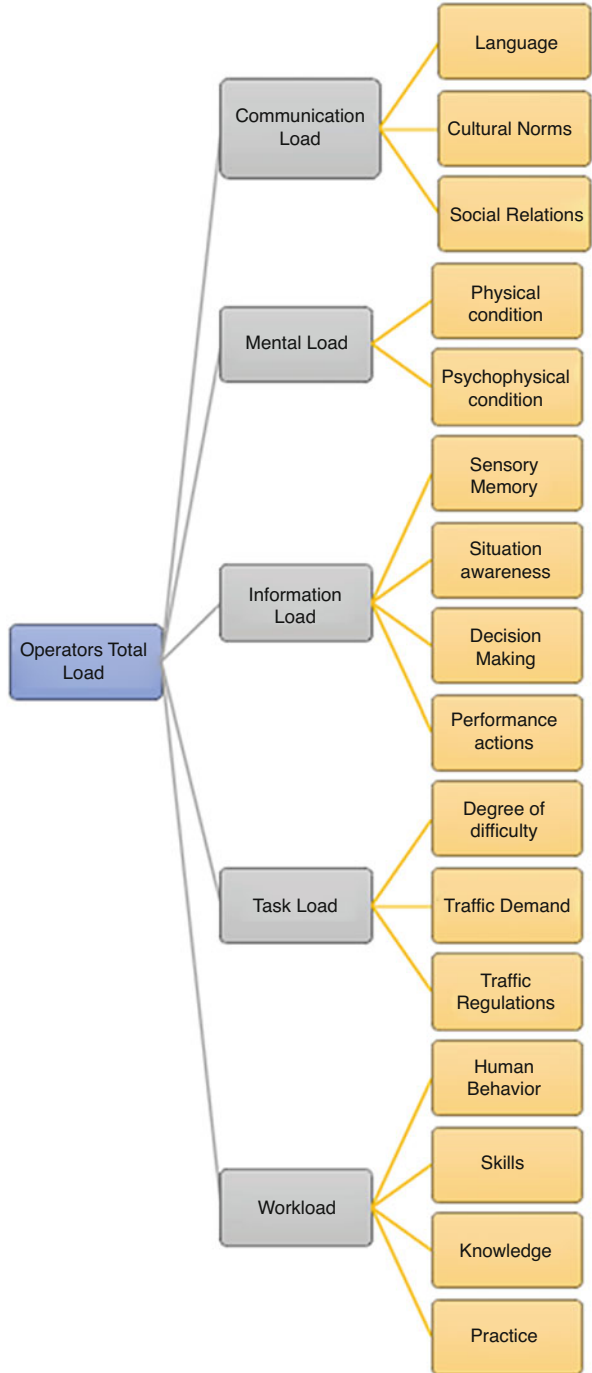


**Table 1** Saaty Fundamental Scale

Numerical values	Verbal scale	Explanation
1	Equal importance of both elements	Two elements contribute equally
3	Moderate importance of one element over another	Experience and judgment favor one element over another
5	Strong importance of one element over another	An element is strongly favored
7	Very strong importance of one element over another	An element is very strongly dominant
9	Extreme importance of one element over another	An element is favored by at least an order of magnitude
2,4,6,8	Intermediate values	Used to compromise between two judgments

$$A = [a_{ij}] = \begin{bmatrix} 1 & a_{12} & \dots & a_{1j} & \dots & a_{1n} \\ \frac{1}{a_{12}} & 1 & \dots & a_{2j} & \dots & a_{2n} \\ \dots & \dots & \dots & \dots & \dots & \dots \\ \frac{1}{a_{1j}} & \frac{1}{a_{2j}} & \dots & a_{ij} & \dots & a_{in} \\ \dots & \dots & \dots & \dots & \dots & \dots \\ \frac{1}{a_{1n}} & \frac{1}{a_{2n}} & \dots & \frac{1}{a_{in}} & \dots & 1 \end{bmatrix} \tag{1}$$

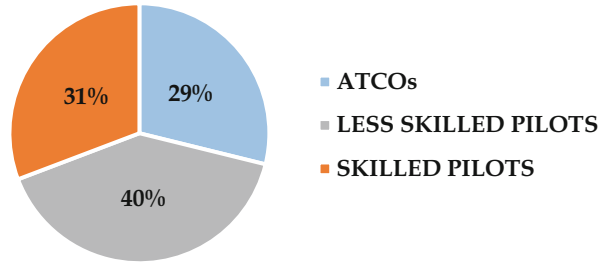
In order to calculate the pairwise comparison matrices to priorities the effect of each aspect in the model within the same level, the geometric mean of each group was utilized. The matrix consistency ratio should be less than 0.1, as most experience matrices are not consistent. CR for groups is calculated.

### 3 Questionnaire

In this research, an online AHP based survey was designed and performed among operators, focusing on the operators’ major characteristics from various perspectives. The purpose of the questionnaire is to quantify the most important issues as seen through the eyes of the operators, based on their experience and knowledge.

The questionnaire was created based on aviation operators (pilots, ATCOs) in this research. There were 52 participants (13 females), 37 pilots, and 15 ATCOs. The participants were arranged into three groups: (i) less skilled pilots (average age 22), (ii) skilled pilots (average age 35), and (iii) ATCOs (average age 34). Figure 2 demonstrates the participant groups’ percentages in the questionnaire.

Fig. 2 Survey participants



## 4 Results and Discussions

After analyzing and visualizing the participants' preferences in the model, there will be some differences between the groups' overviews. AHP method will highlight the critical characteristics based on pairwise comparisons. The responses have been collected and utilized by using the geometric mean.

Based on the collected responses of the three groups of aviation operators and by employing the AHP process, evaluating and weighing the characteristics in each level individually, the following tables (Tables 2, 3, and 4) show the aspects (the weights, final score, and consistency ratio) which have been computed for the first level in the operators' load model characteristics from each group:

Combining the three groups' opinions would show the variations between the groups, which could rise due to the experience level and the type of the job. Comparing different groups of participants would make it easier to evaluate and weigh various individual aspects of aviation operators' total loads from other overviews.

The survey highlighted that the communication loads are the strongest factor in the model in the first hierarchy level, as illustrated by Fig. 3.

Pilots and air traffic controllers in aviation communication do not have face-to-face contact or a visual speech interface to interact with each other; consequently, they must communicate purely through voice. Their communication is primarily done by radio transmissions written in a specific phraseology meant to be as precise and efficient as possible. As a result, their listening and speaking skills are extremely vital.

A noticeable fluctuation of the opinions is clear between the groups in the third and fourth critical factors (information and mental loads) within the first level of the model.

Looking into the second level of the model (see Fig. 4) for the sub-criteria of the communication loads also provides a clear overview of the specific issue from the operators' eyes which is the level of language among aviation operators based on the participants. In fact, communication errors are a main factor in the aviation world accidents, but with the accelerated automation development in the aviation industry, the issue is shifting toward the type and volume of information the aviation operator receives within a specific timeframe.

**Table 2** Less skilled pilots’ PCM for the first level

Less -skilled Pilots						
Operators Total Loads	Comm. Load	Mental Load	Info Load	Task Load	Work Load	Weights
Communication load	1	4.45	4.51	2.89	1.14	39.35%
Mental Load	0.22	1	2.62	2.04	0.48	15.48%
Information Load	0.22	0.38	1	3.16	0.43	11.71%
Task Load	0.35	0.49	0.32	1	0.49	8.38%
Workload	0.88	2.09	2.32	2.05	1	25.08%
CR= 0.096	Sum=					100%

**Table 3** Skilled pilots’ PCM for the first level

Skilled Pilots						
Operators Total Loads	Comm. Load	Mental Load	Info Load	Task Load	Work Load	Weights
Communication load	1	3.98	3.60	4.13	0.82	36.33%
Mental Load	0.25	1	0.95	1.60	0.35	10.91%
Information Load	0.28	1.05	1	3.73	0.45	14.95%
Task Load	0.24	0.63	0.27	1	0.39	7.46%
Workload	1.22	2.84	2.23	2.58	1	30.34%
CR= 0.047	Sum=					100%

**Table 4** ATCOs’ PCM for the first level

ATCOs						
Operators Total Loads	Comm. Load	Mental Load	Info Load	Task Load	Work Load	Weights
Communication load	1	7.05	3.36	5.67	1.01	39.71%
Mental Load	0.14	1	0.61	0.90	0.28	6.99%
Information Load	0.30	1.65	1	4.37	0.33	14.52%
Task Load	0.18	1.12	0.23	1	0.21	6.01%
Workload	0.99	3.53	3.03	4.75	1	32.77%
CR= 0.036	Sum=					100%

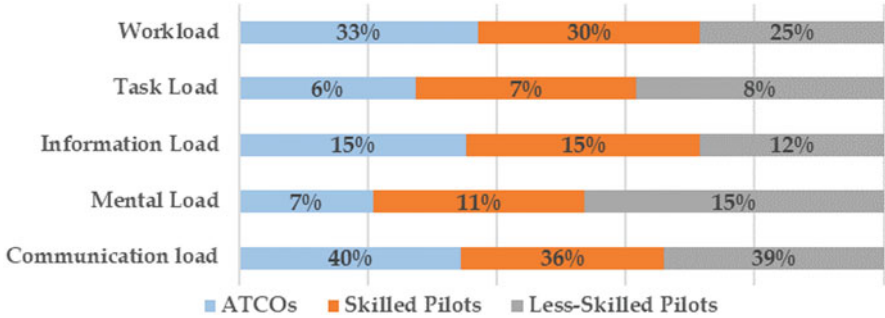


Fig. 3 The total load of the aviation operators

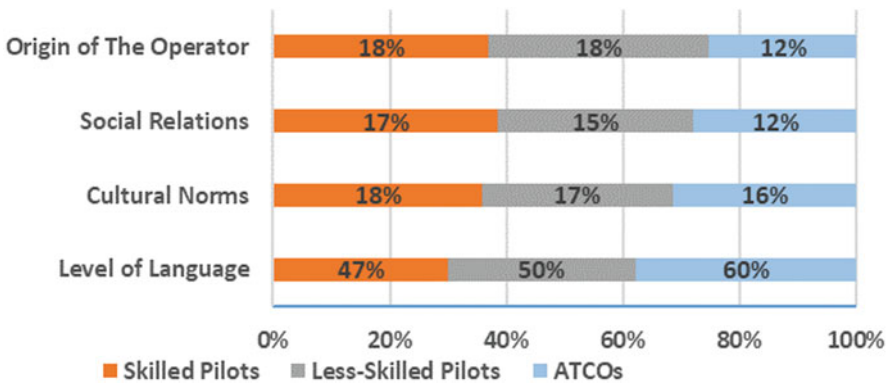


Fig. 4 Sub-criteria of the communication load

Based on the participant’s opinions, the information errors could be the most critical issue for the futuristic pilot environment after the communication, especially with introducing some automated systems in the aviation communication process.

## 5 Conclusion

The findings demonstrated a priority ranking and scaling of the operators’ total loads within each level, which is a great indicator of the significant elements. To better understand the futuristic operators’ environment and manage critical scenarios, employing multi-criteria procedures, specifically AHP, illustrated a critical role. The inconsistencies between the perspectives are shown using quantitative and qualitative criteria using the traditional, classic, and simplified analytical hierarchical process (AHP) technique for decision-making.



The results of this survey were based on a total of 52 participants from 3 groups of aviation operators (less skilled pilots, skilled pilots, and ATCOs), and it should be mentioned that the results could change if more participants and more groups are included.

The results show that the communication load plays a dominant role in the operator total load model from all participants, followed by the operators' workload.

## References

- Bruno, G., Esposito, E., & Genovese, A. (2015). A model for aircraft evaluation to support strategic decisions. *Expert Systems with Applications*, *42*(13), 5580–5590. <https://doi.org/10.1016/j.eswa.2015.02.054>
- Chao, C. C., & Kao, K. T. (2015). Selection of strategic cargo alliance by airlines. *Journal of Air Transport Management*, *43*, 29–36. <https://doi.org/10.1016/j.jairtraman.2015.01.004>
- Chen, C. J., Yang, S. M., & Chang, S. C. (2014). A model integrating fuzzy AHP with QFD for assessing technical factors in aviation safety. *International Journal of Machine Learning and Cybernetics*, *5*(5), 761–774. <https://doi.org/10.1007/S13042-013-0169-1>
- Havle, C. A., & Kılıç, B. (2019). A hybrid approach based on the fuzzy AHP and HFACS framework for identifying and analyzing gross navigation errors during transatlantic flights. *Journal of Air Transport Management*, *76*, 21–30. <https://doi.org/10.1016/j.jairtraman.2019.02.005>
- Jankovics, I., & Kale, U. (2019). Developing the pilots' load measuring system. *Aircraft Engineering and Aerospace Technology*, *91*(2). <https://doi.org/10.1108/AEAT-01-2018-0080>
- Kale, U., Rohács, J., & Rohács, D. (2020). Operators' load monitoring and management. *Sensors (Switzerland)*, *20*(17). <https://doi.org/10.3390/s20174665>
- Kilic, B., & Ucler, C. (2019). Stress among ab-initio pilots: A model of contributing factors by AHP. *Journal of Air Transport Management*, *80*, 101706. <https://doi.org/10.1016/j.jairtraman.2019.101706>
- Nakagawa, T., & Sekitani, K. (2004). A use of analytic network process for supply chain management. *Asia Pacific Management Review*. 成功大學管理學院, *9*(5), 783–800. <https://doi.org/10.6126/apmr.2004.9.5.02>
- Oktal, H., & Onrat, A. (2020). Analytic hierarchy process–based selection method for airline pilot candidates. *International Journal of Aerospace Psychology*. Bellwether Publishing, Ltd, *30*(3–4), 268–281. <https://doi.org/10.1080/24721840.2020.1816469>
- Rezaei, J., Fahim, P. B. M., & Tavasszy, L. (2014). Supplier selection in the airline retail industry using a funnel methodology: Conjunctive screening method and fuzzy AHP. *Expert Systems with Applications*, *41*(18), 8165–8179. <https://doi.org/10.1016/J.ESWA.2014.07.005>
- Saaty, T. L. (1990). How to make a decision: The analytic hierarchy process. *European Journal of Operational Research*, *48*(1), 9–26. [https://doi.org/10.1016/0377-2217\(90\)90057-I](https://doi.org/10.1016/0377-2217(90)90057-I)
- Saaty, T. L. (2008). Decision-making with the analytic hierarchy process. *International Journal of Services Sciences*, *1*(1), 83–98. Available at: <https://www.inderscienceonline.com/doi/abs/10.1504/IJSSci.2008.01759>. Accessed 15 Feb 2022.

# Experimental and Analytical Principles of Improving Waste Management Technologies in the Technosphere



Ihor Trofimov, Sergii Boichenko, Iryna Shkilniuk, Anna Yakovlieva, Sergii Shamanskyi, Tetyana Kondratyuk, and Oksana Tarasiuk

## 1 Introduction

Biosecurity is one of the most important components of Ukraine's environmental and national security. According to the World Health Organization (WHO), the situation with diseases today is more than ever far from stable. Equilibrium in the world of microbes is violated due to population growth, rapid urbanization, intensive methods of agriculture, deterioration of the environment, etc. Opportunities for the rapid international spread of infectious diseases and their carriers are greatly increased due to aviation, which carries more than 2 billion passengers per year.

One of the most serious biosecurity challenges is H5N1, H7N9, and pork H1N1 (as well as H5N8, H7N3, H7N7) viruses, prions, SARS, MERS, Ebola, smallpox, and polio, as well as drug-resistant microorganisms (in particular tuberculosis – M (X)DRTB) and coronavirus infection COVID-19, which was first registered on December 31, 2019, in Wuhan (China). It is necessary to reorganize the economy in such a way that human industrial activity is fully integrated into the effective

---

I. Trofimov (✉)

Scientific-Technical Union of Chemmotologists, Kyiv, Ukraine

Department of Chemistry and Chemical Technology, National Aviation University, Kyiv, Ukraine

S. Boichenko · I. Shkilniuk · A. Yakovlieva · S. Shamanskyi · O. Tarasiuk

Institute of Energy Safety and Energy Management, National Technical University of Ukraine, "Igor Sikorsky Kyiv Polytechnic Institute", Kyiv, Ukraine

Scientific-Technical Union of Chemmotologists, Kyiv, Ukraine

T. Kondratyuk

Scientific-Technical Union of Chemmotologists, Kyiv, Ukraine

Department of Microbiology, National University Named After Taras Shevchenko, Kyiv, Ukraine

environmental infrastructure. Thus, the study of the process of transport waste management in Ukraine and the world is currently relevant.

One of the global environmental problems inherent in Kyiv like the rest of the megacities is the problem of environmental pollution with production, consumption, and transport infrastructure waste. These issues are practically not solved today, which, without a doubt, will lead to new environmental problems – pollution of groundwater with toxic waste, the formation of biogas, changes in the landscape, etc.

Problems associated with the damage of a wide variety of anthropogenically transformed substrates with microscopic fungi are becoming more urgent, extremely important, and acute in terms of city ecological issues, the neutralization of transport infrastructure waste, and the safety of human life. Microscopic fungi particularly are recognized as the main agents of bio-damage in the terrestrial environment.

The article is based on the research carried out within the framework of grant project No. 2020.01/0242 “Experimental and analytical principles of ensuring the safety of humans and society by improving waste management technologies in the technosphere” with the support of the National Research Foundation of Ukraine.

## **2 Statement of the Problem and Purpose of Research**

Today, in Ukraine, the problem of landfills is one of the most important and relevant among the problems of environmental pollution. This issue needs to be addressed immediately, not only in Ukraine but also throughout the world. Each human dwelling produces a huge number of unnecessary materials and products, from old newspapers and magazines, empty cans, bottles, food waste, wrappers, and packages to broken dishes, worn clothes, and broken household or office appliances. Every day, we face waste: at home and on the street. Everywhere we are surrounded by papers, plastic wrappers, glass, cellophane, etc.

Garbage is formed and accumulated not only in residential premises but also in offices, administrative buildings, cinemas and theaters, shops, cafes and restaurants, kindergartens, schools, institutes, clinics and hospitals, hotels, railway stations, markets, or just on the streets.

If not in terms of standard of living, then at least in terms of the amount of household waste, Ukraine does not lag behind the average European indicator. About 10 million tons of garbage accumulate every year. According to the forecasts of both foreign and domestic experts, the environmental situation in Ukraine is approaching critical, because we are engaged in waste processing at a very low level. Official data of the Ministry of Regional Development of Ukraine shows 5500 official landfills with an area of 8500 hectares. This is 0.014% of the total area of Ukraine (60.4 million hectares).

The problem of waste disposal is relevant for Ukraine, as the country is the European leader in the amount of waste per capita. At the same time, the situation with its disposal remains at the same low level. Because the composition of domestic waste is increasingly approaching the Western one (disposable tableware, aluminum

cans for drinks, plastic packaging), its volume has a steady tendency to increase annually. It especially concerns a large volume of polyethylene materials that are almost undegradable. A large amount of packaging material after one-time use is converted into waste, into the garbage.

As you know, transport is an important part of the world economy, as it is a material carrier between states. The specialization of states and their complex development is impossible without a transport system. The transport factor affects the allocation of production sites; without its consideration, it is impossible to achieve rational placement of productive forces. When allocating production sites, the need for transportation, the mass of raw materials of finished products, their transportability, the provision of transport paths, their throughput, etc. are all being considered. Depending on the impact of these components, the decision is made on the enterprises' allocation. Transport is also important in solving social and economic problems. The provision of the territory with a well-developed transport system serves as one of the important factors in attracting the population and production factors, has an important advantage for the placement of productive forces, and gives an integration effect.

Transport infrastructure includes railway, tram, and inland waterways, contact lines, roads, tunnels, overpasses, bridges, railway and bus stations, subways, airfields and airports, communication systems, navigation and vehicle traffic management, as well as others to ensure the functioning of the transport complex of the building, structures, devices, and equipment. Vehicles include aircraft, railway cars, vessels used for trade or navigation, automobiles, and electric urban passenger transport.

The purpose of this stage of research:

Task 1: To identify the landfills of transport infrastructure in the Kyiv and Kyiv region

Task 2: To conduct a taxonomic analysis of a complex of microorganisms isolated from landfills of transport infrastructure in Kyiv

Task 3: To highlight complexes of microorganisms capable of petroleum products hydrocarbons and solid organic waste destruction/degradation

### **3 Environmental Problems of Transport Infrastructure Waste**

In the process of vehicles' exploitation, the particles of worn-down details are being released into the environment, which significantly pollutes it. These pollutants are formed due to the friction of material elements sliding against each other during an operational cycle.

The main sources of this type of pollution are as follows: engine and transmission parts, brake pads, and tires.

As for the wearing down of engine parts and transmission, it can be reduced by timely lubrication with high-quality oils and the use of oils recommended for this vehicle according to the frequency of oil replacement in lubrication systems.

The composition of used petroleum products includes used motor oils, transmission oils, industrial lubricants, as well as petroleum products that are used to wash machinery units.

Studies have shown that the volume of used oils and lubricants have different compositions depending on the modification of cars, their technical condition, rolling stock working conditions, and can range from 13% to 33%.

The decommissioned vehicle left in an abandoned state is a concentrated source of anthropogenic environmental pollution. Despite this, it is difficult to imagine the life of modern society without, for example, automotive or air transport constantly improving engine power, design, safety system, and comfort, and due to technical development, the morphological composition of the vehicle changes, more and more new materials are used for its production.

All those materials that were used during its manufacture remain in the decommissioned vehicle: ferrous and non-ferrous metals, petroleum products, lubricants and coolants, plastics and textiles, rubber products, glass and ceramics, cardboard, wood, etc.

For the proper handling of decommissioned vehicles and the correct selection of processes and methods of their further processing, they are systematized. All these materials can and should become secondary resources to produce new commodity products.

The aircraft consists of millions of components (parts) that must be further recycled after writing off the machine. In other words, an aircraft is a huge number of metal and composite parts that have been synchronously flying at a speed of 900 km/h (0.85 of the speed of sound; this is the typical speed of the Boeing 787 Dreamliner) at an altitude of 10 km.

Based on the situation around the world over the past decades, the use of aviation recycling and disposal processes is an alternative source for obtaining the necessary aviation spare parts and aircraft components.

## **4 Ways to Solve the Problem**

Biotechnology for environmental protection is a low-waste technology with an environmentally friendly technical implementation of the process. Their use is aimed at cleaning the environment from various kinds of pollutants and producing environmentally friendly products with the possibility of secondary resource flows recycling. Therefore, the choice of biologically active systems (BAS) has a conceptual basis associated with the need for deep knowledge in the field of physiology and biochemical processes of growth and metabolism of biological objects, as well as the mandatory sanitary and hygienic evaluation.

Microorganisms that can be used to neutralize solid and liquid waste are very different, and their spectrum is continuously expanding. With the development of industrial processes, there is an accumulation of new types of waste that can be neutralized and converted into useful products by biotechnological methods. Biotechnological industrial areas are currently developing at a rapid pace. Taking into account the problem for Ukraine with landfills and waste in general, it is necessary to develop unconventional, in particular, biotechnological methods of their processing.

It is also worth noting that BAS of these microorganisms can be widely used in industry, medicine, and agriculture to neutralize the waste of these industries. To solve the issues of food safety, conservation, and restoration of natural resources, in particular the fertility of soils contaminated with petroleum products, it is advisable to use biotechnology that does not violate biological equilibrium in nature and contributes to the effective decomposition of pollutants without the formation of toxic and destructive products.

Various manifestations of the adaptation of organisms to stress factors are observed under the conditions of various factors. The manifestation of an active strategy for adapting microorganisms, which allows them not only to maintain viability but also to reproduce and develop in a wide range of environmental factors, is, in particular, their ability to direct their metabolic processes toward the synthesis and accumulation of individual metabolite, in the activation of nonspecific protective mechanisms, that is, to use their powerful potential – to produce important BAS.

Exopolysaccharides of microorganisms can be used as biosurfactants in the detoxification processes of soil contaminated with toxic metals and petroleum products. In recent decades, environmental measures have become widespread ways to use biological technologies that are most acceptable due to their environmental safety, low cost of work, and sufficiently high efficiency, which has been repeatedly demonstrated in solving various environmental problems. The metabolic versatility of these microorganisms plays an important role in important industrial processes as well as in the biological destruction of polluting substances.

Consequently, microorganisms resistant to petroleum products can be used in bioremediation processes, in treatment technology for wastewater, contaminated by petroleum products, etc. Technologies that can be used do not violate biological equilibrium in nature and allow to effectively decompose pollutants without the formation of toxic destructive products, restoring soil fertility.

It is known that most microorganisms form biofilms – more than 99% of all microorganisms on Earth coexist in such groups with different enzymatic activities and various adaptive properties. The expansion of data on the composition of biofilm groups is of great practical importance today in the use of such “biofilm” microorganisms in biotechnology.

## 5 Results and Discussion

During the first phase of the research, analyzing data from the Internet and using Maxar space imagery technology and scientific research, we discovered landfills containing transport infrastructure waste or the ones related to transport infrastructure (Fig. 1).

- Landfills near Boryspil International Airport (a – unauthorized, b – official)
- Landfill in Prolisky village, Boryspil district, Kyiv region
- Unauthorized landfill near the Energia garbage plant
- Waste field of military equipment on the territory of the Kyiv Armored Plant
- Waste field of cranes in the Holoziivskiyi district of Kyiv on the banks of the Dnipro River
- Waste field of buses and trolleybuses KP “Kyivpastrans” in the Darnytskyi district of Kyiv
- Waste field of abandoned cars in Desnianskyi District of Kyiv
- Solid household waste landfill No5, Pidhirtsi village, Obukhiv district

We have compiled a general map of the analyzed landfills of transport infrastructure in the Kyiv and Kyiv region, which is clearly shown in Fig. 1.

For all landfills, space images were analyzed and a map was drawn up. The data and the basic OpenStreetMap were applied (<https://www.openstreetmap.org>). For new, unauthorized landfills that were missing from OpenStreetMap, the authors added the geometry of landfills to its database. In addition, the specified database

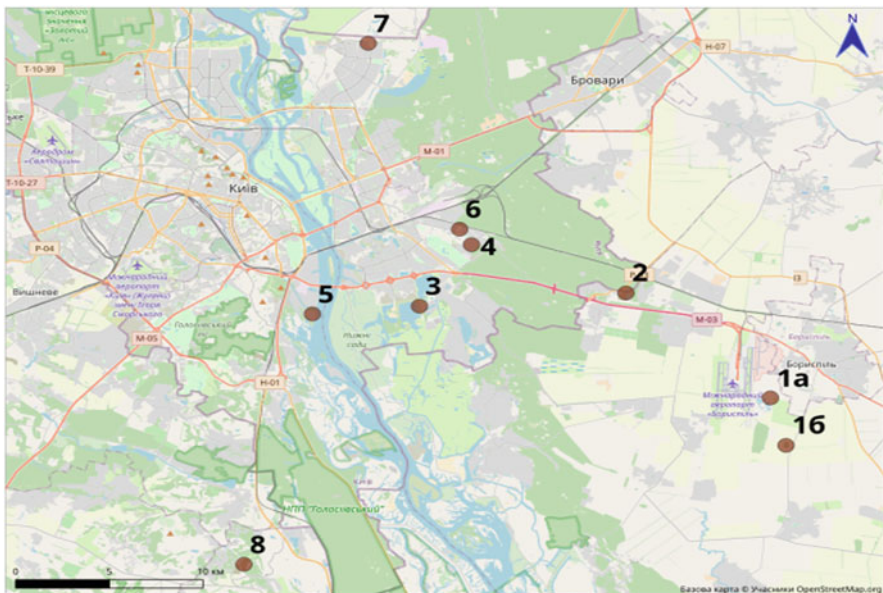


**Fig. 1** Landfills of transport infrastructure of Kyiv and Kyiv region

was supplemented with information about the areas around landfills (land use, roads) obtained by decryption of space images as well as from the information on land cadastre, allowing to draw up detailed maps even for those areas that had little information in the OpenStreetMap database (first of all, it was needed for the outskirts of Boryspil International Airport and the city of Boryspil).

During the second stage of research, we took samples from the landfills of transport infrastructure (shown in Fig. 1) for the taxonomic analysis of microorganisms.

To obtain the accumulative crops of microorganisms, samples were placed on the surface of agarized media: malt extract agar, malt agar (IEA, MA produced by Merck KGaA, Germany), nutrient agar (NA, Sigma), trypticase-soybean agar (TSA), Chapek-Dox agar, and potato glucose agar (KHA or PDA – potato dextrose agar) (HiMedia Laboratories). The release of pure crops of microorganisms from cumulative crops was carried out using standard microbiological cultivation methods on appropriate agarized nutrient media (IEA, PDA, Chapek-Docks).

Isolated pure cultures of microscopic fungi were identified with the help of determinants of domestic and foreign authors. The taxonomic analysis was carried out according to the IX edition of the “Dictionary of Fungi” ([www.Speciesfungorum](http://www.Speciesfungorum)).

As a result of the study, microorganisms capable of growth in the presence of diesel fuel were found in most of the samples studied. However, stable consortiums, microorganisms of which were capable of increasing biomass during five probations, were found in samples taken at a waste dump near the Boryspil airport. With the help of a microscopic study, it was found that consortiums were formed by static and active rod-like bacteria.

The static forms were located in the middle of a drop of diesel fuel, while the active forms either adhered to the outer part of the membrane or moved freely in the liquid between droplets of diesel fuel. We can assume that in sample 2PT, there are pleomorphic bacteria, and in samples 3PT, 4PT, and 5PT, there are capsule-forming, non-spore-forming bacteria that are capable of diesel fuel oxidation. In samples of 3VRZ, 4B, and 5B for 30–40 days of cultivation in the presence of diesel fuel, compact biofilms were formed, resembling a bacterial mat in structure. Bacterial mats are highly integrated microbial ecosystems with significant physicochemical gradients, which resemble the result of the metabolic activity of microorganisms.

During the cultivation of bacteria consortiums of samples 2PT, 3PT, 4 PT, and 5PT on the solid Tauson’s medium (Fig. 2), which contained 100 mkl of diesel fuel, the formation of a powerful bacterial culture in all the samples studied after 24 hours of cultivation at 28 °C was observed. Ten bacteria isolates were obtained from a bacterial consortium of sample 2PT. Their ability to assimilate diesel fuel in monoculture was tested. It was found that five of them could grow during cultivation on Tauson’s liquid medium, which contained 2–4% diesel fuel, which was confirmed by phase-contrast microscopy data and Gould’s sowing results on the R2A medium (Fig. 3).

According to morphological (Fig. 4) and tinctorial (Fig. 5) signs of the bacterium strain, 1–2 can be attributed to the group of corinomorphic bacteria, bacteria of other strains represented by gram-negative sticks. During the study of the ability of



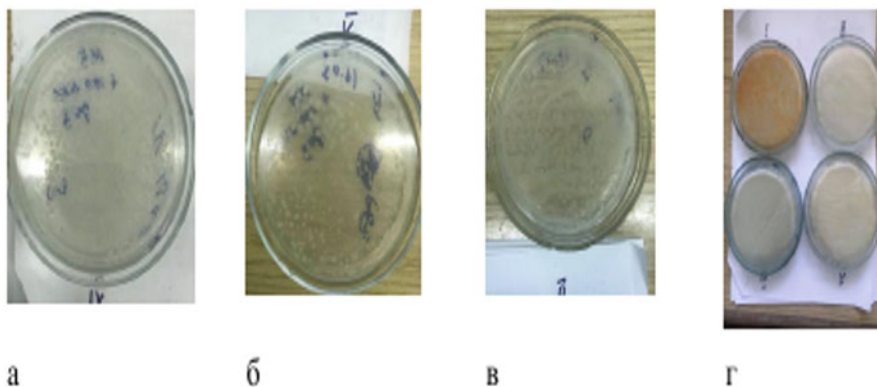


**Fig. 2** Cultivation of bacteria of consortiums 2-4PT on the agarized Tauson's medium in the presence of diesel fuel (explanation in the text)

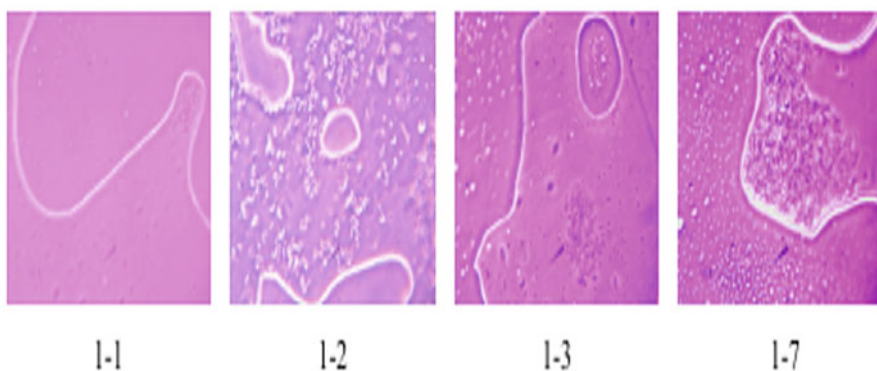


**Fig. 3** Interaction of monocultures of 2PT bacteria consortium with drops of diesel fuel for 4 days of cultivation at a temperature of 28 °C. Phase-contrast microscopy, increase in Ch1600

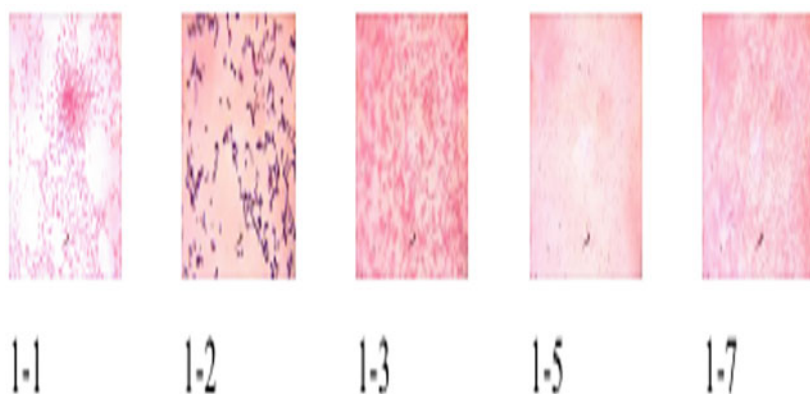


**Fig. 4** Morphological and tinctorial features of monocultures of bacteria isolated from the 2PT sample. R2A cultivation environment, 48 hours, 28 °C. Coloring by gram, light microscopy, magnification H1600

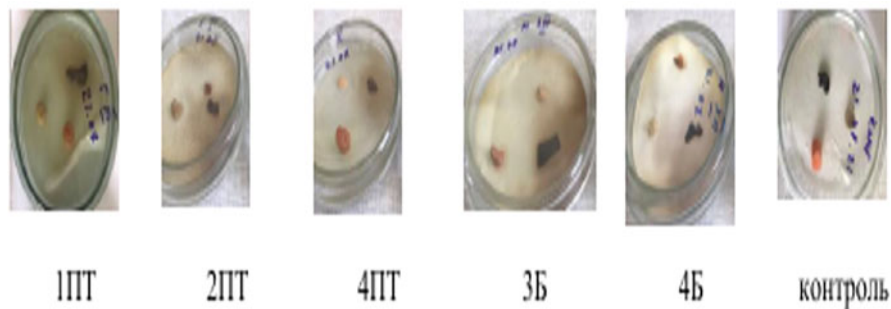


**Fig. 5** Maceration of plant and fungal tissue by consortia of microorganisms from transport waste dumps near the Boryspil airport and Boryspil Auto Plant

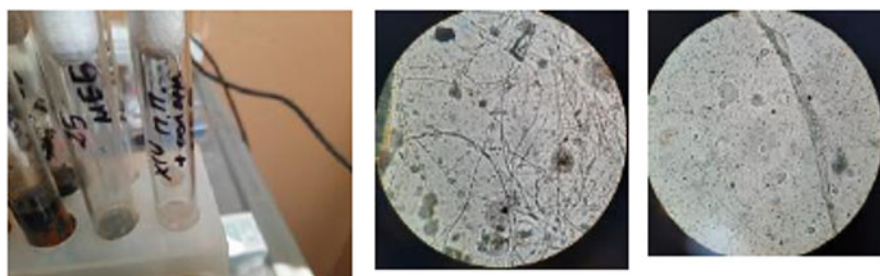


**Fig. 6** Microorganisms (microscopic fungi of *Cladosporium* and *Fusarium* genera) in sample No4B (XIV) (residue of spent motor oil from the landfill of Boryspil Auto Plant)

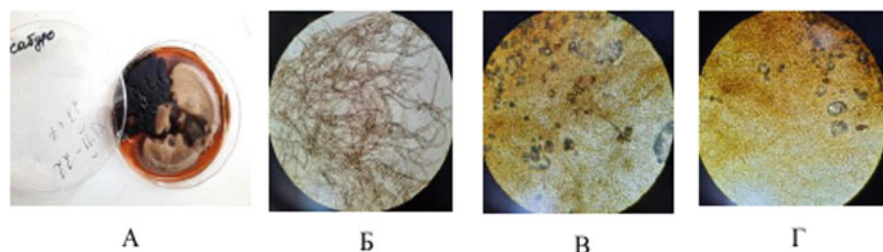


**Fig. 7** Microscopic fungi of the genus *Aureobasidium pullulans* (B) and *Alternaria cf. chlamydospore* (B, D) in sample No. 2B (XVII) (soil sample taken in the decomposition of automotive plastic parts from the landfill of Boryspil automobile plant). A – fungi cultures on the Saburo medium, B–G – increase  $\times 400$

microbial consortia to macerate fungal and plant tissue, stable consortia of bacteria were found in samples selected at the landfills of transport waste near the Boryspil airport and Boryspil Auto Plant. As you can see, hbcyre microorganisms participating in the iron cycle were found in most samples of a landfill of transport waste near the Boryspil airport and the landfill of the central railway station in Kyiv.

Microscopic fungi were identified with the help of the relevant determinants of domestic and foreign authors (Figs. 6 and 7). The taxonomic analysis was carried out

according to the ninth edition of the “Dictionary of Fungi.” This slide shows the families of fungi we have selected. These fungi can actively produce high-molecular-weight extracellular polysaccharides and important enzymes (amylase, xylanase, pectinase), which are widely used in biotechnology.

The analysis of the obtained results shows that microscopic fungi belonging to the following taxonomic groups were found in the samples: groups of the *Zygomycota phyla* (species of the genus *Mucor* and *Rhizopus*), *Basidiomycota phyla* (yeast fungi of the genus *Rhodotorula*), and *Ascomycota phyla* (species of genera *Eurotium*, *Monascus*, *Talaromyces*, etc., in particular substrate-specific fungus *Amorphotheca resinae* (modern synonym *Hormoconis (Cladosporium) resinae*). Representatives of the informal group anamorphic fungi, as well as the group of oomycetes (species of the genus *Phoma*), were also found in the studied samples (species of genera *Acremonium*, *Alternaria*, *Aspergillus*, *Aureobasidium*, *Cladosporium*, *Fusarium*, *Geomyces*, *Gliocladium*, *Exophiala*, *Penicillium*, *Trichoderma*, *Stemphylium*, *Ulocladium*, etc.)

During the third stage of research, we have improved the technological scheme of the process at the bio-remediation site of transport infrastructure waste landfills (Fig. 8).

We have investigated the landfill waste of the transport infrastructure of Kyiv and selected microorganisms, which we recommend to use for the treatment of landfills of transport infrastructure to implement the patented method.

For the destruction of diesel fuel, kerosene, and used oils: bacteria *Rhodococcus erythropolis*; fungi *Fusarium* sp. and their consortium; bacteria *Acinetobacter* sp.;

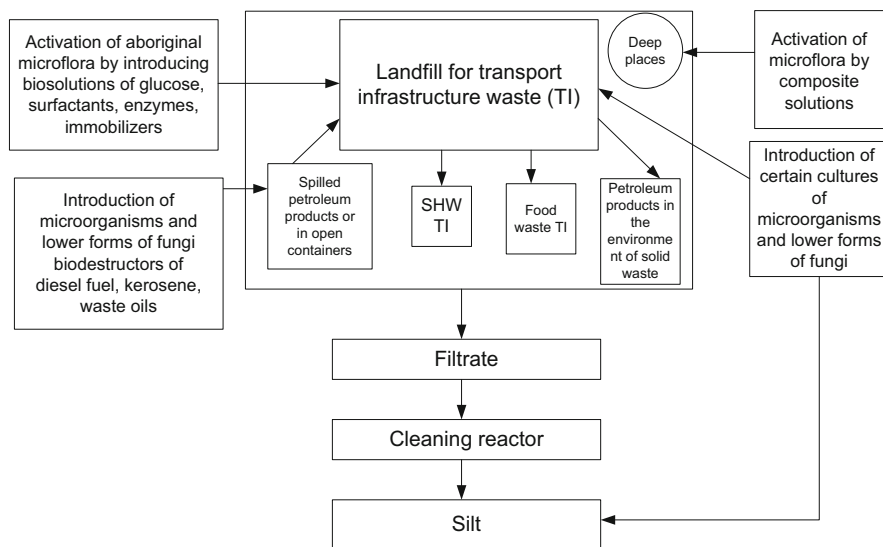


**Fig. 8** Technological scheme of the process at the bio-remediation site of transport infrastructure waste landfills

yeast *Candida maltosa*, bacteria *Dietzia maris*, and their consortium; and aboriginal forms of microorganisms.

To destruct various organic synthesis products: bacteria *Bacillus subtilis*; bacteria *Pseudomonas putida*, *Pseudomonas* sp., *Pseudomonas pseudoalcaligenes*, and *Pseudomonas aeruginosa*; a consortium of bacteria of the genera *Marinobacter*, *Halomonas*, and *Idiomarina*; bacteria *Halomonas* sp.; bacteria *Pseudonocardia dioxanivorans*; bacteria *Acinetobacter calcoaceticus* and *Achromobacter xylooxidans*; bacteria of the genera *Bacillus*, *Pseudomonas*, *Kocuria*, *Stenotrophomonas*, *Proteus*, and *Staphylococcus*; and yeast *Geotrichum* sp.

For the processing of solid food waste: bacteria *Bacillus cereus*; fungi of the genera *Aspergillus*, *Mucor*, *Penicillium*, and *Neurospora*; and fungi *Trametes versicolor*.

Processing of transport infrastructure landfills (by analogy, it is also possible for urban landfills) by microorganisms is recommended to be carried out once a season during the warm period.

The method in Fig. 8 is implemented as follows. First, aboriginal microflora is activated by bringing components to the landfill with the basic media – solutions of surfactants, glucose, and enzymes, creating an optimal environment for the development of microorganisms.

At the same time, mechanical fringing and injections to the soil of the landfill are carried out in separate deep places of composite solutions with the ability to provide an aerobic environment in closed layers. Next, a complex of certain cultures of microorganisms and lower forms of fungi is added to the body of the landfill. If there are large spots of spilled petroleum products (diesel fuel, kerosene, or used motor and transmission oils) at landfills, or if soil is saturated with petroleum products, contribute a complex of microorganisms and lower forms of petroleum products destructor fungi separately for these places, followed by soil slicing to a depth of 5–10 cm. In addition, certain cultures of microorganisms and lower forms of fungi are added to sediment silt.

## 6 Conclusion

Waste from landfills of transport infrastructure of Kyiv is investigated, and microorganisms, which we recommend using to neutralize petroleum products and solid organic waste, are separated.

For the destruction of diesel fuel, kerosene, and used oils: *Rhodococcus erythropolis* bacteria; *Fusarium* sp. fungi and their consortium; *Acinetobacter* sp.; *Candida maltosa*, *Dietzia maris* bacteria, and their consortium; and organic forms of microorganisms.

For the destruction of various organic synthesis products: bacteria *Bacillus subtilis*; bacteria *Pseudomonas putida*, *Pseudomonas* sp., *Pseudomonas pseudoalcaligenes*, and *Pseudomonas aeruginosa*; consortium of *Marinobacter*, *Halomonas*, and *Idiomarina* bacteria; bacteria *Halomonas* sp. and bacteria

*Pseudonocardia dioxanivorans*; bacteria *Acinetobacter calcoaceticus* and *Achromobacter xylosoxidans*; bacteria of the genera *Bacillus*, *Pseudomonas*, *Kocuria*, *Stenotrophomonas*, *Proteus*, and *Staphylococcus*; and yeast *Geotrichum* sp.

For the processing of solid food waste: bacteria *Bacillus cereus*; fungi of the genera *Aspergillus*, *Mucor*, *Penicillium*, and *Neurospora*; and *Trametes versicolor* fungi.

We have established that it is necessary to select strains/bacteria consortiums for the treatment of certain types of waste. From the microorganisms selected at the landfills of the transport infrastructure of Kyiv, those that are best suited for the destruction of petroleum products, products of organic synthesis, and processing of solid household waste are allocated. In general, it is impossible to establish any patterns; microorganisms need to be selected separately for each particular case. The information obtained will be useful in the selection of microorganisms for the processing of petroleum products, solid industrial, and food waste.

## References

- Boichenko, S. V., & Shkilniuk, I. O. (2021). *Cause-and-effect analysis of microbiological contamination of motor fuels and prospects for the rational use of biodegradation in the processes of recycling waste from the technosphere*. Development of scientific, technological and innovation space in Ukraine and EU countries. (3rd ed., pp. 1–19). Baltija Publishing. <https://doi.org/10.30525/978-9934-26-151-0>
- Hallenbeck, P. C. (2017). *Modern topics in the photo-trophic Prokaryotes* (p. 492). Springer International Publ.
- Patent 149576 IPC B09B 3/00 Method of bio-remedication of landfills of waste transport infrastructure / I.L. Trofimov, S.V. Boychenko, I.O. Kovshlyuk, A.V. Yakovleva // applications. 07.07.21.– Valid from 02.12.2021. 2015, 2015, in New No. 48, 2021.
- Roeselers, G., van Loosdrecht, M. C. M., & Muyzer, G. (2008). Phototrophic biofilms and their potential applications. *Journal of Applied Phycology*, 20, 227–235. <https://doi.org/10.1007/s10811-007-9223-2>
- Safi, J., Awad, Y., & El-Nahhal, Y. (2014). Bioremediation of Diuron in soil environment: Influence of cyanobacterial mat. *American Journal of Plant Sciences.*, 5, 1081–1089. <https://doi.org/10.4236/ajps.2014.58120>
- Trofimov, I. L., Boichenko, S. V., Shkilniuk, I. O., Shamanskyi, S. I., Yakovlieva, A. V., & Zelena, P. P. (2021). Vydilennia kompleksu ta chystykh kultur mikroorhanizmv, zdatnykh do destruktsii/dehradatsii vuhlevodniv naftoproduktiv ta tverdykh orhanichnykh vidkhodiv iz prob zvalyshch transportnoi infrastruktury m. Kyieva. Materialy Natsionalnoho forumu «Povodzhennia z vidkhodamy v Ukraini: zakonodavstvo, ekonomika, tekhnolohii». *Tom, I. S.* 88–94.
- Velykodskiy, Y. I., Trofimov, I. L., & Bojchenko, S. V. (2021). Monitoryng, kartografuvannya ta inventaryzaciya zvalyshh m. Kyieva ta Kyivskoyi oblasti, shho mistyat vidxody transportnoyi infrastruktury. *Naukoyemni tekhnolohiyi.*, #3, S. 245–S. 254. <https://doi.org/10.18372/2310-5461.51.15995>
- Volchenko, N. N., & Karaseva, E. V. (2006). Skrynynh uhlevodookysliashiushchykh bakteriyi – produktentov poverkhnostno-aktyvnykh veshchestv byolohycheskoi pryrody y ykh pryomeneny v opyte po remedyatsyy neftezahriaznennoi pochvy y nefeshlama. *Byotekhnolohiya.* №2. – s. 45–60.

# Investigation of Electromagnetic Effect of Lightning on Aircraft by Finite Element Method



Semen Memis, Ozcan Kalenderli, and Ozkan Altay

## Nomenclature

Al	Aluminum
E	Electric field intensity, V/m
E <sub>max</sub>	Maximum electric field intensity, V/m
PTFE	Polytetrafluoroethylene
Ti	Titanium

## 1 Introduction

Lightning causes dangerous events on aircraft (Rupke, 2006). Failure to protect against lightning can result in explosion/ignition of the fuel tank, damage to the radome (front-end part of the aircraft), radar and control surfaces, electrical power losses, damage to the avionics systems, and even loss of aircraft and life. The lightning protection is becoming crucial since aircraft safety is mostly dependent on avionics systems and the development of new materials to replace steel, aluminum, and titanium (Petrov et al., 2012).

The highest electric field intensities occur in the areas where the equipotential lines are closest to each other and the radius of curvature is small, such as the radome, wing, tail, and antenna of the aircraft (Rupke, 2002).

---

S. Memis (✉) · O. Altay  
Turkish Aerospace, Ankara, Türkiye  
e-mail: [semen.memis@tai.com.tr](mailto:semen.memis@tai.com.tr)

O. Kalenderli  
Istanbul Technical University, Department of Electrical Engineering, Maslak, Istanbul, Türkiye  
e-mail: [kalenderli@itu.edu.tr](mailto:kalenderli@itu.edu.tr)

The ARP 5414B (Aircraft Lightning Zone) standard of SAE, which is used to determine lightning zones on aircraft, is not detailed enough. It is insufficient in new-generation aircraft with different geometry, engines, or fuselage materials (ARP, 2018). The lightning strike zones are dependent on aircraft shape, materials, and operational factors.

Finite element model is used to evaluate the electric field intensity on the aircraft. In this study, lightning is modelled considering cloud and earth to be a parallel plate electrode system. Change in the electric field with respect to electric voltage and aircraft position is analyzed by COMSOL (Semen, 2019).

## 2 Model

In order to examine the interactions of lightning strike and aircraft during flight, a three-dimensional electric field simulation model was created and analyzed. The modeled electrical structure is a uniform field, disc-shaped, plane-plane electrode system in which the cloud and ground are a plane electrode (5 km in a diameter) (Fig. 1).

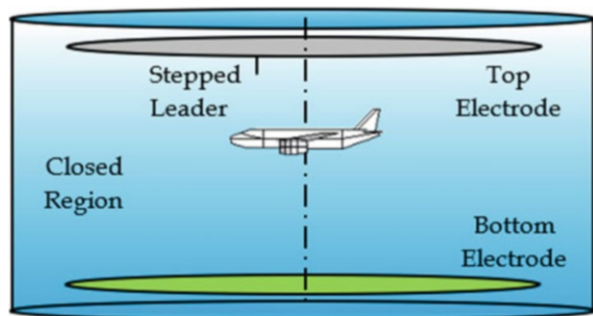
An external cylinder was used in the simulation to make the solution with finite element methods. The cloud potential is assumed as 100 MV and the ground potential as 0 V. The distance between the two plane electrodes was taken as 4 km. The stepped leader attaches to regions where the radius of curvature of the aircraft is small. The model given in Fig. 1 has been considered in the problem definition.

The dimensions of the aircraft used in the model are shown in Fig. 2.

As the second process, the materials in the model were defined. Different types of materials are used in the aircraft. Figure 3 shows the materials used in the aircraft and the regions where they are used (blue regions in the figure).

The mesh used in the model is shown in Fig. 4.

**Fig. 1** Problem structure for COMSOL



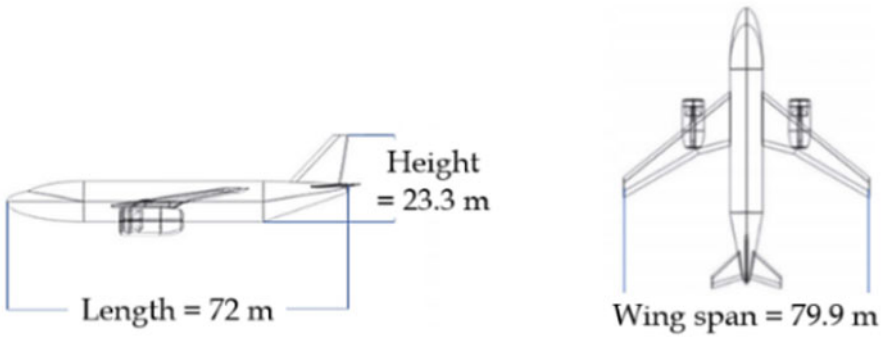


Fig. 2 The dimensions of aircraft used in the model

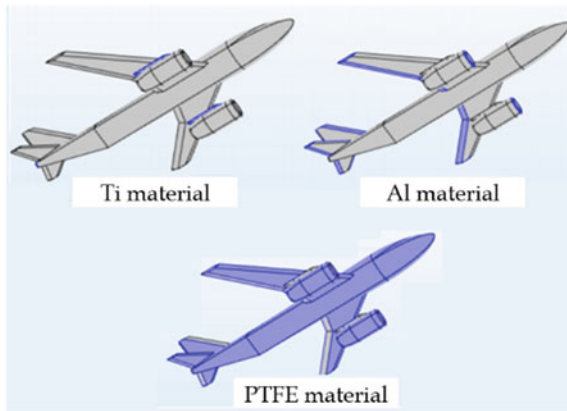


Fig. 3 The material properties on the aircraft

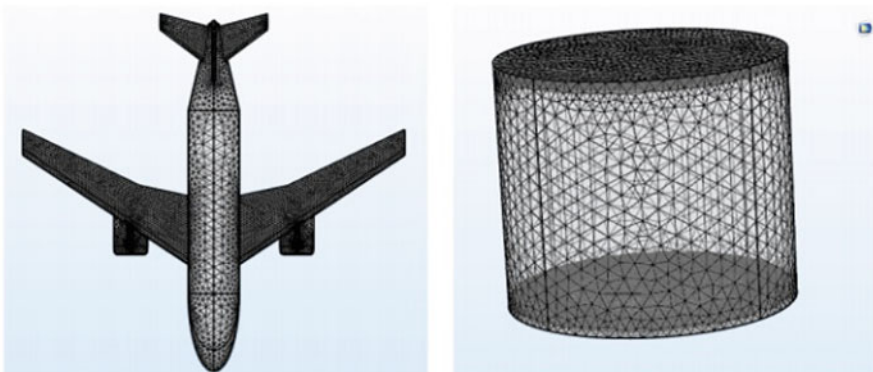


Fig. 4 Finite element mesh used in this study



### 3 Results and Discussion

Depending on the cloud potential, the change in the electrical potential of the aircraft was investigated. The variation of the electrical potential values on the aircraft when the cloud potential is changed between 10 MV and 100 MV is given in Fig. 5.

The electric field distribution obtained when the distance between the lightning cloud and the aircraft is 400 m and the aircraft is 3.6 km above the ground level is shown in Fig. 6. Cloud potential is taken as 100 MV. The potential on the aircraft is calculated as 90 MV.

It was observed that the electric field intensity was maximum at the sharp corners. The maximum electric field intensities on the aircraft tail, engines, wing, and radome are given in Table 1.

Also, the electric field intensity values have changed according to the flight position of the aircraft. The variations in the electric field intensity in the aircraft zones due to pitch and roll angles (Fig. 7) are not the same for each aircraft zone.

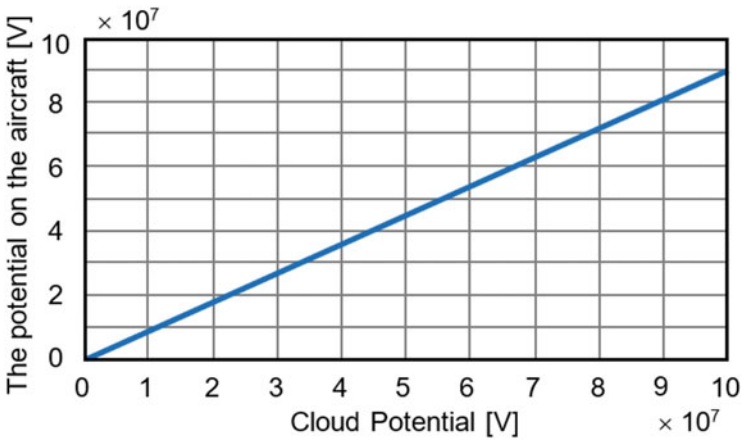


Fig. 5 The variation of the electrical potential on the aircraft with the cloud potential

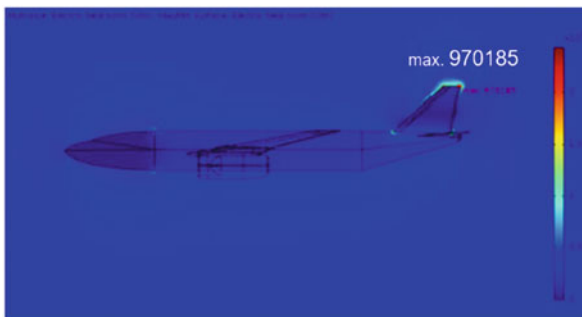
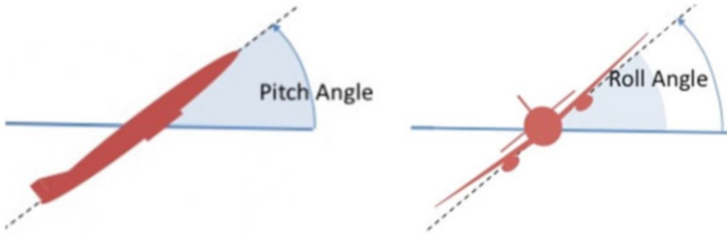


Fig. 6 Distribution of electric field intensity on the aircraft (in the yz-axis)

**Table 1** Electric field distribution on aircraft zones with respect to cloud potential

Cloud potential (MV)	100
The voltage on the aircraft (MV)	90.1
The maximum electric field on the aircraft tail (kV/m)	970.2
The maximum electric field on the aircraft engines (kV/m)	235
The maximum electric field on the aircraft wing (kV/m)	130
The maximum electric field on the aircraft radome (kV/m)	93.2



**Fig. 7** Pitch and roll angles for an aircraft (<https://www.skybrary.aero>, 2021)

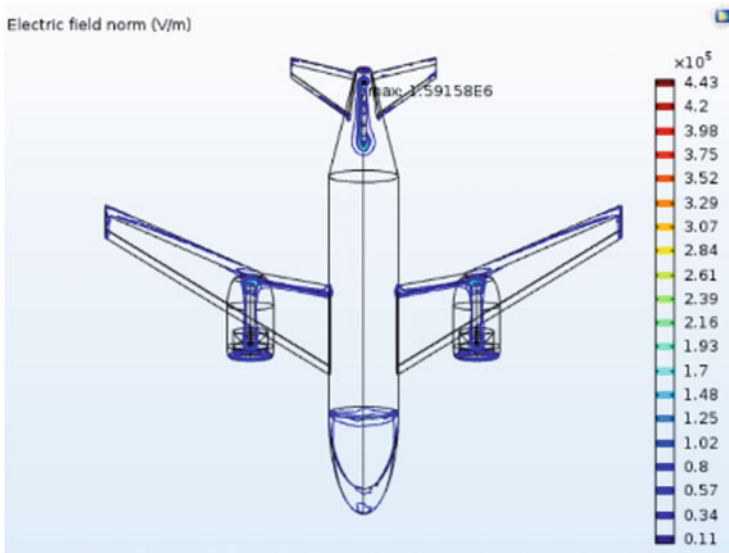


**Fig. 8** Electric field distribution on aircraft with 15 pitch degree

When the pitch angle is selected 15°, the electric field distribution on the aircraft tail is given in Fig. 8.

The pitch angles of the aircraft are selected as 15°, 20°, 25°, and 30° toward the ground. The maximum electric field intensities on the aircraft tail with the cloud potential for different pitch angles are given in Fig. 9.

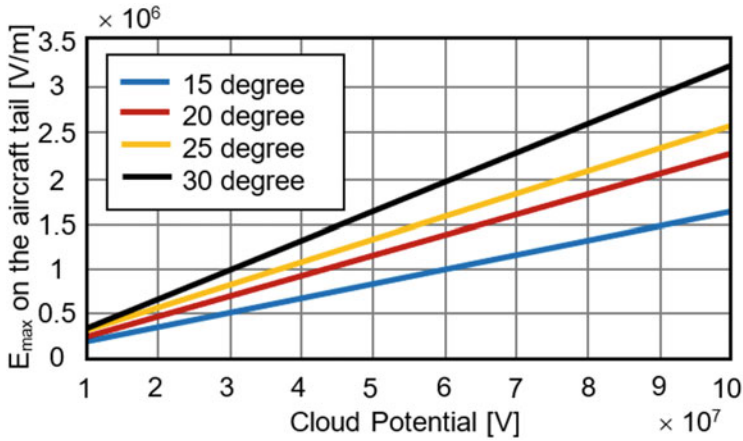


**Fig. 9** The variation of maximum electric field intensity on the aircraft tail with the cloud potential for four different pitch angles of the aircraft

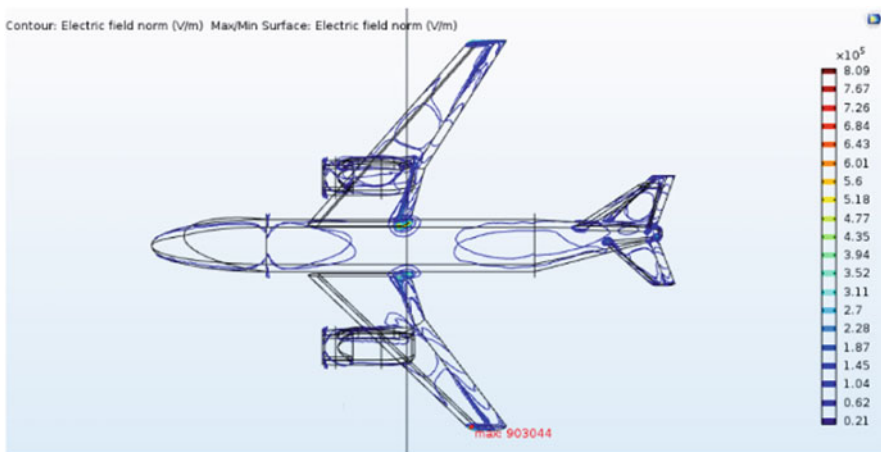


**Fig. 10** Electric field distribution on aircraft with 45 rolling degree

When the pitch angle is set to 30 degrees toward to ground, the maximum electric field density in the aircraft tail is  $3.20 \times 10^6$  V/m, the maximum electric field density in aircraft engines is  $1.5 \times 10^6$  V/m, the maximum electric field density in aircraft wings is  $4.49 \times 10^5$  V/m, and the maximum electric field density in aircraft radome is  $2,58 \times 10^5$  V/m.

The angles of rolling are then changed to 45°, 60°, and 75°, respectively. When the roll angle is selected as 45°, the maximum electric field distribution on aircraft wing is given in Fig. 10.

The maximum electric field intensities ( $E_{max}$ ) on the aircraft wings with respect to roll angles are given in Fig. 11.

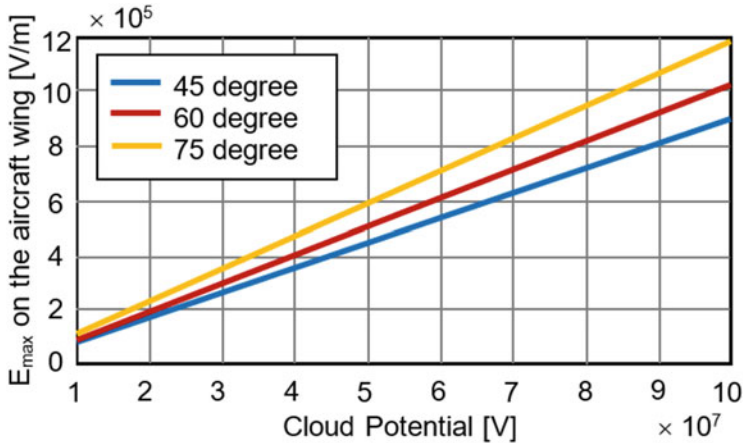


**Fig. 11** The variation of maximum electric field intensity on the aircraft wing with the cloud potential for three different roll angles of the aircraft

When the rolling angle is set to 75 degrees, the maximum electric field density in the aircraft tail is  $7.8 \times 10^5$  V/m, the maximum electric field density in aircraft engines is  $1.2 \times 10^6$  V/m, and the maximum electric field density in aircraft wings is  $1.18 \times 10^6$  V/m.

## 4 Conclusions

In COMSOL, the electric field intensity on the aircraft was calculated by changing the voltage of the lightning cloud from 10 MV to 100 MV. It was observed that the maximum electric field intensity and electrical potential values on the aircraft increased linearly with the increase in the potential of the lightning cloud.

Electric field intensity values were calculated separately for the regions where the radius of curvature of the aircraft is small, such as the tail, wing, engines and radome. It has been observed that the most critical electric field intensity for the aircraft occurs during the pitching motion of the aircraft in the take-off (and thus in the landing).

It is found that the maximum electric field intensities on the aircraft increase linearly with the increase of the potential of the lightning cloud. It has been observed that the rolling and pitching movements of the aircraft increase the probability of lightning strikes to the aircraft.

The use of non-conductive materials in the aircraft fuselage increases the direct and indirect effects on aircraft. Due to the increased lightning effects, the lightning protection levels of aircraft should be increased. Careful screening, grounding, and use of surge suppression devices and electric static discharger can reduce or prevent problems from lightning strike. The results of the simulations can be used in aircraft lightning strike risk assessment studies during design phases.

## References

- Petrov, N. I., Haddad, A., Petrova, G. N., Griffiths, H., & Waters, R. T. (2012). Study of effects of lightning strikes to an aircraft (Chapter 22). In R. K. Agarwal (Ed.), *Recent advances in aircraft technology* (pp. 523–544). N.I. Petrov and R.T. Waters.
- Rupke, E. (2002). *Lightning direct effects handbook*. Lightning Technologies.
- Rupke, E. J. (2006, Aug 14). What happens when lightning strikes an airplane. *Scientific American Newsletters*.
- SAE Aerospace Recommended Practice (ARP) 5414B. (2018). *Revision B - aircraft lightning zone*. SAE Aerospace standard.
- Semen, M. (2019). *The analysis of Lightning Strike effects on aircrafts by finite element method*, M. Sc. Thesis, ITU Graduate School of Science, Engineering and Technology, December 2019. <https://www.skybrary.aero>, accessed on August 15, 2021.

# Research of Tribological Characteristics of Modern Aviation Oils



Oksana Mikosianchyk and Olga Ilina

## Nomenclature

HS	Hydraulic system
SWF	Specific work of friction

## 1 Introduction

Ensuring the highest reliability indicators at all stages of the aircraft life cycle is directly related to the issues of quality control, diagnosis, preventive maintenance, and repair of aircrafts. The role of the problem of ensuring the reliability of modern aircrafts is growing due to their complexity, constant increase in loads, and intensity of use, significantly expanding the range of operation conditions and areas of application and the increasing level of aircraft automation. One of the most important issues in ensuring the reliable operation of aircraft units is using high-quality lubricants. Qualitative analysis of aviation lubricants is an important tool for aircraft maintenance, which should be based on specially developed test methods for assessing their physical, chemical, and operation characteristics. An important aspect of assessing the quality of aviation lubricants is related to expansion of the standardized list of their indicators, which include tribological properties of lubricants (Mnatsakanov et al., 2021). The improvement of the latter should primarily be aimed at protecting the main functional components and mechanisms from premature wear, deformation, and corrosion.

---

O. Mikosianchyk (✉) · O. Ilina  
Department of Applied Mechanics and Materials Engineering, National Aviation University,  
Kyiv, Ukraine

### ***1.1 The Influence of the Quality of Hydraulic Oils on the Reliability of the HS of Aircrafts***

Hydraulic units and devices are widely used in modern aircraft. The aircraft's HS provides control of systems and mechanisms that determine flight safety. HSs are designed to control the stabilizer and rudders, to clean and release the chassis, takeoff and landing machinery, etc. The main disadvantage of HS is the work of the system units under high pressure: as such, it increases the wear of parts, which results in contamination of the working fluid, so the HS must be subjected to timely maintenance.

The HS performance and reliability are significantly affected by the properties of the working fluid. Oils for aviation HS must have an optimal level of viscosity, high viscosity-temperature properties in a wide range of temperatures, oxidation resistance, and anti-foam properties. In addition, they must exhibit high tribological characteristics and be compatible with the structural and sealing materials of the components and units of the HS. Reduced viscosity of hydraulic oil causes intense manifestation of fatigue wear of contacting parts of the HS. Increased viscosity significantly increases the mechanical losses of the drive, complicates the relative movement of pump parts and valves, and makes it impossible to operate HS at low temperatures.

The paper (Obergruber et al., 2018) has analyzed the properties of hydraulic fluids used in A320 aircrafts and provided recommendations for determining the interval of their replacement. However, studies of the quality of oils were based on the assessment of physicochemical parameters of lubricants, such as acid number, density, presence of impurities, and kinematic viscosity of oils. However, the given recommendations on the terms of replacement of hydraulic oils do not include assessment of tribological indicators of the materials considered.

It has been established that AMG-10 oil, like other hydraulic fluids with a thickener of the base fraction, undergo mechanical destruction during operation, which leads to a decrease in their viscosity (Shumilov et al., 2014). The intensity of mechanical destruction depends on the operation conditions – temperature and pressure in the system (and the nature of pressure changes during operation) – as well as on the design of the pump, its performance characteristics, and the volume of the working fluid. In the HSs of modern aircrafts, the service life of AMG-10 oil is much reduced and can be a little more than 100–200 h. Currently, the operation of AMG-10 oil lasts until the drop in its kinematic viscosity at 50 °C to 7 mm<sup>2</sup>/s and the appearance of mechanical impurities in it above the allowable quantities.

Studies for the operational state of aviation hydraulic fluids from phosphoric acid esters based on the principle of probing with using nondestructive infrared absorption have resulted in obtaining the FTIR spectra of absorption lines, depending on the type of pollution (Paul, 2014).

An important factor in ensuring the high performance of friction units is the proper choice of lubricants with high lubrication, antifriction, and antiwear characteristics (Mikosyanchyk et al., 2019). The analysis of publications on the assessment

of these characteristics of oils for HSs showed that comprehensive research in this direction has not yet been carried out. Among various producers of commercial batches of oils, it is important to choose a lubricant that meets not only the required physical and chemical characteristics but also has efficient tribological properties. However, tribological indicators are not standardized for a wide range of lubricants. Therefore, the development of methods for assessing the quality of lubricants in tribological contacts is an important area of research, the results of which may provide recommendations for efficient performance of oils in certain operation modes.

## 2 Method

The study of the oil samples was carried out on a software-hardware complex designed to evaluate the tribological characteristics of triboelements, for which a special software had developed for stepper engine control and online visual evaluation of the kinetics of changes in the main tribological parameters of tribocontact (Mikosyanchik & Mnatsakanov, 2017).

On the software-hardware complex with using a roller analogy, the operation of gears in the conditions of rolling with sliding was modeled. The test oils are as follows: sample 1 is oil “Bora B” AMG-10 according to TU U 19.2-38474081-010: 2016 with change 1 (produced by Bora B LLC, Ukraine); sample 2 is AMG-10 oil according to GOST 6794-75 with changes 1–5 (produced by LLC NPP Kvalitet).

Rollers from steel 30HGSA (HRC 48–52, Ra 0.34  $\mu\text{m}$ ) were used as a material of contact surfaces. Lubrication of contact surfaces was made by immersing the lower roller in a bath of oil.

The study was carried out in nonstationary conditions, which provide cyclic repetition in the start-stationary operation-braking-stop mode. The total duration of the cycle is 80 s.

The maximum speed was 700 rpm for the leading surface and 500 rpm for the lagging surface, while slippage was 30%. The maximum contact load according to hertz is 200 MPa. The total number of cycles in the experiment is as follows: 100 cycles (from the 1st to the 45th cycle at oil temperature 20 °C, from 46 to 50 cycles while heating oil, from 51 to 100 cycles at oil temperature 100 °C).

## 3 Results and Discussion

The studied samples of oils are characterized by effective antifriction characteristics. Sample 1 and sample 2 show high running properties. For sample 1, the average values of the coefficient of friction are 0.012 and 0.013 at an oil temperature of 20 and 100 °C, respectively; the coefficient of friction is stable, and the range of oscillations of this parameter is within 0.01 ... 0.02. Its increase by 1.17 times



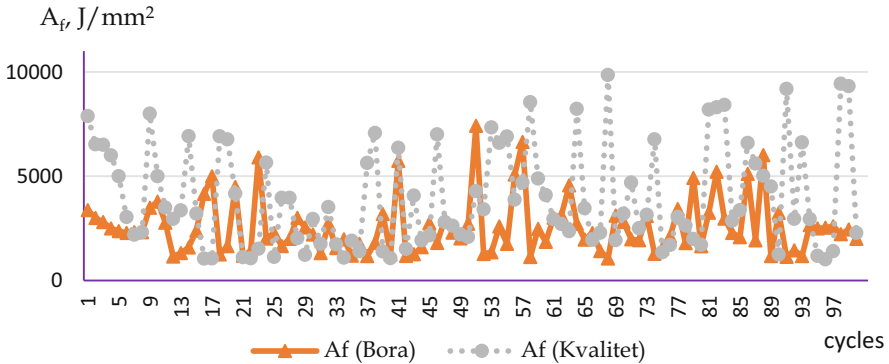


**Fig. 1** The kinetics of changes in SWF ( $A_f$ ) during system operation

during 45–49 cycles is due to the change in the nature of the boundary layers with increasing lubricant temperature. Further stabilization of the coefficient of friction indicates the effective structural adaptability of the tribocontact in nonstationary operation conditions. For sample 2, the average values of the coefficient of friction are 0.0129 and 0.0148 at an oil temperature of 20 and 100 °C, respectively. Thus, at 20 °C, the coefficient of friction is close to that for sample 1, but with rising oil temperature to 100 °C, it is 1.13 times higher than that for sample 1. The increase in oil temperature leads to an increase in the coefficient of friction by 1.46 times during 45–49 cycles of operation. Its abrupt increase to 0.019–0.021 in 10% of the operating cycles indicates the destruction of the boundary layers of the lubricant and the transition of the tribosystem to a semidry mode of lubrication.

An important operation indicator of a tribological contact, which characterizes its dissipative processes and energy load, is SWF ( $A_f$ ).

The obtained experimental values of  $A_f$  for sample 1 in the range 1055–7419 J/mm<sup>2</sup> characterize the operation conditions of the tribosystem with moderate manifestation of energy processes in tribological contact (Fig. 1). With an increase in oil temperature from 20 to 100 °C, that is, with the transition of the tribosystem to more complex conditions of friction, SWF increases slightly, on average, by 1.1 times, and no failure of the lubrication layer occurs. Therefore, the investigated lubricant under such conditions provides predominantly the mixed mode of lubrication at start-up.

For sample 2, SWF for the contact in the initial period of running up to five cycles is at the level of 7880–5000 J/mm<sup>2</sup>, which doubles the same parameter for sample 1. With further operation at 20 °C, SWF reaches, on average, 3578 J/mm<sup>2</sup>, which is 1.49 times higher as compared to sample 1. Under rising oil temperature to 100 °C, SWF increases slightly and equals, on average, 4329 J/mm<sup>2</sup>, which is 1.62 times higher than for sample 1. Also, periods of rapid  $A_f$  increase in contact by 2...3.5 times were recorded, which indicates the intensification of energy processes both at the lubricant-metal boundary and in the surface metal layers. These processes usually lead to intensification of wear of friction pairs, which, in turn, is the main prerequisite for reducing the service life of the tribosystem as a whole.

The total linear wear of 30HGSA steel rollers is 2.31 and 3.63  $\mu\text{m}$  for lubrication friction pairs with oil sample 1 and sample 2, respectively. When using oil sample 2, the wear of friction pairs increases by 1.57 times as compared to sample 1. The wear of the lagging surface is 1.29 (sample 1) and 1.2 (sample 2) times that of the leading surface, which is due, according to K.T. Trubin's theory, to reducing the endurance limit of the lagging surface because of the increase in the rate of fatigue failure in the conditions of different directions of friction forces in contact on the leading and lagging surfaces.

The wear intensity of both leading and lagging surfaces is characterized by low values, which indicates high wear resistance of contact surfaces and effective antiwear characteristics of the studied oils. When friction pairs were lubricated with sample 2, the wear intensity of the leading and lagging surfaces increases by 1.63 and 1.52 times, respectively, compared to sample 1.

The change in the microhardness of the surface layers of steel 30HGSA during 100 cycles of operation depends on the type of test material and differs in the implementation of oppositely running processes. When using sample 1, hardening of both leading and lagging surfaces was recorded. In particular, the microhardness of the metal surface layers increased by 512 and 517 MPa for the leading and lagging surfaces, respectively. As for sample 2, the metal surface layers were softened for the leading surface (the decrease in microhardness after the epy operation was 696 MPa), whereas for the lagging surface, they were hardened (increased microhardness after the operation was 444 MPa).

According to the receipts of the producers of samples 1 and 2, they have identical base (mineral oil based on deeply dearomatized low-solidification fraction, which is obtained from hydrocracking products of a mixture of paraffinic oils and consists of naphthenic and isoparaffinic hydrocarbons) and a densifying additive, a special oil-soluble red dye. The producer of test sample 1 indicates the presence of a complex of multifunctional additives in the oil, whereas the producer of sample 2 indicates the presence of an antioxidant additive only.

It is the composition of the active components of the additives of samples 1 that influences the kinetics of changes in the microhardness of the surface layers due to their activation during friction. The additives present in sample 1 are characterized by more effective antiwear properties and cause an increase in the wear resistance of contact surfaces in conditions of rolling with slipping.

The performed analysis of the main tribological characteristics of the studied hydraulic oils has identified the most significant indicators that affect the linear wear of contact surfaces. Since the experiments were conducted in nonstationary conditions of friction, the variability of the indicators depending on the operating cycles, the range of change of each parameter was analyzed. The most influential of them are the maximum SWF ( $A_{fmax}$ ), the minimum coefficient of friction ( $f_{min}$ ), the minimum effective viscosity of the oil in contact ( $\eta_{ef,min}$ ), and the minimum thickness of the boundary layers of lubricant ( $h_{bmin}$ ) and oil temperature ( $t$ ). The empirical dependence of the linear wear of friction pairs ( $I$ ) on the above parameters is obtained as follows:

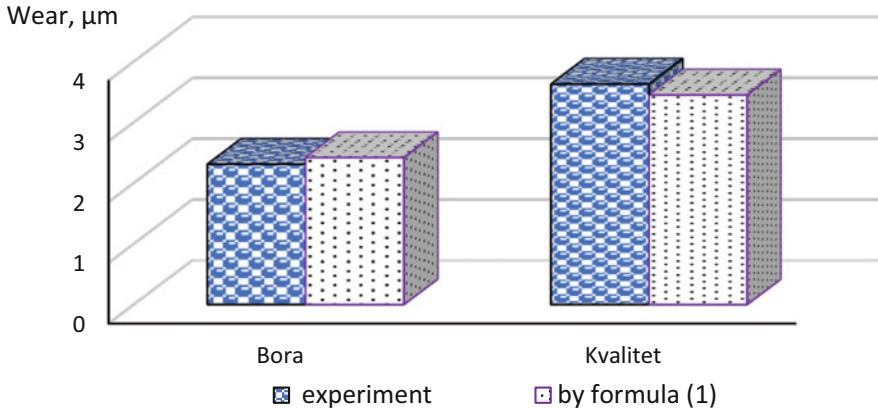


**Fig. 2** The total linear wear of the leading and lagging surfaces lubricated with hydraulic oil AMG-10 from the producers Bora and Kvalitet

$$I = (A_{\text{fmax}}^{0.6} \times f_{\text{min}}) / (\eta_{\text{ef. min}}^{0.125} \times h_{\text{bmin}}^{0.5} \times t^{0.18}) \quad (1)$$

The calculated values of linear wear of contact surfaces in nonstationary friction conditions, obtained by formula (1), are presented in Fig. 2.

A good enough convergence of measurement results (95–97%) of experimental wear parameters of steel 30HGSA lubricated with hydraulic oil AMG-10, alongside with the assessment of wear by the empirical calculation formula, allows one to predict the antiwear properties of lubricants in nonstationary conditions of the tribosystem operation.

## 4 Conclusion

The present research on the software-hardware complex using a roller analogy has simulated the operation of gears in rolling conditions with sliding. The discrepancy from the obtained experimental values of the studied indicators is in the range of 7–10%. The sample of the oil Bora B AMG-10 (producer LLC Bora B, TU U 19.2-38474081-010: 2016) is characterized by more effective tribological characteristics in nonstationary conditions of friction in the mode of rolling with 30% sliding in comparison with AMG-10 oil (producer LLC NPP Kvalitet, GOST 6794-75) according to the following characteristics:

1. *Antifriction properties.* For Bora B oil AMG-10, the average values of the coefficient of friction are 0.012 and 0.013 at 20 and 100 °C, respectively; the coefficient of friction is stable.
2. *Energy characteristics.* The SWF in frictional contact when using oil Bora B AMG-10 is in the range of 1055–7419 J/mm<sup>2</sup>, which characterizes the operation

conditions of the tribosystem with moderate manifestation of energy processes in the tribological contact.

3. *Antiwear characteristics.* The additives present in Bora B oil AMG-10 are characterized by more effective antiwear properties and an increase in the wear resistance of contact surfaces in conditions of rolling with slipping due to the hardening of the surface layers of the metal during operation.

Based on the analysis of the main tribological characteristics of the studied hydraulic oils, the most significant indicators influencing the linear wear of contact surfaces have been determined, and an empirical dependence of the linear wear of friction pairs has been obtained.

## References

- Mikosyanchik, O. A., & Mnatsakanov, R. G. (2017). Tribological characteristics of cast iron with a steel coating in lubrication medium under unsteady modes. *Journal of Friction and Wear*, 38(4), 279–285.
- Mikosyanchyk, O. O., Mnatsakanov, R. H., Lopata, L. A., Marchuk, V. E., & Yakobchuk, O. E. (2019). Wear resistance of 30KhGSA steel under the conditions of rolling with sliding. *Materials Science*, 55(3), 402–408.
- Mnatsakanov, R. G., Mikosianchyk, O. A., Yakobchuk, O. E., & Khalmuradov, B. D. (2021). Lubricating properties of boundary films in tribosystems under critical operation conditions. *Journal of Machinery Manufacture and Reliability*, 50(3), 229–235.
- Obergruber, M., Hönl, V., Procházka, P., & Táborský, J. (2018). Diagnostics of hydraulic fluids used in aviation. *Agronomy Research*, 16(S1), 1133–1141.
- Paul, S. (2014). *Optochemical sensor systems for aerospace applications*. Vollständiger Abdruck der von der Fakultät für Physik der Justus Liebig Universität. Gießen zur Erlangung des akademischen Grades eines.
- Shumilov, I. S., Chursova, L. V., & Sedova, L. S. (2014). Process fluids of aero-HSs and their properties. *Science and Education of the Bauman MSTU*, EL №.FS77-48211, 187–226.

# Evaluation of Nanostructured Materials: PEM Fuel Cell Applications



Murat Ayar, Ozge Yetik, and T. Hikmet Karakoc

## Nomenclature

AHP                      Analytic hierarchy process  
PEMFC                  Proton exchange membrane fuel cells

## 1 Introduction

The energy demand increases day by day due to the increasing population and the increasing needs in parallel. Today, this demand is provided mainly by fossil fuels. However, it is emphasized that the emissions of fossil fuels cause global warming and reduce the quality and duration of life in the world. For this reason, researchers are turning to sustainable and green alternative energy sources.

---

M. Ayar (✉)

Department of Airframe and Powerplant Maintenance, Eskisehir Technical University,  
Eskisehir, Türkiye

e-mail: [muratayar@eskisehir.edu.tr](mailto:muratayar@eskisehir.edu.tr)

O. Yetik

Mechanical Engineering Department, School of Engineering and Architecture, Osmangazi  
University, Eskisehir, Türkiye

e-mail: [oyetik@ogu.edu.tr](mailto:oyetik@ogu.edu.tr)

T. H. Karakoc

Department of Airframe and Powerplant Maintenance, Eskisehir Technical University,  
Eskisehir, Türkiye

Information Technology Research and Application Centre, Istanbul Ticaret University, Istanbul,  
Türkiye

e-mail: [hkarakoc@eskisehir.edu.tr](mailto:hkarakoc@eskisehir.edu.tr)

Among the alternative energy sources, fuel cells stand out with the advantages of zero pollution and broad applications (Zhong et al., 2010). In addition, technical features, high electrical efficiency and fuel flexibility possibilities, and their usability in many areas are being investigated (Abdalla et al., 2018). Technologies with a clean energy conversion and storage capability with almost no environmental impact and higher practical efficiency are seen as an urgent need from the sustainability framework (Kumar & Pillai, 2014). When it comes to fuel cells, low-cost and durable materials have received increasing attention in energy storage and conversion research areas (Liu et al., 2018).

Fuel cells are systems that convert the chemical energy of substances into electrical energy by electrochemical methods. Generally, a fuel cell consists of an anode and a cathode separated by an electrolyte that acts as an ion carrier (Mainardi & Mahalik, 2006). To date, polymer electrolyte membrane fuel cells (PEMFCs) and solid oxide fuel cells (SOFCs) stand out as the most essential and promising options for broad mobile and stationary use. Therefore, PEMFCs and SOFCs are currently the most researched fuel cell technologies (Fan et al., 2018).

With technology development, researchers have achieved significant leaps for proton exchange membrane fuel cells (PEMFCs). Despite this, PEMFCs still have disadvantages such as low power density and fuel usage, related to poor reaction kinetics and methanol permeability through the membrane, respectively. Due to nanomaterials' distinctive physical and chemical properties, it is thought that PEMFCs can remedy these shortcomings (Zhang et al., 2018). Thanks to the properties of nanostructured materials, lighter, thinner, and cheaper electrodes that are more efficient than ordinary electrodes can be made (Ese & Afrand, 2020). The use of nanomaterials in PEMFCs, while improving material efficiency due to their large surface area, may also cause disadvantages such as affecting lifetime and stability (Ellingsen et al., 2016).

The motivation of this study is that PEMFCs will have an important place in the future, especially in mobile energy needs, and that nanomaterials will remedy the bottlenecks of fuel cells. For this purpose, a comparison of the nanomaterials used in PEMFC fuel cells was made within the framework of sustainability. This study provides information about the comparison and properties of nanostructured materials to be used in fuel cells with multi-criteria decision-making method.

## 2 Method

The Analytical Hierarchy Process is a mathematical theory used for measurement and decision making, developed by Thomas L. Saaty in the mid-1970s (Saaty & Niemira, 2006). The preparation stages before the AHP method and the steps of applying the method are briefly shown in Fig. 1.

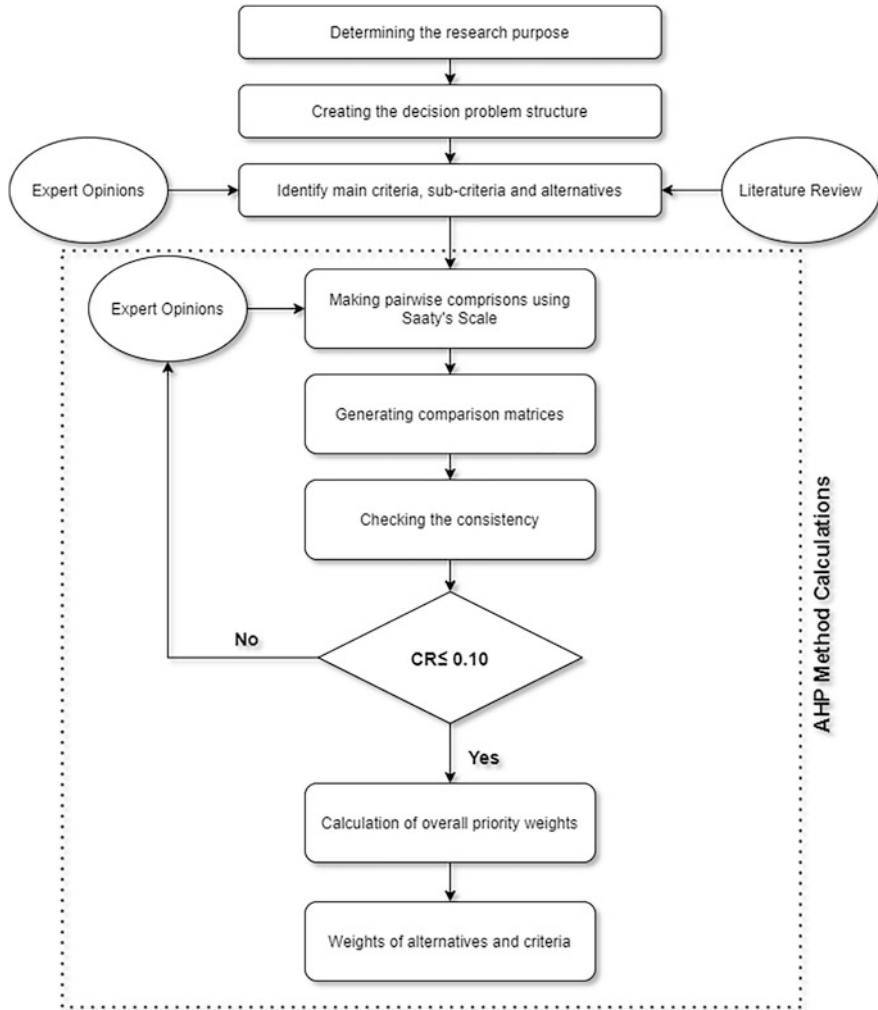


Fig. 1 Steps of the AHP method

In order to make a comparison of nanostructured materials, first of all, the essence of the study was brought into a decision problem structure. The decision problem was identified as “Which Nanostructured Material is most suitable for PEM Fuel Cells.” In the next stage, alternatives and criteria were determined. The decision problem structure to be used in the AHP method, which emerged after these stages, is shown in Fig. 2.

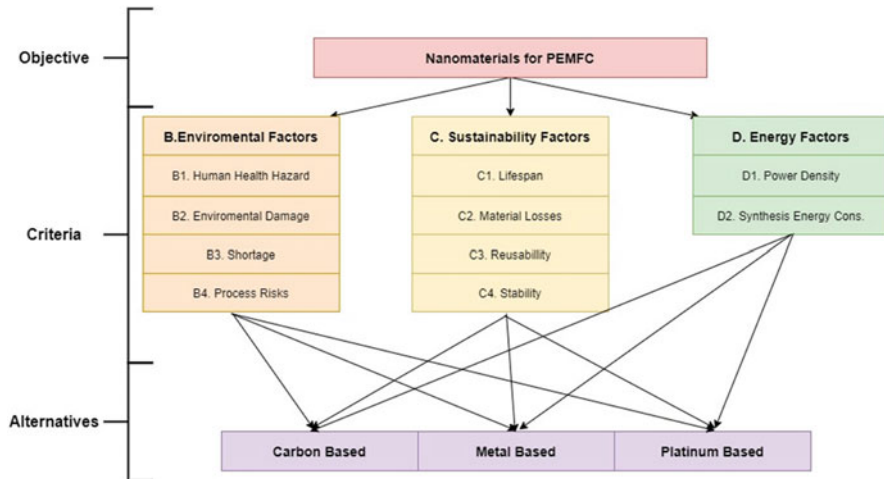


Fig. 2 Structure of the decision problem

### 3 Results and Discussion

We obtained the weights of the alternatives from the matrix obtained after all the calculations, so we have now solved the optimal decision problem. As can be seen in Fig. 3, according to the results, metal-based nanomaterials have emerged as the most suitable material for PEMFCs. Despite being widely preferred, platinum-based nanoparticles remained in second place due to their disadvantages. Carbon-based nanomaterials, on the other hand, lagged behind other options by a large margin with a value of 0.20.

The weight values of the criteria that we can reach from the comparison matrix, which form the values of the alternatives, are presented in Fig. 4. The effect of the criteria we used in our comparison study on the scores of the alternatives can be read from the graph on the screen. According to these results, the most important selection criterion for nanomaterials to be used in PEMFC was power density with a weight of 0.83. For these materials, whose main purpose is cooling, it is an expected result that this criterion related to heat transfer has the highest value. In the second and third rows, lifespan and human health hazard criteria, which have values close to each other, took the values of 0.57 and 0.55, respectively. The criteria with the lowest scores in the evaluation of the alternatives were the shortage, process risks, and stability criteria, which took the values of 0.09, 0.08 and 0.06, respectively.

In solving the decision problem, from a sustainability perspective, the best option to be used in PEMFCs has emerged as metal-based nanostructured materials. In addition, the effect degrees of the criteria on the result were determined with the



**Fig. 3** Weights of the alternatives

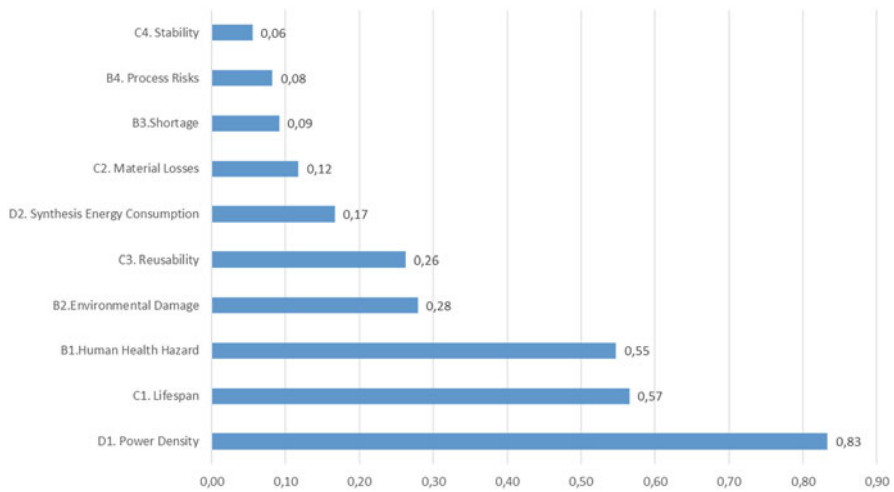
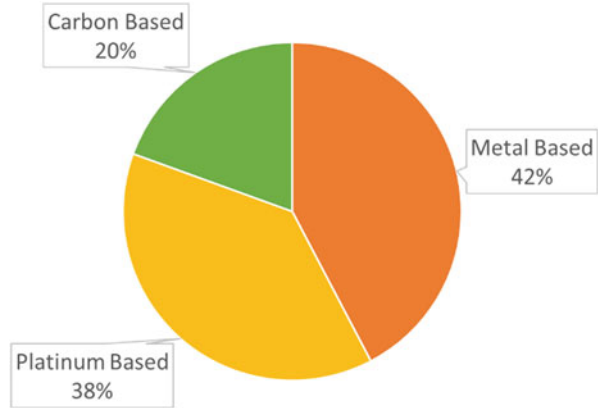


**Fig. 4** Effect weights of criteria on alternative selection

method used. These results will give an idea about the subject to researchers who will study both fuel cells and particles from now on.

## 4 Conclusion

Fuel cell stands out as the greenest option among sustainable fuels. One of the main problems in front of the widespread use of fuel cells is the need for cooling. Nanomaterials are applied by researchers of exceptional solutions in many fields. It has been concluded that it would be more appropriate to prefer metal-based nanostructures instead of the most commonly used platinum for use in fuel cells.

## References

- Abdalla, A. M., Hossain, S., Azad, A. T., Petra, P. M. I., Begum, F., Eriksson, S. G., & Azad, A. K. (2018). Nanomaterials for solid oxide fuel cells: A review. *Renewable and Sustainable Energy Reviews*, *82*, 353–368.
- Ellingsen, L. A. W., Hung, C. R., Majeau-Bettez, G., Singh, B., Chen, Z., Whittingham, M. S., & Strømman, A. H. (2016). Nanotechnology for environmentally sustainable electromobility. *Nature Nanotechnology*, *11*(12), 1039–1051.
- Esfe, M. H., & Afrand, M. (2020). A review on fuel cell types and the application of nanofluid in their cooling. *Journal of Thermal Analysis and Calorimetry*, *140*(4), 1633–1654.
- Fan, L., Zhu, B., Su, P. C., & He, C. (2018). Nanomaterials and technologies for low temperature solid oxide fuel cells: Recent advances, challenges and opportunities. *Nano Energy*, *45*, 148–176.
- Kumar, S. S., & Pillai, V. K. (2014). Low-cost nanomaterials for high-performance polymer electrolyte fuel cells (PEMFCs). In *Low-cost nanomaterials* (pp. 359–394). Springer.
- Liu, M., Zhang, C., & Chen, W. (2018). Novel nanomaterials as electrocatalysts for fuel cells. In *Nanomaterials for green energy* (pp. 169–204). Elsevier.
- Mainardi, D. S., & Mahalik, N. P. (2006). Nanotechnology for fuel cell applications. In *Micromanufacturing and nanotechnology* (pp. 425–440). Springer.
- Saaty, T. L., & Niemira, M. P. (2006). A framework for making a better decision: How to make more effective site selection, store closing and other real estate decisions. *Research Review*, *13*(1), 1–4.
- Zhang, Y., Xue, R., Yuan, W., & Liu, X. (2018). Nanomaterials in proton exchange membrane fuel cells. In *Nanostructured materials for next-generation energy storage and conversion* (pp. 199–226). Springer.
- Zhong, C. J., Luo, J., Fang, B., Wanjala, B. N., Njoki, P. N., Loukrakpam, R., & Yin, J. (2010). Nanostructured catalysts in fuel cells. *Nanotechnology*, *21*(6), 062001.

# Overview of Hydrogen-Powered Air Transportation



Hursit Degirmenci, Alper Uludag, Selcuk Ekici, and T. Hikmet Karakoc

## Nomenclature

ACI-ATI Airports Council International-Aerospace Technology Institute  
BAC Boeing Airplane Company  
LCC Lockheed California Company

## 1 Introduction

The aviation industry is growing at a rapid pace. By 2030, air travel is expected to increase by 5% (Baroutaji et al., 2019). The aviation industry accounts for roughly 12% of all carbon dioxide emissions generated by the transportation industry (Baroutaji et al., 2019). According to the Kyoto Protocol, the global carbon rate increases by 2% every year (Klug & Faass, 2001). Kerosene, a fossil-based fuel, is used as fuel in the aviation sector today. Fossil-based fuels are not environmentally friendly. In addition, the use of a fossil-based fuel in the aviation sector makes a sustainable economy unsustainable due to fossil-based fuels are not renewable energy sources. In order to ensure aviation's long-term sustainability and reduce

---

H. Degirmenci (✉) · A. Uludag

Eskişehir Technical University, Faculty of Aeronautics and Astronautics, Eskişehir, Türkiye  
e-mail: [hursitdegirmenci@eskisehir.edu.tr](mailto:hursitdegirmenci@eskisehir.edu.tr); [alperuludag@eskisehir.edu.tr](mailto:alperuludag@eskisehir.edu.tr)

S. Ekici

Department of Aviation, Iğdır University, Iğdir, Türkiye

T. H. Karakoc

Eskişehir Technical University, Faculty of Aeronautics and Astronautics, Eskişehir, Türkiye

Information Technology Research and Application Centre, Istanbul Ticaret University, Istanbul, Türkiye

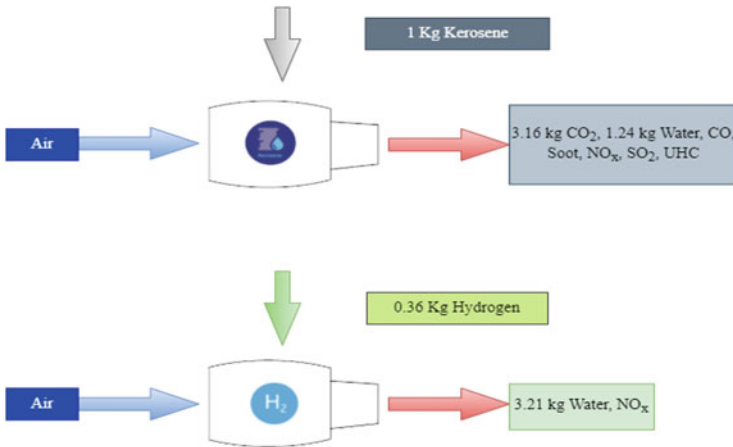


**Fig. 1** Mass energy and emission comparison between kerosene and hydrogen fuel

environmental damage, it's become vital to switch to fuels made from environmentally friendly and renewable resources.

Hydrogen fuel is the most promising fuel for ensuring aviation's long-term sustainability and reducing environmental damage. Hydrogen is one of the universe's most plentiful elements. With the exception of hydrocarbons, it cannot be destroyed, and it simply transforms from water to hydrogen and back to water during consumption (Momirlan & Veziroglu, 2005).

Hydrogen has a high specific effect due to its low molecular weight. This means that with  $1 \text{ kg}\cdot\text{s}^{-1}$  of hydrogen, 450 kg-force thrust is obtained (Cecere et al., 2014). When comparing hydrogen with kerosene, it is clear that hydrogen has approximately three times the energy per unit weight of petroleum and is much more environmentally friendly (Van Zon, 2008). It is shown in Fig. 1.

This article contains an overview of the research utilizing hydrogen energy in airports and aircraft, as well as its future sustainability.

## 2 Hydrogen-Powered Aircraft and Airports

The aviation industry is known for its high levels of safety and security. The Hindenburg disaster in aviation history has generated a sensitivity to hydrogen (Klug & Faass, 2001). The explosion of the hydrogen contained in the airship and its subsequent destruction in a matter of seconds is an iconic moment in aviation history. As a result of the disaster, the aviation industry was negatively affected.

Hans Joachim Pabst von Ohain is the first one to power a turbojet engine with hydrogen in 1936 (Töpler & Lehmann, 2015). It is not because hydrogen fuel is environmentally friendly that it is used (Töpler & Lehmann, 2015). It was chosen because it produces a high reaction and allows for combustion with a lean mixture

(Töpler & Lehmann, 2015). Then he tried the hydrocarbon-based gasoline (Töpler & Lehmann, 2015). Serious research in the aviation industry began in the 1970s (Clean Sky 2, 2020).

## 2.1 NASA “Hydrogen Airport” Project

Korycinski (1978) analyzed two NASA (National Aeronautics and Space Administration) hydrogen airport studies. At Chicago O’Hare International Airport (Airport1), BAC simulated the utilization of LH<sub>2</sub>, while LCC simulated the utilized of LH<sub>2</sub> at San Francisco International Airport (Airport2). Subsonic commercial aircraft with a capacity of 400 passengers and a distance of 5500 nautical miles have been used in this scenario. The reason for investigating at large commercial aircraft as part of the research is that they used a quarter of the fuel used in civil air travel in the United States in 1975. The two airports’ wide-body aircraft traffic was used to assess fuel needs, which were then used to measure the size and capacity of international airports for liquid H<sub>2</sub> production, storing, and delivery. The simulation was assumed in the years 1990–1995. Table 1 shows the characteristics of the airport hydrogen liquefying facility (Korycinski, 1978).

LH<sub>2</sub> ground fuel system expenses are roughly to be \$304 million in Airport2 and \$469 million in Airport1 (Korycinski, 1978).

## 2.2 Tupolev T-155 Project

According to Schmidtchen et al. (1997), the Tupolev T-155 project was performed in the 1980s (Fig. 2). It made its first flight in 1988. It was discovered through this experiment that the unit weight energy of H<sub>2</sub> is 2.8 times more than that of kerosene (Schmidtchen et al., 1997). Furthermore, it has been noted that when hydrogen fuel is used, the turbine output temperature is 37 K lower, which increases engine life and performance (Cecere et al., 2014). To produce an equivalent amount of energy as kerosene, LH<sub>2</sub> needs four times the volume, and low-temperature requirements such as 20 K have increased the cost (Cecere et al., 2014). This is attributable to the fact that the LH<sub>2</sub> system requires additional insulation and cooling systems (Cecere et al., 2014). Due to the high cost of liquid hydrogen, the project was canceled. Later, the

**Table 1** Characteristics of airport hydrogen liquefying facility (Korycinski, 1978)

Airport	Maximum output		Hydrogen liquefying	
	Ton.day <sup>-1</sup>	(tonne.day <sup>-1</sup> )	Size ton.day <sup>-1</sup>	(ton.day <sup>-1</sup> )
Airport2	846	768	250	227
Airport1	800	726	268	243

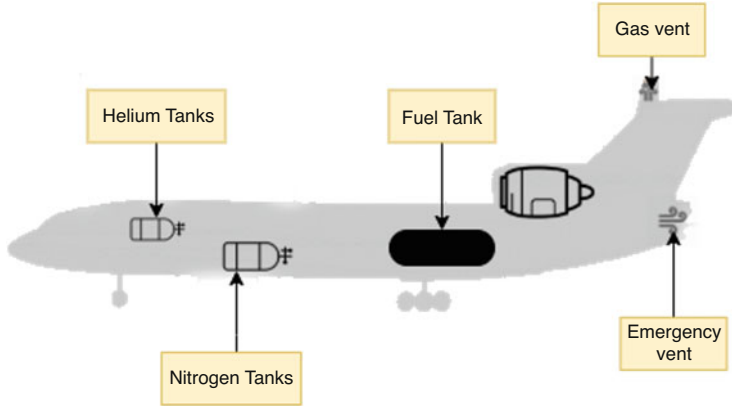


**Fig. 2** TU-155 liquid hydrogen aircraft design

information gathered from this experiment was utilized in the Airbus company's Cryoplane project (Cecere et al., 2014).

### **2.3 Swiss Group “Hydrogen in Air Transportation” Feasibility Study**

The Swiss Group conducted a preliminary investigation of a cargo jet utilizing liquid hydrogen as fuel at Zurich Airport between 1980 and 1984 (Alder, 1987). A feasibility study for refueling 15–30 tons of LH<sub>2</sub> per day was done (Alder, 1987). A route has been established between California, Europe, and Saudi Arabia. Zurich Airport was selected as the European hub (Alder, 1987). Three alternative possibilities were considered (Alder, 1987). It is shown in Fig. 3.

In each case, liquid hydrogen was more expensive than kerosene. Jet A fuel cost LH<sub>2</sub> is by a factor of 2.2–3.8 more expensive (Alder, 1987). The high cost of liquid hydrogen compared to kerosene negatively affected the sustainability of this project (Alder, 1987).

### **2.4 German-Russian “Feasibility Study”: Cryoplane Based on A310 Defined**

Pohl and Malychevc (1997) investigated a project on the use of hydrogen in civil aircraft undertaken under German-Russian cooperation between 1990 and 1993. The base aircraft for passenger aircraft configuration studies was a first-generation LH<sub>2</sub>, an Airbus A310. In the purely tourism-related configuration, this medium-range wide-body aircraft has a maximum takeoff weight of 150 mt and a passenger

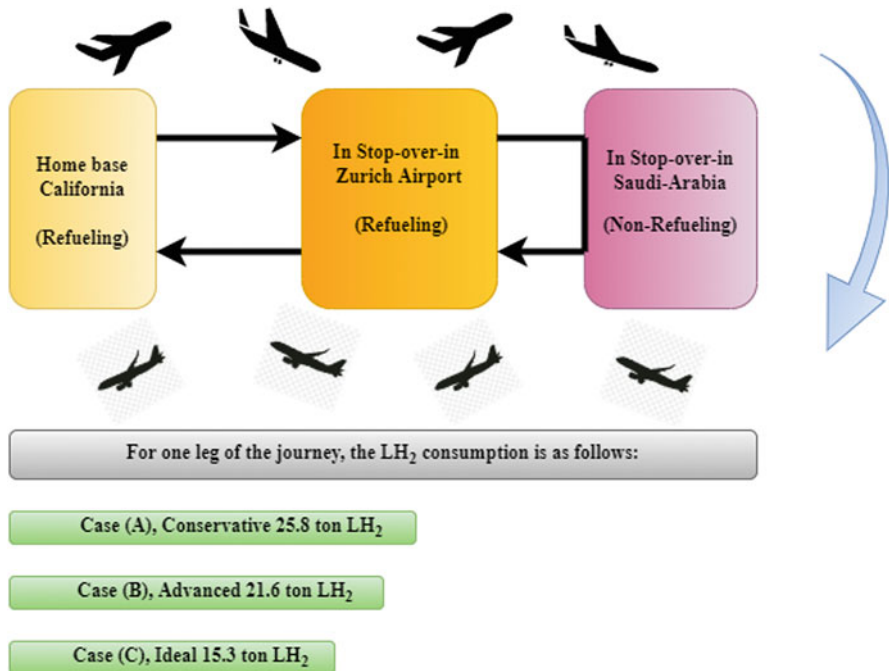
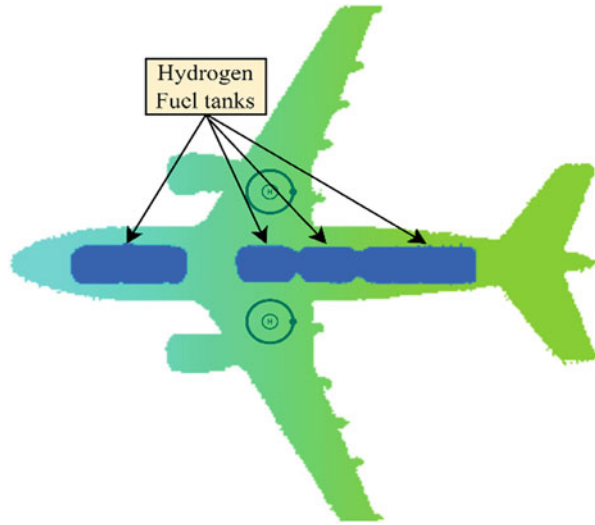


Fig. 3 Three alternative possibilities

capacity of 243. It is propelled by two PW-4152 engines, each having a static thrust of 52,000 pounds. Because the fuel volume is four times that of a jet fuel aircraft and the cryogenic heating rate necessarily requires extremely efficient tank isolation and pressurization, conventional wing tanks are not suitable for LH<sub>2</sub> aircraft. The fuselage-mounted tank arrangement was determined to be the best alternative for replacing an existing aircraft for hydrogen operating condition after considering achievement, operational expenses, ability to handle, and protection. Four different fuel tanks are positioned on the hull's upper side (Pohl & Malychevc, 1997). It is shown Fig. 4.

For a conventional aircraft, the design range requires 15,600 kg of LH<sub>2</sub>, which is equivalent to 37,000 kg of kerosene (Pohl & Malychevc, 1997). With the exception of the cryogenic fuel system, the aircraft's systems are largely unchanged (Pohl & Malychevc, 1997). Major structural modifications include wing reinforcements, fuselage midsection, and fuselage upper surfaces due to tank mounting (Pohl & Malychevc, 1997). If indeed the energy-related cost of LH<sub>2</sub> is less than 110% of that of jet fuel, it can be considered cost-competitive (Pohl & Malychevc, 1997).

**Fig. 4** Liquid hydrogen fuel tank design



## 2.5 Airbus Cryoplane Feasibility Study

The Airbus company investigated the use of liquid  $H_2$  as a fuel in aircraft between 2000 and 2002 (Airbus, 2002). For this study, both conventional and nonconventional configurations were used. Seven different aircraft configurations were used to simulate the use of liquid hydrogen fuel. These aircraft include the business jet, rural propeller aircraft, rural jet aircraft, mid-range aircraft, extended-range aircraft, and also very large long-range Aircraft. Various tank configurations were made according to the aircraft category. The optimal tank arrangement was chosen for each category. The most important point in the tank configuration is the aircraft's center of gravity. It occupies four times more volume than liquid hydrogen kerosene. As a result of this situation, the empty weight of the aircraft is 25% higher than that of kerosene aircraft. The maximum take-off weight decreases due to light  $LH_2$ . Using bulky tanks increases DOC (direct operating costs) by 25% for 1000 nm (Airbus, 2002).

The minimum changes to be made for the  $LH_2$  aircraft are categorized in Fig. 5.

As a result, when compared to liquid hydrogen fuel, kerosene has a lower cost. Depending on the price of hydrogen and kerosene fuel, DOC (direct operating costs) is predicted to be approximately equivalent in 2040 (Liquid Hydrogen Fuelled Aircraft, 2002).



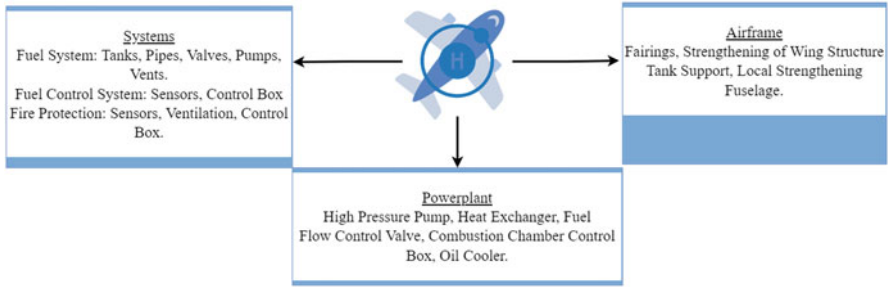


Fig. 5 Minimum change for LH<sub>2</sub> aircraft Cryoplane

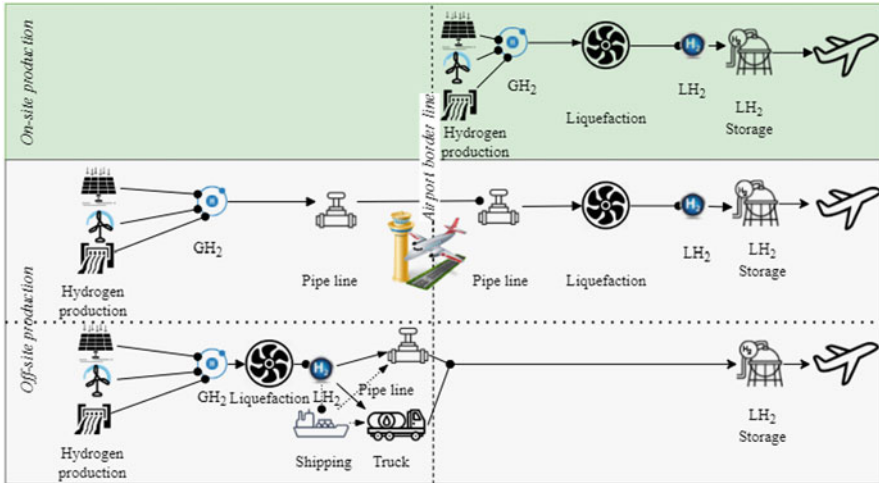


Fig. 6 Hydrogen fuel cell powered commuter segment aircraft

### 3 Future Aspect of Hydrogen-Powered Air Transportation

Fuel cell assisted aircraft (Clean Sky 2, 2020): If aircraft were powered by fuel cells, hydrogen would be refueled at airports, and the hydrogen fuel cell would then start generating electrical energy from the electrical and chemical reaction of hydrogen with oxygen in the air, powering the electrically powered propellers while only emitting water vapor as a by-product. In the next decades, commuter segment (19 passengers and 500 km range) aircraft will be able to use hydrogen fuel. A hydrogen aircraft is powered by a fuel cell, which also handles motors and provides battery energy planning and infrastructure to satisfy transitory loads. To provide thrust, every electric motor gets to drive an impeller (Fig. 6). It reduces the climate effect in the range of 80–90%. Related to the cost per seat available kilometer, the cost rises by 0–5% (CASK). It is foreseen that it will take place physically within 10 years (Clean Sky 2, 2020).

Several ways can be considered for a hydrogen-powered airport (ACI-ATI Report, 2021). LH<sub>2</sub> airport consists of subsections such as production, liquefaction, storage, distribution, and transportation. Firstly, hydrogen production, liquefaction, and storage can be done from the airport. Secondly, a production facility is built near



**Fig. 7** Three primary hydrogen supply chain/pathways into the airport

the airport, gas hydrogen is transported to the airport via pipelines, and liquefaction is done from the airfield. Another way is to produce at a different location, liquefy hydrogen, and transport it to the airport by pipelines, trucks, and ships. Storage is carried out at the airport (ACI-ATI Report, 2021). It is shown in Fig. 7.

## 4 Conclusion

In this study, comprehensive studies on LH<sub>2</sub> are included. These are the following: NASA “Hydrogen Airport” Project, Tupolev T-155 Project, German-Russian “Feasibility Study”-Cryoplane Based on A310 Defined, and Airbus Cryoplane Feasibility Study. The common problem that came across in these studies is that the cost of LH<sub>2</sub> fuel is much higher than kerosene fuel. The most emphasized issue in the studies investigated is the cryogenic storage of hydrogen.

In terms of applicability for a few decades, they are commuter segment (19 passengers and 500 km range) aircraft operating with hydrogen fuel cells. Related to the cost per seat available km in, the cost rises by 0–5%. (CASK). It is foreseen that it will take place physically within 10 years. It is predicted that the use of liquid hydrogen will increase in 2040 depending on fuel prices.

This article contains an overview of the research on hydrogen as a fuel in airports and aircraft, as well as its future feasibility. More research is considered necessary to increase the effectiveness of hydrogen fuel.

## References

- ACI. (2021). *Integration of hydrogen aircraft into the air transport system: An airport operations and infrastructure review*. ACI-ATI Report. [aci.aero/publications/new-releases](https://aci.aero/publications/new-releases)
- Airbus. (2002). *Final technical report of Cryoplane liquid hydrogen fuelled aircraft – System analysis*. Airbus Deutschland GmbH. [https://www.fzt.haw-hamburg.de/pers/Scholz/dglr/hh/text\\_2004\\_02\\_26\\_Cryoplane.pdf](https://www.fzt.haw-hamburg.de/pers/Scholz/dglr/hh/text_2004_02_26_Cryoplane.pdf)
- Alder, H. P. (1987). Hydrogen in air transportation. Feasibility study for Zurich Airport. *International Journal of Hydrogen Energy*, 12(8), 571–585. [https://doi.org/10.1016/0360-3199\(87\)90016-4](https://doi.org/10.1016/0360-3199(87)90016-4)
- Baroutaji, A., Wilberforce, T., Ramadan, M., & Olabi, A. G. (2019). Comprehensive investigation on hydrogen and fuel cell technology in the aviation and aerospace sectors. *Renewable and Sustainable Energy Reviews*, 106, 31–40. <https://doi.org/10.1016/j.rser.2019.02.022>
- Cecere, D., Giacomazzi, E., & Ingenito, A. (2014). A review on hydrogen industrial aerospace applications. *International Journal of Hydrogen Energy*, 39(20), 10731–10747. <https://doi.org/10.1016/j.ijhydene.2014.04.126>
- Clean Sky 2. (2020). *Hydrogen-powered aviation: A fact based study of hydrogen technology, economics, and climate impact by 2050*. Clean Sky 2. <https://doi.org/10.2843/766989>
- Klug, H. G., & Faass, R. (2001). Cryoplane: Hydrogen fuelled aircraft status and challenges. *Air & Space Europe*, 3(3–4), 252–254. [https://doi.org/10.1016/S1290-0958\(01\)90110-8](https://doi.org/10.1016/S1290-0958(01)90110-8)
- Korycynski, P. F. (1978). Air terminals and liquid hydrogen commercial air transports. *International Journal of Hydrogen Energy*, 3(2), 231–250. [https://doi.org/10.1016/0360-3199\(78\)90021-6](https://doi.org/10.1016/0360-3199(78)90021-6)
- Momirlan, M., & Veziroglu, T. N. (2005). The properties of hydrogen as fuel tomorrow in sustainable energy system for a cleaner planet. *International Journal of Hydrogen Energy*, 30, 795–802. <https://doi.org/10.1016/j.ijhydene.2004.10.011>
- Pohl, H. W., & Malychev, V. (1997). Hydrogen in future civil aviation. *International Journal of Hydrogen Energy*, 22(10–11), 1061–1069. [https://doi.org/10.1016/S0360-3199\(95\)00140-9](https://doi.org/10.1016/S0360-3199(95)00140-9)
- Schmidtchen, U., Behrend, E., Pohl, H. W., & Rostek, N. (1997). Hydrogen aircraft and airport safety. *Renewable and Sustainable Energy Reviews*, 1(4), 239–269. [https://doi.org/10.1016/S1364-0321\(97\)00007-5](https://doi.org/10.1016/S1364-0321(97)00007-5)
- Töpler, J., & Lehmann, J. (Eds.). (2015). *Hydrogen and fuel cell technologies and market perspectives*. Springer.
- van Zon, N. (2008). *Liquid hydrogen powered commercial aircraft: Analysis of the technical feasibility of sustainable liquid hydrogen powered commercial aircraft in 2040*, p. 16. <http://www.noutvanzon.nl/files/documents/spaceforinnovation.pdf>

# Evaporative Hydrocarbon Emission of Gasoline During Storage in Horizontal Tanks and Their Energy and Environmental Efficiency



Sergii Boichenko, Dubrovska Viktoriia, Shkyar Viktor, Iryna Shkilniuk, Anna Yakovlieva, and Oksana Tarasiuk

## Nomenclature

GS	Gas space
LFFCS	Light fuel fractions capture systems
MPC	Maximum permissible concentrations
RV	Respiratory valve's
SAA	Surface-active additive
VAM	Vapor-air mixture

## 1 Introduction

As of now, it's known (Boychenko, 2001; Boychenko et al., 2006) that at the refinery, the main losses occur in tanks (17.9% of total losses), during a gas flare process (18.1%), due to equipment's permeation/leakage (16.4%), in oil distributors (5.2%) and in treatment facilities (8.3%).

---

S. Boichenko (✉) · D. Viktoriia · S. Viktor  
Institute of Energy Safety and Energy Management, National Technical University of Ukraine  
Igor Sikorsky Kyiv Polytechnic Institute, Kyiv, Ukraine

Scientific-Technical Union of Chemmotologists, Kyiv, Ukraine

I. Shkilniuk · A. Yakovlieva  
Scientific-Technical Union of Chemmotologists, Kyiv, Ukraine

Ukrainian Scientific-Research and Education Center of Chemmotology and Certification of  
Fuels, Lubricants and Technical Liquids, National Aviation University, Kyiv, Ukraine  
e-mail: [anna.yakovlieva@nau.edu.ua](mailto:anna.yakovlieva@nau.edu.ua)

O. Tarasiuk  
Non-governmental Organization "Institute of Circular and Hydrogen Economics", Kyiv,  
Ukraine

The evaporative emissions of petroleum products during storage and transportation are usually between 1% and 6% of total anthropogenic sources (Skobelev et al., 2018; Magaril, 2013). According to other sources, the gasoline losses make up 1.5–2% of the total amount of petroleum products while moving downstream. Up to 40% of hydrocarbons emitted by road transport evaporate from fuel tanks and fuel systems of vehicles with gasoline engines (Saikomol et al., 2019).

According to some international researches: Germany's gas stations emit 145,000 tons of hydrocarbons vapours annually; gas stations in England emit more than 120,000 tons. French experts estimate the losses from evaporation in the amount of 0.18% of the total operational volume during filling gas station tanks and storing automobile gasoline (Danilov & Shurygin, 2016). German experts estimate these losses at 0.17%. Japanese researchers have determined that due to the stable temperature in the underground tank (in Japan during the year it does not change much, namely, it varies from 15 to 25 °C), the losses from evaporation are 1.08 kg/m<sup>3</sup> of the pumped gasoline (Saikomol et al., 2019; Gallo, 2011). On average, the composition of the vapour mixture emitted from the tanks is as follows: 32% of methane row hydrocarbons, 12% of gasoline fractions and 56% of the air. In the context of the global problem of depletion of energy resources and the associated degradation of the environment, the relevance of this problem is indubitable and only confirms that the reduction of gasoline losses from evaporation remains an important environmental and economic problem (Skobelev et al., 2018).

## 2 The Purpose and the Task of the Study

Hypotheses: Studying the impact of causes, factors and sources on the process of hydrocarbon evaporative emissions from horizontal tanks will improve the technology of calculating the emission of gasoline components, optimize and improve the efficiency of technological operations, save valuable hydrocarbons and minimize man-made environmental impact.

The basic and applied task of this research is to create theoretical principles for improving the methodology for predicting gasoline losses from evaporation and minimizing them during various technological operations.

## 3 Analysis of Recent Researches and Publications

Evaporative losses of hydrocarbons during their storage are caused by the property of oil and petroleum products to evaporate from the open surface. At the same time, the main source of losses from evaporation is the "breathing" rebar of the tanks. The evaporation of petroleum products during their storage constitutes the main share of losses (Boychenko et al., 2006; Magaril, 2013).

For suppliers of petroleum products an important problem is the calculation of their losses. If the processes of inventory records for petroleum products are not established, there is a high probability of financial losses due to the uncertainty of the amount of petroleum products pumped or stored, the absence of real balances and, as a result, the impossibility to correctly prepare an overall balance sheet of the enterprise. In addition, an accurate and thorough record of petroleum products is important for the company's report to end suppliers, consumers and regulatory authorities (Danilov & Shurygin, 2016). The purpose of this rationing is to streamline the calculation of oil loss due to evaporation during the production, processing, storage or transportation, etc. In practice, the most common rate of losses is 0.2–0.3% of the volume of petroleum products. The loss rate of 0.3% for petroleum products is considered the standard value during evaporation process (Skobelev et al., 2018; Magaril, 2013).

However, the accuracy of calculations depends on the capacity of the vessels being in use as the ability to measure the volume and weight of the stored petroleum products depends on it. For example, at large oil storage facilities, 1 mm of the product's surface in the tank weighs more than one tone. In such vessels, the precise records can be maintained up to plus or minus one whole tone (Boichenko & Kalmykova, 2020).

Losses from evaporative emissions of hydrocarbons relate to natural losses (Hakkola & Saarinen, 2000). Natural losses of petroleum products are losses (reduction of mass while maintaining quality within the requirements of normative documents) that are a consequence of the physical and chemical properties of petroleum products, the influence of meteorological factors and the imperfections of the current measures of preventing losses of petroleum products due to evaporation and adhesiveness during transportation, acceptance, storage and shipment (Wixtrom & Brown, 1992).

It should also be noted that natural losses do not include losses of petroleum products caused by violations of the requirements of standards, technical conditions, rules of technical operation and storage and consequences of natural disasters.

The norm of natural losses is the maximum permissible value of irretrievable losses of petroleum products, arising directly from commodity and transport operations as a consequence of accompanying their physical and chemical processes, as well as losses inevitable at this level of the state of the technological equipment used (losses from evaporation due to the inseparability of pumps, retardations, technological equipment), as well as losses from adhering to the internal walls and equipment of tanks, vehicles and pipelines (Gallo, 2011).

There are two ways to make a quantitative assessment (i.e. to predict) of oil products losses: experimental and calculated domestic and foreign methods. Domestic methods for calculating hydrocarbon evaporative losses during storage were proposed by such authors as N. N. Konstantinov, V. I. Chernykin and F. F. Abuzov. These techniques are not adapted to practical use, as they are overwhelmed with unnecessary information, and, most importantly, do not have the status of official normative documents. Also, there is a foreign experience in determining the losses of petroleum products from tanks during storage (Saikomol et al., 2019). Since this

aspect of the problem is not the main task of this work, we will return to a deeper study of this problem in future works (Srivastava et al., 2019).

## 4 Main Part

Stricter European requirements for the quality of motor fuels during exploitation and uncompromising norms of gas emissions (emission of hydrocarbons) into the atmosphere caused the relevance of the scientific and applied task of minimizing the losses of petroleum products from evaporation. To investigate the problem of hydrocarbon emission from horizontal tanks and to identify and study the impact of a set of causes, factors, sources and their consequences, the Ishikawa method was used, which is presented in the form of cause-and-effect relationships.

Detailing of the cause-and-effect diagram of connections has allowed to establish the most significant and problematic factors and sources affecting the process of emission of hydrocarbons from horizontal tanks, to identify the negative consequences of gasoline losses and to predict the methods and means of minimizing and preventing evaporation of hydrocarbons.

The Ishikawa method (Gallo, 2011) of cause-and-effect analysis has allowed to establish and systematize the main factors that mostly affect the amount of losses during gasoline evaporation, namely: ambient temperature, pressure of saturated vapour of petroleum products, wind speed, temperature regime of the tank, type of the tank, stored petroleum products (gasoline has the largest amount of light hydrocarbons), colour of the tank paint, tank volume, turnover of the tank, location effect, roof fittings, serviceability of respiratory valves and presence or absence of means of losses preventive measures.

The main sources of losses of petroleum products during technological operations are fuel vapour emissions during so-called deep and shallow “breathing”, ventilation of gas space, poor quality of seals of technological equipment, violation of the rules of fuel loading and non-compliance with the terms of regulatory work of the tank park (corrosion of the tank surface, “offing”, defects of welds, etc.). In reservoir parks, evaporative losses (natural losses) reach 75% of overall petroleum product losses. The main technological operations with CSG are loading, unloading, storage and pumping. The temperature and density of gasoline changes during pumping due to the fact that the temperature of gasoline inside the tank may vary from the one being pumped (Iakovlieva et al., 2013).

The level of gasoline, its temperature and pressure of saturated vapour in the gas space (GS) of the tank decrease during the loading process. While pumping gasoline off the tank, the process of air absorption and additional evaporation of light hydrocarbons is accompanied by a rise in pressure up to the level of the respiratory valve’s (RV) configuration. If the pressure in the GS exceeds the RV’s setting, there will be a “reverse exhalation”. Storage of petrol is accompanied by a change in temperature, density, level and pressure in GS. The level of gasoline in the tank during storage changes due to the evaporation of light hydrocarbons and

modifications in their density and temperature. Density changes due to evaporation of light hydrocarbons and daytime temperature fluctuations. The temperature of gasoline changes due to the daytime temperature fluctuation. With the increase of pressure in GS up to the level of RV's configuration, there is an emission of light hydrocarbons – “low breathing”. During fuel loading process, the temperature of gasoline changes (the pumped in gasoline is mixed with the residue in the tank). The amount of a replaced vapor-air mixture (VAM) in this case and the concentration of light hydrocarbons in it will be determined by a closed or open flow – the filling occurs. In the case of filling in with the open flow, there is greater surface turbulence and intensification of the evaporation process, hence the increase in the concentration of light hydrocarbons in the replaced VAM. When filling in with a closed flow, the internal layers of liquid are exposed to turbulence, and evaporation from the surface is less intense (Shearston & Hilpert, 2020).

When loading the tank, evaporation losses can reach 0.1% of the total volume. The main consequences identified by us using the method of Ishikawa are the consequences of economic, environmental and technological nature, which was grouped, structured and graphically reflected by the method of system analysis (Fig. 1).

1. Losses from evaporation lead to deterioration of operational properties of petroleum products, for example, starting and anti-detonation ones. Evaporative emission of light hydrocarbons leads to the deterioration of these two most important operational properties of petroleum products – reduction of octane number and deterioration of starting properties of petroleum products, due to the losing of light high-octane components of gasoline, which in turn leads to limitation of technical resource of vehicle engines.
2. Losses from evaporation lead to economic losses. The refining industry provides the needs of different sectors of the economy. Pollution is the cause of two types of material costs: prevention of the impact of a contaminated environment on human health and elimination of such an impact. The sum of these costs is the economic damage of pollution caused to the enterprise and the national economy of the country, as well as the damage caused to people's health. The economic damage from pollution of the environment is determined by the amount of damages caused by individual sources. In determining the expected damage on the basis of variant calculations, a minimum amount is set, which is intended to prevent and compensate for the impact of the polluted environment.
3. Emission of volatile hydrocarbons has a significant impact on the quality of the environment. No less urgent problem today is the pollution of atmospheric air with toxic substances due to the evaporation of petroleum products, which jeopardizes environmental balance and human health, causes material damage and significantly reduces the technical resource of the vehicle engine. The degree and nature of petroleum products evaporation impact on human organism can be tracked down to the concentration of vapour in the air, the duration of stay in the gassed atmosphere, environment temperature, physical condition and physiological features of the organism. However, to prevent pollution and provide human safety, maximum permissible concentrations (MPC) of harmful substances are established.



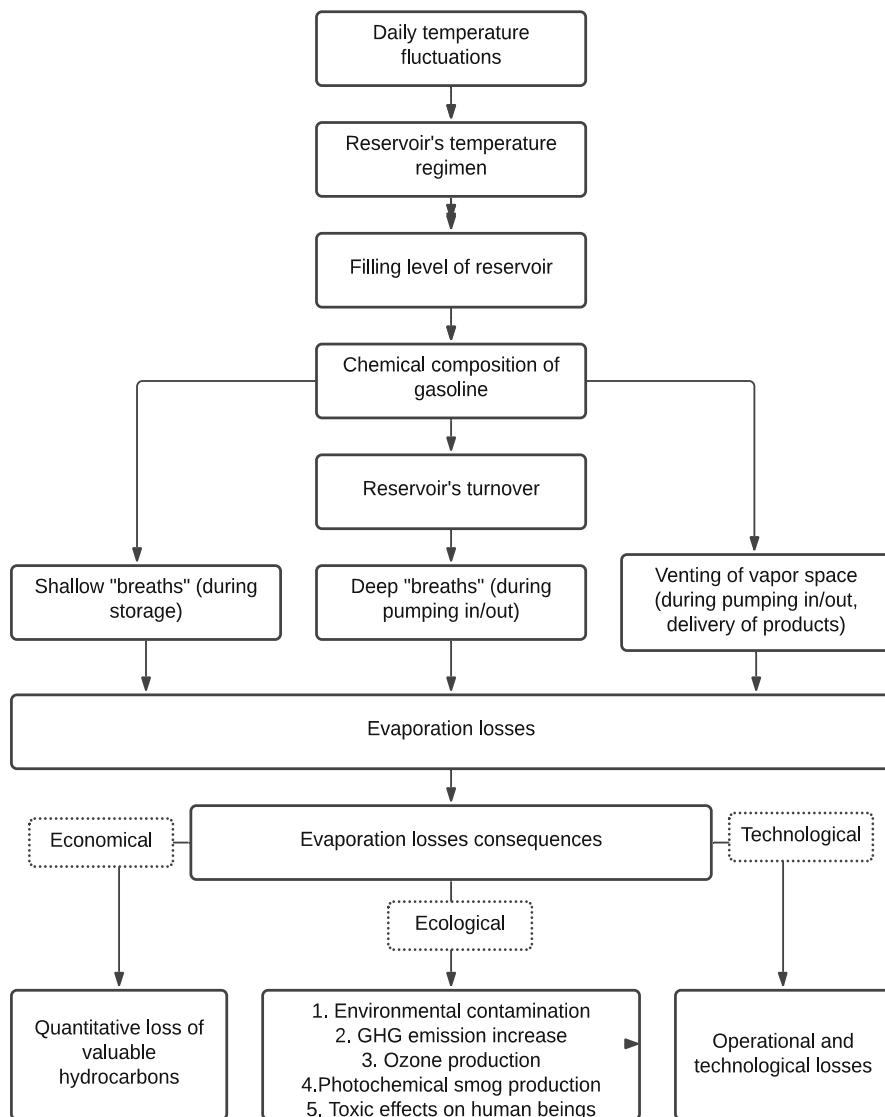


**Fig. 1** Systematic analysis of the causes and consequences of gasoline losses, which leads to the evaporative emission of hydrocarbons during technological operations (Boychenko, 2001)

Evaporation processes occur during pumping, storage, shipment, loading, transportation and direct use of petroleum products, leading to increased greenhouse effect due to the emission of hydrocarbon gases, in particular, methane, ethane, propane, butane, pentane and others, among which methane is the so-called greenhouse gas. Volatile hydrocarbons, like ethane, propane, butane and pentane, are the

main components in the reactions of ozone formation – one of the most common air pollutants. Ozone is formed as a result of the reaction of photosynthesis, with easy inclusion of petroleum products' vapours due to their reactionary ability. In addition, hydrocarbon vapour can enter into a chemical reaction with other pollutants in the atmospheric air due to its reactionary ability and form photochemical smog. In turn, smog affects human health and causes soil contamination and destruction of plants.

The greenhouse effect is associated with global warming, leading to climate change on a planetary scale.

At the same time, the current state of use of means and methods of reducing hydrocarbon losses at oil supply facilities does not meet the main task of the resource and energy-saving and environmental policy in the technosphere, in particular.

This has its own reasons, namely:

The positive economic effect of the use of means of evaporation losses prevention is achieved only if the cost of preventing losses of 1 ton of petroleum products is less than the total cost of 1 ton of petroleum products.

In addition, the situation is complicated by the fact that even morally and technically obsolete technologies are applied irrationally. Advanced technical developments usually require large investments or, at best, are applied locally.

The use of pontoons, floating roofs, SCLF and other methods does not allow to successfully capture light fractions and only prevents small losses hydrocarbons.

Thus, with the rapid cost increase of oil and petroleum products, as well as the adoption of stricter ecological norms, the basic and applied task of minimizing the loss of hydrocarbon raw materials and commodity products through the evaporative emission of hydrocarbons is becoming increasingly important.

One must select loss prevention tools specifically for each tank reservoir. To determine the effectiveness of the use of loss reduction measures, it is necessary to compare the amount of petroleum products that evaporated from the tank reservoir without the established measures with a similar value in the tanks where such measures were introduced.

Various technical solutions can be used to reduce evaporative losses [9]; they are chosen according to technical and economic calculations, taking into account meteorological and industrial conditions, and can be divided into several groups, in particular:

1. Reducing the vapour space above the liquid level (the less the vapour space, the less the losses) with the special design features of tank reservoirs with floating roofs, or pontoons, which allow to minimize losses from deep "breaths" and "reverse exhale" by 70–75% at an annual turnover ratio of up to 60 times a year and by 80–85% at an annual turnover ratio of more than 60 times a year and from shallow "breaths" by 70% compared to conventional tanks with a shielded roof. Calculations show that tanks with a floating roof and pontoon are most effective at an annual turnover ratio of more than 12.

In the future, the economic efficiency of floating roofs and pontoons can be achieved through the use of durable polymeric materials and improvement of the design of sealing shutters.

2. Storage with overpressure. Storage tank reservoirs that withstand varying degrees of pressure without emitting hydrocarbon vapor. According to the equation of losses, in the tank reservoir designed to work with overpressure losses from “shallow breaths” and partly from “deep breaths” can be completely eliminated. However, as the calculations showed, too much of overpressure complicates the design and increases the cost of tanks. The optimum amount of overpressure is strongly influenced by the turnover of the tank reservoir, the physicochemical properties of the oil products and meteorological conditions. Hydrocarbon fuel with a high-pressure level of saturated vapour is advisable to store in tank reservoirs of baggy, teardrop or spherical shape. These tanks allow to keep overpressure within 700–2000 kPa range, which makes it possible to almost completely exclude losses from “shallow breaths”. However, the complexity of their manufacture and high price block their widespread use.
3. Reducing the amplitude of fluctuations in the temperature of vapour space. To create conditions for isothermal storage of petroleum products or a significant reduction in fluctuations in the temperature of vapour space and the surface of the oil, the following measures are used: thermal insulation of tanks, cooling them in the summer water and coating with reflective paint (internal and outer coating of white colour), as well as underground storage. For example, complex coating of the inner and outer surfaces of tanks makes it possible to reduce the evaporative losses of light hydrocarbons by 30–65%. Protective screens, fences, plants and canopies are also installed, defending from gusts of strong wind and precipitation that cause pressure to drop. Given the fact that evaporation occurs mainly on the surface of the liquid under the floating roof of the tank, the surface temperature becomes an important parameter. Any mechanisms that reduce the temperature of the floating roof will directly affect the evaporation rate (e.g. roof insulation will significantly reduce the evaporation loss). Wind speed also affects evaporation. Adding a wind defence system will decrease the evaporation rate.
4. Petroleum products leaking vapour capture system. Basically, it is used in the transportation and storage of fuel. At fuel stations, the best means of reducing losses are systems of light fractions capture on the basis of an ejector heat exchanger (refrigeration ejector systems). The use of equipment with an ejector heat exchanger (nitrogen – to cool the flow of the mixture of air with hydrocarbons in the heat exchanger of the ejector) for condensation of low-oxidation hydrocarbons at oil storage facilities will protect the environment from hydrocarbon vapour (reducing the losses of light fractions to 98%). Vapor-equalizing systems are used to do this. Their use allows to partially reduce losses from “deep breaths”. The effectiveness of loss reduction depends on the rate of pumping in and releasing of hydrocarbons. Losses are reduced by the value of matching operations coefficient. If the pumped in volume of petroleum products exceeds the pumped out one, the excess vapor-air mixture enters the gasholder, which reduces the losses of petroleum products by 90–95%. Conversely, when the volume pumped out of tanks exceeds the inflow of petroleum products, gas-holders “give the vapor-air mixture back” to the system. The vapor-air mixture of the cloud gas can be supplied to the device for extraction (capture) of petroleum

products. Capturing vapours of petroleum products can be carried out by vapour condensation during cooling or absorption process (e.g. with the help of activated coal).

Light fuel fractions capture systems (LFFCS). One of the features of LFFCS is that its design involves non-stop operation in automatic mode and does not require the presence of service personnel. In addition, LFFCS has a self-defence technology against accidental outages, which is able to function continuously in the mode of frequent shutdowns and is operational in aggressive environment.

5. Reducing the pressure of saturated vapours by adding a synthetic fatty acid-based surface-active additive (SAA) to the fuel with significant activity of surfactant. Reducing the pressure of saturated vapour is highly dependent on the concentration of the additive – the maximum effect is observed at the 9.25 mg/kg concentration rate. It turned out that the evaporation rate in the tanks dropped to 47%.

While decreasing the pressure of saturated vapor, the additive has a very weak effect on the initial boiling point of gasoline and does not affect the temperature of 10%, therefore not leading to a deterioration of cold start property.

It should be noted that reducing the pressure of saturated vapour by the introduction of the additive allows to increase the concentration of a high-octane component – butane. The effect of reducing losses decreases with a concentration of additives exceeding 9.25 mg/kg.

Thus, the additive provides:

Reduction of losses from evaporation

Improvement of the mixture formation when starting the engine

Reduces the negative impact on the environment caused by the loss of light hydrocarbons

Improves the operational characteristics of transport (Magaril, 2013).

6. Organizational and technical measures. Work on efficient and rational use of petroleum products begins with the preparation of a plan of organizational and technical measures. Preparation and development of the plan of organizational and technical measures includes:
  - (i) Collection and analysis of normative, planned and factual data on the losses of petroleum products for the reporting period
  - (ii) Identification of all available losses of petroleum products and outlining the directions of their elimination
  - (iii) Preparation of proposals to eliminate irrational losses of petroleum products
  - (iv) Study of proposals received from engineering and technical staff to reduce losses and include them in the plan of organizational and technical measures
  - (v) Appointment of responsible personnel
  - (vi) Determination of funding sources and list of necessary materials and tools to perform the work
  - (vii) Assessment of acceptable costs and effectiveness of all points of the plan of organizational and technical measures

Proper organization of tank reservoir operation is one of the most important measures (means) of reducing the losses of petroleum products, namely:

To reduce losses from “shallow breaths” in open-air tanks, petroleum products must be stored at maximum filling, as in this case the smallest level of vapour space is achieved.

To reduce losses from “deep breaths”, it is necessary to reduce to the maximum the pumping of petroleum products between the tanks within the facility.

The shorter the amount of time between pumping petroleum products out and pumping them into the tank reservoir, the lower the amount of losses from “deep breaths”.

Losses from “shallow breaths” are directly proportional to the areas of evaporation, so highly volatile petroleum products are better stored in tanks of large volume.

Pumping the fuel out of the tank completely at the highest possible speed, and partial release of the products from the tank at a minimum speed. Also, it should be noted that the partial release from the tank (in cases where the tank can be filled again) is at the maximum speed. As for seasonal and daily recommendations, it is recommended to fill the tanks in the summer at night and discharge it during the day. Measurement of fuel level, sub-water and sampling – in the early morning or late evening. Important is the technical condition of tanks and respiratory fittings. Regular check of the tightness of the roof of the tank and the valves can prevent losses from ventilation of the vapour space. During the pumping of petroleum products with high turnover rates, a reduction in losses of up to 25% can be achieved by installing reflector discs under the venting valve. Taking into account the above data and reference data of other sources, we can establish a link between the impact of factors on the sources of loss and the methods and means of preventing the evaporative emission of hydrocarbons.

This study is devoted to the development of technological bases of new economic methods and new energy-conserving equipment based on the prevention of losses from evaporation at storage gasoline.

The main conclusion of this study, which we have formulated here, is the fact that in addition to various technical solutions (methods, measures) to prevent losses from evaporation, the records of hydrocarbon losses and the organization of the system for monitoring these losses play an extremely important role, which is an important measure to reduce them. This study indicated that pentane ( $C_5H_{12}$ ) was the dominant species potentially released from evaporation at storage gasoline. Pentane is a valuable raw material for isomerization. The fraction enriched with isopentanes is used as a component of gasolines or serves to isolate isopentane, a raw material for the production of isoprene, which is a monomer for the synthesis of synthetic rubbers. Also, pentanes in the composition of straight-run gasoline fractions of oil are used in the production of petroleum solvents. This study determines the directions of the further improvement of technology of using gasoline in terms of fuel efficiency.

At the same time that pentane belongs to the substances of the fourth hazard class, it also has reflex and resorptive indicators of harmfulness. Therefore, it is important to increase the level of environmental safety of the fuel tanks.

## 5 Conclusion

This study demonstrates it is important to establish the reasons that will help to quantify the contribution of gasoline vapour emissions from the most common horizontal tanks to environment.

Therefore, the further work that we plan to perform is the improvement of the methodology for calculating (recording) the gasoline evaporative hydrocarbon emission, which will create an opportunity to evaluate the effectiveness of the use of volatile hydrocarbon capture systems and become the main engineering tool for serving the main goal – improving the record system and minimizing quantitative (energy efficiency aspect) and qualitative (environmental efficiency aspect) emissions (losses) from evaporation. In general, increasing the efficiency of using motor fuels today is one of the most realistic areas for solving energy and environmental problems at the same time.

Understanding the prioritization of quantifying emissions = losses and technological schemes to minimize them is also necessary to justify the budget for investing in the implementation of these technologies.

## References

- Boichenko, S., & Kalmykova, N. (2020). Cause and consequence analysis of losses of petroleum products in the tank park. *Science-Based Technologies*, 2(46), 218–235.
- Boichenko, S. (2001). *Rational use of hydrocarbon fuels*. NAU.
- Boychenko, S., Fedorovych, L., Cherniak, L., et al. (2006). Poteri uglevodorodov v hode tehnologicheskikh protsessov pererabotki, transportirovki, hraneniya i zapravki. *Neft I Gaz*, 3, 90–94.
- Danilov, V., & Shurygin, V. (2016). K voprosu o reshenii problem poter' nefteproduktov ot isparenija. *Uspеhi sovremennogo estestvoznaniya*, 3, 141–145.
- Gallo, M. (2011). A fuel surcharge policy for reducing road traffic greenhouse gas emissions. *Transport Policy*, 18(2), 413–424.
- Hakkola, M. A., & Saarinen, L. H. (2000). Customer exposure to gasoline vapors during refueling at service stations. *Applied Occupational and Environmental Hygiene*, 15(9), 677–680.
- Iakovlieva, A., Lejda, K., Vovk, O., & Boichenko, S. (2013). Peculiarities of the development and implementation of aviation biofuels in Ukraine. In World Congress on Petrochemistry and Chemical Engineering. *Journal of Petroleum & Environmental Biotechnology*, 4(6), 47.
- Magaril, E. (2013). The influence of carbonization elimination on the environmental safety and efficiency of vehicle operation. *International Journal of Sustainable Development and Planning*, 8(4), 1–15.
- Saikomol, S., Thepanondh, S., & Laowagul, W. (2019). Emission losses and dispersion of volatile organic compounds from tank farm of petroleum refinery complex. *Journal of Environmental Health Science and Engineering*, 17, 561–570.
- Shearston, J. A., & Hilpert, M. (2020). Gasoline vapor emissions during vehicle refueling events in a vehicle fleet saturated with onboard refueling vapor recovery systems: Need for an exposure assessment. *Frontiers in Public Health*, 8, 18.
- Skobelev, D., Guseva, T., Chechevatova, O., Sanzharovskiy, A., Shchelchikov, K., & Begak, M. (2018). *Comparative analysis of the drawing up and review of reference documents on*

- best available techniques in the European Union and in the Russian Federation* (D. Skobelev, Ed.; published in two languages—Russian and English, 90 pp). Pero.
- Srivastava, M., Srivastava, A., Yadav, A., & Rawat, V. (2019). Source and control of hydrocarbon pollution. In M. Ince & O. K. Ince (Eds.), *Hydrocarbon pollution and its effect on the environment*. IntechOpen. <https://doi.org/10.5772/intechopen.86487>
- Wixtrom, R. N., & Brown, S. L. (1992). Individual and population exposures to gasoline. *Journal of Exposure Analysis and Environmental Epidemiology*, 2(1), 23–78.

# Technologies for Alternative Jet Fuel Production From Alcohols



Anna Yakovlieva, Sergii Boichenko, and Vasyl Boshkov

## Nomenclature

AtJ	Alcohol to jet
GtJ	Gas to jet
OtJ	Oil to jet
StJ	Sugars to jet

## 1 Introduction

Modern fuels for civil aviation must meet a number of requirements related to the economy, reliability, durability of aircraft, and environmental safety of fuels (Trofimov, 2014). At the same time, the world oil reserves are limited, while oil is the main raw material for the production of aviation fuel. Taking into account these factors, the development of alternative technologies for the production of aviation fuel from renewable feedstock becomes relevant. To date, a number of technologies for the production of alternative aviation fuels are already known, which are actively researched and implemented in practice (Trofimov, 2014; Grace, 2004).

Trends in the development of civil aviation indicate the need to increase fuel efficiency and its environmental friendliness (Yakovlieva et al., 2019). The problems with petroleum fuels may be solved by the use of alternative aviation fuels. A

---

A. Yakovlieva (✉) · V. Boshkov  
Technical University of Kosice, Kosice, Slovakia  
e-mail: [anna.yakovlieva@nau.edu.ua](mailto:anna.yakovlieva@nau.edu.ua)

S. Boichenko  
Institute of Energy Safety and Energy Management, National Technical University of Ukraine  
“Igor Sikorsky Kyiv Polytechnic Institute”, Kyiv, Ukraine

National Aviation University, Kyiv, Ukraine



number of companies together with aircraft manufacturers with significant government support are actively developing new fuels (Grace, 2004; Tretiakov, 2008). In the near future, liquefied natural gas, synthetic gasoline, and diesel fuel may be used, and in the future, we can expect the widespread use of hydrogen and power plants with fuel cells (Yakovlieva et al., 2019). Leading representatives of the aviation industry came to a consensus on the need to increase the fuel efficiency of aircraft operated by 1.5% by 2020. One such way is to use alternative fuels. However, the main problem associated with large-scale biofuel production is its cost. At present, biofuels are two to three times more expensive than traditional aviation kerosene. But with the increase in biofuel production, its cost will gradually fall. At the same time, according to analysts, the cost of traditional jet fuel will increase, respectively; over time, these two fuels will probably change their position (Grace, 2004; Boichenko & Yakovlieva, 2020).

## 2 Review of Technologies for Alternative Jet Fuel Production

The basis of any motor fuel, whether traditional or alternative, in particular on the basis of biomass, are hydrocarbons formed by hydrogen and carbon atoms (Han et al., 2013). Differences in the composition of raw materials determine the approaches and technological processes used to convert both types of resources to hydrocarbon fuels. Thus, the nature of petroleum hydrocarbons requires conversion at high temperatures and in the vapor phase. Hydrocarbons derived from biomass are highly reactive and therefore require much lower temperatures for reactions than petroleum compounds (Ghazanfari, 2017). Figure 1 shows the main technological processes of processing biomass into alternative jet fuels.

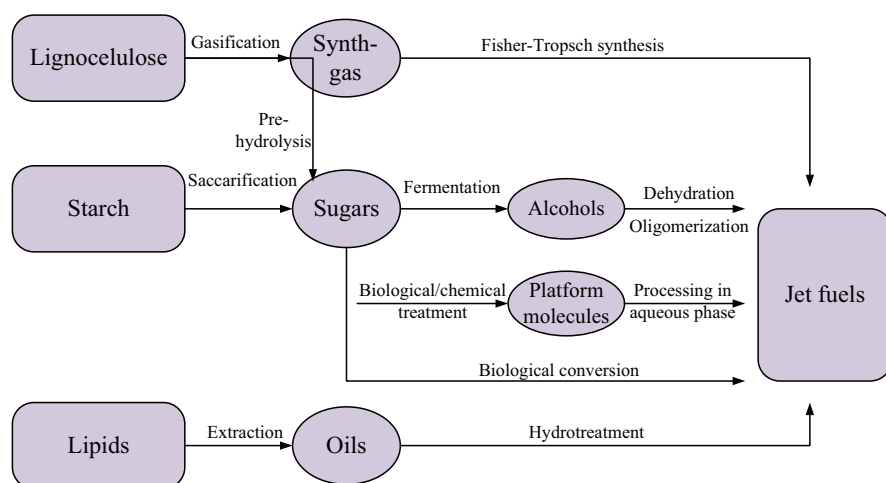


**Fig. 1** The main technological processes of biomass processing into alternative jet fuel (Ghazanfari, 2017)

In all cases, the first stage of grinding is required, which aims to reduce the structural complexity of biomass and obtain oxygen-containing intermediates, less complex and, consequently, more suitable for further production of jet fuels. These intermediates (oils, synthetic gas, alcohols, and sugars) give the name to various directions of conversion of biomass into alternative jet fuels: oil to jet, OtJ; gas to jet, GtJ; alcohol to jet, AtJ; and sugars to jet, StJ (Han et al., 2013; Iakovlieva et al., 2013). To date, a number of technologies for the production of alternative aviation fuels are already known and are being actively researched and put into practice.

### **3 Technological Processes of Alcohol Production as Feedstock for Jet Fuels**

World ethanol production is based on two methods: petrochemical and biotechnological (enzymes or bacteria). The petrochemical method is the hydration of ethylene in the presence of inorganic acids. Simplicity of technological process and high productivity makes this method extremely attractive in the conditions of low cost of the used raw materials (Boichenko & Yakovlieva, 2020; Han et al., 2013).

Glucose fermentation is the oldest method of ethanol production used to make alcoholic beverages. Agricultural products containing sugar, starch and cellulose, as well as wood waste and household waste are used as a feedstock (Ghazanfari, 2017).

There are methods of alcohol production by hydrolysis of cellulose. Cellulose has to be decomposed either with the help of strong chemicals (acids), or with the help of bacterial enzymes (Tretiakov, 2008; Boichenko & Yakovlieva, 2020; Iakovlieva et al., 2013). The process is slow and not cheap: as of 2006, the cost of production of a liter of cellulose alcohol was 60 cents, and at this price in the economy it is equal to oil at a price of not less than \$120 per barrel (Rajagopal & Zilberman, 2008).

Lower alcohols, the main one being bioethanol, can be used as an alternative raw material for the production of motor fuels and other petrochemical products. Processing biomass into ethyl alcohol is one of the most effective ways to use it. It should be noted that 80% of the world's bioethanol is used as automotive fuel in the form of gasoline-ethanol mixture of different composition (Tretiakov, 2008; Han et al., 2013).

### **4 Production of Jet Fuels Based on Alcohols**

AtJ fuel is a fuel derived from alcohols such as methanol, ethanol, butanol, and other long-chain alcohols. In recent years, the conversion of ethanol into a blended jet fuel is a very promising option for the development of alternative aviation fuel. The AtJ process includes three main stages (Rajagopal & Zilberman, 2008):

1. Dehydration of alcohol of biological origin to the corresponding olefin
2. Oligomerization of olefins to a new oligomerized olefin
3. Hydrogenation of oligomerized olefin to saturated hydrocarbon product

These three processes are well-known and widely used in the petrochemical industry. Alcohols commonly used in AtJ technology include small compounds with a number of C<sub>2</sub>–C<sub>4</sub> carbon atoms, such as ethanol and butanol (n-butanol and iso-butanol) (Ghazanfari, 2017; Rajagopal & Zilberman, 2008).

To convert alcohols to jet fuels, they are first dehydrated to a suitable alkene product containing the same number of carbon atoms. The product is then separated from liquid water and impurities by fractionation and fed to the next stage of the process in the form of gas. In the next step, the gaseous material is oligomerized to unsaturated compounds with higher molecular weight. Unsaturated oligomers having a molecular weight approximately compatible with petroleum fuels for separation are separated and further processed in the third main step – hydrogenation over a solid phase catalyst with hydrogen gas. In the final stage, the hydrogenated product is distilled to obtain the final products, among which is the kerosene fraction (Yakovlieva et al., 2019; Rajagopal & Zilberman, 2008).

Today it is accepted to allocate two kinds of technological processes of the production of jet fuel from alcohol. The first of them, described above, is known as AtJ-SPK – alcohol to jet-synthesized paraffinic kerosene. The second process is the production of alternative jet fuels from alcohols containing aromatic hydrocarbons. This technology is called AtJ-SKA – alcohol to jet-synthesized kerosene with aromatics. An alternative fuel based on AtJ-SKA technology, now produced by Swedish Biofuels, is also known by the trade name SB-JP-8 (Yakovlieva et al., 2019). In principle, the technological process of obtaining AtJ-SKA fuel is the same as the technological process of AtJ-SPK, except for the presence of an additional stage of aromatization of hydrocarbons. Depending on the technological capabilities of the fuel production enterprise, the production of aromatic substances can be performed as an integrated flow in the overall production process.

In order to spread the production of alternative jet fuels on the basis of alcohols on a commercial scale, the technological process must pass the procedure of its approval and comply with ASTM standards (Yakovlieva et al., 2019). The blended jet fuel, obtained from alcohols by the ATJ process, has already been approved by the ASTM D7566 standard (Boichenko & Yakovlieva, 2020). Currently, such fuel, which is produced from ethanol or an isobutanol intermediate, is allowed to be compounded with petroleum jet in the amount of up to 50% (vol.).

## 5 Conclusion

Thus, today the world is developing a large number of alternative technologies for the production of aviation fuels using both renewable and nonrenewable feedstock. Analyzing the current situation in the modern oil refining industry, and taking into

account the environmental situation in the world, which is constantly deteriorating – the transition to alternative aviation fuels is obvious.

In addition, the requirements of international organizations, such as ICAO, IATA, and CAEP, for the greening of civil aviation should be taken into account. Among these requirements are the following: reduction of CO<sub>2</sub> emissions by aircraft and reduction of toxicity of their exhaust gases (NO<sub>x</sub>, SO<sub>2</sub>, and other substances).

Given these and other factors, alternative aviation fuels developed and used in the world today must meet the following requirements:

- Be widespread and available worldwide to ensure international flights.
- Long service life of the aircraft (more than 30 years) requires alternative fuels to be compatible with engine parts and do not require significant re-equipment.
- Alternative fuels must undergo a strict certification procedure in order to ensure full compliance with the quality indicators of traditional jet fuels.
- Alternative aviation fuels must be environmentally friendly and able to meet the ever-increasing fuel needs of aviation.

## References

- Boichenko, S., & Yakovlieva, A. (2020). Energy efficient renewable feedstock for alternative motor fuels production: Solutions for Ukraine. In *Systems, decision and control in energy I* (pp. 247–259). Springer.
- Ghazanfari, J. (2017). Limiting factors for the use of palm oil biodiesel in a diesel engine in the context of the ASTM standard. *Cogent Engineering*, 1, 1–17.
- Grace, J. (2004). Understanding and managing the global carbon cycle. *Journal of Ecology*, 92, 189–202.
- Han, J., Elgowainy, A., Cai, H., & Wang, M. Q. (2013). Life-cycle analysis of bio-based aviation fuels. *Bioresources Technology*, 150, 447–456.
- Iakovlieva, A., Lejda, K., Vovk, O., & Boichenko, S. (2013). Peculiarities of the development and implementation of aviation biofuels in Ukraine. *World Congress on Petrochemistry and Chemical Engineering. Journal of Petroleum & Environmental Biotechnology*, 4(6), 47.
- Rajagopal, D., & Zilberman, D. (2008). *Environmental, economic and policy aspects of biofuels* (115 p). New Publishers Inc.
- Tretiakov, V. (2008). Bioethanol – Strategy of development of fuel and oil complex. *Chemistry and Technology*, 1, 8–12.
- Trofimov, I. (2014). Analysis of impact of aviation on atmosphere pollution. *Power Engineering: Economics, Technologies, Ecology*, 1, 119–120.
- Yakovlieva, A., Boichenko, S., Lejda, K., & Vovk, O. (2019). *Modification of jet fuels composition with renewable bio-additives* (Center for Education Literature) (207 p). National Aviation University.

# Analysis of World Practices of Using Liquid Hydrogen as a Motor Fuel for Aviation



Sergii Boichenko, Ihor Trofimov, Anna Yakovlieva, and Oksana Tarasiuk

## 1 Introduction

The European Commission's green deal on carbon neutrality by 2050 also challenges the aviation industry to seek new positions. Given the growing demand for air transportation around the world, it is becoming clear that the goal of decarbonization can only be achieved through new energy sources and innovative aircraft configurations. In addition to carbon dioxide (CO<sub>2</sub>), harmful greenhouse gases released during kerosene combustion include water vapor (H<sub>2</sub>O), carbon monoxide (CO), nitrogen oxides (NO<sub>x</sub>), soot, aerosols, and unheated hydrocarbons (UHC). Two-thirds of CO<sub>2</sub> emissions come from short- and medium-range aircraft, which account for 70% of the world's fleet.

Hydrogen (H<sub>2</sub>) is a universal and clean energy carrier that can be produced by electrolysis. Thus, the "green" H<sub>2</sub> offers a huge potential to promote sustainable development and growth in aviation. and secondary emissions – nitric oxides. Other emissions, such as CO<sub>2</sub>, are eliminated because H<sub>2</sub> is not hydrocarbon fuel. H<sub>2</sub> is also a fuel with a small number of pollutants, significantly reducing particulate

---

S. Boichenko (✉)

National Technical University of Ukraine "Igor Sikorsky Kyiv Polytechnic Institute", Kyiv, Ukraine

Scientific-Technical Union of Chemmotologists, Kyiv, Ukraine

I. Trofimov · A. Yakovlieva

Scientific-Technical Union of Chemmotologists, Kyiv, Ukraine

Ukrainian Scientific-Research and Education Center of Chemmotology and Certification of Fuels, Lubricants and Technical Liquids, National Aviation University, Kyiv, Ukraine

e-mail: [anna.yakovlieva@nau.edu.ua](mailto:anna.yakovlieva@nau.edu.ua)

O. Tarasiuk

Non-governmental Organization "Institute of Circular and Hydrogen Economics", Kyiv, Ukraine

matter in the exhaust gases of the engine. Moreover, in addition to combustion, H<sub>2</sub> offers the possibility of converting into electricity through a fuel cell. H<sub>2</sub> also has a disadvantage when used as fuel, especially in aviation, because its density is much lower than kerosene. H<sub>2</sub> can be stored in different aggregate states and different pressure ranges. Gaseous hydrogen (GW) is stored at ambient temperatures and high pressures of up to 700 bar, although the volume required for the same amount of energy is still seven times higher than that of kerosene (Fuel Cells and Hydrogen, 2020). To obtain a higher density and reduce the pressure to an acceptable level, H<sub>2</sub> is liquefied by cooling to 20 °K at ambient pressure. Liquid hydrogen (LH) requires only four times the volume to store the same amount of energy compared to kerosene (Bruce et al., 2020). Given the increased public awareness of the problem of global warming and greenhouse gas emissions, the question arises as to the extent to which aircraft expansion should be limited and not use renewable energy.

Sustainable aviation fuel (SAP) is a major competitor to hydrogen. Synthetic kerosene produced in the process of “power-to-liquid,” or PtL, is one of the possibilities, assuming that electricity as a source of energy, as well as CO<sub>2</sub>, captured from the air, and water act as the (Goldman, 2018) main resources (Dagget et al., 2006). Using PtL, the design of the aircraft does not change, and the airport does not need new infrastructure. However, CO<sub>2</sub>, which was previously filtered from the air at great cost, is still produced during combustion.

In 2009, all stakeholders of the aviation industry committed to a set of ambitious climate action goals, namely:

- 2009–2020: improving fuel efficiency by 1.5% per annum
- From 2020: reaching net carbon neutral growth
- By the year 2050: reducing global net aviation carbon emissions by 50% relative to 2005

The industry is well on track for the short-term fuel efficiency goal, and ICAO has put in place the CORSIA system (Carbon Offset and Reduction Scheme for International Aviation) to achieve the mid-term carbon neutral growth goal. The long-term 50% carbon reduction goal requires the combined efforts of all aviation stakeholders (aircraft and engine manufacturers, airlines, airports, air navigation service providers, and governments).

## 2 Rationale for Alternative Aviation Fuels

To truly decarbonize, the industry needs new, low-carbon propulsion (Dahl and Suttorp, 1998) technologies:

- (a) Battery- and turboelectric technologies
- (b) Hydrogen combustion in turbines
- (c) Fuel cells that power electric motors
- (d) New fuels

**Table 1** Evaluation matrix for the selected electro-fuels (compared to JET A-1) excellent, 5; good, 4; satisfactory, 3; challenging, 2; problematic, 1

Property	Jet A-1	nC <sub>8</sub> H <sub>18</sub>	CH <sub>3</sub> OH	CH <sub>4</sub>	H <sub>2</sub>	NH <sub>3</sub>	NH <sub>3</sub> /H <sub>2</sub>
CO <sub>2</sub> emission	1	4	4	4	5	5	5
Electrosynthesis	–	3	3	4	5	5	5
Specific energy	4	4	2	4	5	2	2
Energy density	5	5	2	3	1	2	2
Storage	5	5	4	2	1	3	3
Toxicity	3	3	2	4	5	1	1
Combustion properties	5	5	4	5	5	2	5
NOx and soot emissions	2	2	4	4	4	3	4
Drop-in capability (combustion)	5	4	2	2	2	2	4
Turbine power output	4	4	4	4	5	5	5
Drop-in potential (turbine)	5	5	4	3	2	2	3
Structural considerations	4	4	3	3	2	2	3

- (e) Numerous aircraft (airframe and engine) technologies
- (f) Sustainable aviation fuels
- (g) Operational and infrastructural measures.

Since the aviation industry committed to the set of goals in 2009, an impressive number of technological solutions contributing to the 2050 goal have been proposed, and many related projects have been initiated. In a maximum decarbonization scenario, hydrogen aircraft would start to replace all aircraft for ranges of up to 10,000 km after 2028–2038, representing the first conceivable entry-into-service dates with ambitious assumptions. After a ramp-up of manufacturing capacity over 3–4 years, all new aircraft up to a 10,000 km range would be powered by hydrogen. In this scenario, 60% of all aircraft are switched to liquid hydrogen by 2050, and the rest would be powered by synfuel and/or biofuels.

The following Table 1 shows the evaluation matrix, which summarizes the properties of selected electro-fuels, including hydrogen, and compares them to the conventional JET A-1 fuel.

The abovementioned Table 1 uses an evaluation scale from 5 (excellent properties) to 1 (problematic properties), and it could be clearly seen that hydrogen received the most of 5s as to its tested properties. The only problem is energy density and storage technologies, which are currently developing at an advanced pace. Drop-in capability (i.e., readiness to immediate use as a replacement fuel in the airports) is also highly problematic as most of the hydrogen technologies require current infrastructure rebuild. Nevertheless, feasibility and economic analyses show hydrogen can be a major part of aviation's future technology mix, as it proved to be the most efficient one in most cases (IATA, 2019). Hydrogen eliminates CO<sub>2</sub> emissions in flight and can be produced carbon-free. Considering also non-CO<sub>2</sub> emissions and taking into account the uncertainties of these effects, the latest estimates show that hydrogen combustion could reduce climate impact in flight by

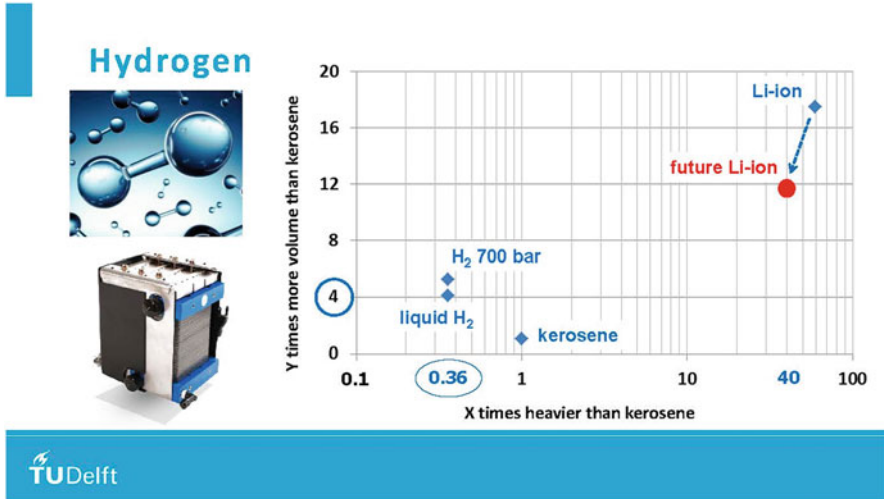


Fig. 1 Energy density of hydrogen

50–75% and fuel cell propulsion by 75–90% (ATAG, 2021). This compares to about 30–60% for synfuels. Figure 1 shows the volumetric and mass density of hydrogen, demonstrating the problem for aviation and the area for scientific researches in the nearest future.

As the main task for the airplane is to have lighter objects, which take less volume on board while using the most efficient fuel, conventional kerosene (Jet A-1 fuel) fully meets these requirements compared to hydrogen that proved to have 4 times more volume, being 0.36 times heavier (which is actually lighter), but the modern world's ecological requirements cannot sustain this kind of fuel any longer. That's why many researchers investigate the ways to cope with the volumetric density disadvantage of hydrogen as a fuel of the future. Cryogenic hydrogen has a superior energy density by mass, compared with kerosene, and produces no CO<sub>2</sub> emissions upon combustion. However, challenges arise with respect to its poor volumetric density. This obstacle may encourage a move away from conventional aircraft designs to models such as the blended wing body, which show promise in improved aerodynamic efficiency and can accommodate larger volumes of fuel. Electric batteries are viewed even less attractive in terms of mass density of energy as they proved to be about 40 times heavier than kerosene (Fig. 1). The *ATAG Waypoint 2050 Report* illustrates the comparative CO<sub>2</sub> emissions reduction for different types of airplanes if they start gradually introducing SAFs and/or electro-fuels from 2020 to 2050. The different types of airplanes are commuters (9–50 seats, less than 60 min flights), regional (50–100 seats, 30–90 min flights), short haul (100–150 seats, 45–120 min flights), medium haul (100–250 seats, 60–150 min flights), and long haul (250+ seats, 150+ min flights). The study shows that by 2050, commuters could contribute to less than 1% of industry CO<sub>2</sub> reduction if SAFs and/or electro-fuels are used by 2025; regional, to 3% if electro-fuels or hydrogen and/or SAFs are used



by 2030; short-haul – to 24% if electro-fuels or hydrogen and/or SAFs are used by 2040; medium haul, to 43% if SAFs and potentially some hydrogen are used by 2050; and long haul, to 30% if SAFs are introduced in 2020 and be in use all the years up to 2050. Hydrogen is considered as not feasible fuel for long-haul types of airplanes at the current technological level. Comparison of new technologies and SAFs in different studies shows that biofuels and synfuels have the main advantages of being drop-in fuels – no change needed to aircraft or infrastructure – but they also have the main disadvantages of limited reduction of non-CO<sub>2</sub> effects. On the other hand, new battery-electric and hydrogen technologies have no climate impact in flight and high CO<sub>2</sub> emissions reduction potential, but they have a huge drawback as of today's technologies development – need in change to infrastructure due to fast charging or battery exchange systems or special infrastructure for hydrogen handling. Moreover, the aircrafts of medium and long-range types would need revolutionary aircraft designs as efficient option for ranges above 10,000 km to introduce hydrogen as main fuel, whereas battery-electric technologies are considered as not applicable for this flight range as of current state of their development.

### **3 The Biggest Impediments to the Introduction of Liquid Hydrogen to the Aviation Industry**

In the case of cryogenic hydrogen, extensive changes will be required to support equipment, such as pumps, supply pipes, and control valves. A heat exchanger will also be required to vaporize liquid hydrogen before entering the combustion chamber. Metals commonly used in aircraft, including aluminum, titanium, and steel, in particular, are all susceptible to hydrogen embrittlement. Minimization of embrittlement will likely add to the cost and complexity of direct hydrogen use. Another primary issue relating to the use of hydrogen concerns the higher combustion temperatures achieved, which promote the production of NO<sub>x</sub> and could result in the degradation of other engine components such as the turbine blades. Addressing this problem requires the premixing of hydrogen with air to reduce operating temperatures. However, this process increases the risk of premature burning or “compressor surge” (which is an uncontrolled upstream propagation of the flame) due to the high reactivity of hydrogen with air. The use and handling of compressed and cryogenic hydrogen onboard aircraft would introduce a new series of safety risks to be managed. These are summarized here in Table 2.

**Table 2** Safety risks with cryogenic hydrogen onboard the aircraft

Risk	Description
Flammability	Hydrogen gas is highly flammable and has a wide flammability range (4.3–75 vol%), requiring very little air to ignite
Leakage	Hydrogen molecules are significantly smaller than other gases and can more easily pass through storage casings, which results in increased leakage rates. This risk is compounded by the fact that hydrogen is also difficult to detect due to it being colorless and odorless. Leakage detection devices would be required to alert personnel
Low energy ignition	Hydrogen can mix easily with air and form flammable mixtures that can ignite with minimal energy (0.017 MJ)
Embrittlement	Hydrogen can cause stress in materials by permeating the surface. This is seen in the case of steel, where cracks may form after continued exposure. Material selection needs to be carefully considered to avoid embrittlement
Exposure	Although not corrosive or poisonous, contact with liquid hydrogen can cause injury. Additionally, in the event of a leak, the inhalation of hydrogen can cause asphyxiation

## 4 Hydrogen Supply Infrastructure Challenges

By 2035 or 2040, there would likely be enough hydrogen supply infrastructure in place for liquid hydrogen aviation to take off, excluding any dedicated liquefaction capacity required at large airports. In the efficient decarbonization scenario, ten million tons of liquid hydrogen would be needed by 2040. This amount represents only 5% of the total projected global demand for hydrogen by 2040. This means that aviation could likely tap into a scaled-up hydrogen supply infrastructure. Here synfuel would actually be at a disadvantage, as any scale-up in synfuel production would have to be driven entirely by demand from aviation, meaning synfuels would capture fewer cost reductions from scaling up production than the liquid hydrogen route.

The biggest current challenges are:

- *Current lack of infrastructure:* safe and reliable LH<sub>2</sub> storage, distribution, and onboard H<sub>2</sub> propulsion.
- Once produced, the hydrogen would need to be either compressed or liquified and then distributed to the airports, through either liquid or compressed hydrogen truck trailers for smaller airports or through a pipeline for larger airports. It can also be shipped in liquid form or converted (e.g., into ammonia or liquid organic hydrogen carriers).
- Once at the airport, the hydrogen would be liquified (if not already liquefied at the source), stored, and ultimately transferred to airplanes via refueling trucks or an alternative refueling method like refueling platforms or aircraft “fuel station” plots.

*Scaling and building parallel infrastructures* during the transition to new aircraft systems unlocks the potential of LH<sub>2</sub> aviation by developing the necessary refueling infrastructure.

## 5 On-Airport Applications for Hydrogen

On or “adjacent” airport activities provide a nearer-term opportunity to introduce clean hydrogen into the commercial aviation *sector*. The use of hydrogen for materials handling (e.g., forklifts) is already being demonstrated within the warehouse operations of several large logistics companies, such as Amazon and Walmart. Here, fuel cell equipment has already been found to be competitive with diesel and battery alternatives on a total cost of ownership basis. Plug Power is one fuel cell equipment manufacturer that is successfully applying its technology to GSE applications, having recently demonstrated the use of fuel cell-operated baggage tugs at Hamburg Airport. The US military has also been active, as demonstrated by the Hawaii Air National Guard who recently retrofitted a U-30 Aircraft Tow Tractor with a fuel cell power system to tow an 84t aircraft. Fuel cell cars and buses are a readily available technology offered by several OEMs, such as Toyota and Hyundai. This readiness is being demonstrated in France with a recent announcement by Toulouse-Blagnac Airport that in 2020, it will host a hydrogen production and public refueling station to fuel four buses (provided by SAFRA) that will transport passengers between car parks, terminals, and aircraft. The following Table 3 demonstrate some examples of current use of hydrogen in aviation infrastructure.

Most publicly available research concentrates on hydrogen propulsion components; a few aircraft-level concepts have also been discussed and a few prototypes built. The required infrastructure, however, has rarely been investigated. In the 1970s, a thorough review highlighted hydrogen-powered aviation’s potential and development needs at that time. In the last 10 years, some early prototypes of hydrogen aircraft have been developed (e.g., the motorized research glider HY4). Startups such as ZeroAvia are also modifying general aviation aircraft with a zero-emission hydrogen-fueled powertrain that could be applied to commuter and

**Table 3** Examples of current use of hydrogen in aviation infrastructure

Category		Examples
Mobility ground support equipment (GSE)	Materials handling	Baggage/cargo tractors, belt loaders, pushback and taxiing tugs/tractors, forklifts
	Transport	Apron bus
	Servicing	Follow-me vehicle, ramp agent, de/anti-icing vehicles, catering vehicles, air conditioning units, refuelers, lavatory service vehicles
Stationary GSE	Power generation	Backup power, ground power units (GPU)
Heat generation		Airport food burners

**Table 4** Component analysis of the technologies for hydrogen storage and transportation at the airports

Innovative technological systems	Efficient refueling systems	Airport and aircraft refueling setup	LH <sub>2</sub> hydrant refueling infrastructure	Tanks for hydrogen storage in liquid ammonia and/or LOHCs
Current technologies and parameters	~500 L/min	Universal hydrogen's modular capsule technology; LH <sub>2</sub> refueling trucks designed for long-distance transfer with low boil-off	Prohibitive costs. Costs >5× those of standard hydrant systems	Storage as a compressed gas Storage in LOHCs. One strong proponent of this technology is the SME Hydrogenious
Required parameters	>1000 L/min	Refueling truck concept fully optimized for airport refueling commercially available by 2030	Hydrant refueling system costs at par with refueling trucks	
Targets for further innovations	Reduce LH <sub>2</sub> refueling times to minimize impact on turnaround times New, more efficient hose connection systems to ensure compatibility with unconventional tank setups (e.g., overhead, from the top) and ensure reliable, safe connections through self-closing quick couplings	Develop a refueling infrastructure with minimal disruptions to current airport operations Modular setup, including the optimal organization of ground operations and infrastructure to allow parallel refueling systems	Determine whether LH <sub>2</sub> hydrant refueling infrastructure is cost-technically possible and could enable economies of scale at large airports	Compressed hydrogen and, to a lesser extent, cryogenic hydrogen, e-LNG, and e-ammonia require heavy tanks to contain the fuel

regional aircraft. Fuel cell systems are being tested as auxiliary power units in commercial aircraft, although they have not been deployed in serial production. Hydrogen propulsion with fuel cell systems is also being tested for urban air mobility (unmanned air vehicles and “taxi”-drones). All of this research offers significant promise; it also agrees on the greatest technology challenges for components, aircraft systems, and integration into the overall aviation infrastructure. In order to have a clear understanding of the current stage of hydrogen technologies implementation to the aviation industry, we have developed the following Tables 4 and 5,

**Table 5** Component analysis of the onboard technologies of hydrogen accumulation and propulsion

Technological systems	Current technological parameters	Required technological parameters	Priorities of further innovations
Onboard LH <sub>2</sub> distribution components and system	No designs for commercial aircraft standards yet	Safe, certified distribution architecture with minimized weight and maintenance costs	Ensure a kerosene level of safety and reliability for LH <sub>2</sub> distribution
High-power fuel cell system/H <sub>2</sub> direct burning turbine	~0.75 kW/kg power density on system level; The most advanced and suitable for aviation today are low-temperature proton-exchange membrane (PEM) fuel cells; A hybrid system of H <sub>2</sub> turbines and fuel cell systems	1.7 kW/kg for up to regional aircraft (<5 MW), 2 kW/kg for short-range and larger aircraft; LH <sub>2</sub> requires cryogenic cooling down to 20 °K. These temperatures must be handled by pipes, valves, and compressors; Boil-off needs to be kept low; and leakage and embrittlement of material are avoided	Enable the use of <i>fuel cell propulsion</i> since it has a higher potential to reduce climate impact than H <sub>2</sub> combustion; <i>H<sub>2</sub> propulsion turbines with low-NO<sub>x</sub> emissions</i> and long lifetimes A hybrid system of H <sub>2</sub> turbines and fuel cell systems
Lightweight and safe LH <sub>2</sub> tanks	15–20% gravimetric index (for tank with less than 1 ton of LH <sub>2</sub> )	35% gravimetric index for short-range (5 tons of LH <sub>2</sub> stored), 38%+ for long-range aircraft (more than 30 tons of LH <sub>2</sub> ); Since LH <sub>2</sub> needs to remain cold and heat transfer must be minimized to avoid vaporization of hydrogen, spherical or cylindrical tanks are required to keep losses low.	<i>Decrease weight of LH<sub>2</sub> tanks</i> to enable more efficient H <sub>2</sub> -powered aircraft and better economics – potentially enabling competitive economics for long-range aircraft

demonstrating the current state of technologies for hydrogen storage and transportation at the airports as well as of onboard technologies for hydrogen accumulation and propulsion.

## 6 Conclusions

- To decarbonize, aviation needs new fuels and propulsion technology. A broad range of technological innovations is under development to improve aircraft fuel efficiency and reduce their CO<sub>2</sub> emissions. Many of the revolutionary aircraft technology concepts offer other benefits than fuel efficiency.

- Investing in SAFs and offsetting emissions through market-based measures, such as CORSIA, may appear easier and cheaper than implementing radically new aircraft and propulsion technologies.
- Hydrogen propulsion could significantly reduce climate impact.
- Assuming these technical developments, H<sub>2</sub> propulsion is best suited for commuter, regional, short range, and medium-range aircraft.
- Long-range aircraft require new aircraft designs for hydrogen.
- Refueling infrastructure is a manageable challenge in early ramp-up years but will require significant coordination.
- A more challenging but not impossible scale-up after 2040 is required.
- To scale hydrogen-powered aircraft, several technological and infrastructural unlocks need to happen, especially within the accumulation and storage technologies. Industry experts project these important advancements are possible within 5–10 years.

## References

- ATAG. (2021). *Balancing growth in connectivity with a comprehensive global air transport response to the climate emergency*. ATAG Waypoint 2050 Report.
- Bruce, S., Temminghoff, M., Hayward, J., Palfreyman, D., Munnings, C., Burke, N., & Creasey, S. (2020). *Opportunities for hydrogen in aviation*. CSIRO.
- Dagget, D., Hendricks, R., Walther, R., & Corporan, E. (2006). *Alternate fuels for use in commercial aircraft*. Boeing Company.
- Dahl, G., & Suttrop, F. (1998). Engine control and low-NO<sub>x</sub> combustion for hydrogen fuelled aircraft gas turbines. *International Journal of Hydrogen Energy*, 23, 695.
- Fuel Cells and Hydrogen 2 Joint Undertaking. (2020, May). *Hydrogen-powered aviation: A fact-based study of hydrogen technology, economics, and climate impact by 2050*.
- Goldmann, A. (2018). A study on electrofuels in aviation. *Energies*, 11(2), 392.
- IATA. (2019). *Aircraft technology roadmap to 2050*. IATA.

# Waste-Free Technology for the Production of Building Materials by Mining and Processing Plants



Oksana Vovk, Kostiantyn Tkachuk, Oksana Tverda, Andrii Syniuk,  
and Eduard Kukuiashnyi

## Nomenclature

$\text{Al}_2\text{O}_3$	Aluminum oxide
$\text{B}_2\text{O}_3$	Boron oxide
$\text{Fe}_2\text{O}_3$	Iron (III) oxide
$\text{MgO}$	Magnesium oxide
$\text{SO}_2$	Silicon dioxide

## 1 Introduction

Mining wastes occupy a special place among the pollution caused by mining complexes; affect the air, groundwater, and surface water; increase the risk of migration of surface contaminants; and require the removal of land that could be used, for example, in agriculture (Tverda et al., 2016).

Solving the problems of ensuring the integrated use of mineral raw materials, waste disposal, and organizing the development of minerals with low-waste or non-waste production remains relevant. Under modern conditions of development and growth rates of the mining industry, shortcomings in the integrated and fuller use of minerals become unacceptable waste (Ivanov & Bilaniuk, 2015).

---

O. Vovk · K. Tkachuk · O. Tverda (✉)

Department of Geoengineering, National Technical University of Ukraine “Igor Sikorsky Kyiv Polytechnic Institute”, Kyiv, Ukraine

A. Syniuk

Department of Coal Industry, Ministry of Energy of Ukraine, Kyiv, Ukraine

E. Kukuiashnyi

State Enterprise “Directorate of Objects Construction”, Novovolynsk, Ukraine

One of the powerful directions of the mining industry is the extraction of nonmetallic minerals and the production of gravel from them (Dyoniak & Tkachuk, 2014). This is due to the need to build infrastructure, the development of urban planning, as well as infrastructural modernization. The construction industry of both Ukraine and other countries, with significant extraction of nonmetallic minerals, accumulates millions of cubic meters of waste, occupying large areas of fertile agricultural land.

Thus, at the average stone-crushing enterprise with a capacity of 3 million m<sup>3</sup> of crushed stone per year, 420–600 thousand m<sup>3</sup> of dropouts are formed, which is 14–20% of the total volume of extracted mining mass. Therefore, the task of the utilization of waste generated during the extraction and processing of nonmetallic minerals is particularly important and relevant (Ivanenko et al., 2012).

The simplest technological option is the utilization of nonmetallic mining waste for the production of construction raw materials and products (Ivanov & Bilaniuk, 2015). It should be noted that current waste is better for the production of building materials, because it retains the original physical and mechanical properties and chemical composition and, in addition, can reach the consumer bypassing all other actions necessary to consolidate waste (transportation, storage, etc.). Waste can be used for various construction works, in particular for the construction of roads, foundations, dams, filling of spent areas, leveling, etc. (Samir et al., 2018).

Gravel dropouts, which are formed in the process of stone crushing and stone processing, are almost universally used as a road construction material. The bulk of the industrial waste that is disposed of is used to fill up the excavated quarries, fill the underground mine workings, and rehabilitate the disturbed arable and pasture lands. Shallow quarries in almost all regions of Ukraine are filled. At the same time, in the process of backfilling not only waste rocks, which cannot be used otherwise, but also such types of industrial waste, which can be processed into useful products, are used (Ivanov & Bilaniuk, 2015). Mining companies use part of the waste to form a stemming of borehole charges for the explosive destruction of rocks (Tverda et al., 2021).

Dropouts can be used as an intensifier of sintering in high-speed firing modes of floor tiles and for the production of bricks instead of fireclay and sand, for the production of ceramic products (Ivanenko et al., 2012). Dropouts with particle sizes less than 5 mm should be used as a filler for the manufacture of aerated concrete and mortars (Popovych et al., 2013).

One of the areas where dropouts can be used is ultrahigh performance concrete (UHPC). UHPC can be a good alternative for recycling gravel waste. In (Vaitkevičius et al., 2013), it is researched how gravel waste affects the main properties of UHPC: viscosity, density, and compressive strength. Gravel waste can be used as a microfiller or to replace some cement.

Gravel waste can also be used to produce alite. One way is to heat the feedstock once to obtain alite. To do this, 3 mol of CaCO<sub>3</sub> is taken per 1 ton of waste and heated to a temperature of 1450 °C; the result is alite (3CaO·SiO<sub>2</sub>). The second is realized by means of two-stage heating. One ton of waste is first heated to a temperature of 1300 °C, using 2 mol of CaCO<sub>3</sub>. The result of firing is 2CaO·SiO<sub>2</sub> –



white. The resulting heat is cooled to 25 °C, and  $\text{Al}_2\text{O}_3$  is leached with soda solution. In this regard, it is necessary to reheat. As heat, you can partially use the heat of the exhaust gases obtained during the first firing. This heating is carried out using 1 mol of  $\text{CaCO}_3$  and occurs to a temperature of 1450 °C to obtain alite (Yefimenko et al., 2014).

In addition, the directions of extraction of silica from the gravel waste are being developed. Silica can be used: as a carrier of catalysts and chemical plant protection products; as sorbents and filter powders for the regeneration of petroleum products; as a high-quality flux in nonferrous metallurgy processes; as a raw material for the production of environmentally friendly glass, glass containers, and crystal; as a filler for paper and cardboard in order to obtain hygienically clean packaging materials for the food industry; as a filter powder for beer, oils, and juices; as a matte admixture to varnishes and paints; to obtain silicon carbide in mechanical engineering (ceramic engines, parts for spacecraft); in order to obtain crystalline silicon for the electronic and electrical industries (ceramic electrical insulators, fiberglass, fiber optics, and superfine fiber); for the synthesis of artificial zeolites in petrochemistry (oil cracking); and as a filler in the production of rubber products as well as plastics (Sugonyako & Zenitova, 2015).

The analysis of methods of utilization of gravel production waste shows that enterprises, selling them, could not only receive additional income but also introduce waste-free production technologies, reduce the impact of accumulated waste on the environment, and reduce penalties for environmental pollution. Areas cleared of waste could allow to expand the front of mining company works.

## 2 Method

The emission spectral analysis method was used to determine the chemical composition of mining waste and substantiate the possibility of using waste as raw material for the production of new products – building materials. Emission spectral analysis is based on the acquisition and study of emission spectra. Qualitative spectral analysis is performed based on the position and relative intensity of individual lines in these spectra. Comparing the intensity of specially selected spectral lines in the spectrum of the sample with the intensity of the same lines in the spectra of the standards, the content of the element is determined, thus performing a quantitative spectral analysis. Qualitative spectral analysis is based on the individuality of the emission spectra of each element and, as a rule, comes down to determining the wavelengths of the lines in the spectrum and establishing the belonging of these lines to one or another element. Deciphering of spectra is carried out either on a steelscope (visually), or on a spectro projector or microscope after photographing the spectra (Vikhariev et al., 2010).

Samples of mining waste (quartzite) of Tovkachiv Mining and Processing Plant were analyzed in a certified laboratory in Kyiv.

## 2.1 Calculation

According to laboratory studies, the mining waste has the following composition: quartzite ( $\text{SiO}_2$ ), 96.9–98.05%; pyrophyllite ( $\text{Al}_2\text{O}_3$ ), 0.77–1.47%; and ore mineral ( $\text{Fe}_2\text{O}_3$ ), 0.24–1%. This chemical composition of mining waste allows them to be used as raw material for the manufacture of fiberglass. According to chemical composition of some glasses for continuous fiber (Gutnikov et al., 2010), the chemical composition of the waste is closest to the chemical composition of glass fiber type D ( $\text{SiO}_2$ , 72–75%;  $\text{B}_2\text{O}_3$ , 21–24%;  $\text{Al}_2\text{O}_3$ , 0–1%;  $\text{CaO}$ , 0–1%;  $\text{MgO}$ , 0.5–0.6%;  $\text{Na}_2\text{O}$ , 0–4%;  $\text{K}_2\text{O}$ , 0–4%;  $\text{Fe}_2\text{O}_3$ , 0.3%), except for  $\text{B}_2\text{O}_3$ ,  $\text{MgO}$ , and excessive content of iron (III) oxide. It should be noted that the chemical composition of waste is not constant and depends on mining and geological conditions. That is why the content ranges of the components are given above. If the content of iron (III) oxide does not exceed 0.3%, then mining waste can be used as raw material for the production of type D fiberglass provided that  $\text{B}_2\text{O}_3$  and  $\text{MgO}$  are added in appropriate proportions. If the content of iron (III) oxide exceeds 0.3%, it must be removed from mining waste.

To remove iron (III) oxide from mining waste, it is proposed to grind the initial rock mass in a fine grinding mill to a fraction size of 0.1–0.5 mm. This is necessary to increase the efficiency of the magnetic separator, which is proposed to be used in the next stage for the extraction of iron (III) oxides, as well as for further technological processes of fiberglass production.

In a magnetic separator due to the action of a magnetic field, iron-containing particles are separated from the bulk of the rock. Modern magnetic separators allow you to remove 95–99% of iron (III) oxides. Assume the chemical composition of mining waste is as follows:  $\text{SiO}_2$ , 97.63%;  $\text{Al}_2\text{O}_3$ , 1.09%; and  $\text{Fe}_2\text{O}_3$ , 1.28%. Given that the magnetic separator allows you to remove at least 95% of iron (III) oxides, 976.3 kg of  $\text{SiO}_2$ , 10.9 kg of  $\text{Al}_2\text{O}_3$ , and 0.64 kg of  $\text{Fe}_2\text{O}_3$  will remain from one ton of waste. According to our calculations, 306.73 kg of  $\text{B}_2\text{O}_3$  and 7.16 kg of  $\text{MgO}$  must be added to obtain raw materials from which type D fiberglass can be made. After that, the total mass of raw materials will be 1301.7 kg, and its chemical composition will be as follows:  $\text{SiO}_2$ , 75%;  $\text{B}_2\text{O}_3$ , 23.56%;  $\text{Al}_2\text{O}_3$ , 0.84%;  $\text{MgO}$ , 0.55%; and  $\text{Fe}_2\text{O}_3$ , 0.049%, which fully meets the requirements for type D fiberglass.

## 3 Results and Discussion

The method of waste utilization with the production of type D fiberglass for mining and processing plants is proposed (Fig. 1). The method includes the extraction of rock from the dumps of stone crushing plants, fine grinding of waste to a fraction of 0.1–0.5 mm, extraction of iron (III) oxides on a magnetic separator, adding  $\text{B}_2\text{O}_3$  and

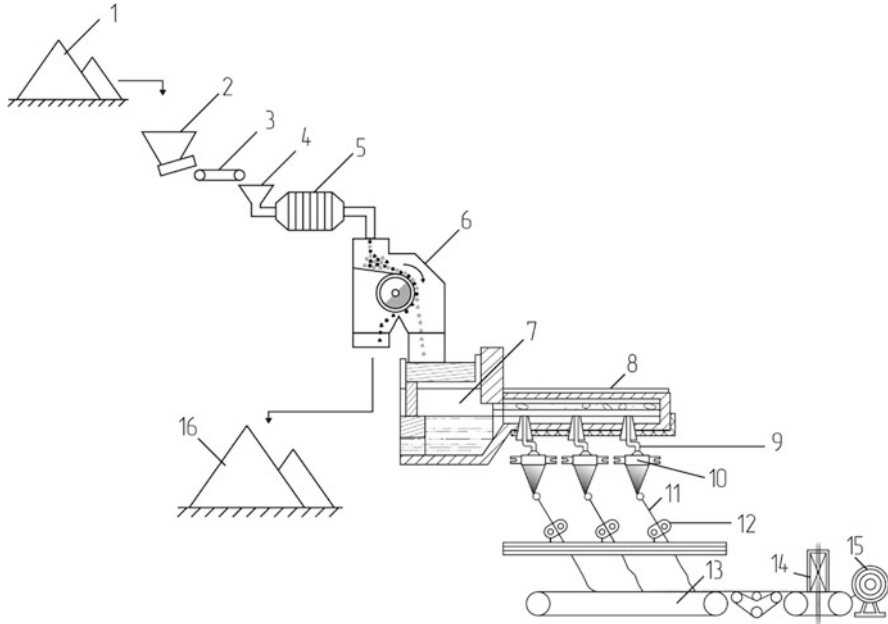


**Fig. 1** Technological scheme of utilization of mining waste to obtain fiberglass: (1) mining waste; (2) power hopper; (3) belt conveyor; (4) the dispenser of a fine grinding mill; (5) a fine grinding mill; (6) magnetic separator; (7) glass furnace; (8) feeder; (9) jet tube; (10) spinneret feeder; (11) fiberglass thread; (12) exhaust rolls; (13) conveyor; (14) drying chamber; (15) glass canvas; (16) removed  $\text{Fe}_2\text{O}_3$

MgO in appropriate proportions, and supply of raw materials to the glass furnace for the production of fiberglass.

Removed  $\text{Fe}_2\text{O}_3$  can be used for the production of pigment for paints. The production of gravel, the production of fiberglass based on the proposed method of waste disposal, and the production of pigment for paints from extracted iron oxide (III) allow to implement by mining and processing plants waste-free technology for the production of building materials.

## 4 Conclusion

The analysis of literature sources and analysis of chemical composition of mining waste showed the possibility of using mining waste to obtain building materials. The analysis of methods of utilization of gravel production waste shows that enterprises, selling them, could not only receive additional income but also introduce waste-free production technologies, reduce the impact of accumulated waste on the environment, and reduce penalties for environmental pollution. Areas cleared of waste could allow to expand the front of mining company works.

The method of waste utilization with the production of type D fiberglass for mining and processing plants is proposed. The method includes extraction of rock from the dumps of stone crushing plants, fine grinding of waste to a fraction of 0.1–0.5 mm, extraction of iron (III) oxides on a magnetic separator, adding  $B_2O_3$  and MgO in appropriate proportions, and supply of raw materials to the glass furnace for the production of fiberglass.

The production of gravel, fiberglass based on the proposed method of waste disposal, and pigment for paints from extracted iron oxide (III) allows implementation by mining and processing plants waste-free technology for the production of building materials.

## References

- Dyniak, S., & Tkachuk, K. (2014). Improving the technology of crushed stone production. *Herald of the National Technical University of Ukraine "Kyiv Polytechnic Institute", Series of "Mining"*, 25, 40–44.
- Gutnikov, S., Lazoriak, B., & Sielieznov, A. (2010). *Glass fibers*. Lomonosov Moscow State University.
- Ivanenko, O., Kravchenko, K., Virnyk, M., & Tytiuk, A. (2012). Use of granite rubble siftings for the production of commercial concrete. *Eastern-European Journal of Enterprise Technologies*, 2(12(56)), 16–18.
- Ivanov, E., & Bilaniuk, V. (2015). The mineral raw materials and mining wastes using efficiency in Ukraine. *Subsoil use in Ukraine. Prospects for investment* (pp. 344–351). The State Commission of Ukraine on Mineral Resources.
- Popovych, O., Zakharko, Y., & Malovanyi, M. (2013). Problems of utilization and processing of construction waste. *Bulletin of Lviv Polytechnic National University, Series Theory and Building Practice*, 755(2013–1), 321–324.
- Samir, M., Alama, F., Buysse, P., van Nylen, T., & Ostanin, O. (2018). *Disposal of mining waste: Classification and international recycling experience*. E3S Web of Conferences 41, 02012: Abstracts of IIIrd International Innovative Mining Symposium.
- Sugonyako, D., & Zenitova, L. (2015). Silicon dioxide as a reinforcing filler for polymeric materials. *Bulletin of the Technological University*, 18(5), 94–100.
- Tverda, O., Tkachuk, K., & Davydenko, Y. (2016). Comparative analysis of methods to minimize dust from granite mine dumps. *Eastern-European Journal of Enterprise Technologies*, 2(10(80)), 40–46.
- Tverda, O., Kofanova, O., Kofanov, O., Tkachuk, K., Polukarov, O., & Pobigaylo, V. (2021). Gas-neutralizing and dust-suppressing stemming of borehole charges for increasing the environmental safety of explosion. *Latvian Journal of Physics and Technical Sciences*, 58(4), 15–27.
- Vaitkevičius, V., Šerelis, E., & Lygutaitė, R. (2013). Production waste of granite rubble utilisation in ultra high performance concrete. *Journal of Sustainable Architecture and Civil Engineering*, 2(3), 54–60.
- Vikhariev, A., Zuikova, S., Chiemieris, N., & Domina, N. (2010). *Physicochemical methods of analysis*. Altai State Technical University.
- Yefimenko, V. I., Yefimenko, V. V., & Yahodkina, O. O. (2014). Analysis of the feasibility of integrated use of waste from mining enterprises for the production of non-metallic building materials. *Journal of the Kryvyi Rih National University*, 36, 145–148.

# Index

## A

Abatement, 15–17, 309, 312  
Additive manufacturing, 99–106, 294  
Aero-engine, 29, 30, 32, 35  
Aerospace, 99–106, 164, 174, 243–247  
Aircraft, 5, 13, 29, 51, 57, 68, 91, 99, 110, 127, 135, 151, 157, 175, 181, 189, 200, 221, 229, 237, 250, 260, 263, 272, 290, 295, 307, 316, 325, 330, 335, 341, 353, 363, 371, 386, 407, 413  
Aircraft line maintenance, 129  
Aircraft maintenance, 127, 263–269, 333, 371  
Aircraft noise, 14, 274, 275, 307–313  
Aircraft systems, 189, 263–265, 269, 419, 420  
Airline market, 287  
Airlines, 3, 5–7, 157–161, 199, 209–213, 244, 258, 263, 275, 285–291, 294–298, 313, 329–333, 335, 336, 342, 414  
Airline services, 209–213  
Air logistics, 109–116  
Airport, 3, 5, 6, 13–17, 29, 43, 110, 128, 152, 154, 155, 199, 205, 206, 211, 243, 257–260, 272, 275, 277–282, 286, 290, 291, 295–298, 307–313, 330, 333, 335, 338, 353, 356, 357, 359, 386–392, 414, 415, 418–421  
Airport infrastructure, 290  
Airport noise contours, 13–17, 311  
Air traffic control officer (ATCO), 38–43, 152–155, 342, 343, 345, 347, 349  
Air transport, 110, 112, 157, 158, 161, 244, 257, 258, 285–291, 296, 354

Air transportation, 3, 29, 158, 257, 294, 295, 312, 335, 385–392, 413  
Alcohol, 59, 61, 217, 407–411  
Alternative aviation fuels, 51–54, 407, 409, 411, 414–417  
Alternative fuel, 52, 158, 230, 234, 236, 408, 410, 411  
Analytical hierarchy process, 342, 380  
Analytic hierarchy process (AHP), 335–339, 341–349, 380, 381  
Annex 16, 222, 271, 272, 274, 310  
Antifriction properties, 376  
Aviation, 4, 29, 39, 51, 57, 110, 127, 135, 151, 157, 175, 181, 189, 199, 212, 221, 229, 237, 243, 250, 258, 272, 277, 286, 293, 301, 307, 315, 321, 329, 339, 341, 351, 371, 385, 407, 413  
Aviation management, 260  
Aviation sustainability, vi, 293–298

## B

BADA model, 316–317  
Biodiesel, 51, 58, 215, 216, 218, 220  
Biomass, 50, 216, 357, 408, 409  
Bio-pollution, 215, 221, 227

## C

Carbon dioxide (CO<sub>2</sub>), 6, 46, 48, 53, 54, 84, 157, 161, 232, 234, 330, 331, 385, 413, 415, 416, 421  
Carbon fiber/epoxy composites, 179

Carbon offset, 6, 414  
 Carbon Offsetting and Reduction Scheme for International Aviation (CORSA), 157, 161, 271–275, 296, 414, 422  
 CFD validation, 91–97  
 14 CFR Part 23, 135, 137, 144  
 Circular cylinder, 77–80  
 Circulation control (CC), 250–251, 256  
 Civil aviation, 151, 200, 202, 206, 271, 272, 274, 275, 287, 288, 311, 330, 335, 407, 411  
 Coanda surface, 250, 254, 255  
 Co axial rotor, 83–87, 89  
 Collaborative decision-making (CDM), 153–155  
 Competition, 3, 127, 209, 229, 285, 286, 288, 298  
 Composite materials, 99, 101, 144, 146, 149, 164, 165, 171, 173, 176, 179–182, 187  
 Composite material testing, 174  
 Composite structure, 172  
 Content analysis, 110, 112, 115, 159, 160, 287  
 Continuous climb (CCO), 316, 318, 319  
 Conversion, 110, 231, 236, 380, 408, 409  
 Correlation type, 65–67  
 Corrosion, 164, 215–220, 371, 398  
 Cycle analysis, 46

## D

Decision-making (DM), 29, 151–155, 204, 243, 295, 342, 343, 348, 380  
 Deep learning, 277, 278, 280, 282, 294  
 Denim textile industry, 47, 48  
 Destructor, 361  
 Diesel fuel, 215, 216, 218–220, 357, 358, 360, 361, 408  
 Differential transformation method (DTM), 21, 22, 26  
 Digitalization, 109–116, 243, 244, 293–298  
 Digital transformation, 110, 112, 243–247, 294, 295, 298  
 Dual radius flap (DRF), 250, 253–256  
 Dye injection, 78

## E

Ecological sustainability, 2  
 Efficiency, 3, 33, 39, 57, 59–61, 145, 149, 155, 158, 159, 190–192, 204, 223–227, 230, 231, 233, 234, 236, 243, 244, 260, 264, 265, 267–269, 295, 296, 312, 313, 330, 331, 333, 355, 380, 396–405, 407, 408, 414, 416, 421, 426

Electrical Vertical Takeoff and Landing (eVTOL), 91, 95  
 Emission, 5–7, 29–35, 47, 48, 51–54, 58, 61, 112, 157–161, 189, 221, 222, 229, 230, 232, 234–236, 258, 260, 296, 297, 311, 315, 316, 321, 330, 331, 379, 385, 386, 396–405, 411, 413–417, 421, 425  
 Emission calculation methods, 29–35  
 Entropy analysis, 223  
 Environment, 2, 29, 45, 46, 48, 51–54, 59, 84, 106, 109, 151, 157, 161, 164, 192, 200, 203, 206, 221–228, 244, 246, 258, 260, 277–282, 288, 294–296, 298, 308, 312, 336, 339, 341, 348, 351–354, 358, 361, 396, 399, 402, 403, 405, 425, 427  
 Environmental and enviro-economic analysis, 51–54  
 Environmental performance, 158, 226, 230, 329–333  
 Environmental quality, 1, 3  
 Environmental sustainability, 2, 3, 5, 293–298, 330, 331, 333  
 Environment report, 159, 161  
 Euler-Bernoulli Beam, 20, 21, 26  
 Evaporation, 33, 34, 58, 59, 396–405  
 Exhaust gas emissions, 215

## F

Face recognition, 278–280, 282, 297  
 Fatigue, 37–39, 41, 43, 127–134, 164, 338, 339, 372, 375  
 Fiberglass production, 426  
 Finite element analysis, 135  
 Finite element method (FEM), 71, 182, 363–369  
 Fixed-wing UAVs, 117–125  
 Flight procedure, 13–17, 312  
 Flight safety, 263, 264, 372  
 Flow control, 79  
 Flow velocity, 65  
 Flux-weakening, 192–193, 197  
 Free vibration, 20, 22, 24–26, 182, 185  
 Fuel, 3, 5, 29, 31–35, 48, 51–54, 57, 106, 110, 136, 154, 160, 161, 199, 215–224, 229, 296–298, 315–320, 322–325, 330, 331, 333, 379–383, 385–388, 390, 392, 398, 399, 402, 404, 405, 413–422  
 Fuel additives, 58  
 Fuel cell, 380, 383, 391, 392, 408, 414, 416, 419, 420  
 Fuel tank, 363, 389, 390, 396, 404  
 Fused Filament Fabrication (FFF), 101–103  
 Future of aviation, 244

**G**

Gasoline, 52, 53, 57–59, 387, 396–405, 408  
 Glass fibers, 146–149, 176, 426  
 Glass microspheres (GMs), 146–149  
 Global warming, 47–50, 157, 223, 294, 321, 322, 379, 401, 414  
 Gradual climb, 315–320  
 Graphite fillers, 176–179  
 Green practices, 157–161

**H**

Hand lay-up, 146, 147, 164, 168, 173, 177  
 Harmful emissions, 45, 57, 61, 215, 294, 413  
 Helicopter, 51, 83–89, 91–97, 117, 136  
 High-lift device, 250–256  
 Hover, 83–85, 87, 89, 91–97, 118  
 Human factors, 128, 200, 203, 244, 298, 339, 341–343  
 Hybrid composites, 176, 179, 180  
 Hybrid engine, 420  
 Hydraulic oil, 372–373, 375–377  
 Hydrocarbons, 30, 353, 375, 386, 396–405, 408, 410, 413  
 Hydrogen, 58, 386, 387, 389, 391, 392, 408, 410, 413–422  
 Hydrogen aircraft, 391, 415, 419  
 Hydrogen airport, 387, 392

**I**

Impact, 5, 29, 45–50, 54, 109, 116, 118, 133, 135, 145, 146, 149, 157, 161, 203, 212, 223, 226, 227, 258, 260, 264, 285, 287, 290, 294, 295, 307, 308, 310–313, 315, 330, 342, 353, 380, 396, 399, 403, 404, 415, 417, 422, 425  
 Index, 5, 29, 31–33, 35, 159, 223, 227, 257–260, 288, 322, 323, 421  
 Internal combustion engines, 51, 58, 61

**J**

Jet flap, 251, 254  
 Jet fuel, 6, 157, 158, 230, 389, 407–411

**L**

Landfills, 46, 352, 353, 355–357, 359–362  
 Liberalisation, 285–287  
 Life cycle assessment (LCA), 45–49  
 Light fraction, 401, 402

Lightning protection zones, 363, 369  
 Lightning strike, 364, 369  
 Limitation, 14, 29–35, 43, 100, 113, 133, 161, 192, 222, 238, 399  
 Liquid hydrogen (LH), 387, 388, 390, 392, 414, 415, 417, 418  
 Lithium-ion battery, 301–305  
 LNG, 230–232, 234–236  
 Longitudinal stability, 117–125  
 Losses from evaporation, 396, 397, 399, 403, 404

**M**

Mars helicopter, 84  
 Maximum battery temperature, 302–305  
 Metal, 47, 48, 58, 100, 106, 187, 216, 217, 219, 354, 355, 374, 375, 377, 417  
 Methanol, 51–54, 59, 380, 409  
 Microhardness, 375  
 Microorganisms complex, 353, 361  
 Mining and processing plant, 423–428  
 Mining waste disposal, 427  
 Mixed fuel, 218, 220  
 Modeling, 35, 72, 83, 118, 151–155  
 More electric aircraft (MEA), 189–197  
 Multi-criteria decision-making (MCDM), 260, 336, 342, 343

**N**

Nanofluid fuels, 57, 59–60  
 Nanoparticles, 58, 60, 382  
 Nanostructured materials, 379–383  
 Natural frequency, 20, 22–26, 182, 186, 187  
 Noise contours map, 13–17  
 Noise map, 14, 310  
 Nomenclature, 13, 19, 51, 57, 77, 91, 117, 145, 151, 163, 175, 181, 189, 199, 215, 237, 249, 257, 263, 271, 277, 293, 301, 307, 315, 321, 335, 341, 363, 371, 379, 385, 395, 407, 423  
 Non-intrusive, 65  
 Non-stochastic models, 155  
 Normal category aircraft, 133–144

**O**

Open-source CFD, 91  
 Operators total loads, 341, 342, 344, 346–348  
 Optimization, 4, 100, 144, 160, 222, 243, 263, 264, 267, 269, 317–320

Organizational readiness, 245  
Oxygenated fuels, 57, 61

## P

Particle image velocimetry (PIV), 65–68, 71–74  
PDCA cycle, 213  
Permanent magnet synchronous machine (PMSM), 191, 192  
Petroleum products, 353–355, 361, 362, 396–404, 425  
Phase change material (PCM), 301–305, 347  
PI controller, 117–125  
Pilot, 129, 152–155, 341–343, 345, 346, 348, 349  
Piston engine, 57, 221, 224, 227, 229–234, 236  
Pitch angle, 87, 92, 97, 118–124, 367, 368  
Ply orientation, 176–180  
Policy impact, 285, 290  
Polymer composite, 146, 147  
Processing, 45, 50, 65, 66, 71, 72, 222, 295, 297, 352, 354, 355, 361, 362, 397, 408, 409, 424  
Production, 45–49, 71, 99, 101, 105, 106, 109, 146, 149, 158, 160, 164, 190, 201, 221, 223, 224, 226, 228–231, 294–296, 352–354, 387, 391, 397, 404, 417–420, 424–428  
Protection, 2, 3, 157, 212, 213, 215, 271–275, 307, 312, 354, 389, 425  
Proton exchange membrane fuel cell (PEMFC), 380, 382

## R

Reliability, 129, 160, 190, 211, 246, 263–265, 341, 371–373, 407, 421  
Renewable energy, 6, 385, 414  
Roster, 39–40, 42  
Rotating frame (RF), 92, 93, 95–97  
Rotor, 83–85, 87–89, 91–97, 192, 193, 230  
Rotorcrafts, 83, 84

## S

Safety culture, 200–202, 205, 206  
Safety management, 199–206  
Sandbag testing, 168, 173  
Schedule, 38, 39, 42, 43, 264  
Service quality, 209–213, 258, 259, 342

Silicon oxide (SO<sub>2</sub>), 411  
SimaPro software, 46–48  
Software, 16, 46, 47, 71, 79, 84, 92, 110–112, 182, 186, 266, 269, 316, 373  
Solar-powered UAV, 163–173  
Span-morphing wings, 19–26  
Spark ignition engine, 52, 59  
Specific work of friction (SWF), 374–376  
Speed control, 78  
Stagger shift, 38  
Starter/generator (SG), 189–197  
Static structure, 168  
Stochastic models, 153  
Strategic alliances, 329–333  
SU2, 84, 87, 89, 91–97  
SU2 solver, 84, 89, 91–97  
Sustainability, 1–3, 5, 58, 100, 106, 109, 236, 257–260, 293, 294, 296–298, 330, 380, 382, 385, 386, 388  
Sustainability commitment, 331  
Sustainable aviation, 1–7, 45–50, 100, 113, 157, 238, 250, 256, 258  
Sustainable aviation fuel (SAF), 157, 161, 315, 331, 414  
Sustainable materials, 99–106

## T

Technology, 3–5, 19, 50, 61, 65, 71, 99–101, 110, 112, 116, 146, 153, 157, 158, 200, 203, 204, 221, 229, 231, 236, 243–247, 250, 290, 294–298, 331, 343, 351–362, 380, 396, 401, 403–405, 407–410, 414, 415, 417, 419–428  
Technosphere, 351–362, 401  
Thai aviation law, 271–275  
Thermal management, 230, 231, 302  
Thermoplastic, 100, 101, 106  
Turbofan engine, 322, 323

## V

Vacuum bagging, 146, 147, 164, 165, 168, 171, 176, 177  
Vapor-air mixture (VAM), 399, 402  
Velocity measurement, 65  
Visualization, 65, 77–80, 238  
Visual tracking, 277, 282  
Vortex breakdown, 237–242  
Vortex hazard, 238  
Vortex instability, 238, 242



**W**

Wake hazard mitigation, 237–242

Waste, 45–47, 50, 100, 158, 160, 161, 215, 258, 260, 294, 296, 298, 330, 351–362, 409, 423–428

Waste-free mining technology, 423–428

Wear, 216, 371, 372, 374–377

Wing spar, 142, 164–170, 172, 173

Wing structural design, 138

Wing structure, 135, 138–144, 164, 181, 182, 184–187

Work shift rotating, 127–134